

POLYMER

*The Chemistry, Physics and Technology of
High Polymers*

Editorial Board

C. H. BAMFORD, PH.D., SC.D.

*Director of Research,
Courtaulds Research Laboratory, Maidenhead*

C. E. H. BAWN, C.B.E., F.R.S.

*Professor of Inorganic and Physical Chemistry,
University of Liverpool*

GEOFFREY GEE, C.B.E., F.R.S.

*Sir Samuel Hall Professor of Chemistry,
University of Manchester*

ROWLAND HILL, PH.D.

*Director of Research
I.C.I. Fibres Division, Harrogate*

REPRINTED 1972 FOR
Wm. DAWSON & SONS Ltd., FOLKESTONE
WITH THE PERMISSION OF
IPC SCIENCE AND TECHNOLOGY PRESS, LTD.

Crystallization of Poly- [3,3-bis(chloromethyl)oxacyclobutane]

MASAHIRO HATANO and SHU KAMBARA

The crystallization phenomena of poly[3,3-bis-(chloromethyl)oxacyclobutane] have been investigated by the methods of X-ray diffraction, dilatometry and infra-red spectroscopy. The rates of crystallization to the α -form of the polymers, having various values of intrinsic viscosity, were measured dilatometrically at the constant crystallization temperature over the range 140°–160°C and the results indicated that a maximum value might exist at a temperature lower than 140°C, probably close to 130°C. The experimental results were used to obtain the k and n values in Avrami's expression. It was found that $n=2$ (except at 145°C), and from Morgan and Keller's theory this would indicate that fibrillar growth follows nucleation which is sporadic in time. The fully extended specimen showed infra-red dichroism in the region 3000–500 cm^{-1} . As the crystallization of polymers proceeded, the absorption band at 897 cm^{-1} increased markedly in intensity, whereas the intensity of the absorption band at 1027 cm^{-1} decreased, suggesting that the former is a crystalline and the latter an amorphous band. The rates of crystallization deduced from plots of the optical densities of these bands against temperature, were in good agreement with those obtained dilatometrically.

INTRODUCTION

AS REPORTED by several workers¹⁻⁴, 3,3-bis(chloromethyl)oxacyclobutane, $(\text{ClCH}_2)_2\overline{\text{CCH}_2\text{OCH}_2}$, can be converted into a high molecular weight polyether by the use of acidic catalysts, such as $\text{BF}_3\text{O}(\text{C}_2\text{H}_5)_2$ and SnCl_4 .

Recently we have found that triethylaluminium, diethylaluminium monochloride and triethylaluminium-alkyl halide are suitable catalysts for the above polymerization^{5, 6}.

The polymer $[-\text{OCH}_2-\text{C}(\text{CH}_2\text{Cl})_2\text{CH}_2-]_n$, obtained from 3,3-bis(chloromethyl)oxacyclobutane has very useful properties, particularly insolubility, crystallinity and chemical stability. In the present work, the crystallization phenomena of this polymer has been investigated by the usual dilatometric methods and by infra-red spectroscopy.

Two crystalline forms of the polymer, denoted by α and β , have been found by X-ray diffraction studies^{7, 8}. The α -form was obtained when the polymer was cooled slowly through the melting point; on the other hand, when it was quenched to temperatures below 0°C an amorphous form was obtained, which crystallized gradually to the β -form at room temperature.

The crystallinity of the α -form polymer obtained by crystallizing at 130°C was much larger than that of the β -form obtained by quenching. By using the dilatometer, rates of crystallization to the α -form of polymers, having various values of intrinsic viscosity, have been measured at constant temperatures over the range 140–160°C. The experimental results were used in Avrami's expression⁹ to obtain the k and n values of that expression. The value of n characterizes the form of nucleation and crystal growth in the molten polymer.

EXPERIMENTAL

Materials

All the samples were prepared by applying the techniques used in earlier investigations⁴. Experimental conditions are shown in *Table 1*.

Table 1. Polymerization conditions and viscosities

<i>Sample No.</i>	786	748	788
[M] (mole/l.)	0.885	1.000	1.000
[Cat] (mole/l.)*	0.072	0.046	0.079
<i>Solvent for polymerization</i>	<i>o</i> -Dichloro- benzene	Ethyl bromide	Ethyl bromide
<i>Reaction temperature</i> (°C)	30	-10	-30
<i>Intrinsic Viscosity</i> † of polymer (cm ³ /g)	0.08	0.23	0.42

*BF₃O(C₂H₅)₂ was used as the polymerization catalyst.

†Viscosity measurements were carried out at 110°C in *o*-dichlorobenzene solution.

Since fractionation of the polymers was difficult owing to their insolubility in common solvents, unfractionated samples were employed in the measurement of rates of crystallization.

Measurements of the rates of crystallization

A dilatometric technique similar to that employed by Bekkedahl¹⁰ was used. The measurements were carried out at constant crystallization temperatures selected to lie in the range 140–160°C.

The density of the specimen used in the present work was 1.388 g/cm³. The capillaries of the dilatometers were calibrated by the usual method before measurements of the rates were made.

A curve of specific volume *versus* time at a constant crystallization temperature, T_c , is illustrated in *Figure 1*, and consists of three parts: a cooling period, an induction period and a crystallization period. The curve corresponding to the crystallization period is assumed to have a sigmoid shape.

The curves of the crystallization periods were analysed by the use of Avrami's expression and will be described later. The induction periods, designated t_i in *Table 2*, lengthened appreciably on raising the crystallization temperature.

In order to estimate the apparent rates of crystallization, reciprocals of the half-value period were calculated from the crystallization curves. The half-value period, designated by $t_{1/2}$ in *Table 2*, is defined as the time required for one half of the crystallizable material to crystallize at a constant temperature.

If any crystal nuclei were not completely destroyed, predetermined nucleation was expected to occur. In order to determine the melting temperature of the specimens, melting temperatures of 180°, 190° and 200°C were selected and the rates of crystallization were measured at 145°C.

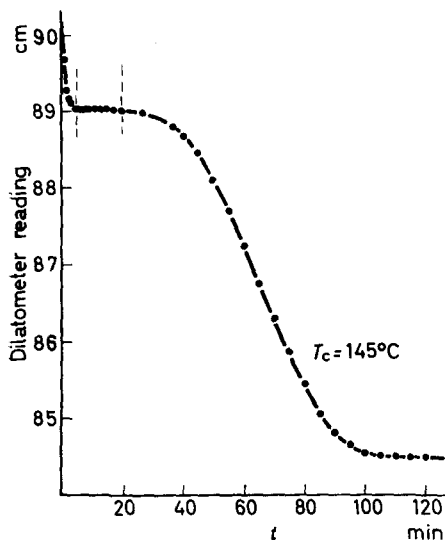


Figure 1—Plot of specific volume versus time at a constant crystallization temperature

The half-value periods found were 4, 12 and 12 min respectively, so that the specimens were known to be completely molten at 190°C, which was the temperature used in the following measurements.

Infra-red absorption measurements

The infra-red absorption measurements were carried out on a Perkin Elmer spectrophotometer, Model 112 (single beam type) using sodium chloride, potassium bromide and calcium fluoride prisms. Dichroisms of the absorption bands of fully (about 300 per cent) extended β -polymers were also measured over the range 3000–500 cm^{-1} , using the above-mentioned prisms and a silver chloride polarizer. To obtain the infra-red spectrum at elevated temperatures, a film of the polymer was sealed together with a thermocouple between sodium chloride plates. This was then placed in a heating cell mounted on the spectrometer.

RESULTS AND DISCUSSION

In order to determine the course of crystallization, several simplifications and assumptions have been made in the statistical treatment.

Avrami has calculated that crystallization processes should in certain limiting cases follow the expression

$$\alpha = e^{-kt^n}$$

where k contains nucleation and growth constants and n has a value of 1, 2, 3 and 4, according to the nature of the nucleation and growth processes. α is the fraction of uncrystallized material and its value at any given time, t , can be calculated from the specific volume at that time, V_t , and the initial and final specific volumes for that crystallization, V_i and V_f , by using the expression

$$\alpha = (V_i - V_t) / (V_i - V_f)$$

Plots of $\log(1/\alpha)$ against t for different crystallization temperatures are shown in Figure 2. They are straight lines, showing that the phase changes conform with Avrami's expression within experimental error.

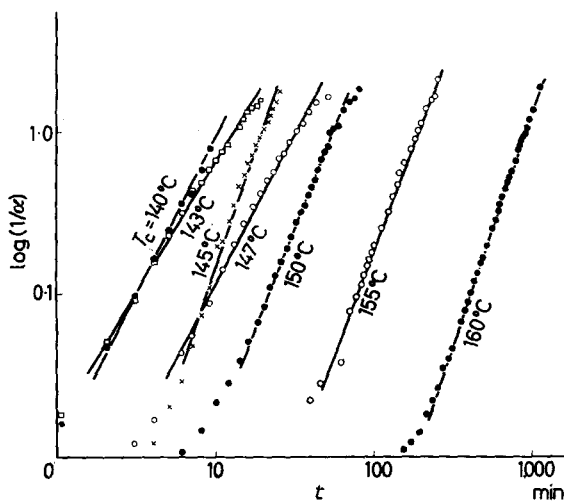


Figure 2—Plots of $\log(1/\alpha)$ against crystallization time, t

Table 2. Rates of crystallization

T_c (°C)	$t_{\frac{1}{2}}$ (min)	$1/t_{\frac{1}{2}}$ (min ⁻¹)	t_1 (min)	n	k
<i>Sample J-786</i> $[\eta]=0.08$ cm ³ /g					
140	8	0.125	0	2.1	8.1×10^{-3}
145	25	0.040	5	3.0	1.6×10^{-4}
150	95	0.0105	35	2.4	3.4×10^{-5}
155	280	0.0038	140	—	—
<i>Sample J-748</i> $[\eta]=0.23$ cm ³ /g					
140	5.5	0.180	0	1.8	2.7×10^{-2}
143	6	0.166	0	1.7	3.5×10^{-2}
145	12	0.083	0	3.3	3.0×10^{-4}
147	17	0.059	8	2.0	3.0×10^{-4}
150	34	0.0294	18	2.4	1.5×10^{-4}
155	114	0.0088	47	2.6	3.2×10^{-6}
160	590	0.0017	140	2.8	2.7×10^{-8}
<i>Sample J-788</i> $[\eta]=0.42$ cm ³ /g					
140	12	0.0835	2	2.2	2.0×10^{-3}
143	24	0.0415	13	2.2	8.3×10^{-4}
145	45	0.0222	15	3.1	3.5×10^{-6}
150	155	0.00645	110	2.4	1.2×10^{-6}

The experimental values of n and k , and the half-value periods for various samples, are summarized in *Table 2*. The relationship between crystallization temperatures and the values of n is shown in *Figure 3*, where it is seen

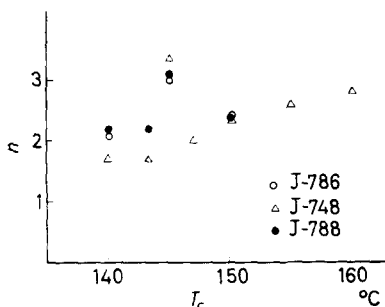


Figure 3—The relationship between crystallization temperatures and the values of n

that n tends to 2 with decreasing crystallization temperature, but at one temperature it has a value of 3. This behaviour was shown by all samples.

According to Keller, Lester and Morgan, the relationship between the form of nucleation and nature of growth in the course of crystallization of the polymers can be summarized as in *Table 3*¹¹. It appears from this

Table 3—Relationship between nucleation and growth in polymers

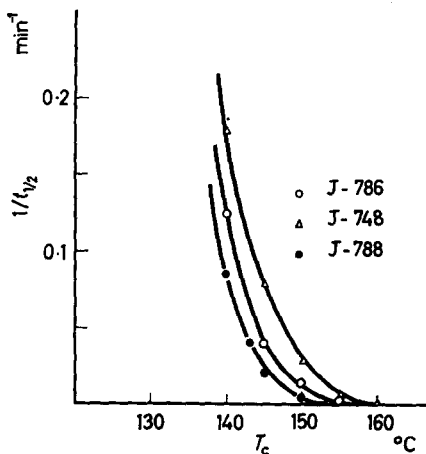
<i>Mechanism of growth</i>	<i>Nucleation</i>	<i>n</i>
Fibrillar	Predetermined	1
	Sporadic in time	2
Fibrillar spherulitic	Predetermined	3
	Sporadic in time	4

that in the crystallization of poly[3,3-bis(chloromethyl)oxacyclobutane], where $n=2$, the nucleation is mainly sporadic in time, and is followed by fibrillar growth. But no explanation can be given for the transition of n from 2 to 3 at 145°C, in all samples.

In order to estimate the apparent rates of crystallization, reciprocals of the half-value periods mentioned above, $t_{1/2}$, were calculated from the crystallization curves. The values of $(1/t_{1/2})$ for different samples are plotted against the crystallization temperature in *Figure 4*. Although the values of $t_{1/2}$ were reproducible in the same sample, it appears that there is no dependence of $t_{1/2}$ on the molecular weight of the polymers. For all samples the curves rose steeply at a crystallization temperature around 140°C. At lower temperatures $(1/t_{1/2})$ was too large to be measured and its maximum value could not be obtained directly. The experimental results indicated that the rate of crystallization might have a maximum value at a crystallization temperature lower than 140°C.

In order to confirm the above-mentioned experimental results, the crystallization of poly[3,3-bis(chloromethyl)oxacyclobutane] has also been investigated by infra-red spectroscopy. The fully extended polymer showed infra-red dichroism in the region 3000–500 cm^{-1} , and some of the

Figure 4—Plot of reciprocals of the half-value periods against the crystallization temperature



absorption bands also showed intensity changes as the crystallization proceeded. It was found that the absorption band at 897 cm^{-1} increased markedly in intensity as the crystallization proceeded, so that this band could be regarded as a crystalline band. On the other hand, the intensity of the absorption band at 1027 cm^{-1} decreased as crystallization proceeded, so that this band could be regarded as an amorphous band.

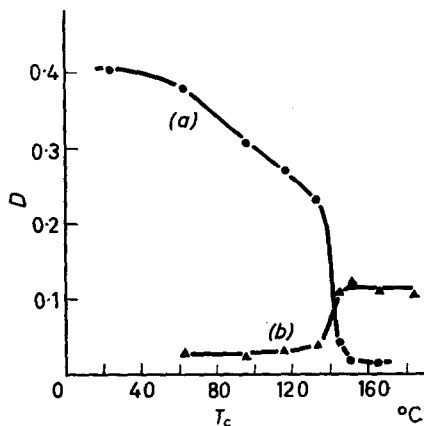
A film of the polymer, 0.03 mm thick, was inserted into the heating cell and cooled from above its melting point to room temperature, and the intensities of the 897 cm^{-1} and 1027 cm^{-1} bands were measured at various temperatures in this region. The plots of intensity against temperature, shown in Figure 5, give a measure of the crystallinity as a function of temperature.

The intensity D was defined as follows:

$$D = \log(I_0/I)$$

where I_0 is the height of the background trace obtained by the base-line method at the peak of the band, and I the height of the band peak. The thickness of the sample was assumed to be constant.

Figure 5—Temperature dependence of the intensities of bands at (a) 897 cm^{-1} and (b) 1027 cm^{-1}



The results obtained from infra-red spectroscopy were in good agreement with the crystallization rates obtained dilatometrically, which are illustrated in *Figure 4*. These results demonstrate that on cooling from melts at 200°C the crystallization of poly[3,3-bis(chloromethyl)oxacyclobutane] commences abruptly at temperatures lower than 140°C, probably close to 130°C, and that the bands at 897 cm⁻¹ and 1027 cm⁻¹ in the spectrum of this polymer are crystallinity-sensitive, the former being a crystalline band and the latter an amorphous band. Detailed results and discussions of the infra-red spectra of poly[3,3-bis(chloromethyl)oxacyclobutane] will be published in the near future¹².

We are also indebted to the Ministry of Education for financial support. Communications Laboratory, Nippon Telegraph and Telephone Public Corporation, for the infra-red spectra, and to Mr Sawatari for his assistance. We are also indebted to the Ministry of Education for financial support.

*Laboratory of Polymer Chemistry,
Tokyo Institute of Technology,
Ookayama, Meguro-Ku,
Tokyo, Japan*

(Received 7th June, 1960.

Revised version received 11th August, 1960)

REFERENCES

- ¹ FARTHING, A. C., *J. chem. Soc.* 1955, p. 3648
- ² FARTHING, A. C., *Brit. Patent 725,777* (2nd February, 1955)
- ³ HULSE, G. E., *U.S. Patent 2,722,520* (1st November, 1955)
- ⁴ KAMBARA, S. and HATANO, M. *J. chem. Soc. Japan, Industr. Chem. Section*, 1957, **60**, 1585
- ⁵ HATANO, M. and KAMBARA, S. *J. Polym. Sci.*, 1959, **35**, 275
- ⁶ HATANO, M. Unpublished data
- ⁷ SANDIFORD, D. J. H. *J. appl. Chem.*, 1958, **8**, 188
- ⁸ HATANO, M. and KAMBARA, S. *J. chem. Soc. Japan, Industr. Chem. Section*, 1959, **62**, 290
- ⁹ AVRAMI, M. *J. chem. Phys.*, 1941, **9**, 117
- ¹⁰ BEKKEDAHL, N. *J. Res. nat. Bur. Stand.* 1949, **43**, 145
- ¹¹ KELLER, A., LESTER, G. and MORGAN, L. *Phil. Trans.* 1954, **274A**, 1
- ¹² HATANO, M. and KAMBARA, S. *J. appl. Polym. Sci.* In press

*The Miscibility of Polymers: II. Miscibility and Heat of Mixing of Liquid Polyisobutenes and Silicones**

GEOFFREY ALLEN, GEOFFREY GEE and J. P. NICHOLSON

Heats of mixing of low molecular weight polyisobutene and poly(dimethyl siloxane) fluids have been measured at 50°C and 100°C over the composition range in which they were miscible. Partial molar heats and entropies of transfer across the phase boundary have also been computed. The heats of mixing are comparable in magnitude with the values predicted by the van Laar-Hildebrand equation, suggesting that random mixing occurs. In sharp contrast to this, the entropies of transfer are much lower than the values calculated on the random mixing approximation, and the Flory-Huggins equation fails to predict the form of the coexistence curve.

PART I of this communication¹ presented values of the polymer-polymer interaction parameter derived from the study of phase equilibria in systems containing two polymers dissolved in a mutual solvent. To compare these parameters with those calculated from phase equilibria in binary mixtures the temperature-composition coexistence curves of three silicones (molecular weights: 850, 1,350, 17,000) with two liquid polyisobutenes (molecular weights: 250, 440) were investigated between 20°C and 180°C. The heats of mixing of two silicones with the lowest molecular weight polyisobutene were measured at 50°C and 100°C over the composition range in which they were miscible.

EXPERIMENTAL

Materials

Two liquid polyisobutenes were supplied by Canadian Polymer Corporation Ltd. Their molecular weights were determined by freezing-point depression measurements in benzene as 250 ± 10 and 440 ± 15 . A liquid silicone of viscosity 428 centistokes and molecular weight 17,000 was supplied by Midland Silicones Ltd, and the other silicone samples were prepared by fractionation of commercial silicone oils by precipitation with methanol from acetone solutions. The bulk viscosities of the fractions were measured in a small Ostwald viscometer which was calibrated with aqueous sucrose solutions. The molecular weights of the silicone fractions were obtained from the molecular weight-bulk viscosity relationships for poly(dimethyl siloxanes) determined by Barry². Densities were determined by weighing against equivalent volumes of distilled water in 10 ml. density bottles.

Phase separation measurements

The polymers were weighed into glass tubes (7 × 120 mm) and heated with vigorous stirring in an oil bath until a clear single-phase solution was

*Part I, *Polymer* 1960, 1 (1), 56

obtained. The reproducibility of the critical solution temperatures varied with the molecular weights and refractive indices of the polymers under examination, but was generally of the order of 2–3 degrees.

Volume changes on mixing

Volumetric tubes (internal dimensions, 250×5 mm) fitted with ground-glass stoppers were prepared from *Veridia* precision bore glass tubing. A small nail sealed in glass was placed in each tube to act as a magnetic stirrer. Each tube was half-filled with silicone by means of a long syringe needle and the polyisobutene was carefully run in to form a separate layer in the same way. The tubes were closed and immersed in a thermostat at 25°C . The position of the polyisobutene–air meniscus relative to a reference mark on the tube was measured with a cathetometer and the two layers of liquid polymer were thoroughly mixed by raising and lowering the internal stirrer thirty or forty times with a magnet. The position of the meniscus relative to the mark was again determined.

Heat of mixing measurements

The calorimeter body consisted of an unsilvered Dewar vessel of internal dimensions 32×120 mm. This was cemented into a *Tufnol* ring which was

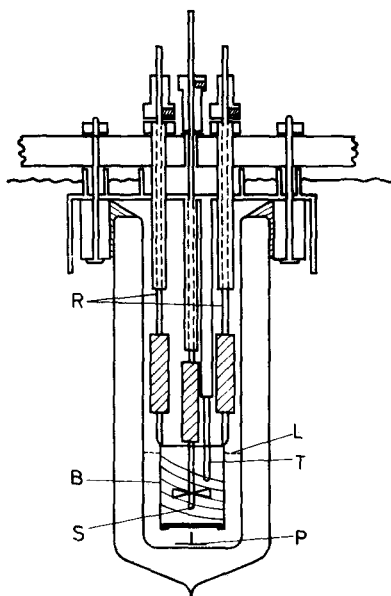


Figure 1—Vertical cross-section of calorimeter: R, control rods; L, liquid level; T, thermistor; P, pin; B, bucket (with heating coil); S, stirrer

bolted to a brass cap to form an oil-tight joint so that the calorimeter could be totally immersed in the liquid-paraffin thermostat (*Figure 1*). Two brass rods passing through the cap supported a 7 ml. bucket formed by a thin

copper cylinder sealed at the bottom with a $\frac{3}{4}$ in.-diameter microscope cover slip. To perform a mixing experiment one polymer was weighed into the bucket and the second into the annular space between the bucket and the wall of the Dewar vessel. The position of the bucket inside the calorimeter could be varied by altering the position of the collars on the supporting rods. These were adjusted so that initially the bucket was immersed as far as possible in the second polymer fluid without actual mixing. The assembled calorimeter was placed in the thermostat and the small propeller stirrer operating inside the bucket was switched on. When temperature equilibrium was reached the polymers were mixed by depressing the control rods so that the bucket became totally immersed in the second polymer and the glass slip forming the bottom of the bucket was broken on a metal pin resting at the bottom of the Dewar. The stirrer circulated the two fluids through the immersed cylinder, now open at both ends, and thorough mixing occurred. The fall in temperature was measured by a thermistor (Standard Telephones Type F1512/300: 6,000 ohm resistance at 100°C) connected in one arm of a Wheatstone net. A coil of *Nichrome* wire was wrapped round the copper cylinder so that the heat absorbed could be measured by the method of electrical compensation.

In each experiment the total volume of polymer fluid in the calorimeter was 15–20 ml. and 1–3 calories were absorbed at each mixing, except at either extreme of the concentration range. The scatter in the heat of mixing results was ± 10 per cent.

RESULTS

Phase relationships

The temperature–composition coexistence curves for the four systems studied are shown in *Figure 2*.

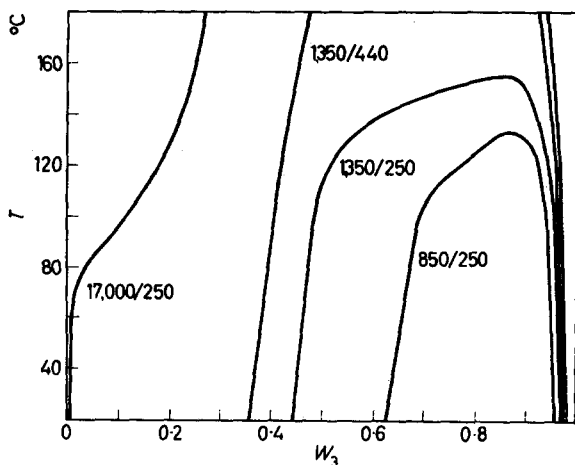


Figure 2—Temperature–composition coexistence curves for silicone (M.Wt. 17,000, 1350, 850) and polyisobutene (M.Wt. 440, 250) mixtures

Volume changes on mixing

The smallest change detectable with the apparatus used was ± 0.01 per cent. No volume change was observed on mixing equal volumes of hexamethylsiliclyl oxide (the silicone 'dimer') and di-isobutene. A contraction of 0.02 per cent of the total volume was found on mixing equal volumes of the silicone-850 and polyisobutene-250.

Heats of mixing

The heats of mixing are plotted in *Figure 3* in terms of the function

$$y = \frac{H_m}{w_2 w_3}$$

where H_m is the heat absorbed (cal/g of mixture) and w_2, w_3 are the weight fractions of polyisobutene and silicone respectively. The very large scatter

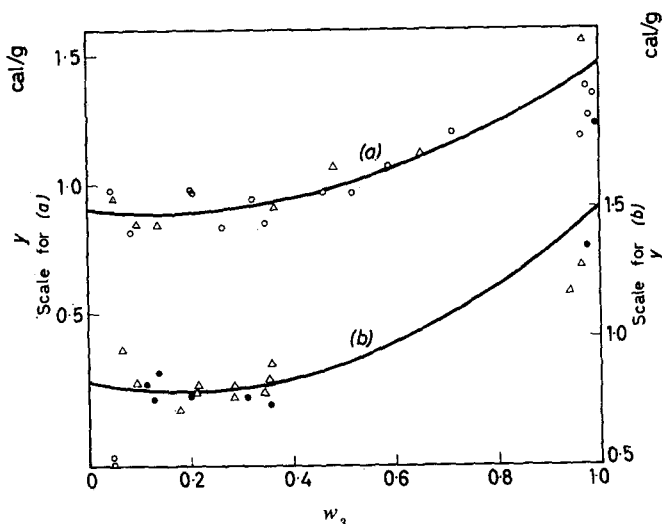


Figure 3—Heat-of-mixing data \circ , \bullet , at 50°C; Δ , at 100°C: (a), silicone-850-polyisobutene-250; (b), silicone-1350-polyisobutene-250

at the extremes of the curves is a consequence of the difficulty of measuring accurately the very small heat absorption in these regions. The shapes of these curves are not well defined by the data, especially for the high molecular weight silicone, where a considerable range of composition is inaccessible owing to incomplete miscibility. The points on each curve refer to observations at two temperatures and it will be seen that there is no evidence of a systematic temperature dependence. A single curve is therefore drawn for each pair of polymers: it is not considered to be more than a reasonable representation of the data.

From the curves of *Figure 3* the partial molar heats of dilution of the system by the two components were derived using the equations

$$\Delta H_2 = M_2 w_3^2 \left(y - w_2 \frac{dy}{dw_3} \right)$$

$$\Delta H_3 = M_3 w_2^2 \left(y + w_3 \frac{dy}{dw_3} \right)$$

The results are shown in *Figures 4 and 5*.

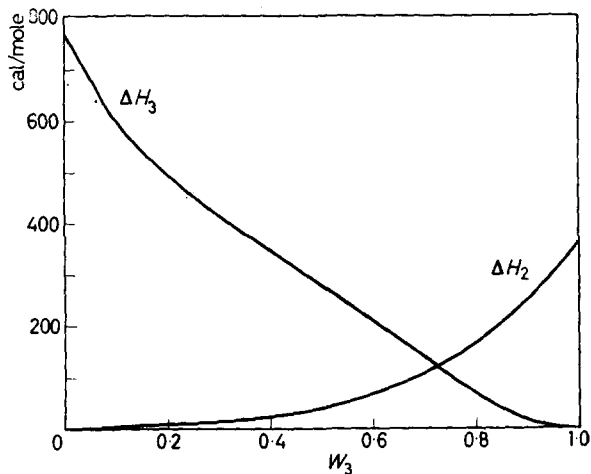


Figure 4—Partial molar heats of dilution: silicone-850-polyisobutene-250

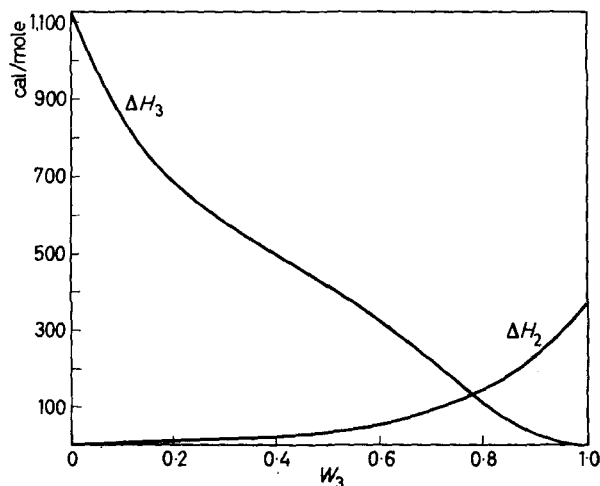


Figure 5—Partial molar heats of dilution: silicone-1350-polyisobutene-250

Densities and coefficients of expansion

The experimental results are expressed in weight fractions and mole fractions but, where necessary for calculations, these were converted to volume fractions using the data in *Table 1*.

Table 1

	Density (g/ml.)	$10^4 \times$ Coeff. of exp. (deg ⁻¹)
Silicone-850	0.911	
Silicone-1,350	0.939	
Silicone-17,000 ³	0.969	9.0
Polyisobutene-250	0.830	
Polyisobutene-440 ³	0.838	7.1

DISCUSSION

Comparison with the Flory-Huggins theory

It has been shown that there is no appreciable volume change on mixing and that the heat of mixing is substantially independent of temperature. The observations encourage the hope that the data can be fitted by the simple Flory-Huggins theory which gives the Gibbs free energy of mixing (ΔG) for this system as

$$\frac{\Delta G}{RT} = n_2 \ln \phi_2 + n_3 \ln \phi_3 + \alpha_{23} V \phi_2 \phi_3 \quad (1)$$

where n_2 moles of component 2 occupy a fraction ϕ_2 of the total volume V .

In this expression the heat of mixing is

$$\Delta H_m = \alpha_{23} RTV \phi_2 \phi_3 \quad (2)$$

and it is implied that α_{23} is proportional to T^{-1} . α_{23} is related to y (Figure 3) by the expression

$$\alpha_{23} = \frac{\rho_2 y}{RT} \left\{ 1 + \frac{(\rho_3 - \rho_2)}{\rho_2} w_2 \right\}$$

where ρ_2 and ρ_3 are the densities of the polymers. In Figure 6 α_{23} is plotted for both systems at 25°C assuming y to be independent of T . As would be expected, the two systems show very similar behaviour, the small differences being almost within experimental error. α_{23} is concentration-dependent, with a value of approximately 1.4 mole/l. in the middle concentration range. Equating this with the van Laar-Hildebrand expression gives 0.9 cal^{1/2} cm^{-3/2} as the calculated difference between the solubility parameters, δ_2 and δ_3 . This is somewhat greater than 0.6, the difference assigned in Part I¹, but is within the limits of accuracy to which these quantities are known. We may conclude therefore that the order of magnitude of the heat of mixing is in accord with the value to be expected on the assumption that the polymers form an essentially random mixture.

The values of α_{23} can also be compared with those obtained from the conditions for critical separation into two phases. If equation (1) holds, no separation can occur unless α_{23} exceeds the critical value

$$\alpha_c = \frac{1}{2} (V_2^{-1} + V_3^{-1})^2 \quad (3)$$

Taking $\alpha_{23} = 420/T$ mole/l., and equating with α_c , we calculate from equation (3) that the upper critical solution temperatures should be -185°C

(silicone-850) and -170°C (silicone-1350). Thus, if the heat of mixing alone is responsible for phase separation in these systems, it would be expected to produce immiscibility some 300 degrees below the observed critical solution temperature.

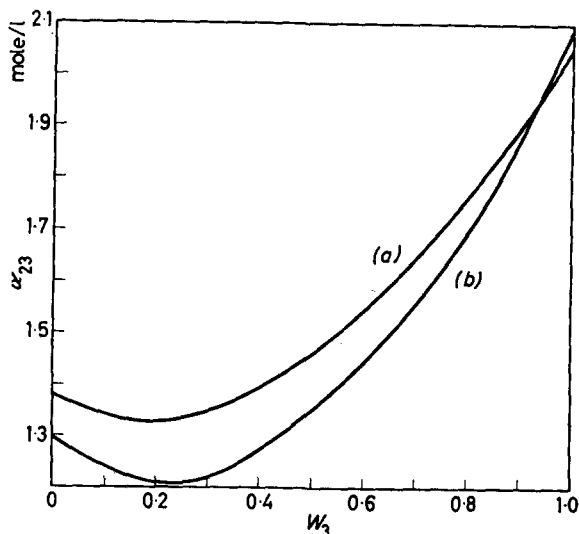


Figure 6—Interaction parameter α_{23} : (a), silicone-850-polyisobutene-250; (b), silicone-1350-polyisobutene-250

The simplest explanation of this discrepancy could be the failure of equation (2). It is possible that the quantity $\alpha_{23}RT\phi_2\phi_3$ in equation (1) also contains an entropy contribution and is not equal to ΔH . A further test of equation (1) has therefore been applied by considering the forms of the coexistence curves. Assuming that at the upper consolute temperature α_{23} has the value given by equation (3) rather than equation (2), we should expect the composition of the critical mixture to be given by

$$\frac{1}{\phi_{3c}} = 1 + \left(\frac{V_3}{V_2}\right)^{\frac{1}{2}} \quad (4)$$

This equation fails completely. The extent of the discrepancy is shown clearly in Figure 7, which compares an experimental coexistence curve with the one calculated from equations (1) and (3).

Entropies of transfer

Although our data do not permit a full thermodynamic analysis of the systems, the entropies of transfer of the components between coexisting phases are readily calculable. If $\Delta S_{2b \rightarrow a}$ and $\Delta H_{2b \rightarrow a}$ are respectively the partial molar entropy and heat of transfer of component 2 from phase 'b' to phase 'a', the condition for coexistence of the two phases requires that

$$T\Delta S_{2b \rightarrow a} = \Delta H_{2b \rightarrow a} = \Delta H_{2a} - \Delta H_{2b} \quad (5)$$

where H_{2a} is the partial molar heat of dilution of 'a' by pure component 3.

Similarly,

$$T\Delta S_{3a \rightarrow b} = \Delta H_{3a \rightarrow b} = \Delta H_{3b} - \Delta H_{3a} \quad (6)$$

Since the heats of dilution have been shown to be independent of temperature, $\Delta S_{2b \rightarrow a}$ and $\Delta S_{3a \rightarrow b}$ will also be independent of temperature and can be calculated from any pair of coexisting phases.

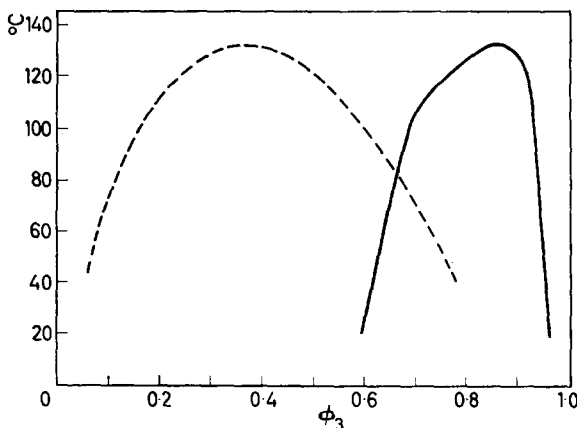


Figure 7—Coexistence curves for silicone-850-polyisobutene-250: - - -, calculated; —, observed

For regular solutions,

$$\begin{aligned} \Delta S_{2b \rightarrow a} &= R \ln (x_{2b}/x_{2a}) \\ \Delta S_{3a \rightarrow b} &= R \ln (x_{3a}/x_{3b}) \end{aligned} \quad (7)$$

while for solutions containing polymer molecules Flory's equation gives

$$-\frac{\Delta S}{R} = n_2 \ln \phi_2 + n_3 \ln \phi_3$$

whence

$$\begin{aligned} \Delta S_{2b \rightarrow a} &= R \ln (\phi_{2b}/\phi_{2a}) + R (\phi_{2a} - \phi_{2b}) (1 - V_2/V_3) \\ \Delta S_{3a \rightarrow b} &= R \ln (\phi_{3a}/\phi_{3b}) + R (\phi_{3b} - \phi_{3a}) (1 - V_3/V_2) \end{aligned} \quad (8)$$

Figures 8 and 9 show the values calculated from the experimental data as a function of $\ln(x_{2a}/x_{2b})$ together with the lines calculated from equations (7) and (8) which are respectively labelled ΔS_{3R} and ΔS_{3F} .

These plots show clearly that some, at least, of the discrepancies observed in trying to fit our experimental results arise from an exceptionally low entropy of mixing. It is not at all obvious to us why there should be such a small increase of entropy when these polymeric fluids mix, since this contrasts sharply with the normal heat of mixing previously noted.

In Part I¹ it was concluded that only very imperfect mixing takes place in ternary solutions containing two polymeric species. In the binary systems discussed in this paper, mixing appears to be substantially complete. The low entropy of mixing may therefore arise from a regular ordering

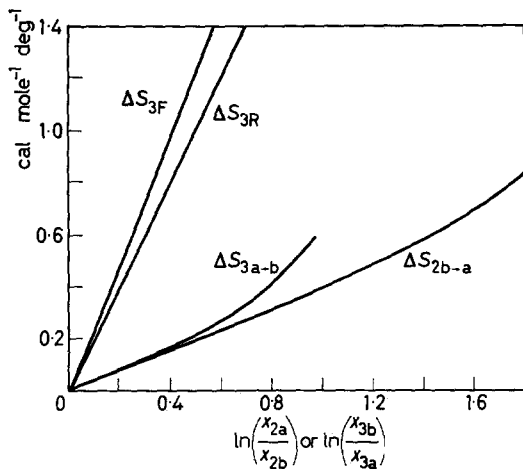


Figure 8—Entropies of transfer: silicone-850-polyisobutene-250

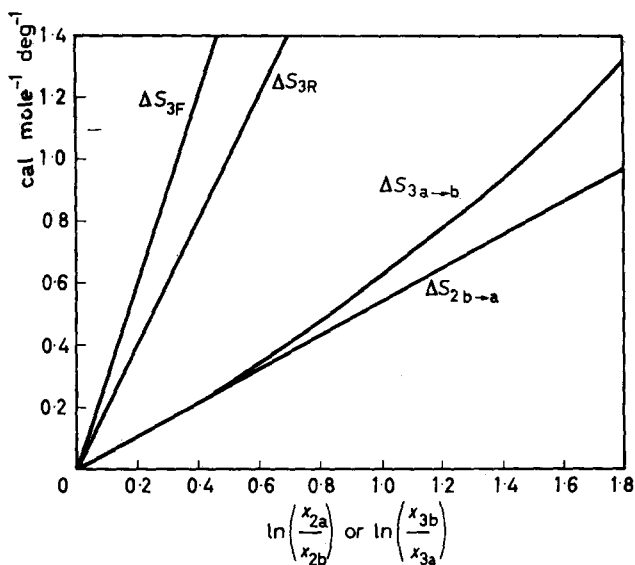


Figure 9—Entropies of transfer: silicone-1350-polyisobutene-250

of the mixture or perhaps from a loss of intramolecular configurational entropy when unlike polymer chains are packed together.

Before speculating further on the significance of these results it is desirable to extend the present investigation to a number of other binary mixtures: this work is now in progress.

*The Chemistry Department,
The University,
Manchester, 13*

(Received 22nd August, 1960)

REFERENCES

- ¹ ALLEN, G., GEE, G. and NICHOLSON, J. P. *Polymer* 1960, **1** (1), 56
- ² BARRY, A. J. *J. appl. Phys.* 1946, **17**, 1020
- ³ MANGARAJ, D. *Ph.D. Thesis*, University of Manchester, 1959

Anion Exchangers Based on Cellulose: I. Preparation and General Properties

A. O. JAKUBOVIC* and B. N. BROOK

A number of ion-exchange derivatives of cellulose have been synthesized by two etherification processes. One of these involves the action of chloroalkylamines upon alkali cellulose, whilst the other is based on the reaction of the latter with aminoalkyl hydrogen sulphates. The reaction yields, based on the amount of aminoalkylating agent used, were rather low (generally about 30 per cent of theoretical) and this was found to be principally due to side-reactions between the reagent and excess alkali present in the reaction mixture. The preparative technique is capable of producing a variety of exchangers having different basic strengths, although no quaternary compounds have been made. All the products were fibrous, having anion-exchange capacities of up to 2 mequiv/g dry cellulose derivative and equilibrium swelling water contents between 55 and 80 per cent.

RECENT WORK in the development of new ion exchangers has been primarily concerned with the production of materials of greater specificity. Most innovations dealt with new functional groups, with only limited reference to changes in the polymer network. The increasing knowledge of polymerization and condensation reactions and products, typified by exchangers based on polystyrene or polyvinyl matrices on the one hand, and aldehyde-phenol or aldehyde-amine condensates on the other, has virtually eliminated the use of naturally occurring substances. On the whole the synthetic matrices employed were hydrophobic. The exchange sites are accessible to electrolytes primarily by virtue of the hydrophilic nature of the functional groups, which make the resins permeable to water, the degree of swelling being controlled by the amount of crosslinking.

It has recently been realized that cellulose derivatives which can act as ion exchangers offer a number of advantages, resulting principally from the fibrous and hydroxylic nature of the polyelectrolyte matrix. These factors exert a considerable influence, especially on the kinetics of exchange. Thus, the functional groups of cellulosic exchangers are more readily accessible; the size of even finely ground resins cannot approach that of the fibre diameter. A particularly important consequence is the far greater capacity for large ions, such as proteins¹ and nucleic acids², which are substantially excluded from resinous exchangers³. Further, the carbohydrate matrix enhances the hydrophilic nature of the system, swelling no longer depending on the functional groups alone. Cellulosic exchangers can also be made into sheets and have thereby given rise to the new analytical technique of ion-exchange paper chromatography⁴.

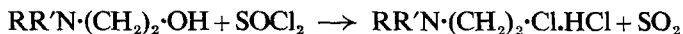
This account deals with the preparation and general characteristics of a range of weakly basic cellulosic anion exchangers. Certain of their fundamental anion-exchange characteristics will be considered in some detail in a subsequent communication¹⁰.

*Present address: Research Laboratories, Jacksons' Millboard & Fibre Co. Ltd, Bourne End, Bucks.

EXPERIMENTAL

Preparation of chloroalkylamines

The method employed followed the general preparative technique of Hall, Stephens and Burckhalter⁵, involving the reaction between thionyl chloride and the requisite alkanolamine according to the equation



where R and R' are hydrogen, alkyl, or similar radicals. The products obtained were off-white, amorphous, and could be further purified by acetone extraction. Some of the higher alkanolamines, for instance di-isopropylaminoethanol, gave viscous liquid products, completely miscible with most solvents and these were not further purified.

A typical preparation was as follows. 75 g of dimethylaminoethanol was added to 113 g of thionyl chloride with continuous stirring and cooling over a period of 40 min. The temperature of the reaction mixture was then maintained at 35°C for a further 10 min before extraction of the reaction mass with acetone. Crystallization from acetone gave a product having a nitrogen content of 9.5 per cent, whilst the calculated value is 9.7 per cent.

Preparation of aminoalkyl hydrogen sulphates

The preparative method was similar to that of Leighton, Perkins and Renquist⁶. The monoalkanolamine concerned was treated with fuming sulphuric acid according to the general equation



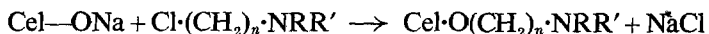
where R and R' again represent hydrogen or alkyl or similar radicals. Monoethanolamine gave a white solid product, but the other alkanolamines produced highly viscous liquids, the reaction mixture displaying a marked tendency to solidify when approximately half the acid (that is an equivalent quantity) had been added. This may well be due to the formation of the di(aminoalkyl) sulphate.

The following illustrates a typical preparation. 115 g of fuming sulphuric acid was gradually added to 51 g of monoethanolamine. The reaction was carried out in an ice bath with continuous stirring. The viscosity of the reaction mixture increased as the reaction proceeded and the crude aminoalkyl hydrogen sulphate formed as a coloured slurry. The reaction time was 60 min. The crude product was extracted with aqueous ethanol and further purified by washing with ethanol on a Buchner filter. The nitrogen content of the crystallized derivative was found to be 9.6 per cent, whilst the calculated figure is 9.9 per cent. The yield was 78 per cent of the theoretical.

Preparation of derivatives using chloroalkylamines

Etherification of cellulose using chloro-compounds is a well-established technique for preparing cellulose derivatives. If the chloro-compound contains a suitable ionizing substituent group, it can be employed for the preparation of ion-exchange celluloses. In the case of chloroalkylamines,

the amino group is the potential ion-exchange site and the preparative reaction can be represented by the equation



In this equation the alkali cellulose is represented by Cel—ONa and n is usually 2.

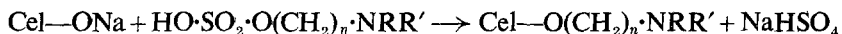
The general preparative technique was to mercerize the cellulose with a suitable sodium hydroxide solution, add an aqueous solution of the reagent, and heat to bring about the etherification. A typical reaction was carried out as follows: 10 g of purified wood cellulose was thoroughly homogenized in the cold with 40 g of 5N sodium hydroxide solution. After mercerization, the cellulose was further treated with an aqueous solution of 12 g of 2-chloroethyl-dibutylamine hydrochloride. The well dispersed mixture was heated at 95°C for 100 min. The cellulosic product was washed with water, then twice cycled with 0.5N hydrochloric acid and 0.2N sodium hydroxide solutions. It was finally washed free of excess alkali.

Another typical preparation, using 2-chloroethyl-isopropyl amine, has been described in a preliminary communication⁷.

Preparation of derivatives by the aminoalkyl hydrogen sulphate technique

The reaction of alkali cellulose with organic sulphates is an alternative method for preparing cellulose ethers⁸. As in the case of halogen compounds, of which the chloro-compound was used as described in the preceding subsection, the choice of a sulphate containing a potential ion-exchange group ensures that the ether formed will be an exchanger.

Reactions of this type can be represented by the equation



In practice, as there is always an excess of sodium hydroxide present, the final by-product will be sodium sulphate and not bisulphate. Further, of course, the reaction is complicated by decomposition of the reagent by the sodium hydroxide present and as this also applies to the chloroalkylamine method it will be dealt with in the discussion section.

The general preparative technique can best be illustrated by quoting a typical example, which was as follows. A 10 g sheet of purified wood cellulose was steeped in a solution having the following composition: 30 per cent of di-isopropylaminoethyl hydrogen sulphate, 14 per cent of sodium hydroxide and 56 per cent of water. The uniformly steeped sheet contained 59 g of this solution and the subsequent reaction was carried out at 105°C for 80 min. The product was washed, cycled, and re-washed as described under the previous heading.

Details of another reaction of this type, employing diethylaminoethyl hydrogen sulphate, have been given elsewhere⁷.

Determination of nitrogen content

The nitrogen contents of the various substances were determined by the standard Kjeldahl method. The error involved in the determination was found to be within ± 2 per cent.

Determination of ion-exchange capacity and titration curves

Direct titration of weak exchangers is rather unsatisfactory since the rate of ionization is generally slow. An equilibration technique was therefore used to obtain the titration curves. About 0.5 g quantities of the exchanger were accurately weighed into 150 ml flasks. To each of these 75 ml. of 0.1N potassium chloride solution was added, together with a varying quantity of 0.1N hydrochloric acid to give suitable degrees of ionization; the acid additions were calculated from the theoretical capacity derived from the nitrogen content. By varying the amount of hydrochloric acid added degrees of neutralization from zero to one can be obtained. Removal of carbon dioxide from the equilibrating mixture and from the free space in the flask was ensured by passing nitrogen. The flasks were then stoppered and agitated for up to ten days. The pH values at equilibrium were measured with a lithium glass electrode and a standard calomel reference electrode. Errors due to any finely suspended insoluble cellulose polyelectrolyte were minimized by decanting the ambient solution for pH measurement. Generally, true equilibrium was reached within 7 days. The experimental capacities were taken to correspond to the quantity of acid taken up by the exchanger when the pH of the solution phase was 5.0.

RESULTS AND DISCUSSION

Preparative considerations

Tables 1 and 2 list, respectively, the derivatives prepared by the reaction of alkali cellulose with chloroalkylamines and aminoalkyl hydrogen sulphates, together with the percentage of nitrogen, degree of substitution, and the calculated and experimental anion-exchange capacities.

Table 1. Derivatives obtained by etherification with chloroalkylamines

Reagent	Nitrogen content (%)	Degree of substitution	Exchange capacity (mequiv/g of dry exchanger)	
			Calculated	Experimental (at pH 5)
Chloroethylamine	0.34	0.04	0.24	0.19
Chloroisopropylamine	0.09	0.01	0.06	—
Chloroethyldimethylamine	0.70	0.08	0.50	0.48
Chloroethyldiethylamine	2.70	0.39	1.91	1.80
Chloroethyldiisopropylamine	2.50	0.37	1.79	1.79
Chloroethyldibutylamine	0.96	0.12	0.69	0.69

It can be seen that there are considerable differences in the extent of substitution of the various cellulose derivatives. As the same type of cellulose and identical mercerization techniques were used in all preparations, this reflects the difference in reactivities of the alkali cellulose with

the various reagents concerned, and in some cases the limited accessibility of the reaction sites to the large substituent groups. However, a further complication arises from the reaction of excess alkali hydroxide (always

Table 2. Derivatives obtained by etherification with aminoalkyl hydrogen sulphates

Aminoalkyl hydrogen sulphate	Nitrogen content (%)	Degree of substitution	Exchange capacity (mequiv/g of dry exchanger)	
			Calculated	Experimental (at pH 5)
Aminoethyl	1.70	0.21	1.21	0.93
Dimethylaminoethyl	0.17	0.02	0.12	—
Diethylaminoethyl	0.89	0.11	0.64	0.56
Di-isopropylaminoethyl	0.75	0.09	0.54	0.53
Dibutylaminoethyl	0.21	0.025	0.15	0.14
Di-2-ethylhexylaminoethyl	0.09	0.01	0.06	—

present in 'mercerized' cellulose) with the reagent. As will be seen later, this is frequently a more efficient process than the desired etherification reaction.

To achieve reasonable substitution, the reaction conditions had to be varied so as to allow for side-reactions and the apparent unreactivity of certain of the aminoalkylating reagents. In this connection the main variables are the time and temperature of the etherification. As an illustration of a simpler case, *Figure 1* shows the variation in capacity with

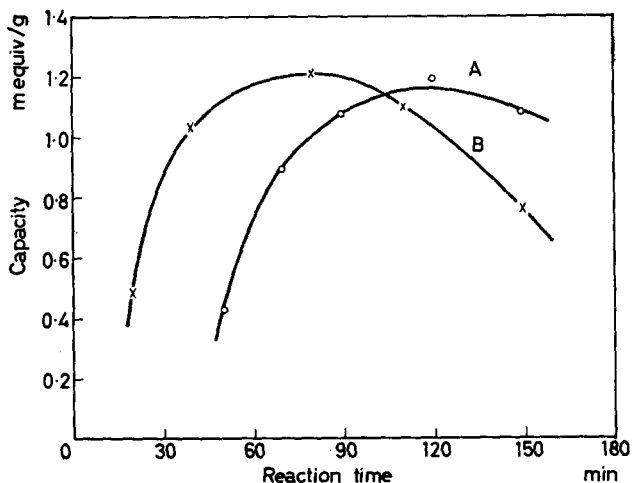


Figure 1—Variation in capacity with reaction time for aminoethylcellulose at: A, 100°C; B, 115°C

duration of the reaction for aminoethylcellulose, prepared by the reaction of sodium cellulose with aminoethyl hydrogen sulphate, at two temperatures. This figure also illustrates another general feature, namely the existence of

upper optima of reaction temperature. It can be seen that at 115°C after some 90 min the capacity of the product begins to fall, indicating that any increase in the degree of substitution is accompanied by losses due to such factors as degradation of the cellulose and derivative solubilization. The results given in the tables refer to fibrous products, but it should be noted that in some cases derivatives of higher substitution could be prepared, though these were in the form of highly swollen gels or even were water soluble. The subject of ion-exchange cellulose gels is outside the scope of this communication and is dealt with elsewhere^{9,10}.

Figure 2 illustrates the variation in capacity which can be brought about by changing the proportion of reagent to cellulose (moles of aminoalkylating compound per monosaccharide unit of the cellulose) in the reaction mixture for two typical derivatives, one prepared by the chloroalkylamine technique and the other by the aminoalkyl hydrogen sulphate method.

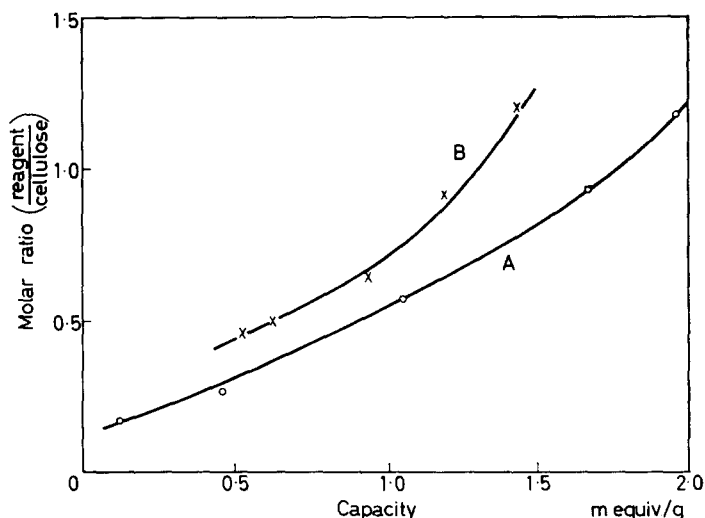


Figure 2—Variation in capacity with the ratio of reagent to cellulose in the reaction mixture for: A, the chloride; B, the sulphate

The extent of substitution possible in the presence of a given amount of reagent can be calculated. The results show that in no case more than 50 per cent of the reagent has combined with the cellulose, the value more generally being between 20 and 30 per cent. The most likely causes responsible for this are (a) thermal decomposition of the reagent; (b) unreactivity of the reagent and (c) side-reactions. (a) was shown not to be the case with most of the reagents used, whilst (b) accounted for the low yield only infrequently, for there was little recovery of the unchanged aminoalkylating agent at the end of the various reactions. Butyl- and octylaminoethyl hydrogen sulphates exhibited a certain degree of unreactivity, probably stemming from their limited water solubility, resulting in substantial immiscibility of the reaction constituents or even phase separation. Clearly, the major cause was the existence of side-reactions.

The main interfering reaction in these etherifications appears to be the decomposition of the reagent by the excess of alkali present in the reaction mixture. This was particularly evident in the case of certain chloroalkylamines, especially the aminoethyl and dimethylaminoethyl compounds, which necessitated the use of very mild reaction conditions to avoid severe decomposition of the chloro-compounds by the sodium hydroxide.

General properties

The titration curves of the exchangers prepared are given in *Figure 3*. Even the limited number of exchangers illustrated clearly show that a

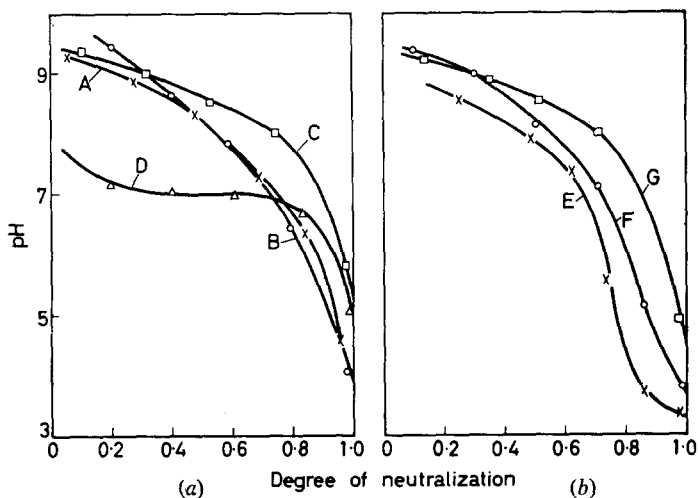


Figure 3—Titration curves of cellulose derivatives prepared (a) by the chloroalkylamine method and (b) by the sulphate method: A, dimethylaminoethyl-; B, diethylaminoethyl-; C, di-isopropylaminoethyl-; D, dibutylaminoethyl-; E, aminoethyl-; F, diethylaminoethyl-; G, di-isopropylaminoethyl-

significant variation in base strength of these derivatives can be achieved. The titration curves show the exchangers to be essentially monofunctional, which agrees with the equations given in the experimental section.

An important consideration is whether the use of the two alternative methods leads to similar exchangers, provided the functional groups (i.e. the alkylamine radicals in the two types of reagent) are the same. To illustrate this point, *Figure 4* juxtaposes the titration curves of diethylaminoethyl- and di-isopropylaminoethylcelluloses, each prepared both by the chloride and the sulphate method. It can be seen that the titration curves of the two diethyl and di-isopropyl derivatives practically coincide, proving that the functional groups of the derivatives are the same whichever preparative technique is used. The very slight differences that can be detected could have arisen from experimental errors in the determination of the titration curve, although they could also be due to slight differences in the degradation of the cellulose during the two different etherification reactions. Nevertheless, the differences are insignificant and in practice

either technique can be used to prepare these exchangers, the more efficient reaction, giving a better yield and a product having a higher degree of substitution being the one generally selected. The various titration curves also illustrate the significant difference between the primary and tertiary amino-derivatives, the former being much weaker exchangers, and this will be considered in detail in a subsequent paper¹⁰.

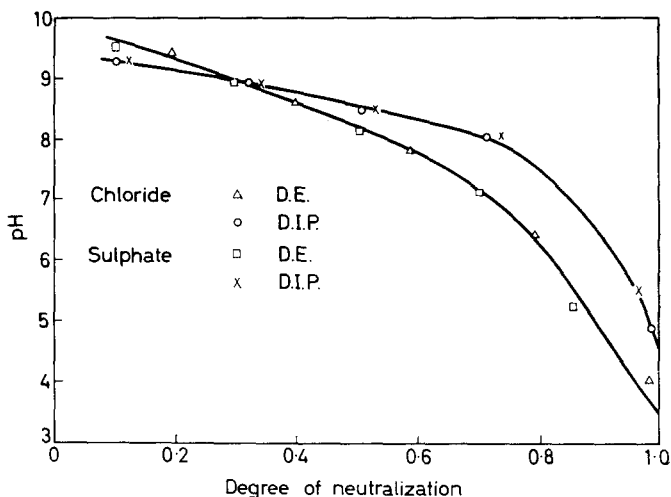


Figure 4—Titration curves of diethylaminoethyl- and di-isopropylaminoethyl celluloses prepared by the chloride and the sulphate method

The equilibrium swelling (weight percentage of water in the swollen exchanger) of these derivatives in the free base form was between 55 and 80 per cent; as expected, in the ionized state (e.g. chloride counter-ionic form) the swelling invariably increased. Whilst in resinous exchangers the swelling is primarily due to the functional groups themselves, the matrix being hydrophobic, in cellulosic exchangers both the ionizable groups and the hydroxylic cellulose network partake in swelling. The complex nature of the swelling of cellulose¹¹ and the effect of mercerization during the preparation make full evaluation of swelling phenomena in these derivatives difficult. It was established, however, that, in addition to the counter-ionic form, the degree of substitution and the nature of the functional group exert a dominant influence on the swelling of these exchangers. There was no evidence of crosslinking in the derivatives, in agreement with the reaction equations given above. The exchanger-water equilibrium will be discussed further¹⁰.

Ion exchangers should be stable to dilute aqueous acids and alkalis as these are frequently used for cycling, regeneration and similar operations. It was found that the prepared cellulose derivatives did not shed their functional groups on prolonged keeping in electrolyte solutions of pH from 0 to 14, which is in accord with the known stability of the glycosidic ether link under such hydrolytic conditions. Stability experiments conducted

over several weeks produced no significant changes in the nitrogen content and capacity of the various exchangers. As the cellulosic nature has been retained in these derivatives, however, stability towards strong oxidizing agents was found not to be of the same high order. Nevertheless, the exchangers were generally unaffected by mild oxidants, such as dilute aqueous chlorate and dichromate solutions.

Thanks are due to Mr R. C. Parsons for experimental assistance and to the Directors of W. & R. Balston Ltd, for permission to publish.

*Whatman Research Laboratory,
W. & R. Balston Ltd,
Maidstone, Kent*

(Received 26th September, 1960.

Revised version received 26th October, 1960)

REFERENCES

- ¹ PETERSON, E. A. and SOBER, H. A. *J. Amer. chem. Soc.* 1956, **78**, 751;
ELLIS, S. and SIMPSON, M. E., *J. biol. Chem.* 1956, **220**, 939
- ² BENDICH, A., FRESKO, J. R., ROSENKRANZ, H. S. and BEISER, S. M. *J. Amer. chem. Soc.* 1955, **77**, 3671
- ³ e.g. CALMON, C. and KRESSMAN, T. R. E. *Ion Exchangers in Organic and Biochemistry* Interscience, New York, 1957
- ⁴ KEMBER, N. F. and WELLS, R. A. *Nature, Lond.* 1955, **175**, 512;
JAKUBOVIC, A. O. in *Chromatographic Techniques* 2nd edn, Heinemann, London, 1960
- ⁵ HALL, L. A. R., STEPHENS, V. C. and BURCKHALTER, J. H. in *Organic Syntheses* 1951, **31**, 37 (Wiley, New York)
- ⁶ LEIGHTON, P. A., PERKINS, W. A. and RENQUIST, M. L. *J. Amer. chem. Soc.* 1947, **69**, 1540
- ⁷ JAKUBOVIC, A. O. *Nature, Lond.* 1959, **184**, 1065
- ⁸ HEUSER, E. *Chemistry of Cellulose* Wiley, New York, 1947
- ⁹ HUEHNS, E. R. and JAKUBOVIC, A. O. *Nature, Lond.* 1960, **186**, 729
- ¹⁰ JAKUBOVIC, A. O. In preparation
- ¹¹ e.g. HONEYMAN, J. *Recent Advances in the Chemistry of Cellulose* Interscience, New York, 1959

Direct Examination of Polymer Degradation by Gas Chromatography:

I. Applications to Polymer Analysis and Characterization

A. BARLOW, R. S. LEHRLE and J. C. ROBB

Two techniques of polymer degradation have independently been incorporated into a conventional gas chromatography apparatus, so arranged that the carrier gas sweeps the degradation products directly into the analysis column. The method involving pyrolysis on a filament has proved most versatile, since any temperature up to 1000°C may be selected for the degradation. The chromatogram series for a given polymer at a number of temperatures gives a rapid and unambiguous characterization of the polymer. Quantitative measurements on the chromatograms of copolymers and polymer mixtures enable their composition to be determined with an accuracy better than 2 per cent.

INTRODUCTION

INFORMATION from polymer degradation studies may conveniently be grouped under two headings: (1) that derived from an examination of the degradation products and (2) that derived from measurements of the rate of evolution of these products, at various temperatures. The techniques and results described here fall under heading (1); the determination of rates and energies of activation will be described in a forthcoming publication.

In most cases the degradation products are fragments characteristic of the original structure; these may be used to characterize unknown structures or to identify polymers. Moreover, a quantitative estimation of the products enables analyses of polymer mixtures and copolymers to be carried out.

Products from polymer degradations have been examined by gas chromatography by various workers¹⁻³, and the present authors have described⁴ the principles of methods by which the degradation could be effected in the gas chromatography flow-stream, so that a pulse of degradation products could be characterized as they were formed. This reduces the possibility of decomposition of the primary products of degradation (which appears to have occurred to a marked extent in the method of Angelis³, for example), and has the added advantage of speed of operation, so that for a given sample the products obtained over a range of temperatures may be quickly measured. More recently, other authors⁵⁻⁷ have described variants of this one-stage method, though in these cases the change in behaviour with temperature of pyrolysis was not utilized as a further parameter for characterization. The application of the method to the study of a wider range of organic compounds has also been described^{8,9}.

Any one-stage method requires that the time of pyrolysis should be short in order that chromatographic resolution of the products shall not be impaired. In the present work two degradation techniques have been used: (a) the sample was used as the dielectric in a condenser and was

broken down by triggering a high-energy discharge between the plates, and (b) the sample was placed on a filament and pyrolysed by passing a predetermined current through the wire for about ten seconds. These two methods are here assessed with respect to their application in polymer characterization and analysis.

METHODS

Gas chromatography apparatus

Detector unit—A katharometer detector unit was constructed to withstand temperatures in the region of 300°C, and the channels in it were arranged so that the gas streams from the columns did not impinge directly upon the tungsten filaments, since earlier designs had indicated that this may be a cause of instability. Effects of the variation in ambient temperature were minimized by fixing the unit within the column heating jacket.

Chromatography tubes—Both the reference and the chromatography tube were of glass, 135 cm long, 4 mm in diameter.

Solid supporting material—Crushed firebrick (Johns Manville *Chromosorb*, mesh 30–60). Both ‘normal’ and ‘acid-washed’ materials were used, with some difference in behaviour to which reference will be made later.

Stationary liquid phase—In some of the earlier work, column temperatures from 150° to 280°C were used, and a number of stationary liquid phases were examined with respect to their stability and resolving power over this temperature range. The two most successful materials proved to be silicone oil and low-molecular weight polyethylene (ex Badisch Anilin and Soda-Fabrik A.G., Ludwigshafen, m.p. 105°C, mol. wt. \approx 2500). The polyethylene column was made up by dissolving the material in refluxing toluene, adding this solution to the charge of firebrick, and distilling off the toluene under low vacuum. The firebrick was introduced into the chromatography tube, which was then run under operating conditions for several days so that equilibrium deposition could be attained. Tests carried out with a large number of organic compounds indicated that the polythene gave better resolution than silicone oil. This conclusion is also supported by the results of Baxter and Keen¹⁰. At column temperatures below 100°C, dinonyl phthalate was used as the stationary liquid phase.

Column heating jacket—This consisted of two concentric glass tubes, surrounded by a cellular asbestos cover, and contained a helical *Brightray* wire heater, the winding being somewhat closer at the lower end of the tube. During operation at 316°C only 1°C temperature difference was measured between top and bottom of the column.

Carrier gas and flow system—B.O.C. ‘White Spot’ nitrogen was used as carrier gas, the flow rate of which was governed by needle valves and estimated with *Rotameter* flow-meters. The flow system for the analysis column was duplicated for the reference column, and 10-litre ballast tanks were incorporated to minimize the disturbance in flow when taps were closed for short periods.

Electrical system—A conventional Wheatstone network was used, driven by a 6 V lead accumulator, and the output was displayed on a Sunvic potentiometric recorder, type RSP-2.

Resolution and sensitivity—The resolution of the apparatus described ranged from 600 to 800 theoretical plates, depending upon operating conditions. Sensitivity was such that less than 10 μg of a component in the range of interest could be detected.

Peak identification—The most reliable method was to condense selectively a peak from the effluent gases by means of a liquid air trap, and to subject the material to mass-spectrometric analysis. A Metropolitan-Vickers type MS2 mass spectrometer was used. In some cases gas chromatography peaks were characterized by adding a small additional quantity of the suspected material to the mixture and noting the increase in peak height.

Sample preparation

Polymer samples were re-precipitated by the methods described by Ceresa¹¹, and polymer mixtures prepared by co-precipitation. (In much of the work described below, the presence of traces of solvent or non-solvent in the polymer is of no importance, since this can be removed by subjecting the sample to a small increase in temperature *in situ* before the degradation. The complete evolution of the solvent can be followed chromatographically, whilst at the same time the chromatogram checks that degradation is not taking place.) When a completely solvent-free sample was desirable, the precipitated polymer was dried under high vacuum for a period of 8–12 h at a temperature below the highest temperature at which there was no detectable degradation. For poly(vinyl chloride), for example, it was felt that the maximum safe temperature was in the region of 80°C. In certain instances freeze-drying techniques were used, but the removal of final traces of solvent was here more difficult.

For some of the work, small disks of polymer were required. Initially, these were obtained by film-casting techniques, but it was subsequently found more convenient to use a disk press of the type used for preparing potassium bromide disks in infra-red work. The preparation of solvent-free specimens is certainly much easier by the latter method.

EXPERIMENTAL PROCEDURE AND RESULTS

(a) *The dielectric breakdown technique*

A few milligrams of the sample, in the form of a disk 0.5–1.0 mm thick, is held between two cylindrical brass electrodes. This arrangement is connected in parallel with a large condenser which is charged up to 3 kV. The energy in the large condenser degrades the polymer sample when induced to discharge through it by triggering an initial path by means of a Tesla coil.

Apparatus—The circuit arrangement is shown in *Figure 1*. The total discharge energy is fixed by selecting one of several condensers A (0.25–168 μF) and charging it to a known voltage. The time-constant of the discharge is fixed by choosing one of the series resistors B (130–51 k Ω). The triggering voltage is supplied by an Edwards leak-tester, model T2.

The experimental arrangement of the electrical connections and the mounting of the sample is shown in *Figure 2*. The two-way tap and alternative flow system is incorporated so that samples with some volatility can be examined, and is not normally used in polymer work, where there

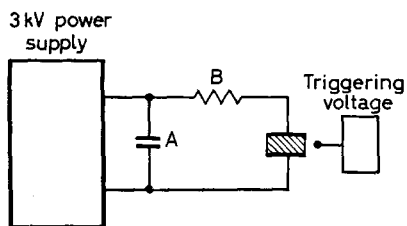


Figure 1—Schematic diagram for dielectric breakdown method

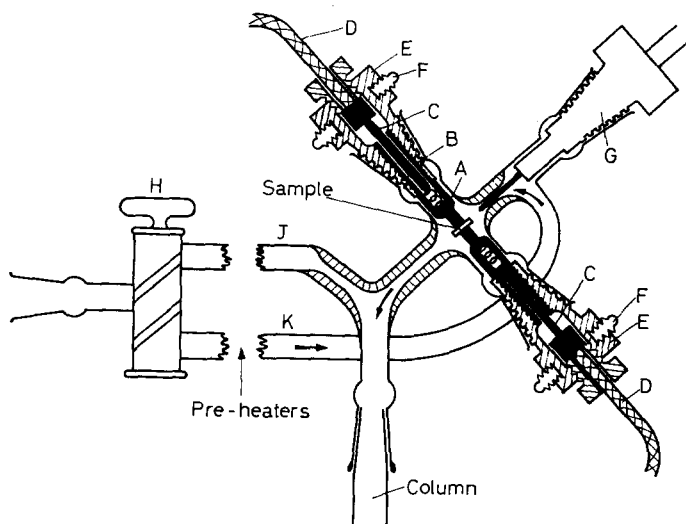


Figure 2—Sample mounting for dielectric breakdown method

is continuous flow in the direction of the arrows. The sample is held between the rods A, the separation of which is pre-adjusted by means of their threaded ends and set by means of the locking-nuts B. Spring-loaded contacts C ensure connection with the H.T. leads D, for all positions of the rods. The B10 cones E are made of polytetrafluoroethylene, and are both held in place by 10 cm springs stretching between the lugs F. No tap-grease is used near the degradation unit. The pre-heaters are simple 'trap' types, electrically heated. Under flow conditions of 2 litres per hour, the gas entering the degradation region was at $\sim 80^{\circ}\text{C}$ when the pre-heaters were maintained at 340°C .

Scope of the method—Preliminary experiments showed that prolonged application of the triggering voltage alone caused no detectable degradation.

Experiments in which no series resistor was used in the discharge circuit resulted in sharp explosions in which the polymer sample was shattered. It was not possible to estimate any degradation products by gas chromatography, but most samples had the appearance of mechanical degradation; they showed no charring and no vapour evolution was observed. Work with cellulose acetate samples showed that a series resistor as low as $130\ \Omega$ in the discharge circuit is sufficient to give a reasonably controlled discharge. The effect was then to produce a small charred hole in the sample, and the

loss in weight was 0.2 mg, with good reproducibility. Although the total energy of discharge is of course known (in the above experiments, 112 J) a realistic estimate of the sample temperature during the discharge is not possible, since the process occurring is too complex. However, it is believed that temperatures of many thousands of degrees are attained; this means, incidentally, that the secondary thermal effects are so predominant that no information about the primary electrical breakdown is derived. The difficulties of temperature estimation and control constitute the severest limitation of this method, and restrict its use to polymer characterization.

Results—The chromatograms obtained for a series of polymer samples are shown in *Figure 3(a)–(g)*. (In each case the experimental conditions were as follows: condenser $A=168\ \mu\text{F}$, charged to 2.8 kV, resistor $B=4.7\ \text{k}\Omega$, chromatography column temperature = 146°C , flow rate 2 l./h. The retention times and relative peak heights of the products from each sample were reproducible; the actual peak heights showed some variation from sample to sample.) All the chromatograms show a very large negative peak of

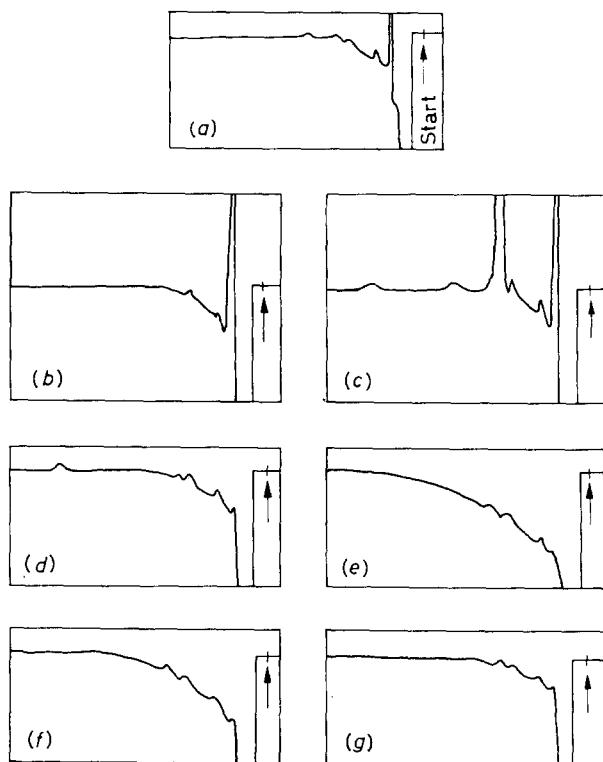


Figure 3—Chromatographs of polymer degradation products obtained by the dielectric breakdown method: (a) poly(vinyl chloride); (b) poly(methyl methacrylate); (c) polystyrene; (d) polyethylene; (e) poly(vinyl alcohol); (f) poly(vinyl acetate); (g) cellulose acetate

short retention time. Mass-spectrometric analysis has shown that this contains a high proportion of acetylene together with mixtures of other low-molecular-weight unsaturated hydrocarbons. The subsequent 'spectrum' consists of a series of very small peaks superimposed on the tail of the negative peak, and for the polymers in *Figure 3(a)–(c)* there are also moderately large positive peaks. (It was found that the retention times of all the peaks were additively modified by changes in the duration of the negative peak; for comparative purposes it was convenient to measure retention times from the end of the negative peak—actually the intercept between the base line and the extrapolation of the peak side.)

In *Figure 3(a)–(c)* the major positive peak in each case is characteristic of the polymer being degraded. Thus for poly(methyl methacrylate) the peak is monomer, for poly(vinyl chloride) the peak is HCl, and for polystyrene the characterized peaks are benzene (later shown to arise principally from adsorbed solvent), toluene, styrene monomer, α -methyl-styrene. Hence each of these polymers may be characterized in a few minutes by subjecting it to degradation in this way.

However, we see in *Figure 3(d)–(g)* that for some polymers the degradation is so severe that characteristic 'spectra' are not obtained, but merely small positive peaks, which are believed to arise from secondary reactions of the primary low-molecular-weight products. Many experiments were carried out to try to achieve less drastic discharge conditions. These included variation of the circuit parameters, sample thickness, and incorporation of graphite in the samples. Non-triggered discharges were also examined. In no case was it possible to achieve an increase in the characteristic fragments at the expense of the small unsaturated fragments. Hence, in some cases this technique is of rather limited applicability since the degradation is so drastic that the resulting chromatograms may not be very different.

(A mass-spectrometric analysis of the products present in the large negative peak of a chromatogram from a polyethylene sample indicated that the principal components were: acetylene 70 per cent, ethylene 14.5 per cent, propene 1.7 per cent, butadiene 1.3 per cent, but-1-ene 0.9 per cent, methyl acetylene 0.8 per cent, propane 0.7 per cent, ethane 0.6 per cent, pentene 0.5 per cent, butane 0.5 per cent, hexene 0.4 per cent. Acetylene was the principal component of this peak for each polymer examined.)

(b) *The filament technique*

The sample is placed on a filament in the carrier-gas stream and the filament is heated for a few seconds, the degradation products being swept directly into the chromatographic column. In this technique, two approaches have been used: (1) the filament temperature may be high enough to degrade the sample completely during the heating period, so that quantitative decomposition of the sample is achieved, and (2) at a lower filament temperature, there will be only partial degradation of the sample, so that some sample remains and is available for subsequent degradation by means of a pulse at higher temperature. By method (2) the same sample may be subjected to a stepped series of temperatures. The application of these two methods is further discussed below.

The filament and sample mounting—The filament unit is shown in Figure 4. It communicates directly with the chromatography column D, and carrier gas enters through C. The rigid tungsten leads A are fused into the plug B, and the filament is spot-welded to them using a nickel intermediate. The filament is wound on a former from 9 cm of 30 s.w.g. Nichrome wire, and has a nominal resistance of 1.94 Ω .

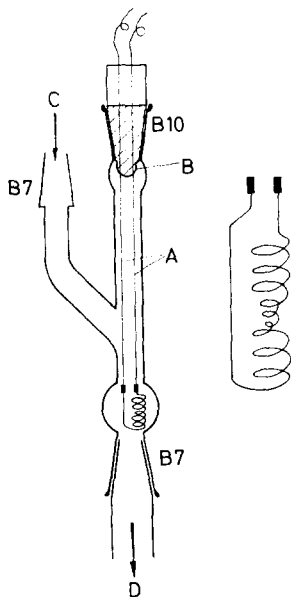


Figure 4—Hot filament degradation unit, and filament showing 'basket' for sample

Since the filament shows a variation in temperature along its length, it is constructed with a 'basket' at the centre, so that polymer samples can be reproducibly mounted on the same turn of the helix.

Two methods of sample mounting were used, according to the problem in hand. The first was to place a drop of polymer solution (or suspension) on the basket, and to allow the solvent to evaporate, first of all in the air, and subsequently in the carrier gas stream. Last traces of solvent were removed by applying a low voltage to the filament, as described previously. The second method was merely to place a weighed piece of polymer in the filament basket, using forceps. Provided the samples are not too large, the polymer melts and coats the wire before the degradation reaction has progressed. Reproducible degradations are achieved if the sample pellet weighs less than 2 mg.

In some cases it has been convenient to prepare the samples by chopping pieces from disks of the dried polymer made in the potassium bromide press. Samples in the weight range 0.1–2.0 mg have usually been chosen, and when necessary, their exact weight has been determined on a microbalance.

The filament timer and voltage control—In the preliminary work the filament voltage was Variac-controlled and the duration of the heating pulse was controlled manually by reference to a stop watch. Although

the reproducibility obtained in this way was satisfactory for many purposes⁴, personal factors have now been eliminated by constructing an automatic timer, in which a pre-set voltage can be supplied to the filament for any chosen period up to 30 sec.

The mode of operation of the timer is shown diagrammatically in *Figure 5*. M_1 and M_2 are microswitches operating relays which start and stop

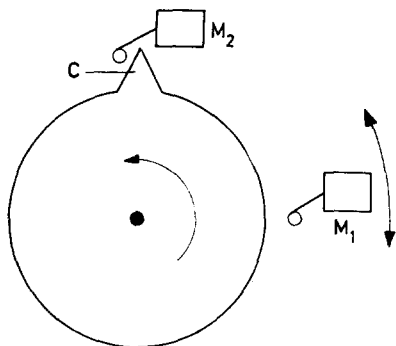


Figure 5—Schematic timer unit, showing how the microswitches are activated by a cam driven by the synchronous motor

the heating pulse respectively. They are activated by cam C which can rotate at 1 rev/min by means of a drive from a synchronous clock motor. Microswitch M_2 is fixed, and M_1 may be set at any position within an arc of 180° by means of a Vernier slow-motion drive control. Hence with this control any pulse duration up to 30 sec can be pre-selected. Provision is also made for continuous filament operation. *Figure 6* shows the circuit which includes the voltage control which enables any one of nine filament voltages to be reproducibly selected. Each one of these voltages can be pre-set by means of its associated rheostat to correspond to any filament temperature up to 1000°C .

Filament temperature calibration—The temperature of the filament basket was calibrated against the supply volts. Up to 800°C , temperatures were estimated by slowly increasing the filament volts until samples of simple standard compounds in the basket just melted. Above 700°C a Foster disappearing-filament optical pyrometer was used. Spot checks with a Cambridge pyrometer gave identical results. (The calibration curve is of similar shape to the resistance-temperature curve, as provided by the manufacturers, for a straight wire, (Nichrome 65/15), but the inflexion temperature is displaced.)

A calibration curve was plotted each time the filament was renewed.

Analysis of copolymers and polymer mixtures by the filament technique—The requirements of the method are (a) that a filament temperature can be chosen so that each constituent pyrolyses completely in 10–15 sec to give at least one characteristic peak which can be completely resolved from the peaks from the other constituent, and (b) these characteristic products must not interact when they are produced simultaneously from the copolymer or polymer mixture. The first requirement can be satisfied by all of the systems studied so far; the second is facilitated by the flow

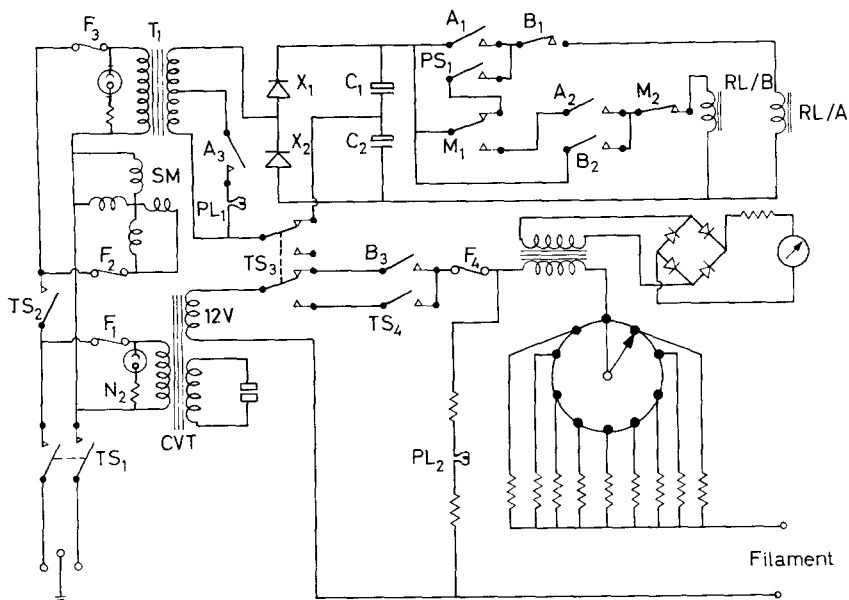


Figure 6—Timer circuit and voltage selector: TS₁, mains switch; TS₂, timer supply switch; when TS₃ is switched as shown, circuit is switched for automatic timing, but is not operational. Mode of operation: (a) depressing PS₁ activates relay A, closing the switches A₁, A₂ and A₃. Lamp PL₁ is now lit, showing circuit is primed. (b) On the next occasion when microswitch M₁ operates, relay B is activated, opening switch B₁ and closing switches B₂ and B₃. Lamp PL₂ lights, showing that current is flowing through the filament. Opening B₁ deactivates relay A and hence switches A₁, A₂ and A₃ are opened. (c) When microswitch M₂ is opened, relay B is deactivated, and the circuit reverts to its original setting as in the figure. When TS₃ is in the alternative position, the filament may be manually switched on and off by TS₄. (SM=synchronous motor; CVT=constant voltage transformer)

conditions, i.e. the products are swept away from the region of high temperature as they are formed.

Identical procedures are used for copolymers and polymer mixtures. First of all, preliminary experiments are carried out to enable the most suitable temperature to be chosen. The criterion adopted has been to choose as high a temperature as possible without causing the production of the small unsaturated fragments characteristic of degradations in the region of 1000°C. In this way the pyrolysis is effected in the shortest possible time. Usually a temperature in the range 550–580°C was found to be suitable. The second stage is to prepare calibration curves of characteristic peak height (or area) vs sample size for each of the pure constituents. These curves enable the sizes of the peaks in the copolymer chromatogram to be translated into masses of the individual monomers present.

Vinyl chloride–vinyl acetate copolymers were the first ones analysed in this way. A filament temperature of 580°C was used, and hydrogen chloride and acetic acid were taken as the characteristic products. A heating period

of fifteen seconds ensured quantitative evolution of these products for all sample sizes. The calibration curves are shown in *Figure 7(a)* and *(b)*, and the results of typical analyses are compared in *Table 1* with the values

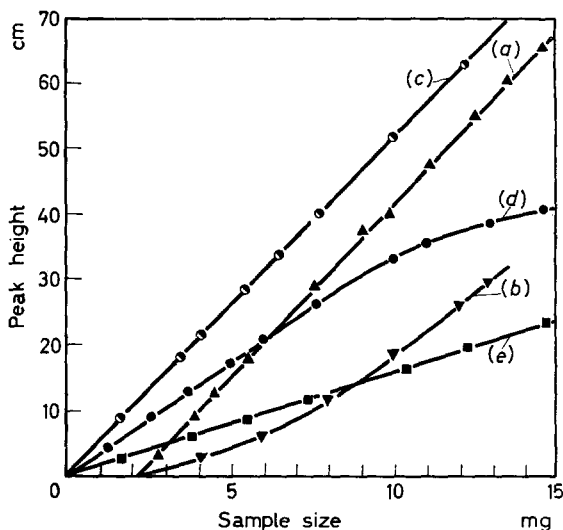


Figure 7—Calibration curves for copolymer and polymer mixtures analysis: (a) poly(vinyl chloride); (b) poly(vinyl acetate); (c) poly(methyl methacrylate); (d) polystyrene; (e) poly(ethyl methacrylate)

Table 1. Percentage of vinyl chloride in vinyl chloride–vinyl acetate copolymers

Copolymer	By chlorine estimation (mean of 2 results)	By I.R. analysis ($\pm 1\%$)	By degradation ($\pm 2\%$)
049	60.8 ± 0.6	54.7	55.8
047	69.4 ± 0.1	64.4	65.2
075	74.1 ± 0.3	72.3	72.2
076	69.1 ± 0.9	66.7	67.8
R46/82	81.8 ± 4.4	84.8	83.9
R51/83	87.9 ± 1.0	89.0	87.7

given by chlorine estimation and infra-red analysis. The standard deviations of the analyses by degradation were usually about 2 per cent. (It is interesting to note that there is a positive intercept on the sample-size axes of the calibration curves for this system. It is thought that this may be caused by some interaction of the acidic products with the material of the column, since the use of acid-washed firebrick reduced the intercepts by a factor of about 2. All other calibration plots extrapolated through the origin.)

Corresponding curves and results for methyl methacrylate–styrene copolymers, a methyl methacrylate–styrene mixture, a methyl methacrylate–vinyl chloride mixture, and methyl methacrylate–ethyl methacrylate mixtures are shown in *Figure 7(a)*, *(c)–(e)* and *Tables 2* and *3*. The results

POLYMER DEGRADATION BY GAS CHROMATOGRAPHY: I

Table 2. Percentage of methyl methacrylate in styrene-methyl methacrylate copolymers

<i>Analysis of polymer by radioactive assay*</i>	<i>By degradation</i>
7.2	7.6 ± 0.2
14.5	13.1 ± 0.3
48.4	46.8 ± 0.9

*Polymer synthesized with labelled methyl methacrylate units.

Table 3. Analyses of polymer mixtures

<i>Polymer A</i>	<i>Polymer B</i>	<i>Percentage of A from original weight taken</i>	<i>Percentage of A by degradation</i>
Vinyl chloride	Methyl methacrylate	80.0	81.7 ± 1.4
Methyl methacrylate	Styrene	50.0	50.8 ± 1.8
Methyl methacrylate	Ethyl methacrylate	75.0	74.3 ± 1.2
Methyl methacrylate	Ethyl methacrylate	51.0	52.2 ± 1.2
Methyl methacrylate	Ethyl methacrylate	30.0	29.7 ± 0.6
Methyl methacrylate	Ethyl methacrylate	25.0	24.5 ± 1.4

are usually within 1 per cent of the expected values. Reproducible results from methyl methacrylate-styrene copolymers were obtained only if the sample size did not exceed 0.5 mg. In all other cases, samples up to 1.5 mg were used.

These results indicate that analyses of copolymers and mixtures may be carried out by degradation to give results which are comparable with those obtained by analytical and infra-red methods; in addition, the speed and facility of the technique renders it quite attractive, especially in cases where a large number of estimations have to be made.

Characterization of polymers, copolymers, and mixtures by the filament technique—Many polymers can be characterized from their degradation chromatogram at a particular temperature. To make this technique of more general application, each sample may be taken through a series of temperatures, and the change in degradation behaviour with temperature used as an additional characterization variable. By this means information about the relative thermal stabilities of polymers is also obtained, and random and block copolymers and mixtures may be distinguished in certain instances. Even for homopolymers the temperatures at which degradation products are first detected may be much more easily recognizable than the product retention times, if these are very close.

The experimental procedure is to mount the sample as for analysis and to subject it to a low temperature for, say, fifteen seconds, using the timer and voltage selector described earlier. The portion of the sample which does not degrade at that temperature (and any involatile degradation product) is available for degradation at the next higher temperature. In most of the work it has been convenient to use nine temperature settings, covering the range 150–950°C.

At the outset, it must be stated that the temperature at which degradation products are first detected will usually be well in excess of the 'ceiling temperature' of the polymer. The reason for this is that the low degradation rates in the region of the ceiling temperatures ensure that in 10–15 sec the quantity of degradation products from a 1 mg sample will be almost infinitesimally small, and beyond the range of detection of the apparatus. Nevertheless, the first products from a series of polymers may be expected to appear at temperatures which follow the order of the ceiling temperatures of the polymers.

In this work, chromatographic column temperatures have been chosen to give best resolution for the products of higher volatility (for example, the temperatures used here do not recognize the possible formation of dimer in a styrene degradation) since these products are usually most characteristic of the polymers examined.

Typical sets of chromatograms are illustrated in *Figure 8*. In some cases (*Figure 8(a)* and (*b*)) the peaks at low and intermediate temperatures correspond to monomer, indicating an 'unzipping' mechanism, whilst more drastic degradation occurs at the highest temperatures, where acetylene is the principal product. Poly(methyl acrylate) behaves similarly (*Figure 8(c)*) but the presence of smaller additional peaks (methanol, ethanol, methyl methacrylate) indicates a more complicated reaction mechanism. The characteristic monomer peak is also observed for polystyrene and for polytetrafluoroethylene (*Figure 7(d)* and (*e*)), the results for polytetrafluoroethylene illustrating the comparatively high thermal stability of this polymer.

Some polymers do not undergo chain scission to small fragments as a primary reaction, but an 'unstripping' reaction occurs, causing loss of side-groups from the chain. Poly(vinyl chloride) (*Figure 8(f)*) and poly(vinyl acetate) (*Figure 8(g)*) illustrate this behaviour, the primary products being hydrogen chloride and acetic acid respectively. The remaining polyacetylene chain is much more stable, and acetylene and small unsaturated molecules are still being produced at the highest temperatures.

These results illustrate that homopolymers may be characterized by considering the variables: (*a*) peaks produced and their retention times, and (*b*) the 'appearance temperatures' of the peaks.

When polymer mixtures are distinguished from copolymers of similar composition, it may happen that the actual degradation products will be identical for both. In these cases the temperature of appearance of the products will frequently distinguish between them, since the presence of foreign monomer in a polymer chain may interrupt chain processes involved in the degradation. Thus the presence of styrene in a methacrylate polymer reduces the amount of methacrylate produced at a given (low) temperature, and this is shown in the chromatographic series (*Figure 8(h)*) for the copolymer as compared with that for the mixture (*Figure 8(i)*). An extension of this principle enables block and random copolymers to be differentiated by means of their degradation behaviour. Provided chain processes play a part in the degradation, the chains will be shorter for the random copolymer than for the block copolymer, which will behave more closely like a mixture of the homopolymers. The particular system vinyl

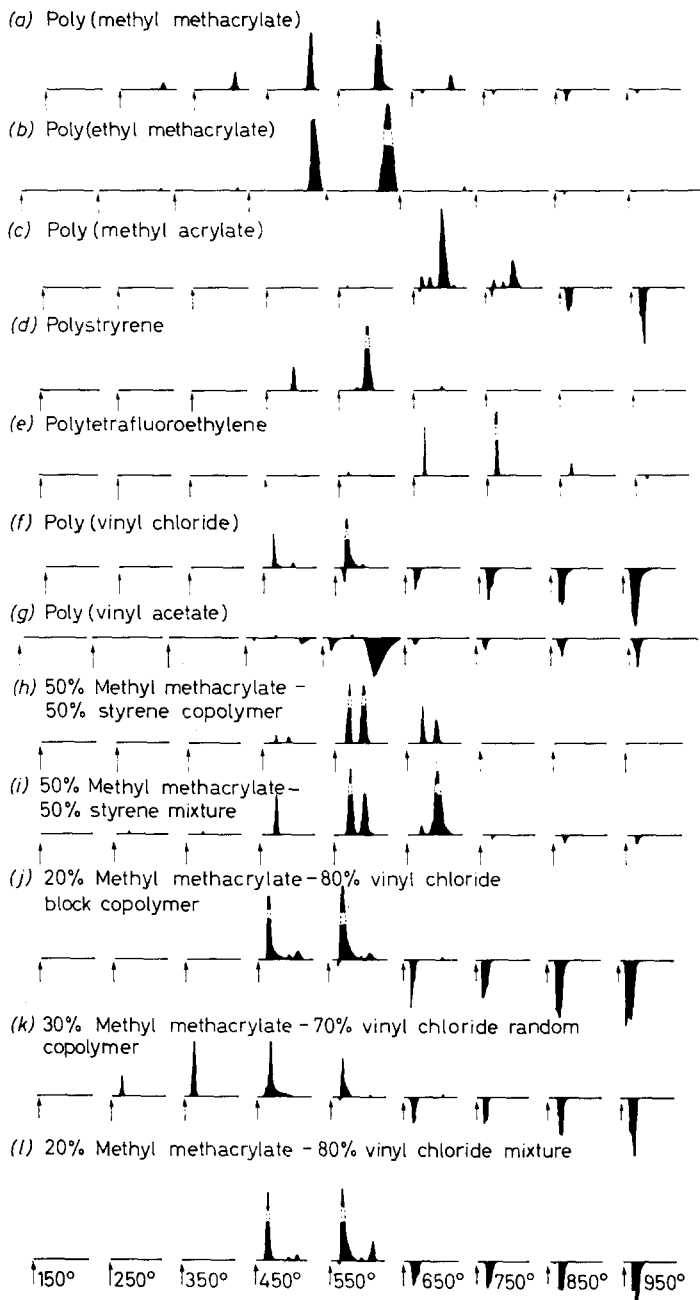


Figure 8—Typical chromatograms obtained by the filament technique

chloride-methyl methacrylate has been examined in this respect, and the difference in behaviour of the block and random copolymers is recognizable (*Figure 8(j)-(l)*). Such characterizations using solution properties or physical properties may be both difficult and lengthy.

In this work, the 'temperature series' experiments have been used as an aid to polymer characterization. A quantitative study of the chromatograms provides information about the rates and temperature dependence of rates of the processes involved. Such applications will be considered in Part II of this series.

CONCLUSIONS

Of the degradation techniques investigated here, the dielectric breakdown method is limited in application to those polymers which do not degrade entirely to small fragments not particularly characteristic of the polymer. Milder degradation conditions are difficult to achieve by this method, since the degree of control is rather limited.

The hot filament technique is of general application, and may be used to analyse polymer mixtures and copolymers more rapidly than analytical methods available at present. The use of a series of degradation temperatures for each polymer sample facilitates the characterization of both homopolymer and copolymer systems by making use of variations in the temperature dependence of the degradation rates.

The authors wish to thank Mr H. Sheard for the construction of the timer unit, and Mr J. K. Allen who provided the labelled polymers. Acknowledgement is also made to Imperial Chemical Industries Ltd who supplied some of the polymer samples used in this work, and to the University of Birmingham who provided a maintenance grant for A.B. One the authors (R.S.L.) wishes to thank the National Coal Board for a fellowship (1957-58), during the tenure of which this work was commenced.

*Chemistry Department,
The University,
Edgbaston,
Birmingham, 15*

(Received 21st July, 1960)

REFERENCES

- ¹ DAVISON, W. H. T., SLANEY, S. and WRAGG, A. L. *Chem. & Ind.* 1954, p. 1356
- ² HASLAM, J., HAMILTON, J. B. and JEFFS, A. R. *Analyst* 1958, **83**, 66
- ³ DE ANGELIS, G., IPPOLITI, P. and SPINA, N. *La Ricerca Scientifica* 1958, **28**, 1444
- ⁴ LEHRLE, R. S. and ROBB, J. C. *Nature (Lond.)* 1959, **183**, 1671
- ⁵ RADELL, E. A. and STRUTZ, H. C. *Anal. Chem.* 1959, **31**, 1890
- ⁶ GUILLET, J. E., WOOTEN, W. C. and COMBS, R. L. *J. appl. Polym. Sci.* 1960, **3**, 61
- ⁷ STRASSBURGER, J., BRAUER, G. H., TRYON, M. and FORZIATI, A. F. *Anal. Chem.* 1960, **32**, 454
- ⁸ JANÁK, J. *Nature (Lond.)* 1960, **185**, 684
- ⁹ JANÁK, J. *Gas Chromatography 1960* (Ed. R. P. W. Scott). Butterworths, London, 1960, p. 233
- ¹⁰ BAXTER, R. A. and KEEN, R. T. *Atomics International Report*, 1959, NAA-SR-3154
- ¹¹ CERESA, R. J. *Techniques of Polymer Characterization* (Ed. P. W. Allen). Butterworths, London, 1959, p. 235

Surface-Chemical Mechanism of Heterogeneous Polymerization and Derivation of Tung's and Wesslau's Molecular Weight Distribution*

MANFRED GORDON† and RYONG-JOON ROE‡

Because Ziegler and Phillips catalysts produce polymers with characteristic broad molecular weight distributions, some general mechanism of heterogeneous catalysis of polymerization may exist. Bresler has suggested independently that this mechanism results from control of the termination step by desorption of the growing chain end from the catalyst surface. In constructing a model mechanism, we assume a random coil configuration for the polymer on the surface (cf. Simha's treatment of sorption equilibria) rather than a linear configuration (cf. Longuet-Higgins's treatment). In order to calculate the termination rate, our model considers the reversible sorption of the growing chain end and of individual chain segments, and the rate of diffusion of the polymer chain as a whole from the surface. We find that the termination rate constant depends on the chain length x as follows:

$$K_t = B/[x^3(x^3 + A)]$$

Application of the Herrington-Robertson steady-state method leads to the molecular weight distribution function subject to the above equation

$$\text{Number fraction, } p(x) \propto 1/[x^3(x^3 + A)^{G+1}]$$

where the constant $G = 2B/K_p$, and K_p is the propagation constant. This distribution is found to fit experimental data previously fitted by two different empirical distribution functions. The relationship between the adjustable parameters G and A , suggested by fitting the data in the literature, is explained in terms of the model.

INTRODUCTION

THE MECHANISM of heterogeneous polymerization must reflect not only rates and mean molecular weights, but also the whole molecular weight distribution. The existence of a phase boundary may impose general mechanisms and distributions independent of the chemical nature of catalyst or polymer (see e.g. Bresler¹), or the observed distributions may arise wholly from the non-uniform chemical (catalytic) activity of surface sites (cf. Natta²). We here propose a general surface-chemical mechanism, unaffected by non-uniformity of the catalyst, which leads to distributions which fit all literature data (so far confined to Ziegler and Phillips polyethylene). We adopt a steady state of polymerization (generally well obeyed, see Natta³) and a termination constant K_t dependent on chain length¹ through control of termination by reversible desorption of the quasi-Gaussian⁴ polymer chain from the surface. Longuet-Higgins recently

*A brief account of this work was presented at the I.U.P.A.C. Symposium on Macromolecules in Wiesbaden, October 1959²⁴.

†Present address: Department of Chemistry, Imperial College, London S.W.7.

‡Present address: Department of Chemistry, Duke University, Durham, N.C., U.S.A.

described⁵ a model for the sorption of polymer on a surface in which successive chain segments could be sorbed or desorbed sequentially, and in which the fully sorbed chain would lie flat on the surface. Simha, Frisch and Eirich⁴ treated a Gaussian chain model, in which polymer chains are sorbed at certain anchor points separated by bridges⁶. We adopt this last pattern, but we represent the configuration by a random walk rather than by a Gaussian chain, a change which will be shown not to affect basic conclusions.

TERMINATION MECHANISM

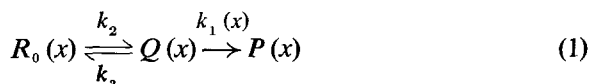
Outline of termination mechanism and steady-state mass law treatment

Consider a chain of length x adsorbed on the catalyst surface. To discuss its possible states, we postulate that the sorption bonds are of two types:

- (a) a rather strong (chemical) bond tying the propagating chain end to the surface, and
- (b) a rather weak (physical) bond tying to the surface some of those segments which happen to lie at the surface.

Both types can be *reversibly* broken. When all the sorption bonds (a) and (b) are broken, the given molecule has a finite chance of becoming terminated by an *irreversible* process which can be diffusion-controlled.

Let $R(x)$ be the number of chains of length x at the surface which have their chemical sorption bond unbroken, and are therefore propagating. Among these $R(x)$ chains, let $R_0(x)$ denote the number of those chains which have their chemical bond unbroken but have no physical bonds to the surface. We denote by $Q(x)$ the number of chains at the surface which have no sorption bonds to the surface, either chemical or physical, and by $P(x)$ the total number of dead polymer chains in the system. The kinetic scheme postulated is:



Here $k_1(x)$ is the rate constant for the slow, irreversible termination process, and depends on the length x of the chain. The rate constants k_2 and k_3 for the breaking and re-forming of the chemical sorption bond of the chain end to the surface are independent of the size of the chain. The rate constants may contain as factors the constant concentrations of other species which influence the reaction rates considered here. We assume that the rate of formation of a chemical bond from a chain end to the surface is much faster than the formation of a physical bond from a chain segment to the surface. This justifies the assumption inherent in (1) that the last bond to be broken is always the chemical bond whenever a chain loses all its attachments* to the surface.

The steady-state solution for (1) is

$$Q(x) = k_2 R_0(x) / (k_1(x) + k_3) \quad (2)$$

*Longuet-Higgins's model⁵ for the desorption rate of polymer implies a similar assumption. Since there all bonds are broken in sequence, the terminal one is the last to break.

The termination rate becomes:

$$dP(x)/dt = k_1(x) Q(x) = k_1(x) k_2 R_0(x) / (k_1(x) + k_3) \quad (3)$$

The overall termination rate constant $K_t(x)$ defined by

$$dP(x)/dt = K_t(x) R(x) \quad (4)$$

is therefore given by

$$K_t(x) = k_1(x) k_2 \rho(x) / (k_1(x) + k_3) \quad (5)$$

where

$$\rho(x) = R_0(x) / R(x) \quad (6)$$

An expression for $\rho(x)$ will be derived in the next section from a random-walk model, and an expression for $k_1(x)$ in the following section from diffusion theory.

The random-walk model for the configuration of sorbed chains

The fraction $\rho(x)$ of chains at the surface attached only by a chemical bond is now calculated from a random-walk model for the configurational probabilities of chains at the surface, with a reflecting barrier to represent the surface. A one-dimensional random walk is sufficient when the surface is planar because the presence of the surface does not introduce any additional configurational changes parallel to it. We identify the unit step in the random walk with a segment of f monomer units of the chain, i.e. the configuration of an x -mer is represented by a random walk of

$$n = x/f \quad (7)$$

steps, where $1/f$ is a measure of chain flexibility. The catalyst surface is represented by a reflecting barrier at the origin, from which the random walk starts (*Figure 1*). The number of possible random walks with r further contact points with the barrier is denoted by $h(n, r)$. The

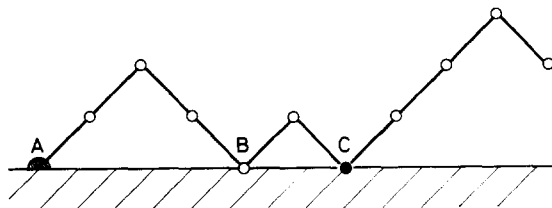


Figure 1—Schematic diagram for random walk: A, propagating chain end (chemical bond); B, contact point without bond formation; C, contact point with physical bond

probability that a physical bond (with constant energy E) is formed at any of the r contact points ($0 \leq r \leq n/2$) is called α . Accordingly,

$$\rho(x) = \frac{\sum_r h(n, r) 2^r (1 - \alpha)^r}{\sum_r \sum_j h(n, r) 2^r (1 - \alpha)^{r-j} \alpha^j \binom{r}{j} \exp -jE/kT} \quad (8)$$

where the denominator enumerates the possible states of surface chains,

each weighted by its Boltzmann factor. Two states are counted as identical, if they have the same random-walk configuration and exactly the same set of segments are engaged in physical bonds. From Feller's result⁷ (cf. Goodrich⁸) for the number of random walks with r returns to the origin in the absence of any barriers,

$$z(n, r) = 2^r \binom{n-r}{n/2} \quad (9)$$

we find the reflection principle:

$$h(n, r) = z(n, r) / 2^{r+1} = \frac{1}{2} \binom{n-r}{n/2} \quad (10)$$

The net heat of sorption E per sorbed segment will be put equal to zero as an approximation (athermal sorption). It may be estimated from data on the sorption of poly(vinyl acetate) on iron⁹ from carbon tetrachloride that the net heat per sorbed segment is < 1 kcal/mole. For the non-polar poly-olefins under consideration, the net heat of sorption per segment from hydrocarbon solvent should be substantially lower. Our calculations will be totally unaffected if $|E| < 0.01$ kcal per mole of sorption bonds. Using the approximation

$$2^{r-n} \binom{n-r}{n/2} \simeq (2/\pi n)^{1/2} \exp(-r^2/2n) \quad (11)$$

which was shown by Feller⁷ to be valid for large n , we thus find from equation (8) with $E=0$:

$$\rho(x) = (2/\pi n)^{1/2} \sum_r (1-\alpha)^r \exp(-r^2/2n) \quad (12)$$

The following limiting cases are manageable:

$$(a) \quad \alpha \gg (2/n)^{1/2} \quad (13)$$

$$(b) \quad \alpha \ll (2/n)^{1/2} \quad (14)$$

Case (a) is of interest for this work, because the mean chain length is large. In this case the first term in (12) dominates and the remaining tail of the summation can be approximated by an integral:

$$\rho(x) \simeq (2/\pi n)^{1/2} \left[1 + \int_1^{\infty} (1-\alpha)^r \exp(-r^2/2n) dr \right] \quad (15)$$

Using the expansion for the error function for values of the argument which are large (in virtue of (13)), equation (15) becomes

$$\rho(x) \simeq (2/\pi n)^{1/2} [1 + (1/\sigma) - (1/n\sigma^3) + \dots] \quad (16)$$

where

$$\sigma = -\ln(1-\alpha) \quad (17)$$

We retain the first two terms of the expansion and substitute for n from (7):

$$\rho(x) \simeq (2f/\pi x)^{1/2} [1 + (1/\sigma)] \quad (18)$$

Thus, in the limiting case under discussion, the probability of finding no physical bond decreases as the inverse square root of the chain length.

The limiting case (b) will be discussed in the Appendix, where various cross-checks are made with related theories of the statistics of chain sorption.

Fick's law treatment for $k_1(x)$ (irreversible termination)

The irreversible process of dead polymer formation with rate constant $k_1(x)$ is composite, being treated as a superposition of diffusion and chemical reaction. Chains which are free from any sorption bonds to the catalyst surface are liable to diffuse away from the surface; moreover they are liable to suffer irreversible chemical termination at their reactive chain end. The diffusion process is characterized by a diffusion constant $D(x)$ depending on chain length; the chemical termination step is characterized by a rate constant k_t independent of chain length. Near the surface there will be a concentration gradient of chains of any given size which have not undergone chemical termination. However, the overall concentration of polymer (including dead polymer) is sensibly uniform throughout the system in the steady state. Therefore the medium through which unterminated chains diffuse is sufficiently uniform for Fick's law with constant $D(x)$ (i.e. independent of distance from the surface) to be used. We take the catalyst surface to be planar, so that the one-dimensional form of Fick's law applies. The concentration of free unterminated x -mer at distance z from the surface and at time t is called $q(x, z, t)$. The steady-state concentration corresponding to $t \rightarrow \infty$ will be denoted simply by $q_0(x, z)$. At the surface, the concentration is related to the number $Q(x)$ of free unterminated x -mer; thus for the steady state:

$$q_0(x, 0) = Q(x) / \theta S \quad (19)$$

where θ is the thickness of the sorption layer and S is the area of the catalyst surface. Two limiting cases arise with respect to stirring (including convection currents): sufficiently fast and sufficiently slow stirring.

(a) *Sufficiently fast stirring*—In this case a Nernst diffusion layer¹⁰ of thickness d exists on the catalyst surface ($d \gg \theta$), through which the unterminated polymer diffuses, and outside which all concentrations are uniform because of stirring:

$$q_0(x, z) = q_0(x, d) \quad z \geq d \quad (20)$$

If the chemical termination constant k_t is not too large, the rate of termination of polymer chains in the diffusion layer may be neglected. Fick's law is solved in the steady state with the boundary conditions (19) and (20) to yield:

$$F = D(x) [q_0(x, 0) - q_0(x, d)] / d \quad (21)$$

where F is the outward flux of unterminated chains of length x . In the steady state, the total influx SF into the stirred volume V is balanced by the rate $dP(x)/dt$ of chemical termination occurring there:

$$dP(x)/dt = k_t V q_0(x, d) \quad (22)$$

$$= SD(x) [q_0(x, 0) - q_0(x, d)] / d \quad (23)$$

which yields, with substitution from (19):

$$dP(x)/dt = k_t V Q(x) D(x) / \theta [k_t V d + SD(x)] \quad (24)$$

If $k_t V d \gg SD(x)$, but k_t is not large enough to violate the assumption made above, we find that the process is purely diffusion-controlled:

$$dP(x)/dt = Q(x) D(x) / \theta d \quad (25)$$

Conversely, if $k_t V d \ll SD(x)$, the process is purely chemically controlled:

$$dP(x)/dt = k_t V Q(x)/S\theta \quad (26)$$

In equations (22)–(26), k_t includes as a factor the constant concentration of the terminating agent. In the case of mutual (bimolecular) termination of chains, this factor is $\sum_x q_0(x, d)$.

(b) *Sufficiently slow stirring*—In this case the Nernst diffusion layer extends (as it were) throughout the reaction volume. The appropriate differential equation is that for diffusion with superposed chemical reaction (termination):

$$\partial q(x, z, t)/\partial t = D(x) \partial^2 q(x, z, t)/\partial x^2 - k_t q(x, z, t) \quad (27)$$

with boundary condition (19). The solution is obtained by Danckwerts's method¹¹ (expounded by Crank¹²); for the steady state it reads:

$$q_0(x, z) = q_0(x, 0) \exp -[k_t/D(x)]^{1/2} z \quad (28)$$

The total rate of dead polymer formation is

$$dP(x)/dt = k_t S \int_0^\infty q_0(x, z) dz = [k_t D(x)]^{1/2} S q_0(x, 0) \quad (29)$$

$$= [k_t D(x)]^{1/2} Q(x)/\theta \quad (30)$$

Equation (30) shows that diffusion and chemical reaction share the rate control in this case, the rate being proportional to both $D(x)^{1/2}$ and $k_t^{1/2}$.

We restrict further consideration to equation (25), applicable for the diffusion-controlled termination when stirring is sufficiently fast, because this is most likely to represent the experimental conditions of the molecular-weight data to be discussed below. It follows from (25) and (3) that the rate constant associated with the irreversible part of the process is proportional to the diffusion constant:

$$k_1(x) = D(x)/\theta d \quad (31)$$

Dependence of diffusion coefficient on molecular weight

At infinite dilution, Flory's¹³ hydrodynamic model theory for diffusion of polymer through solvent leads to

$$D(x) \propto kT/x^{1+a''} \quad (\text{infinite dilution}) \quad (32)$$

where $0 \leq a'' \leq 0.1$. For polyethylene in bulk, McCall, Douglas and Anderson's measurements¹⁴ suggested the relation

$$D(x) \propto 1/x^{5/3} \quad (\text{bulk polymer}) \quad (33)$$

In the range intermediate between infinite dilution and bulk polymer, an inverse power law is appropriate¹⁵ with an exponent intermediate between 1/2 and 5/3. Because in the Nernst diffusion layer of our model the conditions approximate much more closely to infinite dilution than to pure polymer, we require an exponent near to 1/2. For mathematical convenience we adopt the relation:

$$D(x) = K/x^2 \quad (34)$$

where K is the apparent diffusion coefficient of the monomer. By inserting this in (31), we obtain

$$k_1(x) = K/\theta x^{\frac{1}{2}d} \quad (35)$$

Overall termination rate constant

We substitute in (5) for $\rho(x)$ from (18) and for $k_1(x)$ from (35), to find

$$K_t(x) = B/[x^{\frac{1}{2}}(A + x^{\frac{1}{2}})] \quad (36)$$

where

$$A = K/k_3\theta d \quad (37)$$

and

$$B = (2f)^{\frac{1}{2}}k_2K [1 + (1/\sigma)]/\pi^{\frac{1}{2}}k_3\theta d \quad (38)$$

Equation (36) shows that the overall termination rate constant should fall with increasing x as $x^{-\frac{1}{2}}$ for small x and as x^{-1} for large x . This should be contrasted with homogeneous polymerization, where the termination rate constant is not dependent on chain length.

MOLECULAR WEIGHT DISTRIBUTION

Derivation of molecular weight distribution

In addition to the mechanism of termination discussed above, the following kinetic model is postulated for the derivation of molecular weight distribution. Initiation and propagation take place only at the catalyst surface. The initiation rate in the steady state will be taken as constant. The monomer concentration at the catalyst surface is constant, and the catalytic activity of the surface for propagation does not change with time. From the last three postulates follows the constancy of the overall polymerization rate. In practice, this rate in Ziegler polymerizations sometimes declines with conversion, but only very slightly³. The propagation rate constant is taken not to depend on the chain length. The catalytic activity for initiation and propagation may vary from site to site² on the surface. However, the chemical bond between surface and the propagating chain end is repeatedly broken and re-made during its life time, and each chain end thus samples the sites of various propagation activities. Accordingly, it is justified to use, as a good approximation, only the mean propagation rate constant K_p of the sites for all chains in calculating the molecular weight distribution. (In K_p we include, as a factor, the constant concentration of monomer for simplicity of notation.)

The method of Herrington and Robertson¹⁶ is applicable under these conditions, and leads to the following expression for the number fraction of dead x -mer:

$$p(x) = \frac{P(x)}{\sum_x P(x)} \propto \frac{K_t(x)}{K_p} \exp - \int_1^x \frac{K_t(x)}{K_p} dx \quad (39)$$

Substituting for $K_t(x)$ from (36) in (39) and performing the integration, we obtain the required molecular weight distribution function:

$$p(x) = A^G G / [2x^{\frac{1}{2}}(A + x^{\frac{1}{2}})^{G+1}] \quad (40)$$

where

$$G = 2B/K_p \quad (41)$$

The number-average and weight-average D.P.'s and the cumulative weight fraction distribution $I(x)$ are calculated from (40) by standard methods:

$$\text{D.P.}_n = 2A^2 / (G-1)(G-2) \quad (42)$$

$$\text{D.P.}_w = 12A^2 / (G-3)(G-4) \quad (43)$$

$$I(x) = 1 - \frac{1}{2} \left(\frac{A}{A+x^{\frac{1}{2}}} \right)^G \left[G(G-1) \left(\frac{A+x^{\frac{1}{2}}}{A} \right)^2 - 2G(G-2) \left(\frac{A+x^{\frac{1}{2}}}{A} \right) + (G-1)(G-2) \right] \quad (44)$$

In the following section, this last equation is compared with all the experimental results in the literature.

Fitting of experimental molecular weight distributions

The available data are: (a) nine fractionations by Wesslau¹⁷ of polyethylene polymerized at 60°C by Ziegler catalysts, i.e. titanium tetrachloride and various aluminium alkyls and chloroalkyls (his type A catalysts); and further four fractionations of polyethylene polymerized with various combinations of alkoxy aluminium alkyls or titanium alkoxy and titanium chlorides (his type B catalysts); (b) two fractionations of Ziegler-type and one of Marlex 50 polyethylene by Tung¹⁸; (c) two fractionations by Henry¹⁹ of Ziegler polyethylene.

In Figures 2-6 we have followed the presentation of the original authors by plotting x logarithmically, and $I(x)$ on probability paper (Figures 2, 3

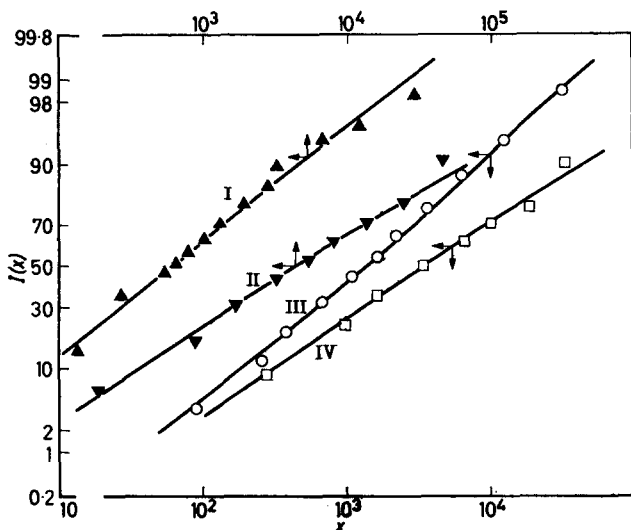


Figure 2—Log-normal plot of data by Wesslau (Table I) with curves calculated from equation (44)

and 6) or $-\log(1-I(x))$ on logarithmic paper (Figures 4 and 5). The curves drawn represent the approximately optimum fit obtainable from equation (44) using the parameters A and G tabulated in Table I. The

MECHANISM OF HETEROGENEOUS POLYMERIZATION

Table 1. Parameters used in fitting Figures 2-6

Run	Catalyst type	A	G	A/G	Fig.	Plot	Ref.
Wesslau's Ma 176	Ziegler A	34	6.0	5.7	2	I	17 a
Wesslau's Ma 192	Ziegler A	37	3.8	9.7	2	II	17 a
Wesslau's Ma 182	Ziegler A	41	4.2	9.8	2	IV	17 a
Wesslau's Ma 116	Ziegler A	62	6.4	9.7	3	I	17 a
Wesslau's Ma 115	Ziegler A	42	5.0	8.4	3	II	17 a
Wesslau's Ma 126	Ziegler A	36	3.8	9.5	3	III	17 a
Wesslau's Ma 169	Ziegler A	64	6.4	10.0	3	IV	17 a
Wesslau's Ma 120	Ziegler A	60	5.0	12.0	3	V	17 a
Wesslau's Versuch 12	Ziegler A	78	8.0	9.8	2	III	17 a
Wesslau's Versuch 7	Ziegler B	570	40	14.5	4	I	17 a
Wesslau's Versuch 1	Ziegler B	2500	100	25.0	4	II	17 a
Wesslau's Versuch 2	Ziegler B	1780	100	17.8	4	III	17 a
Wesslau's Versuch 4	Ziegler B	2500	80	31.5	4	IV	17 a
Tung's Sample C	Phillips	74	8.0	9.3	5	I	18
Tung's Sample A	Ziegler	45	6.4	7.0	5	II	18
Tung's Sample B	Ziegler	27	4.4	6.1	5	III	18
Henry's Sample B	Ziegler	2000	100	20.0	6	I	19
Henry's Sample A	Ziegler	72	7.2	10.0	6	II	19

chain length x has been calculated for Wesslau's data using his viscosity data and his equation²⁰:

$$[\eta] = 3.26 \times 10^{-4} (28x)^{0.77} \quad (45)$$

while in the case of Tung's and Henry's data their own x -values were used.

The degree of fit obtained in Figures 2-6 is considered satisfactory, especially since we use the single equation (44) with two parameters to cover two sets of data previously fitted (with about equal success to ours)

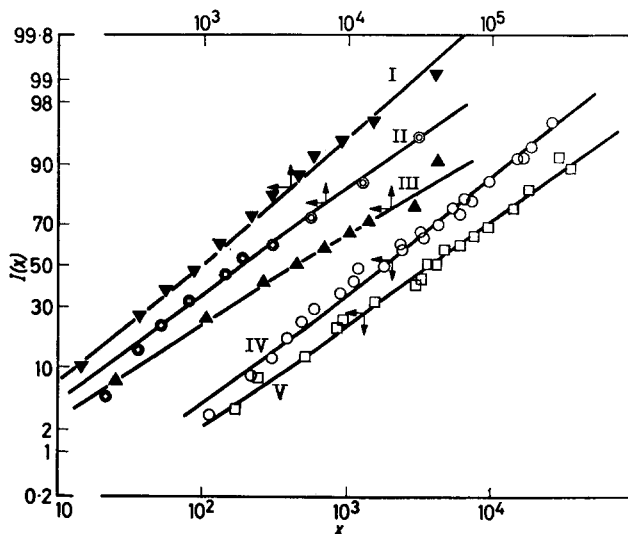


Figure 3—Log-normal plot of data by Wesslau (Table 1) with curves calculated from equation (44)

by two very distinct empirical equations with one and two parameters respectively. These equations were:

$$I(x) = 1 - \exp(-A'x^{B'}) \quad (46)$$

which was originally proposed by Tung²¹ and was applied to polyethylene

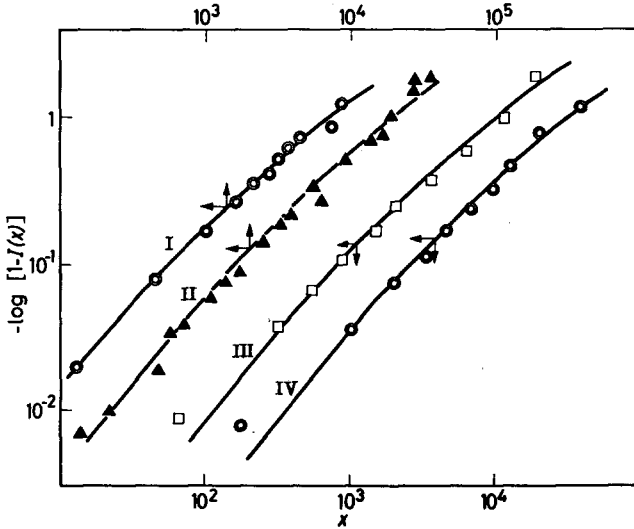


Figure 4—Log-log plot of data by Wesslau (Table I) with curves calculated from equation (44)

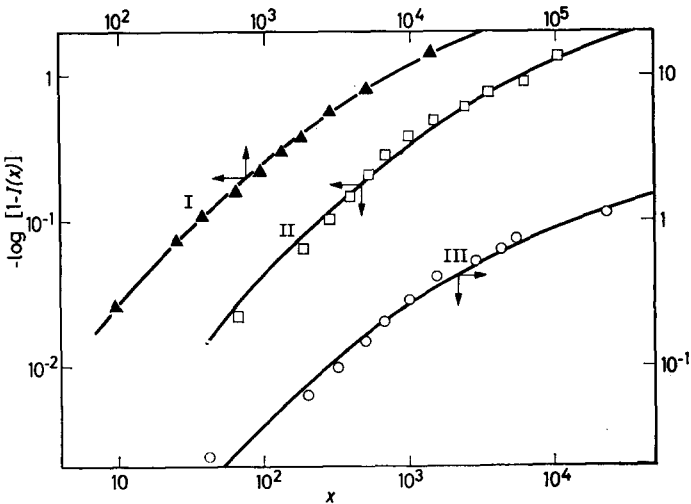


Figure 5—Log-log plot of data by Tung (Table I) with curves calculated from equation (44)

by Wesslau^{17(b)} with $B' = 1$ (thus reducing it to a single-parameter equation) and Wesslau's log-normal distribution^{17(a)}:

$$I(x) = \frac{1}{B''\pi^{1/2}} \int_0^x [\exp - (\ln A''x)^2 / B''^2] dx \quad (47)$$

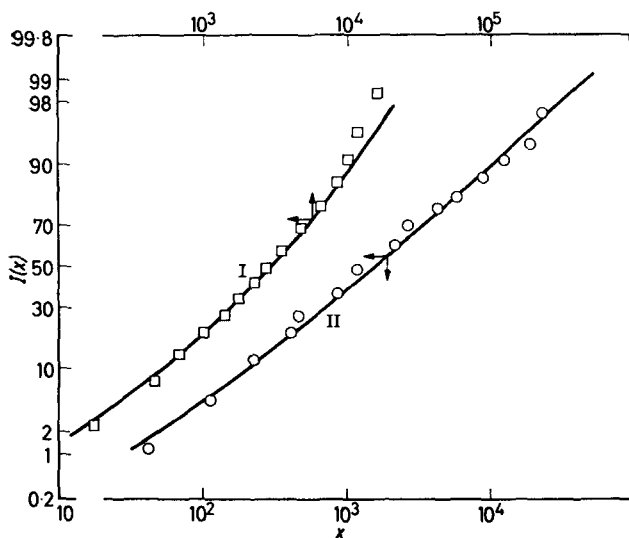


Figure 6—Log-normal plot of data by Henry (Table I) with curves calculated from equation (44)

Tung's equation (46) would give linear plots in Figures 4 and 5, and Wesslau's equation (47) linear plots in Figures 2, 3 and 6.

The empirical Tung (46) and Wesslau (47) distributions have been used to fit many polymer distribution data to which our model is quite inapplicable. The former has been fitted to homogeneously polymerized polystyrene²¹, and to homogeneously polycondensed²¹ nylon 66, and the latter to fractionated polystyrene and to rubber²². However, our theoretical distribution (44) approximates to these two empirical ones only over limited ranges of the parameters. All the examples just quoted would be outside that range, while heterogeneously polymerized polyethylene lies inside. Moreover, while Ziegler polypropylene distribution data are not available in detail, the high ratio of $D.P._w/D.P._n$ observed³ makes it likely that the distribution will resemble that of polyethylene, and could thus be fitted by our scheme.

Relationship between parameters

When fitting his data to the log-normal distribution (47), Wesslau noted a rough empirical relationship between the two parameters, of the form

$$-\log A'' = C_1 B'' + C_2 \quad (48)$$

where C_1 and C_2 are constants, but no theoretical interpretation is available. *Figure 7* shows a plot of our parameters (A against G) for the same data by Wesslau plus those of Tung and of Henry, where the line drawn:

$$A = 9G \quad (49)$$

roughly and significantly correlates the data. Equations (37), (38) and (41) show that according to our theory

$$A/G = \pi^{\frac{1}{2}} K_p / 2 (2f)^{\frac{1}{2}} k_2 [1 + (1/\sigma)] \quad (50)$$

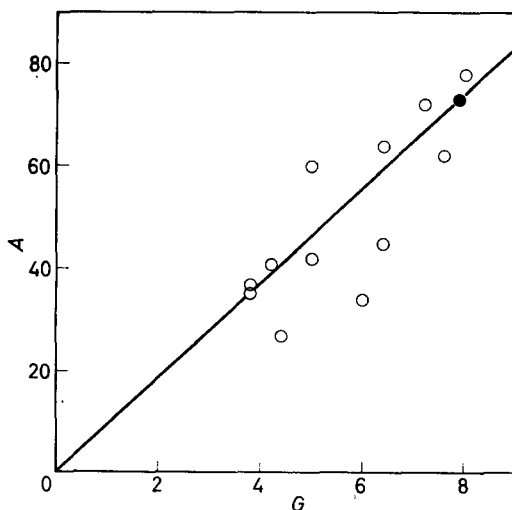


Figure 7—Relation between parameters A and G in Table 1:
○, Ziegler polyethylene; ●, Phillips polyethylene

The flexibility parameter f for polyethylene is constant throughout and σ may also be expected to be constant. Accordingly, the rough constancy of A/G found in (49) reflects the rough constancy of K_p/k_2 . Natta² deduced the constancy of the ratio of K_p to the monomer-transfer constant from his study of the Ziegler polymerization of propylene. Our constant k_2 may be identified with the monomer-transfer constant. The constancy of K_p/k_2 would reflect the fact that the propagation and monomer-transfer reactions involve collisions between the same set of species. If we extend the plot of *Figure 7* to cover the whole of the data in *Table I*, a correlation between A and G persists, since their ratio varies only six-fold over a hundred-fold range of A . There is, however, a danger in considering such a wide range, that apparent correlation may arise in part from the choice of experimental conditions which lead to reasonable average molecular weights.

Molecular weight averages

Tables 2 and *3* give the values of $D.P._w$ and $D.P._n$ calculated from equations (42) and (43), respectively, and also, for comparison, the same averages obtained either from direct measurements or from the empirical

MECHANISM OF HETEROGENEOUS POLYMERIZATION

 Table 2. Comparison of $10^{-3} \times D.P._w$ obtained by different methods

Run	From our eqn	From light scattering	From $[\eta]$ ($D.P._\eta$)	From $[\eta]$ ($D.P._w$)	Summation of fractions	From log-normal eqn	From Tung's eqn
Wesslau's Ma 176	2.31		1.53	1.93	2.18	1.76	
Wesslau's Ma 192	∞		10.9	17.1	13.31	32.51	
Wesslau's Ma 182	84.05		9.5	13.9	9.80	19.01	
Wesslau's Ma 116	5.65		2.25	2.87	2.49	2.60	
Wesslau's Ma 115	10.58		3.51	4.83	5.92	7.60	
Wesslau's Ma 126	∞		10.7	18.1	12.99	40.97	
Wesslau's Ma 169	6.02		3.29	4.42		6.16	
Wesslau's Ma 120	21.60		7.3	10.6		17.59	
Wesslau's V 12	3.65		2.7		2.96*		
Wesslau's V 7	2.93		2.55		2.63*		2.50*
Wesslau's V 1	8.05		7.2		6.56*		7.13*
Wesslau's V 2	4.08		3.9		3.81*		3.57*
Wesslau's V 4	13.02		10.8		10.77*		10.70*
Tung's Sample C	3.29*		2.39*		2.67*	3.55*	3.19*
Tung's Sample A	2.98*		2.03*		2.13*		2.51*
Tung's Sample B	15.62*		4.92*		4.67*		2.77*
Henry's Sample B	5.15*	4.39*	3.43*		4.21*		
Henry's Sample A	4.63*	3.78*	3.09*	4.06	3.81*	4.88*	

 Table 3. Comparison of $D.P._n$ obtained by different methods

Run	From our eqn (42)	Summation of fractions	From log-normal eqn	From Tung's eqn
Wesslau's Ma 176	115	324	233	
Wesslau's Ma 192	543	1062	645	
Wesslau's Ma 182	478	1108	682	
Wesslau's Ma 116	323	441	318	
Wesslau's Ma 115	294	827	470	
Wesslau's Ma 126	514	1115	429	
Wesslau's Ma 169	345		469	
Wesslau's Ma 120	600		681	
Wesslau's V 12	290	428*		
Wesslau's V 7	438	641*		
Wesslau's V 1	1288	1925*		
Wesslau's V 2	653	713*		
Wesslau's V 4	2061	2103*		
Tung's Sample C	261	439*	392*	230*
Tung's Sample A	170	329*		145*
Tung's Sample B	179	364*		187*
Henry's Sample B	825	1283*		
Henry's Sample A	322	481*	453*	

equations (46) and (47). In the tables the figures marked with asterisks are those originally given by the three authors; otherwise they were calculated from their data. The viscosity-average $D.P._\eta$ in the fourth column of Table 2 is based on intrinsic viscosities of unfractionated samples and the relationship (45) between molecular weight and intrinsic viscosity of fractionated samples. Accordingly, for a broad molecular weight distribution, the $D.P._\eta$ values thus calculated will be considerably lower than the true $D.P._w$. The $D.P._w$ values given in the fifth column of Table 2

are, therefore, corrected for the polydispersity according to the method of Chiang²³, assuming the distribution to be log-normal. General trends in *Tables 2* and *3* indicate that equation (39) leads to values of $D.P._w$ mostly higher, and those of $D.P._n$ lower, than the probable real values. This means that our model equation exaggerates both the very high and very low molecular weight fractions lying outside the range accessible to fractionation. The exaggeration at the lower end of the molecular weight may have been introduced partly in the derivation of our equation through the mathematical approximations employed, many of which are not strictly valid for small x . Nevertheless, it is noteworthy that $D.P._n$ values derived from our equation are no worse than those obtained by the two empirical equations. The exaggeration of the high molecular weight fraction is more pronounced and occasionally our equation predicts $D.P._w$ values exceptionally high and even infinite in two cases. It indicates that the model under-estimates the chance of termination of very long chains. In fact, equation (36) shows that the termination constant K_t becomes negligibly small, once a chain has grown to a sufficient size. However, it is likely that such chains would ultimately be terminated by some other mechanism not considered in the model. The effect of any small chance of random termination which does not depend on the chain length will be entirely concealed while the chain length is relatively small, but will begin to manifest itself when the chain grows longer and the desorption-control mechanism fails to terminate it.

Effects of such random termination on the molecular weight averages and distribution will be discussed in the following section.

Superposed random termination

With the superposed random termination of rate constant K'_t independent of chain length, equation (36) is modified to

$$K_t(x) = \{B/[x^{\frac{1}{2}}(A+x^{\frac{1}{2}})]\} + K'_t \quad (51)$$

The number-fraction distribution (40) becomes

$$p(x) = \left[\frac{G}{2x^{\frac{1}{2}}(A+x^{\frac{1}{2}})} + C \right] \left(\frac{A}{A+x^{\frac{1}{2}}} \right)^G \exp -Cx \quad (52)$$

where

$$C = K'_t/K_p \quad (53)$$

It is clear that because of the exponential factor in equation (52) the moments of all order are finite, even for the smallest C . The cumulative weight fraction distribution $I(x)$ and the various averages are difficult to obtain explicitly. However, it is very likely that with small values of the new parameter the calculated $D.P._w$ can be brought within the experimental range without affecting the fit of the experimental cumulative weight fraction curves. This is borne out by the results of a numerical calculation for a set of values of parameters. *Figure 8* shows the variation of $D.P._n$, $D.P._w$ and the ratio $D.P._w/D.P._n$ with different values of C when $A=50$ and $G=4$, and *Figure 9* gives the cumulative weight fraction distributions $I(x)$ plotted on log-probability paper for three different values of C , the values of A and G being the same as in *Figure 8*. The numerical integration was

carried out by either the Gauss-Laguerre method or the 6-point Gauss method for suitable intervals of x . In *Figure 8* the error in the values of $D.P._n$ and $D.P._w$ for $C=4 \times 10^{-5}$ and 4×10^{-4} is estimated to be less than one per cent and for $C=6 \times 10^{-5}$ and 6×10^{-3} less than three per cent.

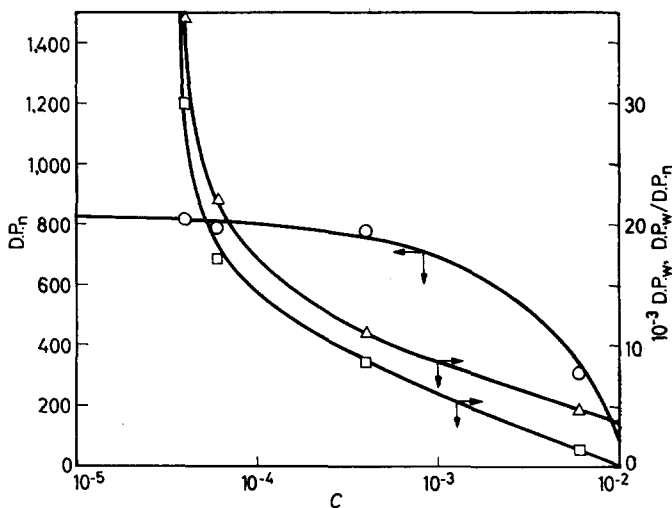


Figure 8—Changes in $D.P._n$ (\circ), $D.P._w$ (\square) and $D.P._w/D.P._n$ (\triangle) with increasing values of superposed random termination component C

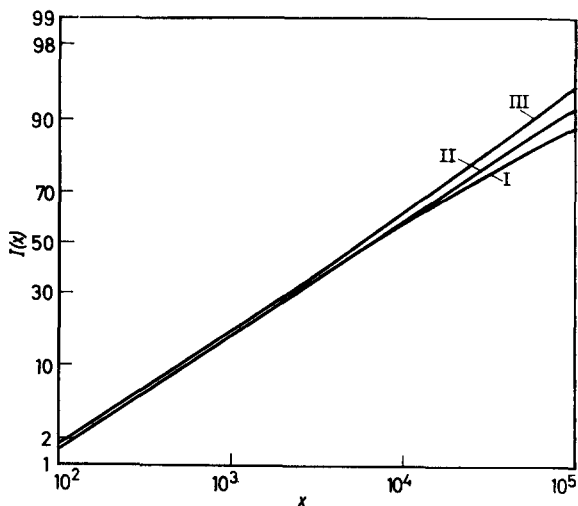


Figure 9—Changes in cumulative weight fraction distribution $I(x)$ with increasing values of superposed random component C : I, $C=0$; II, $C=4 \times 10^{-5}$; III, $C=4 \times 10^{-4}$

It is seen that $D.P._n$ remains effectively constant for values of C smaller than 10^{-3} , whereas $D.P._w$ and, accordingly, $D.P._w/D.P._n$ are drastically reduced from infinity at $C=0$ to those in the experimentally observed range at the value of C as small as 10^{-4} . In *Figure 9* the three curves

plotted are for values of C equal to 0 (curve I), 4×10^{-5} (curve II) and 4×10^{-4} (curve III), respectively. They diverge slightly only for the highest values of x observable experimentally, and the fit of the experimental results is hardly impaired. In fact, curve II for a small value of C is more nearly linear than curve I given by the original equation (44) without the random termination component C , and fits the experimental results better.

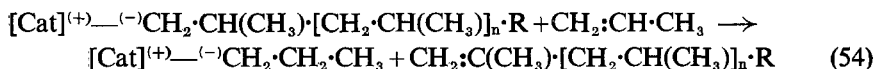
DISCUSSION

Implications of goodness of fit

If the main equation (36) deduced from our model for the dependence of the overall termination rate constant on chain length is mildly changed to related two-parameter forms, e.g. $K_t(x) = B/x^G$ or even $B/[x^t(A+x^t)]$, the overall fit in *Figures 2-6* will be seriously impaired. It is, therefore, gratifying that the theory leads to a specific distribution law which fits the results, though we are far from claiming that all our assumptions are thereby verified. The fit does depend critically on the adoption of a sorption model with random contacts separated by bridges, and a critical comparison of the model with existing theories of polymer sorption is presented in the Appendix.

Chemical nature of termination mechanism

Natta and co-workers² have studied the chemical details of the termination mechanism in the Ziegler polymerization of propylene (which, like ethylene, produces a polymer with wide distribution). In interpreting their experimental results, they postulate four competing termination steps, all of whose rate constants are independent of the chain length. Among these four predominates transfer to monomer, for which the following chemistry has been suggested:



One minor contribution to termination is attributed to a reaction between the chain end and alkylaluminium to yield a polymer both of whose ends are blocked by catalyst fragments, not one end only as for the product in (54). Natta and co-workers also find that the viscosity-average molecular weight is almost independent of monomer pressure and temperature, and explain this in terms of the predominance of the transfer to monomer.

Our model is designed primarily to account for molecular weight distributions. However, the conclusions drawn by Natta and co-workers (using their assumption) from the behaviour of rates and viscosity averages resemble the conclusions we have drawn (using our model) from fractionation data of polyethylene. Thus the transfer step (54) can easily be imagined to be reversible, and become identified with our reversible detachment of the growing chain end from the surface. In that case, the proportionality of the rate of this step to the propagation rate agrees with the conclusion we have drawn from *Figure 7*. The minor contribution made to the chain-cutting processes by alkylaluminium would correspond to our minor random and irreversible termination step with rate constant K_t' .

Two rival kinetic theories for molecular weight distribution

Natta and co-workers² did not attempt to predict distribution functions, but implied that these distributions were dominated by the catalyst site activity distribution. Almost any molecular weight distribution (broader than an exponential distribution) can be fitted *a posteriori* by assuming a suitable distribution of site activities. However, the site activity distribution should be eventually explained in terms of physical and chemical surface characteristics. It should also make plausible the observed correlation between number averages and the widths of the distributions obtained, which is inherent in equation (48) or (49).

Not enough evidence is available for a decisive test between our desorption-kinetic theory and the site-activity theory for molecular weight distributions, partly because the site-activity theory has not been worked out in sufficient detail. Further evidence may be obtained by studying the effect of the addition of substances which terminate the growing chains irreversibly. The practicability of such a test will be illustrated in the following paper²⁵.

APPENDIX

The theory of Longuet-Higgins⁵ for the sorption of polymers on a surface leads to a function $\rho(x)$ very different from our equation (18):

$$\rho(x) = [N_1 / \sum_r N_r] = \rho_0 \exp -x\Delta F/kT \quad (55)$$

where ΔF is the free energy change per sorbed segment, and ρ_0 a normalization constant. His theory rests on a model in which the sorbed chain lies flat on the surface and was not intended for the adsorption of flexible polymer chains whose anchor points are separated by bridges. Simha *et al.*⁴, for different purposes, treat a polymer sorption model closely related to ours. In it one of the chain ends is fixed on the surface and a Gaussian distribution is assumed for the end-to-end distances. This leads to the mean number of sorbed segments per chain

$$\nu(x) = \alpha(2x/\pi f)^{\frac{1}{2}} \quad (x \gg 1) \quad (56)$$

when trivial dimensional corrections are made in their equations (1) and (3). For the athermal case ($E=0$) in our model the same quantity is given (compare equation (8)) by

$$\nu(x) = [\sum_r \alpha r h(n, r) 2^r] / \sum_r h(n, r) 2^r \quad (57)$$

Substitution from (10) for $h(n, r)$ yields

$$\nu(x) = (\alpha/2^n) \sum_r r 2^r \binom{n-r}{n/2} \quad (58)$$

Using the approximation (11), and replacing the summation to $n/2$ by integration to ∞ , which is a good approximation for large n , we find

$$\nu(x) = \alpha(2n/\pi)^{\frac{1}{2}} = \alpha(2x/\pi f)^{\frac{1}{2}} \quad (x \gg 1) \quad (59)$$

This is identical with the result (56) by Simha *et al.* However, their theory cannot be applied to our purpose. In particular, it leads to a function $\rho(x)$ (i.e. $u(0, t)$ in their notation)

$$\rho(x) = \exp - \alpha (2x/\pi f)^{\frac{1}{2}} \quad (60)$$

again very different from (18). This is because (60), unlike (56), involves their explicit additional assumption that the chain segments behave independently through neglect of correlation between neighbouring segments. They recognize that this will be the more nearly true the farther apart the individual anchor points are and accordingly the smaller the value of α . In fact, for $\alpha \ll (2/n)^{\frac{1}{2}}$, i.e. for the limiting case (b) opposite to that treated on p. 44, we can derive from (12)

$$\begin{aligned} \rho(x) &= (\exp n\alpha^2/2) \operatorname{erfc} \alpha(n/2)^{\frac{1}{2}} \\ &= \exp - \alpha (2x/\pi f)^{\frac{1}{2}} \quad (x \ll 2f/\alpha^2) \end{aligned} \quad (61)$$

which agrees exactly with (60).

We have pleasure in thanking Dr R. A. James of the Manchester College of Science and Technology for help with, and advice on, computation.

*Arthur D. Little Research Institute,
Inveresk,
Midlothian*

(Received 19th August, 1960)

REFERENCES

- ¹ BRESLER, E. S. *Disc. Faraday Soc.* 1958, **25**, 199
- ² NATTA, G. *J. Polym. Sci.* 1959, **34**, 21
- ³ NATTA, G., PASQUON, I., GIACHETTI, E. and PAJARO, G. *Chimi. e Industr.* 1958, **40**, 267
- ⁴ SIMHA, R., FRISCH, H. L. and EIRICH, F. R. *J. phys. Chem.* 1953, **57**, 584
- ⁵ LONGUET-HIGGINS, H. C. *Disc. Faraday Soc.* 1958, **25**, 86
- ⁶ JENCKEL, E. and RUMBACH, B. *Z. Elektrochem.* 1951, **55**, 612
- ⁷ FELLER, W. *Probability Theory and its Applications*, Chapman and Hall, London, 1956, p. 82
- ⁸ GOODRICH, F. C. *J. chem. Phys.* 1954, **22**, 588
- ⁹ KORAL, J., ULLMAN, R. and EIRICH, F. R. *J. phys. Chem.* 1958, **62**, 541
- ¹⁰ BIRCUMSHAW, L. L. and RIDDIFORD, A. C. *Quart. Rev. Chem. Soc., Lond.* 1952, **6**, 157
- ¹¹ DANCKWERTS, P. V. *Trans. Faraday Soc.* 1951, **47**, 1014
- ¹² CRANK, J. *The Mathematics of Diffusion*, Clarendon Press, Oxford, 1956, p. 124
- ¹³ FLORY, P. J. *Principles of Polymer Chemistry*, Cornell University Press, Ithaca, New York, 1953, p. 629
- ¹⁴ MCCALL, D. W., DOUGLAS, D. C. and ANDERSON, E. W. *J. chem. Phys.* 1959, **30**, 771
- ¹⁵ GRALÉN, M., *Kolloidzshr.* 1941, **95**, 188
- ¹⁶ HERRINGTON, E. F. G. and ROBERTSON, A. *Trans. Faraday Soc.* 1944, **40**, 236
- ¹⁷ WESSLAU, H. *Makromol. Chem.*, (a) 1956, **20**, 111; (b) 1958, **26**, 102
- ¹⁸ TUNG, L. H. *J. Polym. Sci.* 1957, **24**, 333
- ¹⁹ HENRY, P. M. *J. Polym. Sci.* 1959, **36**, 3

- ²⁰ WESSLAU, H. *Makromol, Chem.* 1958, **26**, 96
²¹ TUNG, L. H. *J. Polym. Sci.* 1956, **20**, 495
²² LANSING, W. D. and KRAEMER, E. O. *J. Amer. chem. Soc.* 1935, **57**, 1369
²³ CHIANG, R. J. *Polym. Sci.* 1959, **36**, 91
²⁴ GORDON, M. and ROE, R.-J. I.U.P.A.C. Symposium on Macromolecules, Wiesbaden, October 1959, Paper IIIA, 4, Weinheim, 1959
²⁵ ROE, R.-J. *Polymer* 1961, **2**(1), 60

A Test between Rival Theories for Molecular Weight Distributions in Heterogeneous Polymerization: The Effect of Added Terminating Agent

RYONG-JOON ROE*

The broad molecular weight distribution in heterogeneous polymerization may arise, as has been suggested by various authors, either because the elementary rate constants vary with chain length or because the catalyst centres are not uniform in their activity. Addition of a terminating agent modifies the molecular weight distribution and can serve as a means of testing these rival proposals. A method is developed by which the expected modification to the molecular weight distribution can be derived for each postulated mechanism of polymerization. With increasing concentration of the added terminating agent, the ratio $D.P._w/D.P._n$ is expected to decrease at first steeply and then slowly towards an asymptotic value of 2, if the termination rate constant is dependent on chain length. On the other hand, the ratio should remain constant, if the catalyst non-uniformity is responsible for the broad distribution. Derivation of these results involves, among others, an assumption concerning the termination reaction by the added agent: its rate constant varies parallel with that of the original termination step, from site to site, but is independent of the chain length. A numerical example is given and its comparison with experimental data in the patent literature suggests that the original termination rate constant is dependent on chain length, as has been proposed in the preceding paper.

INTRODUCTION

RECENT studies have shown that the molecular weight distribution of polymers prepared with heterogeneous catalysts is much broader than that generally obtained in homogeneous polymerization. Ratios of $D.P._w$ to $D.P._n$ much larger than 2 have been reported for polypropylene polymerized with Ziegler-type catalysts¹ and for polystyrene polymerized with Alfin catalysts². Careful fractionation has further established the broad nature of the distributions in detail for linear polyethylene polymerized with Ziegler and Phillips catalysts³⁻⁶ and for polypropylene polymerized with Ziegler catalysts⁷. For industrial purposes the control of the width of the molecular weight distributions is important⁸, and a terminating agent (e.g. hydrogen) is often added in practice to this end⁹⁻¹¹. However, the mechanism responsible for such a broad distribution is not yet clearly understood and the opinions of various authors differ widely^{1, 2, 12-14}. In the preceding paper¹² we proposed a surface-chemical mechanism in which the termination rate constant depends on the chain length through desorption control of the termination reaction. The two-parameter molecular weight distribution derived from this mechanism agrees satisfactorily with the experimental data on linear polyethylene³⁻⁶. On the other hand, Natta¹ and Stockmayer *et al.*²

*Present address: Department of Chemistry, Duke University, Durham, N.C., U.S.A.

attributed the broad distribution to the non-uniformity of catalyst centres with respect to their activities. The practice of adding a terminating agent to control the distribution offers a means of testing these rival mechanisms. With increasing concentrations of the added agent, the molecular weight averages, and the distribution in general, become progressively modified. The pattern of such changes depends on the polymerization mechanism which is responsible for the original broad distribution. Expressions for such changes to be expected from various postulated mechanisms of polymerization are derived in the succeeding sections. A comparison of these expressions with experimental data should, therefore, lead to confirmation of the correct mechanism or to suggestions of new postulates. The derivation of these results involves assumptions concerning the termination reaction by the added agent and these are examined on pp. 65-66.

ORIGINAL MOLECULAR WEIGHT DISTRIBUTION

The postulated mechanisms to be considered in this work fall into two classes, *viz.*, the broad distribution is assumed to arise either (a) because the elementary reaction rate constants K_p and/or K_t depend on the length of the growing chains, or (b) because the activities of catalyst centres are not uniform so that K_p and/or K_t vary from site to site, while at a given site they are not influenced by the lengths of the growing chains. We also assume that the steady state of polymerization is maintained, since in those studies in which data on molecular weights were presented the overall rate of polymerization^{1,9} and the average molecular weights¹⁵ remained effectively constant with time. When the extent of reaction is confined to low conversion, the variation in the concentration of monomer and other chemical species in the reaction system can be neglected, and we therefore include, for convenience of notation, these constant concentrations in the rate constants K_p , K_t and K_i . For example, K_p includes, as factors, the true propagation rate constant, the monomer concentration at the catalyst surface, a quantity proportional to the number of catalyst centres, and the concentrations of soluble 'co-catalysts' if any are involved. Throughout this paper K_t refers to the cessation of growth of polymer chains (and not of kinetic chains), thus including the chain transfer reaction.

Before considering the effect of an added terminating agent, we shall first examine the original molecular weight distribution and its relation to the postulated polymerization mechanisms.

Rate constants dependent on chain length

It is generally accepted that in homogeneous polymerization the elementary rate constants K_p and K_t do not vary with the length of growing chains. The same need not necessarily be true in heterogeneous polymerization, in which the growing chains stay at the phase boundary between the solid catalyst and the solvent medium. Adsorption of growing chains on the catalyst surface, and the process of diffusion of such chains from it, may introduce additional complexity into the termination mechanism, leading to a terminating rate constant dependent on chain lengths, as has been shown in the preceding paper¹². On the other hand, Mussa¹³ postulates a propagation rate proportional to the chain length, a sort of autocatalysis. For the

present purpose, however, we require only the functions $K_p(x)$ and $K_t(x)$ postulated for the dependence of the propagation and termination rate constants on the chain length x , without inquiring into the detailed chemical and physical mechanisms for such a dependence.

Given $K_p(x)$ and $K_t(x)$, one can obtain the number-fraction distribution $p_0(x)$ by means of equation (1), which was derived by Herrington and Robertson¹⁶ for a steady state (in the absence of termination by combination):

$$p_0(x) = P r_0(x) \exp - \int_0^x r_0(x) dx \quad (1)$$

where

$$r_0(x) = K_t(x)/K_p(x) \quad (2)$$

and P is a normalization constant. For most physically realizable systems P is equal to unity. (It can readily be shown that $P=1$ when $\int_0^\infty r_0(x) dx$ diverges.) We therefore simplify our treatment by equating P to unity:

$$p_0(x) = r_0(x) \exp - \int_0^x r_0(x) dx \quad (3)$$

From $p_0(x)$ the averages $D.P._n$ and $D.P._w$ and the cumulative weight fraction distribution $I(x)$ can be calculated by the usual method and compared with the experimental data to test the theory from which the functions $K_p(x)$ and $K_t(x)$ were derived.

Conversely, from the experimentally obtained number-fraction distribution $p_0(x)$, one can deduce the dependence on x of the ratio, $r_0(x)$, of the termination rate constant to the propagation rate constant. Herrington and Robertson¹⁶ give the inversion formula of (3):

$$r_0(x) = \frac{p_0(x)}{\int_x^\infty p_0(x) dx} \quad (4)$$

If, for example, $p_0(x)$ from experimental results is given by the simple exponential distribution:

$$p_0(x) = r e^{-rx} \quad (5)$$

the application of equation (4) leads to the correct conclusion that $r_0(x)$ is equal to r and is independent of x . For broader distributions $p_0(x)$, such as are observed in heterogeneous polymerization, $r_0(x)$ obtained by (4) is usually a monotonic decreasing function of x . For example, the log-normal distribution³

$$p_0(x) = (1/\beta\pi^{1/2}x) \exp - (1/\beta^2) (\ln x/x_0)^2 \quad (6)$$

leads to

$$r_0(x) = \frac{(2/\beta\pi^{1/2}x) \exp - (1/\beta^2) (\ln x/x_0)^2}{\text{erf} = c (1/\beta) (\ln x/x_0)} \quad (7)$$

$$\simeq (2/\beta^2x) (\ln x/x_0) + (x \ln x/x_0)^{-1} + \dots \text{ (large } x) \quad (8)$$

The decrease of $r_0(x)$ with x may mean that either the termination rate decreases with x , or the propagation rate increases with x , or both may occur simultaneously. Thus $r_0(x)$ deduced from the experimental molecular weight distribution by the use of (4) does not give information on the dependence of $K_p(x)$ and $K_t(x)$ on chain lengths individually. The study of the effect of an added terminating agent on the molecular weight distribution can, however, provide a means of deciding which of these rate constants is really dependent on chain length, as will be shown below.

Catalyst activity not uniform

It is well known¹⁷ that the local (microscopic) properties of a solid surface are not uniform over the whole area, possibly owing to fluctuations in the chemical composition, crystal defects, the geometrical shapes, etc. The properties of a solid surface at a given location may also be influenced by the presence of adsorbed substances in its vicinity^{18, 19}. It is therefore conceivable that the heterogeneous nature of the surface of a solid catalyst may manifest itself as non-uniformity of the catalyst activity of active centres. It does not necessarily follow, however, that the broad distribution of polymers obtained by a solid catalyst is the direct consequence of the non-uniformity of catalyst surfaces. Moreover, if the growing end of a chain wanders over a number of catalyst sites during its life-time^{12, 20}, the fluctuation in the propagation activity among them will be averaged out. Even when the chain end remains fixed at a single site throughout its life-time, it can in effect grow at an average propagation rate if the activity at a site drifts rapidly owing to fluctuations in its environment (e.g., changes in the configurations of adsorbed molecules in the immediate vicinity). In order to explain the broad distribution from the postulated variation of the propagation rate constant, it is therefore further assumed in what follows that the growing chain end remains at a single site and the drift in its catalyst activity during the life-time of the chain is so slow as to be negligible.

The character of a catalyst system is defined, for our purpose, by the number fraction distribution $f(K_t^*, K_p^*)$ postulated for the catalyst activity. In other words, $f(K_t^*, K_p^*) dK_t^* dK_p^*$ is proportional to the number of catalyst centres at which the value of the termination rate constant lies between K_t^* and $K_t^* + dK_t^*$ and that of the propagation rate constant between K_p^* and $K_p^* + dK_p^*$. The asterisk is to indicate that the values of these rate constants vary for different centres. These values at a given centre may also drift slowly with time, but $f(K_t^*, K_p^*)$ is not variable with time by virtue of the steady-state condition. A chain initiated at a catalyst centre has a probability $q_0^*(x)$ of growing to length x until its termination:

$$\text{where} \quad q_0^*(x) = r_0^* e^{-r_0^* x} \quad (9)$$

$$r_0^* = K_t^* / K_p^* \quad (10)$$

Assuming for the moment that, on average, an equal number of polymers

is formed from each active centre, we can derive the number-fraction distribution $p_0(x)$ of dead polymer from

$$p_0(x) = \int_0^\infty \int_0^\infty f(K_t^*, K_p^*) q_0^*(x) dK_t^* dK_p^* \quad (11)$$

The average number N^* of polymers formed per unit time at a catalyst centre may in general vary from site to site. The rate N^* is related to the values of the termination and initiation rate constants by

$$N^* = \left(\frac{1}{K_t^*} + \frac{1}{K_i^*} \right)^{-1} \quad (12)$$

Here $1/K_t^*$ is the average life-time of growing chains and $1/K_i^*$ the average length of time which lapses from the moment of termination of a chain till initiation of a new chain at the centre. According to Natta¹ the chain termination is predominantly by transfer to monomer in polymerization of propylene by Ziegler-type catalysts. K_i can therefore be taken as practically infinite and (12) becomes to a good approximation

$$N^* \simeq K_t^* \quad (13)$$

Instead of by (11), the molecular weight distribution $p_0(x)$ is now given by

$$p_0(x) = P \int_0^\infty \int_0^\infty f(K_t^*, K_p^*) K_t^* q_0^*(x) dK_t^* dK_p^* \quad (14)$$

where P is a normalization constant.

It is not possible to obtain the catalyst site distribution $f(K_t^*, K_p^*)$ from the experimental molecular weight distribution $p_0(x)$ by inversion of the general formula (14). Simplification arises, however, in special cases where only one of the two rate constants varies from site to site. When K_t is constant for all sites, the catalyst site distribution can be defined in terms of the single variable K_p^* , and the molecular weight distribution becomes

$$p_0(x) = \int_0^\infty f(K_p^*) (K_t/K_p^*) [\exp - (K_t/K_p^*) x] dK_p^* \quad (15)$$

The inversion of (15) is given by

$$f(K_p^*) = (1/K_p^*) \mathcal{L}_{(K_t/K_p^*)}^{-1} \{p_0(x)\} \quad (16)$$

where \mathcal{L}^{-1} denotes the inverse Laplace transform. For example, from the empirical distribution of linear polyethylene⁴:

$$p_0(x) = P (1/x) e^{-ax} \quad (17)$$

where P is a normalization constant, we obtain by (16)

$$\begin{aligned} f(K_p^*) &= P/K_p^* & K_p^* &\leq K_t/a \\ &= 0 & K_p^* &> K_t/a \end{aligned} \quad (18)$$

On the other hand, when K_t^* alone varies from site to site, K_p being constant (as will be the case when the growing chain end samples a number of catalyst sites during its life-time), the molecular weight distribution is given by

$$p_0(x) = P \int_0^\infty f(K_t^*) (K_t^{*2}/K_p) [\exp - (K_t^*/K_p) x] dK_t^* \quad (19)$$

and its inversion becomes

$$f(K_t^*) = (P'/K_t^{*2}) \mathcal{L}_{(K_t^*/K_p)}^{-1} \{p_0(x)\} \quad (20)$$

In this case, from the empirical distribution (17), we obtain

$$\begin{aligned} f(K_t^*) &= P''/K_t^{*2} & K_t^* &\geq aK_p \\ &= 0 & K_t^* &< aK_p \end{aligned} \quad (21)$$

MODIFIED MOLECULAR WEIGHT DISTRIBUTION

The molecular weight distribution modified by addition of a terminating agent will now be derived for each of the polymerization mechanisms discussed above. In order to preserve a sufficient generality of the final results, the precise chemical nature of the reaction by which the added agent terminates the growing chains will not be specified. Instead, we shall base our analysis on three general assumptions to be examined below.

(a) The overall termination rate constant K_t' in the presence of an added terminating agent is assumed to be the sum of K_t due to the original termination mechanism and K_a due to the added agent. Thus:

$$K_t' = K_t + K_a \quad (22)$$

Here K_a includes the concentration C of the added agent (see below and also p. 61). Natta¹ concluded from his study of propylene polymerization with a radio-isotope tracer that the termination reaction consists of four independent components involving different terminating (or transfer) agents. Except when a complication such as inhibition of the existing termination mechanism is present, the added agent will therefore simply contribute another independent superposed component to the overall termination rate.

(b) K_a is assumed to be proportional to the concentration C , namely,

$$K_a = kC \quad (23)$$

At the catalyst surface where the reaction occurs the local concentration of the terminating agent may not necessarily be the same as its bulk concentration C in the solvent medium. Interference by diffusion control or adsorption of the terminating agent to the catalyst surface cannot be excluded. However, kinetic studies of polymerization of ethylene²¹ and propylene⁹ with Ziegler catalysts have shown that the polymerization rate is proportional to the monomer pressure. This indicates that the monomer concentration at the catalyst surface is proportional, if not actually equal, to

its bulk concentration and the same is here assumed for the concentration of the added terminating agent.

(c) The final results of the present analysis rest critically on the assumptions made for any possible variation of K_a either with chain length or with different catalyst sites. When the original polymerization mechanism postulates the termination rate constant K_t to be invariant, it is natural to assume that K_a also is invariant. The dependence of K_t on the chain length was proposed in the preceding paper¹² from a consideration of the physical processes of desorption and diffusion of growing chains. The simple chemical attack by molecules of the added terminating agent on the growing chain ends should, nevertheless, be random, being determined by the rate of activated collisions as in reactions in homogeneous media. K_a is therefore taken to be constant in spite of the chain-length dependence $K_t(x)$ of the original termination rate. A different consideration applies when a variation in K_t^* due to non-uniformity of catalyst sites is postulated. In this case a similar variation in K_a^* is expected. The postulated variation of K_t^* with catalyst sites will probably have to be attributed to the variation in stability of the bond between the growing chain end and the active centre. If so, the added agent will also have a better chance of terminating those chains growing on a centre of a relatively unstable bond rather than of a stable one. We shall therefore assume that K_a^* varies from site to site exactly as K_t^* does; in other words, the ratio

$$k^*/K_t^* = Q \quad (24)$$

is a true constant for all sites.

The effect of the added terminating agent will now be considered in turn for six of the possible polymerization mechanisms which postulate that (a) K_t alone, (b) K_p alone, and (c) both K_t and K_p vary either (1) with the chain length or (2) from catalyst site to site.

Rate constants dependent on chain length

The Herrington–Robertson formula (3) is still applicable when $r_0(x)$ is replaced by $r(x)$ defined by

$$r(x) = K_t'(x)/K_p(x) \quad (25)$$

Thus the modified number-fraction distribution $p(x)$ is obtained from

$$p(x) = r(x) \exp - \int_0^x r(x) dx \quad (26)$$

(a) $K_t(x)$ alone changes with chain length—In this case K_p and K_a are independent of x . The ratio $r(x)$ becomes

$$r(x) = [K_t(x) + K_a]/K_p = r_0(x) + RC \quad (27)$$

where

$$R = k/K_p \quad (28)$$

which is independent of x . Substitution of (27) in (26) gives

$$p(x) = [r_0(x) + RC] \exp - \int_0^x [r_0(x) + RC] dx \quad (29)$$

which, because of (3) and (4), becomes

$$p(x) = e^{-RCx} \left[p_0(x) + RC \int_x^\infty p_0(x) dx \right] \quad (30)$$

The modification of the given (experimental) initial distribution $p_0(x)$, due to the added terminating agent, can be calculated from (30). Because of the exponential factor $\exp -RCx$, the distribution $p(x)$ is progressively distorted and becomes narrower as C increases. This feature is intuitively obvious, since the effect of random termination will be more pronounced for those long chains for which the chance of termination by the original mechanism is negligibly small.

(b) $K_p(x)$ alone changes with chain length—Both K_t and K_a are now independent of x . The ratio $r(x)$ in (25) becomes

$$\begin{aligned} r(x) &= \frac{(K_t + K_a)}{K_p(x)} = \frac{K_t(K_t + K_a)}{K_p(x)K_t} \\ &= r_0(x)(1 + QC) \end{aligned} \quad (31)$$

where

$$Q = k/K_t \quad (32)$$

which is independent of x . By use of (26), with $r(x)$ given by (31), we obtain the number-fraction distribution

$$\begin{aligned} p(x) &= (1 + QC) r_0(x) \exp - (1 + QC) \int_0^x r_0(x) dx \\ &= (1 + QC) p_0(x) \left[\int_x^\infty p_0(x) dx \right]^{QC} \end{aligned} \quad (33)$$

(c) Both $K_t(x)$ and $K_p(x)$ change with chain length—By writing $r(x)$ in (25) in the form:

$$r(x) = [K_t(x) + K_a]/K_p(x) = r_0(x) + kC/K_p(x) \quad (34)$$

we obtain by (26) the number-fraction distribution

$$\begin{aligned} p(x) &= [r_0(x) + kC/K_p(x)] \exp - \int_0^x [r_0(x) + kC/K_p(x)] dx \\ &= \left[p_0(x) + \int_x^\infty p_0(x) dx kC/K_p(x) \right] \exp - kC \int_0^x [1/K_p(x)] dx \end{aligned} \quad (35)$$

In this case it is not possible to compute $p(x)$ from $p_0(x)$ without an explicit knowledge on the functional dependence of $K_p(x)$ on x . It seems unlikely that in any real system variation with chain length of both $K_t(x)$ and $K_p(x)$ will occur. Nevertheless, if variation of both rate constants is still suspected, a series of accurate experimental determinations of $p(x)$ for different values of C will, upon comparison with equation (35), determine $K_p(x)$ in principle. However, this determination is sensitive to experimental errors in $p(x)$.

Catalyst activity not uniform

(a) K_t^* alone varies from site to site—The original molecular weight distribution $p_0(x)$ as given by equation (19) becomes modified on addition of a terminating agent to

$$p(x) = P \int_0^\infty (K_t) (K_t^{*2}/K_p) \exp -(K_t^{**}/K_t) x dK_t^* \quad (36)$$

The integration is with respect to K_t^* since the catalyst site distribution $f(K_t^*)$ remains unchanged and is still defined in terms of K_t^* alone. The overall termination rate constant K_t^{**} is defined by equations (22), (23) and (24):

$$K_t^{**} = K_t^* + k^*C = K_t^* (1 + QC) \quad (37)$$

where the ratio Q , as given in (24), is a true constant. Substitution of (37) into (36) leads to

$$p(x) = P \int_0^\infty f(K_t^*) (K_t^{*2}/K_p) (1 + QC) \exp -(K_t^*/K_t) (1 + QC) x dK_t^* \quad (38)$$

which, upon comparison with (19) becomes

$$p(x) = (1 + QC) p_0 [x(1 + QC)] \quad (39)$$

$p(x)$ as given by (39) is exactly the same distribution as $p_0(x)$, except that all D.P. averages are reduced by a factor $1/(1 + QC)$, and therefore the ratio D.P._w/D.P._n remains unchanged.

(b) K_p^* alone varies from site to site—In this case both K_t and K_a are constant over all catalyst sites, and the overall termination rate constant K_t' becomes

$$K_t' = K_t + kC = K_t (1 + QC) \quad (40)$$

where

$$Q = k/K_t \quad (41)$$

The modified molecular weight distribution $p(x)$ is obtained from equation (15) after K_t there has been replaced by K_t' :

$$\begin{aligned} p(x) &= \int_0^\infty f(K_p^*) (K_t/K_p^*) (1 + QC) [\exp -(K_t/K_p^*) (1 + QC) x] dK_p^* \\ &= (1 + QC) p_0 [x(1 + QC)] \end{aligned} \quad (42)$$

As in (a) above, $p(x)$ is of exactly the same shape as $p_0(x)$ and is obtainable from the latter by a change of the variable from x to $(1 + QC)x$.

(c) Both K_t^* and K_p^* vary from site to site—From the results of (a) and (b) above it is obvious that in this general case too the addition of a terminating agent fails to modify the shape of the molecular weight distribution and simply reduces the average molecular weights.

DISCUSSION

The analysis presented in the above illustrates the method by which the expected modification to the molecular weight distribution can be derived from a postulated mechanism of polymerization. It was plainly impossible to treat every conceivable variant of polymerization mechanisms which might be postulated to account for the broad molecular weight distribution. The analysis was, however, based on those hypotheses which appeared to be most realistic. The results clearly indicate the practicability of testing these postulated mechanisms by studying the effect of an added terminating agent. The postulate that rate constants are dependent on chain lengths leads to modified molecular weight distributions which become progressively sharper as the concentration of the added agent increases. It thus stands in a significant contrast to the prediction that no modifications to the shape of the distribution and therefore to the ratio $D.P._w/D.P._n$ can be expected when

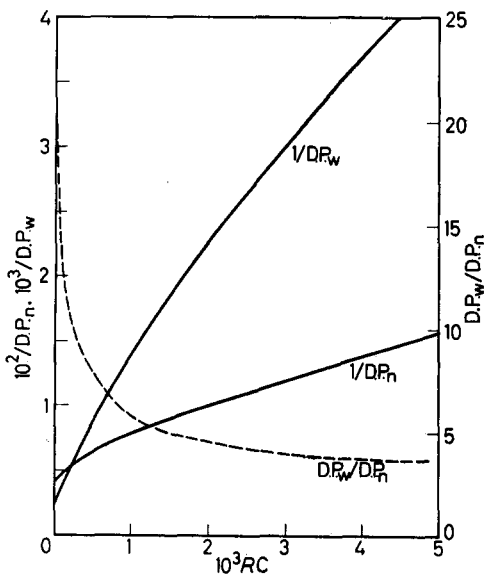


Figure 1 — Theoretical changes in $1/D.P._n$, $1/D.P._w$ and $D.P._w/D.P._n$ with concentration, C , of an added terminating agent, when the termination rate constant varies with chain length (Case 1)

the catalyst non-uniformity is responsible for the original broad distribution. The assumption embodied in equation (24), on which the latter prediction depends (in the case of variable K_t^*), may be an over-simplification. If the ratio Q defined in equation (24) does, in fact, vary to some extent from site to site, the shape of the distribution can no longer be conserved. However, the modification in the shape can only be a mild one if the fluctuation of Q is small. Moreover, with increasing concentration C the fraction of chains terminated by the added agent will increase, and the distribution will eventually approach one which is entirely dictated by the variation of K_a^* from site to site and is therefore again broad although of a different shape.

The results derived on pp. 66–68 can best be illustrated by a concrete numerical example. For this purpose we employ the following ‘original’ distribution $p_0(x)$:

$$p_0(x) = \frac{A^G G}{2x^{\frac{1}{2}} (A + x^{\frac{1}{2}})^{G+1}} \quad (43)$$

with values of the parameters $A=50$ and $G=6$. Equation (43) was originally derived theoretically from the surface-chemical mechanism of heterogeneous polymerization and was shown to fit all the available data of molecular weight distributions of linear polyethylene¹². For the present purpose, however, equation (43) is considered as an empirical equation which closely represents experimental data on molecular weight distributions of polymers prepared without an added terminating agent. Equation (43) is preferred to the log-normal (6) or any other empirical equation because of its more general applicability to experimental data and also because of its convenience for mathematical manipulation. Substitution of (43) into the appropriate expressions derived above for $p(x)$ leads to the following equations, each corresponding to a distinct mechanism postulated for the polymerization.

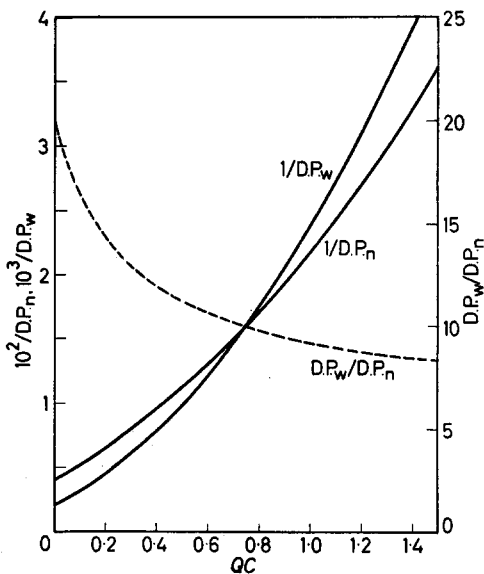


Figure 2 — Theoretical changes in $1/D.P.n$, $1/D.P.w$ and $D.P.w/D.P.n$ with concentration, C , of an added terminating agent, when the propagation rate constant varies with chain length (Case 2)

Case 1— $K_t(x)$ alone changes with chain length (see p. 66). From (30) we obtain

$$p(x) = e^{-RCx} \left[\frac{A^G G}{2x^{\frac{1}{2}} (A + x^{\frac{1}{2}})^{G+1}} + RC \int_x^{\infty} \frac{A^G G}{2x^{\frac{1}{2}} (A + x^{\frac{1}{2}})^{G+1}} dx \right] \quad (44)$$

Case 2— $K_p(x)$ alone changes with chain length (see p. 67). From (33) we obtain

$$p(x) = \frac{A^{G'} G'}{2x^{\frac{1}{2}} (A + x^{\frac{1}{2}})^{G'+1}} \quad (45)$$

$$G' = (1 + QC) G \quad (46)$$

Case 3—The rate constants vary from site to site (see p. 68). From either (39) or (42) we obtain

$$p(x) = \frac{A'^G G}{2x^{\frac{1}{2}} (A' + x^{\frac{1}{2}})^{G+1}} \quad (47)$$

$$A' = A/(1 + QC)^{\frac{1}{2}} \quad (48)$$

$1/D.P._n$, $1/D.P._w$ and $D.P._w/D.P._n$ were computed from equations (44), (45) and (47) and plotted in *Figures 1, 2 and 3*, respectively. $D.P._n$ and $D.P._w$ from equation (44) were computed numerically by 15-point Gauss-Laguerre method²². In these figures the ordinates are all on the same scale, while abscissae are either RC or QC . The proportionality constants R and Q have to be determined experimentally. However, the marked difference between the three cases can easily be recognized even without knowing the

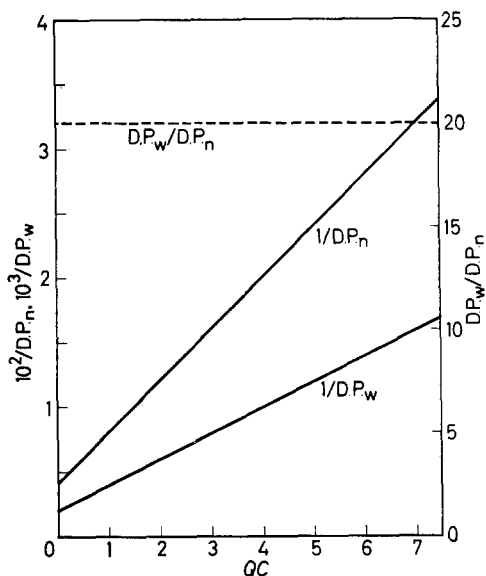


Figure 3 — Theoretical changes in $1/D.P._n$, $1/D.P._w$ and $D.P._w/D.P._n$ with concentration, C , of an added terminating agent, when one or both of the rate constants vary from site to site (Case 3)

absolute values of these constants. For example, the $1/D.P._n$ and $1/D.P._w$ curves are convex upwards, concave upwards and linear for Cases 1, 2, and 3, respectively. Again, the ratio $D.P._w/D.P._n$ remains constant in Case 3, while in Case 1 it at first decreases steeply with increasing concentration C to a value of about 5 and then levels off slowly to the asymptotic value of 2. Therefore, if changes in $D.P._n$ and $D.P._w$ are found experimentally for several concentrations of the terminating agent and the plot is compared with *Figures 1–3*, it should not be difficult to decide which of the three cases represents the true mechanism. Accurate data for this purpose are not available at the moment, but a patent by Hercules Powder Company¹⁰ gives some limited results of such an investigation. *Figure 4* was constructed from Table V of the patent which lists the results of ethylene polymerization catalysed by tri-isobutylaluminium and titanium tetrachloride in the

presence of various proportions of hydrogen. Since the precise conditions of the experiments are not specified and no information is available on $D.P._n$, it would be premature to draw a definite conclusion from *Figure 4*. Nevertheless, it is evident that the experimental curve resembles most closely the

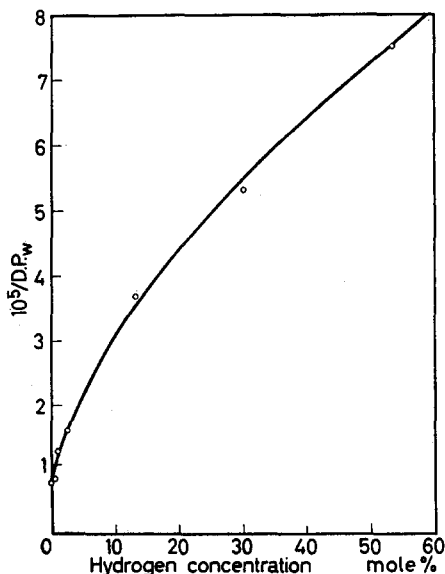


Figure 4— $1/D.P._w$ of polyethylene prepared with tri-isobutylaluminium and titanium tetrachloride in the presence of various proportions of hydrogen¹⁰. The plot resembles the theoretical curve of $1/D.P._w$ in *Figure 1* more closely than those in *Figures 2* and *3*

curve of $1/D.P._w$ in *Figure 1*, that is, the one computed on the assumption that the termination rate constant $K_t(x)$ varies with chain length. It thus seems to support the surface-chemical mechanisms of heterogeneous polymerization proposed in the preceding paper¹².

The author gratefully acknowledges helpful suggestions and encouragement by Dr M. Gordon.

Arthur D. Little Research Institute,
Inveresk,
Midlothian

(Received 19th August, 1960)

REFERENCES

- ¹ NATTA, G. J. *Polym. Sci.* 1959, **34**, 21
- ² CLELAND, R. L., LETSINGER, R. L., MAGAT, E. E. and STOCKMAYER, W. H. *J. Polym. Sci.* 1959, **39**, 249
- ³ WESSLAU, H. *Makromol. Chem.*, 1956, **20**, 111
- ⁴ WESSLAU, H. *Makromol. Chem.* 1958, **26**, 102
- ⁵ TUNG, L. H. *J. Polym. Sci.* 1957, **24**, 333
- ⁶ HENRY, P. M. *J. Polym. Sci.* 1959, **36**, 3
- ⁷ WIJGA, P. W. O., VAN SCHOOTEN, J. and BOERMA, J. *Makromol. Chem.* 1960, **36**, 115
- ⁸ McCORMICK, H. W., BROWER, F. M. and KIN, L. *J. Polym. Sci.* 1959, **39**, 87
- ⁹ NATTA, G. *Chem. & Ind.* 1957, p. 1520

- ¹⁰ Hercules Powder Company, *Austral. Pat.* 217,218 (1956)
- ¹¹ Hercules Powder Company, *Brit. Pat.* 790,399 (1958)
- ¹² GORDON, M. and ROE, R.-J. *Polymer* 1961, **2** (1), 41
- ¹³ MUSSA, I. V., *C. J. appl. Polym. Sci.* 1959, **1**, 300
- ¹⁴ SCHUURMANS, H. J. L. Paper presented at the 136th meeting of the American Chemical Society, Atlantic City, N.J., September 1959
- ¹⁵ WESSLAU, H. Discussion at I.U.P.A.C. Symposium on Macromolecules in Wiesbaden, October 1959; see also Ref. 3
- ¹⁶ HERRINGTON, E. F. G. and ROBERTSON, A. *Trans. Faraday Soc.* 1944, **40**, 236
- ¹⁷ ROGINSKI, S. S. *Adsorption und Katalyse an inhomogenen Oberflächen*, Akademie Verlag, Berlin, 1958
- ¹⁸ LOW, M. J. D. *Chem. Rev.* 1960, **60**, 267
- ¹⁹ HIGUCHI, I., REE, T. and EYRING, H. *J. Amer. chem. Soc.*, 1955, **77**, 4969; *ibid.* 1957, **79**, 1330
- ²⁰ HUGGINS, M. L. Preprint for the International Symposium on Macromolecular Chemistry in Moscow, Section II, 299 (1960)
- ²¹ LUDLUM, D. B., ANDERSON, A. W. and ASHBY, C. E. *J. Amer. chem. Soc.* 1958, **80**, 1380
- ²² 'Tables of Functions and Zeros of Functions', *Nat. Bur. Stand. Applied Mathematics Series*, Vol. 37, U.S. Govt Printing Office, 1954

Thermochemical Aspects of Butadiene–Styrene Copolymerization*

R. J. ORR

Methods are developed so that the entropy and enthalpy changes in the elementary reactions of copolymerization may be calculated from heat capacity data. The methods include isolation of the contributions of the elementary reactions and determination of the residual entropy of copolymers. When applied to the case of butadiene–styrene copolymerization at 5°C, they show that

- (i) *the contribution to the entropy at 0°K by the glassy state is negligible;*
- (ii) *the contribution of the growing polymer chain to entropy and enthalpy changes is determined by the nature of the terminal monomer unit.*

The sum of the entropy changes in the two heteropolymerization reactions is about 50 e.u./mole.

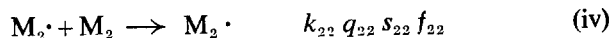
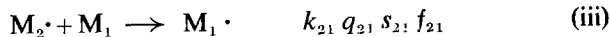
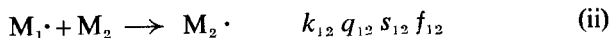
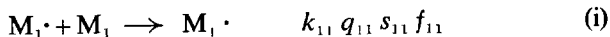
EFFORTS to evaluate heat and entropy changes in copolymerization reactions generally encounter two problems:

- (1) How does one estimate the residual entropy of a copolymer?
- (2) How can the contributions of each of the four elementary reactions of copolymerization be isolated from the overall energy changes?

Contributions to each of these problems have been made by Temperley¹ and Alfrey and Lewis². Temperley dealt with the general problem of residual entropy in polymers but did not give general solutions for the determination of residual entropy in copolymers. Alfrey and Lewis treated the problem of determination of enthalpy changes in copolymerization and provided methods for isolation of the ΔH of the elementary reaction for low conversion copolymers. If the above problems could be solved, all the experimental work necessary to calculate heat, entropy and free-energy changes for butadiene–styrene copolymerization has been done^{3–7}.

THEORETICAL

If the assumption is made that the contribution of the growing polymer chain to the propagation reaction depends only on the nature of the terminal monomeric unit, it becomes possible to describe copolymerization by four elementary reactions, usually written



With each elementary reaction is associated a rate constant k , a heat change q , an entropy change s , and a free-energy change f .

*Presented in part at the Ninth Canadian High Polymer Forum, Toronto, October 1959.

The reactivity ratios r_1 and r_2 are defined as k_{11}/k_{12} and k_{22}/k_{21} respectively. In some instances, it has been found (as far as r_1 and r_2 are concerned) that monomeric units farther back the chain can also contribute to polymer reactivity. If such be the case, the values of the above 'constants' depend on the initial value of $[M_1]/[M_2]$, called the charge ratio. It has been shown with butadiene-styrene polymerization^{8,9} that the reactivity ratios are determined by the nature of the terminal unit in the polymeric chain. The validity of such an assumption in the case of the other energy changes must be tested in a similar way.

Isolation of contributions of elementary reactions

Such an isolation was first made by Alfrey and Lewis² who obtained the expression for the heat of copolymerization (ΔH_c) as

$$\Delta H_c = m_2 P_{21} (\Delta H_{21} + \Delta H_{12} - \Delta H_{11} - \Delta H_{22}) + m_1 \Delta H_{11} + m_2 \Delta H_{22}$$

where $m_2 P_{21}$ is of the form

$$m_2 P_{21} = \frac{1 - [1 - 4m_2(1 - m_2)(1 - r_1 r_2)]^{1/2}}{2(1 - r_1 r_2)}$$

ΔH is the enthalpy change per mole of elementary reaction, and m_1 , m_2 and m are the mole fractions of the two monomers and the copolymer, respectively.

$\Delta H_{21} + \Delta H_{12}$ cannot be determined separately since reactions (ii) and (iii) occur with equal frequency. This particular expression emphasizes the importance of the $r_1 r_2$ product rather than the individual values of r_1 and r_2 .

Insight into the problem and an alternate method of procedure, of greater clarity, may be provided by the following argument. When some specific weight of copolymer is formed, each of the four elementary reactions has occurred some given number of times. Let the number of times that reaction (i) has occurred be represented by Σ_1 and let the other three reactions be similarly represented. Thus, the heat evolution (Q) associated with this weight of polymer, is given by

$$Q = q_{11}\Sigma_1 + q_{22}\Sigma_4 + q_{12}\Sigma_3 + q_{21}\Sigma_2$$

Since $\Sigma_3 = \Sigma_2$,

$$Q = q_{11}\Sigma_1 + q_{22}\Sigma_4 + \Sigma_3 (q_{12} + q_{21}) \quad (1)$$

Similar expressions hold for entropy and free-energy changes.

It can be shown that

$$\frac{\Sigma_1}{\Sigma_2} = \frac{r_1 [M_1]}{[M_2]} \quad \text{and} \quad \frac{\Sigma_4}{\Sigma_3} = \frac{r_2 [M_2]}{[M_1]}$$

The number of moles of monomer 1 and monomer 2 (called A and B respectively) may be determined either from analysis, or from the copolymerization equation and

$$A = \Sigma_1 + \Sigma_2 = \Sigma_1 \left\{ 1 + \frac{[M_2]}{[M_1] r_1} \right\}$$

$$B = \Sigma_3 + \Sigma_4 = \Sigma_4 \left\{ 1 + \frac{[M_1]}{[M_2] r_2} \right\}$$

Hence the values of Σ_1 , Σ_2 , Σ_3 and Σ_4 necessary for use in equation (1) may be determined. If values of q_{11} and q_{22} be known for homopolymerization reactions, $q_{12} + q_{21}$ may be calculated from knowledge of Q .

Treatment of high conversion copolymers—Application of the above equations requires knowledge of $[M_1]/[M_2]$. When the composition of the copolymer differs from that of the monomer mixture which generates it, the value of $[M_1]/[M_2]$ changes as the reaction proceeds. When a high conversion polymer is obtained, it is a blend of copolymers made from a continuously varying charge ratio. In such a case, it is necessary to divide the polymerization into an arbitrary number of successive stages, each of sufficiently short duration that $[M_1]/[M_2]$ may be considered constant. If the initial charge ratio be $[M_1]_0/[M_2]_0$ the charge ratio at the beginning of the second stage is

$$\frac{[M_1]_0 - (m_1)^1}{[M_2]_0 - (m_2)^1}$$

and that at the beginning of the n th is

$$\frac{[M_1]_0 - \sum_{r=1}^{r=n-1} (m_1)^r}{[M_2]_0 - \sum_{r=1}^{r=n-1} (m_2)^r}$$

where $(m_1)^r$ and $(m_2)^r$ are the moles of monomer 1 and 2, respectively, consumed during the r th stage. Such an approximation introduces errors which may be reduced by increasing n .

Phase specifications—The phases in which the monomer and polymer are during reaction must be specified. Values of heat and entropy changes assigned to the elementary reactions will differ with different phase specifications. For a monomer mixture obeying Raoult's law, where ΔS refers to the entropy change on a molar basis

$$(\Delta S_{11})_{sc} = (\Delta S_{11})_{lc} - R \ln \frac{[M_1]}{[M_1] + [M_2]} = (\Delta S_{11})_{lc} + \Delta S_1^M$$

and

$$(\Delta S_{12} + \Delta S_{21})_{sc} = (\Delta S_{12} + \Delta S_{21})_{lc} + \Delta S_1^M + \Delta S_2^M \quad (2)$$

(Terminology according to Dainton*¹⁰ and Hildebrand¹¹).

The necessity for a proper choice of phase is evident in the case of $\Delta S_{12} + \Delta S_{21}$. This value should not depend on the composition of the copolymer under study. Therefore, the $\Delta S_{12} + \Delta S_{21}$ term should only contain contributions from the elementary reactions, and not from the molecular aggregate. Equation (2) shows that the $(\Delta S_{12} + \Delta S_{21})_{sc}$ term does contain contributions from the molecular aggregate. Therefore, the $(\Delta S_{12} + \Delta S_{21})_{lc}$ term is considered to be characteristic of the elementary reactions.

*Dainton's method of phase specification is by subscripts l, c and s, referring to pure monomer, solid polymer and solutions, respectively.

Residual entropy in copolymers

There are three separate aspects to be considered:

- (1) problems arising from use of heat capacity data on the glassy state;
- (2) entropy due to chain configuration;
- (3) entropy due to copolymerization randomness.

Use of data from the glassy state—Heat capacity measurements obtained from glasses may be used as long as the measurements are reproducible and reversible. The argument for this is as follows.

If the glass transformation temperature be T_1 , then the entropy of the stable polymeric form at temperature T_2 (where $T_2 > T_1$) may be given by either of the following expressions:

$$S_{T_2(s)} = \int_{T_1}^{T_2} C_{p(s)} d \ln T + \int_0^{T_1} C_{p(g)} d \ln T + S_{0(g)}$$

or

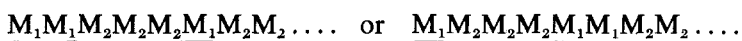
$$S_{T_2(s)} = \int_{T_1}^{T_2} C_{p(s)} d \ln T + \int_0^{T_1} C_{p(s)} d \ln T + S_{0(s)}$$

The subscripts (s) and (g) distinguish the stable and glassy forms of the polymer. The terms $\int_0^{T_1} C_{p(s)} d \ln T$ and $S_{0(s)}$ refer to hypothetical states which cannot be obtained in practice, since at these temperatures a glass is always formed. In the following work $S_{0(s)}$ will be estimated, and when this is used in conjunction with the term $\int_0^{T_1} C_{p(g)} d \ln T$, an error equivalent to $S_{0(g)} - S_{0(s)}$ will result. The assumption is made that this term is negligible. If such an assumption be wrong, then the value of $S_{0(g)} - S_{0(s)}$ may be expected to vary with the polymer composition (since T_1 , the glass transition temperature, varies) and the values of entropy change for the heteropolymerization reactions will appear to depend on the value of the charge ratio. That the term $S_{0(g)} - S_{0(s)}$ is small is also shown from measurements by Bekkedahl¹² who found the difference between the entropy of the crystalline and the amorphous forms of natural rubber at 0°K to be 0.28 cal/°C per mole of bound isoprene. The amorphous form would be a glass at such a temperature. The value contains not only the term $S_{0(g)} - S_{0(s)}$ but also contributions from the configurational entropy.

These latter contributions have been discussed by Temperley¹ who decided they were quite small, a conclusion supported by Bekkedahl's measurement.

Entropy of copolymerization randomness—This is an entropy of mixing, which results from the fact that copolymer molecules generated from a given charge ratio may have different structures.

A copolymer may be pictured as consisting of alternating sequences of the two monomer types in which the sequences may vary in length



Both of the above distinguishable forms may be produced from the same charge ratio.

The probability (P) of a sequence of M_1 units L units in length is given¹³ by

$$P = P_{11}^{L-1} (1 - P_{11})$$

where

$$P_{11} = \frac{r_1 [M_1]/[M_2]}{r_1 [M_1]/[M_2] + 1}$$

A similar relation holds for sequences of M_2 units.

When the number of sequences in a polymer (and the molecular weight) is established, it is possible to calculate the number of sequences of a given monomer unit corresponding to any given length. If the number of sequences per chain be $2n$ (of which half must be M_1 sequences and half M_2 sequences), the number of M_1 sequences of length L is

$$nP_{11}^{L-1} (1 - P_{11})$$

In such a case, let there be a_1 sequences of one M_1 units, a_2 sequences of two M_1 units and a_y sequences of y M_1 units, so that

$$n = a_1 + a_2 + a_3 + \dots + a_y$$

The number of permutations (Ω) open to these M_1 sequences is

$$\Omega = \frac{n!}{a_1! a_2! \dots a_y!}$$

For large values of a

$$\ln \Omega = n \ln n - a_1 \ln a_1 - \dots - a_y \ln a_y$$

The number of M_1 units in the copolymer is

$$a_1 + 2a_2 + 3a_3 + \dots + ya_y$$

The entropy per monomer unit ($k \ln \Omega$ per number of monomer units) is

$$S = k \frac{(n \ln n - a_1 \ln a_1 - \dots - a_y \ln a_y)}{a_1 + 2a_2 + 3a_3 + \dots + ya_y} \quad (3)$$

Provided that y is very large, this equation may be further simplified by expanding in terms of P_{11} or P_{22} . For units of type 1, it may be readily shown that

$$a_1 + 2a_2 + 3a_3 + \dots + ya_y \simeq \frac{n}{1 - P_{11}}$$

and

$$\sum_{i=1}^{i=y} a_i \ln a_i \simeq n \left[\ln n + \ln (1 - P_{11}) + \frac{P_{11}}{1 - P_{11}} \ln P_{11} \right]$$

These equalities become exact only when y is infinite. Appropriate substitution in (3) then shows that

$$S \text{ per monomer unit} = -k [P_{11} \ln P_{11} + (1 - P_{11}) \ln (1 - P_{11})] \quad (4)$$

RESULTS

Reactivity ratios of butadiene-styrene copolymerization at 5°C

Values of r_1 and r_2 for butadiene-styrene copolymerization are known only at 50°C and -18°C^{8,9}. Composition data have been reported for high-conversion butadiene-styrene copolymer prepared for different charge ratios⁶. From these data, values of $r_1=0.44$ and $r_2=1.40$ were calculated (taking styrene as M_1). Such values predict that copolymers at 60 per cent conversion will contain 8.0 per cent and 23.2 per cent of styrene (by weight) when prepared from 90/10 and 71/29 butadiene-styrene copolymers respectively. This may be compared with corresponding values of 8.6 per cent and 22.6 per cent of styrene obtained by direct analysis. Such values also fit well with those predicted for this temperature by a $\log r$ vs $1/T$ plot using data for 50°C and -18°C.

Copolymerization entropy

There was no significant difference in values of copolymerization entropy calculated from equation (3), taking $n=100$ (corresponding to a molecular weight of 100,000) and those calculated from equation (4), assuming infinite molecular weight.

In Table 1 are shown the copolymerization entropies calculated for low-conversion copolymers prepared at 5°C.

Table 1. Residual entropy in low-conversion copolymers

Charge ratio butadiene- styrene	Butadiene in copolymer (at 0% con- version) (%)	Entropy (e.u./mole)		Entropy of copolymer (e.u./g)
		Butadiene	Styrene	
90/10	93.0	0.267	0.166	4.59×10^{-3}
71/29	78.4	0.715	0.596	1.16×10^{-2}
50/50	61.3	1.08	0.932	1.58×10^{-2}
25/75	21.7	1.40	1.29	1.53×10^{-2}

Entropy changes in homopolymerization

The results in Table 2 were calculated from existing data on heat capacities and entropies of polybutadiene and polystyrene and their monomers. Entropy changes shown for polybutadiene are for the micro-structure characteristic of 5°C.

Table 2. Entropy changes in homopolymerization

Temperature (°C)	$-(\Delta S)_{1c}$ (cal °C ⁻¹ mole ⁻¹)	
	Butadiene	Styrene
-23	—	21.58
25	—	24.93
28	—	24.94
30	20.80	—
40	20.95	—
50	21.10	—
60	21.25	—
128	—	27.65
228	—	28.58

Entropy changes in copolymerization

From Table 2 we may obtain values of $(\Delta S_{11})_{lc}$ and $(\Delta S_{22})_{lc}$ so that it becomes possible to determine values of $(\Delta S_{12} + \Delta S_{21})_{lc}$ from heat capacity data on copolymers. Since values of $(\Delta S_{11})_{lc}$ and $(\Delta S_{22})_{lc}$ were not directly available for the temperature of synthesis, 5°C, values of $(\Delta S_{12} + \Delta S_{21})$ were determined at 30°C. These were determined at two charge ratios.

Table 3. Entropy changes for heteropolymerization steps

Charge ratio butadiene- styrene	$-(\Delta S_{12} + \Delta S_{21})_{sc}^*$ (cal °C ⁻¹ mole ⁻¹)	$-(\Delta S_{12} + \Delta S_{21})_{lc}^*$ (cal °C ⁻¹ mole ⁻¹)	$-(\Delta S_{12} + \Delta S_{21})_{lc}$ (cal °C ⁻¹ mole ⁻¹)
90/10	59.2	52.9	53.3
71/29	53.2	49.3	50.6

*Contributions from residual entropy of copolymerization were neglected.

Table 3 shows the lack of agreement between the different charge ratios when using the sc term. This agreement improves when the lc term is used. A further slight improvement was noted when the copolymerization entropy of the copolymer was taken into account. The remaining difference between the two charge ratios is of the same order of magnitude as the precision of the reactivity ratios. It may be concluded that:

(1) four elementary reactions are sufficient to explain entropy changes in copolymerization;

(2) the contribution of the glassy state to the entropy at 0°K is negligible.

Free-energy changes in copolymerization

Nelson¹⁴ has shown the heats of homopolymerization (Q_{11} and Q_{22}) of butadiene and styrene to be 17.8 and 16.8 kcal/mole respectively. The value of $(Q_{12} + Q_{21})_{lc}$ is intermediate and is estimated at 34.6 kcal/mole. Therefore, the free-energy decrease in the two heteropolymerization reactions is about 17 kcal/mole.

Comparison with other copolymerization systems

Neither the reactivity ratios nor energy changes in butadiene-styrene copolymerization contain contributions from the penultimate unit in the copolymer chain.

The copolymerization of acrylonitrile and methyl methacrylate which shows no penultimate unit effect in the reactivity ratios¹⁵ does show such an effect when heats of polymerization are considered¹⁶. Therefore, the fact that four elementary reactions are sufficient to explain copolymerization cannot be deduced only on the basis of reactivity ratio measurements.

Cratic terms in entropy changes in polymerization

Gurney¹⁷ has separated entropy changes during reaction into two terms—unitary and cratic. The cratic term depends only on the number of particles in the various species involved in the reactions. Gurney has applied this

concept to electrolyte dissociation. An analogous situation exists in polymerization. Such cratic terms are characteristic of the elementary reaction and contain no contribution from molecular aggregates. If it is reasonable to assert that the entropy term consists of two parts—unitary and cratic—it is equally reasonable to assert that the cratic term is determined, not only by changes in the total number of particles, but also by changes in the number of physically distinguishable species. Thus, in the exchange reaction $H_2 + D_2 \rightarrow 2HD$, there will be a cratic entropy change caused, not by a change in the total number of particles in the system, but by replacement of a system containing two physically distinguishable species by a system containing only one. Entropy changes in homopolymerization have a cratic component caused by the replacement of a two-particle system by a one-particle system. Heteropolymerization reactions also contain such a term, and in addition should have a term analogous to that in the $H_2 + D_2$ reaction, where two different species have been replaced by a third. (It will be noted that homopolymerization is accompanied by disappearance of only one separate species.) When all unitary terms are equal, the extra cratic contribution to the entropy change in the heteropolymerization reaction (ΔS_{12}) will make it smaller than that in the homopolymerization reaction involving the same monomer (ΔS_{22}) by $R \ln 2$ per mole. It may be noted that in this case $\Delta S_{21} + \Delta S_{12}$ was about $5 \text{ cal } ^\circ\text{C}^{-1} \text{ mole}^{-1}$ smaller than $\Delta S_{11} + \Delta S_{22}$.

The author wishes to thank Polymer Corporation Limited for permission to publish this work. Professor K. J. Laidler, University of Ottawa, Ontario, made valuable comments on the manuscript.

*Research and Development Division,
Polymer Corporation Limited,
Sarnia, Ontario, Canada*

(Received 29th August, 1960.)

Revised version received 17th October, 1960)

REFERENCES

- ¹ TEMPERLEY, H. N. V. *J. Res. nat. Bur. Stand.* 1956, **56**, 55
- ² ALFREY, T. and LEWIS, C. J. *J. Polym. Sci.* 1949, **4**, 221
- ³ SCOTT, R. B., MEYERS, C. H., RAND, R. D. and BRICKWEDDE, F. S. *J. Res. nat. Bur. Stand.* 1945, **35**, 39
- ⁴ FURUKAWA, G. T. and McCOSKEY, R. E. *J. Res. nat. Bur. Stand.* 1953, **51**, 321
- ⁵ BOUNDY, R. W. and BOYER, R. F. *Styrene*, Reinhold, New York, 1952, p. 67
- ⁶ FURUKAWA, G. T., McCOSKEY, R. E. and REILLEY, M. S. *J. Res. nat. Bur. Stand.* 1955, **55**, 127
- ⁷ FURUKAWA, G. T., McCOSKEY, R. E. and KING, G. J. *J. Res. nat. Bur. Stand.* 1953, **50**, 357
- ⁸ ORR, R. J. and WILLIAMS, H. L. *Canad. J. Chem.* 1951, **29**, 270
- ⁹ ALFRED, T., BOHRER, J. J. and MARK, H. *Copolymerization*, Interscience, New York and London, 1952, p. 36
- ¹⁰ DAINTON, F. S. and IVIN, K. J. *Quart. Rev. chem. Soc. Lond.* 1958, **XII**, 61
- ¹¹ HILDEBRAND, J. H. and SCOTT, R. L. *Solubility of Non-electrolytes*, Reinhold, New York, 1950
- ¹² BEKKEDAHL, N. and MATHESON, H. *J. Res. nat. Bur. Stand.* 1935, **15**, 503

- ¹³ ALFREY, T., BOHRER, J. J., MARK, H. *Copolymerization*, Interscience, New York and London, 1952, pp. 133-137
- ¹⁴ NELSON, R. A., JESSUP, R. S. and ROBERTS, D. E. *J. Res. nat. Bur. Stand.* 1952, **48**, 275
- ¹⁵ LEWIS, F. M., MAYO, F. R. and HULSE, W. F. *J. Amer. chem. Soc.* 1945, **67**, 1701
- ¹⁶ BAXENDALE, J. H. and MADARAS, G. W. *J. Polym. Sci.* 1956, **29**, 171
- ¹⁷ GURNEY, R. W. *Ionic Processes in Solution*, McGraw-Hill, New York and London, 1953. p. 90

*Studies on Radiation Polymerization in Solution: III. Effect of Primary Radicals in the Termination Reaction**

S. OKAMURA and T. MANABE

The effect of primary radicals on the termination reactions is discussed theoretically. It is found that the value of the termination rate constant k_t'' between two primary radicals has little effect on the rate and the degree of polymerization under usual conditions, so that a value of k_t'' which satisfies the geometric-mean postulate between the termination rate constants and does not affect actual rate or degree of polymerization may exist. Considering the relation between the rate of polymerization and the primary radical formation, we conclude that the rate constant between growing radicals and primary radicals is much larger than the rate constant between two growing radicals. The ratio $([S\cdot]/[M\cdot])$ of solvent radical concentration to growing radical concentration is proportional to $(1/x-1)^n$, where x is the volume fraction of monomer and n is a constant.

INTRODUCTION

WHEN the concentration of primary radicals is high compared with that of growing radicals, the effects of primary radicals in termination processes must be taken into account. General theoretical solutions for the rate and the degree of polymerization have not yet been obtained. But in the following four special cases the solutions have been attained: (1) neglecting interaction between two primary radicals¹; (2) using the geometric-mean postulate in considering the termination rate constants¹; (3) neglecting interactions both between two growing radicals and between two primary radicals²; (4) neglecting interactions both between two growing radicals and between growing radical and primary radical². To obtain the exact theoretical result, a fourth-order algebraic equation must be solved; the postulates in the special cases mentioned above were used to avoid the troublesome procedure of solving the fourth-order algebraic equation. Exact solutions obtained by means of an electronic digital computer are described in this paper, and the rate and the degree of polymerization are discussed as functions of rate constants.

THEORETICAL

The reaction scheme for polymerization by irradiation in solution may be written as follows³, where M is the monomer, S the solvent, P the polymer formed, and I the radiation intensity:

*Part I, OKAMURA, S. and MANABE, T. *Chem. High Polymers (Tokyo)* 1958, **15**, 688
Part II, MANABE, T., MOTOYAMA, T. and OKAMURA, S. *ibid.* 1958, **15**, 695

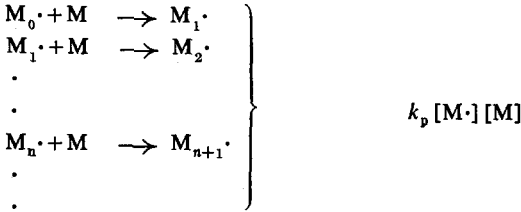
Formation of primary radicals by irradiation Rate



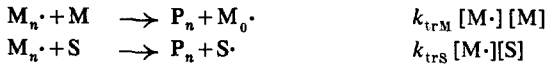
Initiation



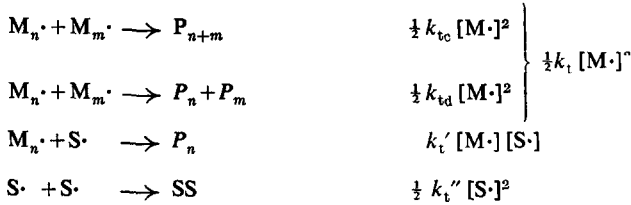
Propagation



Chain transfer



Termination



Assuming a stationary state for $[M\cdot]$ and $[S\cdot]$, the following equations are obtained:

$$\phi_M I [M] + k_p' [S\cdot] [M] - k_t [M\cdot]^2 - k_t' [M\cdot] [S\cdot] - k_{trS} [M\cdot] [S] = 0 \quad (1)$$

$$\phi_S I [S] + k_{trS} [M\cdot] [S] - k_t' [M\cdot] [S\cdot] - k_t'' [S\cdot]^2 - k_p' [S\cdot] [M] = 0 \quad (2)$$

Defining $[M] = [M]_0$ at $[S] = 0$, $[S] = [S]_0$ at $[M] = 0$, we may convert the unknowns $[M\cdot]$ and $[S\cdot]$ into dimensionless quantities in the following way:

$$\left. \begin{array}{l} x = [M] / [M]_0 \\ y = [M\cdot] / [M]_0 \\ z = [S\cdot] / [S]_0 \end{array} \right\} \quad (3)$$

The reaction rate constants are also converted into the dimensionless parameters given below:

$$\left. \begin{aligned} a &= \phi_M I [M]_0 / k_t [M]_0^2 \\ b &= \phi_S I [S]_0 / k_t [M]_0^2 \\ c &= k'_t [M]_0 [S]_0 / k_t [M]_0^2 \\ d &= k''_t [S]_0^2 / k_t [M]_0^2 \\ e &= k_{trS} [M]_0 [S]_0 / k_t [M]_0^2 \\ f &= k'_p [S]_0 [M]_0 / k_t [M]_0^2 \\ g &= k_p / k_t \\ h &= k_{trM} / k_t \\ i &= \frac{1}{2} (1 + k_{td} / k_t) \end{aligned} \right\} \quad (4)$$

Then equations (1) and (2) become:

$$ax + fxz - y^2 - cyz - ey(1-x) = 0 \quad (5)$$

$$b(1-x) + ey(1-x) - cyz - dz^2 - fxz = 0 \quad (6)$$

Eliminating z from the above equations we obtain the following fourth-order algebraic equation:

$$\begin{aligned} &(d - c^2) y^4 + 2e(d - c^2)(1-x) y^3 \\ &+ [(de^2 + f^2 - 2cef) x^2 + (ac^2 + bc^2 + 2cef - 2ad - 2de^2) x + de^2 - bc^2] y^2 \\ &+ 2(bcf - ade)(1-x) xy + (b-a) f^2 x^3 + (a^2 d - bf^2) x^2 = 0 \end{aligned} \quad (7)$$

If y is obtained from equation (7), z may be calculated from either of the following equations (8) which are deduced from equations (5) and (6):

$$\left. \begin{aligned} z &= \frac{ax - e(1-x)y - y^2}{cy - fx} \\ z &= \frac{[(cy + fx)^2 + 4d(1-x)(b + ey)]^{\frac{1}{2}} - (cy + fx)}{2d} \end{aligned} \right\} \quad (8)$$

The ratio (V/V_0) of the solution polymerization rate (V) to the bulk rate (V_0) obtained from equations (3), (4) and (5) is given in (9), in which $[M\cdot]_0$ and $a^{\frac{1}{2}}$ are the values of $[M\cdot]$ and y respectively at $x = 1$:

$$\frac{V}{V_0} = \frac{k_p [M\cdot] [M] + k'_p [S\cdot] [M]}{k_p [M\cdot]_0 [M]_0} = \frac{(gy + fz) x}{ga^{\frac{1}{2}}} \quad (9)$$

The degree of polymerization (\bar{P}_n) is given by:

$$\begin{aligned} \bar{P}_n &= \frac{k_p [M\cdot] [M] + k'_p [S\cdot] [M]}{k_{trM} [M\cdot] [M] + k_{trS} [M\cdot] [S] + \frac{1}{2} k_{tc} [M\cdot]^2 + k_{td} [M\cdot]^2 + k'_t [M\cdot] [S\cdot]} \\ &= \frac{gy + fz}{e + (h - e)x + iy + cz} \cdot \frac{x}{y} \end{aligned} \quad (10)$$

RESULTS

Calculations have been made for the systems shown in *Table 1*.

Table 1. Systems for which calculations have been made

No.	Parameter								
	<i>a</i>	<i>b</i>	<i>c</i>	<i>d</i>	<i>e</i>	<i>f</i>	<i>g</i>	<i>h</i>	<i>i</i>
1	10 ⁻¹⁸	10 ⁻¹⁷	1	2	10 ⁻⁹	10 ⁻⁶	10 ⁻⁶	10 ⁻¹⁰	0.5
2	10 ⁻¹⁸	10 ⁻¹⁷	10	2	10 ⁻⁹	10 ⁻⁶	10 ⁻⁶	10 ⁻¹⁰	0.5
3	10 ⁻¹⁸	10 ⁻¹⁷	100	2	10 ⁻⁹	10 ⁻⁶	10 ⁻⁶	10 ⁻¹⁰	0.5
4	10 ⁻¹⁸	10 ⁻¹⁷	1,000	2	10 ⁻⁹	10 ⁻⁶	10 ⁻⁶	10 ⁻¹⁰	0.5
5	10 ⁻¹⁸	10 ⁻¹⁷	1	1	10 ⁻⁹	10 ⁻⁶	10 ⁻⁶	10 ⁻¹⁰	0.5
6	10 ⁻¹⁸	10 ⁻¹⁷	10	100	10 ⁻⁹	10 ⁻⁶	10 ⁻⁶	10 ⁻¹⁰	0.5
7	10 ⁻¹⁸	10 ⁻¹⁷	100	10,000	10 ⁻⁹	10 ⁻⁶	10 ⁻⁶	10 ⁻¹⁰	0.5
8	10 ⁻¹⁸	10 ⁻¹⁶	1	2	10 ⁻⁹	10 ⁻⁶	10 ⁻⁶	10 ⁻¹⁰	0.5
9	10 ⁻¹⁸	10 ⁻¹⁶	10	2	10 ⁻⁹	10 ⁻⁶	10 ⁻⁶	10 ⁻¹⁰	0.5
10	10 ⁻¹⁸	10 ⁻¹⁶	100	2	10 ⁻⁹	10 ⁻⁶	10 ⁻⁶	10 ⁻¹⁰	0.5
11	10 ⁻¹⁸	10 ⁻¹⁷	1	20	10 ⁻⁹	10 ⁻⁶	10 ⁻⁶	10 ⁻¹⁰	0.5
12	10 ⁻¹⁸	10 ⁻¹⁷	1	200	10 ⁻⁹	10 ⁻⁶	10 ⁻⁶	10 ⁻¹⁰	0.5
13	10 ⁻¹⁸	10 ⁻¹⁷	1	2,000	10 ⁻⁹	10 ⁻⁶	10 ⁻⁶	10 ⁻¹⁰	0.5
14	10 ⁻²⁰	10 ⁻¹⁹	1	2	10 ⁻⁹	10 ⁻⁶	10 ⁻⁶	10 ⁻¹⁰	0.5
15	10 ⁻¹⁶	10 ⁻¹⁵	1	2	10 ⁻⁹	10 ⁻⁶	10 ⁻⁶	10 ⁻¹⁰	0.5
16	10 ⁻¹⁴	10 ⁻¹³	1	2	10 ⁻⁹	10 ⁻⁶	10 ⁻⁶	10 ⁻¹⁰	0.5
17	10 ⁻¹⁸	10 ⁻¹⁷	1	2	10 ⁻⁹	10 ⁻⁸	10 ⁻⁶	10 ⁻¹⁰	0.5
18	10 ⁻¹⁸	10 ⁻¹⁷	1	2	10 ⁻⁹	10 ⁻⁴	10 ⁻⁶	10 ⁻¹⁰	0.5
19	10 ⁻¹⁸	10 ⁻¹⁷	1	2	10 ⁻⁹	10 ⁻²	10 ⁻⁶	10 ⁻¹⁰	0.5
20	10 ⁻¹⁸	10 ⁻¹⁷	1	2	10 ⁻¹²	10 ⁻⁶	10 ⁻⁶	10 ⁻¹⁰	0.5
21	10 ⁻¹⁸	10 ⁻¹⁷	1	2	10 ⁻⁶	10 ⁻⁶	10 ⁻⁶	10 ⁻¹⁰	0.5

When the monomer is styrene and the radiation intensity is 10,000 rad/h, parameter *a* becomes 10⁻¹⁸ approximately. In No. 1-7, 11-13 and 17-21, the G_{R} -values of the solvent are about 10 times larger than that of monomer, while they are about 100 times larger in No. 8-10. In considering No. 1-4, we shall examine the effect of termination between solvent radicals and growing chains (rate constant k_t'). In No. 5-7 the geometric-mean postulate between termination rate constants

$$c^2 - d = 0 \text{ or } k_t'^2 - k_t k_t'' = 0 \quad (11)$$

will be assumed, and, from the examples in No. 11-13, the effect of interprimary-radical termination (rate constant k_t'') may be estimated. The effects of changes in the radiation intensity, of the efficiency of initiation by the solvent radicals and of solvent transfer are shown in examples 14-16, 17-19 and 20-21 respectively. The results obtained are given in *Tables 2-4*.

Since *y* is proportional to the growing-radical concentration $[M\cdot]$ (see equation 3), the following conclusions may be drawn from *Table 2*.

From the results for No. 1-4, it follows that $[M\cdot]$ changes little even when k'_t becomes 10 times larger than k_t , provided that $x > 0.5$. The volume fraction of monomer where $[M\cdot]$ is a maximum skews to larger values when k'_t becomes larger. $[M\cdot]$ is proportional to x when k'_t becomes 1,000 times larger than k_t .

Table 2. Values of 10^9y for different values of x

No.	x							
	0.05	0.10	0.30	0.50	0.70	0.90	0.95	1.00
1	2.85	2.90	2.67	2.33	1.92	1.38	1.20	1.00
2	1.85	2.25	2.45	2.23	1.87	1.37	1.20	1.00
3	0.445	0.779	1.45	1.63	1.56	1.27	1.15	1.00
4	0.050	0.100	0.300	0.500	0.700	0.900	0.950	1.00
5	2.86	2.90	2.67	2.33	1.92	1.38	1.20	1.00
6	1.71	2.17	2.44	2.23	1.87	1.37	1.20	1.00
7	0.351	0.634	1.31	1.56	1.54	1.27	1.15	1.00
8	7.93	8.57	8.14	7.00	5.50	3.29	2.43	1.00
9	3.57	5.10	6.59	6.22	5.14	3.19	2.39	1.00
10	0.493	0.963	2.44	3.20	3.30	2.53	2.04	1.00
11	2.74	2.87	2.67	2.33	1.92	1.38	1.20	1.00
12	2.19	2.62	2.64	2.33	1.92	1.38	1.20	1.00
13	1.34	1.87	2.44	2.27	1.91	1.38	1.20	1.00
14	0.301	0.298	0.269	0.232	0.190	0.134	0.118	0.100
15	18.2	22.6	24.8	22.5	18.8	13.7	12.0	10.0
16	42.9	73.9	141	162	157	128	116	100
17	0.322	0.582	1.24	1.51	1.51	1.27	1.15	1.00
18	3.09	3.02	2.70	2.35	1.92	1.38	1.20	1.00
19	3.09	3.02	2.70	2.35	1.92	1.38	1.20	1.00
20	2.91	2.93	2.68	2.34	1.92	1.38	1.20	1.00
21	0.070	0.183	0.655	1.04	1.29	1.23	1.14	1.00

The geometric-mean postulate (see equation 11) is assumed in No. 5-7 but not in No. 1-3. However, we see that the results for these two sets of examples are the same. This finding will be discussed later.

Comparing the results for No. 8-10 with those for No. 1-3, we see that the effect of k'_t on the growing-radical concentration becomes more apparent as the G_R -value of the solvent increases. This would be expected since, when the G_R -value of the solvent becomes larger, the concentration of solvent radicals increases.

The effect of k'_t on $[M\cdot]$ may be seen by comparing No. 1, 11, 12 and 13. The difference in $[M\cdot]$ between the values in No. 1 and No. 12 is less than 1 per cent (while k'_t in the latter is 100 times larger), provided that the volume fraction of monomer is larger than 0.3.

The effect of the radiation intensity on $[M\cdot]$ may be seen by comparing No. 1, 14, 15 and 16. The growing-radical concentration is proportional

to the square root of the radiation intensity in the range $a < 10^{-16}$ even when the solvent concentration is rather large.

The effect on $[M\cdot]$ of the value of the initiation rate constant of solvent radicals may be seen by comparing No. 1, 17, 18 and 19. The growing-radical concentration changes little when k_p'/k_t is in the range 10^{-6} – 10^{-2} , but it decreases appreciably when k_p'/k_t falls to 10^{-8} .

Table 3. Values of V/V_0 for different values of x

No.	x							
	0.05	0.10	0.30	0.50	0.70	0.90	0.95	1.00
1	0.154	0.301	0.811	1.17	1.35	1.24	1.14	1.00
2	0.101	0.234	0.742	1.12	1.32	1.23	1.14	1.00
3	0.0275	0.0833	0.439	0.818	1.10	1.15	1.10	1.00
4	0.0073	0.0145	0.0936	0.253	0.492	0.811	0.903	1.00
5	0.155	0.302	0.811	1.17	1.35	1.24	1.14	1.00
6	0.0926	0.226	0.739	1.12	1.32	1.23	1.14	1.00
7	0.0189	0.0658	0.398	0.783	1.08	1.14	1.09	1.00
8	0.480	0.945	2.51	3.55	3.88	2.97	2.32	1.00
9	0.234	0.572	2.04	3.16	3.62	2.88	2.27	1.00
10	0.0718	0.142	0.772	1.63	2.33	2.28	1.94	1.00
11	0.147	0.298	0.810	1.17	1.35	1.24	1.14	1.00
12	0.117	0.271	0.801	1.17	1.35	1.24	1.14	1.00
13	0.0698	0.193	0.739	1.14	1.34	1.24	1.14	1.00
14	0.154	0.301	0.810	1.16	1.33	1.21	1.12	1.00
15	0.145	0.294	0.808	1.17	1.35	1.24	1.14	1.00
16	0.119	0.247	0.744	1.13	1.33	1.24	1.14	1.00
17	0.0171	0.0600	0.375	0.757	1.06	1.14	1.09	1.00
18	0.167	0.313	0.819	1.18	1.35	1.24	1.14	1.00
19	0.167	0.313	0.819	1.18	1.35	1.24	1.14	1.00
20	0.154	0.302	0.811	1.17	1.35	1.24	1.14	1.00
21	0.0698	0.183	0.657	1.05	1.29	1.23	1.14	1.00

From the results in No. 1, 20 and 21 the effect of solvent chain transfer on the growing-radical concentration may be deduced. The growing-radical concentration changes little when k_{trs}/k_t is in the range 10^{-12} – 10^{-9} , but it decreases considerably when k_{trs}/k_t becomes 10^{-6} .

From Table 3 the values of the ratio V/V_0 in various systems may be deduced similarly; the results resemble those in Table 2.

The bulk polymerization rate is proportional to $a^{\frac{1}{2}}$. In No. 14, 15 and 16, a has the values 10^{-20} , 10^{-16} and 10^{-14} respectively, but in the other cases $a = 10^{-18}$. Thus, in order to obtain the relative solution polymerization rates, we must multiply the values given for No. 14, 15 and 16 in Table 3 by 0.1, 10 and 100 respectively.

From Table 4 the degrees of polymerization in various systems may be deduced similarly.

STUDIES ON RADIATION POLYMERIZATION IN SOLUTION: III

 Table 4. Values of \bar{P}_n for different values of x

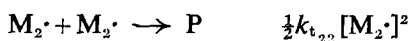
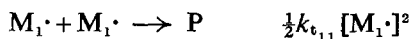
No.	x							
	0.05	0.10	0.30	0.50	0.70	0.90	0.95	1.00
1	20.7	42.0	145	291	526	1,020	1,270	1,670
2	15.5	35.5	137	282	517	1,020	1,270	1,670
3	5.30	15.9	93.3	224	451	962	1,230	1,670
4	1.51	3.13	24.2	83.5	233	723	1,050	1,670
5	20.7	42.0	145	291	526	1,020	1,270	1,670
6	16.9	36.6	137	282	517	1,020	1,270	1,670
7	13.9	28.7	109	237	460	965	1,230	1,670
8	9.18	18.2	61.3	122	223	489	696	1,670
9	4.72	11.6	51.0	110	210	476	684	1,670
10	1.52	3.11	20.9	60.4	141	385	593	1,670
11	21.3	42.3	145	291	526	1,020	1,270	1,670
12	24.3	44.8	146	291	526	1,020	1,270	1,670
13	31.1	54.1	153	296	529	1,020	1,270	1,670
14	46.0	95.2	348	751	1,510	3,500	4,650	6,670
15	3.82	6.84	21.4	40.9	70.2	127	154	196
16	1.27	1.58	2.96	4.79	7.58	13.1	15.8	20
17	17.0	34.1	119	248	468	968	1,230	1,670
18	21.6	43.0	146	292	527	1,020	1,270	1,670
19	21.6	43.0	146	292	527	1,020	1,270	1,670
20	32.4	65.9	217	409	678	1,150	1,360	1,670
21	1.05	1.11	1.43	2.00	3.32	9.92	19.7	1,670

DISCUSSION

The geometric-mean postulate

To obtain the exact theoretical value, the fourth-order algebraic equation (equation 7) must be solved. If the geometric-mean relation (equation 11) between the termination rate constants (k_t , k'_t and k''_t) is assumed, the fourth-order equation can be reduced to one of second order so that the troublesome procedure is avoided. Bamford *et al.*¹ assumed this relation and compared the calculated with the experimental values. Good agreement was obtained between theory and experiment, but the geometric-mean postulate was not justified theoretically. In termination reactions for copolymerization, the ratio ϕ of the cross-termination rate constant to the geometric mean of the constants for the terminations involving like radicals is defined as the following:

$$\phi = k_{t_{12}} / k_{t_{11}}^{1/2} k_{t_{22}}^{1/2} \quad (12)$$



If the geometric-mean postulate holds for these termination rate constants ϕ must be unity. It is found, however, that ϕ is generally considerably larger than unity (Table 5)⁴.

Table 5. Cross-termination rate ratios

System	ϕ
Styrene-methyl methacrylate	13-14
Styrene-methyl acrylate	50
Styrene-butyl acrylate	~ 100
Styrene- <i>p</i> -methoxystyrene	1
Methyl methacrylate- <i>p</i> -methoxystyrene	~ 20

Considering these facts, we may conclude that the agreement between theory and experiment obtained by Bamford *et al.*¹ is not due to the essential correctness of the geometric-mean postulate but to another reason, which we shall now discuss.

From the results for No. 1-3, 5-7, 11 and 12 in Table 3, the effect of k_t'' on the rate of polymerization may be estimated. These results are represented in Figure 1, and show that k_t'' has little effect on the polymerization rate. In other words, a value of k_t'' may exist which satisfies the geometric-mean relation (see equation 11), but which does not affect the actual rate or the degree of polymerization; this may explain the

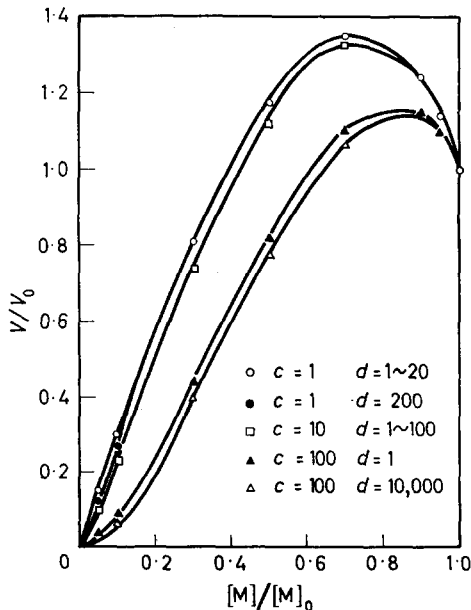


Figure 1—Effect of primary radical on termination reaction. d (or k_t'') has little effect on the polymerization rate but c (or k_t') has a marked effect

agreement between theory and experiment in solution polymerization which was obtained by Bamford *et al.*¹. Indeed, the latter authors deduced from the similar values obtained for their parameters Δ and Σ that the interaction

between primary radicals is negligible compared with normal termination, and with termination between growing chains and primary radicals, under practical conditions.

Radiation intensity and polymerization rate

Only the solvent radicals (but not the monomer radicals) may be treated here as the primary radicals. The concentration of the monomer radicals may be neglected in comparison with that of the growing radicals ($[M_0\cdot] \ll [M\cdot]$). Moreover, the concentration of monomer radicals may be considerably less than that of solvent radicals when the volume fraction of monomer is greater than 0.5, because the G_R -value of solvent is about 10 (or 100) times larger than that of monomer ($b/a=10$ or 100). Then the solution polymerization rate can be discussed as a function of the formation rate of solvent radicals. Defining A and B as follows, we see that A and B are proportional to the rate of formation of primary radicals (mole $l^{-1} \text{ sec}^{-1}$) and the rate of solution polymerization (percentage/sec) respectively.

$$A = \phi_s I [S] / k_t [M]_0^2 = b(1-x) \quad (13)$$

$$B = \frac{k_p [M\cdot] [M] + k'_p [S\cdot] [M]}{k_p [M]_0 [M]} = y + \frac{fz}{g} \quad (14)$$

In Figure 2 the relation between A and B is plotted. It appears that B is proportional to $A^{1/2}$ when $c=1$, $x \geq 0.5$ and $A < 10^{-13}$. In the bulk polymerization of styrene, deviation from the simple theory (polymerization

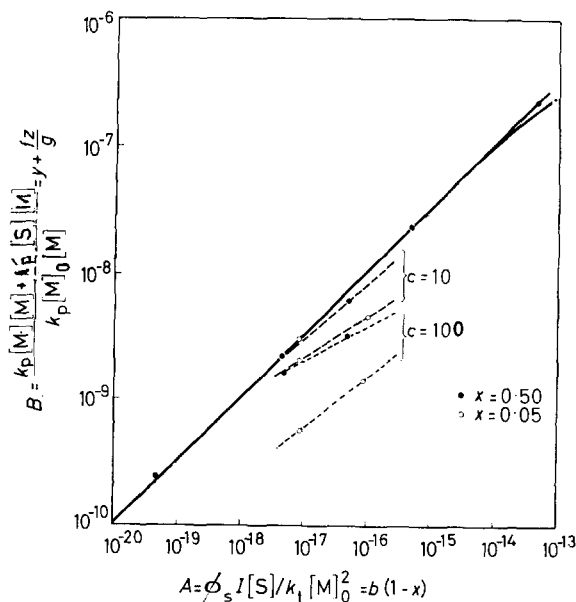


Figure 2—Effect of primary radical formation rate (mole $l^{-1} \text{ sec}^{-1}$) on polymerization rate (percentage/sec)

rate proportional to the square root of the radiation intensity) appears when⁵ $I > 100$ rad/min. The condition is equivalent to

$$A = \phi_M I [M]_0 / k_t [M]_0^2 > 2.5 \times 10^{-19}$$

The rate at which deviation appears ($A_c = 2.5 \times 10^{-19}$) may be less in solution polymerization. The difference between theory ($A_c \approx 10^{-13}$) and experiment ($A_c < 2.5 \times 10^{-19}$) may be due to the assumption that $k'_t/k_t \approx 1$; in other words, k'_t may be considerably larger than k_t . From Figure 2 it is found that the deviation from the square-root rule (solid straight line) increases with increasing k'_t/k_t ($\approx c$).

$[S\cdot]/[M\cdot]$ as a function of x

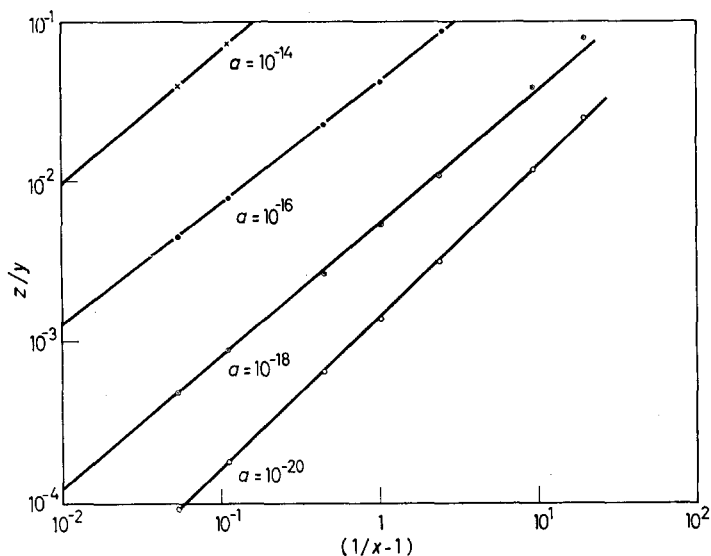
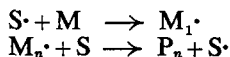


Figure 3— z/y as a function of $(1/x-1)$. The effect of the radiation intensity on the parameters k and n is shown, since $z/y = k(1/x-1)^n$

If the ratio of the concentrations of solvent radicals and growing radicals could be expressed as a simple function of monomer concentration it would be convenient for kinetic considerations. Concentrations of the growing and the solvent radicals could then be obtained by the assumption of a steady-state total concentration:

$$\frac{d([M\cdot] + [S\cdot])}{dt} = 0$$

together with the relation³ of $[S\cdot]/[M\cdot]$ versus x . The interchange reactions between two kinds of radicals:



would then not affect calculation of the concentrations. It was found that the following relation of $[S\cdot]/[M\cdot]$ and monomer concentration

$$\frac{[S]/[S]_0}{[M]/[M]_0} = k \left(\frac{[S]/[S]_0}{[M]/[M]_0} \right)^n \quad (15)$$

is suitable for representation of experimental results³. The relation has not, however, been proved kinetically. By using equation (3) we may convert equation (15) into:

$$\frac{z}{y} = k \left(\frac{1}{x} - 1 \right)^n \quad (16)$$

In *Figure 3* the relation of z/y to $(1/x - 1)$ under various conditions is represented.

From *Figure 3* it is found that the relation expressed by equation (16) is correct over a wide range of x ($0.05 < x < 0.95$). The parameter k

Table 6. k , n and range of x over which relation (16) holds

No.	k	$0.57 \frac{a^{0.04} b^{0.43}}{1.005f - e}$	n	$0.94a^{0.087} b^{-0.094} e^{0.010}$	Range of x where relation (16) is established
1	0.0053	0.0053	0.81	0.82	0.10-0.95
2	0.0055	0.0053	0.83	0.82	0.10-0.95
3	0.0055	0.0053	0.85	0.82	0.30-0.95
4	0.0095	0.0053	1.18	0.82	0.50-0.95
5	0.0053	0.0053	0.81	0.82	0.10-0.95
6	0.0055	0.0053	0.83	0.82	0.10-0.95
7	0.0053	0.0053	0.83	0.82	0.10-0.95
8	0.0015	0.0014	0.66	0.66	0.30-0.95
9	0.0015	0.0014	0.66	0.66	0.30-0.95
10	0.0017	0.0014	0.70	0.66	0.50-0.95
11	0.0053	0.0053	0.81	0.82	0.10-0.95
12	0.0053	0.0053	0.81	0.82	0.10-0.95
13	0.0051	0.0053	0.79	0.82	0.10-0.95
14	0.0015	0.00061	0.95	0.85	0.05-0.95
15	0.045	0.046	0.78	0.80	0.10-0.95
16	0.40	0.42	0.77	0.77	0.05-0.95
17	0.49	0.59	0.83	0.82	0.05-0.95
18	0.000053	0.000053	0.81	0.82	0.10-0.95
19	0.0000053	0.0000053	0.81	0.82	0.10-0.95
20	0.0044	0.0053	0.79	0.77	0.10-0.95
21	1.00	1.06	1.00	0.88	0.00-1.00

in equation (16) varies widely according to the reaction rate constants, while n is considered to be more nearly constant. The parameters k and n are expressed approximately as functions of the rate constants by the following relations:

$$k = 0.57 \frac{a^{0.04} b^{0.43}}{1.005f - e} \quad (17)$$

$$n = 0.94 a^{0.087} b^{-0.094} e^{0.010} \quad (18)$$

Values of k and n are shown in *Table 6*.

The authors are indebted to Dr C. H. Bamford for his advice and helpful discussions.

*Department of Textile Chemistry,
Faculty of Engineering,
Kyoto University,
Kyoto, Japan*

(Received 12th October, 1960)

REFERENCES

- ¹ BAMFORD, C. H., JENKINS, A. D. and JOHNSTON, R. *Trans. Faraday Soc.* 1959, **55**, 1451
- ² CHAPIRO, A., MAGAT, M., SEBBAN, J. and WAHL, P. International Symposium on Macromolecular Chemistry, Milano-Torino, 1954, *Proceedings* p. 73
- ³ OKAMURA, S. and MANABE, T. *Chem. High Polymers (Tokyo)* 1958, **15**, 688
- ⁴ FLORY, P. J. *Principles of Polymer Chemistry*, Cornell University Press, Ithaca, N.Y. 1953, p. 202
- ⁵ BOUBY, L., CHAPIRO, A., MAGAT, M., MIGIRDICYAN, E., PREVOT-BERNAS, A., REINISH, L. and SEBBAN, J. *Proceedings of the International Conference on the Peaceful Uses of Atomic Energy, Geneva, August 1955*, Vol. 7, p. 526, United Nations, New York, 1956
- ⁶ CHAPIRO, A. and MAGAT, M. *Actions Chimiques et Biologiques des Radiations* (Ed. M. HAISSINSKY), Masson et Cie, Paris, 1958, pp. 88, 100

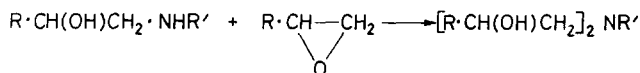
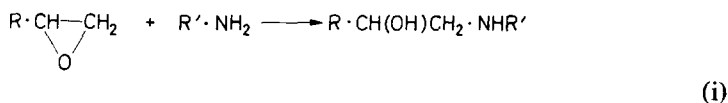
The Mechanism of the Crosslinking of Epoxide Resins by Amines

IEUAN T. SMITH*

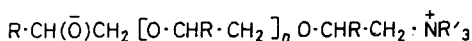
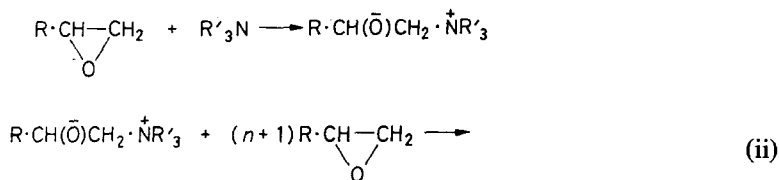
Previous work on the kinetics and mechanism of the reaction between amines and epoxides is reviewed, and it is considered that a termolecular mechanism is to be preferred to a bimolecular mechanism. The hypothesis that these reactions proceed via a termolecular hydrogen-bonded transition state is treated kinetically, and is shown to be consistent with previously published work. Energies of activation and entropies of activation of some amine-epoxide polymerizations have been studied by isothermal gel-point measurements, and by the observation of temperature changes during crosslinking. The results are consistent with the conclusion that the transition state is hydrogen bonded. This mechanism, it is concluded, applies to amine-epoxide reactions under all conditions previously studied, and the second-order kinetics reported from studies on dilute aqueous and dilute alcoholic solutions may therefore not be regarded as diagnostic of a bimolecular reaction mechanism.

INTRODUCTION

THE HARDENING of epoxide resins by amines occurs *via* reactions which are usually written as in (i).



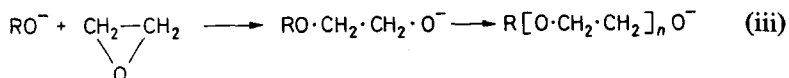
Curing can be effected by some tertiary amines, and the first study of the mechanism was reported by Narracott¹. He found that the polymer formed by treating phenyl glycidyl ether with triethylamine appeared, by analysis, to be a low molecular weight polymer containing about one hydroxyl group per molecule (5-6 monomer units) together with a small percentage of nitrogen. The rate of the polymerization was increased by traces of water or alcohol. Narracott considered that the mechanism could be represented by (ii).



*Present address: Research Association of British Paint Colour and Varnish Manufacturers, The Jordan Laboratory, Paint Research Station, Waldegrave Road, Teddington, Middlesex.

O'Neill and Cole² have shown by infra-red spectroscopy that the only significant reaction during the cure of an epoxide resin by ethylenediamine and by a reactive polyamide was that of epoxide groups with amino hydrogen atoms. This has recently been confirmed, in effect, by the demonstration that the development of a three-dimensional structure is associated with the formation of tertiary amine groups during the curing by aromatic and aliphatic amines³.

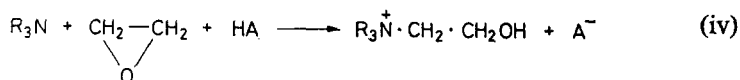
Just as Narracott found that hydroxylic compounds could increase the rate of the tertiary-amine-initiated polymerization of phenyl glycidyl ether, so Allen and Hunter⁴ found that bis(*N,N'*-hydroxyethyl) ethylenediamine cured a low molecular weight epoxide resin much more rapidly than ethylenediamine itself. The latter authors conclude that hydrogen bonding by the hydroxyl groups played a part in the mechanism. Bruin⁵ has criticized the mechanism of Narracott for the tertiary-amine-initiated reactions. However, this mechanism is quite consistent with the known facts about these reactions. The comparatively large quantities of tertiary amine required for complete hardening are consistent with a reaction having a small kinetic chain length, and the mechanism is directly analogous to the polymerization of ethylene oxide by alcoholic alkoxide solutions, which is known⁶ to proceed according to (iii).



Further evidence of the powerful effect of hydroxyl groups on amine-epoxide reactions has been provided by Ingberman and Walton⁷. A number of hydroxyalkylated amines were found to react more rapidly than the parent amine, and phenols were found to accelerate the reaction.

The kinetics of reactions between simple epoxides and many amines (and ammonia) have been studied by various workers. Most of the reactions were studied in dilute aqueous or dilute alcoholic solution, and second-order kinetics have invariably been established⁸. Consideration of the kinetics of these reactions, the orientation of the products and the stereochemistry of ring opening have led to the view that an S_N2 mechanism is followed^{8(j,k)}.

Cromwell and Barker^{8(e)} found that the reaction of epoxybenzylacetophenone with morpholine, and with piperidine, in benzene or ether solution was extremely slow and gave low yields. In methanol solution smooth reactions were observed at room temperature. Eastham and his co-workers^{8(h,i)}, considered that the reactions of ethylene oxide with amines all followed the same course (iv) whether or not the amine contained hydrogen attached to nitrogen.



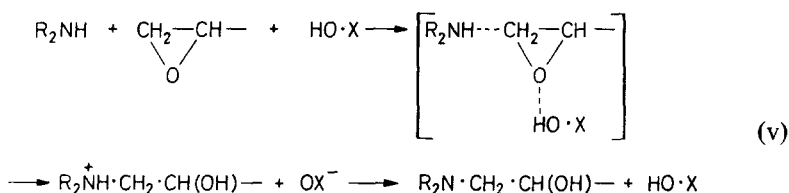
In aqueous solution the reactions were independent of the proton source; when the reactions were conducted in pure amine solution they were sensitive to the source of protons and the rate was given by

$$\frac{-d[\text{Oxide}]}{dt} = k[\text{Oxide}][\text{HA}]$$

Recently it has been shown that the rate of the reaction of ethylene oxide with aniline (in solutions of the latter) in the presence of water was proportional to the concentration of the water⁹; the catalytic influence of acids was proportional to their strength¹⁰, and the rate was given by

$$\frac{-d[\text{Oxide}]}{dt} = (k_0 + k_1)[\text{PhNH}_3^+] + k_2[\text{HX}][\text{Oxide}]$$

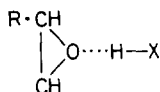
Shechter, Wynstra and Kurkij¹¹ studied the reaction of diethylamine with phenyl glycidyl ether in the absence of solvents, and in concentrated solutions. They showed it to be free from side reactions, and, in the absence of solvent sigmoidal concentration *versus* time curves were obtained. Benzene or acetone slowed the reaction by an amount consistent with the dilution of the reactants, but isopropanol, nitromethane and water accelerated the reaction, and the sigmoidal form of the concentration curves was lost. Phenol was found to be a particularly powerful accelerator. These authors considered that the solvent molecules must be involved in the transition state, and they wrote it as (v) (by analogy with Swain's 'push-pull' mechanism).



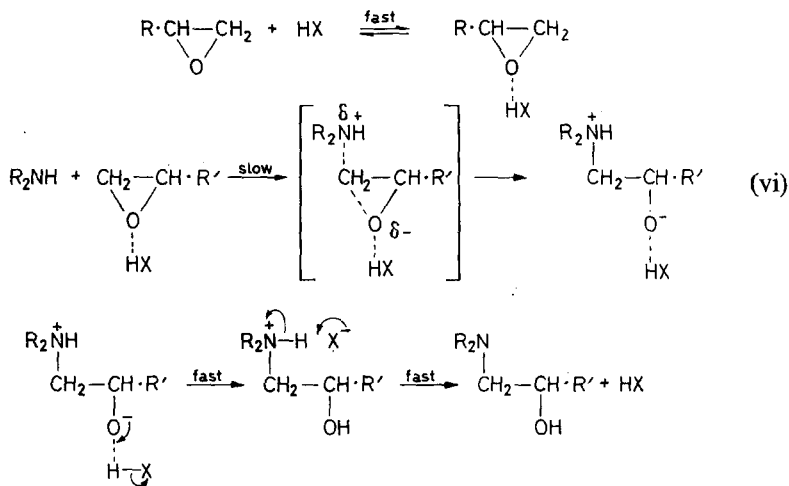
The sigmoidal form of the concentration curves was considered to be due to autocatalysis caused by the hydroxyl group in the product. The above mechanism permits a ready explanation of the fact that ethylene oxide and ammonia do not react under anhydrous conditions¹², a small quantity of water being required to initiate the reaction. Similarly, dry diethylamine and ethylene oxide do not react¹³, although the reaction proceeds readily in the presence of water, methanol or ethanol.

Recently, further support has been obtained for a mechanism of the type indicated by Shechter and his co-workers. The crosslinking of a low molecular weight epoxide resin by a polyamino-compound was found to be accelerated by a large number of compounds capable of acting as hydrogen-bond donors (alcohols, phenols, acids, amides and sulphonamides), but retarded by molecules capable of acting as hydrogen-bond acceptors (ethyl methyl ketone, ethyl acetate, dimethylformamide and compounds containing π -electrons)¹⁰. Further, the acceleration was dependent upon the concentration of the hydrogen-bond donor.

Infra-red spectra measurements and studies of the heat of mixing with chloroform have demonstrated that α -epoxides form hydrogen bonds with a number of donor molecules¹⁴. Since it is unusual for more than two atoms to be involved in a hydrogen bond, and the preferred arrangement is that in which the donor atom, the hydrogen atom and the lone pair electrons of the acceptor atom are in a straight line, we should expect a hydrogen-bonded epoxide molecule to be represented by



in which the H—X bond and the C—O bonds are somewhat weakened. Hence it might be expected that a nucleophilic reagent would react more readily with a hydrogen-bonded epoxide molecule than with a normal epoxide molecule. It appears, therefore, that a hydrogen-bonded transition state is consistent with the properties of the epoxide group, and also with the effect of polar compounds on the rate of the reaction between amines and epoxides. The properties of the hydrogen bond lead us to expect that such a transition state would be termolecular, and can be represented by the reaction scheme (vi).

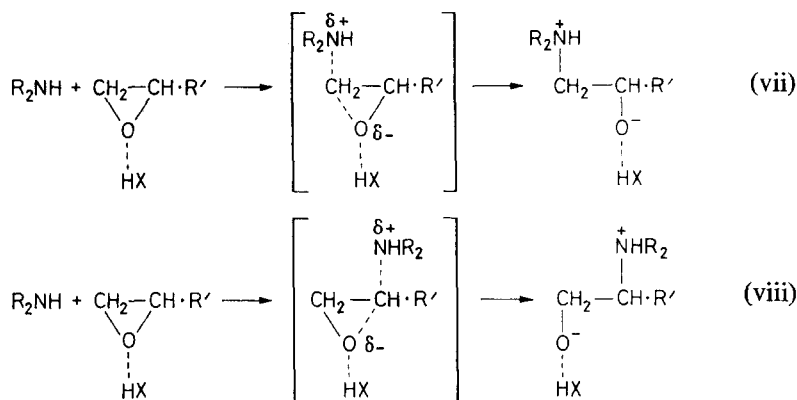


A concerted termolecular reaction mechanism, as suggested by Shechter, Wynstra and Kurkky, is also possible, but we consider this is less likely than the above rate-controlling step which involves only two-body collisions.

In the following sections it will be shown that the kinetics of amine-epoxide reactions are consistent with the above scheme, and that kinetic parameters derived for the crosslinking of epoxide resins by an alkenyl-substituted heterocyclic polyamine (*Synolide 960*, obtained from Cray Valley Products Ltd) support the validity of the hydrogen-bonded transition state.

KINETICS OF AMINE-EPOXIDE REACTIONS

It will be assumed that the rate-controlling steps for the reaction between a secondary amine and an epoxide may be represented by equations (vii) and (viii) where HX is any hydrogen-bond donor molecule:



If the reactions are autocatalytic, as indicated by Shechter and his co-workers, then both the normal reaction (vii) and the abnormal reaction (viii) will have two rate constants. These will be designated k_1 for reaction (vii) accelerated by HX, k_2 for reaction (vii) accelerated by the product, k_3 for reaction (viii) accelerated by HX, and k_4 for reaction (viii) accelerated by the product. In the majority of cases only one product has actually been isolated^{8(j,k)}, but our equations will describe the general case. If the further assumption is made that the ratio of normal to abnormal product is constant, we may define new rate constants, k and k' , given by

$$k = k_1 + k_3 \quad (\text{for hydrogen bonding by HX})$$

$$k' = k_2 + k_4 \quad (\text{for hydrogen bonding by the products})$$

It will also be assumed that the molecule HX and the product(s) function as true catalysts and are not consumed in any side reactions.

Let a be the initial concentration of amine, b the initial concentration of epoxide, c the concentration of HX, x the epoxide consumed after time t , and x' the value of x when d^2x/dt^2 is zero. The rate of consumption of epoxide is given by

$$\frac{dx}{dt} = (a-x)(b-x)(kc+k'x) \quad (1)$$

Integration of equation (1) gives

$$t = \frac{\ln[(b-x)/b]}{(kc+k'b)(b-a)} - \frac{\ln[(a-x)/a]}{(kc+k'a)(b-a)} + \frac{k' \ln[(kc+k'x)/kc]}{(kc+k'a)(kc+k'b)} \quad (2)$$

Equation (2) gives sigmoidal plots of x versus t under certain conditions, and the position of the inflection is obtained by equating d^2x/dt^2 to zero.

Hence

$$6k'x'' = -[2kc - 2k'(a+b)] \pm \{[2kc - 2k'(a+b)]^2 - 12k'[k'ab - kc(a+b)]\}^{\frac{1}{2}} \quad (3)$$

Equation (3) only gives simple solutions under special conditions (see below). When $a=b$, equation (1) becomes

$$dx/dt = (a-x)^2 (kc + k'x) \quad (4)$$

Integration of equation (4) then gives

$$t = \frac{x}{a(a-x)(kc+k'a)} + \frac{k'}{(kc+k'a)^2} \ln \frac{(kc+k'x)a}{(a-x)kc} \quad (5)$$

Now, putting $a=b$ in equation (3) and solving shows that the inflection in the curve described by equation (5) occurs at

$$x'' = (k'a - 2kc)/3k' \quad (6)$$

Equation (6) shows that an inflection can only appear when $2kc < k'a$, and it is seen that this point lies within the limits $0 \leq x \leq a/3$. Hence, if $2kc > k'a$, the sigmoidal form of the concentration curves disappears. This situation is most likely to occur when the reaction is conducted in the presence of a powerful hydrogen-bond donor (k is large), or when c is large compared with a (as long as k' is not much larger than k).

Considering equation (2), and assuming that $k'a$, $k'b$ and $k'x$ may be ignored compared with kc , it is easily shown that—under these conditions—

$$t \simeq \frac{1}{kc(b-a)} \ln \frac{a(b-x)}{b(a-x)} \quad (7)$$

which represents pseudo-second-order behaviour. The case when stoichiometric quantities of amine and epoxide are used is described by equation (5), and it can be shown that if c is increased for given values of k and k' , then the second term of the right-hand side of this equation becomes negligible compared with the first term. Thus as c is made larger, equation (5) tends to

$$t \simeq x/[a(a-x)(kc+k'a)] \quad (8)$$

If, now, $k'a$ is negligible compared with kc we find that

$$t \simeq x/[kca(a-x)] \quad (9)$$

Equations (8) and (9) are, like equation (7), in second-order form. We see, therefore, that the third-order kinetics of equations (2) and (5) will tend towards pseudo-second-order kinetics as k and/or c becomes large. Second-order kinetics would, naturally, be expected in very dilute solutions, but, as we shall see later, these equations allow the conclusion that second-order kinetics may be shown in quite concentrated solutions. The above equations indicate that the most favourable condition for the observation of second-order kinetics will be the presence of water, phenols, alcohols or other compounds capable of associating with an epoxide oxygen atom.

It has been shown¹⁵ that the rate constants shown in *Table 1*, when substituted into equations (2) and (5), reproduce the results of Shechter, Wynstra and Kurkijy¹¹ with reasonable accuracy. The term kc for the reactions carried out in the absence of added solvent may be attributed to traces of impurity (e.g. water) in the systems.

Table 1. Rate constants for the reaction of diethylamine with phenyl glycidyl ether at 50°C

<i>Solvent</i>	$10^5 k'$ ($l.^2 \text{ mole}^{-2} \text{ sec}^{-1}$)	$10^6 kc$ ($l. \text{ mole}^{-1} \text{ sec}^{-1}$)	$10^6 k$ ($l.^2 \text{ mole}^{-2} \text{ sec}^{-1}$)
—	2.6	6.0	—
Water	2.6	340	88
Isopropanol	2.6	210	66
Nitromethane	2.6	29	8.5

We shall now use the rate constants of *Table 1* for the reaction of diethylamine with phenyl glycidyl ether in the presence of water in order to investigate the effect of further dilution on the kinetics. A comparison of the results predicted by equations (5), (8) and (9) for a reaction in which water is present in a quantity equal to the combined weight of the reactants, demonstrates that equation (8) gives excellent agreement, and equation (9) gives good agreement with equation (5). For example, the values of t for 97 per cent conversion are 1.613, 1.609 and 1.647 h for equations (5), (8) and (9) respectively. We can, therefore, confidently state that the treatment presented in this paper indicates that, if this system is homogeneous in the presence of 50 per cent of water, then pseudo-second-order kinetics should be observed.

GEL POINT EXPERIMENTS

It has been deduced¹⁶ that

$$\ln G = \ln(A/X) + E/RT \quad (10)$$

where G is the gel time measured under isothermal conditions, X is the Arrhenius frequency factor, E is the overall apparent energy of activation, R is the gas constant, T is the absolute temperature, and A is a constant dependent upon the form of the kinetics and the degree of reaction at the gel point in a given case. The gel time had previously been used to obtain kinetic information in polymer problems¹⁷.

Equation (10) has now been used to study the crosslinking of *Epikote 828* (Shell Chemical Co.) by *Synolide 960* (Cray Valley Products Ltd) in the presence of various polar compounds, and in the presence of an inert diluent. The apparatus and method used in this work were exactly as described in a previous paper¹⁶. The nitrobenzene was of analytical grade, the *o*-allyl phenol was a commercial sample, and the remainder of the additives were laboratory-grade materials. The plot of $\log G$ versus $1/T$ was linear in all cases, and the parameters shown in *Table 2* (with maximum deviations) have been calculated by the method of least squares.

EXOTHERM EXPERIMENTS

The development of a pronounced exotherm during the crosslinking of an epoxide resin by amines is a process of considerable technological importance. However, no theoretical interpretation of this effect has appeared in the literature on epoxides, although the use of the rate of heating as a measure of the reactivity of a system has been described¹⁸. A general discussion of adiabatic reaction kinetics has been given by Gordon¹⁹, and his equations have been successfully applied to a study of the heating effect accompanying the vulcanization of *Buna S*²⁰. Bengough and Melville have pointed out that thermal studies are particularly useful when dealing with

Table 2. Gel-point experiments on: 60 per cent of epoxide resin, 35 per cent of curing agent; 5 per cent of additive

Additive	<i>E</i> (kcal/mole)	$-\log(A/X)$
[40% curing agent]	14.7 ± 0.2	6.1 ± 0.3
Benzyl alcohol	15.4 ± 0.7	6.5 ± 0.8
<i>m</i> -Cresol	15.3 ± 0.3	6.7 ± 0.4
Nitrobenzene	14.7 ± 0.1	6.0 ± 0.2
Liquid paraffin (sp. gr. 0.870-0.895)	13.7 ± 0.3	5.5 ± 0.4
<i>o</i> -Allyl phenol	15.6 ± 0.5	6.8 ± 0.5
Glycol	15.0 ± 0.8	6.6 ± 1.0
Acetophenone	14.0 ± 0.2	5.6 ± 0.5

very viscous or gelled products since reactants need not be removed from the system, and adiabatic measurements were used to study the non-stationary state of liquid-phase polymerizations²¹.

Gordon¹⁹ deduced that

$$\pm dT/dt = X(C/H)^{n-1}(T_f - T)^n e^{-E/RT} \quad (11)$$

where T is the absolute temperature, t , the time, X , the Arrhenius frequency factor, C , the mean specific heat of the system, H , the heat of reaction, n , the order of reaction, T_f , the final temperature reached by the system, E , the apparent energy of activation of the reaction and R is the gas constant. For the case of an exothermic reaction we may take the positive sign, and rearrangement of equation (11) gives

$$\ln[(T_f - T)^{-n} dT/dt] = \ln[X(C/H)^{n-1}] - E/RT \quad (12)$$

The position of the inflection in the heating curve (when the temperature is T'') is given¹⁹ by

$$(T_f - T'') = nRT''^2/E \quad (13)$$

There are two ways in which an epoxide resin-amine curing agent system may be allowed to polymerize under reasonably adiabatic conditions without the use of a special calorimeter. First, a very large mass of material may be employed; and secondly, the reaction may be accelerated by hydrogen-bond donors so that a minimum period of time is available for heat to be lost to the surroundings.

MECHANISM OF THE CROSSLINKING OF EPOXIDE RESINS BY AMINES

In our first experiments, a sufficiently large bulk of resin was used to justify the assumption that a further increase in the size of the sample would have made little difference to the final temperature reached. The reactants were thoroughly mixed and poured into a large can which was shielded from draughts. Timing was started from the instant of mixing and the temperature recorded by means of a thermometer contained in a small glycerol-filled seal, arranged so that the thermometer bulb was at the centre of the resin mass. In the remaining experiments a smaller quantity of reactants was used, and the reaction was accelerated by various additives. The quantities used are shown in *Table 3*, together with the peak temperatures and inflections (T''). Typical heating curves are shown in *Figure 1*.

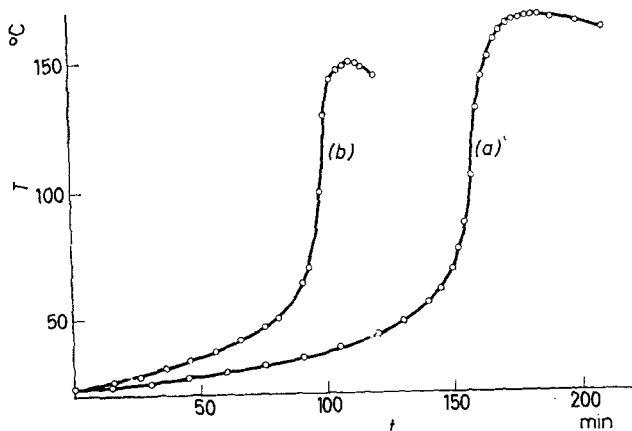


Figure 1—Heating curves for the crosslinking of an epoxide resin: (a), no additive; (b), with added benzenesulphonamide

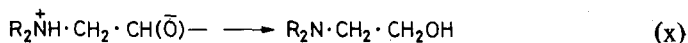
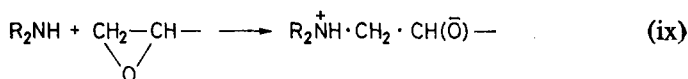
If the values of T'' are substituted into equation (13) and the resulting values of E are compared with the values obtained by the gel-point technique (*Table 2*), then it appears that a value of $n=2$ gives approximately consistent results. Now, from the kinetic treatment presented earlier in this paper, under a variety of experimental conditions second-order kinetics would be expected, particularly in the accelerated polymerization; hence the value $n=2$ is reasonable.

Table 3. Exotherm data

Accelerator	Weight of curing agent + accelerator, (α) (g)	Weight of epoxide resin, (β) (g)	Weight of accelerator as percentage of (α)	T_1 (°K)	T'' (°K)
—	1,100	2,400	—	439.5	393
—	1,800	2,700	—	432.5	393
Water	170	255	5.0	432.5	393
<i>p</i> -Toluene-sulphonic acid monohydrate	170	255	5.0	424.0	393
Benzene-sulphonamide	170	255	5.6	422.0	383
Triethanolamine	170	255	20.0	406.0	373

However, it should be borne in mind that this value refers to the step which gives rise to the heating effect¹⁹, and further discussion is required in order to clarify this point.

Since hydrogen-bond donors appear to act as true catalysts, the heat of reaction is a constant for a given amine-epoxide combination¹⁰, and is unaffected by the presence of accelerators. The change to which the heating effect is due may therefore be represented by the equations



Now the second step is a simple proton transfer, which is a relatively facile process, frequently involving a minimum of disturbance in the remainder of the molecule²². It therefore appears reasonable to ignore the energy changes due to proton transfers compared with the energy change due to the charge separation in reaction (ix).

Thus the heat of reaction is effectively due to a bimolecular process, and, under conditions such that the change of concentration of the reactants associated with this process follows a second-order law, we may anticipate that Gordon's equations may be obeyed. Values of $\log [(T_1 - T)^{-2} dT/dt]$ were therefore calculated from the heating curves for numerous values of $1/T$, and these figures were fitted to equation (12) by the method of least squares to give the parameters shown in *Table 4*. The best fit and the worst fit are illustrated in *Figure 2*.

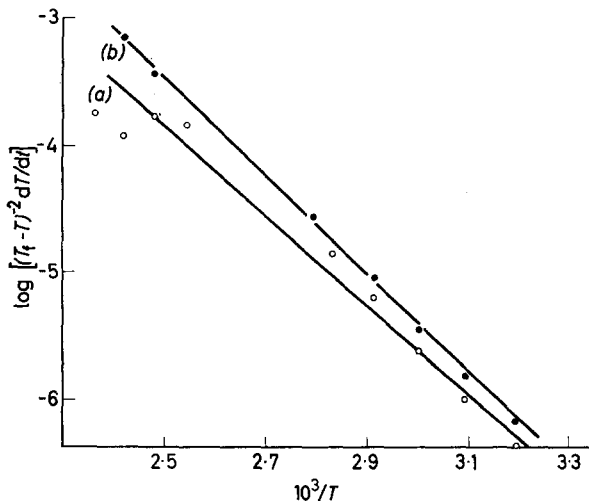


Figure 2—Application of equation (12): (a), no additive; (b), added benzenesulphonamide

DISCUSSION

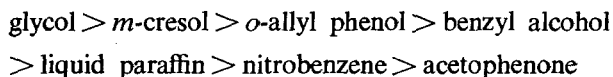
The overall view of the kinetics of the reaction between amines and epoxides provided by equations (1) to (9) indicates that previously published work is in no way inconsistent with the hypothesis that the rate-controlling step is termolecular. In the presence of a very small quantity of a hydrogen-bond donor compound, third-order autocatalytic kinetics may be observed with a sigmoidal concentration *versus* time plot, and equations (2) and (5) should be applicable. On the other hand, in dilute solution in a hydrogen-bond donor solvent, the effect of the solvent in the transition state completely obscures any effect that the reaction product might be capable of exhibiting,

Table 4. Kinetic parameters from exotherm data

Additive	<i>E</i> (kcal/mole)	log (<i>XC/H</i>)
—	15.6 ± 2.2	4.5 ± 2.7
—	16.2 ± 2.1	5.0 ± 2.6
Water	15.1 ± 1.0	4.5 ± 1.2
Benzenesulphonamide	17.3 ± 0.4	5.9 ± 0.5
<i>p</i> -Toluenesulphonic acid monohydrate	16.3 ± 0.8	5.4 ± 1.0
Triethanolamine	15.7 ± 0.6	5.3 ± 0.7

owing simply to the greater concentration of the solvent. Under these conditions second-order kinetics will, of course, be observed. At some intermediate stage (dependent upon the nature of the reactants and the solvent), both the solvent-assisted and the autocatalytic reactions contribute to the overall reaction rate. Nevertheless, second-order kinetics may still be observed as equation (8) is obeyed. In the presence of small quantities of a hydrogen-bond donor, HX, an increase in the concentration of HX will cause an increase in the overall rate of reaction. However, a maximum rate must be expected since, at some stage, a further increase in the concentration of HX will cause a decrease in rate, because the decrease in the concentration of the reactants will be more important than the effect of the solvent in the transition state.

From the gel-point experiments it was observed that the effect of additives on the rate of polymerization was:



Thus there is no simple relationship between the rate of crosslinking and the polarity of an added compound. The results agree well with the hypothesis of a hydrogen-bonded transition state, and it is noted that acetophenone and nitrobenzene retard the reactions studied, confirming earlier findings¹⁰ that hydrogen-bond acceptor molecules slow down amine-epoxide reactions. The values of $-\log(A/X)$ in Table 2 may be regarded as proportional to the entropy of activation, and decrease in the order which might be predicted from a consideration of the hydrogen-bonding potentialities of the additives. When hydrogen-bond donors are not added,

this factor decreases as the polar nature of the additive decreases in the manner expected for a reaction involving an ionic intermediate formed from neutral reactants. The intermediate value of $-\log(A/X)$ for the experiments in which no compound was added at all, suggests that some hydrogen-bond donor groups are present, and these could be due to traces of moisture in the reactants and hydroxyl groups in the epoxide resin and the reaction products.

In view of the approximations made, the exotherm results are regarded as satisfactory. It will be noted that the values of E are in good agreement with the values given in *Table 2*, and that a noticeably better fit to equation (12) is obtained for the accelerated reactions compared with those conducted in the absence of an additive. This is interpreted as indicating that the former reactions show pseudo-second-order kinetics, as might be expected from our kinetic scheme, whereas the latter reactions are probably partially autocatalytic (and third-order) in form. A further point of interest is that there does not appear to be any discontinuity near the gel point ($1/T \approx 2.85 \times 10^{-3}$ to 2.90×10^{-3}), indicating that diffusion control of the charge separation is unimportant at this stage.

The specific heat of the product of an unaccelerated reaction at 80°C (approximately half of the estimated adiabatic temperature rise—to about 170°C) was found to be $0.51 \text{ cal g}^{-1} \text{ }^\circ\text{C}^{-1}$ by the method of mixtures, in reasonable agreement with results published by Warfield²³. From this the heat of reaction can be estimated as $\sim 59 \text{ kcal/mole}$.

The values of $\log(XC/H)$ shown in *Table 4* may be taken as a measure of the entropy of activation, as long as C does not vary too much during the experiments. These figures show the same qualitative trend as the values of $-\log(A/X)$, although the value for the water-accelerated reaction appears to be anomalous and is not understood. Substitution of the above mean value for the specific heat into these terms indicates that the Arrhenius frequency factor is about 10^7 . The uncertainty of this estimate may be quite large, but the value appears to be quite consistent with the reaction mechanism.

Integration of equation (11) (with $n=2$) gives

$$\alpha t = (e^Q/Q) [1! / Q + 2! / Q^2 + 3! / Q^3 + \dots] \quad Q > 1$$

where $\alpha = -[XCRT_i^2 (-\exp E/RT_i)/EH]$ and $Q = (E/RT)(1/T - 1/T_i)$.

Unfortunately, for the experiments described here, the series in square brackets does not converge sufficiently rapidly to allow an exact analytical solution. We have, therefore, failed to reproduce the actual heating curves by means of a theoretical equation, which would have provided a final verification of the validity of the present treatment of the exotherm problem.

CONCLUSIONS

The function of a solvent in the reaction between amines and epoxides may be complex, since it may (a) weaken the C—O bonds by hydrogen bonding to the epoxide oxygen atom, (b) affect the ease of charge separation in the transition state, and (c) take part in proton exchanges (with the amine and with the product). The product may also take part in hydrogen bonding

to the epoxide, so that if the concentration of HX is small enough, auto-catalysis may be observed. The use of a non-polar solvent and pure dry reactants may result in a negligible reaction rate, because not only is the weakening of the C—O bonds not achieved, but the work required to separate the charges on passing through the transition state is now a maximum. This is consistent with the work of Cromwell and Barker^{8(e)}. A highly polar solvent may be used, such as nitrobenzene, which can function as a hydrogen-bond acceptor. In this case opening of the epoxide ring is not facilitated, and some association between the amine and the solvent may occur, reducing the nucleophilic strength of the former. However, the polar nature of such a solvent should aid the charge separation and in this respect may still assist the reaction. In systems containing impurities (and most industrial applications of epoxide resins fall under this heading), such a solvent may act as a 'proton scavenger'. Thus traces of water, or other potentially catalytic impurities, may become preferentially bonded to the solvent. If, in such a complex system, a certain amount of reaction can occur, the product may become associated with the solvent, and autocatalysis will not occur.

Grateful acknowledgement is made to the Directors of Cray Valley Products Limited for permission to report the experimental work.

*Research Department,
Cray Valley Products Ltd,
St. Mary Cray, Kent*

(Received 17th October, 1960)

REFERENCES

- ¹ NARRACOTT, E. S. *Brit. Plast.* 1953, **26**, 120
- ² O'NEILL, L. A. and COLE, C. P. *J. appl. Chem.* 1956, **6**, 356, 399
- ³ GOLUBENKOVA, L. I., KOVARSKAYA, B. M., LEVANTOVSKAYA, I. I. and AXUTIN, M. S. *Vysokomolekulyarnye Soedineniya*, 1959, **1**, 103
- ⁴ ALLEN, F. J. and HUNTER, W. M. *J. appl. Chem.* 1957, **7**, 86
- ⁵ BRUIN, P. Paper presented at the 4th Congress of the Fédération d'Associations de Techniciens des Industries de Peintures, Vernis, Emaux et Encre d'Imprimerie de l'Europe Continentale, Lucerne, 1957
- ⁶ (a) GEE, G. *Chem. & Ind.* **1959**, p. 678
(b) GEE, G., HIGGINSON, W. C. E., LEVESLEY, P. and TAYLOR, E. J. *J. chem. Soc.* **1959**, p. 1338
- ⁷ INGBERMAN, A. K. and WALTON, R. K. *J. Polym. Sci.* 1958, **28**, 468
- ⁸ (a) SMITH, L., MATTSON, S. and ANDERSSON, S. *K. fysiogr. Sällsk. Lund Förh.* 1946, **42**, 1
(b) BERBÉ, F. and FLAMME, L. R. *Bull. Soc. chim. Belg.* 1947, **56**, 349
(c) POTTER, C. and McLAUGHLIN, R. R. *Canad. J. Res.* 1947, **25B**, 405
(d) HANSSON, J. *Svensk kem. Tidskr.* 1948, **60**, 183
(e) CROMWELL, N. H. and BARKER, N. G. *J. Amer. chem. Soc.* 1950, **72**, 4110
(f) BERBÉ, F. *Chim. et Industr.* 1950, **63**, 492
(g) CROMWELL, N. H. and BARKER, N. G. *J. Amer. chem. Soc.* 1951, **73**, 1051
(h) EASTHAM, A. M., DARWENT, B. DE B. and BEAUBIEN, P. E. *Canad. J. Chem.* 1951, **29**, 575
(i) EASTHAM, A. M. and DARWENT, B. DE B. *Canad. Y. Chem.* 1951, **29**, 585
(j) ISAACS, N. S. and PARKER, R. E. *Chem. Rev.* 1959, **59**, 737
(k) CHAPMAN, N. B., ISAACS, N. S. and PARKER, R. E. *J. chem. Soc.* **1959**, p. 1925

- ⁹ LEBEDEV, N. N. and SMIRNOVA, M. M. *Izvest. vysshikh ucheb. Zaved., Khimii i Khim. Teknol.*, 1960, **3**, 104
- ¹⁰ GOUGH, L. J. and SMITH, I. T. *J. Oil Col. Chem. Ass.* 1960, **43**, 409
- ¹¹ SHECHTER, L., WYNSTRA, J. and KURKJY, R. P. *Industr. Engng Chem.* 1956, **48**, 94
- ¹² KNORR, L. *Ber. dtsh. chem. Ges.* 1899, **32**, 729
- ¹³ HORNE, W. H. and SHRINER, R. L. *J. Amer. chem. Soc.* 1932, **54**, 2925
- ¹⁴ (a) SEARLES, S. and TAMRES, M. *J. Amer. chem. Soc.* 1951, **73**, 3704
(b) SEARLES, S., TAMRES, M. and LIPPINCOTT, E. R. *J. Amer. chem. Soc.* 1953, **75**, 2775
(c) GUTOWSKY, H. S., RUTLEDGE, R. L., TAMRES, M. and SEARLES, S. *J. Amer. chem. Soc.* 1954, **76**, 4242
- ¹⁵ SMITH, I. T. *M.Sc. Thesis*, University of London, October 1960
- ¹⁶ GOUGH, L. J. and SMITH, I. T. *J. appl. Polym. Sci.* 1960, **3**, 362
- ¹⁷ (a) GORDON, M., GRIEVESON, B. M. and McMILLAN, I. D. *Trans. Faraday Soc.* 1956, **52**, 1012
(b) HIROYOSHI KAMOGAWA. *Kobunshi Kagaku* 1958, **15**, 238
- ¹⁸ EDWARDS, G. R. *Brit. Plast.* 1960, **33**, 203
- ¹⁹ GORDON, M. *Trans. Faraday Soc.* 1948, **44**, 198
- ²⁰ GORDON, M. *J. Polym. Sci.* 1948, **3**, 438
- ²¹ (a) BENGOUGH, W. I. and MELLVILLE, H. W. *Proc. roy. Soc. A* 1954, **225**, 330; 1955, **230**, 429; 1959, **249**, 445
(b) HAYDEN, P. and MELLVILLE, SIR HARRY. *J. Polym. Sci.* 1960, **43**, 201, 215
- ²² BELL, R. P. *Quart. Rev.* 1959, **13**, 169
- ²³ (a) WARFIELD, R. W., PETREE, M. C. and DONOVAN, P. *S.P.E. Journal* 1959, **15**, 1
(b) AUKWARD, J. A., WARFIELD, R. W., PETREE, M. C. and DONOVAN, P. *Rev. sci. Instrum.* 1959, **30**, 597

Note

The Morphology of Multilayer Polymer Crystals

It is now an established fact that polymers can be crystallized from solution in the form of lamellar crystals¹. The basic layers are about 100 Å thick and consist of folded molecules. The crystals thicken by an accretion of these layers forming a spiral terraced structure *via* the well known screw-dislocation growth mechanism. It has been inferred that the simplest monolayer crystals were likely to be hollow pyramids when in the liquid, but that these flatten when dried down for the usual morphological examinations². This non-planar habit has been attributed to various kinds of staggers of the folds within the monolayer³⁻⁵. It has also been inferred⁵ that the pyramids are not flat-based.

The recognition of the non-planarity of the crystals called for methods suited for observing the crystals in their uncollapsed form. Direct observations in the liquid should only be practicable by light microscopy, phase-contrast in particular (though an indirect electron-microscopic technique has been described⁶). The phase shift by a 100 Å layer in air is about 1/100 wavelength, which can be exploited by good commercial phase-contrast optics; with 100 Å layers floating in the liquid, however, this phase shift becomes much smaller and the limit of detectable contrast is reached. Normally no layers but only sheaf-type objects were seen in the liquid, and these were associated with the confused irregular thickenings, sometimes attributed to incipient spherulitic development^{6,7}, often seen in the centre of dried crystals.

Improvement in the viewing conditions was achieved by a combination of three factors. In the first place, the crystals could be made to rotate. This technique, developed by one of us (S. Mitsuhashi), consists of placing the suspension on a cavity slide and adding a few drops of another volatile miscible liquid to it. Then a cover-glass is placed on the cavity so as to leave a small air bubble in the centre. Convection currents, presumably caused by differential evaporation at the cover-glass edges, cause the crystal to rotate near the central bubble. Secondly, the visibility was improved by choosing a second liquid of refractive index as widely differing from that of the crystallizing liquid as possible. For various reasons acetone proved to be the most favourable. The retardation of 0.002–0.003 wavelength produced by the 100 Å layers could be seen as a noticeable darkening with our Zeiss phase-contrast equipment. Thirdly, special preparations consisting of unusually large layers were used which, with some thickenings in the form of a row of tiny growth spirals along the edges, greatly facilitated observations.

In addition to confirming the hollow pyramidal habit directly, our observations have led to new conclusions. A full account of this work (in collaboration with D. C. Bassett) will be given later. The present note

refers to the way the successive terraces are stacked on top of each other in multilayer crystals, as shown in *Figure 1*. It is clear that the familiar layers in *Figure 1(b)* splay when seen edgewise. Thus the consecutive terraces are not grown together, and in fact the crystal is more like a single helicoidal ribbon (tighter at the centre than at the edges) than a solid spiral pyramid. The central (and presumably initial) layer may appear in the edge-on view, either straight or bent at an angle (corresponding to pyramidal dishing):

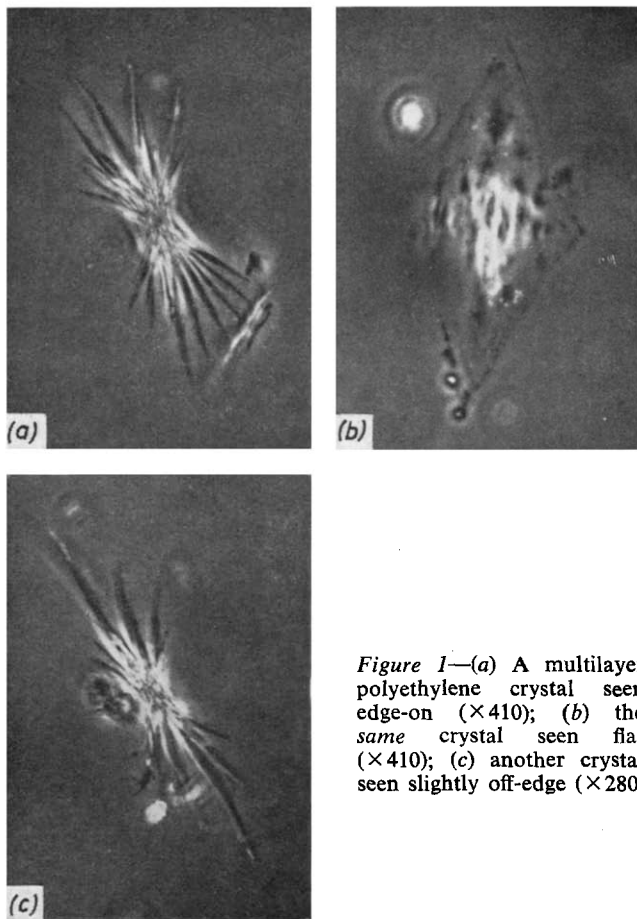


Figure 1—(a) A multilayer polyethylene crystal seen edge-on ($\times 410$); (b) the same crystal seen flat ($\times 410$); (c) another crystal seen slightly off-edge ($\times 280$)

the outer layers are always bent outwards from it. The maximum splaying is that of the long lozenge diagonals (or rather the corresponding pyramid edges). This corresponds to the steeper edges in the non-flat-based pyramidal model for the monolayers⁵. The crystals in *Figure 1(a)* and (c) are unusually regular; generally the edge-on view presents a picture of less straight, somewhat irregularly curving layers, particularly in the case of the most strongly splaying outermost layers, the whole assembly being more like the sheaves reported previously⁷. Accordingly, the sheaves

previously seen might well have been splaying layers seen edge-on. When lying down flat after drying, the outer, most strongly splaying layers often form an apparently irregular mass which accounts for the frequently observed central confusion in such crystals. Consequently, such partially confused crystals would still consist entirely of regular chain folded layers throughout, which was by no means certain from observations on dried crystals. It is tempting to associate the sheafing growth of layers with the formation of spherulites. However, the spherulites (two-dimensional in this case) formed *via* such sheaves would have a radial *a* instead of the usually found radial *b*-axis orientation. No further comments can be made on this point at present. While the splaying layers observed above appear to be widespread, we do not wish to imply that contiguous stacking of layers does not exist. These points will be covered in the comprehensive publication.

Unexpectedly, current findings with low-angle X-ray scattering seem to tie up with morphological observations. As is known, the layer thickness, and consequently the corresponding fold length, can be readily assessed by low-angle X-ray diffraction⁸. In favourable cases the layers give rise to four orders of a discrete reflection. The width of the reflections and the number of orders are variable. Usually the patterns were less well defined when crystallization occurred from more concentrated solutions; in fact, in such cases the number of orders could decrease to only one or two, and even these could largely merge with a strong diffuse background. This was the more puzzling to us as the first observation ever of four sharp orders was made on a specimen from a concentrated solution (1 per cent)⁸, an observation which has not been repeated since. However, it was noticed that filtration in that first experiment was unusually slow. Lately, we have been using different filters giving widely varying filtration speeds. We noticed that the definition of the low-angle X-ray reflections became unusually variable even for dilute solution specimens. In one instance of very fast filtering the discrete reflection was hardly recognizable. The remaining still unfiltered portions of the *same* suspension were then filtered slowly, and the usual reflections appeared. Clearly, the structure of the crystals could not be different in the two cases as the only variable was the physical process of sedimentation. This result ties up with the observed splaying of the crystal layers. Accordingly, the periodicity responsible for the discrete low-angle maxima may not be originally present in the crystal, but may arise through the laying down of the consecutive but spatially separated turns of the helicoid. Consequently, the regularity of the layer stacking, and hence that of the periodicity, very largely depends on the mode of sedimentation. This means that the uniformity of the layer, and therefore that of the folding, cannot be automatically inferred from the low-angle patterns, as has sometimes been attempted in the past⁹. This would only give a lower limit. In principle, the folds could be much more uniform than indicated by the X-ray pattern. In fact, regular folding could still be present, even when discrete reflections are absent, as this absence could arise through irregular stacking, possibly crumpling, of the layers. This is more likely to happen in more concentrated systems, which could account for the larger variability of the X-ray pattern. Hence the

more poorly defined low-angle X-ray patterns often observed in such systems do not necessarily imply that the structure is not folded, or even that it is less regularly folded. The same argument is, at least in principle, valid for melt-crystallized systems, where low-angle reflections (usually not as well defined as those in the solution-crystallized systems) are often invoked in arguments concerning the molecular texture.

S. MITSUHASHI and A. KELLER

*H. H. Wills Physics Laboratory,
University of Bristol,
Bristol 8*

(Received 2nd December, 1960)

REFERENCES

- ¹ e.g. KELLER, A. *Makromol. Chem.* 1959, **34**, 1
- ² BASSETT, D. C., FRANK, F. C. and KELLER, A. *Nature, Lond.* 1959, **184**, 810
- ³ RENEKER, D. H. and GEIL, P. H. *J. Appl. Phys.* 1960, **31**, 1916
- ⁴ NEIGISCH, W. D. and SWAN, P. R. *J. Appl. Phys.* 1960, **31**, 1906
- ⁵ BASSETT, D. C. and KELLER, A. *Phil. Mag.* In press
- ⁶ KELLER, A. *Phil. Mag.* 1957, **2**, 1171
- ⁷ KELLER, A. and BASSETT, D. C. *J. R. micr. Soc., Series III* 1960, **79**, 293
- ⁸ KELLER, A. and O'CONNOR, A. *Nature, Lond.* 1957, **180**, 1289
- ⁹ EPPE, R., FISCHER, E. W and STUART, H. A. *J. Polym. Sci.* 1959, **34**, 721

Contributions to Polymer

*Papers accepted for future issues of
Polymer include the following:*

- Electron Spin Resonance Studies of Irradiated Polymers: I. Factors Affecting the Electron Spin Resonance Spectra of Irradiated Polymers*—SHUN-ICHI OHNISHI, YUICHI IKEDA, MICHIO KASHIWAGI and ISAMU NITTA
- An Infra-red Study of the Crystallization of Poly(vinyl chloride)*—A. KAWASAKI, J. FURUKAWA, T. TSURUTA and S. SHIOTANI
- Anionic Polymerization of Styrene*—CYRIL STRETCH and GEOFFREY ALLEN
- Physical and Mechanical Properties of Polypropylene Fractions*—J. VAN SCHOOTEN, H. VAN HOORN and J. BOERMA
- Polymorphism of Crystalline Polypropylene*—(Miss) E. J. ADDINK and J. BEINTEMA
- Rheological Properties of Concentrated Polymer Solutions: I. Growth of Pressure Fluctuations during Prolonged Shear Flow*—A. S. LODGE
- Proton Magnetic Resonance in Nylon 66*—D. W. JONES
- The Synthesis of Block and Graft Copolymers of Cellulose and its Derivatives*—R. J. CERESA
- A New Method for Following Rapid Rates of Crystallization: I. Poly(hexamethylene adipamide)*—J. H. MAGILL
- The Dielectric and Dynamic Mechanical Properties of Polyoxymethylene (Delrin)*—B. E. READ and GRAHAM WILLIAMS
- Streaming Birefringence of Soft Linear Macromolecules with Finite Chain Length*—A. PETERLIN
- Tracer Studies of Di-anisoyl Peroxide and the Anisoyloxy Radical*—J. K. ALLEN and J. C. BEVINGTON
- The Effect of High-Frequency Discharge on the Surfaces of Solids: I. The Production of Surface Radicals on Polymers*—C. H. BAMFORD and J. C. WARD

Branched Polymers: I. Molecular Weight Distribution—T. A. OROFINO

Branched Polymers: II. Dimensions in Non-interacting Media—T. A. OROFINO

The Crystallization of Poly(ethylene terephthalate) by Organic Liquids
—W. R. MOORE and R. P. SHELDON

CONTRIBUTIONS should be addressed to the Editors, *Polymer*, 4-5 Bell Yard, London, W.C.2.

Authors are solely responsible for the factual accuracy of their papers. All papers will be read by one or more referees, whose names will not normally be disclosed to authors. On acceptance for publication papers are subject to editorial amendment.

If any tables or illustrations have been published elsewhere, the editors must be informed so that they can obtain the necessary permission from the original publishers.

All communications should be expressed in clear and direct English, using the minimum number of words consistent with clarity. Papers in other languages can only be accepted in very exceptional circumstances.

A leaflet of instructions to contributors is available on application to the editorial office.

Book Reviews

Properties and Structure of Polymers

ARTHUR V. TOBOLSKY

John Wiley & Sons: London and New York, 1960.

(x + 331 pp.; 9 in. by 6 in.), 116s.; \$14.50.

THE SUBJECT of the mechanical properties of high polymers is still so new and so imperfectly understood that its presentation in the form of a textbook is a formidable undertaking. The choice of subject-matter must be to some extent arbitrary and will inevitably reflect the main interests of the author. It is not surprising that the main theme of the present work is the representation of the time-dependent properties of polymers (and more particularly of amorphous polymers) in the most complete manner possible, a subject which owes so much to the strikingly original experimental approach of Professor Tobolsky and his associates, and one of great interest to those who are concerned either with the production of polymers or with their use in science and industry.

The introductory chapters are concerned with the basic elastic properties of materials and the way in which these are related to their molecular structure. This leads on to the discussion of the phenomena of rubber elasticity, the processes of crystallization in polymers, the transition to the glassy state, and the mechanism of flow. Chapter 3 presents a very clear outline of the mathematical basis of linear viscoelastic theory which forms the framework for the treatment of the mechanical properties of polymers; this chapter includes also the relation between alternative methods of representation and discusses the significance of certain specific types of distribution function and the properties with which they are associated. The following chapter deals explicitly with the actual behaviour of a variety of polymeric materials. The key to the interpretation of these properties is the time-temperature superposition principle, whereby the whole range of properties of a given polymer may be represented in terms of a single master curve definable by certain characteristic parameters. Although this method has had considerable success, its limitations are not to be overlooked; these limitations are also considered and illustrated by data for crystalline polymers, which have so far defied attempts to reduce them to a single consistent scheme.

The subject-matter of the last two chapters is not very closely related to the main theme of the book. Chapter 5 is concerned with what is sometimes called 'chemo-rheology', i.e. the relation between mechanical behaviour (stress relaxation, creep or flow) and chemical reactions involving the breakdown and re-formation of a molecular network. This problem is of particular importance in rubber-like materials, where a purely chemical estimation of the processes of chain scission and crosslinking reactions is frequently a matter of extreme difficulty. The final chapter, on polymerization equilibria, seems to the reviewer to be rather out of place.

The book is well written, and although full consideration is given to the mathematical basis of the subject, this is presented in such a way that contact with physical reality is maintained throughout. In places, the material could perhaps have been arranged with more consideration for continuity of development. Thus, for example, the sections on the conformations of a polymer

chain, on the elasticity of ideal rubber networks, and on the kinetic theory of rubber elasticity might have been brought together, while the section on the Maxwell model would surely be more appropriately included in the chapter on linear viscoelasticity.

The production is of excellent quality, though the space allotted to headings and simple diagrams is excessive; also, the allocation of 39 pages to Appendices is of questionable advantage. It is unfortunate that w is used throughout for circular frequency in place of the almost universal ω .

The only point of substance which the reviewer would contest is concerned with the concept of chain stiffness. By postulating an ideal chain of random links which has the same mean-square length and the same fully-extended length as a given polymer chain it is possible to define an 'equivalent random link'. This has a length equal to a definite number (x) of monomer units in the fully-extended state. The optical anisotropy of the random link must then be equal to x times the optical anisotropy of the monomer unit, *measured in the fully-extended configuration*. On this basis it is not permissible to assume free rotation about bonds in the calculation of the optical anisotropy of the monomer unit (p. 218).

An alternative definition of chain stiffness is given (p. 42) in terms of the ratio of the root-mean-square length of the polymer chain to that for a random chain having the same number of links of the same length. This definition is clear for a simple chain of the paraffin type, but cannot be directly applied to a chain containing double bonds, rings, or other more complex structures.

These, however, are minor criticisms, and the book as a whole can be confidently recommended.

L. R. G. TRELOAR

Isotope Effects on Reaction Rates

LARS MELANDER

The Ronald Press Company: New York, 1960.

(vi + 181 pp.; 8 in. by 5½ in.), \$6.00.

THE EFFECT of isotopic replacement on a reaction rate is a valuable diagnostic tool for the study of reaction mechanisms. Although a review of 'Isotope Effects in Chemical Kinetics' has been given by Bigeleisen and Wolfsberg (*Advances in Chemical Physics* Vol. 1, 1958), it deals more with theoretical principles and does not consider in detail the application of the effect. The appearance of Melander's book corrects this omission.

Melander, like Bigeleisen, has produced one of the most comprehensive and successful theoretical treatments of kinetic isotope effects based on transition-state theory. He has also made extensive experimental contributions to the subject, and was the first to show conclusively by hydrogen isotope effects that the elimination of a proton is not the rate-controlling step in the nitration of benzene. The present book has, therefore, the hall-mark of authority and, as expected, provides a very clear statement of Melander's theoretical treatment.

At the outset the author makes it clear that 'much has to be assumed to be familiar to the reader', and this evidently includes the idea of what an isotope effect is because no explicit definition is given, nor is an historical introduction provided. If we accept this, however, and pass on to the second chapter on 'Prediction of rate-constant ratios from molecular data', our confidence in the book grows. Rigid expressions for treatment of the effect are derived, and very clearly and systematically the need for approximations is indicated in those cases where parameters cannot be evaluated. The approximations, depending

chain, on the elasticity of ideal rubber networks, and on the kinetic theory of rubber elasticity might have been brought together, while the section on the Maxwell model would surely be more appropriately included in the chapter on linear viscoelasticity.

The production is of excellent quality, though the space allotted to headings and simple diagrams is excessive; also, the allocation of 39 pages to Appendices is of questionable advantage. It is unfortunate that w is used throughout for circular frequency in place of the almost universal ω .

The only point of substance which the reviewer would contest is concerned with the concept of chain stiffness. By postulating an ideal chain of random links which has the same mean-square length and the same fully-extended length as a given polymer chain it is possible to define an 'equivalent random link'. This has a length equal to a definite number (x) of monomer units in the fully-extended state. The optical anisotropy of the random link must then be equal to x times the optical anisotropy of the monomer unit, *measured in the fully-extended configuration*. On this basis it is not permissible to assume free rotation about bonds in the calculation of the optical anisotropy of the monomer unit (p. 218).

An alternative definition of chain stiffness is given (p. 42) in terms of the ratio of the root-mean-square length of the polymer chain to that for a random chain having the same number of links of the same length. This definition is clear for a simple chain of the paraffin type, but cannot be directly applied to a chain containing double bonds, rings, or other more complex structures.

These, however, are minor criticisms, and the book as a whole can be confidently recommended.

L. R. G. TRELOAR

Isotope Effects on Reaction Rates

LARS MELANDER

The Ronald Press Company: New York, 1960.

(vi + 181 pp.; 8 in. by 5½ in.), \$6.00.

THE EFFECT of isotopic replacement on a reaction rate is a valuable diagnostic tool for the study of reaction mechanisms. Although a review of 'Isotope Effects in Chemical Kinetics' has been given by Bigeleisen and Wolfsberg (*Advances in Chemical Physics* Vol. 1, 1958), it deals more with theoretical principles and does not consider in detail the application of the effect. The appearance of Melander's book corrects this omission.

Melander, like Bigeleisen, has produced one of the most comprehensive and successful theoretical treatments of kinetic isotope effects based on transition-state theory. He has also made extensive experimental contributions to the subject, and was the first to show conclusively by hydrogen isotope effects that the elimination of a proton is not the rate-controlling step in the nitration of benzene. The present book has, therefore, the hall-mark of authority and, as expected, provides a very clear statement of Melander's theoretical treatment.

At the outset the author makes it clear that 'much has to be assumed to be familiar to the reader', and this evidently includes the idea of what an isotope effect is because no explicit definition is given, nor is an historical introduction provided. If we accept this, however, and pass on to the second chapter on 'Prediction of rate-constant ratios from molecular data', our confidence in the book grows. Rigid expressions for treatment of the effect are derived, and very clearly and systematically the need for approximations is indicated in those cases where parameters cannot be evaluated. The approximations, depending

on the type of isotope and transition state being considered, lead to quite a number of theoretical expressions which have been usefully summarized and interrelated by means of a full-page chart.

The third chapter sets out the 'Evaluation of rate-constant ratios from experimental data' much along the lines followed by Bigeleisen and Wolfsberg, but with a more practical bias. Here ends the similarity between the review mentioned above and the book under discussion.

The ensuing chapters are on the following topics: 'Primary hydrogen isotope effect and single reaction steps', 'Secondary hydrogen isotope effects', 'Hydrogen isotope effects and reaction mechanisms', 'Carbon isotope effects in single reaction steps', 'Carbon isotope effects and reaction mechanisms', 'Isotope effects with elements heavier than carbon'. They provide examples of the use of the theoretical expressions derived in the earlier chapters to calculate isotope effects, which are compared with the experimental results. The use of these results in deriving a reaction mechanism is discussed, and this provides a very valuable feature of the book. As a pedagogical exercise these chapters are very good and could be read with profit by the undergraduate in his final year.

A few criticisms ought to be made. It is not clear why Chapter 8, which occupies little more than two pages, could not have been merged with the discussion of mechanisms in Chapter 7. On p. 87 we read that 'systems of pure σ -bonds relay . . . effects from one part of a molecule to another. This . . . is interpreted in terms of inductive and hyperconjugative effects'. Surely hyperconjugation involves π -bonds also, as it is a form of conjugation in which σ -bonds can function as π -bonds and become delocalized into the π -orbitals of a double bond. Perhaps this is what the author means as the correct definition is implied on p. 93. The style in places is strange and unidiomatic owing, no doubt, to the fact that the author is not writing in his native tongue and this makes certain paragraphs difficult to follow. There are also some strange errors. On p. 88 the word 'not' should be deleted from the sentence '. . . the isotopic atom is not involved . . .' and, on p. 100, 2-propanol-2-d is not reduced but oxidized.

These are minor blemishes, however, which are more than compensated for by the critical attitude of the author and his constructive suggestions. The value of isotope effects in unravelling the intimate mechanisms of reactions is clearly indicated when Melander suggests that the secondary hydrogen isotope effect could diagnose the transition from S_N1 to S_N2 substitutions. The elucidation of reaction mechanisms is only one service given by the isotope effect to chemical kinetics. It has proved valuable in the study of fundamental theories of kinetics, and perhaps some mention of this aspect could be included in a future edition of the book.

The book is well produced but the price is high.

E. P. GOODINGS

The Chemistry of Nucleic Acids

D. O. JORDAN

Butterworths: London, 1960. (x + 358 pp.; 8½ in. by 5½ in.), 60s.

THE STUDY of nucleic acids is a subject which can, in the strictest sense of the word, be called vital. It has progressed rapidly, in a little over twenty years, from an empirical, descriptive science, to a position where some insight into the complexities of heredity and the relationships between the chemistry of nucleic acids and the central problems of genetics can be gained.

on the type of isotope and transition state being considered, lead to quite a number of theoretical expressions which have been usefully summarized and interrelated by means of a full-page chart.

The third chapter sets out the 'Evaluation of rate-constant ratios from experimental data' much along the lines followed by Bigeleisen and Wolfsberg, but with a more practical bias. Here ends the similarity between the review mentioned above and the book under discussion.

The ensuing chapters are on the following topics: 'Primary hydrogen isotope effect and single reaction steps', 'Secondary hydrogen isotope effects', 'Hydrogen isotope effects and reaction mechanisms', 'Carbon isotope effects in single reaction steps', 'Carbon isotope effects and reaction mechanisms', 'Isotope effects with elements heavier than carbon'. They provide examples of the use of the theoretical expressions derived in the earlier chapters to calculate isotope effects, which are compared with the experimental results. The use of these results in deriving a reaction mechanism is discussed, and this provides a very valuable feature of the book. As a pedagogical exercise these chapters are very good and could be read with profit by the undergraduate in his final year.

A few criticisms ought to be made. It is not clear why Chapter 8, which occupies little more than two pages, could not have been merged with the discussion of mechanisms in Chapter 7. On p. 87 we read that 'systems of pure σ -bonds relay . . . effects from one part of a molecule to another. This . . . is interpreted in terms of inductive and hyperconjugative effects'. Surely hyperconjugation involves π -bonds also, as it is a form of conjugation in which σ -bonds can function as π -bonds and become delocalized into the π -orbitals of a double bond. Perhaps this is what the author means as the correct definition is implied on p. 93. The style in places is strange and unidiomatic owing, no doubt, to the fact that the author is not writing in his native tongue and this makes certain paragraphs difficult to follow. There are also some strange errors. On p. 88 the word 'not' should be deleted from the sentence '. . . the isotopic atom is not involved . . .' and, on p. 100, 2-propanol-2-d is not reduced but oxidized.

These are minor blemishes, however, which are more than compensated for by the critical attitude of the author and his constructive suggestions. The value of isotope effects in unravelling the intimate mechanisms of reactions is clearly indicated when Melander suggests that the secondary hydrogen isotope effect could diagnose the transition from S_N1 to S_N2 substitutions. The elucidation of reaction mechanisms is only one service given by the isotope effect to chemical kinetics. It has proved valuable in the study of fundamental theories of kinetics, and perhaps some mention of this aspect could be included in a future edition of the book.

The book is well produced but the price is high.

E. P. GOODINGS

The Chemistry of Nucleic Acids

D. O. JORDAN

Butterworths: London, 1960. (x + 358 pp.; 8½ in. by 5½ in.), 60s.

THE STUDY of nucleic acids is a subject which can, in the strictest sense of the word, be called vital. It has progressed rapidly, in a little over twenty years, from an empirical, descriptive science, to a position where some insight into the complexities of heredity and the relationships between the chemistry of nucleic acids and the central problems of genetics can be gained.

In recent years there has been a reduced emphasis on the organic chemistry of nucleic acids, whilst more work has appeared, from many sources, on the physicochemical and biophysical behaviour of nucleotides. It is on these aspects that Professor Jordan has concentrated in this excellent survey, which has many points of interest to polymer scientists. In the initial chapters, the difficult problems of preparing consistent samples of the various nucleoproteins are discussed, with critical accounts of several of the published procedures. The resulting products are heterodisperse, and may be examined by the established methods used for many other polymers of this nature. The information given by sedimentation and fractionation of deoxypentose nucleic acid and pentose nucleic acid obtained from several sources is conveniently summarized. Following this, a chapter on the composition of nucleic acids discusses the isolation of the component purines, pyrimidines, nucleosides and nucleotides by carefully controlled hydrolysis.

The nature of the products thus isolated by paper chromatography is then described, followed by an account of the synthesis of the nucleosides, and of their phosphoric esters, the nucleotides.

A brief survey of acid-base properties is followed by six chapters on various aspects of the structure of nucleic acids. The nature of the bond between nucleotides in pentose and deoxypentose nucleic acids is first considered. The X-ray diffraction and electrometric titration data are discussed in terms of the Watson-Crick structure for deoxyribose nucleic acid; some possible modifications are suggested. After this, in the longest chapter of the book, containing work with which the author has been closely connected, the extensive data on the size, shape, molecular weight and configuration of the deoxypentose nucleate ion are collected together, and discussed in relation to the acid-base and electron-charge properties of the ion, and the interaction of deoxypentose nucleic acid with metal ions and with organic cations.

The complex subject of denaturation is described at length, followed by a discussion of the molecular configuration of pentose nucleic acids, and the size and shape of the corresponding ion in solution. Next, the nucleotide sequence in deoxypentose and pentose nucleic acids, and the nature of the terminal phosphate groups are described.

The two final chapters comprise an account of the preparation and properties of the synthetic polynucleotides, and a brief, but stimulating, note on the helical structure and replication of nucleic acids.

The book is well illustrated, and adequately up-to-date in documentation. It represents a most useful and assimilable survey of an important topic.

C. A. FINCH

Erratum

Intermolecular Forces and Chain Flexibilities in Polymers: I. Internal Pressures and Cohesive Energy Densities of Simple Liquids—GEOFFREY ALLEN, GEOFFREY GEE and GEOFFREY J. WILSON, *Polymer*, 1960 1(4), 456.

Page 458, Table 1. The entry 2,2,3-Trimethylpentane should read: 2,2,3-Trimethylbutane.

In recent years there has been a reduced emphasis on the organic chemistry of nucleic acids, whilst more work has appeared, from many sources, on the physicochemical and biophysical behaviour of nucleotides. It is on these aspects that Professor Jordan has concentrated in this excellent survey, which has many points of interest to polymer scientists. In the initial chapters, the difficult problems of preparing consistent samples of the various nucleoproteins are discussed, with critical accounts of several of the published procedures. The resulting products are heterodisperse, and may be examined by the established methods used for many other polymers of this nature. The information given by sedimentation and fractionation of deoxypentose nucleic acid and pentose nucleic acid obtained from several sources is conveniently summarized. Following this, a chapter on the composition of nucleic acids discusses the isolation of the component purines, pyrimidines, nucleosides and nucleotides by carefully controlled hydrolysis.

The nature of the products thus isolated by paper chromatography is then described, followed by an account of the synthesis of the nucleosides, and of their phosphoric esters, the nucleotides.

A brief survey of acid-base properties is followed by six chapters on various aspects of the structure of nucleic acids. The nature of the bond between nucleotides in pentose and deoxypentose nucleic acids is first considered. The X-ray diffraction and electrometric titration data are discussed in terms of the Watson-Crick structure for deoxyribose nucleic acid; some possible modifications are suggested. After this, in the longest chapter of the book, containing work with which the author has been closely connected, the extensive data on the size, shape, molecular weight and configuration of the deoxypentose nucleate ion are collected together, and discussed in relation to the acid-base and electron-charge properties of the ion, and the interaction of deoxypentose nucleic acid with metal ions and with organic cations.

The complex subject of denaturation is described at length, followed by a discussion of the molecular configuration of pentose nucleic acids, and the size and shape of the corresponding ion in solution. Next, the nucleotide sequence in deoxypentose and pentose nucleic acids, and the nature of the terminal phosphate groups are described.

The two final chapters comprise an account of the preparation and properties of the synthetic polynucleotides, and a brief, but stimulating, note on the helical structure and replication of nucleic acids.

The book is well illustrated, and adequately up-to-date in documentation. It represents a most useful and assimilable survey of an important topic.

C. A. FINCH

Erratum

Intermolecular Forces and Chain Flexibilities in Polymers: I. Internal Pressures and Cohesive Energy Densities of Simple Liquids—GEOFFREY ALLEN, GEOFFREY GEE and GEOFFREY J. WILSON, *Polymer*, 1960 1(4), 456.

Page 458, Table 1. The entry 2,2,3-Trimethylpentane should read: 2,2,3-Trimethylbutane.

*Electron Spin Resonance Studies of Irradiated Polymers I. Factors Affecting the Electron Spin Resonance Spectra of Irradiated Polymers**

SHUN-ICHI OHNISHI, YUICHI IKEDA†, MICHIO KASHIWAGI‡ and ISAMU NITTA

Electron spin resonance spectra of the trapped intermediates at room temperatures in irradiated polymers have been measured for fourteen kinds of polymers in order to obtain information on the mechanism of radiation chemical processes. The present report concerns the identification of radical species from the spectral shape. Radicals trapped in irradiated polyethylene, polypropylene and poly(vinyl alcohol) have been identified tentatively. The following factors were found to affect and complicate the observed spectral shape: (1) coexistence of several kinds of radicals; (2) effect of state of aggregation of polymer on the spectra; (3) effect of irradiation dose and dose rate on the spectra.

INTRODUCTION

THE INITIAL changes produced in solid high polymers by the action of ionizing radiations are the formation of ions (including electrons), free radicals, excited molecules, and so on. The primary products are then involved in complicated secondary reactions which result in radiation-chemical effects such as crosslinking, main-chain degradation, gas evolution, unsaturation in chemical bonding, etc. There are some established methods for the study of the secondary products, and these have yielded much information on the radiation chemistry of high polymers. On the other hand, in order to clarify the reaction mechanism, it is also important to study the primary products themselves. Among the several techniques for such study, electron spin resonance (E.S.R.) experiments seem to be one of the most direct and informative methods, because the hyperfine structure of E.S.R. spectra can provide detailed information about the nature of the radicals, while the E.S.R. absorption intensity gives a measure of their concentration.

We have measured the spectra of the trapped intermediates in irradiated polymers at room temperatures. The results of our E.S.R. studies and discussions will be reported in a series of papers. Part I concerns the attempt to identify the radicals from the spectral shape and a discussion is given of some factors affecting the spectra which make the identification difficult. Part II will deal with a kinetic study of radical formation and decay. The *G*-values for radical formation and the lifetime of trapped radicals have been estimated. One of the advantages of the E.S.R. method is that it makes

*This work was presented for the most part at the Conference on the Uses of Large Radiation Sources in Industry, Warsaw, September 1959¹.

†On leave from Fuji Spinning Co., Ltd.

‡On leave from Toyo Rayon Co., Ltd.

it possible to follow chemical changes which occur in half a minute or longer. Reactions of the trapped radicals with some reagents, such as oxygen, will be reported in Part III.

EXPERIMENTAL PROCEDURE

In most of our experiments polymers were irradiated *in vacuo* ($\sim 10^{-5}$ mm Hg) at room temperature with γ -rays from a ^{60}Co source of 1,000 curies. The highest dose rate available was 7×10^5 rad/h and, unless any special description be given, it is to be taken that all the samples were irradiated at this dose rate. Irradiation *in vacuo* with electrons accelerated by a 2 MeV Van de Graaff accelerator was also carried out in few cases. During the electron irradiations, samples were dipped in dry-ice-methanol mixture to prevent heating.

After irradiation, the end of the glass tube, into which the polymers had been tipped for determination of their spectra, was heated in a bunsen flame (while the samples were located at the other end), to remove colour centres produced in the glass by irradiation. A device with a *Nichrome* heater was also used to remove the colour centres.

Resonances were investigated at room temperatures with a microwave bridge-type apparatus (*Varian Model V-4500 Spectrometer*). The operating frequency was determined to be 9,480 Mc/s. The magnet was an electromagnet made by Japan Electron Optics Laboratory Co., Ltd (JNM-3 type). Hyperfine separations were determined from the splitting values of the eight lines of vanadyl acetyl acetonate in benzene as a standard or by referring to the values of the six lines of a dilute solid solution of manganous chloride in cadmium chloride. The hyperfine splitting values of these two compounds are already well known, being ~ 110 gauss for the former² and ~ 86 gauss for the latter³. The values obtained from both determinations were, of course, found to be equal.

The spectrometer can feed microwave power up to about 100 mW to the samples in the cavity. Spectra of most free radicals trapped in polymers have been found to show saturation broadening at such high power levels^{4, 5}. Since radicals trapped in different polymers and also radicals of different kinds trapped in the same polymer have generally different spin-lattice relaxation times (T_1), the microwave power levels from which the saturation broadening starts are different among the radicals. We have measured the spectra of the radicals at their optimum power levels, which ranged from about 1 to 5 mW.

Materials

Samples were obtained from commercial sources.

(1) *Polyethylene*—(A) *Marlex-50* film, and (B) a low density polyethylene film, thickness about 30 μ . (a) *Virgin samples*: these were films produced by the inflation process. In this technique the film is stretched to some extent at a high temperature and then rapidly cooled, and thus has some internal strains. When the inflated film is put into boiling water, it expands by about 5 per cent in the direction of extrusion. In some experiments the films were further stretched and heat-set. (b) *Annealed sample*: in some experiments pellets were used which were melted *in vacuo* and cooled gradually (annealed block).

(2) *Polypropylene*—*Moplen A2* powder produced by Montecatini Co. (a) *Virgin sample*. (b) *Catalyst-free sample*: the trace of catalyst remaining in the powder was removed completely in our laboratory by bubbling hydrogen chloride gas through the *Moplen A2* powder suspension in methanol. (c) *Residue of toluene extraction from the catalyst-free sample (b)*: this was melted *in vacuo* and cooled slowly in the form of a rod. (d) *Yarn*: *Moplen*

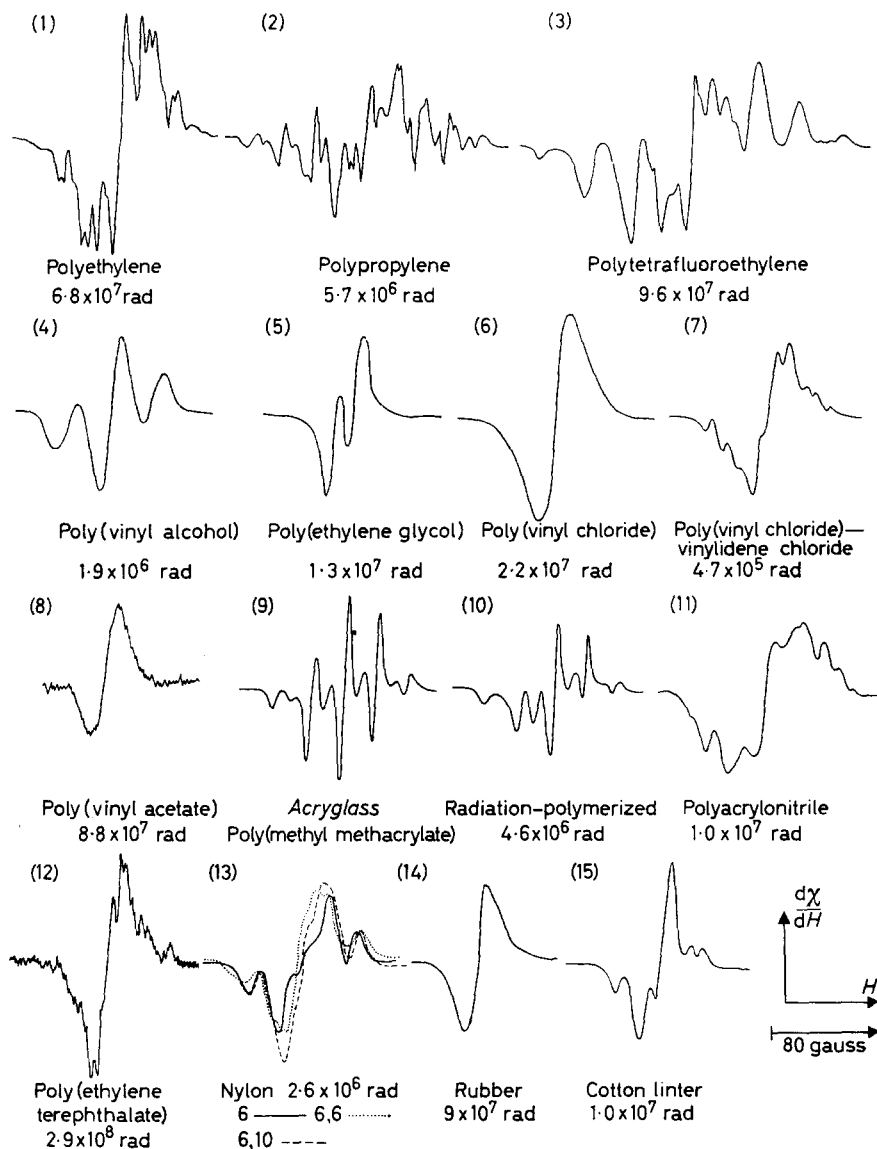


Figure 1—E.S.R. spectra of γ -irradiated polymers in derivative form. In this and the following figures the ordinate scale for each curve is arbitrary unless a special description is given

A2 powder was melted and extruded in the form of a monofilament of about 1 mm diameter. In some experiments this was cold-drawn and heat-set in order to see the effect on the spectrum of mechanical and heat treatment.

(3) *Polytetrafluoroethylene—Teflon No. 1* powder produced by E. I. du Pont de Nemours & Co., Inc.

(4) *Poly(vinyl alcohol)*—Powder sample produced by Dainippon Spinning Co., Ltd, with an average degree of polymerization of 1,450 and a residual acetyl group content of 0.02 mole per cent. In some experiments the films used were prepared from aqueous solution. (a) *Virgin sample*. (b) *Heat-treated sample*: the sample (a) was heated at 180°C in silicone oil for 30 min to give a material whose degree of crystallinity (x) was 65 per cent. These samples were normally evacuated at 60°C for 2 days or more to remove water.

(5) *Poly(ethylene glycol)*—(A) *Carbowax 6000* of average molecular weight 6,000–7,500, and (B) *Polyox WSR-301*, with a viscosity in aqueous (1 per cent) solution of 2,000–4,000 centipoise. These are both products of Union Carbide Chemicals Co.

(6) *Poly(vinyl chloride)*—*A-3250*, a commercial powder product containing no plasticizers, obtained from Nippon Carbide Industry Co., Inc.

(7) *Poly(vinyl chloride-vinylidene chloride)*—A film named *Krehalon* produced by Kurehakei Co., Ltd.

(8) *Poly(vinyl acetate)*—A product of the Nippon Synthetic Chemical Industry Co., Ltd.

(9) *Poly(methyl methacrylate) (P.M.M.A.)*—(A) *Acryglass*: a commercial P.M.M.A. plate, produced by Nitto Chemical Co., Ltd, of average molecular weight $7-9 \times 10^5$. (B) *Acrycon*: a commercial powder product of Mitsubishi Rayon Co., Ltd, prepared by suspension polymerization, of average molecular weight $6-8 \times 10^5$. (C) A radiation-polymerized sample prepared in our laboratory according to the following procedure. The degassed monomer was irradiated at a dose rate of 4,700 rad/h for 5 h. After irradiation, the polymer was precipitated with methanol and, after repeated washing with methanol, it was dissolved in chloroform and then precipitated again with methanol. Solvent was removed by evacuation for two days. Before E.S.R. measurements were made, the sample was heated at about 70°C under a vacuum (10^{-4} mm Hg) for 2 days to remove the solvent completely. In *Figure 1*, (9)(C) is given by (10).

(11) *Polyacrylonitrile*—A radiation-polymerized sample prepared in our laboratory.

(12) *Poly(ethylene terephthalate)*—Commercial samples named *Tetoron*, produced by both Toyo Rayon Co., Ltd and Teikoku Rayon Co., Ltd, were used. In order to examine the effect of the state of aggregation of polymer on the spectrum, we used seven kinds of *Tetoron* samples. (a) *Pellets*: produced by Teikoku Rayon Co., Ltd with $d_{21^\circ\text{C}}$ (density at 21°C) = 1.3410, $x = 5$ per cent. (b) *Pellets (a) after heat-treatment*: the properties of this sample were $d_{21^\circ\text{C}} = 1.3795$, $x = 39$ per cent. (c) *Films*: produced by Toyo Rayon Co., Ltd, $d_{21^\circ\text{C}} = 1.341_5$, $x = 6$ per cent. (d) *Stretched film*: the

sample (c) was drawn at some temperature higher than room temperature, giving material of $d_{21^\circ\text{C}} = 1.3630$, $x = 25$ per cent. (e) *Heat-treated film*: this had the properties $d_{21^\circ\text{C}} = 1.384$, $x = 43$ per cent. (f) *Cold-drawn film*: the density of this film was $d_{21^\circ\text{C}} = 1.0120$ to 1.0465 . (g) *Stretched and rolled film*: film (d) was rolled at about 100°C to give a sample of $d_{21^\circ\text{C}} = 1.390_5$, $x = 48$ per cent.

(13) *Nylon*—(A) *Nylon 6*, (B) *Nylon 66* and (C) *Nylon 610* samples given by Toyo Rayon Co., Ltd. (a) *Virgin sample*. (b) *Stretched Nylon 6 yarn*: the sample was 500 per cent cold-drawn. (c) *Heat-treated Nylon 6 yarn*: the degree of crystallinity of this material was $x = 36$ per cent.

RESULTS AND DISCUSSION

The spectra of the derivative form of the irradiated polymers are shown in *Figure 1*. Since, in most cases, the dose or dose rate of irradiation affects the spectra as will be discussed later, radiation doses are also given in *Figure 1*.

In the case of polyethylene, *Marlex-50* [sample (1)(A)(a)] and a low density polyethylene [(1)(B)(a)] gave similar spectra. The spectrum of irradiated polypropylene, *Moplen A2* [(2)(a)], showed a broad background when measured at a high microwave power level (100 mW); the derivative curve did not come back to the zero line on the higher field side. That this was due to the presence of catalyst was confirmed by the fact that the catalyst-free sample [(2)(b)] actually gave the spectrum with no background. It is remarkable that the spectrum of *Acryglass* [(9)(A)] is clearly different from that of the radiation-polymerized P.M.M.A. The difference will be described in more detail later and might be considered to be due to impurities such as residual monomer or solvent. Spectra of poly(vinyl acetate) could not be obtained easily at room temperatures, a finding which may be associated with the fact that the glass transition temperature (T_g) of this polymer lies near room temperature. Generally it might be supposed that radicals trapped in the amorphous part of the polymer have more chance of encountering and reacting with other radicals or molecules above T_g , since the brownian motion becomes violent. Radicals which are chemically less reactive can have longer lifetimes even above T_g . Irradiated rubber, whose T_g lies near -70°C , at room temperature gave the spectrum shown in *Figure 1*(14). The singlet spectrum of rubber has been tentatively assigned to the radicals of polyenyl type⁸, which might be chemically less reactive species stabilized by bond resonances. The reason why the radical could be observed at room temperature in the irradiated rubber might be said not to be physical, i.e. radical trapping by reduced motion, but chemical in nature. The spectra of *Nylon 6*, *66* and *610* seem to differ to some extent from each other.

From inspection of our experimental results, we have found several factors which affect and complicate the observed spectral shape and which make the identification of the radicals difficult. Despite this, these spectra may still be said to be 'fingerprints' of the polymers and, in fact, could be used for their identification. Three of the complicating factors are discussed below.

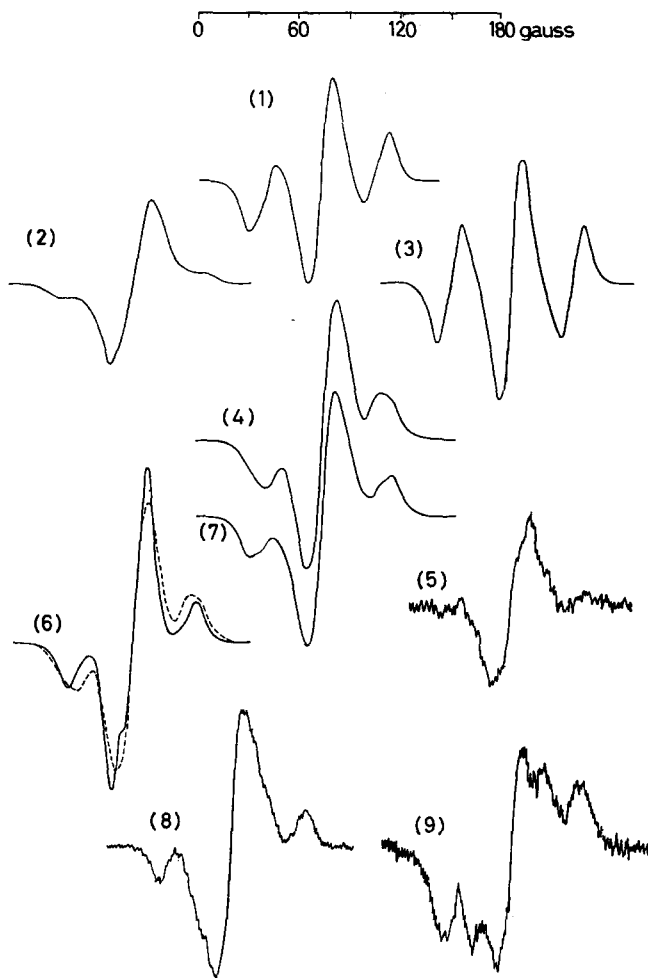


Figure 2—E.S.R. spectra of poly(vinyl alcohol) γ -irradiated with 10 Mrad: (1) untreated powder sample ($x=49.9$ per cent); (2) the derivative after 2 months *in vacuo*; (3) the derivative after 2.5 h in the presence of water vapour; (4) film cast from aqueous solution ($x=41.3$ per cent); (5) the derivative after heating the irradiated film at 88°C for 8 min; (6) the film stretched uni-axially (before irradiation) to six times its original length in the presence of steam ($x=49.9$ per cent); the dotted curve shows the derivative for the unstretched film, i.e. the same as (4); (7) heat-treated film ($x=69.7$ per cent); (8) the derivative after heating the heat-treated film at 88°C for 8 min after irradiation; (9) the derivative after heating the other heat-treated film ($x=65$ per cent) at about 88°C for 5.5 h after irradiation with 43 Mrad. All the spectra were measured at a microwave power of ~ 1 mW except spectrum (9), which was measured at ~ 100 mW and is consequently somewhat broadened by the saturation effects

(1) *Coexistence of several kinds of radicals*

When several kinds of radicals are formed by irradiation, the observed spectrum is, naturally, a superposition of that of each component. This may complicate the spectrum: the splitting and the intensity ratio of the hyperfine structure will be apparently different from those required by simple theory.

Poly(vinyl alcohol) (P.V.A.)—When the spectrum of γ -irradiated P.V.A. [(4)(a)] was observed soon after irradiation, it was a triplet and the intensity

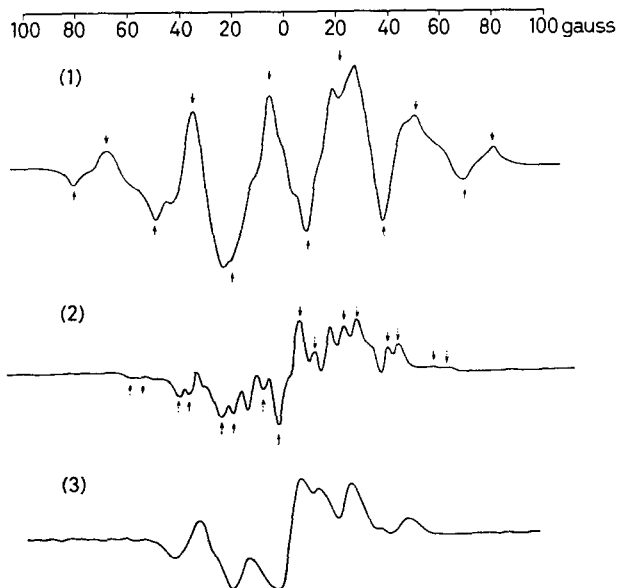


Figure 3—E.S.R. spectrum of electron-irradiated polyethylene (*Marlex-50* inflation film [(1)(A)(b)] annealed at 125°C for 20 h) and its change after irradiation at room temperatures: (1) the derivative obtained at 25 min after irradiation; (2) after 1290 min. Irradiation condition: *in vacuo*, 1.5 MeV, 100 μ A, 50 sec \times 2, 47 Mrad. (3) E.S.R. spectrum of electron-irradiated polyethylene (*Marlex-50* inflation film [(1)(A)(b)] heated to the pre-melting state and annealed at 125°C) at 17,615 min after irradiation. Irradiation condition: *in vacuo*, 1.5 MeV, 100 μ A, 20 sec \times 3, 28 Mrad. During irradiation the samples were dipped in dry-ice-methanol mixture to prevent heating. The spectra were measured under the following conditions: input microwave power level \sim 1mW, the modulation field 1.2 G peak to peak, the field scanning rate 248 G/10 min, time-constant of the integrating filter 0.8 sec. The ordinate scale is the same for the three spectra

ratio was about 1:3:1. The ratio, however, gradually changed, and after 2 months peaks on both sides disappeared almost entirely, as seen from Figures 2(1) and 2(2)^{6,7}. A similar change was observed when the irradiated sample was heated after irradiation. As an example, the change in the

spectrum of an irradiated film produced by heating at 88°C is shown in Figures 2(4) and 2(5). Such behaviour indicates the existence of more than one kind of radical in the irradiated P.V.A. The central part of the spectrum has a longer lifetime than that of the others, which are mainly composed of side peaks. The long-lived singlet component might be assigned tentatively to a radical with conjugated double bonds⁶. On the other hand, when water vapour was introduced to the irradiated P.V.A. powder [(4)(a)], the change in the spectrum was somewhat different⁷. The total absorption intensity decreased faster than in the above case; the half-life of the total intensities was about 10 days *in vacuo* and about 1.5 h in the presence of water vapour. The intensity ratio of the triplet changed from the initial value (about 1:3:1) to 1:2:1 asymptotically as time passed. At the same time, each peak of

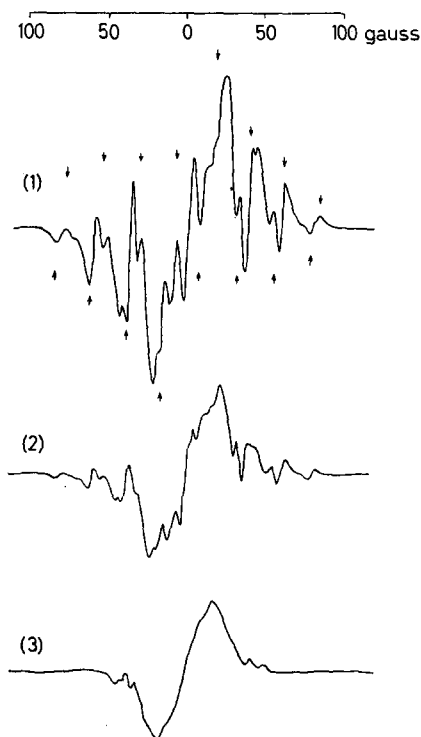


Figure 4—E.S.R. spectrum of electron-irradiated polypropylene, annealed block [(2)(c)] and its change after irradiation: (1) the derivative obtained at 20 min after irradiation; (2) after 1,231 min; (3) after 8,414 min. Irradiation condition: *in vacuo*, 1.5 MeV, 100 μ A, 30 sec, 14 Mrad, dipped in dry-ice-methanol mixture. The ordinate scale is the same for the three spectra

the triplet was narrowed, though the line width at maximum slope (ΔH_{msl}), remained approximately constant (~ 15 G). The narrowing might be due to partial averaging of the anisotropic dipolar hyperfine interaction by a plasticizing action of water molecules. Thus the spectrum observed at 2.5 h after introduction of water vapour was a narrowed and well-resolved one, the intensity ratio being about 1:2:1, the ΔH_{msl} of each peak 15 G, and the hyperfine separation 36 G [see Figure 2(3)]. After this the spectrum decayed without further change in its shape. This is in contrast with the case of P.V.A. *in vacuo*, where the intensity ratio increased from 1:3:1 and finally only a singlet spectrum remained. Identification of the spectrum observed after 2.5 h in the presence of water seems to be difficult. Although

the well-resolved typical triplet spectrum suggests a radical whose unpaired electron interacts equally with two protons, the hyperfine splitting value (36 G) is definitely larger than that expected for organic radicals, i.e. in the range 25 to 32 G.

Polyethylene (P.E.)—Irradiated polyethylenes gave superposed spectra consisting of several components. In order to obtain short-lived components among others, irradiations at higher dose rate, or at lower doses, or at lower temperatures would be generally more favourable, as is discussed below in Section (3). Accordingly, P.E. was irradiated *in vacuo* with the electron beam from the Van de Graaff accelerator. During the irradiation, the sample was dipped in dry-ice-methanol mixture to prevent heating. The irradiated polyethylene (*Marlex-50* inflated film, annealed [(1)(A)(b)]; 1.5 MeV, 100 μ A, 50 sec \times 2, \sim 47 Mrad) gave the spectrum shown in *Figure 3(1)*. As time elapsed, the absorption intensity decreased and the spectral shape changed as shown in *Figure 3(2)*, which was obtained at 21.5 h after

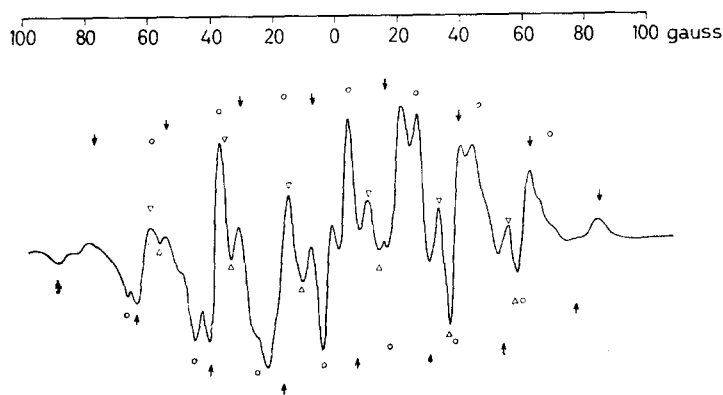


Figure 5—E.S.R. spectrum of electron-irradiated polypropylene yarn [(2)(d)] cold-drawn to 5 times its original length and then heat-treated at 150°C for 4.5 h without tension at 10 min after irradiation. Irradiation condition: *in vacuo*, 1.5 MeV, 100 μ A, 30 sec, 14 Mrad, dipped in dry-ice-methanol mixture. E.S.R. measurement: input microwave power 1 mW, the modulation field 1.8 G peak to peak, the field scanning rate 248 G/10 min, time-constant of the integrating filter 0.8 sec

irradiation. The spectrum (2) had a longer lifetime, of the order of a month. This result indicates that the spectrum (1) observed soon after irradiation consists of at least two components, one of which decays faster (in about one day) than the other. To find the short-lived component, subtraction of the spectrum (2) from spectrum (1) was carried out, and the result suggests that the short-lived component is a sextet, as indicated by arrows in *Figure 3(1)*. This sextet spectrum, the hyperfine splitting value of which is 30 G and the ΔH_{ml} value of each line about 13 G, might be

assigned to a radical $-\text{CH}_2-\dot{\text{C}}\text{H}-\text{CH}_2-$, which seems to decay almost completely in one day as *Figure 3(2)* shows. The sextet spectrum has also been obtained from electron-irradiated polyethylene by Powell *et al.*⁴ and Koritzky *et al.*⁵, and from γ -irradiated polyethylene at 77°K by Smaller

*et al.*¹⁰. The hyperfine splitting value was found to be 32 G by Powell *et al.* and 31 G by Smaller *et al.* We identified the sextet spectrum in the same way as these authors.

The spectrum (2) in *Figure 3* seems to be complex. It appears, however, from inspection of various spectra obtained under different conditions of measurement or irradiation [e.g. spectrum (3) in *Figure 3*, which was obtained 12 days after electron irradiation of the other annealed inflation film], that it has a seven-line spectrum, indicated by arrows in *Figure 3(2)*, as the main component. The seven-line spectrum, of which the line separation was estimated to be about 18 G, might be assigned to a radical $-\text{CH}_2-\dot{\text{C}}\text{H}-\text{CH}=\text{CH}-\text{CH}_2-$ as was done by Koritzky *et al.*⁹. Although the outermost peaks of the seven-line spectrum are not clearly visible in *Figure 3(2)*, which was recorded at a low amplification factor, they were

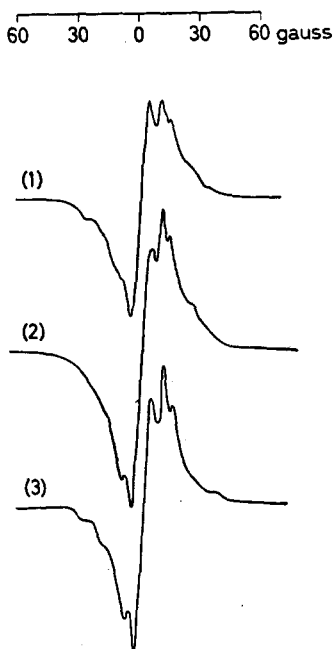


Figure 6—E.S.R. spectra of γ -irradiated polyethylene terephthalate [Tetoron (11)] treated under various conditions: (1) untreated film, $x=6.0$ per cent; (2) heat-treated film, $x=43.0$ per cent; (3) stretched to 3.6 times its original length, $x=28.3$ per cent. Dose 170 Mrad

readily observable when the spectrum was recorded at a higher gain. Calculations of the theoretical unpaired electron density on the allyl radical by Lefkovitz *et al.*¹¹ have shown that the densities on the three carbon atoms are 0.622, -0.231 and 0.622 respectively. According to this result it can be inferred that the $-\text{CH}_2-\dot{\text{C}}\text{H}-\text{CH}=\text{CH}-\text{CH}_2-$ radical gives a septet spectrum, the hyperfine splitting value being $30 \times 0.622 = 18.7$ G, and that each peak of the septet spectrum is split further into a doublet, the doublet splitting value being $30 \times 0.231 = 6.9$ G. Our value of the seven-line splitting (18 G) agrees well with the theoretical value. Full interpretation of the complex fine structure observed in spectrum (2) in *Figure 3* besides the seven-line component seems impossible at present. Some possible interpretations are: (i) there might be a possibility that the doublet splitting

mentioned above (6.9 G) is observable, since each line of the spectrum (2) has a very narrow width (~ 5 G); the peaks indicated by dotted arrows in Figure 3(2) might be components of the doublet; (ii) a small but definite 'kink' in the centre of the spectrum (2) might suggest that there are some radical species whose spectra consist of even numbers of hyperfine lines; (iii) as will be discussed later, we have found a very stable radical species in highly irradiated polyethylene, which had a singlet spectrum ($\Delta H_{msl} = 22.5$ G), and which was assigned to a radical of polyenyl type⁸; this singlet spectrum might be contained in the spectrum (2) and give a background to it.

Koritzky *et al.* have observed a spectrum similar to that in Figure 3(2), but their spectrum seems to be somewhat broadened by the power saturation effect and only the seven-line component can be observed, the complex fine

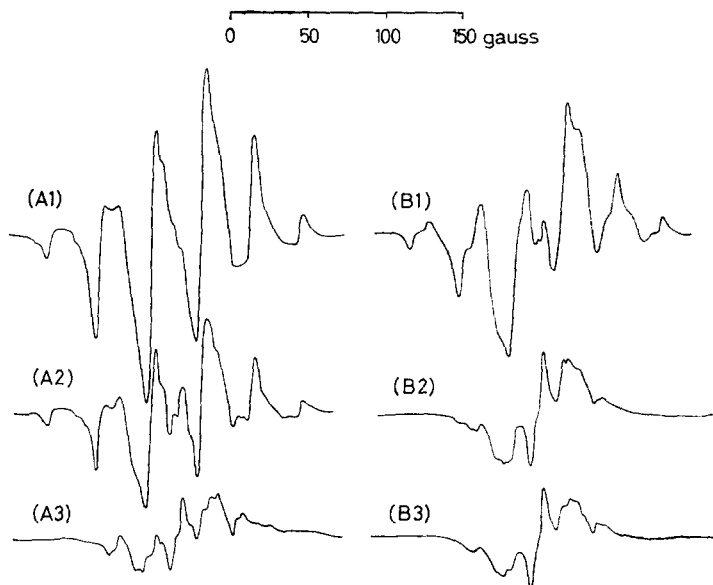


Figure 7—E.S.R. spectra of electron-irradiated polyethylene (*Marlex-50* inflation film) and their decay after irradiation: (A) for the film stretched at 100°C to about 3 times its original length, heat-set for 10 min, and then heat-treated at 125°C for 20 h; and B for the cold-drawn (to about 3 times its original length) film. (A1) 3 min, (A2) 147 min, (A3) 1,181 min; and (B1) 3 min, (B2) 254 min, (B3) 1,491 min after irradiation. Irradiation: *in vacuo*, 1.5 MeV, $100\mu\text{A}$, 20 sec $\times 3$, 28 Mrad, dipped in dry-ice-methanol mixture

structure observed in our case being so broadened that it cannot be distinguished. Koritzky *et al.* obtained a value of 15 G as the line interval, but this seems to be too small. Results of our saturation study⁵ of free radicals in irradiated polymers showed that the spectrum (2) became saturation-broadened when the input microwave power level exceeded 1 mW, and the line interval estimated from the saturated spectrum was not correct. Indeed, the spectrum measured at a microwave power of 10 mW was seven-line with no sign of the complex fine structure and a changed intensity ratio. The value of the line interval obtained from this spectrum

was 13 G, which does not seem to be the correct one. Powell *et al.* have also observed a spectrum similar to *Figure 3(2)*.

Polypropylene (P.P.)—Several kinds of radicals coexist in irradiated P.P. *Figure 4* shows the result of electron-irradiation (1.5 MeV, 100 μ A, 30 sec, 14 Mrad, dipped in dry-ice-methanol mixture) of P.P. rod [(2)(c)] *in vacuo*. In *Figure 4*, spectrum (1) was obtained at 20 min after irradiation, spectrum (2) after 2 h, and spectrum (3) after 6 days. Spectrum (3), mainly singlet, had a long lifetime. Subtraction of spectrum (3) from spectrum (1) suggested that the short-lived component which decays in nearly 6 days consists mainly of an eight-line spectrum indicated by arrows in *Figure 4(1)*, the line separation being about 24 G. The eight-line spectrum might be assigned to a radical $-\text{CH}_2-\dot{\text{C}}(\text{CH}_3)-\text{CH}_2-$.

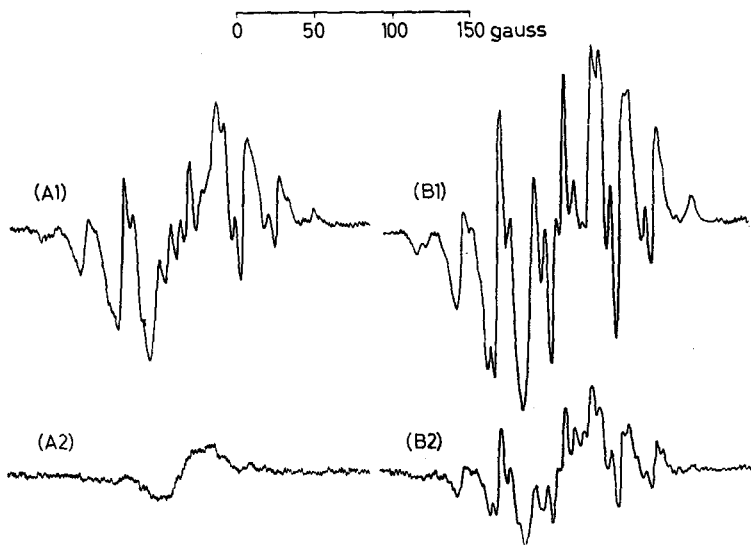


Figure 8—E.S.R. spectra of electron-irradiated polypropylene yarn [(2)(d)] and their decay after irradiation: *A* for the cold-drawn (to 5 times its original length) yarn; and *B* for the yarn which was cold-drawn (to 5 times its original length) and then heat-set at 150°C for 4.5 h without tension; (1) the spectra obtained at 3.5 min after irradiation, (2) after 1,482 min. Irradiation: *in vacuo*, 1.5 MeV, 100 μ A, 30 sec, 14 Mrad, dipped in dry-ice-methanol mixture

In addition to the above eight-line spectrum, other short-lived components [e.g. the sharp-line component in the centre of spectrum (1) in *Figure 4*] are present. These new components were observed in greater proportion in the spectrum shown in *Figure 5*, which was obtained from electron-irradiated P.P. yarn [(2)(d)] cold-drawn to 5 times its original length and then heat-treated at 150°C for 4.5 h without tension]. Inspection of *Figure 5* suggests that, in addition to the above-mentioned eight-line spectrum indicated by the arrows, there is also an odd-membered (presumably seven-line) component, indicated by small circles in the spectrum. The hyperfine splitting value was estimated to be approximately 21 G. The radical corresponding

to this odd-membered component might be $-\text{CH}_2-\dot{\text{C}}\text{H}-\text{CH}_3$. There may also be another component present, indicated by small triangles, which is even-membered (presumably six-line), and the hyperfine splitting value of this component is approximately 22 G. This component might correspond to a radical $-\text{CH}_2-\dot{\text{C}}\text{H}-\text{CH}_2-$. Besides these three components, the singlet spectrum shown in *Figure 4(3)* might also be contained in the spectrum illustrated in *Figure 5*. In summary it is suggested that the spectrum of irradiated P.P. consists of eight-line, odd-membered (presumably seven-line), even-membered (presumably six-line), and singlet components.

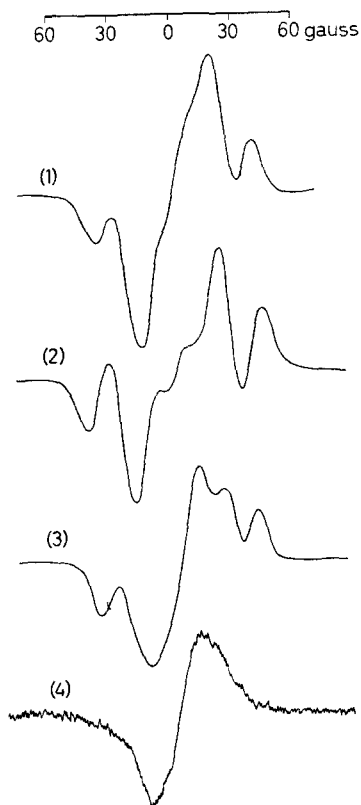


Figure 9—E.S.R. spectra of γ -irradiated Nylon 6 film treated under various conditions: (1) untreated ($x=19$ per cent), (2) heat-treated ($x=41$ per cent), (3) cold-drawn to 5 times its original length ($x=25$ per cent), (4) the derivative obtained after heating the irradiated sample which gave spectrum (1) at 60°C for 20 min. All the samples were irradiated at a dose of 13 Mrad

The hyperfine splitting values obtained for irradiated P.P. (21–24 G) are smaller than that of the sextet spectrum obtained from irradiated P.E. (30 G). This difference might be associated with the different molecular configurations in their crystalline regions: P.E. has a planar zig-zag chain structure and P.P. a three-fold helical structure.

It should be noted that the hyperfine splitting values of the aliphatic radicals¹⁰ produced in methane, ethane, propane, n-butane, n-hexane and n-nonane by γ -irradiation at 77°K range from 25 to 29 G, close to that of irradiated polypropylene, while the radicals in higher hydrocarbons such as n-octadecane, n-octacosane and *Marlex-50* give splitting values of 31 to 33 G.

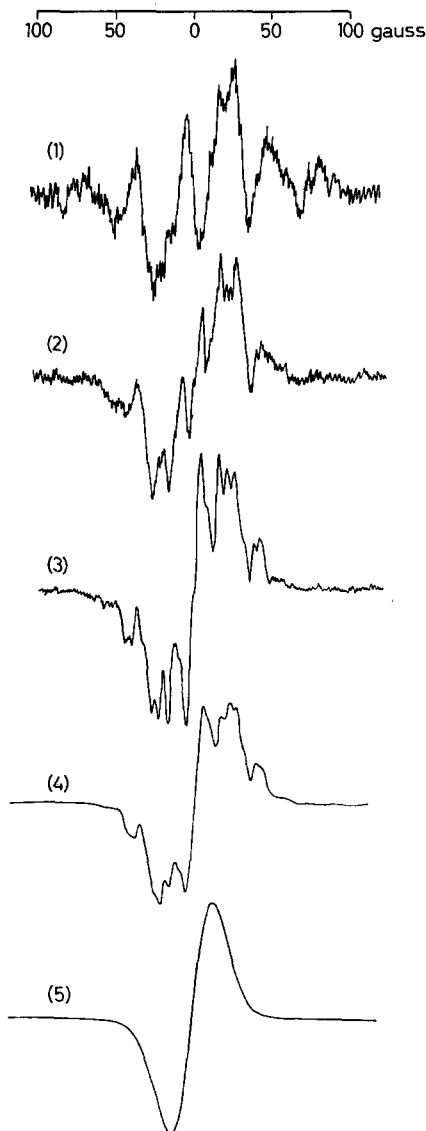


Figure 10—Change of the spectral shape of the γ -irradiated Marlex-50 annealed block [(1)(A)(b)] with dose: (1) 3.7×10^5 rad, (2) 6.0 Mrad, (3) 68 Mrad, (4) 550 Mrad, (5) 3,000 Mrad

(2) *Effect of state of aggregation of polymer on E.S.R. spectra*

We have carried out some experiments to find out whether or not the same kind of radical trapped in different states of aggregation of a polymer will give the same E.S.R. hyperfine structure, and also whether or not the radiation-chemical primary processes are the same in the different states of aggregation.

Poly(ethylene terephthalate)—The spectra of the irradiated *Tetoron* samples [(11)(c), (11)(d) and (11)(e)] were only slightly different, as is shown in Figure 6. When the irradiated samples [(11)(c) and (11)(e)] were heated at 90°C for 40 min, the spectra decayed by about 5 per cent and 44 per cent

respectively. These figures are comparable with the respective degrees of crystallinity (6 per cent and 43 per cent). After heating the samples, the shape of the spectrum was the same in the case of [(11)(c)], and slightly changed in the case of [(11)(e)]. This result may indicate that radicals trapped in the amorphous part of *Tetoron* are removed by heating the irradiated sample above the glass transition temperature (70°C). The spectrum obtained after heating will correspond to radicals trapped mainly in the crystalline region.

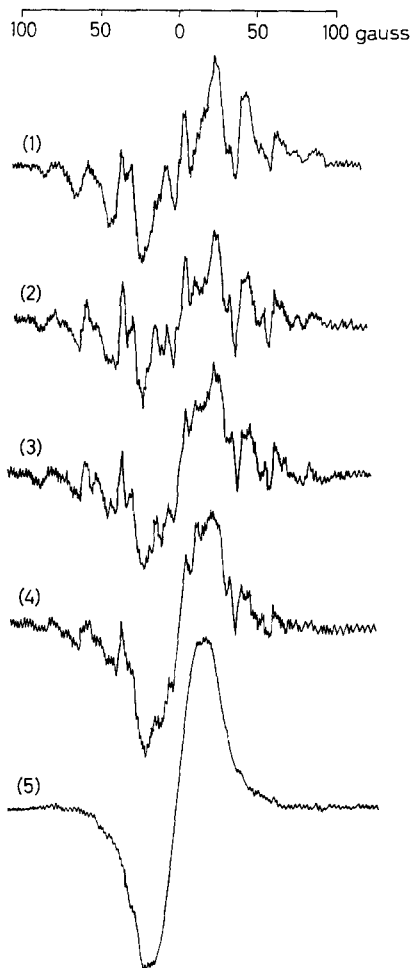


Figure 11—Change of the spectral shape of γ -irradiated polypropylene *Moplen A2* [(2)(c)] with dose: (1) 6.4×10^5 rad, (2) 5.7 Mrad, (3) 15 Mrad, (4) 28 Mrad, (5) 290 Mrad. The spectrum (1) was measured at a microwave power of ~ 3.2 mW and at a modulation field of 3.6 G. The other spectra were measured at ~ 1 mW with a modulation field of 1.8 G

Poly(vinyl alcohol)—The spectrum changed on heating the irradiated specimen at 88°C (i.e. above T_g) for 8 min, as shown in Figure 2, in which the change of curve (4) to (5) is for the untreated P.V.A. film (4)(a) and the change of curve (7) to (8) is for the heat-treated P.V.A. film (4)(b). In this case the change has somewhat complicated features, for untreated and treated samples behave differently on heating. The spectrum of the untreated sample changed little, while in the latter case a shoulder appeared in the

central peak. The intensity of the shoulder peak, however, varied with independent heat-treatments of samples which came from the same P.V.A. powder. In some experiments, the spectrum shown in *Figure 2(9)* was

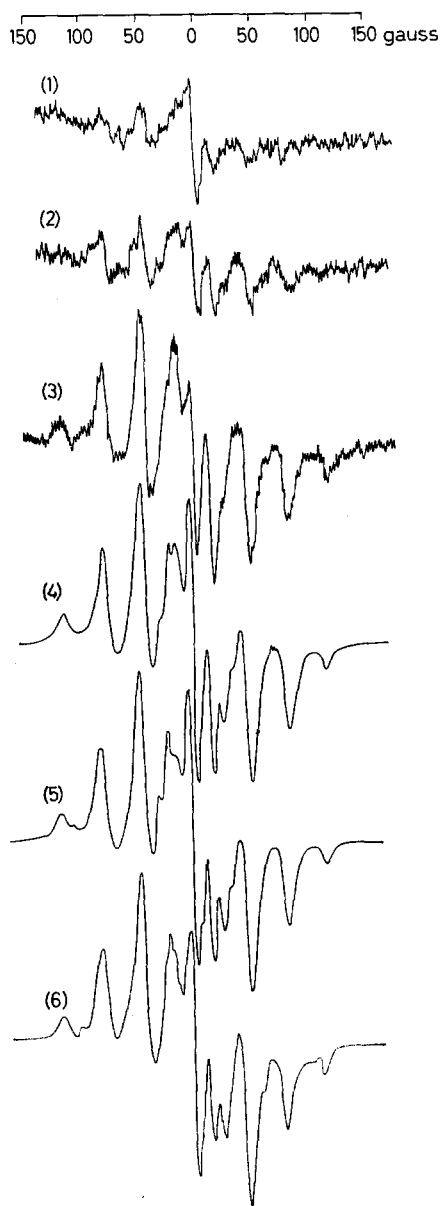


Figure 12—Change of the spectral shape of γ -irradiated poly(tetrafluoroethylene) with dose: (1) 3.7×10^5 rad, (2) 1.1 Mrad, (3) 3.6 Mrad, (4) 41 Mrad, (5) 96 Mrad, (6) 290 Mrad

observed after heating. Although spectrum (9) is somewhat broadened by the saturation effect, since it was measured at full microwave power level (~ 100 mW), the shoulder peak is clearly observable as a resolved peak. It

is tentatively suggested that the apparent five-line spectrum thus obtained consists of a quintet spectrum and of a triplet with doublet structure¹. The quintet component was assigned to a radical $-\text{CH}_2-\dot{\text{C}}(\text{OH})-\text{CH}_2-$ and the triplet to $\dot{\text{C}}\text{H}_2-\text{CH}(\text{OH})-$, on the questionable assumption that in the latter the interaction of the electron with α -hydrogen is weaker than that with the two β -hydrogens. Since the intensity of the shoulder peak was found to vary from sample to sample, the above interpretation might not be valid. The shoulder peak might be due to products of pyrolysis during heat-treatments. Heating the irradiated samples at 88°C for 30 min caused the spectra of the untreated and the heat-treated samples to decay to the

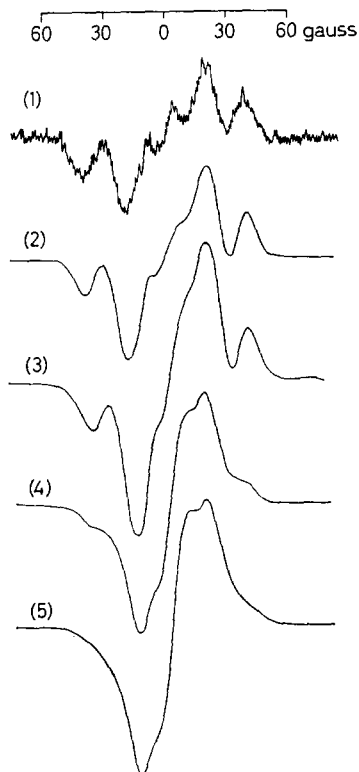


Figure 13—Change of the spectral shape of γ -irradiated Nylon 6 film [untreated sample (12) (A) (a)] with dose: (1) 1.4×10^5 rad, (2) 4.0 Mrad, (3) 13 Mrad, (4) 89 Mrad, (5) 250 Mrad

extent of about 6 per cent and 26 per cent respectively. These figures are not directly comparable with the degrees of crystallinity (41 per cent and 70 per cent) as in the case of *Tetoron*.

Stretching of P.V.A. film affected the spectrum, as shown in Figure 2(6). Comparison with the spectrum of the untreated film (dotted curve) indicates a sharpening of each peak. The stretching treatment will orient the crystallites in the direction of stretching and, as a result, the angle-dependent part of the dipolar hyperfine interaction will become ordered to some extent. Each line of the spectrum which was broadened by anisotropic dipolar interaction would become sharpened. In this connection it would be interesting to investigate the angular dependence of the spectrum on the external magnetic field for the doubly oriented specimen.

Polyethylene—Stretching and heat-treatment of *Marlex-50* before irradiation affects the decay of the sextet spectrum and also seems to affect slightly the spectral shape of each component of the sextet. Experimental results of electron-irradiation on 11 kinds of inflation films, which had been stretched and then heat-treated under different conditions, showed that the sextet spectrum had a longer lifetime when the samples were stretched and heat-treated at higher temperatures. For example, the sextet component of the electron-irradiated cold-drawn film (1.5 MeV, 100 μ A, 20 sec \times 3, 28 Mrad, dipped in dry-ice-methanol mixture) had decayed almost completely after 254 min at room temperature, while that of the film which had been stretched at 100°C, heat-set at that temperature for 10 min, and then heat-treated at 125°C for 20 h, decayed only after 1181 min (see *Figure 7*). This result suggests that heat-treatment will convert a smaller or imperfect crystalline

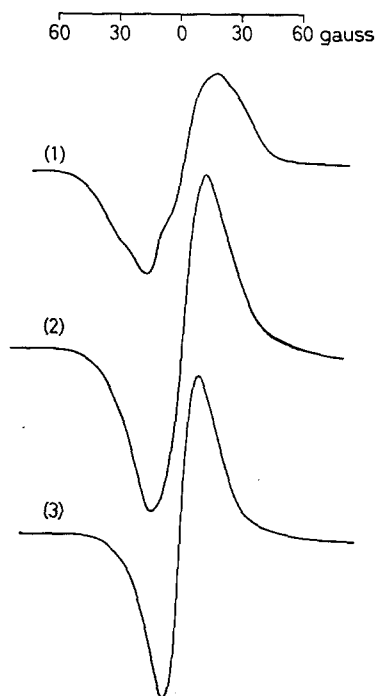


Figure 14—Change of the spectral shape of γ -irradiated poly(vinyl chloride) with dose: (1) 4.9×10^5 rad, (2) 25 Mrad, (3) 95 Mrad

region into a larger or more nearly perfect one. Results of electron-irradiation on a *Marlex-50* block prepared from pellets by melting *in vacuo* were somewhat different. The spectrum of the completely annealed block (1)(A)(b) obtained immediately after electron-irradiation (the same irradiation as above) showed mainly the septet, the sextet component having decayed almost entirely, and was quite similar to the spectra shown in *Figures 3(2)*, *7(A3)*, and *7(B3)*. A similar spectral difference between the inflation film and the block was observed in the case of γ -irradiation. The septet component appeared in the spectrum of the block to a greater extent than in that of the inflation film when the samples were irradiated with smaller doses (~ 1 Mrad). These results suggest that the sextet component,

i.e. the radical $-\text{CH}_2-\dot{\text{C}}\text{H}-\text{CH}_2-$, decays or reacts faster in the block sample.

On heating the irradiated P.E. at higher temperatures, the spectra changed in a similar fashion, as shown in *Figure 10*: the spectrum (3) changed gradually to (4) and then finally to (5). Since heating will cause partial melting of small crystallite or 'soft' crystalline regions but not of large crystallites or 'rigid' crystalline regions, it might be supposed that the spectra obtained after heating correspond to the radicals in the larger crystallites or 'rigid' crystalline regions. However, since we have recently assigned the singlet spectrum to a polyenyl radical or radicals⁸, a better interpretation of the observed changes might be that radicals which are chemically more reactive disappear during heating. The radical $-\text{CH}_2-\dot{\text{C}}\text{H}-\text{CH}_2-$ disappears first, the $-\text{CH}_2-\text{CH}=\dot{\text{C}}\text{H}-\text{CH}_2-$ radical follows, and the $-\text{CH}_2-\dot{\text{C}}\text{H}-(\text{CH}=\text{CH})_n-\text{CH}_2-$ radicals ($n \sim 5$) stabilized by bond resonances remain after heating.

Polypropylene—Stretching and heat-treatment of P.P. yarn before irradiation affected the shape as well as decay of the spectrum. *Figure 8 (A1)* was obtained from the electron-irradiated (1.5 MeV, 100 μA , 30 sec, 14 Mrad, dipped in dry-ice-methanol) yarn (2)(d) which had been cold-drawn to 5 times its original length; *Figure 8 (B1)* was obtained from the electron-irradiated (under the same conditions) yarn which had been stretched to 5 times its original length and then heat-set at 150°C for 4.5 h without tension. [It will be noticed that *Figure 8(B1)* is the same as *Figure 5* where the scale of the abscissa is doubled.] In the latter spectrum (B1), the seven-line component, discussed in Section (I) above, is obtained in greater proportion. The short-lived components decayed faster in the cold-drawn sample, as can be seen in *Figures 8(A2)* and (B2). The spectrum obtained from the electron-irradiated (under the same conditions as above) P.P. block [(2)(c)] contained the seven-line component with an intensity intermediate between the two mentioned above [see *Figure 4(I)*]. The radicals observed in the irradiated P.P. at room temperature will be those trapped in the crystalline regions, since T_g of *Moplen A2* lies near -35°C. Recently, a new crystal phase has been reported¹² to exist in stretched P.P., and this may account for the observed difference in the spectra.

Nylon 6—The spectra of untreated, heat-treated, and stretched films of Nylon 6 are shown in *Figures 9(1)*, *9(2)* and *9(3)* respectively. *Figure 9(4)* was obtained after heating the sample which gave spectrum (1) at 60°C (above T_g) for 20 min. On the other hand, when the heat-treated sample was heated after irradiation, the spectral shape was unchanged.

(3) Effect of irradiation dose and dose rate on E.S.R. spectra

Variation of the spectral shape of irradiated polymers with different doses has been observed for a number of polymers, and the results are shown in *Figures 10-16*.

In the cases of polyethylene, polypropylene, Nylon 6, *Acryglass*, poly(vinyl chloride) and poly(vinyl alcohol), changes of spectral shape after different doses are well defined: the structure of the spectra tends to disappear as the dose increases so that at higher doses they become broad singlets with little

sign of structure (cf. assumption of polyenyl radical). In the case of poly(vinyl chloride), the ΔH_{msl} value of the singlet spectrum decreased asymptotically to 16 G as the dose was increased. The spectrum of poly(ethylene glycol) [which is a doublet, as shown in *Figure 1(5)*, the hyperfine splitting value being 15 gauss] did not show marked change up to about 200 Mrad, except the slight broadening of each peak of the doublet spectrum. In the case of polytetrafluoroethylene, the shape of the outer quintet components of the spectrum, which have been assigned to the radical $-\text{CF}_2-\dot{\text{C}}\text{F}-\text{CF}_2-$ by Rexroad *et al.*¹³, did not change with dose, although some complicated changes were observed in the central part of the spectrum (see *Figure 12*).

Several causes for this behaviour might be postulated. For instance, structural changes, such as lowering of the degree of crystallinity or the formation of the crosslinks, or changes in radiation-chemical processes, such as gas evolution, might occur. However, as the following experimental results will show, such changes do not seem to have a direct effect on the E.S.R. spectrum.

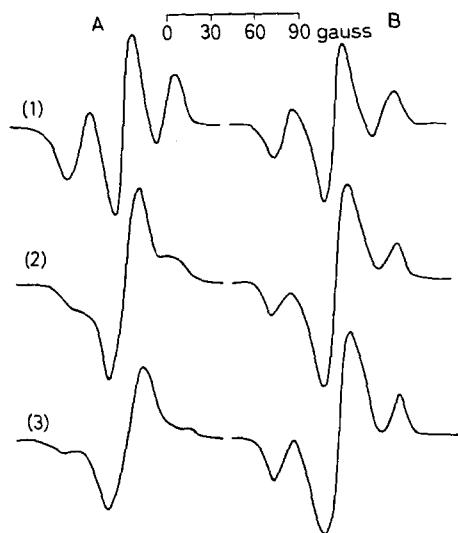


Figure 15—Change of the spectral shape of γ -irradiated poly(vinyl alcohol) with dose: A for the untreated film ($x=41$ per cent); and B for the heat-treated film ($x=70$ per cent): (1) 3.1×10^5 rad, (2) 45 Mrad, (3) 400 Mrad

In the case of poly(ethylene glycol), Nitta *et al.*¹⁴ have found that the crystallization-sensitive bands of the infra-red spectrum disappear almost entirely near 200 Mrad, the melting point begins to drop near a dose of 30 Mrad and the gel-point is at 370 Mrad, whereas, in the E.S.R. spectrum of poly(ethylene glycol), no marked change was found near any of these doses. In the case of *Acryglass*, we found no change in the chemical composition of the evolved gas, and found also a continuous decrease in viscosity near the dose of 11 Mrad at which its E.S.R. spectrum began to change.

Another interpretation might be that two kinds of radicals with different rates of formation or decay are formed by irradiation; with lower doses or higher dose rates, the relative concentration of the short-lived radicals will

be greater, whilst that of the long-lived radicals will become larger as the dose is increased or the dose rate is lowered.

We suggest that the change of the spectra of irradiated polyethylene, polypropylene, Nylon 6, poly(vinyl chloride) and poly(vinyl alcohol) can be explained reasonably in these terms.

For instance, in the case of P.E. annealed block (1)(A)(b), we have found at least three kinds of radicals produced by irradiation [see Section (1)]: a sextet spectrum ($-\text{CH}_2-\dot{\text{C}}\text{H}-\text{CH}_2-$), a seven-line spectrum ($-\text{CH}_2-\dot{\text{C}}\text{H}-\text{CH}=\text{CH}-\text{CH}_2-$), and [$-\text{CH}_2-\dot{\text{C}}\text{H}-(\text{CH}=\text{CH})_n-\text{CH}_2-$ where $n \sim 5$] a singlet spectrum. The lifetimes of these radicals increase in that order. Thus, in the initial range of irradiation, the spectrum should be mainly the sextet, and the actual spectrum observed at a dose of 3.7×10^5 rad was nearly sextet, as shown in Figure 10(1). As the dose is increased, the relative concentration of the $-\text{CH}_2-\dot{\text{C}}\text{H}-\text{CH}=\text{CH}-\text{CH}_2-$ radical will become larger and the spectrum observed at a dose of 68 Mrad was mainly the septet

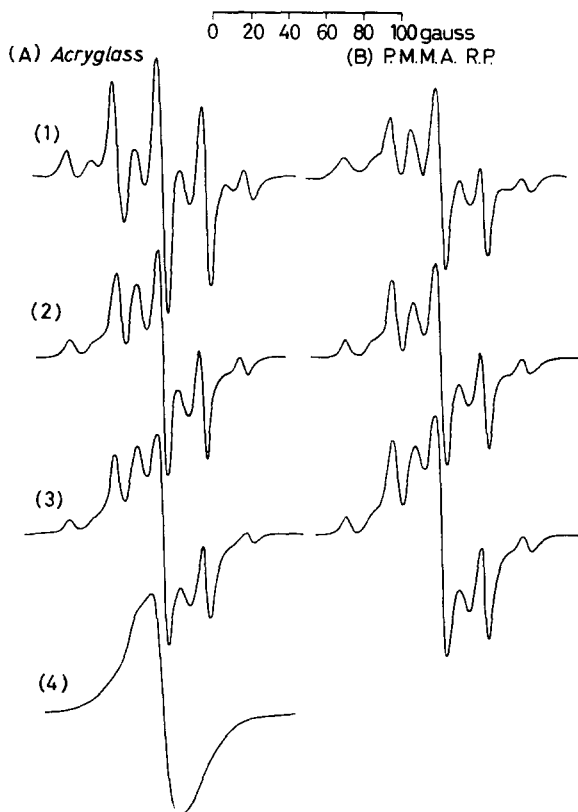


Figure 16—Change of the spectral shape of γ -irradiated poly(methyl methacrylate): A for Acryglass (9) (A); and B for the radiation-polymerized sample (9) (C): (1) < 10 Mrad, (2) 28 Mrad, (3) 82 Mrad, (4) 400 Mrad

[see *Figure 10(3)*]. In the higher dose range, the concentration of the stable polyenyl radical will become larger, and the spectrum observed at a dose of 3,000 Mrad was actually a singlet.

In contrast to the result with γ -irradiation at a dose of 10 Mrad the spectrum of the electron-irradiated P.E. (annealed inflation film) at approximately the same dose was mainly sextet. This is because the dose rate was very much higher in this instance.

The change of the spectrum of P.P. (*Figure 11*) might be interpreted in a similar way. The spectrum of the so-called short-lived eight-line, seven-line and six-line components [see Section (I)], observed in the initial stage of irradiations, changed gradually to the singlet spectrum of long lifetime as the dose increased. The spectra of Nylon 6, poly(vinyl chloride) and poly(vinyl alcohol) might also be interpreted in a similar way. In these cases the spectra of highly irradiated samples were found to be quite similar to those obtained after heating the samples which had been irradiated at lower doses.

The effect of dose on the spectra of irradiated poly(methyl methacrylate) is somewhat different from the above examples. As is clearly seen from *Figure 16*, the spectral shapes of *Acryglass* [(9)(A)] and the radiation-polymerized P.M.M.A. [(9)(C)] are different from each other up to doses of about 10 Mrad, while above this level the spectra become increasingly similar, and at a dose of 82 Mrad they are indistinguishable. At the same time, the radical-formation curves (concentration of the radicals produced *versus* dose) are also somewhat different in the above two samples, as will be shown in Part II. The curve for the radiation-polymerized sample increases monotonically at the lower doses until it finally reaches saturation. On the other hand, that for *Acryglass* is a curve in which the radical concentration in the initial range of irradiation up to about 7 Mrad is about 60 per cent greater and then, above that dose, it begins to become smaller, the spectral shape becoming similar to that of the radiation-polymerized P.M.M.A. Finally, above a dose of 100 Mrad, the curves for both kinds of P.M.M.A. coincide (at the point where the spectral shapes become the same as well).

The result of heating *Acryglass* after irradiation, and also the results¹⁵ of γ - and ultra-violet-irradiations of *Acryglass* containing benzophenone as an additive, suggest that the spectrum of P.M.M.A. consists of two components; the spectrum of the short-lived component is mainly that shown in *Figure 16(A1)*, which is well known for P.M.M.A. and has been assigned to the radical $-\text{CH}_2-\dot{\text{C}}(\text{CH}_3)-\text{COOCH}_3$ by Abraham *et al.*¹⁶, and the spectrum of the long-lived component is a singlet, as shown in *Figure 16(A4)*. While the change of the spectrum of radiation-polymerized P.M.M.A. might be reasonably interpreted in a similar way to that for P.E., P.P., etc., that of *Acryglass* may not, since the concentration of the short-lived radical is abnormally large in the initial stage of irradiation. In accordance with Ovenall's result¹⁷ that the spectrum (A1) in *Figure 16* (i.e. of the radical $-\text{CH}_2-\dot{\text{C}}(\text{CH}_3)-\text{COOCH}_3$), is due to the residual monomer, *Acryglass* might contain more of this residual monomer.

The authors would like to express their sincere thanks to Dr R. S. Powell of the General Electric Research Laboratory for his kind advice on the power saturation effect, to Dr Kazuo Morigaki of Osaka University for supplying manganous chloride samples, and also to Mr Shun-ichi Sugimoto for his help in a part of our experiments.

Osaka Laboratories,
Japanese Association for Radiation Research on Polymers,
Mii, Neyagawa City,
Osaka, Japan

(Received 2nd February, 1960.

Revised version received 26th September, 1960)

REFERENCES

- ¹ OHNISHI, S., KASHIWAGI, M., IKEDA, Y. and NITTA, I. Paper presented at the Conference on the Uses of Large Radiation Sources in Industry, CW/IIA/31, Warsaw, September 1959
- ² PIETTE, L. H. Private communication
- ³ KOGA, H., HÔRAI, K. and MATSUMURA, O. Paper presented at the 14th Annual Meeting of the Japan Physical Society, October 1959
- ⁴ POWELL, R. S., LAWTON, E. J. and BALWIT, G. S. Paper presented at the 1959 Spring Meeting of the American Physical Society
- ⁵ OHNISHI, S. *et al.* To be published
- ⁶ ABRAHAM, R. J. and WHIFFEN, D. H. *Trans. Faraday Soc.* 1958, **54**, 1291
- ⁷ OHNISHI, S., KASHIWAGI, M. and NITTA, I. *Doitai to Hoshasen (Isotopes and Radiation)*, 1958, **1**, 209
- ⁸ OHNISHI, S., IKEDA, Y., SUGIMOTO, S. and NITTA, I. *J. Polym. Sci.* 1960, **47**, 503
- ⁹ KORITZKY, A. T., MOLIN, YU. N., SHAMSHEV, V. N., BOUBEN, N. YA. and VOEVODSKY, V. V. *Vysokomolekularnye Soedineniya*, 1959, **1**, 1182
- ¹⁰ SMALLER, B. and MATHESON, M. S. *J. chem. Phys.* 1958, **28**, 1169
- ¹¹ LEFKOVITZ, H. C., FAIN, J. and MATSEN, F. A. *J. chem. Phys.* 1955, **23**, 1690
- ¹² SOBUE, H. and TABATA, Y. Unpublished data
- ¹³ REXROAD, H. N. and GORDY, W. *J. chem. Phys.* 1959, **30**, 399
- ¹⁴ NITTA, I., OHNISHI, S. and FUJIMOTO, S. Paper presented at the 12th Annual Meeting of the Chemical Society of Japan, April 1959
- ¹⁵ OHNISHI, S. and NITTA, I. Paper presented at the 9th Annual Meeting of the Society of Polymer Science, Japan, May 1960
- ¹⁶ ABRAHAM, R. J., MELVILLE, H. W., OVENALL, D. W. and WHIFFEN, D. H. *Trans. Faraday Soc.* 1958, **54**, 1133
- ¹⁷ OVENALL, D. W. *J. Polym. Sci.* 1959, **39**, 21

An Infra-red Study of the Crystallization of Poly(vinyl chloride)*

A. KAWASAKI, J. FURUKAWA, T. TSURUTA and S. SHIOTANI

We have studied infra-red spectral changes in the 3,000–800 cm^{-1} region on crystallizing poly(vinyl chloride) specimens. The optical densities of the 1,428, 1,333, 1,254, 1,226 and 955 cm^{-1} bands increase linearly with increasing specific gravity or crystallinity. The 1,434 cm^{-1} band is assigned to both the δ (CH_2) mode of disordered, and the δ (CH_2)_i(A₁) mode of the syndiotactic, portions of the polymer molecule. The crystallization-sensitive band at 1,428 cm^{-1} is ascribed to interactions in the crystalline regions of the polymer. The 1,226 cm^{-1} band may be assigned to the γ_w (CH_2)_i(B₂) or γ_w (CH)_i(B₂) modes. Though the infra-red dichroism is questionable, the 955 cm^{-1} band may be due to the γ_r (CH_2)_i(B₁) mode in the crystalline regions. The shoulder at 965 cm^{-1} is assignable to the γ_r (CH_2) mode of amorphous regions.

INTRODUCTION

THERE have been several papers concerned with the infra-red spectrum of poly(vinyl chloride). Recently, Grisenthwaite *et al.*^{1, 4}, Krimm *et al.*^{2, 5} and Shimanouchi *et al.*^{3, 7} have discussed the infra-red spectral changes in the C—Cl stretching region on crystallizing poly(vinyl chloride) specimens. Narita *et al.*⁶ reported that the intensity of the band at 837 cm^{-1} decreased on melting the specimen.

In a previous communication⁸ we reported the absorption bands which changed their intensity in the 3,000–800 cm^{-1} region on crystallizing. This paper is a detailed version of that communication.

EXPERIMENTAL

The infra-red spectra were measured on a Shimadzu AR-275 double-beam spectrometer with a rock-salt prism and a Koken DS-301 double-beam spectrometer with a rock-salt prism.

Poly(vinyl chloride) was prepared with a binary mixture of triethyl-aluminium and di-tert-butyl peroxide⁹ as catalyst at room temperature. The viscosity-average molecular weight of the polymer was 32,000. Specimens were prepared from a tetrahydrofuran solution of the polymer in the form of thin solid films. The solvent remaining in the film was removed by extraction with carbon disulphide at room temperature until tetrahydrofuran was no longer detected in the infra-red spectrum of the polymer film. To ensure that the polymer film had the highest crystalline content, the extracting agent was evaporated off slowly. After this treatment, the film was dried under vacuum at room temperature to remove carbon disulphide completely. The specific gravity of the film was measured by the flotation method in zinc chloride solution. By varying the conditions of heat treatment in Wood's alloy, the specific gravity, d_4^{30} , of the sample

*The outline of this paper was presented before the Symposium on Raman and Infra-red Spectra at Kyoto, 16th October 1958 and at Tokyo, 11th September 1959.

could be raised in the range 1.3887 to 1.4022. The sample was found to show the highest density when it had not been heat-treated.

In our laboratory, a study of the polymerization of poly(vinyl chloride) by various organo-metallic compounds is now in progress, and some interesting results have been obtained. For example, a sample of poly(vinyl chloride) (mol. wt., 111,000), prepared at -65°C with a binary mixture of triethylboron and cumene hydroperoxide⁹ as catalyst, was found to contain a fraction (50 per cent by weight) which was sparingly soluble in boiling tetrahydrofuran. This fraction, however, was soluble in cyclohexanone at 100°C . To avoid dehydrochlorination, it is recommended that the insoluble fraction be heated under nitrogen for about three hours. Films of this fraction were made by casting from a cyclohexanone solution, and the solvent was removed in the manner described above. These films showed higher densities than those prepared at room temperature from a binary mixture of triethylaluminium and di-tert-butyl peroxide as catalyst.

RESULTS AND DISCUSSION

The examination of the infra-red spectra of specimens having various specific gravities has shown that the ratios of any two optical densities of the bands at 2,920, 1,375, 1,196 and 1,092 cm^{-1} remain nearly unchanged irrespective of the change in the specific gravity of the polymer samples. This result suggests either that each of these bands is independent of the specific gravity, or that they are all dependent upon it to the same extent.

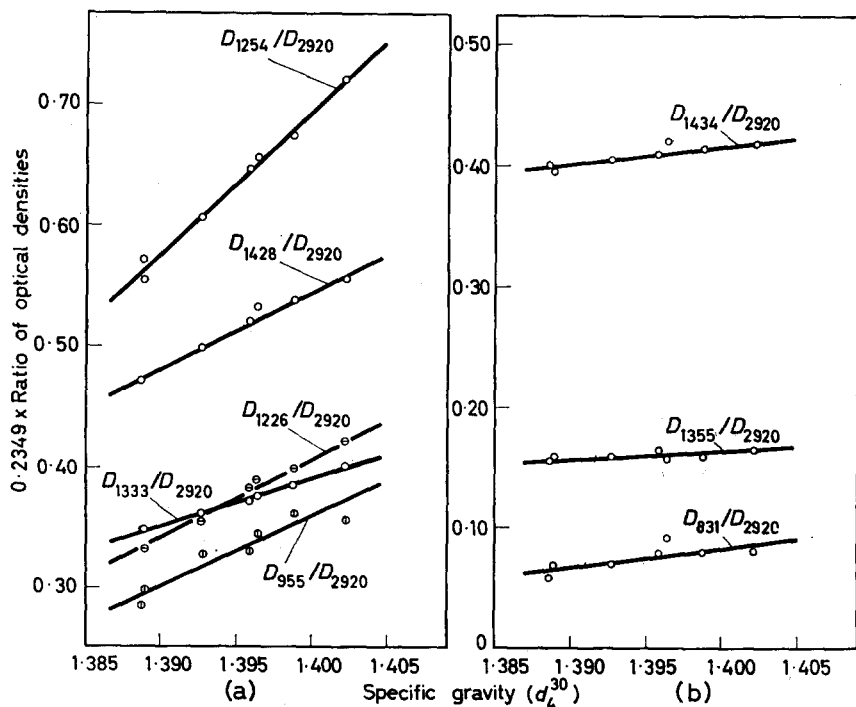


Figure 1—Relation between optical density and specific gravity⁸.
(By courtesy of The Chemical Society of Japan)

We have taken the band at $2,920\text{ cm}^{-1}$ as standard and have calculated the relative optical densities of every absorption band.

It can be seen from *Figure 1a* that the ratios of optical densities at $1,428$, $1,333$, $1,254$, $1,226$ and 955 cm^{-1} to the $2,920\text{ cm}^{-1}$ band increase linearly with increasing specific gravity. Though the same behaviour was observed also for the absorption bands at $1,434$, $1,355$ and 831 cm^{-1} , the dependence of the optical density upon the specific gravity was much less marked (*Figure 1b*). These results indicate that the former five bands can be correlated with the changes of specific gravity or crystallinity of the sample to a larger extent than the other bands.

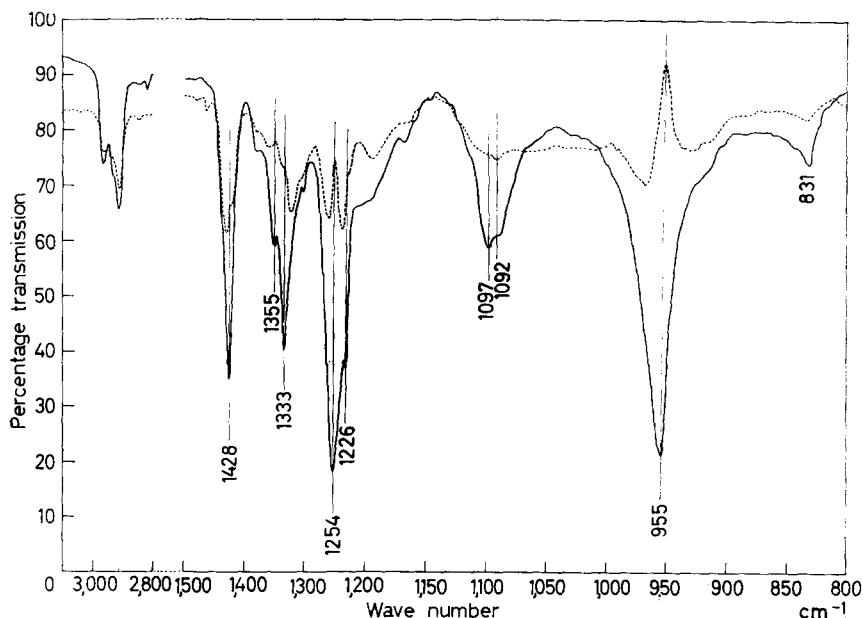


Figure 2—Differential infra-red spectra of poly(vinyl chloride)⁸: ——— reference, lower-density polymer ($d_4^{30}=1.3877$); - - - - - reference, higher-density polymer ($d_4^{30}=1.4031$). (By courtesy of The Chemical Society of Japan)

Figure 2 shows the differential infra-red spectra of two polymers having different specific gravity. In *Figure 2*, the full line is obtained by putting the lower-density film in the reference beam and the higher-density film in the sample beam of the double-beam spectrometer. In the full line the intensities of the bands which are ascribed to the amorphous modes are decreased and the line shows a spectrum of an imaginary sample whose crystallinity is considered to be higher than that of the above higher-density sample. In contrast with the full line spectrum the dotted line was obtained by putting the higher-density film in the reference beam and the lower-density film in the sample beam. In the dotted line the intensities of the bands which are ascribed to the crystalline modes are decreased. In both cases, the thickness of the film which was put in the sample beam was greater than that of the film which was put in the reference beam. *Figure*

2 shows clearly the correlation of the absorption bands at 1,428, 1,333, 1,254, 1,226 and 955 cm^{-1} with the specific gravity of the sample.

Figure 3 shows the infra-red spectrum of the tetrahydrofuran-insoluble, highly crystalline poly(vinyl chloride) ($d_4^{30}=1.4031$) prepared at -65°C with a binary mixture of triethylboron and cumene hydroperoxide as catalyst. In this spectrum, the absorptions at 1,428, 1,333, 1,254, 1,226 and 955 cm^{-1} have become much sharper.

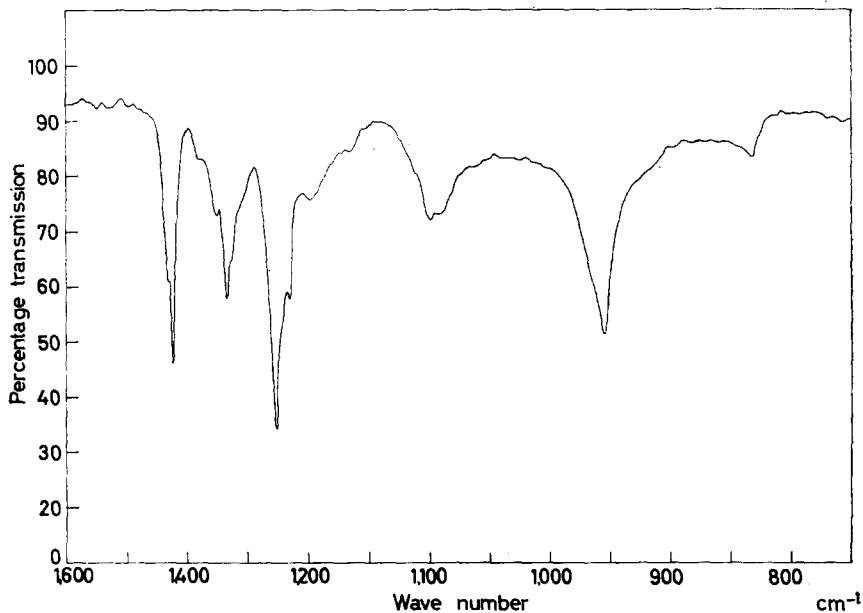


Figure 3—Infra-red spectrum of high-density poly(vinyl chloride) ($d_4^{30}=1.4031$)

Krimm *et al.*² stated that the component at 1,430 cm^{-1} became weaker relative to that at 1,423 cm^{-1} on crystallization and therefore the 1,423 cm^{-1} band should be ascribed to the $\delta(\text{CH}_2)$ mode of syndiotactic portions of the material and the 1,430 cm^{-1} band to the disordered portions of the polymer. However, as can be seen from Figures 1a and 1b, the behaviour of the 1,428 and 1,434 cm^{-1} bands seems different from that found by Krimm *et al.*². The intensity of the 1,434 cm^{-1} band increases gradually on crystallization and a more prominent enhancement of band intensity is observed at 1,428 cm^{-1} . Consequently, the 1,434 cm^{-1} band may be associated not with the $\delta(\text{CH}_2)$ mode of the disordered portions of the polymer alone, but with both the $\delta(\text{CH}_2)_i(\text{A}_1)$ mode of the syndiotactic and the $\delta(\text{CH}_2)$ mode of the disordered portions of the material. It is also possible that the crystallization-sensitive band at 1,428 cm^{-1} may be due to interactions in the crystalline regions of the polymer. The $\delta(\text{CH}_2)_o(\text{A}_2)$ mode is infra-red inactive*.

The intensity of the 1,226 cm^{-1} band is also enhanced by crystallization. This band was found to be a distinct parallel band as reported before¹⁰.

*Notation of Krimm and Liang¹¹, in which subscript i refers to in-phase and o to out-of-phase movement of the two CH_2 groups in the repeat unit.

From the discussion in Krimm's paper¹¹, we assume that this parallel band can be assigned to the wagging modes of CH₂ or CH groups which arise from B₂ species, i.e. the $\gamma_w(\text{CH}_2)_i(\text{B}_2)$ or $\gamma_w(\text{CH})_i(\text{B}_2)$ modes. Krimm *et al.*¹¹ decided that the $\gamma_w(\text{CH})_o$ and $\gamma_w(\text{CCl})_o$ modes were due to B₂ species, but it is correct to consider that these modes are due to A₂ species and therefore the $\gamma_w(\text{CH})_i$ and $\gamma_w(\text{CCl})_i$ modes should be due to B₂ species. In contrast with our assignment Krimm *et al.*¹¹ assigned the 1,352 cm⁻¹ band to the $\gamma_w(\text{CH}_2)_i(\text{B}_2)$ mode and the 1,197 cm⁻¹ band to the $\gamma_w(\text{CH})_o(\text{B}_2)$ mode (as stated above the latter mode should be $\gamma_w(\text{CH})_i(\text{B}_2)$). The modes which are expected to be seen in this region and moreover show parallel dichroism are the $\gamma_w(\text{CH}_2)_i$, $\gamma_w(\text{CH})_i$ and parallel chain-stretching modes¹². As can be seen in Figure 4 the bands at 1,375, 1,226 and 1,196 cm⁻¹ show parallel dichroism. The ratios of optical densities at 1,226 and 1,355 cm⁻¹ to that of the 2,920 cm⁻¹ band increased linearly with increasing specific gravity, but the ratios of optical densities at 1,196 and 1,375 cm⁻¹ to that of the 2,920 cm⁻¹ band remained nearly unchanged irrespective of the change in the specific gravity of the polymer samples. It may be reasonable to consider that with the change of polymer crystallinity the intensity of the band which is ascribed to the hydrogen bending mode is more changeable than that of the chain-stretching mode. Consequently the 1,226 cm⁻¹ band should be ascribed to the $\gamma_w(\text{CH}_2)_i$ or $\gamma_w(\text{CH})_i$ mode. From its infra-red dichroism the 1,375 cm⁻¹ band may be assigned to the $\gamma_w(\text{CH}_2)_i$ or $\gamma_w(\text{CH})_i$ mode. Similarly from its intensity change with the change of specific gravity of the samples the 1,355 cm⁻¹ band may also be assigned to the $\gamma_w(\text{CH}_2)_i$ or $\gamma_w(\text{CH})_i$ mode. The 1,355 cm⁻¹ band, however, shows perpendicular dichroism, as can be seen in Figure 4 and therefore it is impossible to deter-

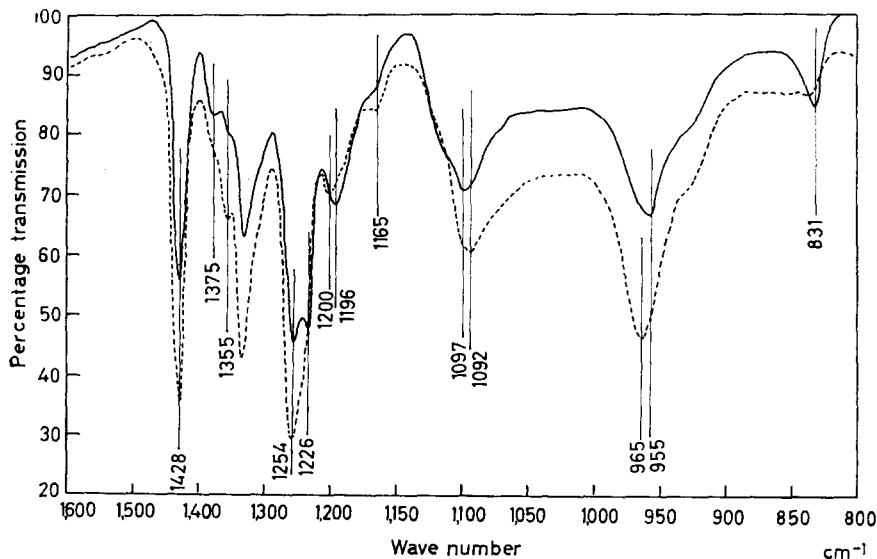


Figure 4—Infra-red spectrum of oriented poly(vinyl chloride): - - - - radiation with electric vector perpendicular to direction of orientation; ——— radiation with electric vector parallel to direction of orientation

mine which band is to be assigned to which of the two hydrogen bending modes. The $1,196\text{ cm}^{-1}$ band which Krimm *et al.* assigned to the $\gamma_w(\text{CH})_i$ mode is assigned to the parallel chain-stretching mode. Of the other modes expected in this region, the $\gamma_w(\text{CH}_2)_o(\text{B}_1)$ mode, if it could be observed, should be a very weak band and show perpendicular dichroism. The $\gamma_w(\text{CH})_o(\text{A}_2)$ mode is infra-red inactive. The $\gamma_t(\text{CH})_2$ modes may also be expected in this region, but the $\gamma_t(\text{CH}_2)_i(\text{A}_2)$ mode is infra-red inactive and the $\gamma_t(\text{CH}_2)_o(\text{A}_1)$ mode should exhibit perpendicular dichroism. Moreover, the latter $\gamma_t(\text{CH}_2)_o(\text{A}_1)$ mode may be observed as a very weak band. Thus the modes $\gamma_t(\text{CH}_2)$, $\gamma_w(\text{CH})_o(\text{A}_2)$ and $\gamma_w(\text{CH}_2)_o(\text{B}_1)$ are ruled out. In the infra-red spectrum of deuterated poly(vinyl chloride), $(\text{CD}_2\text{CDCl})_n$, Narita *et al.*⁶ observed a parallel band at 937 cm^{-1} which, it was suggested, corresponds to the 969 cm^{-1} band of poly(vinyl chloride). But from its wave number ($937 \times 1.31 = 1,227$) we consider that the 937 cm^{-1} band of deuterated poly(vinyl chloride) may correspond to the parallel band at $1,226\text{ cm}^{-1}$ of poly(vinyl chloride).

A remarkable shoulder is observed at about $1,240\text{ cm}^{-1}$ in the spectrum of the low-density polymer, but it almost disappears on crystallization. Thus the shoulder may be ascribed to the overtone of the amorphous band³ at 615 cm^{-1} , as was suggested by Krimm *et al.*².

Low-density polymers have another shoulder at about 965 cm^{-1} , the intensity of which is nearly equal to that of the 955 cm^{-1} band. On crystallization the 955 cm^{-1} is enhanced, whereas the shoulder decreases and eventually disappears. Krimm *et al.*¹¹ observed only one perpendicular band at 963 cm^{-1} in this region and Narita *et al.*⁶ also observed only a perpendicular band at 969 cm^{-1} . The 955 cm^{-1} band was observed as a parallel band and the 965 cm^{-1} shoulder was a perpendicular band, as was reported by Shimanouchi *et al.*⁷. For these bands, three different interpretations have been presented. Krimm *et al.*¹¹ assigned their 963 cm^{-1} band to the chain-stretching mode, Shimanouchi *et al.*⁷ assigned their 962 (perpendicular dichroism) and 958 cm^{-1} (parallel dichroism) bands to the $\gamma_t(\text{CH}_2)$ modes without any discussion and Narita *et al.*⁶ assigned their 969 cm^{-1} band to the overlapping of the $\gamma_t(\text{CH}_2)$ and C—C skeletal modes from their spectrum of deuterated poly(vinyl chloride). But as we discussed above, we consider that the parallel band at 937 cm^{-1} in the deuterated poly(vinyl chloride)⁶ corresponds to the $1,226\text{ cm}^{-1}$ band of poly(vinyl chloride), and it may therefore be reasonable to assume that the 965 cm^{-1} band can be assigned to the $\gamma_t(\text{CH}_2)$ mode alone. The perpendicular 787 cm^{-1} band in the deuterated poly(vinyl chloride) probably corresponds to the perpendicular 965 cm^{-1} band of poly(vinyl chloride). In the deuterated poly(vinyl chloride)⁶ the parallel band which corresponds to the parallel 955 cm^{-1} band of poly(vinyl chloride) was not observed. The deuterated poly(vinyl chloride)⁶, however, was prepared with azo-bis-isobutyronitrile as catalyst at 50°C and therefore the polymer might be mainly amorphous. In a crystalline deuterated poly(vinyl chloride) the band which corresponds to the 955 cm^{-1} band of poly(vinyl chloride) may be expected to be seen. Consequently it may be reasonable to assume that the 965 and 955 cm^{-1} bands can both be assigned to the $\gamma_t(\text{CH}_2)$ modes. As we described above, since on crystallization the intensity of the

965 cm^{-1} band decreases and eventually disappears, the band may be assigned to the $\gamma_r(\text{CH}_2)$ mode which is presented in the amorphous regions. The $\gamma_r(\text{CH}_2)_o(\text{B}_2)$ and $\gamma_r(\text{CH}_2)_i(\text{B}_1)$ modes are infra-red active: the former mode should show parallel dichroism and the latter shows perpendicular dichroism. From its infra-red dichroism only, the 955 cm^{-1} band may be assigned to the $\gamma_r(\text{CH}_2)_o$ mode, but the mode may be observed as a very weak band, if it can be detected¹¹, and therefore the intensity of the band is too strong to be assigned to the $\gamma_r(\text{CH}_2)_o$ mode. Thus we assigned the 955 cm^{-1} band to the $\gamma_r(\text{CH}_2)_i$ mode, although its infra-red dichroism is questionable. However, the infra-red dichroism of the 955 cm^{-1} band may probably be affected by the degree of orientation or crystallinity of the polymer sample.

As can be seen in *Figure 2* or *3* the 1,092 cm^{-1} band involved another band at 1,097 cm^{-1} . The former (1,092 cm^{-1}) band showed perpendicular dichroism and the latter (1,097 cm^{-1}) band showed parallel dichroism. On crystallization the intensity of the 1,097 cm^{-1} band was enhanced. In the highly crystalline sample the intensity of the 1,097 cm^{-1} band is stronger than that of the 1,092 cm^{-1} band. These bands may probably be ascribed to the skeletal stretching modes^{6, 11}.

*Department of Synthetic Chemistry,
Faculty of Engineering, Kyoto University,
Yoshida, Kyoto, Japan*

(Received 27th April, 1960.

Revised version received 19th September, 1960)

REFERENCES

- ¹ GRISENTHWAITE, R. J. and HUNTER, R. F. *Chem. & Ind.* 1958, p. 719
- ² KRIMM, S., BERENS, A. R., FOLT, V. L. and SHIPMAN, J. J. *Chem. & Ind.* 1958, p. 1512
- ³ SHIMANOUCI, T., TSUCHIYA, T. and MIZUSHIMA, S. *J. chem. Phys.* 1959, **30**, 1365
- ⁴ GRISENTHWAITE, R. J. and HUNTER, R. F. *Chem. & Ind.* 1959, p. 433
- ⁵ KRIMM, S., BERENS, A. R., FOLT, V. L. and SHIPMAN, J. J. *Chem. & Ind.* 1959, p. 433
- ⁶ NARITA, S., ICHINOHE, S. and ENOMOTO, S. *J. Polym. Sci.* 1959, **37**, 237, 281
- ⁷ SHIMANOUCI, T., TSUCHIYA, S. and MIZUSHIMA, S. *Kobunshi Kagaku* 1958,, **8**, 202
- ⁸ KAWASAKI, A., SHIOTANI, S., FURUKAWA, J. and TSURUTA, T. *Bull. chem. Soc. Japan* 1959, **31**, 1149
- ⁹ FURUKAWA, J., TSURUTA, T., SHIOTANI, S. and KAWASAKI, A. *J. chem. Soc. Japan, Ind. Chem. Section*, 1959, **62**, 268
- ¹⁰ FURUKAWA, J., TSURUTA, T., KAWASAKI, A. and SHIOTANI, S. *J. chem. Soc. Japan, Ind. Chem. Section*, 1958, **61**, 1362
- ¹¹ KRIMM, S. and LIANG, C. Y. *J. Polym. Sci.* 1956, **22**, 95
- ¹² LIANG, C. Y., KRIMM, S. and SUTHERLAND, G. B. B. M. *J. chem. Phys.* 1956, **25**, 543

Anionic Polymerization of Styrene

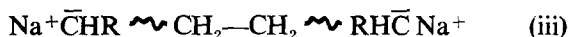
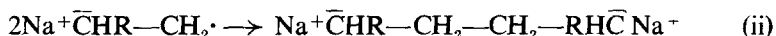
CYRIL STRETCH and GEOFFREY ALLEN

Polymerization of styrene initiated by sodium naphthalene in dioxane solution yields polymers with sharp molecular weight distributions and degrees of polymerization in agreement with Szwarc's mechanism. At complex concentrations of 10^{-3} mole l^{-1} the half-life of the reaction is approximately 2 min at room temperature. The overall activation energy is approximately 9 kcal mole $^{-1}$. The reaction rate is first order with respect to monomer and directly proportional to the concentration of complex. Anionic propagation appears to be the rate-controlling reaction.

POLYMERIZATION of vinyl monomers by sodium naphthalene in ethereal solutions is reported^{1,2} to involve electron transfer to the monomer,



followed by dimerization of the radical-ions and subsequently by anionic propagation:



No termination reaction occurs and the polymeric anions grow until equilibrium with residual monomer is attained. The implications of this mechanism are (a) an average degree of polymerization given by

$$\bar{P}_n = 2 \times \frac{\text{Number of molecules of monomer reacted}}{\text{Number of molecules of complex}} \quad (1)$$

and (b) an initial molecular weight distribution of the Poisson type followed by a relaxation to a 'most probable' distribution when the polymeric di-anions are allowed to remain in equilibrium with the monomer.

A number of recent publications³⁻⁵ have dealt with the polymerization of styrene (and in one instance⁶ of α -methylstyrene) initiated with sodium naphthalene in tetrahydrofuran solution. Provided that careful selection and control of the polymerization conditions are exercised it is clear that products with extremely sharp molecular weight distributions can be obtained. In particular Wenger³ has shown that in low temperature polymerizations it is advantageous to begin by treating the initiating complex with a small amount of monomer at room temperature, adding the rest of the monomer at the lower temperature. A one-step low temperature polymerization was satisfactory only when sodium biphenyl was used as the initiator.

Concurrently we have been investigating the styrene-sodium naphthalene system in solution in dioxane. Because the rate of polymerization is lower than in tetrahydrofuran, we are able to report both kinetic and molecular weight studies.

EXPERIMENTAL

Warhurst and Morantz⁷ have described in detail the precautions required for a quantitative investigation of the reactions of sodium-hydrocarbon complexes in dioxane. We have used similar apparatus and experimental techniques. Thus all operations involving the formation or reaction of naphthalene or polystyryl anions were carried out in a high-vacuum system which could be pumped to 10^{-5} mm Hg. Dry nitrogen, free from CO_2 and O_2 , was used to transfer the solutions within the apparatus.

Sodium naphthalene solutions

A stock solution of the complex was formed by siphoning a solution of naphthalene in dioxane on to a film of sodium which was freshly prepared by decomposing sodium azide crystals in an evacuated flask. The reagents were left in contact overnight and the green solution of $\text{Na}^+\text{C}_{10}\text{H}_8^-$ was then transferred through a glass sinter to a reservoir. Since the reaction between the naphthalene and the sodium film was not quantitative, the stock solution was standardized by titration with a solution of methyl iodide in dioxane.

In early experiments benzoic acid was used to standardize the stock solution but this reaction was non-stoichiometric.

Purification of styrene

Hydroquinone inhibitor was removed by washing twice with a 10 per cent solution of caustic potash, followed by 10 washes with equal quantities of water. Preliminary drying was effected by shaking overnight with barium oxide and then the monomer was passed through a column of 100-mesh chromatographic alumina and collected over more barium oxide. It was introduced into the main apparatus whilst still in contact with barium oxide, outgassed and then distilled freshly from its reservoir when required.

Polymerization reactions

Four identical reaction vessels equipped with magnetic stirrers were available for each run. They were charged with equal quantities of complex solution from the main reservoir and a standardization was performed on one sample, leaving three identical solutions for polymerization reactions. The absence of a significant amount of impurity was proved by titrating the red polystyryl anions produced by adding monomer to the sodium naphthalene solution. The concentration of styryl anions was < 2 per cent below that of the initiator solution.

For the purpose of testing the molecular weight relationships a series of polymers with molecular weights ranging from 2×10^4 to 2×10^5 was produced at room temperature.

Rapid addition of 1 to 4 ml of styrene to 20 or 40 ml of approximately 10^{-3} M solutions of sodium naphthalene was followed some ten minutes later by the addition of benzoic acid to terminate the polystyryl anions. This procedure allowed time for almost complete reaction and prevented appreciable relaxation of the molecular weight distribution. (Although the rate of depropagation is not accurately known, it must be very much lower

than the rate of propagation since at equilibrium the amount of free monomer is very small.) The polymers were precipitated by methanol, dried at 60°C, and weighed to ascertain that polymerization was quantitative within the limits of experimental error.

In kinetic runs three of the reaction vessels were charged with the same reaction mixture and the reaction was stopped after different time intervals by adding benzoic acid. The weight of polymer produced in each flask was determined and the molecular weights of the products were also measured to give independent estimates of the amounts of monomer consumed. All runs were performed at a constant monomer/solvent ratio (2 : 40 by volume) to avoid dielectric effects. Rate constants were measured in the range 11° to 40°C.

Molecular weight measurements

The molecular weights of all products were determined by viscometry in benzene solution at 25°C from the relation⁸

$$[\eta] = 1.12 \times 10^{-4} M_w^{0.73} \quad (2)$$

In three cases, where M_w was also determined by the light scattering technique, corresponding values agreed within experimental error. For six polymers M_n was determined; Ultracella filter *aller feinst* membranes were used in Pinner-Stabin-type osmometers, the solvent being benzene.

The molecular weight distributions for four polymers were analysed using a Baker-Williams⁹ gradient elution column. Molecular weight averages were also computed from these data, since

$$\bar{M}_w = \sum_i W_i M_i$$

$$\bar{M}_n = \left[\sum_i \left(\frac{W_i}{M_i} \right) \right]^{-1}$$

where W_i is the fractional weight and M_i the average molecular weight of the i th fraction. This type of analysis assumes that fractions with very sharp molecular weight distributions are isolated.

The probable error in molecular weight measurements is considered to be not greater than ± 10 per cent.

RESULTS

Molecular weight relationships

Table 1 summarizes the results of molecular weight measurements made on ten different samples; the ratio M_w/M_n is close to 1.0 for the majority of the samples and consistent with a Poisson-type distribution of molecular weight.

Three of these polymers were fractionated by the gradient elution technique and one by fractional precipitation. Of the former, sample 8 had a simple sharp distribution but the other two samples (6 and 7) had two-peak distributions. In both cases approximately 75 per cent of the polymer had a very sharp distribution ($M_w/M_n = 1.0$) centred at a molecular weight very close to that calculated from equation 1. The remaining

Table I. Molecular weight measurements*

Sample No.	$10^3 M$ (Eq. 1)	$10^3 M_n$		$10^3 M_w$		
		(a)	(b)	(b)	(c)	(d)
1	118				110	104
2	103	86			106	
3†	‡	103	106	166	163	170
4	75	68			71	
5	66	64			65	
6§	‡		42	52	56	
7§	‡‡		37	45	45	
8	‡		49	51	48	
9	40	31			35	
10	37	36			34	

* (a) Osmometry, (b) fractionation, (c) viscometry, (d) light scattering.

† Polymerized in viscous solution.

‡ Complex solution standardized with benzoic acid.

§ Two-peak distributions.

25 per cent appeared as a low molecular weight peak of half the calculated molecular weight. This minor peak could be attributed to a slow dimerization of the radical-ions [reaction (ii)] or to the presence of a radical scavenger which would prevent dimerization of some radical-ions. Since the main distribution is sharp and the molecular weight of the second peak is half of the expected value, we exclude the first possibility on the ground that it would lead to a broad molecular-weight distribution and a different relationship between the two components. The two polymers were in fact produced in consecutive runs from the same batch of monomer and we believe that an unidentified impurity caused the anomalous distributions. Wenger³ points out that a small secondary peak may be an integral feature of the reaction mechanism; unfortunately our fractionation data do not definitely resolve this point.

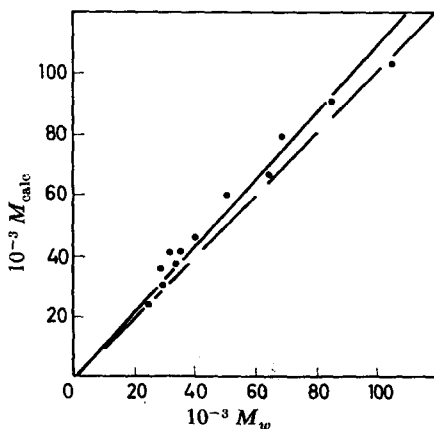


Figure 1—Comparison of observed (M_w) and calculated (M_{calc}) molecular weights

Sample 3 was polymerized in a solution which became viscous. For this polymer fractionation showed a single peak distribution with $M_w/M_n=1.5$ and it is probable that the reaction became diffusion-controlled owing to inadequate stirring. In subsequent experiments care was taken to regulate the viscosity of the solutions and broad distributions were not then encountered.

Since $M_n=M_w$ within experimental error, the validity of equation 1 can be tested by plotting the molecular weight measured viscometrically against the values calculated from the relative concentrations of monomer

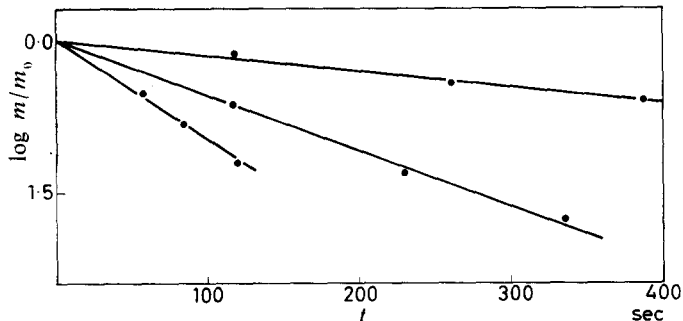


Figure 2—Typical kinetic runs showing the first-order dependence of reaction rate on monomer concentration

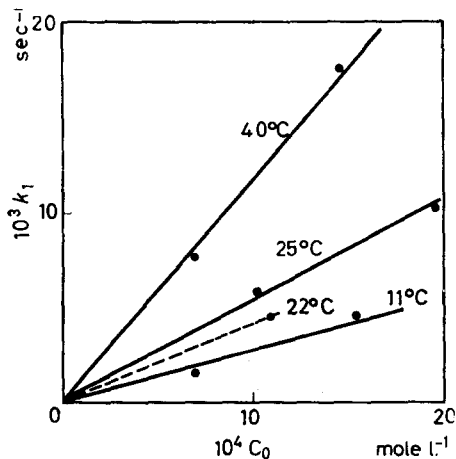


Figure 3—Plot of first-order rate constants (k_1) as a function of temperature and complex concentration (C_0)

and complex. *Figure 1* shows that the observed molecular weights are on the average lower by about 10 per cent but, in view of the experimental uncertainties associated with the use of equations 1 and 2, this can be regarded as satisfactory agreement.

Kinetic studies

Under our experimental conditions the reactions had a half-life of

approximately 2 min. The overall rate of polymerization determined

(a) from the rate of consumption of monomer

and

(b) from the molecular weights of the polymer produced after different time intervals,

was first-order with respect to monomer concentration (see *Figure 2*). At a given temperature, these first-order rate constants (k_1) were proportional to C_0 , the concentration of sodium naphthalene initiator, as shown in *Figure 3*. The temperature dependence of the second-order rate constants ($k_2 = k_1/C_0$) obtained from the slopes of the plots given in *Figure 3* gives

$$E_{\text{act.}} = 9 \pm 3 \text{ kcal mole}^{-1}$$

$$A = 10^7 \text{ l. mole}^{-1} \text{ sec}^{-1}$$

It will be noted that, because the reactions were very fast, the errors in the rate constants which arise mainly from the time required to mix the reactants (approx. 10 sec) were of the order of ± 15 per cent. Termination of polymerization could be determined more precisely since this corresponds to the disappearance of the red colour of the polystyryl anions.

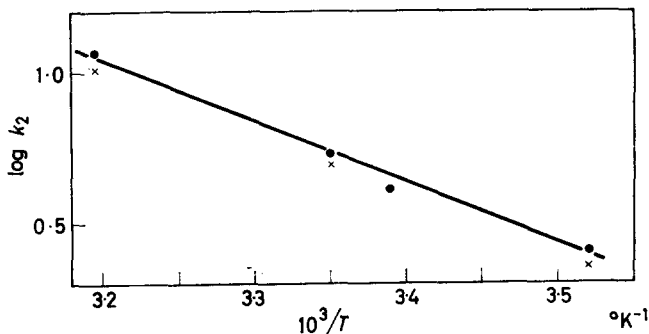


Figure 4—Temperature dependence of the second-order rate constants (k_2)

In a set of subsidiary experiments, the initiator was first treated with a drop of styrene (about 0.1 ml). The red solution was allowed to stand for 1 or 2 h to ensure a virtually complete dimerization of the radical-ions and then 2.0 ml of monomer was added. A series of kinetic runs was performed and the first- and second-order rate constants were determined. The second-order rate constants are included in *Table 2*; they are estimated to be reliable to ± 25 per cent.

Table 2. Second order rate constants (k_2 , $\text{l. mole}^{-1} \text{ sec}^{-1}$)*

Temp. (°C)	Sodium naphthalene		Polystyryl anions
	(a)	(b)	(b)
11.0	2.2	2.6	2.0
25.0	5.0	5.4	4.0
40.0	10.4	11.7	
Error (%)	± 15	± 15	± 25

*Calculated from (a) molecular weight data, (b) percentage conversion of monomer.

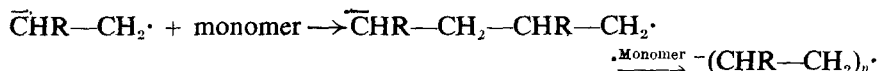
DISCUSSION

All our results are compatible with the mechanism proposed by Szwarc^{1,2}. The fact that equation 1 predicts the molecular weight of polystyrene produced in the sodium naphthalene-dioxane system demonstrates

- (a) that the initial electron transfer reaction is substantially complete, and
 (b) the absence of a termination reaction.

Since the molecular weight distributions are sharp (and, within experimental error, of the Poisson type) it is further implied that the initial electron transfer reaction (i) and also the dimerization reaction (ii) are both fast relative to the anionic propagation reaction (iii). These conclusions are substantiated by the observation that polymerization of styrene initiated by polystyryl di-anions proceeds at a rate closely similar to the overall rate of the reaction initiated by sodium naphthalene.

One minor modification required of Szwarc's mechanism seems to be the recognition that radical dimerization may also occur through poly-radical-ions. Levy and Szwarc¹⁰ conclude that in tetrahydrofuran solution styrene monomer radical-ions dimerize at a slow rate. Since the rate of radical reactions should be similar in tetrahydrofuran and dioxane this appears to be contrary to our conclusion given above. However, Szwarc and Levy point out that, unlike polymerization reactions, their experiments were carried out under conditions in which reactions of the type



are slow. Thus both sets of data can be reconciled if radical dimerization occurs through poly-radical-ions $-(\text{R}\cdot\text{CH}\cdot\text{CH}_2)_n\cdot$, provided that the bulk of the dimerization proceeds at low values of n . An independent argument leads Wenger³ to the same conclusion; he points out that the polymeric radical-ions will combine more rapidly than the monomeric species because of the true separation of charge in the former.

Anionic propagation

Although it seems clear that the overall rate of polymerization is principally determined by the rate of anionic propagation, it is possible that both free-radical and anionic propagation mechanisms operate in the early stages of polymerization. The amount of free-radical propagation will depend, of course, on the rate of dimerization of the radical-ions.

Consider the rate of consumption of monomer t seconds after initiation (assuming the latter to be complete and instantaneous), then

$$-\frac{dm}{dt} = k_1 mc + k_2 m C_0 \quad (3)$$

where m = concentration of monomer

c = concentration of radical ends

C_0 = concentration of initiating naphthalene ions

k_1 = rate constant for free radical propagation of styrene

k_2 = rate constant for anionic propagation of styrene

Let k_d be the bimolecular rate constant for the dimerization of the radical anions. Then, ignoring disproportionation and chain transfer reactions,

$$c = \frac{C_0}{(1 + k_d C_0 t)} \quad (4)$$

since C_0 will also be the initial concentration of radical ends. Integration of the equation obtained by substituting 4 in 3 gives

$$-\ln \frac{m}{m_0} = k_t C_0 t + \frac{k_t}{k_d} \ln (1 + k_d C_0 t) \quad (5)$$

from which the weight fraction of polymer produced by free-radical propagation (x_t) can be calculated. In computing x_t we have assumed:

$$\begin{aligned} k_t &= 20 \text{ l. mole}^{-1} \text{ sec}^{-1(12)} \\ k_i &= 5 \text{ l. mole}^{-1} \text{ sec}^{-1} \\ C_0 &= 1 \times 10^{-3} \text{ mole l.}^{-1} \end{aligned}$$

In selecting values for k_d we have been guided by the fact that k_d for uncharged polystyryl radicals is approximately¹¹ $10^7 \text{ l. mole}^{-1} \text{ sec}^{-1}$ and that the rate of dimerization of radical-ions may reasonably be expected to be slower. Values of x_t are presented in *Table 3* and, bearing in mind that our kinetic measurements were made in the time interval $t = 50$ to 400 sec , it will be seen that the amount of free-radical propagation can probably be ignored. This conclusion is further supported by our observation that the rate of polymerization is similar for initiation by naphthalene ions and polystyryl anions.

Table 3. Weight fraction (x_t) of polymer produced by free radical propagation

k_d (l. mole ⁻¹ sec ⁻¹)	t (sec)	x_t
10 ⁶	10	0.004
10 ⁵	10	0.027
10 ⁴	10	0.156
10 ⁴	50	0.052

Having identified the overall rate of polymerization as being essentially the rate of anionic propagation we must now consider the nature of the propagating species. In dioxane the sodium polystyryl salt will be incompletely dissociated and so anionic propagation may occur through the free anions or the ion pairs.

Case I—If the ion pair is inactive then the rate of polymerization is

$$\begin{aligned} -\frac{dm}{dt} &= k_2 m [\text{free anions}] \\ &= k_2 m K^{\frac{1}{2}} C_0^{\frac{1}{2}} \end{aligned} \quad (6)$$

where K is the dissociation constant of the salt (assumed to be only slightly dissociated):

Case II—When the anions and ion pairs are of the same order of reactivity or if the amount of free anion is negligibly small, then

$$-\frac{dm}{dt} = k_2''mC_0 \quad (7)$$

$$= k_1'm \quad (8)$$

since C_0 is constant in the absence of a termination reaction.

The overall reaction is first order with respect to monomer (cf. *Figure 3*) and the first-order rate constant is directly proportional to C_0 , suggesting that k_1 should be identified with k_1'' of equation 8. The second-order rate constant k_2 can then be identified with k_2'' in equation 7. The temperature dependence of k_2 gives an activation energy of 9 ± 3 kcal and pre-exponential factor of 10^7 l. mole⁻¹ sec⁻¹ for anionic propagation of styrene in dioxane.

Unfortunately, our results cannot be compared directly with other data relating to the polymerization of styrene. The only comparable data on anionic propagation are those of Worsfold and Bywater¹² for the polymerization of α -methylstyrene by sodium naphthalene in tetrahydrofuran. They report an activation energy of 2–3 kcal from the temperature dependence of the second-order rate constant (k_2'' in our notation). Both the monomer and the solvent will influence the rate of reaction and with the limited data available it is difficult to separate out the two factors.

No data for the free-radical propagation of styrene in dioxane have been published but in hydrocarbon solvents

$$E_{\text{act.}} \approx 7 \text{ kcal}$$

$$A \approx 10^6 \text{ l. mole}^{-1} \text{ sec}^{-1}$$

At room temperature the rate constant of the free-radical propagation step is somewhat higher than our value for anionic propagation. The overall rate of free-radical polymerization is lower, owing to the operation of chain-termination mechanisms which are absent from our system.

Our thanks are due to Mr M. N. Jones (Manchester) for molecular weight determinations and to Mr B. Robinson (Manchester) and Mr H. Burger (Physical Chemical Institute, Vienna University) for fractionation data. We also acknowledge helpful comments from Professor G. Gee, who suggested this work.

*The Chemistry Department,
The University of Manchester,
Manchester, 13*

(Received 22nd August, 1960)

REFERENCES

- ¹ SZWARC, M., LEVY, M. and MILKOVITCH, R. *J. Amer. chem. Soc.* 1956, **78**, 2656
- ² SZWARC, M. *Nature, Lond.* 1956, **178**, 1168
- ³ WENGER, F. *Makromol. Chem.* 1960, **34**, 200; 1960, **37**, 143
- ⁴ LYSSY, T. *Helv. chim. Acta*, 1959, **42**, 2245
- ⁵ MEYERHOFF, G. *Z. phys. Chem. (N.F.)*, 1960, **23**, 100

- ⁶ SIRIANNI, A. F., WORSFOLD, D. J. and BYWATER, S. *Trans. Faraday. Soc.* 1959, **55**, 2124
- ⁷ MORANTZ, D. and WARHURST, E. *Trans. Faraday Soc.* 1955, **51**, 1375
- ⁸ GREEN, J. H. S. *J. Polym. Sci.* 1959, **34**, 514
- ⁹ BAKER, D. D. and WILLIAMS, D. D. *J. chem. Soc.* 1956, p. 2352
- ¹⁰ LEVY, M. and SZWARC, M. *J. Amer. chem. Soc.* 1960, **82**, 521
- ¹¹ See, for example; BAMFORD, C. H., BARB, W., JENKINS, A. D. and ONYON, P. F. *The Kinetics of Vinyl Polymerization by Radical Mechanisms*, Butterworths, London, 1958, p. 71, Table 3.1
- ¹² WORSFOLD, D. J. and BYWATER, S. *Canad. J. Chem.* 1959, **36**, 1141

Physical and Mechanical Properties of Polypropylene Fractions

J. VAN SCHOOTEN, H. VAN HOORN and J. BOERMA

A large-scale fractionation of polypropylene according to molecular weight as well as to crystallinity has been carried out. The fractions obtained differed widely in properties. A fraction of low crystallinity, known as a 'stereoblock copolymer', possessed rubberlike properties. Evaluation of the fractions and of mixtures thereof showed that yield stress, dynamic modulus, drop in dynamic modulus at the transition point, mechanical damping and hardness depend only on the degree of crystallinity, whereas impact strength and elongation at break also depend on molecular weight and molecular weight distribution. A high impact strength requires a high molecular weight and a narrow molecular weight distribution. A correlation was found between tensile impact strength and loss factor at the glass transition point. The morphological structure of the various fractions is described.

THE RELATION between structure and properties of polypropylene has been extensively discussed in recent publications¹⁻³. These papers deal mainly with the effect of average crystallinity and average molecular weight on mechanical properties. However, it is known for other polymers, e.g. for polyethylene⁵, that molecular weight distribution and crystallinity distribution also influence the mechanical properties. In order to investigate the effect of these variables in the case of polypropylene a fractionation of polypropylene has been carried out on a preparative scale, which has yielded a number of fractions varying in average molecular weight and in average crystallinity. The results of the study of the properties of these fractions and of mixtures thereof are discussed below.

EXPERIMENTAL

Sample properties

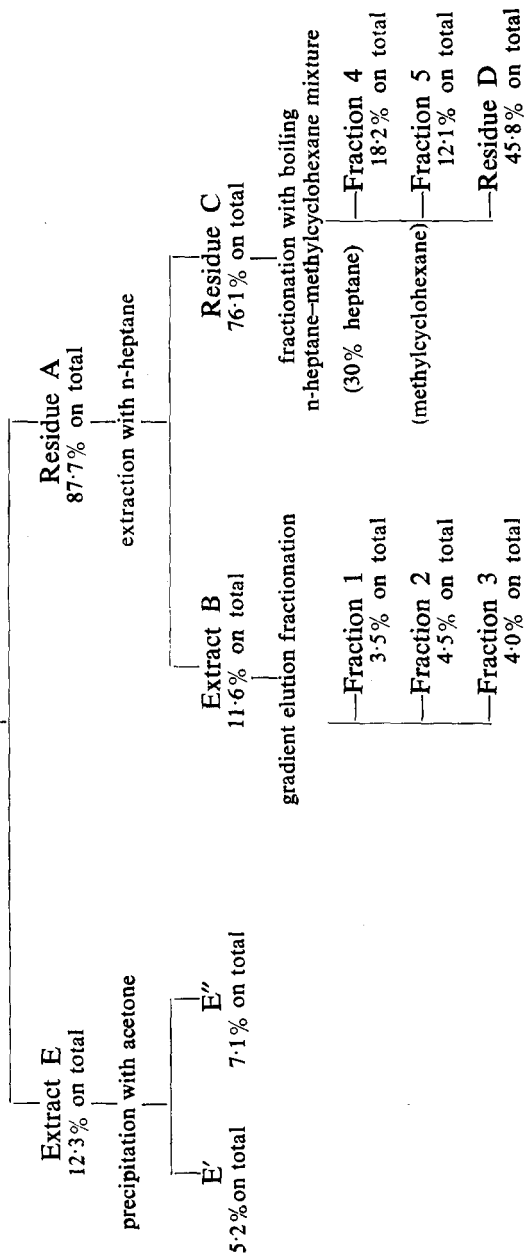
The sample used in this investigation was obtained with a γ -TiCl₃-AlEt₃ catalyst system. Some of its properties were: inherent viscosity (determined at 0.1% w/w in decalin at 135°C): 3.76, density at 20°C: 0.900.

General fractionation procedure

1000 g of polypropylene was first extracted with boiling ether (b.p. 34.6°C) in order to separate the amorphous, readily soluble material from the crystalline polymer. The ether extract was split into two fractions by partial precipitation with acetone. The crystalline residue was extracted with boiling n-heptane (b.p. 98.4°C). Extract and residue were fractionated according to molecular weight into three fractions each, the extract by elution fractionation using a column technique, the residue by successively boiling with an n-heptane-methylcyclohexane mixture (30/70) and methyl-

Table 1. Fractionation scheme

Sample M
extraction with ether



cyclohexane* (b.p. 100.3°C). The entire procedure can be represented by the schemes in *Table 1*.

Extraction with boiling solvents

(a) *Extraction with ether*—Four 250 g portions of polypropylene were boiled under reflux with 2 l. of ether on a steam bath for 1 h. The residue was filtered off on a fluted filter and extracted again. This was repeated till no more polymer was extracted. The extracts were combined and the ether removed by distillation. The ether extract (E) and residue (A) were then dried in a vacuum oven at room temperature. 50 g of the extract E was re-dissolved in ether and partly precipitated with acetone. After settling of the precipitate the clear supernatant liquid was removed by decantation. The precipitate was dried in a vacuum oven, giving fraction E', which was a rubbery solid. The non-precipitated part, isolated from the ether-acetone solution after evaporation of the solvents consisted of a waxy solid E'' which was not investigated further.

(b) *Extraction with n-heptane*—660 g of the ether residue A was extracted in four portions with boiling n-heptane with gentle stirring.

The residue was filtered through a fluted filter suspended in condensing heptane vapour. For this purpose, a 5-litre beaker was placed on an electric hot-plate on a thin sheet of asbestos. On top of this was placed a conical funnel with a short wide stem and a diameter only slightly larger than that of the beaker. The funnel was covered with a watch-glass. The heptane in the beaker was heated at such a rate that the condensing vapours barely reached the watch-glass.

The n-heptane extractions were repeated till no more precipitate was formed on dilution of the filtrate with an equal volume of acetone. The combined extracts were cooled to room temperature, diluted with acetone and the precipitate filtered off. The heptane extract B and residue C were dried in a vacuum oven at 60°C.

(c) *Extraction of residue C*—Two 75 g portions of the heptane residue C were extracted with a boiling heptane-methylcyclohexane (30/70) mixture in the same way as described under (b) for the heptane extraction. The extract (fraction 4) and the corresponding residue were also worked up in the same manner.

The combined residues of these extractions were now extracted with boiling methylcyclohexane, giving fraction 5 and residue D.

Fractionation of fraction B

Fraction B, which is known to be very heterogeneous⁴, was fractionated according to molecular weight in the manner described earlier.

In order to establish the conditions for the separation of fraction B into three sub-fractions of about equal size, a small-scale fractionation of 1 g of polymer was carried out first.

A solution of 1 g of fraction B in 86 ml of n-heptane at 100°C was mixed with 43 g of *Sil-O-Cel* (50–80 mesh), preheated to the same temperature.

*All solvents contained 0.1 per cent of Ionol (2,6-di-tert-butyl-4-methylphenol) as an antioxidant.

The mixture was then cooled to room temperature and the n-heptane removed by distillation in vacuum. The dry mixture was brought into the column filled with cold *Butylcarbitol** (boiling range 220–235°C). Elution was carried out at 150°C with *Butylcarbitol*–kerosine mixtures containing 0, 10, 20, 30 and 40 per cent of kerosine (boiling range 185–210°C), respectively (see *Table 2*).

Table 2. Analytical elution fractionation of fraction B
 Σw_i (inh. visc.)_i = 1.16, inherent viscosity of fraction B = 1.24

Fraction	Solvent 140 F in eluent (%)	Weight (%)	Inherent viscosity at 135°C (in decalin)	Crystallinity† (%)
i	0	28.7	0.20	50
ii	10	13.1	0.41	36
iii	20	26.0	0.74	30
iv	30	26.5	2.26	9
v	40	5.7	4.44	7

† According to infra-red spectrometry.

Subsequently, two 30 g portions of fraction B were fractionated as described above at 150°C with *Butylcarbitol*–kerosine mixtures containing 5, 20 and 50 per cent of kerosine, respectively.

General evaluation of the fractions

The fractions were evaluated by measuring inherent viscosity, percentage crystallinity (from density), melting point, melt index, tensile properties and tensile impact strength. Izod impact resistance measurements were only carried out on the total sample and on the two residues C and D.

All samples were stabilized with 0.2 per cent of 2246 [2, 2'-methylenebis(4-methyl-6-tert-butylphenol)].

(a) *Inherent viscosity*—The molecular weight of the fractions was estimated by measuring the viscosities of dilute solutions in decalin at 135°C in Ubbelohde viscometers. Instead of determining intrinsic viscosities by extrapolation of reduced or inherent viscosities to zero concentration we used inherent viscosities at a concentration of 0.100 g per 100 ml. The solutions were stabilized with 0.1 per cent of 2246.

(b) *Crystallinity*—The crystallinity of the fractions was determined from density according to Natta and co-workers⁶:

$$\text{Percentage crystallinity} = \frac{0.983 + 9(t + 180) \times 10^{-4} - 1/d}{4.8(t + 180) \times 10^{-6}}$$

where d = density measured at temperature t °C.

The densities of the fractions were determined on compression-moulded sheets at 23°C after 3 hours annealing at 130°C in a density-gradient column.

(c) *Melting point*—Melting points were determined on a hot-stage microscope as the temperature at which the birefringence between crossed

* Monobutyl ether of diethylene glycol (Carbide and Carbon Chemicals Company).

PROPERTIES OF POLYPROPYLENE FRACTIONS

nicols had completely disappeared. The samples were prepared by melting between microscope slides followed by crystallization for 3 h at 130°C.

(d) *Melt index*—The flow of the molten polymer is characterized by the melt index, determined according to a modified British Standard method BS 2782 I/C. The melt index is given in grammes extruded in 10 min and determined with a charge of about 4 g and a 2.16 kg weight at 250°C.

(e) *Tensile properties*—Yield stress, tensile strength and elongation at break were determined at 20°C according to BS 903 (dumb-bell C) with a cross-head speed of 10 cm/min.

(f) *Tensile impact strength*⁷—This test is a high-speed tensile test by impact on the free end of a dumb-bell, clamped at the other end. The test is carried out with dumb-bell C of BS 903 on a normal 40 kg cm Izod impact machine. The hammer of the machine swings in its normal course, but breaks the specimen in tension.

(g) *Izod impact strength*—This test is carried out on notched bars, according to BS 2782 Pt 3 (1957).

(h) *Shore hardness D*—The Shore hardness was measured according to ASTM method D 1484-57 T.

PHYSICAL AND MECHANICAL PROPERTIES OF FRACTIONS

Inherent viscosity, crystallinity and melting point

The results of the general evaluation are listed in *Table 3*.

Inherent viscosities were measured on the fractions as isolated as well as on the compression-moulded sheets*.

Table 3. Inherent viscosity, crystallinity and melting point of polypropylene fractions

Fraction	Inherent viscosity		Density (g/cm ³)	Crystal- linity (%)	Melting point (°C)
	Powder	Moulded sheet			
Total sample M	3.76	3.24	0.900	56	168–170
Ether extract E	0.69	—	0.861	4	—
Fraction E'	1.39	—	—	—	—
Ether residue A	4.26	3.91	0.904	61	168–170
n-Heptane extract B	1.24	1.23	0.887	39	150
fraction 1	0.17	0.18	0.907	65	154
fraction 2	0.63	0.64	0.886	38	142–144
fraction 3	2.70	2.75	0.871	18	~115
n-Heptane residue C	4.65	4.07	0.907	65	168–170
fraction 4	1.80	1.74	0.906	64	165–167
fraction 5	2.53	2.42	0.910	69	167–168
Me-cyclohexane residue D	6.08	4.65	0.909	68	170

Fraction E'', which is not mentioned in *Table 3*, was completely amorphous. Its inherent viscosity can be calculated from the inherent viscosities of the total extract and fraction E' to be about 0.17.

*The unexpectedly serious breakdown at the pressing temperature (230–250°C) has been the subject of a paper by J. van Schooten and P. W. O. Wijga presented at the Society of Chemical Industry Symposium on High Temperature Resistance and Thermal Degradation of Polymers, London, 21st–23rd September 1960.

The properties of the various fractions show very large differences. The ether extract is almost completely amorphous; the n-heptane residue, on the other hand, is highly crystalline, the n-heptane extract being of intermediate crystallinity. This extract could, however, be split up into three fractions of widely different molecular weight and crystallinity (see also Ref. 4). Fraction 1, having high crystallinity and low molecular weight, appeared to be very brittle; fraction 3, having low crystallinity and high molecular weight (stereoblock copolymer) had very distinct rubberlike properties, while fraction 2 was intermediate in crystallinity and molecular weight. The compensating effect of molecular weight and crystallinity on solubility is apparent from a comparison of the properties of fractions 1, 2 and 3.

TENSILE PROPERTIES, FLOW AND HARDNESS

The mechanical properties of the fractions are listed in *Table 4* and in *Figures 1-4*.

Table 4. Mechanical properties of the fractions

Fraction	Yield stress (kg/cm ²)	Tensile strength (kg/cm ²)	Elongation at break (%)	Set at break (%)	Tensile impact strength (kg cm/cm ²)	Izod impact strength (kg cm/cm ²)	Melt index at 250°C (g/10 min)	Shore hardness D
Total sample M	254	260	690	—	321	11.3	1.4	65
Ether residue A	336	369	680	—	161	7.0	0.9	70
n-Heptane extract B	102*	177	625	350	409	—	> 100	48
fraction 1	too brittle to measure							
fraction 2	100	101	500	280	409	—	too high	47
fraction 3	47*	222	710	25	flows	—	1.3	33
n-Heptane residue C	381	220	100	—	153	6.4	0.7	73
fraction 4	380	—	—†	—	70	—	~ 40	72
fraction 5	372	—	—†	—	103	—	7.3	72
Me-cyclohexane residue D	362	213	200	—	161	—	0.4	74

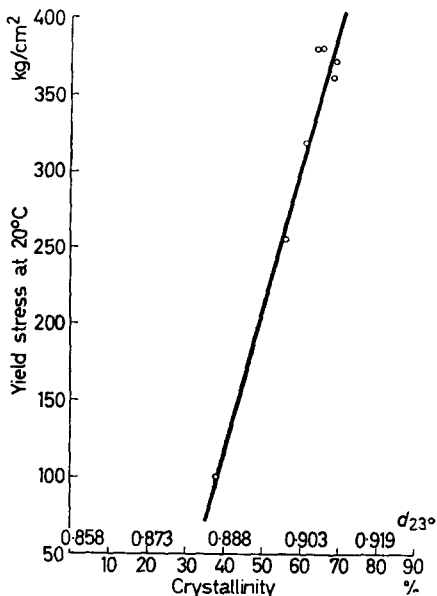
*No yield point, stress at 20 per cent elongation is reported here.
 †Break at yield point.

As was found earlier¹, the yield stress depends linearly on crystallinity (*Figure 1*). The same holds for the Shore hardness D (*Figure 2*). A linear relation between the logarithm of the melt index (measured at 250°C) and the inherent viscosity of the fractions¹ was found to hold roughly (see *Figure 3*). *Figure 3* also contains data on mixtures of fractions, which will be discussed below. The various relations can be expressed by the following formulae:

$$\begin{aligned} \text{Yield stress (kg/cm}^2\text{)} &= 9.18 \times \text{Percentage crystallinity} - 248 \\ \text{or Yield stress (kg/cm}^2\text{)} &= 11,430 \times \text{Density} - 10,030 \\ \text{Shore hardness D} &= 0.88 \times \text{Percentage crystallinity} + 15.3 \\ \text{or Shore hardness D} &= 1,098 \times \text{Density} - 927 \\ \log \text{ MI (250}^\circ\text{C)} &= 2.725 - 0.704 \times \text{Inherent viscosity} \end{aligned}$$

The data of *Table 4* further show that the tensile impact strength is strongly dependent on both crystallinity and molecular weight. While at

Figure 1—Relation between yield stress and crystallinity of polypropylene fractions



roughly constant crystallinity it increases with increasing molecular weight (Figure 4), the data taken from Table 4 and collected in Table 5 clearly show that at constant inherent viscosity it greatly increases with decreasing crystallinity. Furthermore, it is interesting to compare the properties of the ether residue A with those of the heptane residue C, the latter being essentially A from which the medium crystalline material (extract B) has

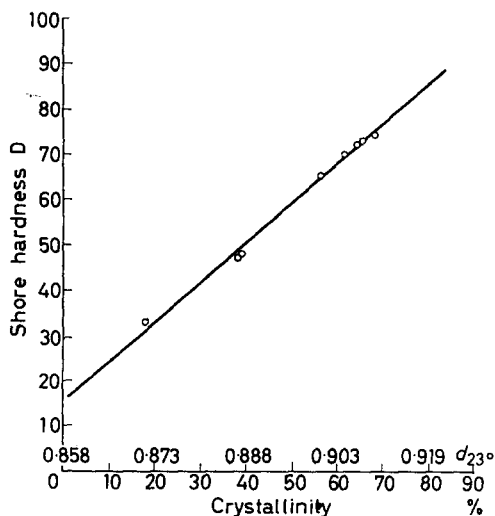


Figure 2—Relation between Shore hardness D and crystallinity

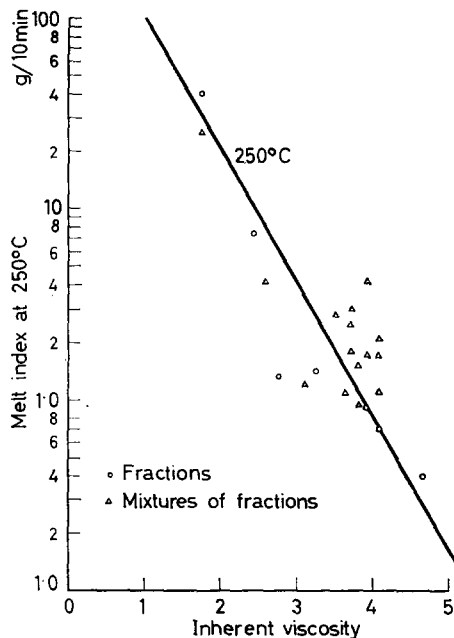
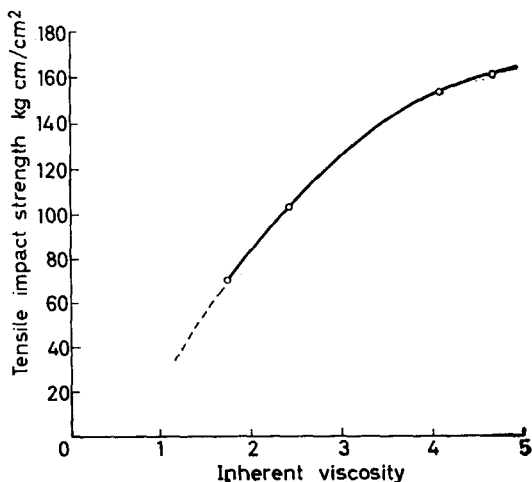


Figure 3—Relation between melt index and inherent viscosity

been removed (Table 6). This removal results in a slight increase in crystallinity and yield stress, a small decrease in tensile impact strength, but a very large decrease in tensile strength and ultimate elongation.

Evidently, the presence of B has a favourable effect on the tensile properties of highly crystalline polymer. However, the very heterogeneous nature of this fraction rendered it desirable to investigate separately the contribu-

Figure 4—Relation between tensile impact strength and inherent viscosity for highly crystalline fractions (yield stress 360–380 kg/cm²)



PROPERTIES OF POLYPROPYLENE FRACTIONS

Table 5. Tensile impact strength as influenced by crystallinity

Inherent viscosity	Crystallinity (%)			
	67	56	39	18
3.24	132*	321		
2.75	116*			flows
1.23	35*		409	

*Taken from Figure 4

Table 6. Comparison of properties of residues A and C

Residue	Crystallinity (%)	Yield stress (kg/cm ²)	Tensile strength (kg/cm ²)	Elongation at break (%)	Tensile impact strength (kg cm/cm ²)	Izod impact strength (kg cm/cm ²)
A (=C+B)	61	336	369	680	161	7.0
C (=A-B)	65	381	220	100	153	6.4

tion of its various components to the mechanical properties when added to C.

MECHANICAL PROPERTIES OF MIXTURES OF FRACTIONS

The influence of molecular weight distribution and of crystallinity distribution on product properties was studied on mixtures of fractions. The composition and properties of the mixtures and of their components are given in Table 7.

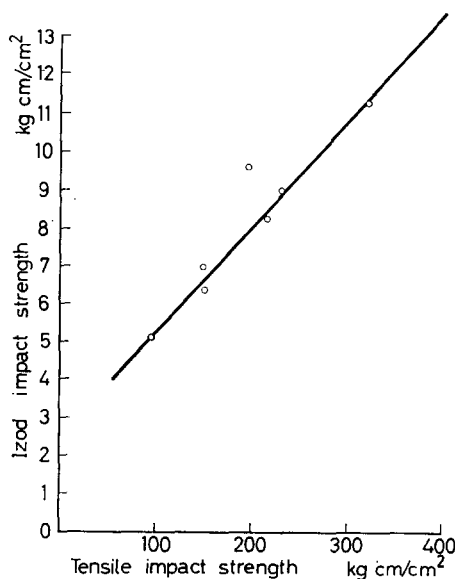


Figure 5—Relation between Izod and tensile impact strengths

Table 7. Properties of mixtures of fractions and of their components

Sample designation	Composition	Inherent visc.		Density (g/cm ³)	Crystal- linity (%)	Yield stress (kg/cm ²)	Tensile strength (kg/cm ²)	Elongation at break (%)	Tensile impact strength (kgcm/cm ²)	Melt index at 250°C (g/10 min)	Shard hardness D	Izod† impact strength (kgcm/cm ²)
		Moulded sheet	Impact bar									
E	See Table 3*	—	—	0.861	4	—	—	—	—	—	—	—
E'	—	—	—	—	—	—	—	—	—	—	—	—
C	See Table 3	4.07	3.87	0.907	65	381	220	100	153	0.7	73	6.4
D	"	4.65	—	0.909	68	362	213	200	161	0.4	74	(6.9)
1	"	0.18	—	0.907	65	too brittle	—	—	—	—	—	—
3	"	2.75	—	0.871	18	47	222	710	flows	1.3	33	—
4	"	1.74	—	0.906	64	380	†	—	70	~40	72	(4.3)
5	"	2.42	—	0.910	69	372	†	—	103	7.3	72	(5.3)
MA	97.5% C + 2.5% E	3.90	—	0.907	65	379	†	—	149	4.2	74	(6.4)
MB	95.0% C + 5.0% E	3.70	—	—	—	340	240	80	186	3.0	72	(7.5)
MC	92.5% C + 7.5% E	3.63	—	—	—	297	297	680	217	1.1	72	8.6
MD	85.0% C + 15.0% E	3.69	3.93	0.902	59	321	—	666	230	1.8	68	9.0
ME	95.0% C + 5.0% E	4.03	3.58	0.906	64	360	—	—	167	2.1	72	(7.1)
MF	90.0% C + 10.0% E	4.05	—	0.904	61	340	260	420	197	1.7	71	9.6
MG	85.0% C + 15.0% E	3.80	—	0.903	60	317	338	670	252	0.94	69	(9.4)
MH	95.0% C + 5.0% E	3.90	—	0.908	66	392	—	—	128	1.75	74	(5.9)
MI	90.0% C + 10.0% E	3.69	3.49	0.907	65	379	—	—	97	2.5	74	5.1
MJ	85.0% C + 15.0% E	3.49	—	0.908	66	378	—	—	80	2.8	74	(4.6)
MK	90.0% C + 10.0% E	1.74	—	0.906	64	340	—	—	125	~25	69	(5.9)
MM	50.0% C + 50.0% D	3.10	—	0.906	64	363	—	—	98	1.4	73	(5.1)
MN	30.0% C + 70.0% D	4.07	—	0.909	68	363	—	—	113	1.1	74	(5.6)
MO	70.0% C + 30.0% D	—	—	0.898	54	257	196	330	151	4.2	62	(6.6)
ML	90.0% C + 10.0% E'	3.78	—	0.905	62.5	317	216	250	239	1.5	69	(9.0)

† Figures in parentheses have been estimated with the aid of Figure 3

‡ Sample breaks at yield point

* See Table 1

Most of the fractions were too small for their Izod impact strength to be measured. Therefore, tensile impact strength was measured on all samples and Izod impact resistance on only a few. From these data a curve relating Izod and tensile impact strength was constructed (*Figure 5*).

The effect of various additions to the heptane residue C on yield stress and on tensile impact strength is illustrated in *Figure 6*. Addition of highly crystalline material of low molecular weight is seen to have a deleterious effect on impact strength without, however, affecting the yield stress. Addition of amorphous polymer or stereoblock copolymer lowers the yield stress, but results in a marked gain in impact strength. These additions also result in an increase in tensile strength and ultimate elongation.

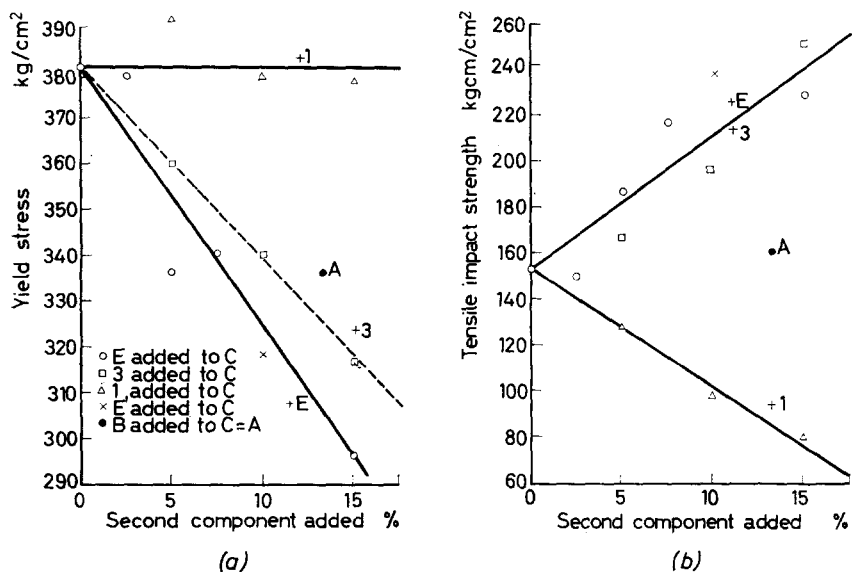


Figure 6—Influence of addition of a second component to residue C on (a) yield stress and (b) tensile impact strength

Reverting to the difference between residues A and C we find that A has a definitely lower yield stress as compared with C owing to the presence of the stereoblock copolymer, with only a marginally better impact strength. This small difference is evidently due to the simultaneous presence of low-molecular-weight, highly crystalline material (fraction 1), whose absence is therefore even more important than the presence of material of low crystallinity to attain superior impact properties.

The relationship between tensile impact strength and inherent viscosity for the various mixtures and their components is given in *Figure 7*.

Here again the favourable effect of addition of amorphous polymer, E, or stereoblock copolymer, fraction 3, is demonstrated, although at additive concentrations higher than 10 per cent this gain is accompanied by a definite decrease in yield stress.

Two types of mixtures shown in *Figure 7* have about constant yield stress, viz. the mixtures of heptane residue C and fraction 1 and the mixtures of

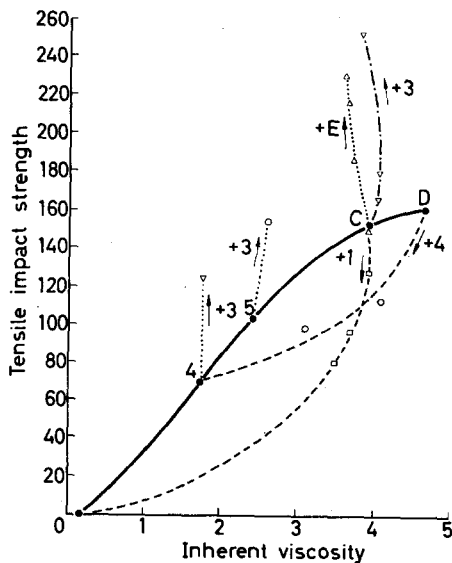


Figure 7—Tensile impact strength as a function of inherent viscosity

fractions D and 4. In these cases all mixtures appear to have lower tensile impact strengths than is to be expected at comparable inherent viscosity levels from the curve obtained for the individual fractions. This leads to the conclusion that a wide molecular weight distribution will be detrimental to optimum impact properties at constant crystallinity or yield stress.

There seems to be a tendency for mixtures to have higher melt indices than the fractions of equal inherent viscosity (see *Figure 3*). This might indicate that at equal viscosity-average molecular weight a wider molecular weight distribution gives better flow properties.

DYNAMIC MODULI AND MECHANICAL LOSS FACTORS

Most of the fractions and some of their mixtures have been tested for their dynamic mechanical behaviour in the temperature range from -30°C to $+50^{\circ}\text{C}$. Modulus of elasticity and mechanical damping were measured in bending vibration experiments in the frequency range $20\text{--}120\text{ sec}^{-1}$. The technique used was similar to that described in the literature^{8, 9}.

Figure 8 shows a typical example of the results. The data on all samples have been collected in *Table 8*. Three values are given for both modulus (E) and mechanical damping ($\tan \delta$): those at -30°C and $+50^{\circ}\text{C}$ and those measured at the temperature (T_p) where the major damping peak was found. The last-mentioned values are denoted as E_p and $\tan \delta_p$. In addition, the values of T_p and the frequencies at which the damping peak values were measured are given.

Temperatures of damping maximum

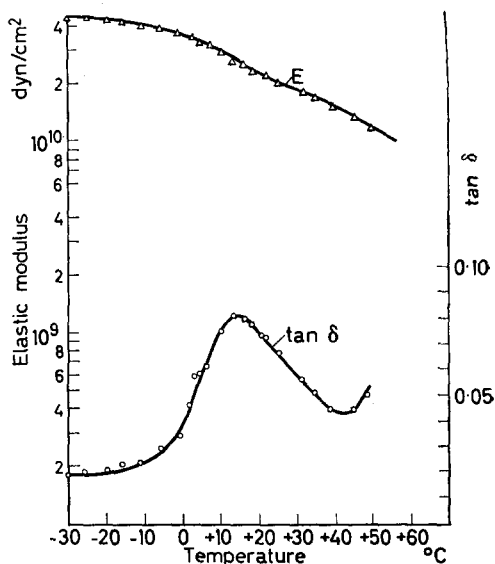
The differences found between the temperatures T_p for the various fractions amount to a few degrees centigrade only. The comparatively low

PROPERTIES OF POLYPROPYLENE FRACTIONS

Table 8. Dynamic modulus and mechanical loss factor measurements

Sample	Inherent viscosity	Density (g/cm ³)	Crystallinity (%)	T _p (°C)	Frequency at T _p (sec ⁻¹)	Elastic modulus (10 ⁹ dyne/cm ²)			Mechanical damping (tan δ)			Remarks
						at -30°C	at +50°C	at T _p	at -30°C	at +50°C	at T _p	
Total sample M	3.24	0.900	56	8	51	28	5.0	15	0.015	0.07	0.145	too brittle for sample preparation
Ether residue A	3.50	0.904	61	12	43	45	10.5	26	0.015	0.05	0.091	
n-Heptane extract B	1.23	0.887	39	12	60	28	1.2	7.5	0.014	0.09	0.304	
Fraction 1	0.184	0.907	65									
Fraction 2	0.64	0.886	38	12	69	28	1.0	7.0	0.014	0.11	0.336	damping not measurable above -2°C
Fraction 3	2.75	0.871	18			3	<0.4	~1.4	0.022	—	≥0.3	
n-Heptane residue C	3.92	0.907	65	15	49	35	9.0	21	0.025	0.05	0.076	=D ₁ after annealing for 2 h at 130°C
Fraction 4	1.74	0.906	64	14	76	30	8.0	17	0.025	0.048	0.085	
Fraction 5	2.42	0.910	69	14	57	38	10.0	22	0.025	0.045	0.074	
Residue D	4.65	0.909	68	14	56	41	12.5	26	0.030	0.04	0.085	
Residue D	4.65	0.911	70	14	57	48	14	30	0.025	0.04	0.078	
MH=95% residue C + 5% fraction 1	3.90	0.908	66	13.8	47.5	45	13	25	0.018	0.05	0.083	considerable spread in measured values
MI=90% residue C + 10% fraction 1	3.69	0.907	65	13.5	52	45	12.6	28	0.015	0.04	0.074	
MJ=85% residue C + 15% fraction 1	3.49	0.908	66	14.5	53.5	45	12.2	25	0.015	0.04	0.075	
ME=95% residue C + 5% fraction 3	4.03	0.906	64	14	45	45	11	26	0.020	0.051	0.080	
MF=90% residue C + 10% fraction 3	4.05	0.904	61	13	45	46	10.5	25.5	0.021	0.052	0.097	
MG=85% residue C + 15% fraction 3	3.80	0.903	60	14.8	40	38	8.1	17.4	0.022	0.057	0.109	
ML=90% residue C + 10% fraction E'	3.78	0.905	62.5	11	50	39	9.5	22	0.020	0.045	0.105	
MO=70% residue 5 + 30% fraction 3	2.58	0.898	54	12	60	40	7.0	20	0.023	0.054	0.127	

Figure 8—Measurement of elastic modulus and mechanical loss factor (mixture ME, see Table 7)



value found for the total sample M can be ascribed to the presence of the low-molecular-weight amorphous material. Extraction of low-molecular-weight amorphous and medium-crystalline polymer, resulting in products A and C, leads to higher peak temperatures. This is in line with earlier results (unpublished) from torsional vibration experiments, where for strongly crystalline material a higher peak temperature was found than for amorphous samples. However, in that case the damping maxima were found at temperatures around 0°C owing to the lower frequencies employed ($\sim 0.1 \text{ sec}^{-1}$).

Modulus values

Around the transition point large changes in modulus value occur. The percentage change correlates with crystallinity, as is shown in Figure 9,

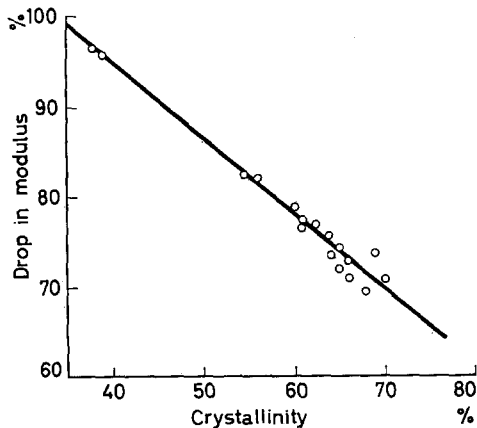


Figure 9—Relation between drop in elastic modulus from -30°C to +50°C and crystallinity

where the percentage drop relative to the value at -30°C is plotted against percentage crystallinity.

Damping values

The transition point is characterized also by a maximum of the mechanical damping or loss factor. The height of the maximum or its value corrected for background* correlates with crystallinity, as shown in *Figure 10*. A similar relation is obtained when the differences in damping at -30°C and $+50^{\circ}\text{C}$ are plotted against crystallinity.

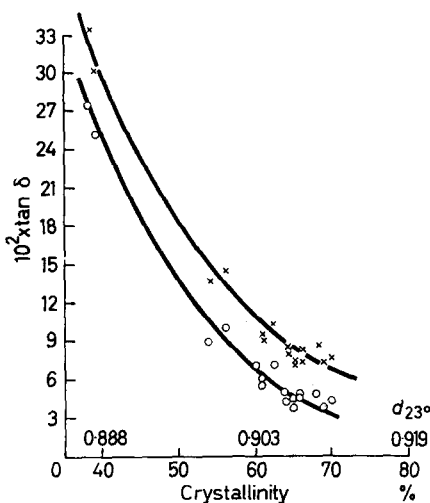


Figure 10—x, Relation between mechanical damping at the transition temperature and crystallinity; o, Corrected damping peak value as a function of crystallinity

Apparently, the damping is caused mainly by the amorphous parts of the polymer. It is known already that in amorphous polymers large damping peaks occur at the glass-rubber transition^{8, 10} and moreover that in partly crystalline polymers the height of the damping peak is proportional to the non-crystalline part of the polymer^{8, 11}.

Impact resistance in relation to mechanical damping

Although there exists no general theory describing breaking phenomena, the dissipation of energy in shock loading may reasonably be expected to be closely related to that in loading cycles, as studied in vibration techniques. A detailed analysis of this relationship would require knowledge of modulus and loss factor over a wide range of frequencies; the present study constitutes a first step in this direction.

To this end tensile impact data have been compared with mechanical damping peak value. As appears from *Figure 11*, there is general correlation, in that low loss factors are found for fractions with a low tensile impact resistance, which confirms the above expectation.

*The mean value of $\tan \delta$ at -30°C and $+50^{\circ}\text{C}$ was used as 'background'.

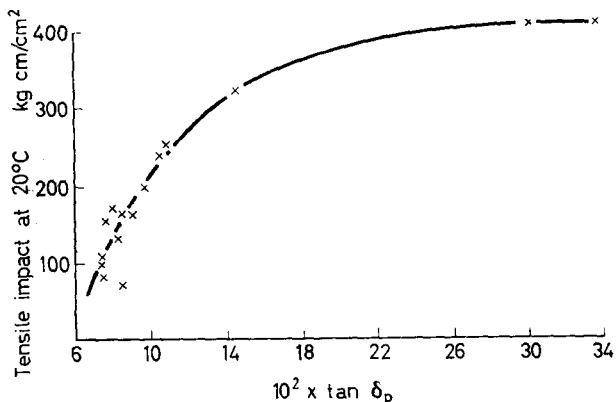


Figure 11—Tensile impact strength versus damping peak value

A closer consideration of the results obtained on the fractions of relatively high crystallinity shows that there is still some spread in the values around the drawn line. From *Figure 7* it may be expected that not only damping but also molecular weight influences impact resistance. Several attempts were made to find a relationship between tensile impact and a mixed function of inherent viscosity and $\tan \delta$, but so far these have been only partly successful.

There is, however, good reason to believe that the use of a lower molecular-weight average, such as the number-average molecular weight, might be more successful. On the other hand, there are indications, that higher-frequency damping, which is to a large extent equivalent to low-temperature damping, may have to be considered more closely in connection with the short loading times involved in impact testing.



Figure 12—Total sample M, crystallized at 130°C, between crossed nicols ($\times 62$)

MORPHOLOGICAL STRUCTURE OF THE FRACTIONS *

In order to illustrate the differences in crystalline structure of the various fractions a number of photographs are given of thin samples under the polarizing microscope between crossed nicols. The thin films were made



Figure 13—Ether residue A, crystallized at 130°C, between crossed nicols ($\times 62$)

by heating a small quantity of the carefully dried polymer at about 230°C on an electrically heated plate between an object and cover glass and pressing to a thin film. This temperature was considered high enough to destroy any 'memory' of its previous structure.

Figures 12-20 are photographs of samples crystallized for three hours at 130°C. Sample M, ether residue A, fractions 4, 5 and D show large

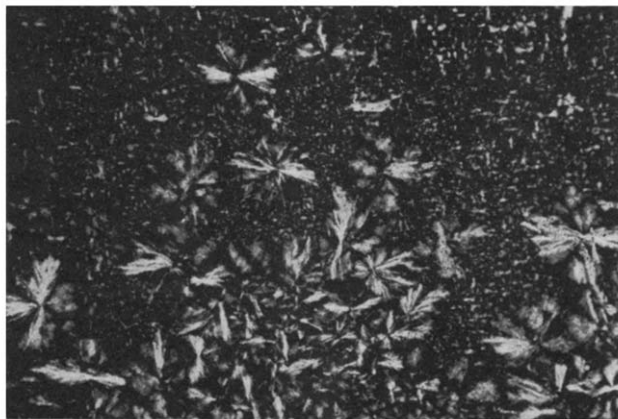


Figure 14—n-Heptane extract B, crystallized at 130°C, between crossed nicols ($\times 62$)

*Identical results on similar fractions were first observed by Dr G. Schuur (private communication).

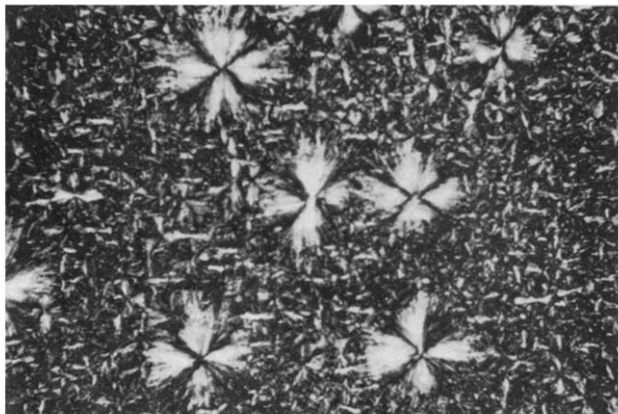


Figure 15—Fraction 1, crystallized at 130°C, between crossed nicols ($\times 62$)

spherulites, of which it is difficult to say whether they are positive or negative. These spherulites are called 'mixed' forms by Padden and Keith¹². There is a definite trend for the spherulite size to be larger for the lower-molecular-weight fractions. In the samples A, 4 and 5 smaller, brighter spherulites are also observed. These are of the form designated type III by Padden and Keith.

Fractions B, 1 and 2 show large positive spherulites, consisting of needles (*Figures 14–16*), called type I spherulites by Padden and Keith. This type appears to be formed especially in highly crystalline fractions of low molecular weight. The larger spherulites in *Figures 14–16* have probably



Figure 16—Fraction 2, crystallized at 130°C, between crossed nicols ($\times 62$)

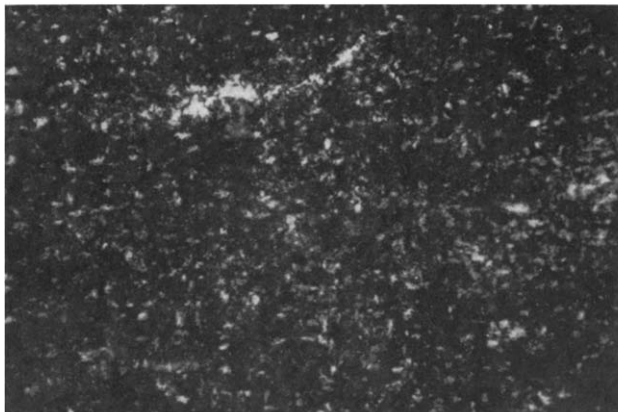


Figure 17—Fraction 3, crystallized at 100°C, between crossed nicols ($\times 62$)



Figure 18—Fraction 4, crystallized at 130°C; between crossed nicols ($\times 62$)



Figure 19—Fraction 5, crystallized at 130°C, between crossed nicols ($\times 62$)

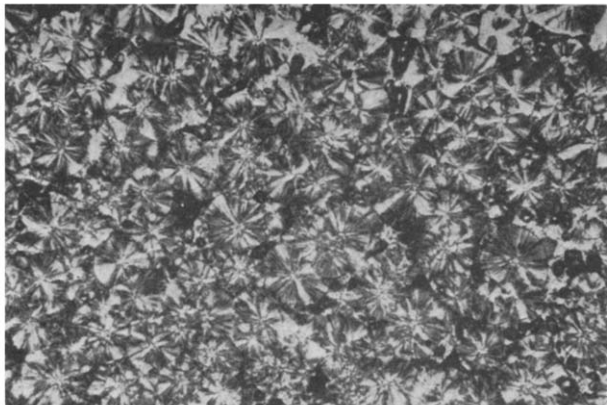


Figure 20—Fraction D, crystallized at 130°C, between crossed nicols ($\times 62$)

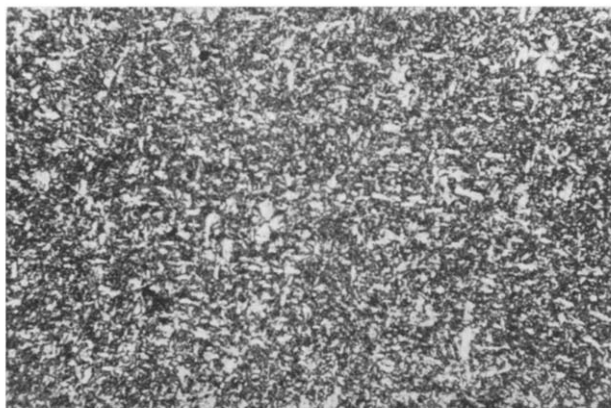


Figure 21—Fraction 1, cooled in air, between crossed nicols ($\times 62$)



Figure 22—Fraction 2, cooled in air, between crossed nicols ($\times 62$)

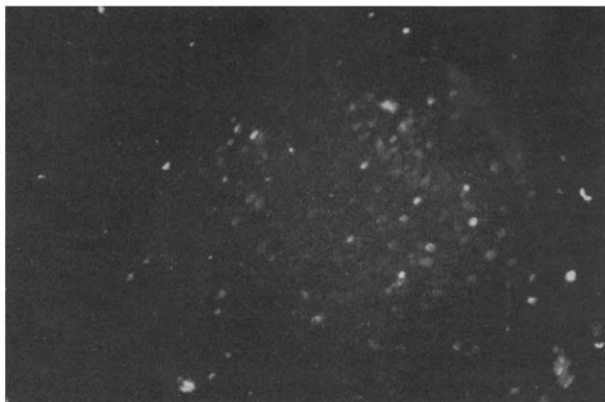


Figure 23—Fraction 3, cooled in air, between crossed nicols ($\times 62$)

been formed at 130°C , whereas the finer structure has been formed during cooling.

Fraction 3 did not crystallize at all at 130°C and showed only a grainy structure when crystallized for 3 h at 100°C (Figure 17).

In Figures 21–26 the structure is shown of samples which were cooled in air after melting on a glass slide. The structure of the lower-molecular-weight fractions is still rather coarse (Figures 21 and 24). Fraction 3 is hardly crystallized (Figure 23). The higher-molecular-weight fractions 5 and D showed a large number of type-III spherulites when prepared in this way, whereas in fraction 4 only a few type-III spherulites are formed. This suggests that type-III spherulites are formed more readily in higher-molecular-weight polymer.

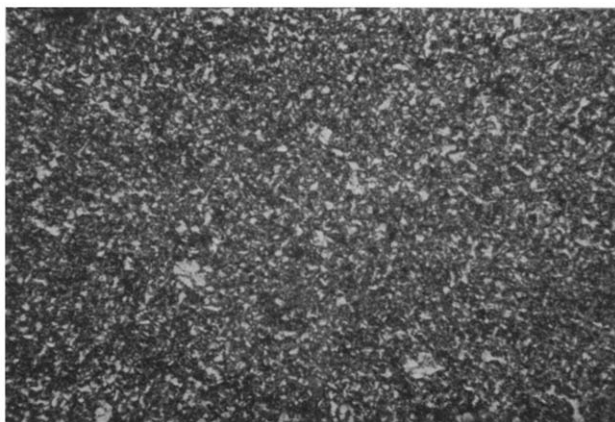


Figure 24—Fraction 4, cooled slowly in air, between crossed nicols ($\times 62$)

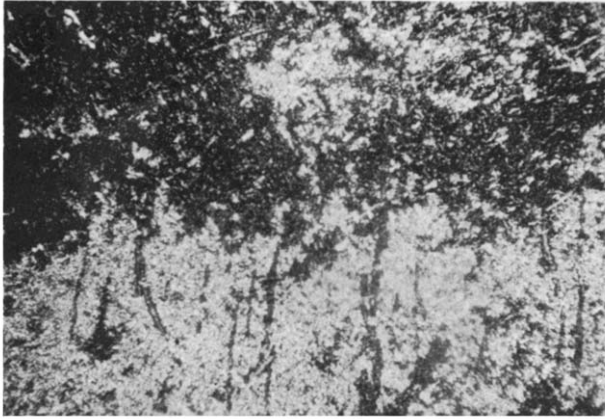


Figure 25—Fraction 5, cooled slowly in air, between crossed nicols ($\times 62$)

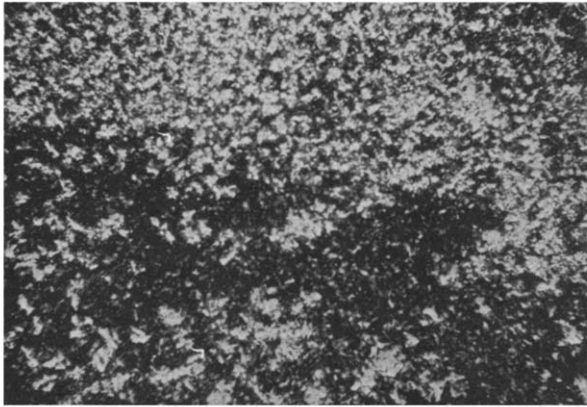


Figure 26—Fraction D, cooled slowly in air, between crossed nicols ($\times 62$)

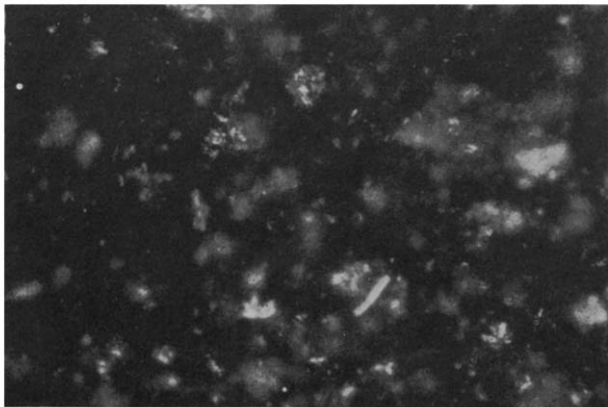


Figure 27—Moulded sheet of fraction 1, between crossed nicols ($\times 62$)

The structure of the compression-moulded sheets was examined for a few fractions by cutting thin slices with a microtome. The samples and the knife of the microtome were cooled in solid carbon dioxide before cutting. Because fraction 1 was too brittle to allow cutting with a microtome, the compression-moulded sheet was examined as such (*Figures 27-30*). It is

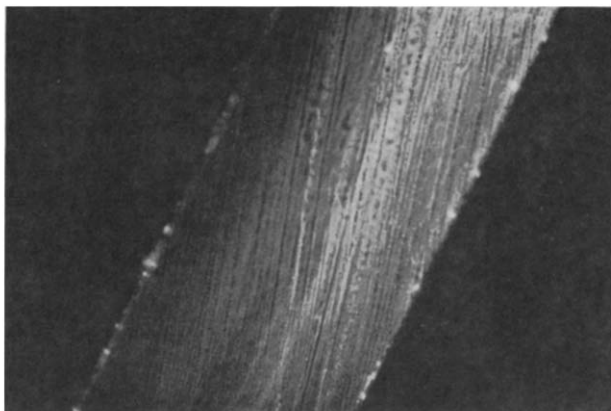


Figure 28—Microtome section of moulded sheet of fraction 3, between crossed nicols ($\times 62$)

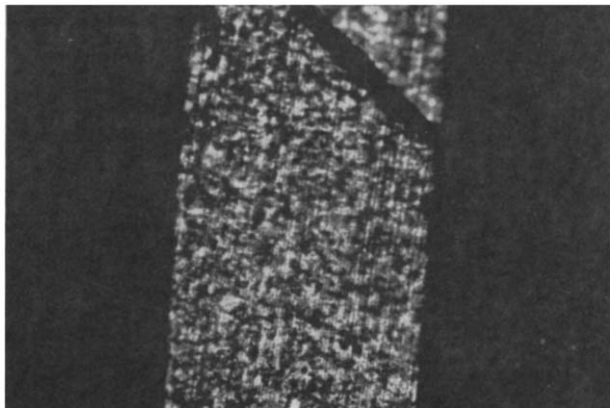


Figure 29—Microtome section of moulded sheet of ether residue A, between crossed nicols ($\times 62$)

still possible to see that a rather coarse crystalline structure is present in fraction 1. Fraction D contains type-III spherulites, which were not found in the microtome cuttings of the lower-molecular-weight fractions.

The differences found in spherulitic structure go hand in hand with differences in mechanical properties, e.g. the tensile impact resistance is higher according as the spherulite size is smaller, for fractions of equal crystallinity (see fractions 4, 5 and D).

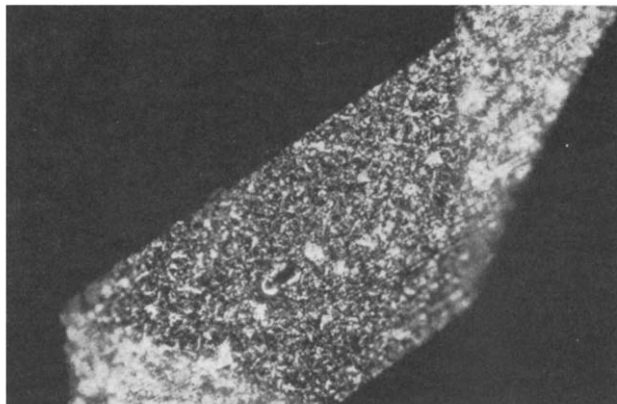


Figure 30—Microtome section of moulded sheet of fraction D, between crossed nicols ($\times 62$)

Furthermore, the lower-molecular-weight fractions, which cause brittleness, crystallize easily in large positive spherulites.

The differences in spherulitic structure are also reflected in differences in the X-ray diagrams, as will be discussed in a separate paper¹³.

The authors wish to thank Dr P. W. O. Wijga for discussions in the course of this investigation and for his helpful comments.

*Koninklijke/Shell-Laboratorium, Amsterdam,
(Shell Internationale Research Maatschappij, N.V.),
Badhuisweg 3, Amsterdam-N, Holland*

(Received 26th October, 1960.

Revised version received 28th November, 1960)

REFERENCES

- ¹ WIJGA, P. W. O. Paper presented at The Physical Properties of Polymers, Society Chemical Industry Symposium, London, 15th–17th April 1958
- ² GOPPEL, J. M. Paper presented at the International Plastics Convention, London, 17th–27th June 1959.
- ³ CRESPI, G. and RANALLI, F. *Trans. Plast. Inst., Lond.* 1959, **27**, No. 68, 55–73
- ⁴ WIJGA, P. W. O., VAN SCHOOTEN, J. and BOERMA, J. *Makromol. Chem.* 1960, **36**, 115–132
- ⁵ TUNG, L. H. *S.P.E. JI*, 1959, **14** (7), 25–28
- ⁶ DANUSSO, F., MORAGLIO, G. and NATTA, G. *Industr. Plast. mod.* Jan. 1958, p. 40
- ⁷ BRAGLAW, C. G. *Mod. Plast.* 1956, **34**, 199
- ⁸ WOODWARD, A. E. and SAUER, J. A. 'The dynamic mechanical properties of high polymers at low temperatures', *Fortschr. Hochpolym. Forsch.* Bd 1, pp. 114 ff
- ⁹ ATKINSON, E. B. and EAGLING, R. F. 'Some applications of dynamic elastic measurements in polymer systems', paper presented at The Physical Properties of Polymers, Society of Chemical Industry Symposium, London, 15th–17th April 1958 *Preprints* p. 99
- ¹⁰ STUART, H. A. *Die Physik der Hochpolymeren*, Vol. IV, Springer: Berlin, 1956, pp. 48–53
- ¹¹ McCRUM, N. G. *J. Polym. Sci.* 1959, **34**, 355–369
- ¹² PADDEN Jr., F. J. and KEITH, H. D. *J. appl. Phys.* 1959, **30**, 1479
- ¹³ ADDINK, E. J. (Miss) and BEINTEMA, J. *Polymer*, 1961, **2** (2), 185

Polymorphism of Crystalline Polypropylene

(MISS) E. J. ADDINK and J. BEINTEMA

The X-ray diagrams of polypropylene specimens of widely varying properties have revealed the existence of three modifications besides the normal modification studied by Natta and co-workers. One of these modifications has been described in the literature. For this modification a modified tentative structure is proposed which is more consistent with the available data than the tentative structure suggested in the literature.

INTRODUCTION

IN THE course of the work on polypropylene carried out in this Laboratory several samples of this polymer of widely varying properties have been investigated by X-ray diffraction. The majority of these samples resulted from a fractionation of polypropylene described by van Schooten *et al.*¹.

Many of the diagrams obtained showed, besides the well-known diffraction diagram of crystalline isotactic polypropylene, one or more extra reflections which could not be explained by the crystal structure published by Natta and co-workers^{2, 3}. In fact, evidence was obtained of the existence of at least three more crystalline modifications. The occurrence of these modifications seems to be dependent on the molecular weight, the degree of isotacticity, and the thermal treatment of the samples.

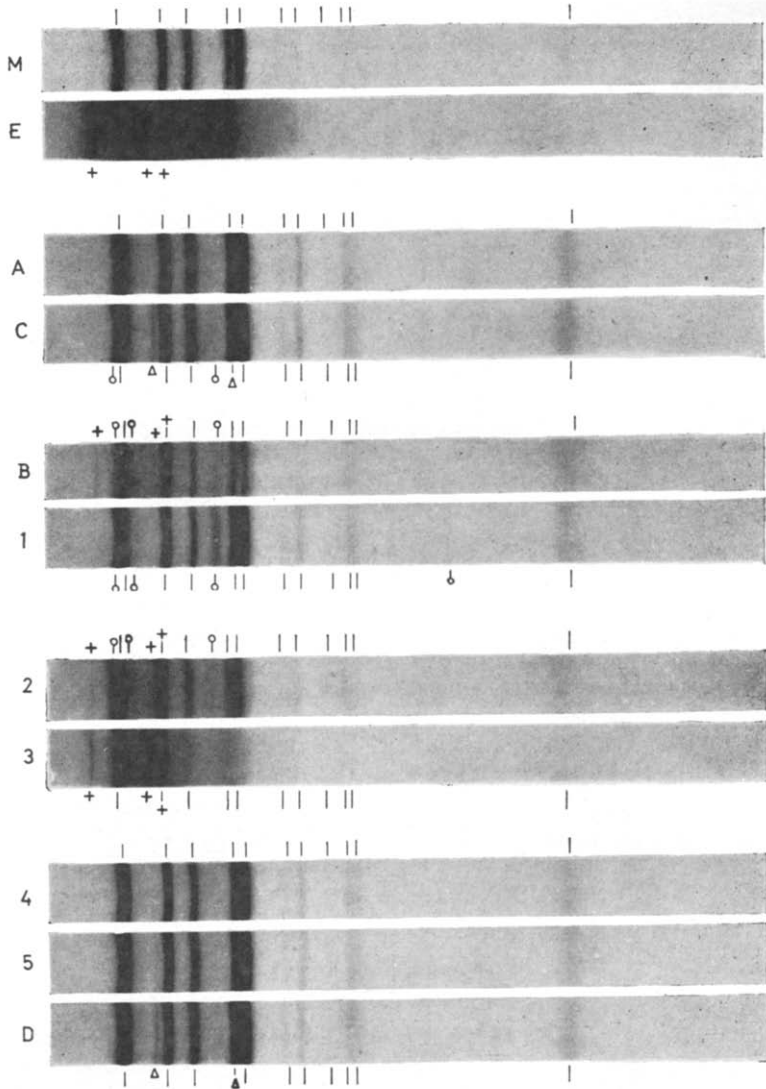
One of the crystalline modifications has since been described by Keith *et al.*⁴ and an explanation of the features of the X-ray diagrams based on a tentative structure has been given. As the very scanty X-ray data did not allow of a detailed investigation, this structure was given with all reserve, and actually, as will be shown in the following, a slightly different structure is more consistent with the X-ray data and with symmetry considerations.

EXPERIMENTAL

The polypropylene samples used in the investigations had been prepared in the fractionation described in a previous publication¹, to which the reader is referred for their properties. The fractions will be designated here by the letters and numbers used in Ref. 1.

The X-ray diagrams were obtained from pressed sheets in a focusing Guinier camera according to de Wolff⁵. To study the orientation effect by stretching, a number of diagrams were recorded in a flat-film camera of conventional design.

The X-ray diagrams of the polypropylene fractions, together with that of the total sample are given in *Figure 1*. The diagram of the total sample (M) is essentially identical with that given by Natta^{2, 3} for normal isotactic polypropylene henceforth called the α -modification. The diagrams of the fractions, however, show, besides the lines of this α -modification, some reflections which cannot be accounted for by the structure given by Natta. These extra reflections can be divided into three groups, presumably due



- l : α -modification; normal isotactic polypropylene lattice, described by Natta
- Δ : β -modification; occurring in highly crystalline material
- γ : γ -modification; occurring in material of low molecular weight and high crystallinity
- + : δ -modification; occurring in material of low crystallinity

Figure 1—X-ray diagrams of total sample (M) and fractions

POLYMORPHISM OF CRYSTALLINE POLYPROPYLENE

Table 1. Lattice spacings of the various modifications of polypropylene

α -modification			β -modification			γ -modification			δ -modification		
<i>hkl</i>	<i>Int.</i>	<i>d</i> (Å)	<i>hkl</i>	<i>Int.</i>	<i>d</i> (Å)	<i>hkl</i>	<i>Int.</i>	<i>d</i> (Å)	<i>hkl</i>	<i>Int.</i>	<i>d</i> (Å)
020	vw	10.4									
							m	6.4	200	s	7.1
110	vs	6.25					mw	5.8			
			100	s	5.5				110	m	5.5
040	vs	5.25							201	s	5.25
130	s	4.75					vs	4.4			
111	s	4.20	101	ms	4.2						
131̄	vs	4.05									
041̄											
131	mw	3.62							400	w	3.56
060	m	3.48									
150											
200	w	3.28					w	3.18			
220	m	3.13									
112̄	mw	3.05									
111̄								mw	2.80		
241̄	vw	2.66									
221̄								m	2.54		
171̄	vw	2.54					w	2.46			
	w	2.42									
	w	2.28									
							w	2.22			
	m	2.10					mw	2.12			
	w	2.02									

to three different modifications, distinguished as β -, γ -, and δ -modification. The lattice spacings observed are listed in Table 1.

β -Modification

The reflections ascribed to the β -modification were observed in fractions of high degree of isotacticity, particularly in the n-heptane residue C and the final residue D. That there is an extra reflection with $d=4.2$ Å, which coincides with the 111 reflection of the normal α -polypropylene diagram, was concluded from the markedly increased intensity of this reflection.

In an X-ray diagram of oriented material obtained by stretching, at least the reflection with $d=5.5$ Å was present in the equator. For the other reflection the diagram did not allow of any definite conclusion in this respect, as it could not be resolved from the α -polypropylene reflections.

These two reflections had already been observed previously in diagrams of sheets which on microscopical inspection showed a number of highly birefringent spherulites, and their intensity showed a correlation with the number of these spherulites. After heating to near the melting point and cooling down, the spherulites had lost their high birefringence and the extra reflections had disappeared.

γ -Modification

The γ -modification is observed only in polypropylene with low molecular weight and having a degree of isotacticity which is not too low. The strongest reflections of this diagram had previously been observed in solid pyrolysis products of polypropylene with even lower molecular weight⁶. The diagrams of these fractions were reproducible. The extra reflections reappeared after melting and recrystallization.

The reflections of the α -modification proved to have shifted somewhat in these samples. Obviously the short chains allow of closer packing, in particular in the direction of the *b*-axis.

The brittleness of these low-molecular-weight fractions made it impossible to stretch the samples for study in the oriented form.

 δ -Modification

The reflections of the δ -modification are observed only in material of very low crystallinity: the ether extract E, the *n*-heptane extract B, and in the fractions of the latter with the lowest crystallinity. The reflection with $d=5.25$ Å coincides with the 040 reflection of the normal crystalline isotactic polymer (α -modification) (compare diagrams M and E in *Figure 1*). From the absence of the other reflections of the latter in diagram E and from the relatively high intensity of the reflection in question, particularly in the diagram of fraction 3, it may be concluded that this reflection belongs to the diagram of the δ -modification.

In diagrams of stretched samples of E and 3 the reflection $d=7.1$ Å was more intense near the equator; the reflection $d=5.25$ Å, on the contrary, was more intense near the poles.

DISCUSSION

Normal α -modification

The structure of the normal modification has been investigated by Natta and co-workers^{2, 3}. Before discussing the β -, γ - and δ -modifications it may be useful to draw attention to some aspects of the polypropylene chain as present in this structure. These aspects concerning the interrelation of the various types of helices have, as far as we know, never been explicitly discussed in literature.

It should be kept in mind that with isolated isotactic polypropylene chains no difference in configuration can be distinguished, provided it is assumed that the atoms can rotate freely around the single C—C bonds.

We imagine the main chain spread out as a zigzag in the vertical plane, extending in the vertical direction, with the CH₃ side-chains, if one is looking in a direction normal to the plane, attached to the left row of chain carbon atoms.

The C—CH₃ bonds projecting from the plane can point either all forward or all to the rear. By a rotation over 180° around a horizontal axis, turning the entire chain upside down, a chain with rear side-chains is converted into one with forward side-chains. Both positions therefore can be realized with the same chain.

In the case of a bundle of polymer chains with a common main direction such a rotation of a single chain is unlikely to occur. The two types of

chains with different orientation may be found together in this bundle. They can be distinguished from each other by imagining the chains spread out in a plane as described above. To facilitate discussion we can label these two types of chains A- and B-chains. It is obvious that the difference between A-chains and B-chains has nothing to do with right- or left-handed screw symmetry. By rotating the entire bundle over 180° around an axis perpendicular to the main direction all A-chains are converted into B-chains and *vice versa*. Screw axes, on the contrary, would retain their sense of rotation.

Actually this flat zigzag chain, which is present in crystalline polyethylene, cannot be realized with isotactic polypropylene. The mutual distance of the CH_3 groups would be too small. Accordingly Natta *et al.* have described the structure of crystalline isotactic polypropylene as consisting of helical chains. From the X-ray data it follows that the identity period in the main direction of the chain comprises three monomer units. The shape of the helix is determined by a number of conditions that must be fulfilled: its repetition period (6.5 Å), the known values of the length of aliphatic carbon bonds and of the angle between these bonds, the principle of staggered single bonds, together with the minimum mutual distance of the CH_3 groups. The proper symmetry of the resulting helix is characterized by a threefold screw axis. Consequently right- and left-handed helices are possible, and in the structure in question right- and left-handed helices are arranged in a regular pattern.

It is obvious from the above discussion that the formation of a right-handed or a left-handed helix is not an intrinsic property of the isotactic chain, but depends only on the way in which the chain is spiralized.

Still, right-handed helices formed from A- and B-chains show a different configuration. The shape of the helices is such that the C—C bonds within the main chain alternatively are in the direction of the helix axis (the *c*-axis in the crystallite) and in a direction making an angle with it that is determined by the tetrahedral angle of the C—C bonds.

If the helix axis is again supposed to be vertical, it can be shown that in an A-chain forming a right-handed helix, the CH_3 side-chains are attached to the lower one of each pair of carbon atoms connected by a vertical bond. The C— CH_3 bonds, forming an angle of about 20° with the horizontal plane, are pointing downwards. If, on the contrary, this chain forms a left-handed helix the CH_3 side-chains are attached to the upper one of each pair of carbon atoms and consequently the C— CH_3 bonds will point upwards. In the same way a B-chain can form either a right-handed helix with the side-chains pointing upwards or a left-handed helix with the side-chains pointing downwards.

The helices in which the C— CH_3 bonds make an angle $\phi < 90^\circ$ with a prefixed direction of the *c*-axis have been named anaclic by Natta and co-workers, the helices in which this angle is $(180^\circ - \phi)$ cataclinc.

The outer shape of a helix is determined principally by the arrangement of the CH_3 groups relative to each other, that is, by the sense of rotation. Accordingly anaclic and cataclinc helices are assumed to be placed more or less at random in the structure proposed, whereas left-handed and

right-handed helices are arranged regularly, a left-handed helix always facing a right-handed one.

The fact that each isotactic chain can be incorporated into the crystal lattice as a right-handed or as a left-handed helix just as required, may greatly facilitate the crystallization of this modification.

β -Modification

Our conclusion that the β -modification, characterized by the reflections $d=5.5 \text{ \AA}$ and $d=4.2 \text{ \AA}$, is present in the strongly birefringent spherulites, is confirmed by the publication of Keith, Padden, Walter and Wyckoff⁴. Using a very fine X-ray beam these authors succeeded in obtaining an oriented diagram of this modification, free from the normal α -modification, from a part of a single spherulite of the strongly birefringent type. Their diagram also shows two reflections, for which the d values 5.35 \AA and 4.127 \AA are given. It suggests a hexagonal (or trigonal) symmetry with one of the lateral axes of the crystallites in the direction of the radius of the spherulite. Both reflections are observed in the equator as well as in the first layer line.

Our diagram of a stretched sample suggests that the reflection with $d=5.35 \text{ \AA}$ belongs to the zone of the c -axis. Assuming the a -axis to be parallel to the radius of the spherulite, this reflection has to be indexed 100. The second reflection ($d=4.127 \text{ \AA}$) should be indexed 101 (Keith and co-workers assume an a -axis twice as long and so give the indices 200 and 201). From Keith's d -values the c -axis can be calculated to be 6.35 \AA , practically the same as the value given by Natta for the α -modification (6.50 \AA). This strongly suggests that both modifications consist of the same type of helices. This assumption is supported by the observation that by a thermal treatment the strongly birefringent spherulites can be converted into less birefringent ones.

Admitting the impossibility of basing a detailed interpretation of the structure upon two observed X-ray reflections, Keith, Padden, Walter and Wyckoff propose a tentative structure, showing a regular arrangement of left- and right-handed helices in a 'hexagonal' (or, rather, trigonal) pattern, into which Natta's structure can be transformed with only a slight lateral rearrangement.

Closer inspection of their figure showing the projection of the structure on a plane normal to the principal axis reveals, however, from the way in which right- and left-handed helices are arranged that the structure they propose is actually neither hexagonal nor trigonal, but orthorhombic. It can even be shown to be impossible to arrange equal numbers of two types of chains regularly in a hexagonal or trigonal pattern. Moreover the calculated distance between some of the methyl groups belonging to neighbouring left-handed and right-handed helices is about 3.6 \AA , essentially shorter, therefore, than the generally postulated minimum values (4.0 \AA) and the values in Natta's structure (4.35 \AA). Because of this short interatomic distance in particular the structure proposed by these authors seems highly improbable and has to be revised.

Several other structures might be imagined which can account for the two reflections observed. If we assume that the crystal symmetry is hexagonal

or trigonal and that the polymer chains in this modification actually have the same helical shape and the same dimensions as those in the α -modification, the number of possibilities is more limited. The helices have to be arranged in a hexagonal or trigonal pattern at a mutual distance as given by the inner reflection, indexed 100, so that the methyl-methyl distances between the chains are at least 4.0 Å. Thus one arrives at a structure slightly different from the one above as the simplest one that satisfies these conditions. In this structure each crystallite contains either only right-handed or only left-handed helices as is shown in *Figure 2*. The

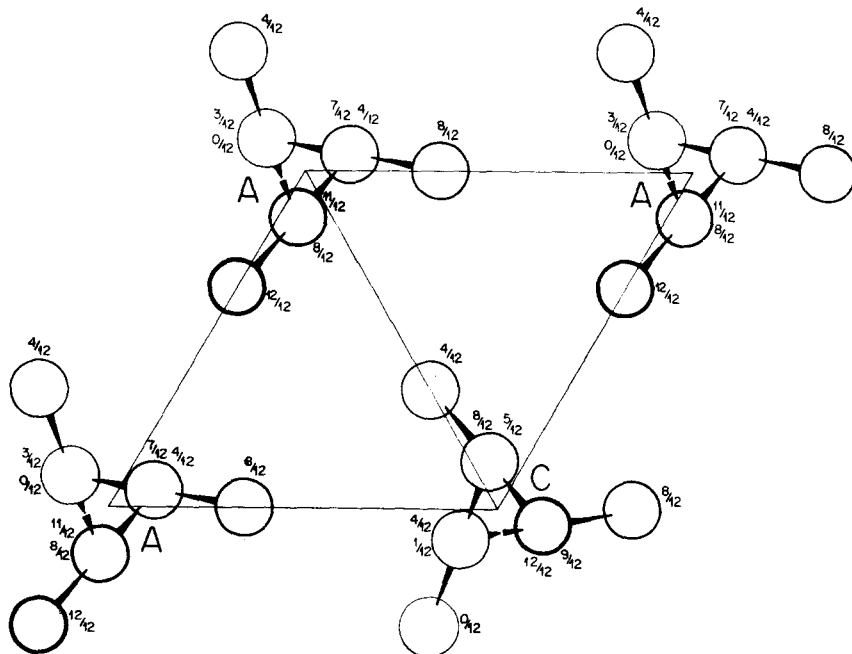


Figure 2—Projection of tentative structure of β -modification: anaclitic (A) and cataclitic (C) chains randomly distributed

methyl-methyl distances between neighbouring chains are now about 4.2 Å. At first sight a structure with all chains having the same sense of rotation seems improbable, as one would suppose right- and left-handed helices to be present in equal numbers. As was discussed above, however, each polymer chain can be incorporated in the crystal lattice in the shape of a right-handed helix as well as in the shape of a left-handed one, provided that no distinction need be made between anaclitic and cataclitic helices. Assuming that, as in Natta's structure, anaclitic and cataclitic helices can be arranged at random, a crystallite with only right-handed (or only left-handed) helices can, from this point of view, easily be realized.

The parameters of the trigonal elementary cell (space group $P3_121-D_3^4$ or $P3_221-D_3^6$) are $a=6.38$ Å: $c=6.33$ Å. With all the helices having the same sense of rotation there is no reason for doubling the a -axis as was proposed by Keith, Padden, Walter and Wyckoff.

If the dimensions of the helices are assumed to be identical with those given in Natta's structure, a calculation of the structure factors shows that the two reflections 100 and 101 actually are the most intense reflections to be expected.

Though this structure is put forward with all reserve, it seems to be consistent with the scanty experimental X-ray data and with the generally accepted ideas on the structure of this type of compounds.

γ -Modification

The γ -modification is observed only in specimens of low molecular weight. Perhaps high mobility of the polymer chains is a condition for this modification to be formed. As it was not possible to study oriented samples the experimental data do not suffice to establish a structure, even though more reflections could be observed than with the β - and δ -modifications.

δ -Modification

The δ -modification is observed only in specimens with a high percentage of amorphous material, separated from the bulk of isotactic material by extraction. This suggests the possibility of these reflections being due not to isotactic but to syndiotactic polymer.

Syndiotactic polypropylene has been obtained by Natta⁵ and its crystal structure has been described. X-ray data, however, have as yet not been published. From this structure with a base-centred orthorhombic cell ($a=14.50$ Å, $b=5.81$ Å, $c=7.3$ Å) it may be expected that the most intense reflections will be those with the indices 200 ($d=7.25$ Å), 110 ($d=5.39$ Å) and 201 ($d=5.14$ Å). Though the values we found are slightly different (7.1, 5.5 and 5.25 Å) they are close enough to the predicted ones to support the assumption that these reflections are due to this modification and that in the essentially atactic material some syndiotactic fragments of polymer chains have crystallized. The observation that in the diagram of an oriented sample the reflection with $d=7.1$ Å is intensified on the equator and that with $d=5.25$ Å off the equator, is in accordance with this assumption. The behaviour of the reflection with 5.5 Å could not be studied, as in the heavy halo of the amorphous material it was not resolved from the 5.25 Å reflection. To the weak reflection with $d=3.56$ Å the indices 400 may be assigned.

Admittedly, the identification of the δ -modification with the syndiotactic polypropylene is far from certain as the diagrams could not be compared directly with the X-ray data of the syndiotactic polymer. Indeed the differences in d values are perhaps greater than would be expected from the accuracy of the measurements. With this modification, too, the explanation of the diagram has, therefore, to be considered as only tentative.

CONCLUSION

From the work reported here it is clear that polypropylene can exist in at least four crystalline modifications, one of which perhaps contains other than isotactic chains. The situation is similar to that for other polymers, e.g. polyethylene⁷, trans-1, 4- polybutadiene and poly- α -butene⁸, for which also more than one modification have been observed. As these phenomena

will probably influence the mechanical properties of the polymers, their further investigation may be of interest also from an applicational point of view.

(Shell Internationale Research Maatschappij N.V.),
 Koninklijke/Shell-Laboratorium, Amsterdam,
 Badhuisweg 3, Amsterdam-N, Holland

(Received 17th November, 1960.

Revised version received 30th January, 1961)

REFERENCES

- ¹ VAN SCHOOTEN, J., VAN HOORN, H. and BOERMA, J. *Polymer*, 1961, **2** (2), 161
- ² NATTA, G. and CORRADINI, P. and CESARI, M. *R.C. Accad. Lincei*, 1936, **21**, 24
- ³ NATTA, G. and CORRADINI, P. *Nuovo Cim. Suppl.* 1960, **15**, 1
- ⁴ KEITH, H. D., PADDEN JR., F. J., WALTER, N. N. and WYCKOFF, H. W. *J. appl. Phys.* 1959, **30**, 1485
- ⁵ DE WOLFF, P. M. *Acta cryst.* 1948, **1**, 207
- ⁶ VAN SCHOOTEN, J. and WIJGA, P. W. O. Symposium on High Temperature Resistance and Thermal Degradation of Polymers. Plastics and Polymer Group, Society of Chemical Industry: London, 21st-23rd September 1960
- ⁷ TEARE, P. W. and HOLMES, D. R. *J. Polym. Sci.* 1957, **107**, 496
- ⁸ NATTA, G. *Makromol. Chem.* 1960, **35**, 94

NOTE ADDED IN PROOF

Since this paper was submitted it came to our notice that Natta in Irish Patent Application 430/60 (filed June 1960) mentioned an infra-red absorption band at 11.53μ , characteristic for syndiotactic polypropylene. Fraction 3 actually showed this band clearly. This, therefore, confirms the supposed identity of the δ -modification with syndiotactic polypropylene.

Rheological Properties of Concentrated Polymer Solutions I. Growth of Pressure Fluctuations during Prolonged Shear Flow

A. S. LODGE*

A new apparatus, similar to the Weissenberg Rheogoniometer, has been developed for the determination of the differences of normal stress components in steady shear flow. The liquid is sheared between a rotating cone and a fixed plate, the pressure distribution on the latter being measured by means of a diaphragm-capacity gauge having a response time (about 0.1 sec) considerably shorter than those (about 1 h) of the capillary gauges which have been used hitherto. Preliminary experiments reported here have revealed the unexpected result that with certain systems [poly(methyl methacrylate) in dimethylphthalate, polystyrene in dimethylphthalate] the observed pressure during prolonged shear flow (20 min at 20 sec⁻¹) develops a random fluctuation with 'periods' of up to 0.4 sec and amplitudes up to about one third of the shear stress. A liquid mixture of polydimethylsiloxanes showed no fluctuations under similar conditions. The growth of pressure fluctuations was accompanied by the development, in the free liquid surface near the rotating cone, of irregularities or ruffling visible to the naked eye. The observations may possibly be explained in terms of structural changes in the solutions leading to the growth of inhomogeneities or gel particles of dimensions (about 0.4 mm) comparable to the gap between cone and plate.

INTRODUCTION

RHEOLOGICAL PROPERTIES of moderately concentrated polymer solutions are not completely characterized by values of the viscosity alone: in steady shear flow, it is also necessary to know the values of the differences of the three normal components of stress acting on the shearing planes, on planes normal to the lines of flow, and on planes normal to both these sets of planes¹. Following the work of Weissenberg¹ and others^{2, 3}, increasing attention is now being given to the problem of measuring these differences. Non-zero values for these differences give rise to characteristic pressures on the walls of viscometers: in a cone-and-plate rotational viscometer, for example, the pressure on the plate increases towards the axis of rotation, the rate of increase $dp/d(\ln r)$ (where p = pressure and r = distance from the axis) being a constant (for a given shear rate) equal to one combination of the required differences of normal stress components.

Such pressure distributions have been measured by means of capillary gauges^{3, 4}, but these usually take an hour or more to reach equilibrium owing to the appreciable viscosity of the solutions used, and therefore mask any effects which might arise from more rapid changes in the state or structure of the flowing solutions. A quick-response gauge has recently been developed⁵ to replace the capillary gauges and is now being used for systematic measurements of pressure distributions in cone-and-plate and in

*Present address: Department of Mathematics, The Manchester College of Science and Technology, Manchester, 1.

parallel plate rotational systems. The results of these measurements together with a detailed description of the apparatus used are to be published elsewhere. The present paper deals solely with certain new and unexpected effects which have been observed in preliminary measurements performed with a prototype cone-and-plate apparatus embodying a pressure gauge with a response time of the order of 0.1 sec. These effects appear to arise from reversible changes of structure induced by slow, steady flow.

EXPERIMENTAL

Apparatus

A schematic diagram of the apparatus used is given in *Figure 1*. The liquid under investigation is sheared in the narrow gap between a fixed horizontal duralumin plate and a wide-angled mild steel cone rotating about

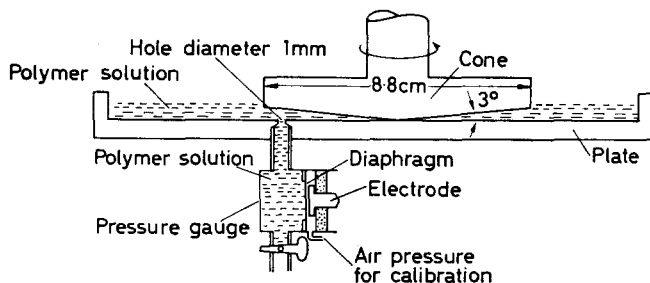


Figure 1—Schematic diagram of cone-and-plate apparatus with pressure gauge. The plate and gauge assembly can be moved in a horizontal plane to measure pressures at different distances from the cone axis

its axis which is vertical. The pressure on the plate is measured by means of a diaphragm-capacitance gauge connected to a small hole, 1 mm in diameter, in the plate. Values of pressure at different distances from the cone axis are obtained by moving the lower plate and pressure gauge horizontally.

The pressure gauge consists of a chamber, filled from below with the liquid under test; one wall is a circular beryllium-copper diaphragm, 18 mm \times 0.002 in. whose deflection in response to a change of pressure gives rise to a capacity change to an electrode about 0.001 in. away. The capacity change is measured by means of a Fielden Proximity Meter Type PM2 slightly modified so as to give an improved response to quick changes of input. The output (about 1 V for a pressure change of 130 dyn/cm²) from the Fielden is fed through another d.c. amplifier to a Siemens-Ediswan pen oscillograph which gave the traces shown in *Figures 2* and *3*. The pressure gauge (and the rest of the apparatus) used here was of a provisional design used to give information on which a finalized design was prepared. A detailed description of the finalized design of pressure gauge has been published elsewhere⁵: this gauge differs only in minor details (e.g. in having a fixed instead of a movable electrode) from the gauge used in obtaining the results reported below.

Calibration

The whole pressure-measuring system was calibrated with regard to sensitivity and response time by applying and then suddenly removing a known air pressure to the electrode side of the diaphragm, the gauge and the gap between cone and plate being filled with liquid ready for measurement. The calibration traces obtained for each liquid used are included in *Figures 2* and *3*. From these traces it will be seen that the response times are of the order 0.02 sec to 0.1 sec, depending on the liquid used. It is to be expected that the response time, which is essentially determined by the movement of liquid through the small hole in the plate, will depend on the viscosity of the liquid used. The small oscillations observed in the

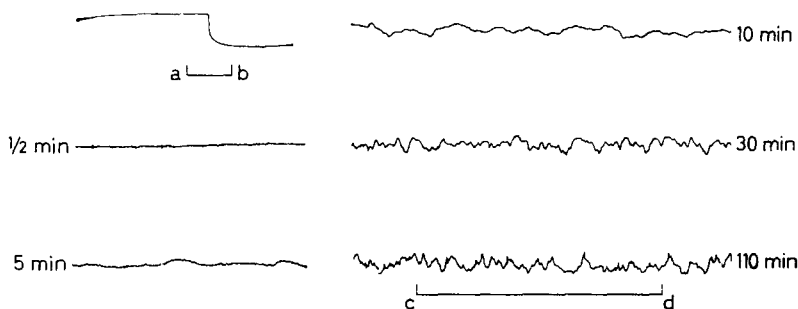


Figure 2—Growth of pressure fluctuations in solution A. Shear rate 20 sec^{-1} . Times of shearing shown in minutes. First trace shows response to sudden change of pressure 160 dyn/cm^2 . $ab=1 \text{ sec}$; cd =period of rotation of cone. Distance between hole and cone axis= 4.2 cm (cone radius= 4.4 cm)

calibration traces for two of the three liquids used may be due to oscillations in air pressure induced by the sudden change, and are in any case unimportant for present purposes. (It should be noted that the time scale for the calibration traces of *Figure 3* is expanded by a factor of 4 in comparison with the time scale for all the other traces of *Figures 2* and *3*.) It can also be seen that the response time is independent of the distance of the hole from the cone axis.

Materials

Solution A contained 2 g of poly(methyl methacrylate) of number-average molecular weight 10^6 in 100 ml of dimethylphthalate. Solution B contained 3 g of polystyrene of viscosity-average molecular weight 5×10^6 in 100 ml of dimethylphthalate. Dimethylphthalate was a comparatively poor solvent for these polymers; dissolution of the polymer was accelerated by slow rotation of a flask with tilted axis in an oven at 60°C to 90°C for a few days. When cooled to room temperature, both solutions exhibited marked elasticity, as judged by the observed recoil of air bubbles following cessation of a sudden rotation of the solutions. Solution C was a mixture of two *MS 200* (polydimethylsiloxane) fluids: 60 per cent (by weight) of the *12,500 CS* fluid and 40 per cent of the *1000 CS* fluid. This mixture was

chosen to give an inelastic liquid of viscosity roughly comparable to those of solutions A and B. The viscosities given in *Table 1* were estimates made by the falling-ball method; the viscosity of B was (unfortunately) not measured, but appeared to be similar to that of A.

RESULTS

Pressure fluctuations

A sample of solution A which had been at rest for several days was subjected to a constant shear rate in the apparatus. Pressure records taken at various times after the commencement of shear flow are given in *Figure 2*. They show that the pressure is steady at first and begins to

Table 1

Solution	Gauge response time (sec)	Pressure fluctuations		$\frac{dp}{d(\ln r)}$ (dyn/cm ²)	Viscosity (poise)
		Greatest period (sec)	Greatest amplitude (dyn/cm ²)		
A	0.02	0.4	120	900	20
B	0.05	0.4	60	1000	
C	0.1	—	<6	<40	50

fluctuate after a few minutes shearing; the fluctuations appear to be random and increase in amplitude and frequency during the first 30 min or so, after which they reach a more or less steady pattern.

Some pressure records for solution A are reproduced in *Figure 3* for comparison with pressure records taken under similar conditions for solutions B and C. It will be seen that similar fluctuations, though somewhat smaller in amplitude, are obtained with solution B and that none are obtained with solution C. The two lower traces for solution C show periodic variations having the same period as the rotation of the cone; it is believed that these variations are an artefact of the apparatus, arising from small axial translations of the cone due to end-movement in its bearing. As is to be expected on this explanation, the amplitude of these variations is greater at points nearer the cone axis. A similar but smaller periodic variation is discernible in the lower traces for solutions A and B in *Figure 3*; the fact that this variation is smaller for A and B than for C is consistent with the fact that the viscosities of A and B are smaller than the viscosity of C. There is no difficulty in seeing that these periodic variations are quite separate effects from the random fluctuations.

Normal stress components

The greatest amplitudes of the pressure fluctuations, estimated from the traces, are given in *Table 1*. It is desirable to have some other pressure value as a standard of comparison with these amplitudes, and for this purpose the values of $dp/d(\ln r)$ are also given in *Table 1*. These were obtained as the slopes of graphs of mean pressure p plotted as a function of $\ln r$, where r denotes distance from the cone axis; the graphs were substantially linear. As mentioned in the Introduction it can be shown that

(under suitable conditions) these values give a certain combination of differences of normal stress components in shear flow and represent a fundamental property (quite distinct from viscosity) of the liquids concerned⁴.

Visible heterogeneities

A further observation, qualitative but significant, was made. It was observed that, during the first 5 to 15 minutes shearing of solutions A and B, the appearance of the free liquid surface near the rim of the cone changed from smooth to rough as if small gel-like particles were being formed in the solution. The size of these particles or heterogeneities, estimated by eye, was of the order of $\frac{1}{4}$ or $\frac{1}{2}$ mm. No such effect was ever observed with solution C.

Time dependence of mean pressure

It was also observed that, during the first few minutes shearing of solutions A and B, the mean pressure at a point (i.e. the pressure with any fluctuations averaged out) increased to a maximum and then more slowly decreased to a more or less steady value. No such effect was observed with solution C: indeed, the pressure variations with both time and position were barely significant for this liquid.

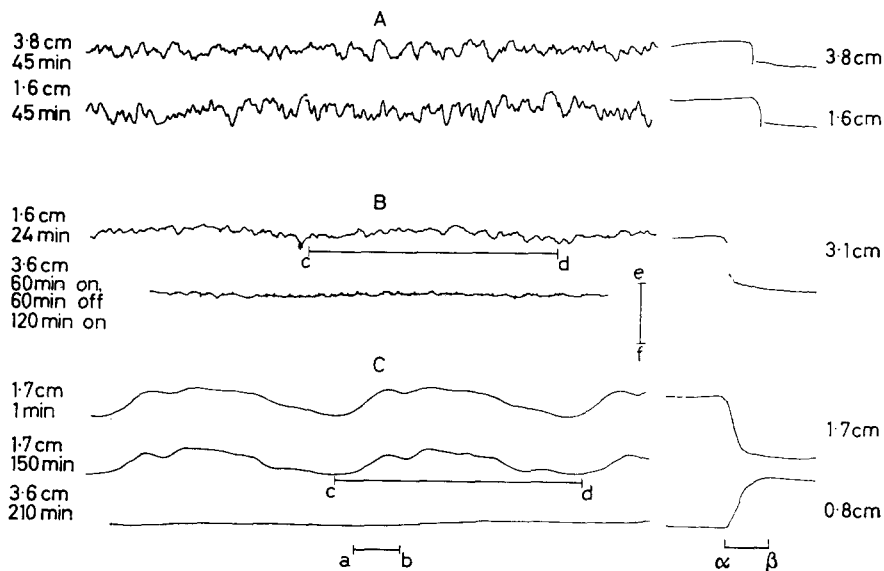


Figure 3—Pressure records for solutions A, B and C. Distances between hole and cone axis in centimetres. Times of shearing in minutes. Shear rate 20 sec^{-1} . Sensitivity $ef=500 \text{ dyn/cm}^2$ for all traces. Time scale: $ab=1 \text{ sec}$ for left-hand traces, $\alpha\beta=\frac{1}{2} \text{ sec}$ for right-hand (response time) traces; cd =period of rotation of cone

Reversibility

When the shear flow was stopped for a short time (a few minutes), after prolonged shearing so that the pressure fluctuations had been developed,

and then started again, the pressure fluctuations and visual heterogeneities appeared at once, apparently unchanged. A rest period of 1 or 2 days, however, was sufficient to restore the solutions (A and B) to their original state, i.e. that in which pressure fluctuations and visual heterogeneities did not occur at the start of shear flow.

DISCUSSION

In view of the facts that pressure fluctuations occur (with solutions A and B) only after prolonged shearing, and that they never occur at all with solution C, it seems certain that the fluctuations must be regarded as arising from some material property of solutions A and B and that they cannot be dismissed as artefacts of the apparatus. It might be objected that the viscosity of C was in fact $2\frac{1}{2}$ times larger than the viscosity of A and that in consequence the response time of the gauge when filled with C would be too long to resolve the fluctuations, but inspection of the calibration traces shows that this is not so: the response time with C though longer than those with A or B is still short enough to resolve fluctuations of the type found with A and B. In any case, fluctuations attributable to the apparatus may be seen in the $\frac{1}{2}$ min trace of *Figure 2* and are evidently very much smaller than those occurring after prolonged shearing. It should be noted that the rate of flow is very much too low for turbulence (in any accepted sense of the word) to occur.

A possible explanation of the pressure fluctuations is that during prolonged shear flow the structure of the solution (or state of dispersion of the polymer) undergoes changes (by some mechanism as yet unknown) in such a manner that gel particles or regions of higher polymer concentration, surrounded by regions of lower concentration, are formed. When such a particle moves past the hole in the plate, it is reasonable to expect it to give rise to a transient change of pressure in the hole; the apparently random nature of the observed fluctuations would result from the superposition of pressure transients of various amplitudes and durations caused by particles not only of various sizes but also moving past the hole at various heights (and therefore at various speeds) above it. A simple calculation shows that the size of particle necessary to produce the widest peaks in the pressure records (a 0.4 mm diameter particle moving past the hole at a height of 0.2 mm above the plate) is not inconsistent with the sizes of surface irregularities (about 0.1 to 0.5 mm) observed near the cone rim.

The literature contains other evidence for the occurrence of time-dependent changes of structure induced by steady flow: the shear stress for the rubber-decalin system, for example, increases to a maximum and then decreases to a steady value⁶. Some evidence (based on the diffusion of dye) also exists for the occurrence of heterogeneities ('rheological units') in the shear flow of raw rubber⁷; in this case the largest heterogeneities are only 0.01 mm in diameter. The evidence offered in the present paper appears to be rather more direct than any previously published and is, moreover, remarkable in that structural changes occur at a polymer concentration as low as 2 per cent and at a shear rate as low as 20 sec^{-1} .

The effects described in this paper are considered to be important for the

following reasons: they represent a new source of information concerning the structure of polymers in solution; they give renewed warning of fundamental difficulties⁸ in rheological investigations of certain polymer-solvent systems, viz. the occurrence of heterogeneity on a scale comparable with the apparatus dimensions; and, if they occur in fibre-forming systems (e.g. in the slow flow through feed pipes to a spinneret), they may influence the properties of the spun fibre.

It is a pleasure to thank my former colleagues, Dr D. W. Saunders and Mr K. J. Butler, for their continual assistance in developing the apparatus used here.

*The British Rayon Research Association,
Heald Green Laboratories,
Wythenshawe,
Manchester, 22*

(Received 18th November, 1960)

REFERENCES

- ¹ WEISSENBERG, K. *Nature, Lond.* 1947, **159**, 310
- ² JOBLING, A. and ROBERTS, J. E. *J. Polym. Sci.* 1959, **36**, 421
- ³ GARNER, F. H., NISSAN, A. H. and WOOD, G. F. *Phil. Trans. A*, 1950, **243**, 37
GREENSMITH, H. W. and RIVLIN, R. S. *Phil. Trans. A*, 1953, **245**, 399
- ⁴ ROBERTS, J. E. *Proceedings of 2nd International Congress on Rheology*, Butterworths, London, 1954, pp. 91-98
- ⁵ LODGE, A. S. *J. sci. Instrum.* 1960, **37**, 401
- ⁶ TRAPEZNIKOV, A. A. and ASSONOVA, T. V. *Colloid J. Voronezh*, 1958, **20**, 376
- ⁷ MOONEY, M. and WOLSTENHOLME, W. E. *J. appl. Phys.* 1954, **25**, 1098
- ⁸ BONDI, A. *Trans. Soc. Rheology*, 1958, **2**, 303

Proton Magnetic Resonance in Nylon 66

D. W. JONES*

Broad-line proton magnetic resonance spectra have been recorded from a dry sample of nylon 66 chip of viscosity-average molecular weight 14,800. The measurements covered the overall range 20° to 400°K but were made at close temperature intervals above 300°K in order to investigate the change in line shape. Under the conditions of these experiments, no composite structure was detected in the derivative signal but there were small changes in line shape near 320° and near 360°K; the ratio of $\Delta H_{m,sl}$ to r.m.s. moment was approximately halved between 350° and 365°K. An apparent activation energy of 30 kcal/mole has been derived for the line-narrowing process near 360°K on the assumption that it is governed by a single correlation time. This value is compared with those derived from mechanical and dielectric measurements and seems consistent with the interpretation of the marked line narrowing as arising from large torsional motions of the hydrocarbon chains. Over the whole temperature range studied, both $\Delta H_{m,sl}$ and second-moment values of the nuclear resonance absorption line are smaller than those reported previously for nylon 66 samples. Neither the second moment nor the line width changes significantly from the values at 77°K of 21.5G² and 14.5G, respectively, when the temperature is reduced to 20°K.

INTRODUCTION

FOR SEVERAL linear polymers which contain methylene groups, whether in long chains as in polymethylene¹ or in short sequences as in *Terylene* and related polyesters², the proton magnetic resonance (p.m.r.) absorption curve becomes composite at sufficiently high temperatures. The presence of such a compound structure implies that there are present in the polymer regions possessing markedly different correlation times³. A very narrow line attributed to moisture has been obtained⁴ from nylon 6, but there is no evidence in polyamides for the co-existence of a narrow line, arising from the amide group or from enhanced molecular motions of the methylene groups, with a broader resonance. Although the absence of such fine structure in the spectra renders the assignment of nuclear resonance transitions to particular regions of the polymer more difficult, the pronounced high-temperature line narrowing in polyamides has been ascribed to composite motions of paraffin segments⁵ in the less well ordered regions.

The present account describes an attempt to follow the width and shape of the p.m.r. line from solid poly-(hexamethylene adipamide), or nylon 66, at closely spaced points in the transition region above room temperature and at wider temperature intervals between room temperature and liquid hydrogen temperature.

EXPERIMENTAL

Proton resonance spectra of nylon 66 were measured by means of an Anderson bridge circuit which was fed from a 16.435 Mc/s oscillator and followed by a r.f. amplifier, detector, lock-in amplifier, and Kent recorder⁶ so as to yield the derivative of the absorption signal. The magnetic field

*Seconded from the British Rayon Research Association, Heald Green Laboratories, Wythenshawe, Manchester, 22.

was scanned at a rate of about 3 G min^{-1} , and modulated at 25 c/s with an amplitude typically of 1.1 G so that the modulation correction to the second moment was small. Although the field homogeneity was about 0.5 G , a 16 sec time-constant was needed on the recording system for the high temperature spectra and it was not possible to measure line widths below 3 G . A r.f. level to the bridge of 150 mV was generally used; this corresponds to an H_1 field estimated to be below 2 milligauss . Spectra recorded at twice this r.f. level at 77°K and 300°K showed no significant change in line width or second moment.

For measurements in the range $300^\circ\text{--}400^\circ\text{K}$, the temperature was controlled by passing a stream of warmed air over the sample coil⁷ and measured by means of a thermocouple placed next to the coil and within the lagged tube enclosing the p.m.r. coil assembly. For the measurements at lower fixed temperatures, another resonance coil enclosed in a copper shield was successively immersed in refrigerants of ice, solid carbon dioxide and acetone, liquid nitrogen, and liquid hydrogen.

Additional room-temperature spectra of nylon 66 and 610 were recorded at 14.1 Mc/s for a range of r.f. levels up to 1.0 V on a Pound-Watkins spectrometer described previously⁸. At each level the nuclear resonance signal amplitude was compared with that from a standard dummy signal fed to the tuned circuit.

The samples of polymer chip were obtained from Dr J. Mann and were sealed in 0.4 in. -diameter glass tubes after drying under vacuum. The nylon 66 was specified as free of inorganic impurities (such as titanium dioxide) and with an ash content below 0.05 per cent . It was found to have a viscometric molecular weight of $14,800$, as derived⁹ by Dr W. R. Moore from his intrinsic viscosity measurement of 1.10 in *m*-cresol at 25°C , and a density, as measured at room temperature by flotation and without allowing time for liquid penetration, of 1.135 g cm^{-3} , corresponding¹⁰ to an estimated crystallinity of 45 per cent . The density of the nylon 610 sample was 1.074 g cm^{-3} . Both samples may contain up to 5 per cent monomer.

RESULTS

Figure 1 shows the temperature dependence of $\Delta H_{m,sl.}$, the peak-to-peak width of the first derivative of the p.m.r. absorption curve, in nylon 66 between 20° and 400°K . The corresponding variation in apparent¹¹ second moment of the absorption line, computed from the experimental ordinates of the derivative curve at 0.5 G intervals and corrected for the integrating time constant of measurement, is shown in *Figure 2*. The cut-off points on each derivative curve were estimated as intersections with the mean background-noise lines on the trace, and the integrations were performed separately for each half-spectrum on a Pegasus computer⁸. Experimental points on both graphs are generally the means from about three acceptable spectra; in cases where more measurements have been made at a single temperature, the standard deviations calculated from the spread of results are represented by vertical lines in *Figures 1* and *2*.

Despite the use of a r.f. level of 150 mV and a minimum modulation width of 1 G , resolution of the p.m.r. line into broad and narrow components

(as predicted by McCall and Anderson¹²) was not detected. Modulation amplitudes covered the range 1.0–1.7 G at room temperature and 1.0–1.5 G at higher temperatures. Although the resolution of narrow lines was low, the measurements appear to exclude the persistence above 360°K in an appreciable part of the polymer of the 9 G component which is present at

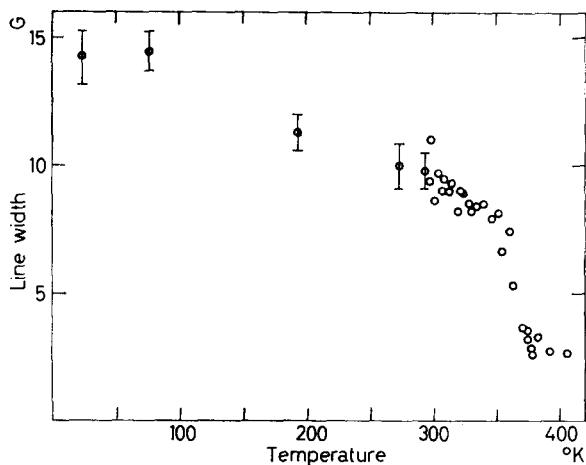


Figure 1—Variation with temperature of peak-to-peak line width, $\Delta H_{m,sl}$.

room temperature. Some sharpening of the central portion of the experimental curve was apparent near 370°K (Figure 3). Further evidence of a change in line shape is supplied by the comparatively small drop in second moment in the 360°K region accompanying the reduction of line width to

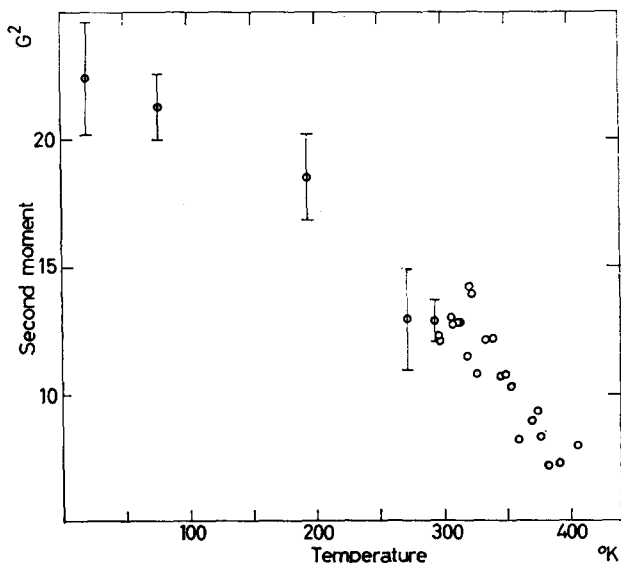


Figure 2—Variation with temperature of second moment of resonance absorption curve

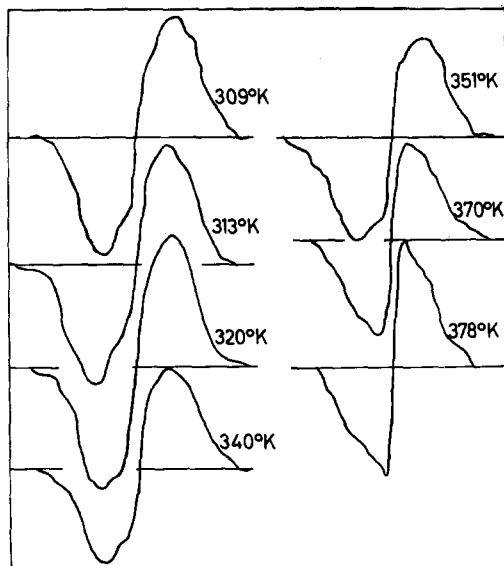
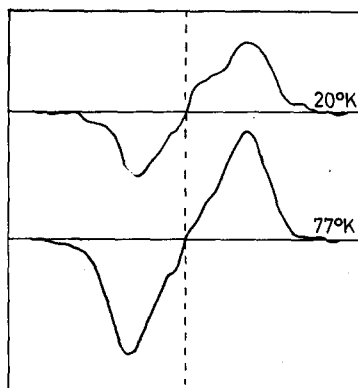


Figure 3—Experimental derivative curve shapes above room temperature

the limit of our measurements. As the temperature increases from 20°K, the ratio of $\Delta H_{m,sl}$ to r.m.s. moment slowly drops from 3.0 to about 2.5 at room temperature, but it remains above the Gaussian value (2.0) at about 2.4 until a rapid fall to half this value begins at 350°K. Further, the ratio of squared half-width, $\Delta H_{\frac{1}{2}}^2$, to second moment (5.5 for a Gaussian

Figure 4—Experimental derivative curve shapes at low temperatures



curve) drops from 6.9 at 320° to 5.3 at 334°K and then later, as the rapid line narrowing occurs, falls again to reach, for example, 4.2 at 370°K. Small outer shoulders disappear from the differential curve at about 320°K (Figure 3).

In the r.f. spectrometer measurements, saturation was absent at r.f. levels above 0.3 V r.f. in nylon 66 but was evident down to 0.03 V in nylon 610. Comparison with ammonium chloride spectra recorded under similar conditions led to estimates of T_1 for the broad line in the samples used of 0.07 sec (dried sample) and 0.02 sec (sample containing equilibrium moisture) for nylon 66, and 0.15 sec for nylon 610, all at room temperature.

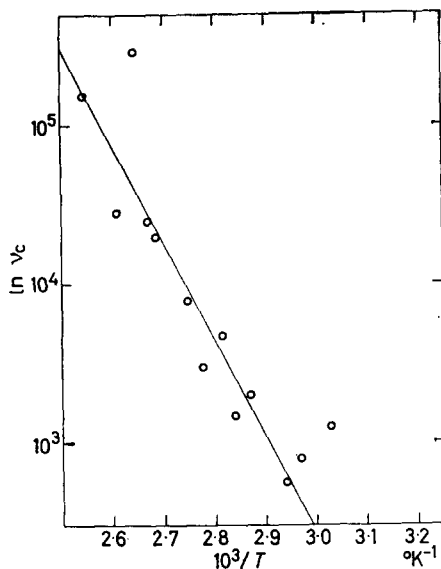


Figure 5—Variation with temperature of correlation frequencies near 360°K ($B=2.6\text{G}$; $C=8.3\text{G}$)

DISCUSSION

Below room temperature, the measurements of absorption line-width in nylon 66 presented here lie between 1 and 2 G below those reported by Slichter¹³, which in turn are below the values given by Glick *et al.*¹⁴. (For dry nylon 610, our measurement for $\Delta H_{m,el}$, of 8.2 G at 305°K falls on Slichter's curve for this polymer⁵.) The location of the marked reduction in line width at 350°–370°K, i.e. about 180° below the crystalline melting point, is in agreement with the p.m.r. results of Slichter¹³ rather than those of Glick *et al.*¹⁴, in which the drop was centred on 350°K for dry nylon 66. The higher temperature is comparable with that for the α p.m.r. transition (360°–380°) in polymethylenes polymerized from diazomethane⁷. While the same process is not necessarily responsible for mechanical loss maxima and what may be termed 'nuclear resonance transitions' at similar temperatures, it is of interest that at low audio-frequencies a damping maximum has been reported in various specimens of dry unirradiated nylon 66 at 351°K (0.3 c/s)¹⁵, 338°K (3 c/s)¹⁶, 350°K (650 c/s)¹⁷, 365°K (700 c/s)¹⁸, and 370°K (1250 c/s)¹⁹. These occur within the range of the principal dynamic loss transition which starts at 325° and extends up to 430°K for the dry polymer. The correlation frequency of about 5 kc/s for the p.m.r. line narrowing near 360°K would be consistent with a rather higher temperature for the mechanical loss transition if the same motion is involved.

From the absence of a sharp change in the amide infra-red frequencies in the temperature region of marked line narrowing and almost up to the melting point, Cannon²⁰ and others have emphasized that the variation in the degree of CONH dipolar association (or hydrogen bonding²¹) with temperature—or, indeed, with nature of polyamide²²—must be only slight. Also, at room temperature, the interaction between the amide groups is evidently almost as marked in amorphous as in crystalline regions. Although the relatively loose packing of the chains can still permit torsional

motion of the methylene groups, the infra-red evidence would appear to contradict the specific interpretation of the α' mechanical dispersion region as arising from segmental motion¹⁹ associated with disruption of hydrogen bonds²³ (or amide-dipolar interactions). Further, Glick *et al.*¹⁴ have shown that replacement of the amide protons by deuterium in nylon 66 causes remarkably little change in second moment over a wide temperature range.

It is possible that the slight fall in $\Delta H_{m,sl}$ starting near 325°K (*Figure 1*) and the small change in shape of the differential curve (*Figure 3*) are related to the change observed by Roseveare²⁴ from retractive force measurements (and designated a second-order transition) and also reported earlier from thermal expansion measurements²⁵. In addition, there is some suggestion at this temperature of an abnormality in the second moment (*Figure 2*): individual values determined include 11.2, 13.5, and 13.7 G² at 315°K; 14.0, 13.9, and 14.7 G² at 322°K; and 11.2 and 10.5 G² at 328°K. Such phenomena accompany nuclear resonance transitions in polymethylenes; one near 330°K has been tentatively assigned to groups of seven CH₂ groups⁷ which do not, of course, occur in the present polymer. Instead, one might hope to discern, especially from second-moment data, regions where motion in the sets of six and four CH₂ groups is successively unfrozen as the temperature is raised. Over the range 20°–280°K, the temperature intervals of the present measurements are such that only a gradual diminution of broadening with increasing temperature is apparent. The data for poly(hexamethylene adipamide) obtained at closer intervals in this region by Glick *et al.*¹⁴ suggest that the first stage of second-moment reduction occurs over a wide temperature range around 200°K. There is no plateau region so that, if there are two distinct processes, then evidently their correlation frequencies are not very different. Some earlier results⁵ on poly(hexamethylene sebacamide), for which the experimental uncertainty quoted is between 1 and 2 G², could be interpreted as demonstrating a second-moment contraction at 200°K in this polymer also.

It is difficult to assess accurately the reliability from the uncertainty in estimates because of systematic errors arising from the uncertainty in defining the limits of the spectrum, but it is considered that the present

Table 1. Experimental values for second moments (G²) in nylon 66 at various temperatures

<i>Author</i>	77°K	298°K	350°K
Slichter ⁵	26	18	—
Glick <i>et al.</i> ¹⁴	28	17	14
Present work*	21.0 ± 1.3	12.5 ± 0.8	11.0 ± 0.7

*Quoted e.s.d.'s are derived from spread of observations only.

second-moment values are reliable to ± 15 per cent. Over the whole temperature range studied, they are at least this amount below the values reported by Glick *et al.*¹⁴ for a polymer which is presumed to be rod¹⁹ with a number-average molecular weight of 15,800 and a density of 1.145 g cm⁻³. Such a discrepancy (*Table 1*) seems surprisingly large in view of the approximate similarity in molecular weights of the samples. In fact, the experimental points in *Figure 2* are distributed about a line

intermediate between those reported for nylon 610⁵ and nylon 66¹⁴. The negligible increase in $\langle \Delta H^2 \rangle$ when the temperature is reduced below 77°K would suggest that molecular motion is already substantially quenched at that temperature; the similarity in line shapes at liquid nitrogen and hydrogen temperatures can be seen from *Figure 4*. Few p.m.r. measurements have been made on polymers at so low a temperature but the smallness of the change is not unexpected in a polymer without side groups. However, the maximum magnitude measured for the second moment of 22 G² is 3 G² below the rigid-lattice value calculated by Slichter on the basis of tetrahedral bond angles and with a C—H distance of 1.094 Å but without a correction for molecular oscillations.

By means of the Gutowsky–Pake equation²⁶

$$2\pi\nu_c = \frac{4819 \Delta H_{m.sl.}}{\tan \left[\frac{\pi}{2} \left(\frac{\Delta H_{m.sl.}^2 - B^2}{C^2} \right) \right]}$$

which involves the line width, $\Delta H_{m.sl.}$, in the region of a diminution of nuclear resonance width from C to B , it is possible to determine a single correlation frequency, ν_c , at each temperature. One may then make the specific assumption that the corresponding correlation time, τ_c , represents the dominant process responsible for the p.m.r. line narrowing, in so far as this is manifested by the movements of $H-H$ vectors in the specimen. Changes in line shape above 350° have already been mentioned and these may make the use of $\Delta H_{m.sl.}$ in the Gutowsky–Pake relationship misleading. This risk has been preferred to that of using second moments, which may involve temperature-dependent side band effects. Two sets of values have been taken for the line widths at temperatures above and below the 350°–370° transition region: $B=2.6$ (instrumental limitation) and $C=8.3$ G, and $B=0$ and $C=8.3$ G. If these data at several temperatures are fitted to an Arrhenius rate process relation

$$\nu_c = \nu_0 \exp \{ -E^*/RT \}$$

the frequency factor, ν_0 , has the large value of 10²² and the apparent activation energy, E^* , is estimated to be 30 kcal/mole if $B=2.6$, as in *Figure 5*, or 20 kcal/mole if $B=0$. If one makes the approximation of a single correlation frequency, where a range of values would have been more appropriate, ΔE^* may be underestimated²⁷. As they stand, these potential energies are nearer to the value of 21 kcal/mole reported by Woodward *et al.*¹⁷ for the mechanical loss β dispersion (damping maximum at 250°K and 1000 c/s) than to these authors' value of 73 kcal/mole for the α' dispersion; more recent dynamical measurements by Woodward *et al.*¹⁹, however, indicate that the β peak virtually disappears if the sample is thoroughly dried. From the variation in direct current conductivity, ascribed mainly to motion of the amide protons in amorphous regions above room temperature, McCall and Anderson¹² deduce 40 kcal/mole for the activation energy of the dipole rotation process in nylon 66. Boyd finds²⁸ that this value drops to 22 kcal/mole if a dry sample is moistened.

In semi-crystalline polymers devoid of side groups, it is not always possible to associate mechanical dispersions or p.m.r. changes with the

motions of specific structural groups. Even when a p.m.r. line is composite, as happens under appropriate conditions in some polyesters², one component line may arise from re-orientations of protons in more than one kind of environment. In the case of polyamides, it may be an oversimplification to split up the gradual increase in molecular flexibility shown by the second moment changes occurring over a wide temperature range into distinct molecular processes. The fact that a graph of $\ln \nu_c$ against $1/T$ (Figure 5) yields a single straight line suggests that the magnetic relaxation mechanism does not change appreciably in the 350°–370° region. A separate broad signal was not observed at high temperatures in nylon 66 but the change in line shape demonstrated by the large value of $\langle \Delta H^2 \rangle$ in comparison with $\Delta H_{m.sl.}$ and ΔH_1 suggests that weak outer wings may have escaped detection.

In view of the approximations involved, agreement between the several estimates of the apparent activation energy for the re-orientation process in the 360°K region is fair. The magnitude of this energy is consistent with the assignment of the major transition in nylon 66 to torsional segmental motions of the hydrocarbon chains, whether or not the amide–amide junctions remain fixed. One cannot be sure, however, which regions of the polymers are involved.

The author is grateful to Dr W. R. Moore for kindly carrying out the molecular weight determination, to Dr J. A. S. Smith for much advice and for the use of apparatus, and to Dr J. Mann for supplying the material and for helpful discussions. He would also like to thank the British Rayon Research Association for financial support before and during the course of this work.

School of Chemistry,
The University,
Leeds, 2

(Received 28th November, 1960)

REFERENCES

- ¹ SMITH, J. A. S. *Chem. Soc. Special Publ.* No. 12, 1958, p. 199
- ² WARD, I. M. *Trans. Faraday Soc.* 1960, **56**, 648
- ³ SLICHTER, W. P. and MCCALL, D. W. *J. Polym. Sci.* 1957, **25**, 230
- ⁴ COOMBES, R. J. Reported by POWLES, J. G. and KAIL, J. A. E. *Trans. Faraday Soc.* 1959, **55**, 1996
- ⁵ SLICHTER, W. P. *J. appl. Phys.* 1955, **26**, 1099
- ⁶ SMITH, J. A. S. *Disc. Faraday Soc.* 1955, **19**, 207
- ⁷ HERRING, M. J. and SMITH, J. A. S. *J. chem. Soc.* 1960, p. 273
- ⁸ JONES, D. W. and SMITH, J. A. S. *Trans. Faraday Soc.* 1960, **56**, 638
- ⁹ TAYLOR, G. B. *J. Amer. chem. Soc.* 1947, **69**, 635
- ¹⁰ STARKWEATHER, H. W., Jr, and MOYNIHAN, R. E. *J. Polym. Sci.* 1956, **22**, 363
- ¹¹ ANDREW, E. R. and NEWING, R. A. *Proc. phys. Soc., Lond.* 1958, **72**, 959
- ¹² MCCALL, D. W. and ANDERSON, E. W. *J. chem. Phys.* 1960, **32**, 237
- ¹³ SLICHTER, W. P. *J. Polym. Sci.* 1959, **35**, 77
- ¹⁴ GLICK, R. E., GUPTA, R. P., SAUER, J. A. and WOODWARD, A. E. *J. Polym. Sci.* 1960, **42**, 271
- ¹⁵ THOMAS, A. M. *Nature, Lond.* 1957, **179**, 862
- ¹⁶ SCHMIEDER, K. and WOLF, K. *Kolloidzshr.* 1953, **134**, 149

- ¹⁷ WOODWARD, A. E., SAUER, J. A., DEELEY, C. W. and KLINE, D. E. *J. Colloid Sci.* 1957, **12**, 363
- ¹⁸ DEELEY, C. W., WOODWARD, A. E. and SAUER, J. A. *J. appl. Phys.* 1957, **28**, 1124
- ¹⁹ WOODWARD, A. E., CRISSMAN, J. M. and SAUER, J. A. *J. Polym. Sci.* 1960, **44**, 23
- ²⁰ CANNON, C. G. *Spectrochim. Acta*, 1960, **16**, 302
- ²¹ TRIFAN, D. S. and TERENCEZI, J. F. *J. Polym. Sci.* 1958, **28**, 443
- ²² MIYAKE, A. *J. Polym. Sci.* 1960, **44**, 223
- ²³ WOODWARD, A. E. and SAUER, J. A. *Fortschr. Hochpolymer-Forsch.* 1958, **1**, 114
- ²⁴ ROSEVEARE, W. E. Reported in Ref. 17
- ²⁵ BOYER, R. F. and SPENCER, R. S. *J. appl. Phys.* 1944, **15**, 398
- ²⁶ GUTOWSKY, H. S. and PAKE, G. E. *J. chem. Phys.* 1950, **18**, 162
- ²⁷ POWLES, J. G. I.U.P.A.C. Symposium on Macromolecules, Wiesbaden 1959, **1A**, 10
- ²⁸ BOYD, R. H. *J. chem. Phys.* 1959, **30**, 1276

The Synthesis of Block and Graft Copolymers of Cellulose and its Derivatives

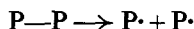
R. J. CERESA

The mechanical rupture of polymer chains into polymer free radicals is one of the basic processes for synthesizing linear block copolymers. Three mechanochemical syntheses have been applied to cellulose and its derivatives. These are: (1) the mastication of methyl-, ethyl- and benzylcelluloses, cellulose acetate and starch with polymerizable vinyl monomers; (2) the vapour-phase swelling of cellulose acetate with acrylonitrile monomer; and (3) the freezing and thawing of starch-acrylonitrile emulsions. The isolation and characterization of the block copolymeric fractions for specific systems is presented.

OF THE methods developed at this College for the synthesis of linear and grafted block copolymers three have been found suitable for the copolymeric modification of cellulose and its derivatives. Full experimental data for each method of synthesis have been published¹⁻⁶ and therefore an outline only of the experimental conditions will be given for each general system. The three processes to be considered are: (1) the mastication of cellulose derivatives with a polymerizable vinyl monomer; (2) the vapour phase swelling of cellulose derivatives with polymerizable monomers; and (3) the freezing of starch monomer emulsions.

MASTICATION BLOCK COPOLYMERIZATION

It has been shown⁷⁻¹⁰ that in general polymers in a visco-elastic state when subjected to mechanical working, such as occurs during mastication, extrusion or milling, undergo main-chain scission to form polymeric free radicals:

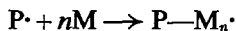


The active free-electron sites are therefore in terminal chain positions. The fate of these polymeric radicals depends upon the conditions in operation during their formation. Thus, if oxygen is present, polymeric peroxides or hydroperoxides are formed, as in the case of the mastication of natural rubber in the presence of air:



If extensive hydrogen abstraction occurs as the primary polymeric free-radical reaction reactive sites along the backbone of the polymer are formed which may lead to branching and eventual gelation, particularly if the main chain contains unsaturated olefinic bonds^{11,12}.

When mastication is carried out in the presence of a polymerizable monomer present in sufficient concentration to yield a visco-elastic material, and in the absence of a high concentration of atmospheric oxygen, the primary reaction of the polymeric free radicals is the initiation of block copolymerization^{13,14}:



If the termination step of the polymerization is combination, disproportionation or transfer to monomer, essentially linear block copolymers are formed. Transfer to polymer, however, produces free-radical sites randomly placed along the polymer backbone and therefore under these conditions complex 'block-grafts' are formed. Transfer reactions, if they occur, result in the formation of homopolymer fractions:



Mechanical scission of the block-copolymerized monomer is an additional source of homopolymer. It was found that cellulose esters and ethers when plasticized with vinyl monomers and masticated under block-copolymerization conditions yielded substantial fractions of block copolymer with relatively little homopolymer of the block-copolymerized monomer (Table 1).

Table 1. The mastication of cellulose derivatives with vinyl monomers

Polymer A	Monomer B	B (%)	Masti- cation (min)	Conventional percentage	Composition		
					Poly A	Poly B	Block AB
Methyl cellulose	Acrylonitrile	23.7	25	89	29.0	—	71.0
Ethyl cellulose	Methyl methacrylate	38.5	30	93	49.9	4.9	45.2
Benzyl cellulose	Styrene	35.1	20	87	42.9	1.1	56
Cellulose acetate	Vinyl acetate	25.0	25	95	39.6	14.4	46.0
Starch	Methyl methacrylate	20.2	20	98	35.4	6.0	58.6

Methyl cellulose-acrylonitrile

The mastication of a high-molecular weight-polymer with acrylonitrile monomer leads in general to the formation of 'pseudo' crosslinked block copolymers^{15,16}. The aggregation of the polyacrylonitrile chains of the block-copolymer fractions results in the formation of swollen gels when the polymerization products are extracted with solvents for the initial polymer. Thus with the system: methyl cellulose-acrylonitrile the hot aqueous extraction of the mastication product removed unchanged methyl cellulose from the highly swollen but insoluble block-copolymer fraction. The latter fraction was soluble in dimethyl formamide and the solution when fractionally precipitated with methanol gave only one fraction which was precipitated over a narrow range. The addition of free methyl cellulose to this solution, before precipitation, yielded two clear-cut fractions without appreciable coprecipitation (Table 2).

Table 2. The fractional precipitation of methyl cellulose-polyacrylonitrile block copolymer

Solution	1st fraction	2nd fraction
Block copolymer	—	99.6% cont. 8.05% N
Block copolymer + methyl cellulose	51.2% cont. 0.2% N	48.6% cont. 7.90% N

The absence of homopolymeric polyacrylonitrile from the block-copolymer fractions was confirmed by the ammonium thiocyanate extraction method^{15, 16}. The composition of the block-copolymer fraction was, therefore, 69.6 per cent of methyl cellulose and 30.4 per cent of polyacrylonitrile.

Ethyl cellulose-methyl methacrylate

The products from the mastication experiments were dissolved in acetone and fractionally precipitated with methanol (*Table 3*).

Table 3. The fractional precipitation of ethyl cellulose-methyl methacrylate block copolymer

Fraction	Weight (%)	Composition	
		Ethyl cellulose (%)	Poly(methyl methacrylate)* (%)
I	4.8	0.5	99.5
II	25.3	20.1	79.9
III	29.9	46.3	53.7
IV†	40.0	99.5	0.5

*Poly(methyl methacrylate) contents were determined by infra-red spectrography.

†This fraction was not precipitated by methanol from acetone solution and it was recovered by solvent evaporation at low temperature under vacuum.

Block-copolymer fraction II had a limiting viscosity number, $[\eta]$, in benzene of 252, whilst block-copolymer fraction III had $\eta = 165$. The higher value corresponded to a larger average chain length of the poly(methyl methacrylate) segments, which is in agreement with the earlier precipitation of the fraction. Thus the differences in solution behaviour between the block-copolymer fractions II and III were a reflection of the differences in composition, relative chain lengths and segment distributions.

Benzyl cellulose-styrene

Fractional precipitation from benzene solutions with methanol gave three distinct fractions (*Table 4*).

Table 4. The fractional precipitation of benzyl cellulose-styrene block copolymers

Fraction	Weight (%)	Composition	
		Benzyl cellulose (%)	Polystyrene* (%)
I	1.1	—	98.5
II	56.0	47.5	52.5
III	42.9	98.0	2.0

*Polystyrene content measured by infra-red adsorption.

From *Table 4* it can be seen that from this system a single block-copolymer fraction was isolated with an approximate composition of 1:1. Osmotic pressure measurements in benzene solutions of the block-copolymer fraction II gave an average molecular weight value of $(1.6 \pm 0.2) \times 10^5$.

Cellulose acetate-vinyl acetate

In this system Soxhlet extraction with methanol removed homopolymeric vinyl acetate. The residue, after extraction to constant weight, was reprecipitated from benzene solution with methanol with a recovery in excess of 98.5 per cent. No coprecipitation occurred when up to 15 per cent of poly(vinyl acetate) was added to the benzene solutions before precipitation with methanol. The Soxhlet extraction was therefore considered to be complete. The residual mixture of cellulose acetate and block copolymer, after reprecipitation, was fractionated from benzene solution by methanol addition. Two clear-cut fractions were obtained (*Table 5*).

Table 5. The fractional precipitation of cellulose acetate-vinyl acetate block copolymers

Fraction	Weight %	Composition	
		Cellulose acetate (%)	Poly(vinyl acetate)* (%)
I	39.6	97	—
II	46.0	87.9	12.1
III†	14.4	—	99.5

*From infra-red spectrography.
†Methanol extraction.

The osmotic molecular weight of the block-copolymer fraction II was measured as $(2.3 \pm 0.22) \times 10^5$ and the limiting viscosity number, $[\eta]$, in benzene as 135.

Starch-methyl methacrylate

The visco-elastic state cannot be achieved by the plasticization of starch with vinyl monomers. However, the polymeric chains are easily degraded mechanically by frictional forces¹⁷ to give free radicals which will initiate block copolymerization. The application of rotational shearing forces to starch-monomer mixtures in the fully filled mastication chamber gave rise to sufficient mechanical degradation to initiate the required block copolymerization.

In mastication products containing more than 20 per cent of vinyl polymer, aqueous extraction of the residual starch fraction is only partially due to the low degree of swelling of the products in boiling water. Soxhlet extraction of the vinyl homopolymer, in this case poly(methyl methacrylate), is, as a rule, practically complete. 6.0 per cent of poly(methyl methacrylate) was recovered by Soxhlet extraction with benzene and the remaining fractions in the residue were separated by methanol precipitation from aqueous dimethyl formamide solutions¹⁴ (*Table 6*).

VAPOUR-PHASE SWELLING BLOCK
COPOLYMERIZATION

This synthesis of block copolymers was first used with poly(methyl methacrylate) as the base polymer, but it has since been extended to a range of high-molecular-weight and lightly crosslinked polymers⁵. The mechanism and experimental techniques of this synthesis have recently been published¹⁸ in full. The essential stages are: (1) vapour-phase swelling of

the high-molecular-weight polymer by the free-radical-polymerizable monomer; (2) rupture of carbon-carbon, or other weaker linkages, in the polymer by forces set up when a critical degree of swelling is attained; (3) block copolymerization of the monomer in the swollen polymer by the polymeric free radicals produced *in situ*; and (4) removal of unpolymerized monomer.

Table 6

Fraction	Weight (%)	Composition	
		Starch* (%)	Poly(methyl methacrylate)† (%)
I	35.4	99.0	—
II	58.6	85.0	21.1
III‡	6.0	—	97.5

*Determined from the iodine value.
 †Determined from infra-red spectrography.
 ‡Benzene extraction.

A sample of cellulose acetate with an acetate content of 37.1 per cent was found to swell in the vapour of acrylonitrile at a measurable rate at 30°C. The characteristic increase in the rate of swelling, which was an essential feature of the process, occurred after 40 minutes swelling at a monomer uptake of 15 per cent. Moulded specimens of the polymer swollen to 15 per cent and higher extents were insoluble in chloroform at 15°C, owing to the presence of the block-copolymerized acrylonitrile. Soxhlet extraction with chloroform removed both unpolymerized monomer and residual cellulose acetate. No block polymerization occurred until the critical degree of swelling was attained (Table 7).

Table 7

Swelling (min)	Monomer (%)	Polymerization (%)	Composition	
			Cellulose acetate (%)	Block copolymer (%)
10	6.8	nil	100	—
20	10.9	nil	100	—
30	14.6	nil	100	—
40	15.1	1.6	86.2	13.8
50	19.4	3.8	80.6	19.4
60	24.6	13.4	64.1	35.9

The degree of swelling of the block-copolymer fractions in chloroform decreased with increasing times of initial swelling in the monomer vapour. Thus at 40 min the 'pseudo-gel'¹⁵⁻¹⁶ had a swelling index in chloroform in excess of 60 g of solvent per gramme of block copolymer. At 50 min the gel swelling index was reduced to 19 and at 60 min to 13. This trend was associated with the increasing polyacrylonitrile contents and with the shorter chain lengths of the cellulose acetate segments.

FREEZING OF POLYMER-MONOMER EMULSIONS

Berlin and Penskaya^{19,20} have shown that the freezing and defreezing of starch solutions is accompanied by free-radical degradation processes. The mechanical forces associated with the phase transitions and growth of ice crystals are sufficient to cause rupture of the starch macromolecules. When emulsions of starch with free-radical-polymerizable monomers are subjected to repeated freezing to -200°C and subsequent thawing to room temperature, block copolymerization occurs, provided that oxygen has been removed by degassing. For these experiments acrylonitrile was used as the monomer owing to the ease of separating the insoluble block copolymer fraction. The results for this system are summarized in *Table 8*.

Table 8

<i>Starch: Acrylonitrile in 10% emulsion*</i>	<i>No. of freezing cycles</i>	<i>Percentage block copolymerization</i>
1:1	5	3.5
	10	6.8
	15	8.2
	20	13.4
	25	26.8
1:3	5	4.9
	10	11.2
	15	13.7
	20	21.7
	25	38.9
3:1	5	2.4
	10	8.9
	15	11.7
	20	26.3
	25	27.4

*The emulsion was stabilized with 0.25 per cent of a block copolymer of starch and methyl methacrylate synthesized by the mastication method.

CONCLUSION

In the three methods of synthesizing block polymers of cellulose and its derivatives which have been described, the basic principle is the mechanical scission of polymer chains in the macromolecule to give polymeric radicals which initiate the block copolymerization of a vinyl monomer. The energy required to rupture the molecules has, in the instances reported, been supplied by mechanical action, solvent swelling forces and aqueous freezing forces. It can therefore be postulated that any process which causes the rupture of cellulose molecules should be capable of being adapted to the synthesis of block copolymers. Ultrasonic, gamma, X-ray and sensitized ultra-violet irradiation, milling, grinding, high speed stirring and shaking are all basic methods which it should be possible to adapt, and in fact several of these have been successfully adapted, to block copolymerization techniques for cellulose and its derivatives.

*National College of Rubber Technology,
Holloway Road,
London, N.7*

(Received 30th November, 1960)

REFERENCES

- ¹ ANGIER, D. J., CERESA, R. J. and WATSON, W. F. *Chem. & Ind.* 1958, p. 593
- ² CERESA, R. J. and WATSON, W. F. *J. appl. Polym. Sci.* 1959, **1**, 101
- ³ ANGIER, D. J., CERESA, R. J. and WATSON, W. F. *I.R.I. Trans.* 1958, **34**, 8
- ⁴ ANGIER, D. J., CERESA, R. J. and WATSON, W. F. *J. Polym. Sci.* 1959, **34**, 699
- ⁵ CERESA, R. J. *Polymer*, 1960, **1** (3), 397
- ⁶ CERESA, R. J. *Polymer*, 1960, **1** (1), 72
- ⁷ ANGIER, D. J. and WATSON, W. F. *I.R.I. Trans.* 1957, **33**, 22
- ⁸ CERESA, R. J. *I.R.I. Trans.* 1960, **36**, 45
- ⁹ CERESA, R. J. and WATSON, W. F. *I.R.I. Trans.* 1959, **35**, 19
- ¹⁰ CERESA, R. J. *Trans. Plast. Inst. Lond.* In press
- ¹¹ ANGIER, D. J. and WATSON, W. F. *J. Polym. Sci.* 1955, **18**, 129
- ¹² ANGIER, D. J. and WATSON, W. F. *J. Polym. Sci.* 1956, **20**, 235
- ¹³ ANGIER, D. J., FARLIE, F. O. and WATSON, W. F. *I.R.I. Trans.* 1958, **34**, 8
- ¹⁴ CERESA, R. J. I.U.P.A.C. Symposium on Macromolecules, Moscow, June 1960
- ¹⁵ CERESA, R. J. *Polymer*, 1960, **1** (4), 477
- ¹⁶ CERESA, R. J. *Polymer*, 1960, **1** (4), 488
- ¹⁷ CERESA, R. J. and WATSON, W. F. I.U.P.A.C. Symposium on Macromolecules, Nottingham, September 1958
- ¹⁸ CERESA, R. J. and GRAY, M. A. 10th Canadian High Polymer Forum, Montreal, September 1960
- ¹⁹ BERLIN, A. A. and PENSKEYA, E. A. *Dokl. Akad. Nauk S.S.S.R.* 1956, **120**, 585
- ²⁰ BERLIN, A. A., PENSKEYA, E. A. and VOLKOVA, G. I. I.U.P.A.C. Symposium on Macromolecules, Moscow, June 1960

A New Method for Following Rapid Rates of Crystallization

I. Poly(hexamethylene adipamide)

J. H. MAGILL

A new technique is described for following rates of crystallization in birefringent systems. It consists, essentially, in following the increase in depolarization of plane-polarized light by the crystallizing specimen. Birefringence and crystallinity do not occur concurrently under all conditions, but when transformation from the melt to the more ordered solid phase takes place in the absence of external stresses, the rate of light depolarization is believed to be associated with the development of crystallinity. The method is applicable to a study of fast rates but the slow equilibration of the melt sample to the crystallization temperature imposes a limitation on measurements when the undercooling is large. The paper describes rate measurements on poly(hexamethylene adipamide), (nylon 66), in the range 250°–160°C after melting at 300°C before crystallization. These rate measurements show that the mechanism of nucleation and growth is in substantial agreement with the morphology of crystallized specimens to within a few degrees of 250°C. Results obtained are presented and discussed in the light of current knowledge.

METHODS used for studying the development of crystallinity in substances utilize the change in some physical property with time. Measurements of the changes in density, specific volume or rate of growth of spherulites in the supercooled melt are most frequently employed. Studies of the change of intensity of the crystallinity bands in the infra-red have also been made^{2,3}. Each method has its respective experimental advantages and disadvantages. Sometimes there has been a disparity of results obtained by different methods for the same substance. Recent reviews⁴⁻⁶ on crystallization kinetics in polymeric systems deal with these techniques.

With the exception of the microscope-ciné-camera technique⁷, current methods are not applicable to a study of fast rates of crystallization. The light-depolarization method⁸ developed in these laboratories is applicable to materials of any crystalline texture which exhibit birefringence on crystallization. Ideally, the change from the melt to the solid phase should occur under stress-free conditions.

Complementary studies of the morphology of crystallized specimens should always be made in conjunction with the kinetic measurements and the two approaches should yield consistent information.

EXPERIMENTAL

Materials

The poly(hexamethylene adipamide) polymer had the following analysis:
Relative viscosity of 8.4 per cent solution of polymer, w/w, in 90 per cent formic acid = 32.1
TiO₂ content = nil

Amine end-groups = 40.6 μ equiv./g
Carboxyl end-groups = 78.6 μ equiv./g
Molecular weight (number average) = 12.7×10^3
Ash content = 20 p.p.m.

Apparatus

The apparatus consisted of a Köfler hot-stage mounted on a polarizing microscope (Cooke, Troughton and Simms). The microscope, fitted with a $\times 10$ objective, was pre-focused on a crystallized sample of polymer representative of the thickness of samples to be investigated. Then the eyepiece was removed and the ocular tube of the microscope coupled direct to a Mazda 27 M1 photomultiplier fed with an 800 V E.H.T. supply from an Ediswan power unit, type *R1184*. The photomultiplier was connected to a Solartron cathode-ray oscillograph, type *CD513*. Recordings of the c.r.o. spot were made on *R20* Kodak film with a Cossor camera, model *1428, Mk II A*, fitted with a Cossor variable-drive unit, model *1431*. In the absence of a pulse generator, a Sangamo synchronous motor, model *S7*, 3600 rev/h, operated a micro-switch which interrupted the photomultiplier output to the oscillograph, thus superimposing a time base on the photographic trace. A 24 V Point-O-Lite source supplied from an Advance Components Ltd stabilized power unit, type *DC/24/5*, was used to illuminate the specimen on the Köfler hot-stage. The melt thermostat was a Gallenkamp hot-stage situated vicinally to the Köfler crystallizing hot-stage.

Methods

Sections of polymer chip were dried at 160°C under 10^{-2} mm Hg pressure for three hours and stored in a desiccator over phosphorus pentoxide until ready for use. These sections were mounted in degassed *MS550* silicone oil between clean, $\frac{5}{8}$ in.-diameter, No. 1 cover slips. The samples were melted at $300^\circ \pm 3^\circ\text{C}$ on a Gallenkamp hot-stage for 30 min and then transferred rapidly to the Köfler hot-stage thermostated to within $\pm 0.5^\circ\text{C}$ at the crystallization temperature. When viewed through crossed polarizers immediately after this transfer, the amorphous polymer melt showed a uniformly dark field corresponding to 'zero' photomultiplier output. A finite induction period, τ , elapsed during which no depolarization of transmitted light occurred. With the observable onset of crystallization, the photomultiplier output increased almost autocatalytically and exponentially to a maximum rate at t_1 , after which the rate decreased and fell off asymptotically to a pseudo-equilibrium level. This change was indicated by the deflection of the spot on the c.r.o. screen. The course of this spot was recorded by the 35 mm camera. At the same time, the c.r.o. screen was also viewed through a suitable orange-coloured filter placed over the opening of the camera collimator.

Calibration of photomultiplier

The photomultiplier was calibrated to ensure that its response was linear and stable over the working range. With a $\times 10$ objective lens at its normal working distance from the hot-stage, the light flux passing to the

phototube was adjusted to a fixed level corresponding to a $50 \mu\text{A}$ output, with only the polarizer in position. Intermediate calibration points were obtained by using three standardized Kodak neutral density filters. The maximum operative level was always considerably less than $50 \mu\text{A}$.

Sample thickness

Although sample thickness was found to be less critical than was imagined in the early stages of this work, control was still exercised in this respect. Film thickness was measured or controlled:

- (1) with a screw micrometer for determining average thickness $> 50 \mu$;
- (2) microscopically by remounting the crystallized film, after rate measurements, in a dilute TiO_2 suspension in *MS550* silicone oil (the apparent depth between the two planes of TiO_2 particles, $\times 1.5$, gave the film thickness in microns);
- (3) by mounting the polymer section between cover slips, using another cover slip, with a $\frac{1}{4}$ in. diameter hole cut in its centre, as a spacer.

Most kinetic measurements were made on thick films, $150 \pm 20 \mu$, so as to minimize the influence of surface effects.

RESULTS

Crystallization kinetics

Typical transmitted depolarized light versus time recordings are shown in *Figure 1*(a) and (b). These sigmoidal curves are peculiar to each crystallization temperature and are representative of rate processes.

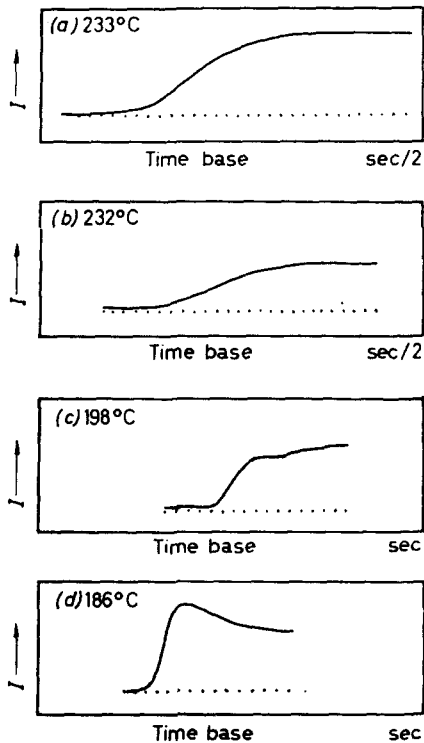


Figure 1--Light transmission/time recordings

Sometimes abnormal light transmission-time, (I/t), recordings were obtained. One observed effect illustrated in *Figure 1(c)* is not unlike the secondary crystallization phenomenon mentioned by Morgan⁹ and others¹⁰. After the primary crystallization process, which is normally associated with the growth of morphological structures, the arrest point or inflexion in *Figure 1(c)*, prior to the secondary ordering process, is often absent in these measurements. In such cases, this 'after-process' is manifest as a smooth change from the primary process gradually levelling off with time. Another effect shown in *Figure 1(d)* is seldom noted, and then only when the crystallization is rapid.

Half-times of crystallization, $t_{1/2}$, may be interpolated directly from the I versus t recordings. Alternatively and preferably, normalized plots of these recordings in the form $(I_0 - I_t)/(I_0 - I_c)$ versus $\log t$, can be used to obtain $t_{1/2}$ values for each isotherm, where I_0 = initial photomultiplier output; I_c = final photomultiplier output and I_t = photomultiplier output after time t (sec). The shape of these graphs also gives information about the nature of the mechanism of nucleation and crystallization. Typical plots are given in *Figure 2*.

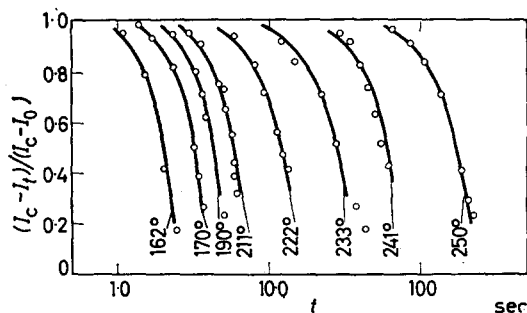


Figure 2—Normalized light transmission/time plots

An attempt was made to measure the induction period for each crystallization temperature and the results are shown in *Figure 3*. Considerable scatter is observed, especially at the lower crystallization temperatures. Here, the τ/T graph begins to flatten off instead of passing through the anticipated minimum in the region where the rate constant is believed to be a maximum. The reason for this observation will be discussed later.

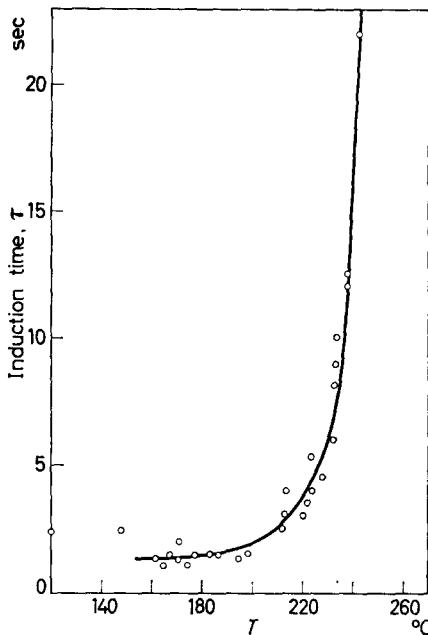
Outside the variability in the observed τ , reproducibility of the normalized I versus t photographic traces was about 5 per cent. However, it was possible to circumvent, to some degree, this difficulty arising out of spurious τ values, by assigning the average τ at a given temperature interpolated from the induction time/temperature plot, to the corresponding isotherm. Adopting this procedure, we calculate rate constants using the Avrami relationship

$$\theta = e^{-kt^n}$$

where θ = fraction of untransformed material; k = rate constant; t = time; n = an integer characteristic of the type of nucleation.

Parameters k and n were arrived at in several ways, already outlined by other authors^{11,12}. In this work, n was most conveniently obtained

Figure 3—Induction time versus crystallization temperature



from the slope of the $\ln(-\ln \theta)$ versus $\ln t$ graphs. This derived value was then used to calculate k from the appropriate $t_{\frac{1}{2}}$ values assuming first-order kinetics. Alternatively, rate constants were derived from the slope of the initial straight-line portion of the $-\ln \theta/t^n$ graphs. The value of τ

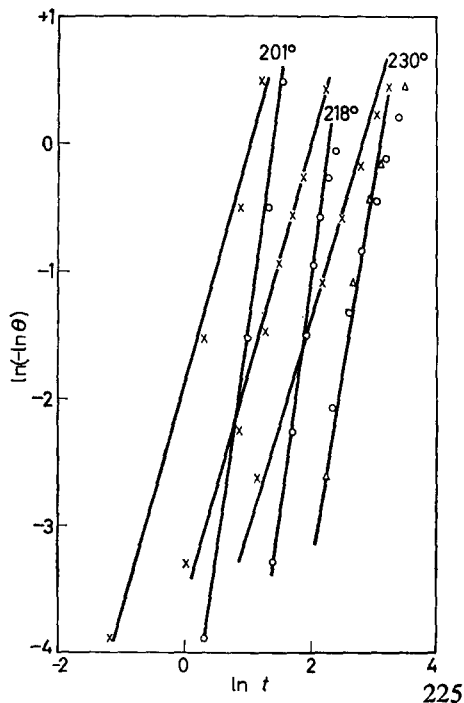


Figure 4—Avrami crystallization isotherms: ○, △ with induction time ($n=3$); ×, without induction time ($n=2$)

must not be omitted in these calculations⁹ since this leads to an erroneous value of $n=2$, instead of $n=3$, for the crystallization temperature range studied. Examples given in *Figure 4* illustrate this point.

Some further experimental evidence for the correlation between the light depolarization and spherulitic growth rate measurements has been obtained in addition to that presented in an earlier communication⁸. Photographic exposures of a crystallizing specimen made at pre-set intervals with a Shackman time-lapse camera, show that the radial growth rate, G , of spherulites is linear with time. Densitometer measurements of the same series of consecutive exposures on the developed film give a sigmoidal curve similar to the I/t traces in the light depolarization method. Plots in *Figure 5* of $D^{1/2}$ versus G , where D is the average optical density of each consecutive exposure, are linear over a considerable range. D is equivalent to the I values in the I/t recordings.

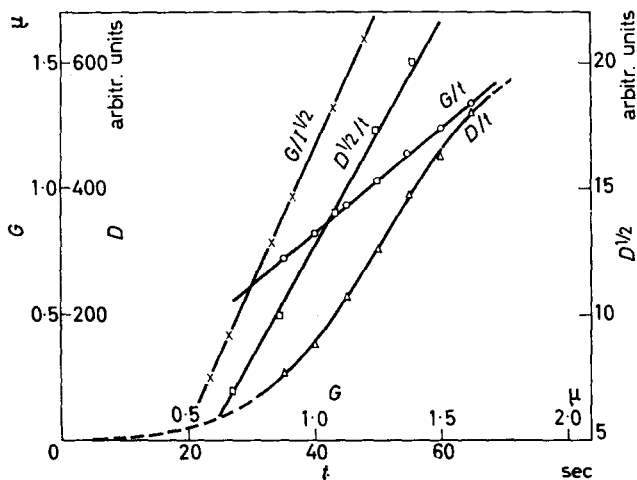


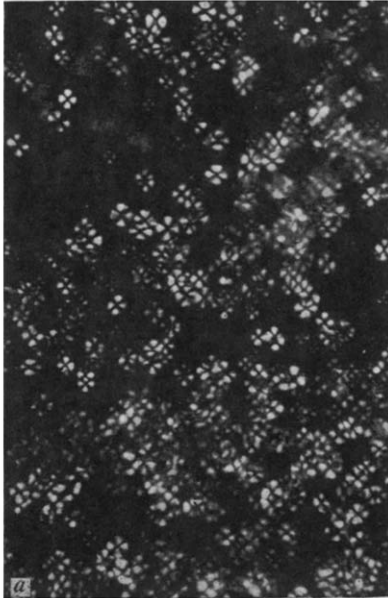
Figure 5—Light transmission/spherulitic growth and rate/time relationships

Morphology of crystallized specimens

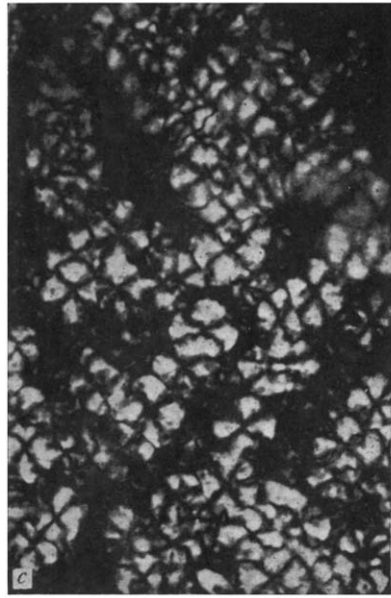
The textures of crystallized samples were examined with the polarizing microscope. Nucleation was predominantly predetermined, and subsequent growth spherulitic down to 160°C. However, within samples, variations of spherulite sizes were observed, i.e. there were areas within a sample having spherulites of a size peculiar to that zone but differing from the spherulite size in another zone. These variations within samples were less pronounced when the crystallization process was arrested by quenching at -30°C in acetone (see *Figure 6*). The granular background associated with these quenched samples is due to perceptible growth at lower temperatures.

X-ray diffraction

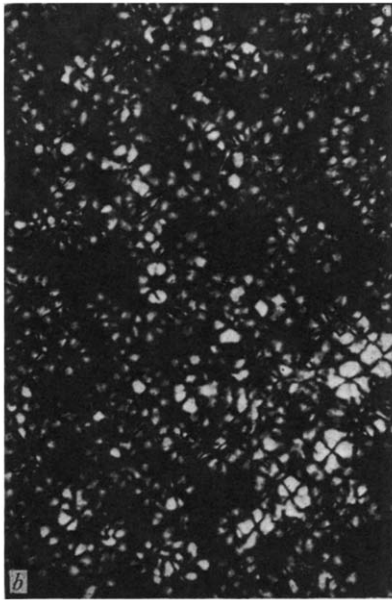
A few samples selected at random were examined. These revealed that crystalline perfection was higher for samples grown at the higher crystallization temperatures, ca. 240°C. Little or no difference could be detected for samples crystallized in the range 200°C to 160°C.



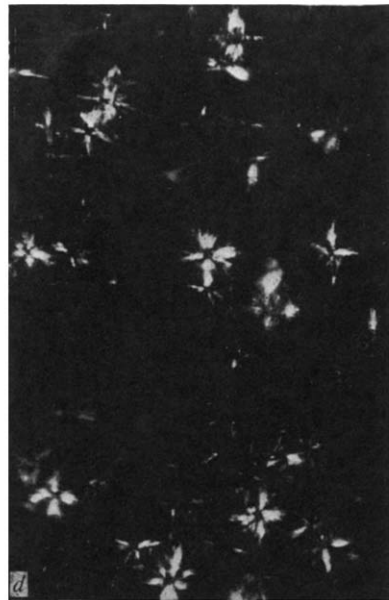
(a)—Crystallization for *ca.* 1 sec at 163°C (predetermined nucleation)



(c)—Crystallization for *ca.* 8 sec at 221°C (predetermined nucleation)



(b)—Crystallization for *ca.* 4 sec at 203°C (predetermined nucleation)



(d)—Crystallization for *ca.* 3 min at 248°C (predominantly sporadic nucleation)

Figure 6—Morphology of specimens melted for 30 min at 300°C, then crystallized and quenched

DISCUSSION

Results of different experimental methods for following crystallization rates are not always in agreement with each other. Differences have been noted for the same polymer, and the results obtained appear to depend on the method used. The variability may be due to the crystallinity detector and the extent to which it is able to follow the changes in arrangements of crystalline and amorphous regions during the phase change. Inconsistencies between polymers depend on numerous factors, notably the fabrication of the polymer itself and its melt history. The crystallization kinetics and morphology may also be affected by the polymer stability, adventitious impurities, and extraneous or intrinsically formed nuclei resulting from thermal degradation at the melt temperature.

Treatment of results

The technique developed in these laboratories appears analogous to the other methods for following rates of crystallization. The accelerated manner in which the light depolarization alters with time as the crystallization proceeds is a direct consequence of the proportionality between the rate of volume increase of the transformed material and its surface area, in agreement with the direct microscopic observation that the spherulitic radius increases linearly with time. *Figure 5* provides direct experimental evidence on this point. In the method, account is taken of the low initial growth of observable nuclei before their development to spherical entities²⁰.

Evans's¹³ and Morgan's¹¹ treatment of the theory of expanding spheres in a study of spherical growth of a new phase from nuclei which appear:

- (a) randomly in time and space
- (b) non-randomly in time and space

can be used to describe the spherulitic growth in a polymer melt lamella. The rate of nucleation and growth of these macroscale organized bodies is directly proportional to the depolarization intensity of transmitted light, since it is assumed here that only the birefringent sheaves and spherulites are contributory in this respect. Following Poisson's equation¹⁴, Evans points out that the fraction of unchanged volume in unit volume equals e^{-E} after time t ; where E is the expected number of spheres passing any point. It therefore follows that the fraction of changed volume equals $1 - e^{-E}$. For a particular I/t recording, let I_t be the depolarization intensity after a time t , ($t > \tau$), then

$$I_t \propto 1 - e^{-E}$$

since it is assumed that the rate of depolarization is intimately associated with the growing species, i.e.

$$I_t \propto (1 - \theta) = k(1 - \theta)$$

Let $I_t = I_0$ initially, when $\theta = 1$, and $I_t = I_c$ finally when $\theta \rightarrow 0$. In addition, the function, $(I_c - I_t)/(I_c - I_0)$, can be deduced and represents the fraction of unchanged material remaining at any time, t . This normalization process reduces all I/t recordings to the same scale (zero to unity). The derived function is dimensionless and representative of the Avrami θ in the same

way as corresponding volume, density or infra-red intensity function, whence

$$\frac{I_c - I_t}{I_c - I_0} = e^{-kt^n}$$

A plot of $(I_c - I_t)/(I_c - I_0)$ versus $\log t$ minimizes differences arising out of light intensity and sample thickness variations. For each sample, the change is analysed in terms of the fraction of transformed material for that particular crystallization temperature. It is not analysed in terms of the fraction of completely transformed crystalline substance. In the absence of refractive index data on nylon 66 through the phase transformation region, a more detailed analysis cannot be put forward. It is therefore assumed that the refractive index of the melt is not very different from the average refractive index of the crystallized polymer. On this model, the mechanism of nucleation and crystal growth can be found from these plots. Under appropriate conditions it can be applied to non-spherulitic growth¹⁷.

It is recognized that birefringence and crystallinity do not occur concomitantly under all conditions¹⁹. However, under stress-free conditions, where the ultimate spherulite size is less than the sample thickness, the rate of depolarization of transmitted polarized light is thought to parallel the development of crystallinity. In these circumstances, no contribution from factors causing extraneous depolarization would be superimposed on the depolarization arising only from the development of spherulites. In any case, it seems that in the early stages of the crystallization process, where the amorphous phase is in excess, a good parallelism exists, allowing the Avrami expression to be applied. Deviations have been noted for values of $\theta < 0.5$ determined from density measurements⁴, but there are also examples which appear to be exceptions to this observation¹¹. *Figure 7* shows typical examples of the agreement between theoretical and observed values obtained in this work.

Morphology

Microscopic examination of some of the crystallized specimens from the kinetic studies shows a distribution of spherulite sizes between areas in the same sample. These variations may lead to erroneous conclusions about the mechanism of nucleation. In controlled tests, where the sample was quenched after an initial period of growth, uniformity of spherulitic size was generally observed for the early stages of the crystallization. It can therefore be concluded that the morphology of these specimens indicates that nucleation and growth are spherulitic and primarily predetermined in the temperature range 160°C to 245°C (approximately), in general agreement with the kinetic measurements. Typical photographs of these crystallizations are shown in *Figure 6*.

The observed decrease in grain size with lowering of the crystallization temperature is not as consistently reproducible and well defined in nylon 66 as it is in isotactic polypropylene¹⁷ and poly(ethylene terephthalate)¹⁸ polymers. On the basis of crystallization theory a reproducible picture is to be expected, since, as the temperature is lowered, more fruitful nuclei are formed at the lower temperature.

Ordinary X-ray diffraction patterns of a few samples indicate, as expected, that perfection of the crystal lattice was greater at the higher crystallization temperature but no further conclusions were permissible, since organization on the crystallite scale revealed by these patterns does not permit comparison with the macro-spherulitic entities observed microscopically.

Kinetic results

The majority of the $(I_0 - I_t)/(I_0 - I_\infty)$ isotherms (*Figure 2*) obtained from I/t recordings can be brought into coincidence by a shift of the time scale. This behaviour is a unique property of the crystallization of homopolymers, showing the invariant nature of the temperature coefficient throughout the major part of the crystallization process. In these circumstances the integer, n , in the Avrami equation remains constant. For nylon 66, predominantly predetermined nucleation and growth are obtained over the temperature range studied. The various approaches to the calculation of n and k gave consistent results except when the induction times were omitted. In this instance, erroneous values for n were obtained as the time from the invisible to the visible onset of crystallization appreciably influences the kinetics. In the absence of a value or values for n , the half-times of crystallization may be used instead of k for comparative purposes, since $t_{1/2}$ is a rate parameter: as

$$k = \frac{\ln 2}{(t_{1/2})^n}$$

However, it must also be remembered that in any study of the crystallization kinetics of polymers the equilibrium nucleation process is not independent of the melt history, as is implied on the basis of first-order kinetics. Morgan¹⁶ has pointed out that the previous melt history, as well as melt

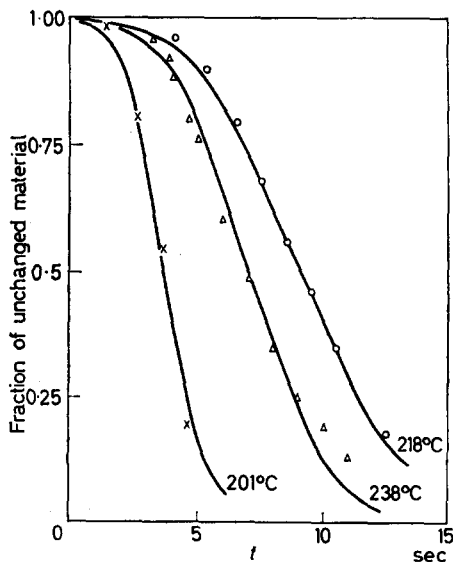
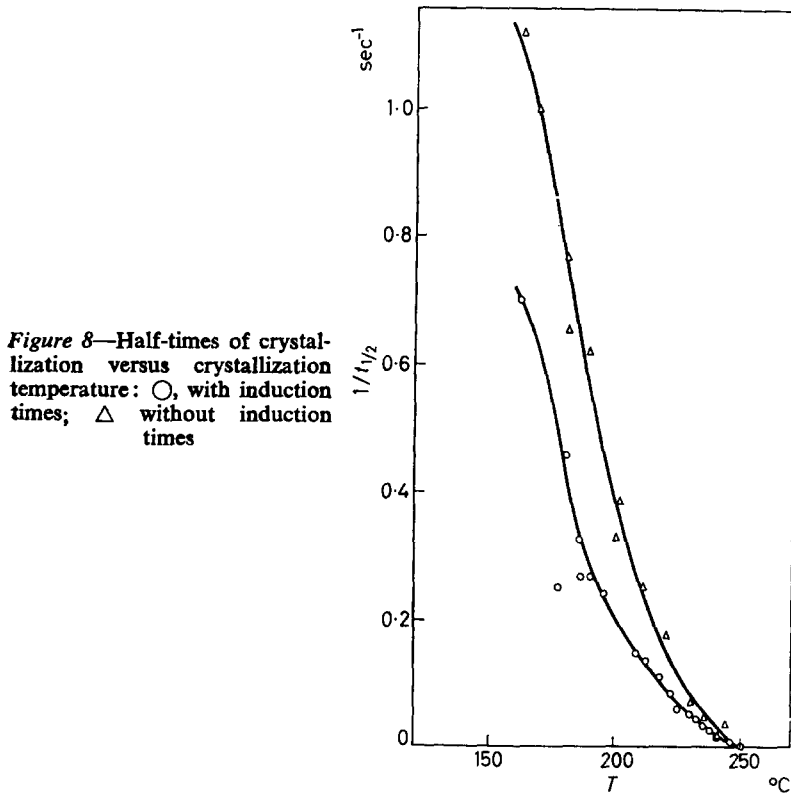


Figure 7—Fraction of unchanged material versus time. Time scale for 238°C plot is sec/5. The theoretical line is superimposed on the observed results

time, has a very significant effect on the subsequent crystallization. A detailed study¹⁵ of the influence of melt temperature on the measured induction time for crystallization of nylon 66 shows that a linear relationship between the plot of $\log \tau$ versus $\log (\Delta T)$, where ΔT denotes the extent of the undercooling, only exists above melt temperatures of 290°C.

Since the induction time, τ , is intimately associated with the rapid attainment of the steady-state nuclei and slow initial observable rates of growth of these nuclei, factors which affect the measured or apparent



induction time are likely to influence the kinetic rate parameter. The levelling-out of the induction time in *Figure 3* as the crystallization temperature is lowered is due to the slow rate of equilibration of the melted sample to the hot-stage crystallization temperature. The attainment of the true crystallization temperature is precluded by poor heat transfer and presents one of the most difficult experimental problems encountered in work of this nature. Rapid cooling of a sample followed by good thermostating at the desired crystallization temperature seem almost, if not entirely, incompatible and unattainable.

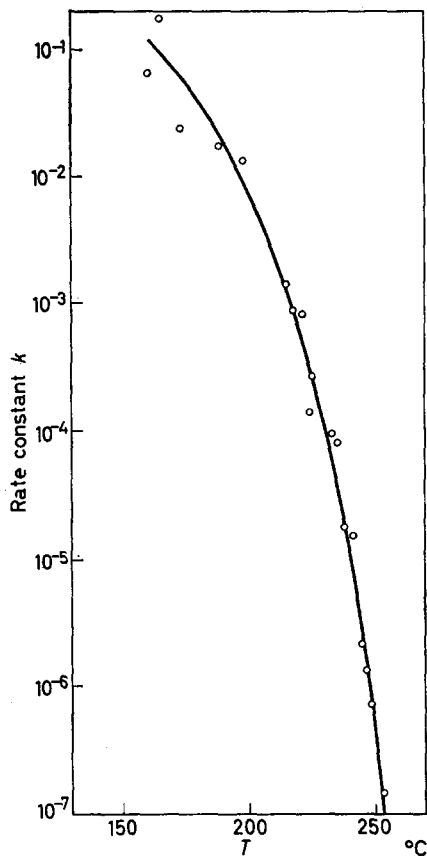


Figure 9—Rate constants versus crystallization temperature

The rate constants obtained in this paper are of the same order of magnitude as McLaren's microscopical measurements¹⁵, and consistently on the higher side of Morgan's⁹ density-balance data obtained in the temperature range 235°–255°C. At present, no satisfactory explanation can be suggested for this difference. It is realized, however, that for the lower temperatures (say, below 210°C), the $t_{\frac{1}{2}}$ or rate values shown in Figures 8 and 9 correspond to some temperature, δT degrees above the observed crystallization hot-stage temperature. (δT is a parameter increasing in magnitude with the degree of supercooling.) The same conclusion follows immediately from an analysis of the induction times. Clearly, the poor rate of equilibration of the sample to the true crystallization temperature is responsible. At the lower crystallization temperatures, where the induction time becomes comparable with the rate of cooling, experimental results can only be considered to be proportional to the true rate parameters.

In an earlier communication⁸, agreement was obtained between the spherulitic growth rate data of Burnett and McDevit⁷ and the light-depolarization $t_{\frac{1}{2}}$ values, from which the induction times were purposely eliminated. In this respect, the validity of this technique is substantiated.

The author thanks Mr J. A. Nixon for assistance with experimental details and Dr T. C. Tranter for X-ray diffraction and densitometer measurements.

*Research Department,
British Nylon Spinners Limited,
Portypool, Mon.*

(Received 2nd January, 1961)

REFERENCES

- ¹ MANDELKERN, L. in *Growth and Perfection of Crystals* (Ed. DOREMUS, R. H., ROBERTS, B. W. and TURNBULL, D.), Wiley, New York, 1958, pp. 467-95
- ² REDING, F. P. and BROWN, A. *J. appl. Phys.* 1954, **25**, 848
- ³ BUCHDAHL, R., MILLER, R. L. and NEWMAN, S. *J. Polym. Sci.* 1959, **36**, 215
- ⁴ MANDELKERN, L. *Chem. Rev.* 1956, **56**, 903
- ⁵ MANDELKERN, L. *Rubb. Chem. Technol.* 1959, **32**, 1392
- ⁶ MANDELKERN, L. *S.P.E. J.* 1959, **15**, No. 1
- ⁷ BURNETT, B. B. and McDEVIT, W. F. *J. appl. Phys.* 1957, **28**, 1101
- ⁸ MAGILL, J. H. *Nature, Lond.* 1960, **187**, 770
- ⁹ HARTLEY, F. D., LORD, F. W. and MORGAN, L. B. International Symposium on Macromolecular Chemistry, Milano-Torino September-October 1954, p. 577
- ¹⁰ RYBNIKAR, F. *J. Polym. Sci.* 1960, **44**, 517
- ¹¹ MORGAN, L. B. *Phil. Trans. A*, 1954, **247**, 13
- ¹² MARKER, L., HAY, P. M., TILLEY, G. P., EARLY, T. M. and SWEETING, O. J. *J. Polym. Sci.* 1959, **38**, 33
- ¹³ EVANS, U. R. *Trans. Faraday Soc.* 1945, **41**, 365
- ¹⁴ POISSON, S. D. *Recherches sur la Probabilité des Jugements en matière criminelle et en matière civile* Bachelier, Paris, 1837, p. 206
- ¹⁵ McLAREN, J. V. Unpublished work
- ¹⁶ MORGAN, L. B. *J. appl. Chem.* 1954, **4**, 160
- ¹⁷ MAGILL, J. H. Unpublished work
- ¹⁸ HARTLEY, F. D., LORD, F. W. and MORGAN, L. B. *Phil. Trans. A*, 1954, **247**, 23
- ¹⁹ BUNN, C. W. Chapter 10 in *Fibres from Synthetic Polymers* (Ed. R. HILL), Elsevier, Amsterdam, 1953
- ²⁰ BYRANT, W. D., PIERCE, B. H. H., LINDERGREN, C. R. and ROBERTS, R. *J. Polym. Sci.* 1955, **16**, 131

Note

Fractionation of Radiation-branched Polybutadiene

In the preparation of branched polybutadiene fractions, samples of butyl-lithium-catalysed polybutadiene of narrow molecular weight distribution ($\overline{M}_w/\overline{M}_n=1.25$) were exposed to gamma radiation from a cobalt-60 source for doses below the gelation point. Air was excluded by closely wrapping the samples in polyethylene film but they were not outgassed before irradiation. The irradiated polymers were then fractionated from benzene with acetone as precipitant and the fractions examined by light scattering, viscometry and osmometry. Rather surprisingly it was found that the irradiated polymers could be separated into branched polymer of high molecular weight and a substantially linear polymer of molecular weight similar to that of the original polymer. The data are shown in *Table 1*. Light scattering measurements were carried out with cyclohexane as solvent, while for viscosity and osmotic measurements the solvent was benzene. The extent of branching is shown by g' , which is the ratio of the intrinsic viscosity of the polymer to that of a linear polymer of the same weight-average molecular weight. (The viscosity versus molecular weight relationship for linear polybutadiene fractions prepared with butyl-lithium as catalyst is¹ $[\eta]=1.45 \times 10^{-4} M^{0.76}$.)

The fact that crosslinking is apparently restricted to a fraction of the polymer which increases rapidly in molecular weight with dose suggests that several molecules are linked together by a short-chain reaction following the primary formation of a radical. If the crosslinking mechanism involved recombination of two adjacent free radicals, a random increase in

Table 1. Molecular weights of irradiated polymer fractions

Polymer	Irradiation dose (R)	Normalized weight fraction	$10^{-5} \overline{M}_w$	$10^{-5} \overline{M}_n$	$[\eta]$	k'	g'
Original	0	1.0	2.56	2.05	1.86	0.38	1.0
A	3×10^5	0.53	9.09	7.06	2.75	0.51	0.58
		0.19	2.54	1.67	1.51	0.46	0.82
		0.10	1.85	1.27	1.32	0.46	0.91
		0.18	1.42	0.73	1.00	0.44	0.84
B	3.5×10^5	0.33	42.3	>10*	4.02	0.52	0.26
		0.21	3.34	3.08	2.16	0.51	0.92
		0.37	2.53	1.76	1.64	0.49	0.89
		0.09	1.94	1.13	1.38	0.39	0.92
C	6×10^5	0.57	107.0	>10*	3.80	0.62	0.12
		0.27	2.82	1.99	1.79	0.43	0.90
		0.11	2.58	1.39	1.48	0.45	0.80
		0.05	1.63	0.91	1.16	0.45	0.87

*Extrapolation to infinite dilution unreliable for molecular weights above 10^6 .

molecular weight throughout the sample would have been anticipated. Gel was formed after a dose of about 10^6 R. It must be remembered, however, that oxygen was not vigorously excluded in these experiments and may have influenced the reaction to some extent.

Since each crosslink is accompanied by the disappearance of one molecule and each chain scission results in an extra molecule, it is possible from fractionation data before and after irradiation to obtain some estimate, $G(X)$, of the extent to which crosslinking predominates over chain scission. The net decrease in number of molecules gives

$$G(X) = \left[\frac{100N}{D} \frac{1}{\bar{M}_n} - \sum f_i/M_i \right]$$

where \bar{M}_n is the initial number average molecular weight, f_i and M_i are weight fraction and molecular weight of the i th fraction after irradiation, D is the dose in eV/g and N is Avogadro's number. This calculation applied to sample A shows an increase in the number of molecules after irradiation, a result which may be attributed either to inadequate fractionation of the polymer, or to the participation of dissolved oxygen in the polybutadiene. The data from samples B and C give values of $G(X)$ in the region of 4.

The primary radical-forming reaction resulting in hydrogen evolution has not been studied, but it might be expected to be similar to that observed for natural rubber, where² $G(H_2) = 0.64$. A value of this order for polybutadiene would show that each primary radical must be followed by a short-chain reaction linking at least three polymer molecules. This estimate is not greatly different from the value of 5, which has been obtained from crosslink density measurements on highly purified butadiene-styrene copolymers³.

The data presented in this note demonstrate that with the ready availability of polymers of narrow molecular weight distribution, useful information can be gained on the mechanism of radiation crosslinking in the early stages of reaction before gelation has occurred. The main advantage of this method is that it does not require the initial molecular weight distribution to be defined by the mathematical equations on which the calculations from sol and gel fractions are based.

We thank the Dunlop Rubber Company Limited for permission to publish.

G. VAUGHAN, D. E. EAVES and W. COOPER

*Chemical Research Department,
Central Research,
Dunlop Rubber Co. Ltd,
Erdington,
Birmingham, 24*

(Received 20th April, 1961)

REFERENCES

- ¹ COOPER, W., VAUGHAN, G. and EAVES, D. E. *J. Polym. Sci.* In press
- ² TURNER, D. T. *Polymer*, 1960, 1 (1), 27
- ³ PEARSON, R. W. Unpublished results

Contributions to Polymer

*Papers accepted for future issues of
POLYMER include the following:*

The Dielectric and Dynamic Mechanical Properties of Polyoxymethylene (Delrin)—B. E. READ and G. WILLIAMS

Streaming Birefringence of Soft Linear Macromolecules with Finite Chain Length—A. PETERLIN

Tracer Studies of Di-anisoyl Peroxide and the Anisoyloxy Radical—J. K. ALLEN and J. C. BEVINGTON

The Effect of the High-frequency Discharge on the Surfaces of Solids I. The Production of Surface Radicals on Polymers—C. H. BAMFORD and J. C. WARD

Branched Polymers I. Molecular Weight Distributions—T. A. OROFINO

Branched Polymers II. Dimensions in Non-interacting Media—T. A. OROFINO

The Crystallization of Polyethylene Terephthalate by Organic Liquids—W. R. MOORE and R. P. SHELDON

The Assignment of the Infra-red Absorption Bands and the Measurement of Tacticity in Polypropylene—M. P. McDONALD and I. M. WARD

The Thermal Depolymerization of Polystyrene IV. Depolymerization in Naphthalene and Tetralin Solutions—G. G. CAMERON and N. GRASSIE

The Constitution of Ethylene-Propylene Copolymers—J. VAN SCHOOTEN, E. W. DUCK and R. BERKENBOSCH

Intermolecular Forces and Chain Flexibilities in Polymers III. Internal Pressures of Polymers below the Glass Transition Temperature—G. ALLEN, D. SIMS and G. J. WILSON

The Rate of Cure of Network Polymers and the Superposition Principle—M. GORDON and W. SIMPSON

CONTRIBUTIONS should be addressed to the Editors, *Polymer*, 4-5 Bell Yard, London, W.C.2.

Authors are solely responsible for the factual accuracy of their papers. All papers will be read by one or more referees, whose names will not normally be disclosed to authors. On acceptance for publication papers are subject to editorial amendment.

If any tables or illustrations have been published elsewhere, the editors must be informed so that they can obtain the necessary permission from the original publishers.

All communications should be expressed in clear and direct English, using the minimum number of words consistent with clarity. Papers in other languages can only be accepted in very exceptional circumstances.

A leaflet of instructions to contributors is available on application to the editorial office.

The Dielectric and Dynamic Mechanical Properties of Polyoxymethylene (Delrin)

B. E. READ and G. WILLIAMS

The dielectric and dynamic mechanical properties of polyoxymethylene (Delrin) have been measured in order to investigate molecular motions in this polymer. The dynamic shear modulus and loss factor have been determined in the frequency range from 0.05 to 1 c/s, from -190°C up to the melting point (180°C). Two loss maxima have been observed at about -77°C and 87°C respectively. The dielectric properties have been investigated over the frequency range 120 c/s to 9 kMc/s and the temperature range -80°C to $+150^{\circ}\text{C}$. A single broad relaxation absorption was observed which correlates with the low temperature mechanical relaxation. The effect on these relaxations of swelling the polymer with dioxan is consistent with motions occurring in the amorphous regions of the polymer only.

INTRODUCTION

POLYOXYMETHYLENE is a highly crystalline polymer having the chemical structure $(-\text{CH}_2\text{O}-)_n$. Since the ether group has a dipole moment, molecular motions occurring in this polymer may be investigated experimentally by both dielectric and dynamic mechanical methods. The long chain molecules do not contain side branches, so that the motions observed will be associated with the chain backbone or end groups. In this paper it is shown that the molecular motions probably occur in the disordered regions of the polymer whereas the chain segments in the crystallites are rigidly fixed in position.

As this work was being completed, dielectric measurements on polyoxymethylene, confined to low temperatures and frequencies were published by Ishida¹ and by Michailov and Eidelnant² and their conclusions regarding the exact origin of the dielectric relaxation are not in accord with the findings of the present work. After the completion of this work, measurements by Thurn³ were communicated to the authors and the results generally agreed with those presented here.

MATERIAL

The polyoxymethylene used in these experiments was Du Pont *Delrin 500*. The number average molecular weight of the polymer lies in the range 30 000 to 50 000. The density of the polymer, which was determined by hydrostatic weighings, was 1.420 ± 0.005 , equivalent to 70.0 per cent crystallinity by weight⁴. After annealing a sample in an evacuated tube at 160°C for three days, its density was found to be 1.434 ± 0.004 corresponding to 75.5 per cent crystallinity. On account of the rapid rate of crystallization in this polymer, attempts to produce wholly amorphous material by quenching from the melt were unsuccessful. In order to study the effect of absorbed liquid at low temperatures, a specimen was heated in

dioxan at 60°C for three days, after which about six per cent by weight of the solvent had been absorbed. The total weight of sample and absorbed dioxan was unchanged after the completion of the mechanical and dielectric measurements at low temperatures.

EXPERIMENTAL

(1) *Dynamic mechanical measurements*

The dynamic shear modulus and damping were measured in the frequency range 0.05 to 1 c/s from -190°C up to the melting point (180°C). The apparatus used was a torsion pendulum similar to that described by McCrum⁵. The polymer strips were clamped at their upper end to a rigid support and an inertia bar freely suspended from below. The inertia bar was pulsed electromagnetically and the period and amplitude of free torsional oscillations observed by means of a mirror, lamp-and-scale arrangement. The variation and measurement of temperature was effected by a method similar to that used by McCrum⁵. The frequency of measurement was varied by altering the positions of weights attached to the inertia bar, thus maintaining the tensile load on the specimen constant.

The logarithmic decrement, Δ , and the real and imaginary components, G' and G'' respectively, of a complex shear modulus were evaluated from standard equations⁶. Corrections were applied for the effect of load on the period of oscillation. Δ was found to decrease with increasing load although G'' was independent of load within experimental error.

The error involved in the evaluation of absolute values of G' was about 5 per cent, arising mainly from inaccuracies in determining the sample dimensions. However, excluding dimensional changes, which were not taken into account in calculating the modulus, the variation of G' with temperature for any given specimen was accurate to within 0.5 per cent. The absolute errors in G'' and Δ were about 5 per cent.

(2) *Dielectric measurements*

For the electrical measurements, discs 50 mm in diameter and 1 to 2 mm thick were made by moulding *Delrin* pellets under pressure. For the high frequency measurements coaxial samples were directly machined from *Delrin* rods giving samples about 5 cm long, 1.6 cm outside diameter and 0.5 cm inside diameter. All samples were heated at 100°C under 0.1 mm of mercury pressure over silica gel in order to remove small traces of water from the polymer.

Measurements were made between 120 c/s and 9 kMc/s by a variety of methods. In the range 120 c/s to 10 kc/s a Schering bridge was employed in conjunction with a guarded electrode cell. Temperatures between -80°C and room temperature were obtained using methanol-solid carbon dioxide mixtures, while temperatures up to 150°C were obtained using an oven. A Hartshorn-Ward instrument⁷ was used in the frequency range 300 kc/s to 100 Mc/s. Temperature variation between -80°C and 150°C was made using a two terminal cell but the frequency upper limit was about 5 Mc/s owing to the anomalous effects of stray inductance and capacitance at higher frequencies. A *G.R. Slotted Line*⁸ was used in the frequency range

200 Mc/s to 2 kMc/s, temperature variation being achieved in the same way as in the Schering bridge method. At 9 kMc/s a $H_{0,1n}$ cavity resonator was employed. It is estimated that the dielectric constant and loss were measured to an accuracy of ± 1 per cent and ± 3 per cent respectively over the entire frequency range. The temperature of samples was known to $\pm 0.5^\circ\text{C}$.

RESULTS

Mechanical data

A summary of mechanical data is presented in *Figures 1* to *3* and *Table 1*.

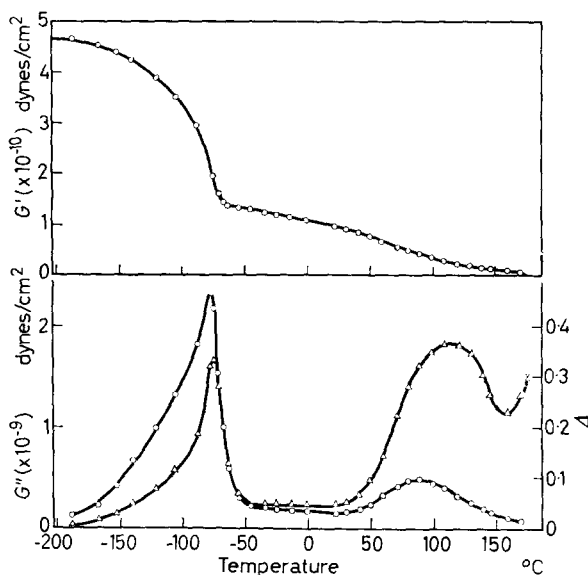


Figure 1—Plot of G' , G'' and the logarithmic decrement (Δ) as a function of temperature. Δ is represented by the triangles

Typical curves of G' , Δ and G'' versus temperature are plotted in *Figure 1*. The frequency of measurement decreased with decreasing modulus, ranging from 0.3 to 0.1 c/s, although the experiments can be regarded as being performed essentially at constant frequency. The specimen used for runs below room temperature had a smaller cross section than that used above room temperature in order to keep the experimental frequency within the above convenient range.

It can be seen from *Figure 1* that polyoxymethylene exhibits two relaxations. The low temperature relaxation corresponds to sharp maxima in the Δ and G'' curves at -75°C (0.176 c/s) and -77°C (0.186 c/s) respectively. G''_{max} occurs at the same temperature (T_{max}) as the inflection point in the G' plot. On the high temperature side of the relaxation the changes in both the modulus and loss curves are far more abrupt than on the low temperature side where a long tail is observed.

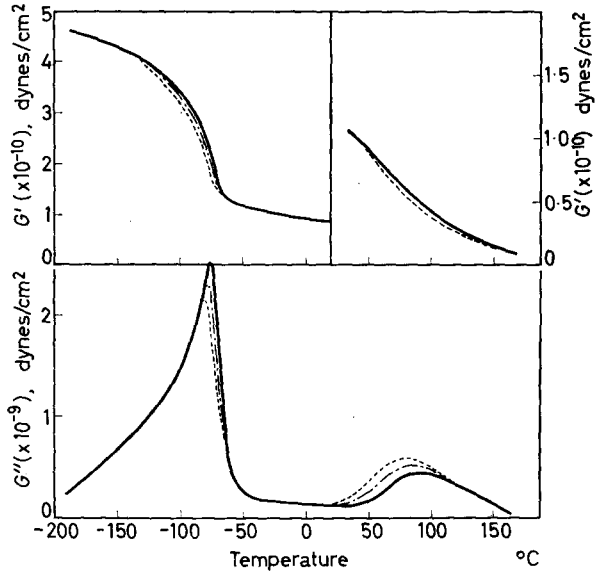


Figure 2—Curves of G' and G'' versus temperature at three frequencies: full line 0.42 c/s, chain-dotted, 0.16 c/s, dashed 0.08 c/s. Note the scale change for G' above room temperature

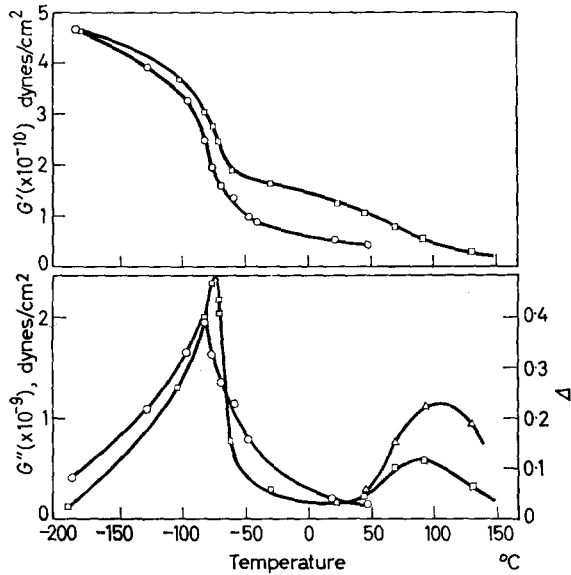


Figure 3—Plots showing the effects of adding 5.7 per cent dioxan (O) and also of annealing (□) on the modulus and losses for polyoxymethylene. For the annealed sample above room temperature energy losses are shown both as G'' (□) and Δ (Δ)

Above room temperature the logarithmic decrement shows a broad peak roughly equal in height to the low temperature maximum, and centred at 115°C (0.150 c/s). G''_{\max} occurs at 89°C (0.188 c/s), but is considerably lower than the G''_{\max} of the low temperature loss peak. An increase in Δ is observed between 157°C and the melting point.

Figure 2 shows the variation of G' and G'' with temperature at three frequencies. The variation of T_{\max} with frequency is shown in Table 1.

Table 1. Summary of dynamic mechanical data

Material and diagram	Crystallinity (wt per cent)	Low temperature relaxation			
		T_{\max} (°C)	Frequency (c/s)	$G'_{-190} - G'_{20}$ dynes/cm ² × 10 ⁻¹⁰	$2G''_{\max}$
					$G'_{-190} - G'_{20}$ (= β)
Unannealed	70.0				
Figure 1	70.0	-77	0.186	3.70	0.125
Figure 2					
(a)	70.0	-76	0.427	3.70	0.137
(b)	70.0	-78	0.160	3.70	0.126
(c)	70.0	-80	0.077	3.70	0.116
+ Dioxan (5.7%)					
Figure 3	70.0	-85	0.364	4.14	0.097
Annealed					
Figure 3	75.5	-74	0.164	3.38	0.141
Material and diagram	Crystallinity (wt per cent)	High temperature relaxation			
		T_{\max} (°C)	Frequency (c/s)	$G'_{20} - G'_{147}$ dynes/cm ² × 10 ⁻¹⁰	$2G''_{\max}$
					$G'_{20} - G'_{147}$ (= β)
Unannealed	70.0				
Figure 1	70.0	89	0.188	0.810	0.119
Figure 2					
(a)	70.0	94	0.412	0.962	0.094
(b)	70.0	87	0.161	0.988	0.107
(c)	70.0	77	0.081	0.986	0.122
+ Dioxan (5.7%)					
Figure 3	70.0				
Annealed					
Figure 3	75.5	87	0.070	1.070	0.112

(a) Since G' is not constant either side of each dispersion, the modulus increments are defined in terms of arbitrary temperatures denoted by the appropriate subscripts.

(b) β is an empirical parameter analogous to that defined in the dielectric section.

Results obtained for the swollen and annealed samples are illustrated in Figure 3. The swelling agent shifts the low temperature loss maximum down by 9°C (at constant frequency) and broadens the dispersion on the high temperature side. Both modulus and loss curves are now relatively symmetrical compared with the dry polymer. In the intermediate temperature

range, G' for the swollen polymer is less than that of the dry material by a factor of about two. Although it was not possible to make accurate measurements above 30°C , owing to loss of solvent, qualitative experiments showed that in the presence of some swelling agent the high temperature loss peak was considerably depressed.

Increase of crystallinity leads to a slight reduction of the modulus increment, $G'_{-190} - G'_{20}$, of the low temperature relaxation (*Table 1*). In addition the dispersion is slightly narrowed and shifted by 4°C to higher temperatures. The annealing process leads to a decrease in Δ_{max} in the high temperature transition region, whilst G''_{max} maintains about the same level but is moved by about 10°C to higher temperatures.

Dielectric data

A single strong dielectric relaxation process was observed, the curves being broader in the frequency plane (i.e. constant temperature) than that expected for a single relaxation time.

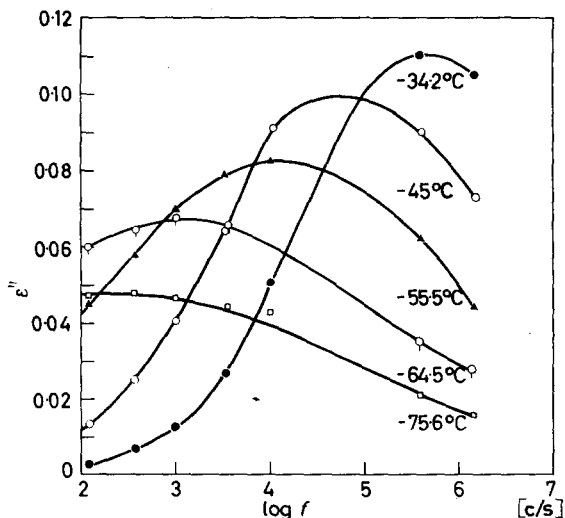


Figure 4—The dielectric loss factor as a function of frequency at low frequencies

The results for low frequencies are shown in *Figure 4*. It is seen that the relaxation maxima are obtained at low temperatures. As the temperature decreases the curves broaden rapidly and decrease in height. This behaviour is consistent with a distribution of relaxation times that changes rapidly with temperature, the distribution being wider the lower the temperature.

The low frequency results are plotted in the temperature plane in *Figure 5* and again it is seen that the loss is smaller at lower temperatures and lower frequencies. The shape of the curves varies over the range, the higher frequency curves being fairly symmetrical whereas the lower frequency curves are much broader on the low temperature side of maximum loss.

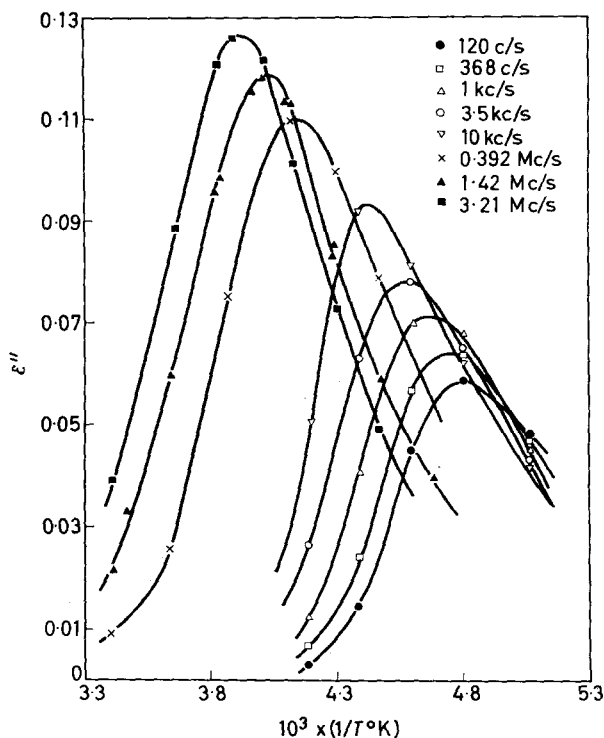


Figure 5—The dielectric loss factor as a function of temperature at low frequencies

The non-symmetry of these curves can be explained in terms of the changing distribution of relaxation times.

The higher frequency curves are shown in *Figures 6 and 7* and are similar to the low frequency curves except that in *Figure 7* the curves are more symmetrical than those in *Figure 5*.

We may attempt to analyse the data in terms of the formal dielectric parameters.

The incremental dielectric constant

The dielectric constant increment is $(\epsilon_0 - \epsilon_\infty)$ where ϵ_0 and ϵ_∞ are the low and high frequency dielectric constants at a given temperature. The value of $(\epsilon_0 - \epsilon_\infty)$ was evaluated using two methods; (a) the difference between the observed low and high frequency dielectric constants; (b) the area below the loss factor versus log frequency curve⁹. Values for $(\epsilon_0 - \epsilon_\infty)$ are shown in *Figure 8* and it is seen that it increases with increasing temperature, which is converse to the behaviour predicted by Onsager¹⁰. It was found that ϵ_∞ had the value 2.87 which was independent of temperature within experimental error. The low frequency dielectric constant at 20°C was 3.48.

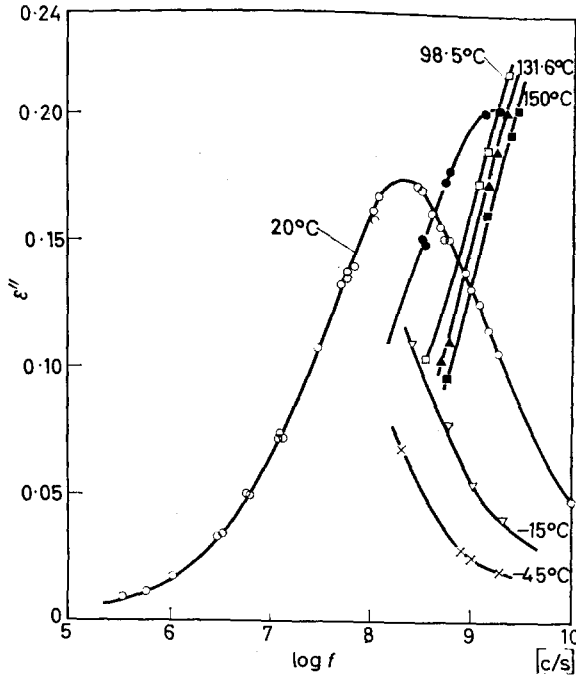


Figure 6—The dielectric loss factor as a function of frequency at high frequencies

The distribution of relaxation times

Fuoss and Kirkwood¹¹ have derived a semi-empirical relation between the loss factor and frequency for a symmetrical distribution of relaxation times

$$\epsilon'' = \epsilon''_m \operatorname{sech} \beta \ln \omega \tau \tag{1}$$

ω is the angular frequency, τ is the apparent relaxation time, ϵ''_m is the maximum loss factor and β is an empirical distribution parameter which is equal to unity for a single relaxation time and for a distribution lies between zero and unity. At the maximum in the frequency plane we have

$$\epsilon''_m = (\epsilon_0 - \epsilon_\infty) \frac{1}{2} \beta \tag{2}$$

Rearranging (1) gives

$$\epsilon'' = [2\epsilon''_m \cdot (\omega\tau)^\beta] / [1 + (\omega\tau)^{2\beta}] \tag{3}$$

Thus a plot of $\log \epsilon''$ against \log frequency has slope β at low frequencies, and $-\beta$ at high frequencies.

A further method of evaluating β is the plot $\cosh^{-1} (\epsilon''_m / \epsilon'')$ against \log frequency which has a slope β over the entire range of frequency.

Where the maximum loss was observable, β was evaluated using relation (2) and the test plots of $\cosh^{-1} (\epsilon''_m / \epsilon'')$ versus \log frequency. At higher temperatures the maximum loss was not observed so β was evaluated from plots of $\log \epsilon''$ versus \log frequency.

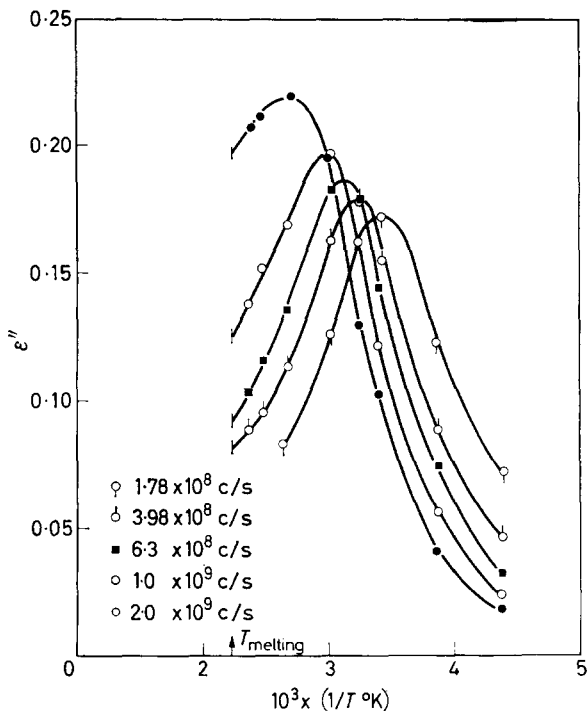


Figure 7—The dielectric loss factor as a function of temperature at high frequencies

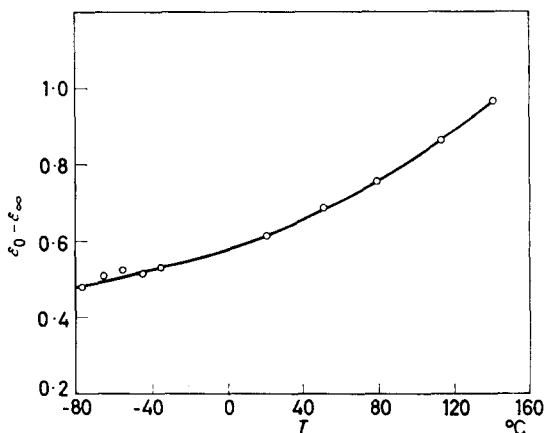


Figure 8—The dielectric increment as a function of temperature

The results for β are shown in *Figure 9*. It is seen that it is reasonably constant over the higher temperature range at a value of about 0.65. As the temperature is lowered, β decreases rapidly and reaches a very small value in the region of -90°C .

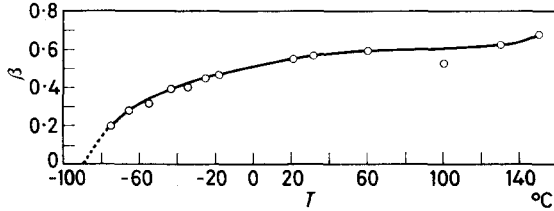


Figure 9—The variation of β with temperature for the dielectric relaxation

The activation energy

The activation energy of the relaxation process may be assumed to be related to the relaxation time by the Arrhenius equation

$$\tau = \frac{1}{2\pi f_m} = \tau_0 \exp\left(\frac{\Delta H}{RT}\right) \tag{4}$$

where f_m is the frequency of maximum loss for a given temperature, τ_0 is a constant and T is the temperature ($^{\circ}\text{K}$).

ΔH was evaluated in the present work from the slope of the plot $\log f_m$ versus $1/T$ which has slope $\Delta H/2.303R$.

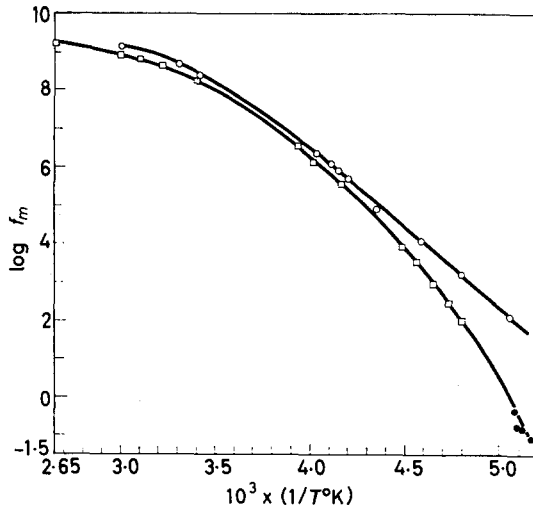


Figure 10— $\log f_m$ plotted against reciprocal temperature. Squares represent the temperatures of maximum loss obtained at constant frequencies. Open circles represent the frequencies of maximum loss obtained at constant temperatures. Filled circles correspond to the mechanical measurements obtained at constant frequencies

In Figure 10 the circles represent points taken from Figures 4 and 6 and the squares represent points taken from Figures 5 and 7. It is seen that the two curves are parallel at higher frequencies and temperatures but there is a

pronounced divergence at the lower temperatures. This divergence almost certainly arises from the rapid broadening of the distribution of relaxation times at lower temperatures.

The divergence emphasizes the facts that the activation energy should be derived from the results in the frequency plane since under these conditions the distribution is then constant. In the temperature plane, variation of temperature also varies the distribution and the combined variation may give very different results from those observed at constant temperatures. The main difference between the two curves is that in the frequency plane $\omega\tau=1$ at the maximum loss for a symmetrical distribution of relaxation times, but $\omega\tau \neq 1$ at the maximum loss in the temperature plane and this leads to the divergence shown in *Figure 10*.

The activation energies obtained from the frequency plane show a temperature dependence. At lower temperatures up to about 20°C, ΔH is a constant at about 19.3 ± 0.5 kcal/mole. At higher temperatures and above 1 Mc/s there is a continuous decrease in ΔH . It is to be noted that at the higher temperatures the two curves in *Figure 10* are parallel, thus the activation energy may be calculated from the frequency or temperature plane results. This is due to the fact that the distribution as estimated by β is changing only slowly at higher temperatures.

Influence of solvent

Samples were immersed in A.R. dioxan, and maintained at 60°C for a period of days. A maximum uptake of about six per cent solvent was obtained.

The solvent influenced the dielectric relaxation curves, shifting the loss factor maximum to higher frequencies at a given temperature. Also the loss factor maximum in the temperature plane (i.e. constant frequency) was shifted to lower temperatures. The shift was accompanied by a decrease in the maximum loss and a broadening of the curve which is consistent with a broadening in the distribution of relaxation times. *Figure 11* shows the results obtained at 1.42 Mc/s for varying amounts of dioxan absorbed by the polymer. *Table 2* gives the temperatures at which the loss factor reaches the maximum value as the dioxan concentration is varied.

Table 2. Temperature of maximum loss ϵ''_m for varying concentrations (weight per cent) of dioxan at 1.42 Mc/s

<i>Dioxan conc.</i>	T_m (°C)
0	-25.5
2.67	-30.0
6.10	-34.1

Influence of water

It was found that the polymer absorbed about 0.2 per cent of water and this had the effect of increasing the loss over the frequency range at a given temperature, the effect being more marked at low frequencies. The effect was a minor one since the absorption increased by only three or four per

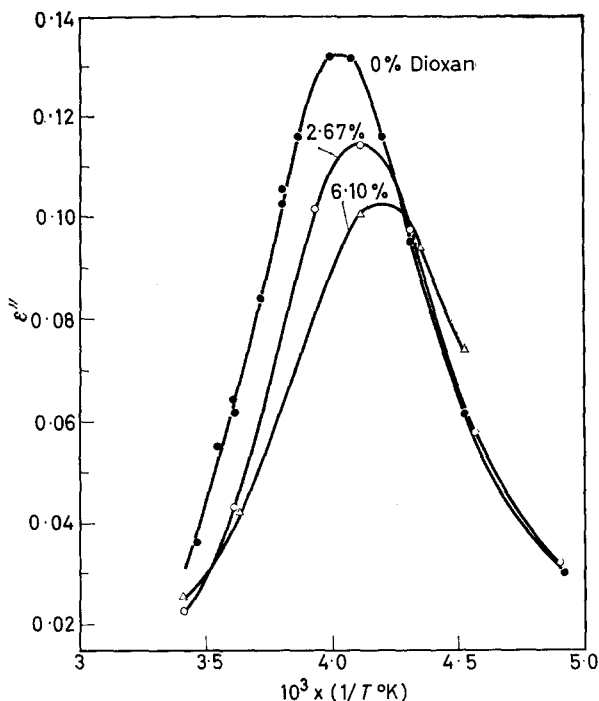


Figure 11—The dielectric loss factor curves at 1.42 Mc/s for different amounts of absorbed dioxan

cent, but the precaution was taken to dry all samples over silica gel at 100°C at 0.1 mm of mercury for 24 hours before measurements were made.

DISCUSSION

The limiting value of G' at low temperatures (4.65×10^{10} dynes/cm²) is higher than the value of about 2×10^{10} dynes/cm² observed for polyethylene, polytetrafluoroethylene and for many amorphous polymers in the glassy state. This may be due to the relatively high force constants for deforming the C—O bond and the C—O—C valence angle, compared with the corresponding force constants for the carbon-carbon chain¹². In addition the close packed structure would suggest a high contribution to the modulus from intermolecular forces. On account of thermal expansion, G' decreases generally with increasing temperature, but shows the largest decreases in the two relaxation regions where onset of molecular mobility occurs. The rise in Δ in the 157°C to 180°C range is undoubtedly due to the motions of chain segments accompanying the melting of crystallites. This is confirmed by X-ray⁴ and heat capacity data¹³.

The dielectric and low temperature mechanical relaxations

There appears to be a strong correlation between the dielectric relaxation process and the low temperature dynamic mechanical relaxation. It is seen

in *Figure 10* that the mechanical points fall on a smooth extrapolation of the dielectric curve. Also the effect of dioxan on the two relaxations is to lower the temperature at which the maximum loss occurs and broaden the distribution of relaxation times. There is also an apparent correlation between the distribution parameter β obtained for the two relaxations.

The dielectric process may be due to several mechanisms. The possibility of Maxwell-Wagner loss¹⁴ arising from conducting impurities is unlikely since all samples were highly pure¹⁵ and also water was eliminated from the polymer by drying. The relaxation might arise from the terminal ester groups, which would be the same mechanism for the amorphous and crystalline regions. However, Alsup, Punderson and Leverett¹⁶ have shown that solvents are selectively absorbed into the amorphous regions; thus if the dielectric mechanism is due to end groups in both the amorphous and crystalline regions, it would be expected that dioxan (plasticizer) would affect the amorphous relaxation, moving it to lower temperatures and the two absorptions would be resolved. This is not observed. Thus the dielectric relaxation arises only from the amorphous regions and may be due to either end group motions or backbone motions of the chain. We may estimate the contribution of the end groups to the dielectric increment ($\epsilon_0 - \epsilon_\infty$) in the following way. The dipole moment μ of dipolar molecules dissolved in a non-polar solvent is given by⁹

$$\mu^2 = \frac{27kT}{4\pi N} \frac{\epsilon_0 - \epsilon_\infty}{(\epsilon_0 + 2)(\epsilon_\infty + 2)} \quad (5)$$

The molecular weight of the polymer is between 30 and 50 000 and assuming all the end groups are in the amorphous region we have $N = 4.2 \times 10^4$ dipoles/cm³. Taking the dipole moment of the ester end group as 2.3D, we obtain from (5) a value $(\epsilon_0 - \epsilon_\infty) = 0.06$ at 20°C. This value is an overestimation but is still only one tenth of the observed value at this temperature. Thus the main relaxation process is not due to the end groups in the polymer. A similar value for $(\epsilon_0 - \epsilon_\infty)$ is obtained using the Onsager equation¹⁰. It is therefore suggested that the dielectric relaxation process is due to the motion of backbone segments in the amorphous regions.

The low temperature mechanical process could not be explained by the motion of end groups in the amorphous regions owing to the large modulus change observed. Thus due to the observed effect of dioxan on the relaxation, the low temperature mechanical process is due to the motion of backbone segments in the amorphous regions of the polymer. The small decrease in the modulus increment as the crystallinity is increased is also indicative of an amorphous relaxation.

If the proposed mechanism is correct then, since the low temperature mechanical relaxation shows the largest modulus increment and the highest G''_{\max} , we would expect, by analogy with amorphous polymers, a glass transition temperature in the region of -85°C. Values of T_g determined by low frequency mechanical tests are usually only a few degrees higher than those obtained from dilatometric and heat capacity studies. T_g for this polymer has not been determined dilatometrically and this measurement is to be undertaken in this laboratory. On the basis of brittle tests, however,

Linton and Goodman¹³ have estimated that T_g should lie between -40°C and -60°C . Since brittle tests are essentially a high frequency experiment ($f \approx 1 \text{ kc/s}$) they generally yield high values for T_g . From the dielectric data, an estimate of T_g may be obtained from the temperature at which the distribution parameter β becomes extremely small. For example Fuoss¹¹ found for polyvinyl chloride that β decreased to a very small value in the region of 75°C at which temperature a glass transition is observed by mechanical measurements. According to *Figure 9* we would predict by this method a glass transition for polyoxymethylene in the region of -90°C .

It is of interest to compare the temperature of the mechanical loss maximum in this polymer with the temperatures of the low temperature relaxations observed in the crystalline polymers shown in *Table 3*. Temperatures of the loss maxima are estimated at a frequency of about 100 c/s .

Table 3. Temperatures (in $^\circ\text{C}$) of loss maxima for a series of related polymers

Polymer	Structural unit	$T_{\text{max.}}$	
		A	B
Polyoxymethylene	$(-\text{CH}_2-\text{O}-)_n$		-65
Polyethyleneoxide	$(-\text{CH}_2-\text{CH}_2-\text{O}-)_n$		-50
Polytrimethyleneoxide	$(-\text{CH}_2-\text{CH}_2-\text{CH}_2-\text{O}-)_n$	-110	-45
Polytetramethyleneoxide	$(-\text{CH}_2-\text{CH}_2-\text{CH}_2-\text{CH}_2-\text{O}-)_n$	-110	-55
Polymethylene	$(-\text{CH}_2-)_n$	-110	

The loss maxima observed for polytrimethyleneoxide, polytetramethyleneoxide and polymethylene at -110°C (Column A) have been attributed by Willbourn¹⁷ to the motions of $(-\text{CH}_2-)_n$ segments containing a minimum of about three $-\text{CH}_2-$ units. This view is supported by the fact that polyoxymethylene does not show a peak at this temperature. The peaks exhibited by polytrimethyleneoxide and polytetramethyleneoxide at -45°C and -55°C respectively, have been interpreted by essentially regarding these materials as block copolymers. Apparently the incorporation of oxygen atoms into a hydrocarbon chain causes a local decrease of the mobility of short chain segments which include these atoms. These loss peaks may correspond to the low-temperature peak in polyoxymethylene (Column B) and also to a peak in polyethyleneoxide some 15°C higher¹⁸. A detailed comparison of $T_{\text{max.}}$ values shown in Column B would require a knowledge of the energy barriers opposing rotation about $-\text{C}-\text{O}-$ bonds and also the resistance of the surrounding medium to the motions of chain segments.

The structure of the crystalline regions of the polymer has been established by X-ray methods⁴ and it is shown that the backbone has a helical structure, the unit cell contains two polymer chains each of which contains nine monomer units. Lower molecular weight polyoxymethylenes have been examined in the vapour and dilute solutions by Kubo *et al.*¹⁹ and they have shown that the dipole moment work is consistent with a helical chain structure to a first approximation. The helix arises since the gauche

configuration is 1.74 kcal/mole lower in energy than the trans. If the gauche configurations are represented as G and G' , then they show that G and G' taking place in successive single bonds is sterically hindered, thus the chain has a preferred GGG or $G'G'G'$ etc. leading to a helix. Although their results are in accord with a helical structure, the temperature dependence of μ and $(\epsilon_0 - \epsilon_\infty)$ can only be explained by an increased probability of trans configurations at higher temperatures.

We may thus suggest that the chain structure in the amorphous regions of polyoxymethylene is predominantly helical with an increased probability of trans defects at higher temperatures. In the present work $(\epsilon_0 - \epsilon_\infty)$ increased with temperature and this is consistent with increased trans configurations at high temperatures. Also the apparent activation energy is small at high temperatures increasing to a constant value of 19 kcal/mole at lower temperatures. This is to be correlated to two effects; as the temperature decreases the free volume available to the reorienting unit decreases and leads to an increased activation energy. Also at high temperatures it is considered that reorientation is confined to small units of the backbone which in the limit is probably the reorientation of an ether unit from the gauche to the trans position. As the temperature decreases the length of the dipolar segment increases, the reorientation possibly taking place about trans defects in the helix, and the segmental motion of the longer unit has a larger activation energy.

Ishida¹ has determined the dielectric properties of *Delrin* in the frequency range 10 c/s to 1 Mc/s and the results of this work and the present study are in agreement regarding the positions of the loss in the temperature and frequency plane but at all temperatures Ishida finds loss factors which are about 30 per cent larger than those in the present work. This may be due to sample preparation (e.g. water content) or a different crystallinity or molecular weight of sample. Ishida was unable to assign the origin of the observed relaxation. Michailov and Eidelnant² have also investigated the polymer in the frequency range 100 c/s to 1 Mc/s and have obtained results similar to those of Ishida and of the present work. Michailov has considered the shape of the ϵ'' versus temperature curves for two frequencies and since the curves are not symmetrical has assigned the relaxation as the superposition of two distinct relaxation processes and further has suggested their origins. However, it is known that if two distinct relaxations are involved then they will be resolved in the frequency plane, the ϵ'' against frequency curves will be either non-symmetrical or show two peaks. In the present work a symmetrical distribution of relaxation times was adequate to fit the data at constant temperatures which would indicate strongly the absence of two distinct absorptions. Also it was realized that since the distribution parameter is strongly dependent upon temperature then the loss factor in the temperature plane will not be symmetrical because two parameters are varying, namely the temperature and the distribution of relaxation times. It can be shown that if the distribution is independent of temperature then the ϵ'' against $(1/T)$ plot is symmetrical, but if the distribution is broadening as the temperature is lowered then the high temperature half-width of the curve is smaller than the low temperature

half-width, i.e. the curve is non-symmetrical. Thus it would appear that the resolution of the loss curve into two components by Michailov is not valid for polyoxymethylene.

The high-temperature mechanical relaxation

Our present data do not show conclusively whether the high-temperature mechanical loss peak arises from motions in the crystalline regions of the polymer, or in the amorphous regions, or both. The peak lies in a temperature region where a crystalline peak might be expected, and also the shift of G''_{\max} to higher temperatures following heat treatment may be thought to indicate a crystalline peak since annealing is known to increase the size of crystallites. However, since the amorphous regions of the polymer must be under stress from the surrounding crystallites, increasing the crystallinity could have a similar effect on an amorphous peak. The decrease in Δ_{\max} upon annealing is usually regarded as indicating an amorphous peak and this evidence is supported here by the qualitative observation that the loss peak is depressed in the presence of plasticizer. Furthermore, heat capacity¹³ and X-ray data⁴ on this material give no indication of a crystalline change below about 135°C. Although the possibility of a crystalline mechanism cannot be entirely excluded, we consider that part at least of the loss peak arises from motions of large chain segments in the disordered regions of the polymer. On this basis activation energies ranging from 65 kcal/mole at 0.08 c/s to 92 kcal/mole at 0.42 c/s were estimated from areas beneath G'' versus $1/T$ curves. The qualitative features of our data, particularly the abrupt cut-off on the high temperature side of the main low temperature dispersion, and the contrasting effect of frequency on G''_{\max} for the two mechanical loss peaks, have suggested that part of the high temperature dispersion may be a delayed tail to the low temperature dispersion. In the temperature region between the two dispersions the amorphous regions must be under stress, otherwise they would crystallize. This may hinder the motions of the largest chain segments which would not therefore occur until the higher temperatures. In the presence of solvent the stresses may be relieved to some extent. Hence, the effect of solvent in broadening the *high temperature side* of the main dispersion and in depressing the high temperature loss peak may be significant.

CONCLUSION

The dielectric and dynamic mechanical properties of polyoxymethylene (*Delrin*) have been measured over a frequency and temperature range. A single broad dielectric relaxation process was observed which is correlated with the low temperature mechanical relaxation. The proposed mechanism for this relaxation is that there is segmental motion of the polymer backbone in the amorphous regions of the polymer. At high temperatures the dipole relaxation is associated with motions of small backbone segments while at low temperatures the moving segments become larger and the activation energy increases until finally the dipoles are unable to rotate below a temperature corresponding to the glass transition temperature.

The mechanism leading to the high temperature mechanical loss is not clearly understood but there is evidence to suggest that the amorphous regions are involved to some extent.

The authors acknowledge discussion with Dr D. H. Whiffen, and wish to acknowledge the assistance of Messrs D. A. Hughes and G. Fillery with the experimental work.

The work described above has been carried out as part of the research programme of the National Physical Laboratory, and is published by permission of the Director of the Laboratory.

*Basic Physics Division,
National Physical Laboratory,
Teddington, Middlesex.*

(Received January 1961)

REFERENCES

- ¹ ISHIDA, Y. *Kolloidzshr.* 1960, **171**, 149
- ² MICHAILOV, G. P. and EIDELNANT, M. P. *Vyosokomol. Socdineniya*, 1960, **10**, 1552
- ³ THURN, H. Private communication
- ⁴ HAMMER, C. F., KOCH, T. A. and WHITNEY, I. F. *J. appl. Polym. Sci.* 1959, **1**, 169
- ⁵ MCCRUM, N. G. *J. Polym. Sci.* 1959, **34**, 355
- ⁶ NIELSEN, L. E. *Bull. Amer. Soc. Test. Mat. No. 165*, 1950, 48
- ⁷ HARTSHORN, L. and WARD, W. H. *J. Instn elect. Engrs*, 1936, **79**, 597
- ⁸ WILLIAMS, G. *J. phys. Chem.* 1959, **63**, 534
- ⁹ BÖTTICHER, C. J. F. *Theory of Electric Polarization*. Elsevier: Amsterdam and London, 1952
- ¹⁰ ONSAGER, L. *J. Amer. chem. Soc.* 1936, **58**, 1486
- ¹¹ FUOSS, R. M. and KIRKWOOD, J. G. *J. Amer. chem. Soc.* 1941, **63**, 378 and 385; *J. chem. Phys.* 1941, **9**, 327
- ¹² TRELOAR, L. R. G. *Polymer, Lond.* 1960, **1**, 290
- ¹³ LINTON, W. H. and GOODMAN, H. H. *J. appl. Polym. Sci.* 1959, **1**, 179
- ¹⁴ SILLARS, R. W. *J. Instn elect. Engrs*, 1937, **80**, 378
- ¹⁵ DU PONT CO. (U.K). Private communication
- ¹⁶ ALSUP, R. G., PUNDERSON, J. O. and LEVERETT, G. F. *J. appl. Polym. Sci.* 1959, **1**, 185
- ¹⁷ WILLBOURN, A. H. *Trans. Faraday Soc.* 1958, **54**, 717
- ¹⁸ READ, B. E. and WILLIAMS, G. Unpublished work
- ¹⁹ UCHIDA, T., KURITA, Y. and KUBO, M. *J. Polym. Sci.* 1956, **19**, 365

Streaming Birefringence of Soft Linear Macromolecules with Finite Chain Length

A. PETERLIN

The change of hydrodynamic interaction with coil expansion in laminar flow together with saturation effects due to finite chain length influences the streaming birefringence. The latter initially has values obtained by the former theories with zero gradient interaction parameters. The further increase in birefringence and deviation of extinction angle from 45° with increasing gradient, however, is slower. The shorter the chain, the faster the birefringence approaches saturation. The effect of finite chain length on extinction angle, however, is very small.

THE CHANGE of hydrodynamic interaction with coil expansion in laminar flow yields an initial decrease of intrinsic viscosity with increasing gradient in good agreement with experimental evidence^{1, 2}. With an infinitely long and perfectly flexible macromolecule the relative viscosity $[\eta]/[\eta]_0$ then goes through a minimum and after that rises again as a consequence of steadily decreasing hydrodynamic interaction in the expanding coil (dilatancy). The finite length of actual macromolecules, however, leads to saturation effects³. With sufficiently short chains the minimum and the subsequent increase in intrinsic viscosity completely disappear. It is very likely that in usual solvents the finite resistivity of actual macromolecules so limits the coil extension that also with longer chains a similar behaviour is observed. Eventually in exceptional cases of extremely high solvent viscosity the expansion by hydrodynamical forces may still be so strong that the solution shows dilatancy effects⁴.

The model can also be applied to streaming birefringence⁵. Chains of infinite length yield a steady, nearly quadratic, increase in birefringence which does not differ appreciably from that obtained without considering either hydrodynamic interaction at all or its change with coil expansion. When plotted over the gradient the initial slope is the same in both cases. But the birefringence then turns out to be smaller with varying interaction up to the point where the intrinsic viscosity again reaches its initial value. After that it is larger than in the case of constant interaction. The situation is similar with a deviation of extinction angle from 45°. In what follows the influence of finite chain length on streaming birefringence will be considered. The random-walk model used corresponds to macromolecular coils in an ideal solvent (at Flory's Θ temperature). Without appreciable modifications it cannot be applied to coils with marked excluded volume effect, i.e. to macromolecules in good solvents.

With one end fixed the free end distribution function

$$\begin{aligned}\Phi(r) &= (\mu_0/\pi)^{3/2} \exp(-\mu_0 r^2) \\ \mu_0 &= 1.5/h_0^2 \\ h_0^2 &= \langle r^2 \rangle = Zb^2\end{aligned}\tag{1}$$

for a chain with Z statistically independent elements of length b may be obtained as a solution of the corresponding diffusion equation

$$\begin{aligned}(\mathbf{F}/\eta_0 W) \Phi - D \text{grad } \Phi &= 0 \\ \mathbf{F} &= -2\mu_0 r k T \\ D &= kT/\eta_0 W\end{aligned}\quad (2)$$

where W is the resistance coefficient of the free end, and η_0 is the viscosity of the solvent. Actually the validity of equation 1 is confined to either small end-to-end distance r or very long molecules so that one has

$$r \ll L \quad (3)$$

Here $L = Zb$, the length of the extended macromolecule. When r approaches L , the restoring force \mathbf{F} has to increase more than linearly with r and to become infinitely large at $r = L$. Such a modification of \mathbf{F} reads⁶

$$\begin{aligned}\mathbf{F} &= -2\mu_0 r k T E \\ E &= \mathcal{L}^{-1}(t)/3t \\ t &= r/L \quad 0 \leq t \leq 1\end{aligned}\quad (4)$$

In the above \mathcal{L}^{-1} is the inverse Langevin function. The function E is shown in *Figure 1*. As a consequence of equation (4) the root mean square

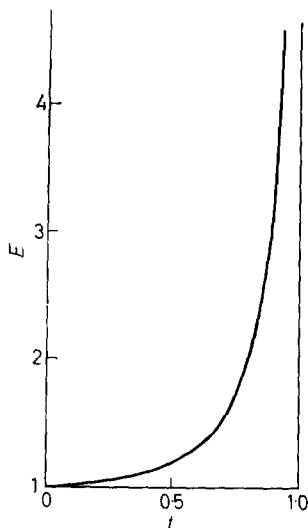


Figure 1—The function $E(t)$ according to equation (4)

end-to-end distance h_0 is smaller than that given by equation (1). The difference does not matter with very large Z but it cannot be completely neglected with shorter chains. From this inconsistency one may conclude that equation (4) for the restoring force does not represent a very correct extension of equation (2). The error, however, is relatively small and does not influence appreciably the usefulness of the modified restoring force at higher values of t .

In laminar flow

$$\mathbf{v} = (0, Gx, 0) \quad (5)$$

the diffusion equation reads

$$\text{div}(\mathbf{v}\Phi - 2\mu_0 \mathbf{r}DE\Phi - D \text{grad} \Phi) = 0 \quad (6)$$

The coefficients W or D and E depend on the actual end-to-end distance r which during one full rotation of the macromolecule in laminar flow goes twice from maximum to minimum and back. In the usual treatment of hydrodynamic interaction^{1, 7-9} one completely neglects this variation of intramolecular distances and simply introduces averages $\langle r_{jk} \rangle$ and $\langle 1/r_{jk} \rangle$. To a large extent this procedure is justified by the fact that the average shape of the molecule and also the space density of the chain elements do not change in spite of the fact that the segments present in any space element are continually exchanged. By such a treatment E and D or W turn out to be constants depending on the average end-to-end distance h which in turn is determined by the parameter β

$$\begin{aligned} \beta &= G/4\mu_0 DE = G/4\mu D \\ \mu &= \mu_0 E \end{aligned} \quad (7)$$

The corresponding solution of equation (6) then reads¹⁰

$$\Phi(\mathbf{r}) = \frac{(\mu/\pi)^{3/2}}{(1+\beta^2)^{1/2}} \exp\{-\mu[(1+2\beta^2)x^2 - 2\beta xy + y^2 + (1+\beta^2)z^2]/(1+\beta^2)\} \quad (8)$$

The whole change by comparison with the infinitely long molecule is in the new definition of the parameters μ and β according to equation (7).

The streaming birefringence is determined by the optical polarizability tensor of the isolated macromolecule in laminar flow

$$\begin{array}{ccc} \alpha_{xx} & \alpha_{xy} & 0 \\ \alpha_{yx} & \alpha_{yy} & 0 \\ 0 & 0 & \alpha_{zz} \end{array} \quad (9)$$

yielding

$$\begin{aligned} \Delta n/c &= 2\pi \{(n^2 + 2)/3n\}^2 (N_A/M) \Delta\alpha \\ \Delta\alpha &= \{(\alpha_{yy} - \alpha_{xx})^2 + 4\alpha_{xy}^2\}^{1/2} \\ \cot 2\chi &= (\alpha_{yy} - \alpha_{xx})/2\alpha_{xy} \end{aligned} \quad (10)$$

Here c denotes concentration in g/cm³, N_A is Avogadro's number, and M is the molecular weight. The average values of α in equation (9) turn out to be

$$\begin{aligned} \alpha_{xx} &= \langle \alpha_1^* x^2/r^2 \rangle + \langle \alpha_2^* (1-x^2)/r^2 \rangle \\ \alpha_{xy} &= \langle (\alpha_1^* - \alpha_2^*) xy/r^2 \rangle \\ \alpha_{yy} &= \langle \alpha_1^* y^2/r^2 \rangle + \langle \alpha_2^* (1-y^2)/r^2 \rangle \end{aligned} \quad (11)$$

with⁶

$$\begin{aligned} \alpha_1^* &= \frac{1}{3}Z(\alpha_1 + 2\alpha_2) + \frac{2}{3}Z(\alpha_1 - \alpha_2)(1 - 1/E) \\ \alpha_2^* &= \frac{1}{3}Z(\alpha_1 + 2\alpha_2) - \frac{1}{3}Z(\alpha_1 - \alpha_2)(1 - 1/E) \end{aligned} \quad (12)$$

These are the main polarizabilities of the chain parallel and perpendicular to the end-to-end vector r respectively, averaged over all configurations compatible with the chosen r . α_1 and α_2 are polarizabilities of the single chain element parallel and perpendicular to its axis respectively. The factor containing E reads

$$1 - 1/E = \frac{2}{3} t^2 \gamma(t) = \frac{2}{3} t^2 (1 + \frac{1}{3} \frac{2}{3} t^2 + \dots) \quad t \ll 1$$

$$= 1 - 3t + 3t^2 \quad t \sim 1 \quad (13)$$

The function γ starts with the value 1 at $t=0$ and reaches $5/3$ at $t=1$ (Figure 2). The averages wanted in equation (10) turn out to be

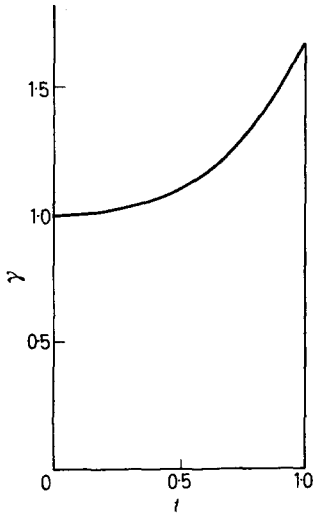


Figure 2—The function $\gamma(t)$ according to equation (13)

$$\alpha_{yy} - \alpha_{xx} = \frac{2}{3} (\alpha_1 - \alpha_2) \langle (y^2 - x^2) \gamma(r/L) \rangle$$

$$\alpha_{xy} = \frac{2}{3} (\alpha_1 - \alpha_2) \langle xy \gamma(r/L) \rangle \quad (14)$$

In agreement with the usual treatment of hydrodynamic interaction where averages of D and E for a given β were used, without considering the variation of molecular shape during coil rotation one has in the correction factor γ to introduce the mean value of the arguments, i.e. $t=h/L$

$$h^2 = \langle r^2 \rangle = \langle x^2 + y^2 + z^2 \rangle$$

$$= (1/2\mu) (3 + 2\beta^2)$$

$$t = h/L = \{(1 + 2\beta^2/3)/EZ\}^{\frac{1}{2}} \quad (15)$$

With

$$\langle y^2 - x^2 \rangle = \beta^2 / \mu$$

$$\langle xy \rangle = \beta / \mu \quad (16)$$

one then obtains

$$\Delta n / nc = \frac{2}{3} \pi \{(n^2 + 2)/3n\}^2 (N_A/M) (\alpha_1 - \alpha_2) \beta (1 + \beta^2)^{\frac{1}{2}} \gamma / E \quad (17)$$

$$\text{ctg } 2\chi = \beta$$

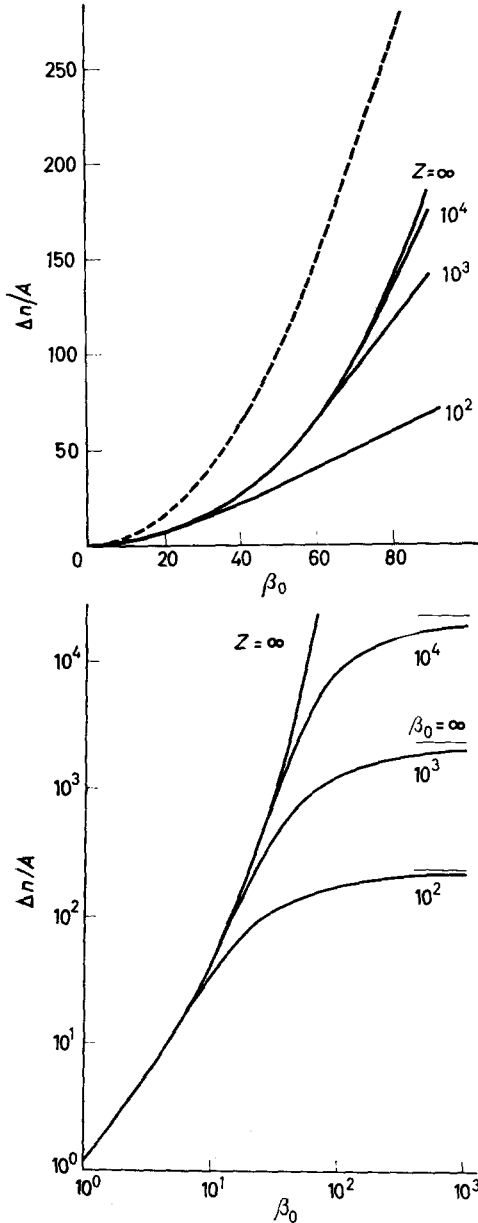


Figure 3—Streaming birefringence ($\Delta n/nc$): $(4\pi/5) [(n^2 + 2)/3n]^2 N_A/M$ for $Z=10^2, 10^3, 10^4$ and ∞ : (a) linear scale, (b) logarithmic scale. The broken line in (a) corresponds to constant interaction and $Z=\infty$

In Figures 3 and 4 the birefringence and the extinction angle χ respectively are plotted over β_0 .

$$\beta_0 = \beta [\eta]_0 / [\eta] = \eta_0 G / 4\mu_0 D = (M [\eta]_0 / N_A kT) \eta_0 G \quad (18)$$

The ratio $[\eta]_0 / [\eta]$ as a function of β has been calculated before³. This change from β to β_0 is in agreement with the usual procedure of plotting Δn and χ over $\eta_0 G$. The proportionality factor from equation (18) just makes the

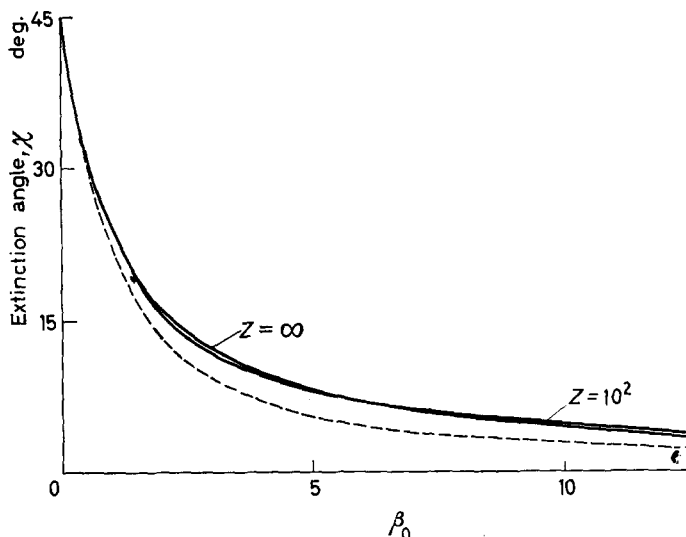


Figure 4—Extinction angle χ for $Z=10^2$ and ∞ . The broken line corresponds to constant interaction and $Z=\infty$

curves coincide, at least in the initial part, for different molecular weights and solvent viscosities.

The initial specific birefringence (specific Maxwell constant)

$$M_{sp} = \left(\frac{\Delta n}{nc\eta_0 G} \right)_{c \rightarrow 0, G \rightarrow 0} = \frac{4\pi}{5} \left(\frac{n^2 + 2}{3n} \right)^2 \frac{\alpha_1 - \alpha_2}{kT} [\eta]_0 \quad (19)$$

agrees with that previously determined with constant hydrodynamic interaction⁸. The birefringence then increases nearly in the same way as with infinitely long chains⁵. Saturation effects occur earlier the shorter the chain. In Figure 3(a) the differences in streaming birefringence dependence on the gradient for different Z are very obvious. With $Z=10^2$ the limited coil expansion possibilities have already markedly reduced Δn , whereas the curves for $Z=10^3$, 10^4 and ∞ very nearly coincide. The limiting values for the asymptotes ($\beta_0 = \infty$) in Figure 3(b) correspond to fully stretched macromolecules

$$\Delta n_\infty / nc = 2\pi \left\{ (n^2 + 2) / 3n \right\}^2 (N_A / M) (\alpha_1 - \alpha_2) Z. \quad (20)$$

Of course, in the calculation presented here the changes of internal optical field with coil extension, yielding the shape anisotropy contribution of streaming birefringence¹¹, were completely neglected and throughout the Lorentz-Lorenz local field was assumed as may be seen from the factor $\{(n^2 + 2) / 3n\}^2$.

The effect of finite chain length is very nearly negligible in the extinction angle. The differences between the curve for $Z=\infty$ and the respective curves for $Z=10^2$, 10^3 , 10^4 are so small that they can hardly be shown on a graph like that of Figure 4. But there is a net difference between the cases with constant and with variable hydrodynamic interaction due to the difference⁵ between β and β_0 .

With the present treatment, considering only the first mode of Rouse's model, one must not expect to obtain an explanation of the orientation effect discovered by Cerf¹² and very thoroughly studied by Leray¹³. They found two regions according to the solvent viscosity. When η_0 is small they have

$$-(d\chi/dG)_{G=0} = A\eta_0 \quad (21)$$

corresponding to a nearly rigid coil, and at higher η_0

$$-(d\chi/dG)_{G=0} = A'\eta_0 + B \quad (22)$$

corresponding to the continuous transition to a perfectly soft molecule. According to equation (17), however, one obtains

$$-(d\chi/dG)_{G=0} = (M [\eta]_0 / 2N_A kT) \eta_0 \quad (23)$$

The same value results in the case of constant hydrodynamic interaction. When higher modes are considered⁹ the factor $\frac{1}{2}$ has to be replaced by a value between $\frac{1}{3}$ (free draining coil) and $\frac{1}{9.76}$ (complete solvent immobilization), but no term independent of solvent viscosity appears. By introducing partial coil rigidity into Rouse's model, however, Cerf¹⁴ was able to show the existence of two limiting cases corresponding to equations (21) and (22). His treatment, of course, is limited to initial values of Δn and χ because he completely neglects the effects of coil expansion on hydrodynamic interaction.

Comparing different theories presented so far for the gradient dependence of intrinsic viscosity and for streaming birefringence and trying to test them by existing experimental data one first notes that most experiments were performed on macromolecular solutions in good solvents where, due to the strong interaction effects, the macromolecular coils are more expanded than in the ideal solvent, i.e. at Flory's Θ temperature. All theoretical treatments, however, start with the random walk model without any excluded volume effect and therefore are strictly applicable only to ideal solutions. As a general consequence with very few exceptions the comparison of experimental data with theoretical predictions and eventual agreement are subject to criticism and may hardly be used as a convincing test of correctness of any theory presented so far although they may add confidence in the soundness of single assumptions. At least in some limiting cases one already knows their respective effects so that one has the impression that a final synthesis including the variation of hydrodynamic interaction with coil expansion, the limitation of coil expansion by finite length and partial rigidity of actual macromolecules, and the excluded volume effect is not too remote. The present contribution is intended to show the influence of limited coil expansion on hydrodynamic interaction in the special case of the ideal solvent. It is likely that the treatment may be extended easily to the case of the finite excluded volume effect. The simple model used, considering only the first mode of Rouse's chain with Z elements, permits a fairly accurate treatment of the hydrodynamic problem even with more complicated coil geometry where the mathematical

difficulties with Rouse's model would already be prohibitive. The results, at least in intrinsic viscosity and streaming birefringence, seem not to deviate markedly from those obtained by the model with Z modes. The situation is less satisfying with the extinction angle. Further deviations have to be expected with β approaching infinity where according to the simplified model the fully extended macromolecule gets perfectly oriented in the flow direction and therefore the intrinsic viscosity decreases to zero.

*Physikalisches Institut,
Technische Hochschule München,
Germany*

(Received January 1961)

REFERENCES

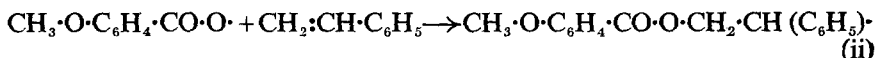
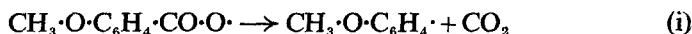
- ¹ ZIMM, B. H. Paper read at the New York Academy Symposium on Mechanics and Thermodynamics of Polymer Solutions, May 1960
- ² PETERLIN, A. *J. chem. Phys.* 1960, **33**, 1799
- ³ PETERLIN, A. *Makromol. Chem.* 1961, **44-46**, 338
- ⁴ SELBY, T. W. and HUNSTAD, N. A. Paper read at the A.S.T.M. Symposium on Non-Newtonian Viscosity, Washington, D.C., October 1960
- ⁵ PETERLIN, A. *J. Phys. Radium*. In press
- ⁶ KUHN, W. and KUHN, F. *Kolloidzshr.* 1942, **101**, 248
- ⁷ KIRKWOOD, J. G. and RISEMAN, J. *J. chem. Phys.* 1948, **16**, 565
- ⁸ PETERLIN, A. *Les Grosses Molécules en Solution*, p 70. Collège de France: Paris, 1948
- ⁹ ZIMM, B. H. *J. chem. Phys.* 1956, **24**, 269
- ¹⁰ HERMANS, J. J. *Physica, 'sGrav.* 1944, **10**, 777
- ¹¹ ČOPIĆ, M. *Bull. sci. Yougoslavie*, 1953, **1**, 103; *J. Polym. Sci.* 1956, **20**, 593; *J. chem. Phys.* 1957, **26**, 1382
- ¹² CERF, R. *Thèse*. Strasbourg, 1951
- ¹³ LERAY, J. *J. Polym. Sci.* 1959, **23**, 167
- ¹⁴ CERF, R. *J. Phys. Radium*, 1958, **19**, 122

Tracer Studies of Di-anisoyl Peroxide and the Anisoyloxy Radical

J. K. ALLEN and J. C. BEVINGTON

The decomposition of di-anisoyl peroxide in dilute solutions in benzene has been followed by analyses for carbon dioxide produced by dissociation of the anisoyloxy radicals formed in the primary dissociation. The rates of initiation of the polymerizations of methyl methacrylate, vinyl acetate and acrylonitrile by di-anisoyl peroxide have been measured by determining the rates of incorporation of initiator fragments in polymers. The arrangement of monomers in order of reactivity towards the anisoyloxy radical is the same as that found when the benzoyloxy radical is used for reference.

LABELLED di-anisoyl peroxide has already been used as the initiator for the radical polymerization of styrene¹. The ratio of the velocity constants for the competing reactions



was determined both at 60°C and 80°C by analysis of polymers for anisyl and anisoyloxy end-groups. In this paper, the results of similar studies with other monomers are reported; the monomers have been arranged in order of reactivity towards the anisoyloxy radical.

The decomposition of dibenzoyl peroxide in solution can be followed by measurements of the carbon dioxide produced by dissociation of the benzoyloxy radicals. If labelled peroxide is used and the carbon dioxide is determined by isotope dilution analysis, very dilute solutions of the peroxide can be used. In unreactive solvents, induced decomposition of the peroxide is absent and the rate of the direct dissociation of the peroxide into radicals can be measured². This technique has now been applied to di-anisoyl peroxide.

In the work reported here, two types of ¹⁴C-di-anisoyl peroxide were used, one labelled at the carboxyl carbon sites and the other in the methoxy groups; they are referred to as C- and M-peroxide respectively. The relationships between the specific activities (in μc/g of carbon) of the two types of peroxide and those of various derivatives are shown in Table 1.

Table 1. Specific activities of peroxides and derivatives

Reactant	C-peroxide	M-peroxide
Di-anisoyl peroxide	<i>c</i>	<i>m</i>
Anisoyloxy radical	<i>c</i>	<i>m</i>
Anisic acid	<i>c</i>	<i>m</i>
Anisyl radical	0	8 <i>m</i> /7
Carbon dioxide	8 <i>c</i>	0

A polymer prepared with M-peroxide as initiator contains both labelled anisoyloxy and anisyl groups; if initiator fragments enter the polymer only as a result of initiation and if initiation is solely by attachment of these fragments to the monomer, the carbon content of the kinetic chain can be represented as

$$(C_8)_x (C_7)_{1-x} (C_n)_v \quad (\text{iii})$$

where n is the number of carbon atoms in each monomer unit and v is the kinetic chain length; x denotes (number of anisoyloxy end-groups)/(total number of end-groups derived from the initiator). The specific activities of the polymer and peroxide, p and m respectively in $\mu\text{c/g}$ of carbon, are related thus

$$p = \frac{8xm + 7(1-x)8m/7}{8x + 7(1-x) + nv} \quad (1)$$

For all except very low polymers, the first and second terms in the denominator can be neglected so that

$$v = 8m/np \quad (2)$$

If there is mutual termination of reaction chains

$$v = k_p^2 [M]^2 / 2k_t R_p \quad (3)$$

where k_p and k_t are the velocity constants for chain growth and termination, $[M]$ is the concentration of monomer, and R_p is the rate of polymerization. From equations (3) and (4)

$$p/m = 16k_t R_p / nk_p^2 [M]^2 \quad (4)$$

Similarly for C-peroxide

$$p/c = 16xk_t R_p / nk_p^2 [M]^2 \quad (5)$$

If two series of polymers are prepared, one with M-peroxide and the other with C-peroxide, plots of p/m and p/c against R_p for a fixed concentration of monomer should be linear; from the slopes, k_t/k_p^2 and x can be evaluated.

The fraction x can also be determined by a procedure involving the use of M-peroxide only. The specific activity of a polymer is measured before and after detachment of the anisoyloxy groups by hydrolysis; this procedure was employed in the previous work using the peroxide as a sensitizer for the polymerization of styrene. It is essential that all the ester end-groups should be removed during the hydrolysis and this can be tested by submitting to the treatment polymers prepared using C-peroxide; in such polymers only the anisoyloxy end-groups are labelled and so hydrolysis should cause the specific activity to fall to zero. A complication arises when the monomer units contain groups sensitive to hydrolytic agents. Consider the case of methyl methacrylate polymerized using M-peroxide; before hydrolysis, the kinetic chain can be represented as

$$(C_8)_x (C_7)_{1-x} (C_5)_v \quad (\text{iv})$$

Suppose that during hydrolysis, all the anisoyloxy end-groups are removed

and that a fraction h of the monomer units is hydrolysed; the carbon content of the kinetic chain is changed to

$$(C_7)_{1-x} (C_5)_{\nu(1-h)} (C_4)_{\nu h} \quad (v)$$

and

$$\frac{\text{specific activity of polymer after hydrolysis}}{\text{specific activity of polymer before hydrolysis}} = \frac{7(1-x)8m/7}{5\nu(1-h)+4\nu h} \times \frac{5\nu}{8xm+7(1-x)8m/7} = 5(1-x)/(5-h) \quad (6)$$

Only about one per cent of the ester groups in the monomer units of polyvinyl acetate remained unaffected by the hydrolysis³; experiments with polymers prepared using C-peroxide showed that some of the anisoyloxy end-groups also survived the treatment. Before hydrolysis, the kinetic chain in such a polymer can be represented as

$$(C_8)_x (C_7)_{1-x} (C_4)_\nu \quad (vi)$$

Unless ν is small, the specific activity (p) of the polymer is related to that (c) of the peroxide thus

$$p = 2xc/\nu \quad (7)$$

After hydrolysis, the kinetic chain can be represented as

$$(C_8)_{xj} (C_7)_{1-x} (C_2)_{0.99\nu} (C_4)_{0.01\nu} \quad (vii)$$

and the specific activity (q) of the resulting polyvinyl alcohol is given by

$$q = 3.96xjc/\nu \quad (8)$$

For a polymer prepared with M-peroxide, hydrolysis causes the specific activity to change from

$$p = 2m/\nu \quad \text{to} \quad q = 3.96\{1-x(1-j)\}m/\nu \quad (9)$$

The value of j can be determined from experiments with polymers prepared using C-peroxide and it can then be used in the determination of x for polymers made with M-peroxide.

If all the anisyl radicals formed in (i) subsequently enter polymer

$$1/x = 1 + k_1/k_2 [M] \quad (10)$$

and k_1/k_2 can be evaluated⁴; k_1 and k_2 are the velocity constants for reactions (i) and (ii) respectively. The value of k_1 is independent of the nature of the monomer and so it is possible to assign relative values for k_2 .

The kinetic chain length, as measured by the tracer method, is equal to R_p/R_i where R_i is the rate of initiation by incorporation of initiator fragments in polymer and so from (2)

$$R_i = npR_p/8m \quad (11)$$

If it is assumed that every anisoyloxy radical (or derived anisyl radical) becomes incorporated in polymer, then

$$R_i = 2k_d [I] \quad (12)$$

where k_d denotes velocity constant for dissociation of peroxide into radicals, and $[I]$ is the concentration of initiator. Hence k_d can be evaluated⁴.

EXPERIMENTAL

Most of the experimental procedures used in this work have been described previously and only minor modifications were made. The C-peroxide was made from carboxyl-¹⁴C-anisic acid prepared by the method of Reid and Jones⁵. The procedure for hydrolysis of samples of polyvinyl acetate was as follows. The polymer (100 mg) was dissolved in methanol (15 cm³) and added to a solution of caustic soda (1 g) in methanol (7 cm³). After 5 min, the precipitate was recovered and dried; it was dissolved in water (30 cm³) containing caustic soda (1 g) and the solution was refluxed for 3 h. The polyvinyl alcohol was recovered by precipitation in methanol and purified by further precipitation from aqueous solution.

RESULTS

Decomposition of di-anisoyl peroxide in benzene at 60°C

Two concentrations of C-peroxide, viz. 0.50 g/l. and 0.01 g/l., were used. The results of isotope dilution analyses for carbon dioxide are plotted in *Figure 1*. Line A is drawn for a first order process with a half-life of 30 h (corresponding to $k = 6.5 \times 10^{-6} \text{ sec}^{-1}$) and supposing that the weight of carbon dioxide produced at infinite time is 0.180 mg for an initial weight of 1.000 mg of peroxide; this corresponds to a 61.8 per cent yield of carbon dioxide. There is a fair fit of the line to the experimental points. The weights of carbon dioxide found in experiments lasting over 640 h were 0.174, 0.170, 0.185, 0.175, 0.176, 0.178 and 0.185 mg. Line B in *Figure 1* refers to the weights of anisic acid found by isotope dilution analysis and is drawn for a first-order process with half-life of 30 h and a final yield of 0.17 mg of anisic acid per mg of peroxide; the weights of the acid found after 766 and 807 h at 60° were 0.207 and 0.157 mg.

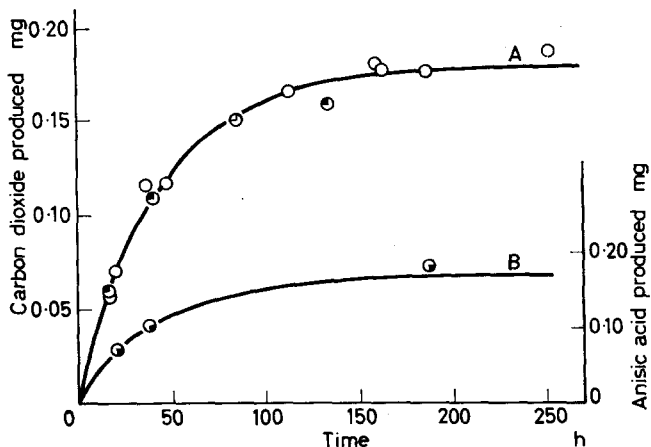


Figure 1—Amounts of carbon dioxide and anisic acid produced during the decomposition of di-anisoyl peroxide in benzene at 60° for an initial weight of 1 mg of peroxide. CO₂ yields: ○ 0.50 g peroxide/l.; ● 0.01 g peroxide/l. Anisic acid yields: ● 0.50 g peroxide/l.

Polymerization of methyl methacrylate

Polymerizations were performed at 60° and 80° using various concentrations of monomer in benzene; the order with respect to initiator was close to 0.5. From the slopes of the lines referring to M-peroxide in *Figure 2* the following values of k_i/k_p^2 (in mole. l.⁻¹ sec) were derived:

at 60°, 47.6 and 37.8 for monomer concentrations of 0.90
and 1.80 mole l.⁻¹ respectively;

at 80°, 25.5 and 23.4 for monomer concentrations of 0.88
and 1.76 mole l.⁻¹ respectively.

Taking the values as 42.7 at 60° and 24.5 at 80°, $(2E_p - E_t)$ is 6.5 kcal mole⁻¹.

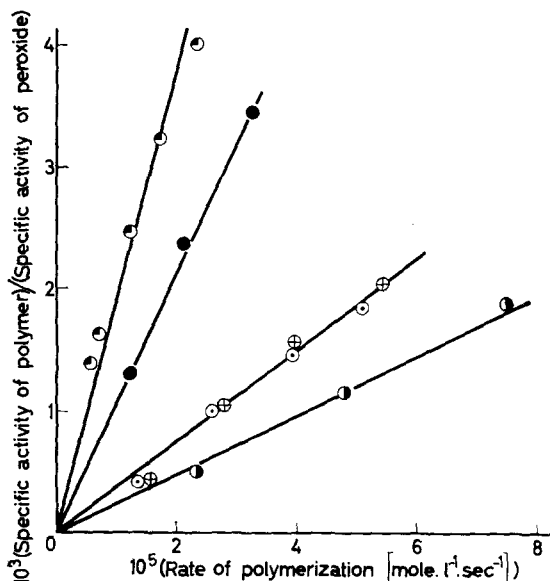


Figure 2—Plots of (specific activity of polymer)/(specific activity of peroxide) against rate of polymerization of methyl methacrylate in benzene.

- M-peroxide, [monomer]=0.90 mole/l., 60°,
- ⊙ C-peroxide, [monomer]=1.80 mole/l., 60°,
- ⊕ M-peroxide, [monomer]=1.80 mole/l., 60°,
- M-peroxide, [monomer]=0.88 mole/l., 80°,
- ⊙ M-peroxide, [monomer]=1.76 mole/l., 80°.

The rate of initiation was directly proportional to the concentration of initiator but there was evidence for a slight dependence upon concentration of monomer (see *Figure 3*). Derived values for k_a are 5.4×10^{-6} sec⁻¹ at 60° and 8.3×10^{-5} sec⁻¹ at 80° for the higher concentrations of monomer.

It was shown, using a sample of polymethyl methacrylate prepared using C-peroxide, that complete removal of anisoyloxy end-groups can be achieved. Experiments with polymers prepared with labelled methyl methacrylate³ showed that h in (6) can be taken as 0.03. Values of the fraction x have been found from the results of experiments in which polymers

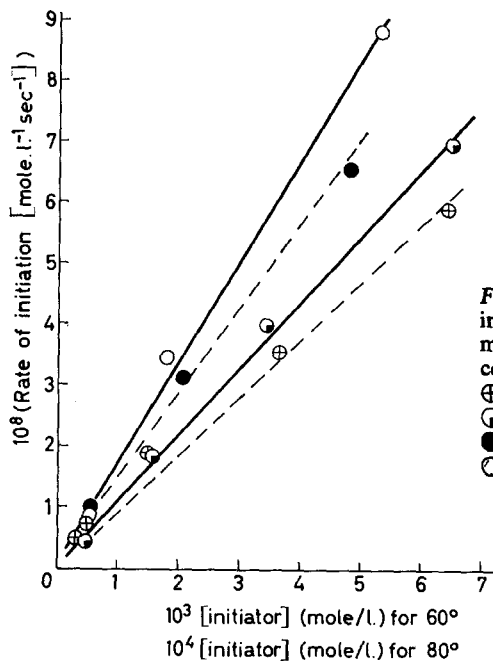


Figure 3—Dependence of rate of initiation of polymerization of methyl methacrylate upon concentration of di-anisoyl peroxide.
 ⊕ 60°, [monomer]=0.90 mole/l.,
 ⊙ 60°, [monomer]=1.80 mole/l.,
 ● 80°, [monomer]=0.88 mole/l.,
 ○ 80°, [monomer]=1.76 mole/l.

prepared using M-peroxide were hydrolysed. At each monomer concentration, several experiments were performed and average values of x have been plotted in Figure 4; all values of x were within 5 per cent of the appropriate average value. From (10), the values of k_1/k_2 are 0.16 and 0.39 mole l.⁻¹ at 60° and 80° respectively, so that $(E_1 - E_2)$ is 10.5 kcal mole⁻¹.

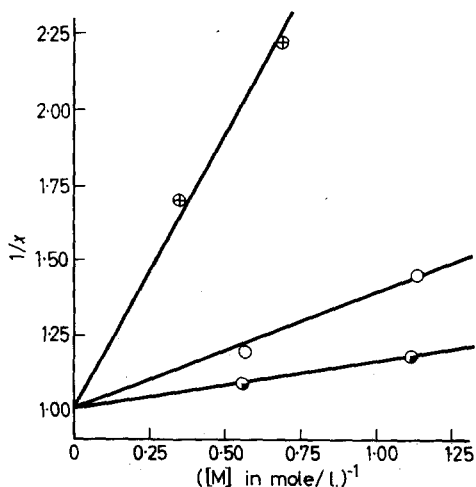


Figure 4—Dependence of x upon concentration of monomer.
 ⊙ methyl methacrylate at 60°,
 ○ methyl methacrylate at 80°,
 ⊕ acrylonitrile at 60°.

Polymerization of acrylonitrile

Acrylonitrile in dimethylformamide was polymerized using both C- and M-peroxide; the order with respect to initiator was close to 0.5 (see Figure 5). From a comparison of the slopes of the lines for C- and M-peroxide in Figure 6, x has the values 0.45 and 0.59 for monomer concentrations of 1.45 and 2.90 mole l.⁻¹. These results are included in Figure 4 and lead to a value of 1.8 mole l.⁻¹ for k_1/k_2 at 60°. From the results obtained using M-peroxide, k_d is found to be 0.8×10^{-6} sec⁻¹ at 60° and k_t/k_p^2 for acrylonitrile about 5 mole l.⁻¹ sec; for reasons discussed later, these values cannot be accepted.

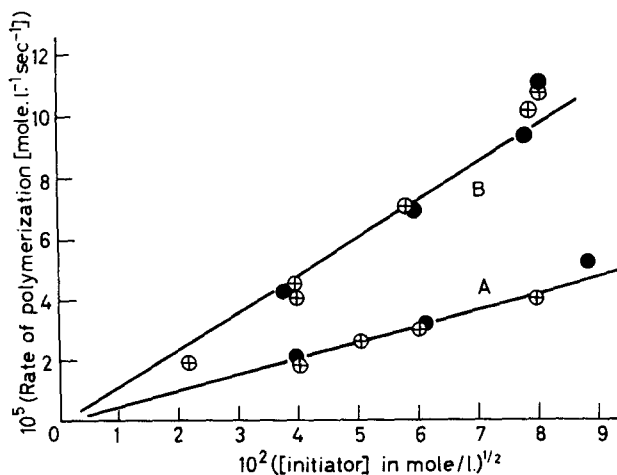


Figure 5—Dependence of rate of polymerization of acrylonitrile in dimethylformamide upon the concentration of di-anisoyl peroxide.

Line A [monomer]=1.45 mole/l.,
 line B [monomer]=2.90 mole/l.,
 ● C-peroxide,
 ⊕ M-peroxide.

Polymerization of vinyl acetate

Tests on the separation of unlabelled polyvinyl acetate from labelled di-anisoyl peroxide showed that traces of the peroxide might be occluded in the polymer even after four precipitations in *n*-hexane. Correction for this effect would be very uncertain but the specific activities of the polymers prepared with labelled peroxides were quite high and serious errors are not introduced by supposing that there is complete separation of polymer and undecomposed initiator.

For a sample of polymer prepared using C-peroxide, the ratio of specific activities of the polymer before and after hydrolysis was 27 so that j is about 0.02. The results of two experiments at 60° with vinyl acetate at 2.06 mole l.⁻¹ in benzene are summarized in Table 2. The specific activity of the M-peroxide was 27.89 $\mu\text{c/g}$ of carbon.

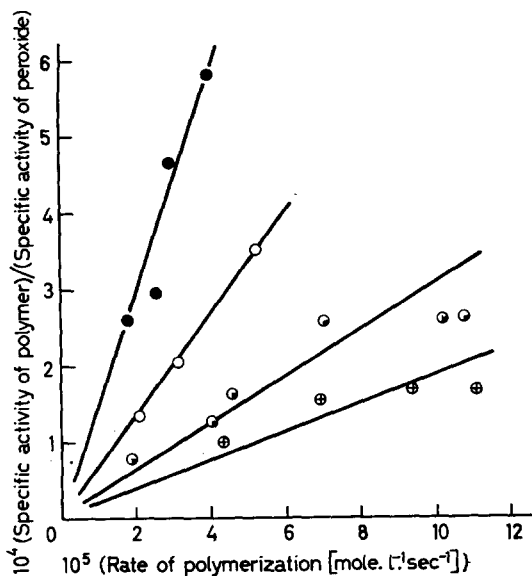


Figure 6—Plots of (specific activity of polymer)/(specific activity of peroxide) against rate of polymerization of acrylonitrile in dimethylformamide.

- C-peroxide,
- M-peroxide for [monomer]=1.45 mole/l.,
- ⊕ C-peroxide,
- ⊙ M-peroxide for [monomer]=2.90 mole/l.

Table 2. Experiments with vinyl acetate

[M-peroxide] × 10 ³ (mole l. ⁻¹)	6.35	3.60
R _p × 10 ⁵ (mole l. ⁻¹ sec. ⁻¹)	2.83	1.97
Spec. act. of polymer (μc/g of carbon)	0.216	0.173
Spec. act. of polymer after hydrolysis (μc/g of carbon)	0.013	0.010
k _t /k _p ² (mole l. ⁻¹ sec) calc. using (5)	290	334
x	0.99	0.99
R _t × 10 ⁷ (mole l. ⁻¹ sec. ⁻¹) calc. using (9)	1.1	0.6
k _d × 10 ⁶ (sec. ⁻¹)	8.7	8.3

If equation (10) is satisfied, these values of x indicate that k_1/k_2 is about 0.05 mole l.⁻¹ for vinyl acetate at 60°.

DISCUSSION

The yields of carbon dioxide during the thermal decomposition of di-anisoyl peroxide in dilute solutions in benzene at 60° are quite high but are lower than for dibenzoyl peroxide; the yields of anisic acid are higher than those of benzoic acid. The presence of monomers markedly suppresses the formation of carbon dioxide. The results clearly confirm that the primary dissociation of the peroxide gives anisoyloxy radicals only; some carbon dioxide is, however, produced directly during photo-dissociation⁶. Values obtained by tracer techniques for k_d for di-anisoyl peroxide are collected in Table 3.

Table 3. Dissociation of di-anisoyl peroxide

Process	$10^6 \times k_d$ (sec^{-1})	
	at 60°	at 80°
Analysis for carbon dioxide	6.5	—
Polymerization of styrene	5.4	70.0
Polymerization of methyl methacrylate	5.4	83.0
Polymerization of vinyl acetate	8.5	—
Polymerization of acrylonitrile	0.8	—

The magnitude of the difference between the extents of solvation in the initial and transition states is likely to depend to some extent upon the nature of the solvent, and therefore it is reasonable to expect small differences between the values of k_d in the various systems. Calculations of rates of initiation of polymerization and so of k_d depend upon the conversion of rates of contraction of reaction mixtures into absolute rates of polymerization; the necessary conversion factors are, in some cases, not known with great accuracy. These effects, however, could not be responsible for the very low value of k_d found when acrylonitrile is used as scavenger. As with dibenzoyl peroxide⁷, it is thought that primary radical transfer occurs so that some of the radicals derived from the peroxide do not become incorporated in polymer although they may initiate polymerization. The initiator fragment method therefore leads to low values for the rate of initiation for acrylonitrile in dimethylformamide, and values of k_i/k_p^2 derived for this monomer must be less than the true value. The value of k_d derived from the experiments with methyl methacrylate also may be a little lower than the true value; the slight dependence of rate of initiation upon concentration of monomer (see *Figure 3*) indicates that even at the higher concentration the efficiency of initiation may have been a little less than 100 per cent or alternatively that there may have been a small loss of comparatively small polymer molecules during recovery and purification. The results collected in *Table 3* are all significantly lower than some of the published values^{8, 9} of k_d for di-anisoyl peroxide which were obtained from experiments involving rather high concentrations of peroxide and low concentrations of monomer, and in which there may well have been significant contributions from induced decomposition of the peroxide.

There is a substantial discrepancy between the values of k_i/k_p^2 obtained for the two concentrations of methyl methacrylate at 60° but otherwise the values for this quantity are reasonable. The value of k_i/k_p^2 for vinyl acetate agrees with that found for a similar concentration of monomer using dibenzoyl peroxide as initiator, but there is a marked dependence upon concentration of monomer⁷ so that the quantity has no precise significance.

Primary radical transfer causes the values of x for acrylonitrile to be uncertain. It was pointed out in connection with dibenzoyl peroxide⁷, that if the aryloxy radical only engages in this type of transfer, the value of x is unaffected although the rates of initiation appear to be low; if, however, the aryl radical is involved in primary radical transfer, equation (8) must be modified to

$$1/x = 1 + k_1 k_a / k_2 \{ (k_a + k_b) [M] + k_s [S] \} \quad (13)$$

where k_a is the velocity constant for addition of the aryl radical to monomer, k_b and k_s are velocity constants for the radical displacements involving the aryl radical and monomer and solvent respectively, and $[S]$ is the concentration of solvent. The true value of k_1/k_2 may therefore be greater than that derived from (10).

The values obtained for k_1/k_2 for the benzoyloxy and aroyloxy radicals with various monomers at 60° are collected in *Table 4*, which shows also the relative values of k_2 for the systems.

Table 4. Reactivities of monomers towards aroyloxy radicals

<i>Monomer</i>	<i>Benzoyloxy radical</i>		<i>Anisoyloxy radical</i>	
	k_1/k_2	mole l ⁻¹ k_2 (relative)	k_1/k_2	mole l ⁻¹ k_2 (relative)
Styrene	0.4	1.00	0.02	1.00
Vinyl acetate	1.1	0.36	0.05	0.40
Methyl methacrylate	3.3	0.12	0.16	0.12
Acrylonitrile	≥8.0	≤0.05	≥1.8	≤0.01

The arrangement of these monomers in order of reactivity towards the anisoyloxy radical is the same as that obtained for reaction with the benzoyloxy radical. In all cases the relative importance of initiation by the aroyloxy radical is much greater for di-anisoyl peroxide than for dibenzoyl peroxide so that a higher proportion of the resulting polymer molecules have ester end-groups.

Bamford, Jenkins and Johnston¹⁰ have developed a treatment for correlating the velocity constants for the reactions of polymer radicals with substrates, both monomers and transfer agents. The velocity constant for such a reaction is expressed by

$$\log k = \log k_T + \alpha\sigma + \beta \quad (14)$$

where k_T is the velocity constant for the abstraction of hydrogen from toluene by the radical in question, σ depends upon the nature of the radical, and α and β depend upon the nature of the substrate. If the treatment can be extended to reactions of aroyloxy radicals, for which the unpaired electron is on an oxygen atom, the equation above can be modified to

$$\log (k_2/k_1) = \log (k_T/k_1) + \alpha\sigma + \beta \quad (15)$$

where k_T refers to the reaction between the aroyloxy radical and toluene. Taking the quoted values¹⁰ for α and β for styrene, vinyl acetate and methyl methacrylate, the data in *Table 4* can be used to calculate values of k_1/k_T and σ for the benzoyloxy and anisoyloxy radicals; discrepancies are found but the following approximate results are obtained:

$$\begin{aligned} \text{benzoyloxy radical } k_1/k_T &= 6 \times 10^3 \text{ mole l.}^{-1}, \sigma = 1 \\ \text{anisoyloxy radical } k_1/k_T &= 3 \times 10^2 \text{ mole l.}^{-1}, \sigma = 1.2 \end{aligned}$$

It would be possible to estimate a value of k_1/k_2 for the reaction of another monomer or transfer agent with one of these radicals, provided that the appropriate values of α and β are known. For example, for acrylonitrile

with the benzoyloxy and anisoyloxy radicals, the calculated values of k_1/k_2 are 36 and 8 mole l.⁻¹ respectively, both of which satisfy the experimental results.

J.K.A. thanks the Department of Scientific and Industrial Research for a maintenance grant. The sample of M-peroxide was prepared by Drs J. Toole and L. Trossarelli.

*Department of Chemistry,
University of Birmingham*

(Received February 1961)

REFERENCES

- ¹ BEVINGTON, J. C., TOOLE, J. and TROSSARELLI, L. *Trans. Faraday Soc.* 1958, **54**, 863
- ² BARSON, C. A. and BEVINGTON, J. C. *Tetrahedron*, 1958, **4**, 147
- ³ BEVINGTON, J. C., EAVES, D. E. and VALE, R. L. *J. Polym. Sci.* 1958, **32**, 317
- ⁴ BEVINGTON, J. C. *Proc. Roy. Soc. A*, 1957, **239**, 420
- ⁵ REID, J. C. and JONES, H. B. *J. biol. Chem.* 1948, **174**, 427
- ⁶ BEVINGTON, J. C. and LEWIS, T. D. *Trans. Faraday Soc.* 1958, **54**, 1340
- ⁷ BARSON, C. A., BEVINGTON, J. C. and EAVES, D. E. *Trans. Faraday Soc.* 1958, **54**, 1678
- ⁸ SWAIN, C. G., STOCKMAYER, W. H. and CLARKE, J. T. *J. Amer. chem. Soc.* 1950, **72**, 5426
- ⁹ BLOMQUIST, A. T. and BUSELLI, A. J. *J. Amer. chem. Soc.* 1951, **73**, 3883
- ¹⁰ BAMFORD, C. H., JENKINS, A. D. and JOHNSTON R. *Trans. Faraday Soc.* 1959, **55**, 418

The Effect of the High-frequency Discharge on the Surfaces of Solids. I—The Production of Surface Radicals on Polymers

C. H. BAMFORD and J. C. WARD

It has been shown that many polymers, when submitted to the action of a high-frequency electric discharge through hydrogen at low pressure, produce radicals characteristic of the polymer in a surface layer less than 1μ thick. The formation and properties of the radicals have been studied by e.s.r. spectroscopy, with particular reference to the effect of increases of temperature and the action of oxygen. We have used these surface radicals to obtain grafts of vinyl polymers on the surfaces of polyethylene and polypropylene. With a few exceptions, the radicals appear to be similar to those obtained by irradiation with γ -rays or high-energy electrons, but the new technique has the practical advantages of speed and simplicity as well as other features which are discussed.

INTRODUCTION

IN A previous report¹ we have shown that free radicals can be produced on the surfaces of many solids by subjecting them to a high-frequency electric discharge through a gas at low pressure. These radicals are formed from the solids by the direct action of the discharge and give electron spin resonance (e.s.r.) spectra characteristic of the corresponding radicals and independent of the nature of the gas carrying the discharge. The process of radical formation is therefore quite different from that previously employed by many workers^{2, 3} in which radicals formed in the gas phase are condensed and thereby stabilized in an inert matrix.

Our technique is of interest in three respects: (i) It provides a simple method of forming radicals for study by e.s.r., practically no special equipment being required. (ii) By following the decay of the radical concentration as a function of time and temperature and the changes in hyperfine structure brought about by the addition of vapours of reactive substances information about the nature of surface processes may be derived. (iii) The radicals derived from polymeric substrates may be used, either directly or indirectly, to initiate graft polymerizations. The technique therefore provides one of the simplest methods of grafting one polymer on to the surface of another. The high-frequency discharge can be used to produce radicals on surfaces of many different kinds; in this paper we discuss mainly polymeric substrates.

EXPERIMENTAL

E.s.r. spectrometer

The instrument was constructed in the laboratory. It employed a modulation frequency of 30 c/s. Superheterodyne detection at 45 Mc/s was followed by amplification at this frequency, then by amplification and phase-sensitive

detection at 30 c/s and finally by d.c. amplification. The first or 'signal' klystron was stabilized by means of frequency modulation at 500 kc/s, a phase-sensitive detector being used to supply a d.c. correcting voltage. The cavity used for most of the experiments was a gold-plated rectangular H_{014} reflection unit surrounded by a jacket which could be filled with refrigerant (generally liquid nitrogen). The sample tubes, of 4 mm internal diameter, were of fused silica, since this material does not produce any spectrum after exposure to the high-frequency discharge. Radical concentrations were estimated by comparison with a calibrated coal sample diluted with pure polyacrylonitrile powder, a diluent which was found to be free from unpaired spins within the limits of measurement.

Technique

The following procedure was used to produce the radicals. The sample of polymer was placed in a specimen tube, which was then carefully evacuated. Hydrogen at a pressure of about 0.1 mm of mercury was admitted and the tube sealed off. The probe of an ordinary laboratory leak-tester was applied to the base of the tube, which could be cooled at intervals of about 3 seconds in liquid nitrogen if desired. Generally the intensity of the spectrum did not increase significantly after the specimen had been treated for a period of 30 seconds.

RESULTS AND DISCUSSION

(1) Polyethylene

Low- and high-density powdered polyethylene samples gave similar six-line spectra of the type shown in *Figure 1* when submitted to the discharge at 77°K. The separation between adjacent lines is approximately 26 gauss. This

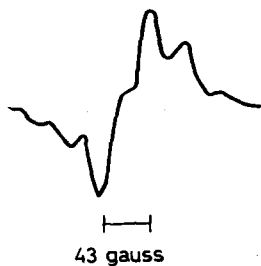


Figure 1—E.s.r. spectrum of high density polyethylene at 77°K after treatment by high-frequency discharge at 77°K

spectrum resembles that of unstretched polyethylene⁴ irradiated by 2 MeV electrons at 77°K. Abraham and Whiffen⁶ obtained somewhat different results on γ -irradiation at room temperature; with low-density polymer their spectrum was similar to that in *Figure 1*, but the central shoulder was split into two, while no spectrum was obtained by γ -irradiation of high-density polyethylene in the absence of oxygen at room temperature. According to current views⁵ the spectrum of *Figure 1* arises mainly from the radical $\sim\text{CH}_2-\dot{\text{C}}\text{H}-\text{CH}_2\sim$.

Loy's work⁷ on γ -irradiation of low-pressure polyethylene at 88°K gave results similar to ours. However, the central shoulder of the low temperature

spectrum was found to split on warming the specimen to room temperature, whereas in our case this did not occur.

The concentration of radicals at saturation at 77°K in our experiments approximates to 5×10^{-4} mol. l.⁻¹ (based on the total volume of the powder). On raising the temperature the signal decays comparatively rapidly, without change of shape, to a value characteristic of the temperature and subsequent decay is much slower. At -80°C and 20°C the values reached after a few minutes are approximately 70 per cent and 20 per cent of the initial values respectively. These results are reminiscent of those of Loy⁷ and of Onishi and Nitta⁸. The latter authors worked with γ -irradiated polymethyl methacrylate and obtained decay curves corresponding to a second order destruction reaction.

The polyethylene radicals react readily with oxygen to give the spectrum shown in *Figure 2*, which was obtained by admitting oxygen to the specimen at -80°C for 1 min and recooling to 77°K to record the spectrum. *Figure 2* shows the asymmetry characteristic of radical-oxygen adducts. The peroxy-



Figure 2—E.s.r. spectrum of peroxy-radical from polyethylene at 77°K produced by admitting to the specimen of *Figure 1* at -80°C

radical concentration also decays on raising the temperature, reaching about 10 per cent of its initial value in ten minutes at 20°C by a reaction which leads to the formation of surface peroxide groups, as will be shown below.

Surface grafting

Reaction of the polyethylene radicals with other monomers was studied in two ways. In the first the high-frequency discharge was applied to polyethylene powder in dilatometers containing hydrogen at a pressure of 0.1 mm of mercury and the radical concentrations measured by e.s.r. In some cases oxygen was then admitted and the dilatometers allowed to stand at room temperature until the spectrum of the peroxy-radical had decayed to zero (about two hours). The products of this reaction are subsequently referred to as the 'peroxidized material'. In the other cases the dilatometers were allowed to warm up to room temperature without admitting oxygen.

The dilatometers were then filled with degassed acrylonitrile from a side-arm and the subsequent polymerization at 80°C followed by observing the contraction. After completion of the reaction the solid was washed four times with ethylene carbonate at 80°C to free it from acrylonitrile homopolymer, and analysed for nitrogen. The polyethylene was also weighed before and after grafting.

Up to 50 per cent w/w grafting of polyacrylonitrile on to polyethylene powder was obtained.

The results of typical dilatometer experiments at 80°C are shown in *Figure 3*. Although pure acrylonitrile has no detectable thermal rate of polymerization at 80°C a slow reaction occurred in the presence of untreated poly-

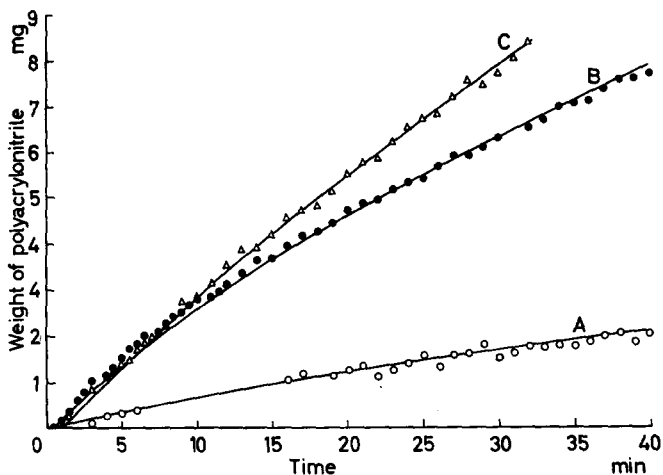


Figure 3—Graft polymerization of acrylonitrile on to high-density polyethylene at 80°C. A Untreated polyethylene (71.5 mg): B Polyethylene (103 mg) submitted to the discharge at 77°K: C As B, but the specimen (130 mg) was subsequently allowed to oxidize in air at 20°C for 17h. Zero time in these experiments was difficult to determine because extensive bumping often occurred when the dilatometers were immersed in the thermostat at 80°C

ethylene (curve A), indicating the presence of some catalytic species, perhaps surface peroxides (see below). The polyethylene specimens which had been submitted to the discharge gave appreciably higher rates of reaction (curves B, C). A surprising feature is the similarity of curves B, C. The peroxidized material presumably contains structures of the type POOH and POOP formed by autoxidation reactions involving the initial P· radicals and POO· radicals as described e.g. by Chapiro⁹. Thermal decomposition of these peroxides produces radicals which initiate grafting in the familiar manner. It might be expected that, in the absence of oxygen, grafting from the initial P· radicals would occur on a shorter time scale and probably to a reduced extent. The results in *Figure 3* are understandable if the radicals are initially somewhat occluded, or rapidly become occluded in the early stages of

grafting. In the former case the radicals cannot be confined to the surface and radical formation by the discharge must penetrate the polymer to some extent. It was therefore of interest to compare the reactivity of polyethylene radicals with radicals produced by the same technique on the surface of a crystalline solid, since the discharge is less likely to penetrate the crystal lattice than the solid polymer. Itaconic acid was chosen for this purpose because a high radical concentration may readily be produced, and the compound does not readily homopolymerize. The e.s.r. spectrum of itaconic acid radicals is shown in *Figure 4*. The radicals are remarkably stable; their concentration does not change appreciably during several days at room



Figure 4—E.s.r. spectrum of crystalline itaconic acid at 20°C after treatment by high-frequency discharge at room temperature

—|—
43 gauss

temperatures and their e.s.r. spectrum is unchanged after admission of oxygen. Nevertheless, a significant reaction occurs between these radicals and liquid acrylonitrile in a dilatometer at 25°C (*Figure 5*) and on heating at 60°C for half an hour weighable quantities of polyacrylonitrile may be obtained after extracting residual itaconic acid with methanol. In a typical experiment the initial radical concentration in the system itaconic acid + acrylonitrile was approximately 10^{-4} mol. l.⁻¹ and the conversion of acrylonitrile 0.5 mol. l.⁻¹ after half an hour. The mean kinetic chain length was therefore 1 500. The results indicate that occlusion phenomena, reducing the termination coefficient in the polymerization, are important in these reactions; if there were no occlusion the time scale in *Figure 5* would be much shorter, and it may easily be calculated that the conversion in the experiment at 60°C would be about 200 times less than observed. Characteristic occlusion phenomena were also observed in the following experiment. Four tubes each containing 1 g of itaconic acid were submitted to the discharge in the usual way and 3 ml degassed acrylonitrile distilled into each. The tubes were heated as indicated in *Table 1* and the weights of polyacrylonitrile measured. Reaction was

complete after one hour at any of the temperatures used. *Table 1* shows that greater yields of polymer at 60°C or 40°C are obtained if the mixture has previously been maintained at a lower temperature until reaction has ceased.

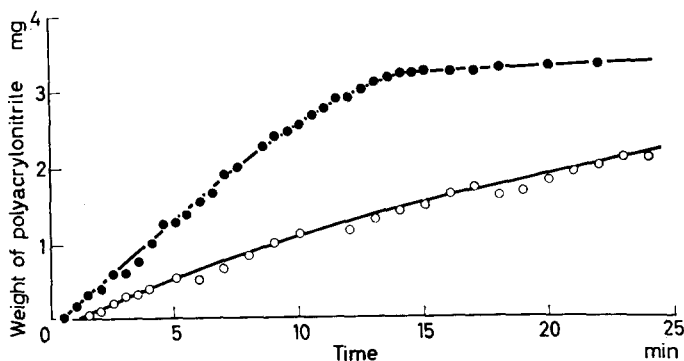


Figure 5—Graft polymerization of acrylonitrile on to itaconic acid crystals after treatment described under *Figure 4*. ● 25°C, 355 mg itaconic acid; ○ reaction at 60°C after 17 min at 40°C, 297 mg itaconic acid

This behaviour is typical of self-occluding systems¹⁰; clearly after reaction has ceased at one of the lower temperatures the radicals survive in a highly occluded state, and must become accessible again when the temperature is raised. *Figure 5* also shows the progress of a reaction in a dilatometer at 60°C after treatment with acrylonitrile for 17 min at 40°C. The initial rate is less than at 25°C probably on account of additional occlusion occurring at 40°C.

Table 1. Weights of polyacrylonitrile grafted to 1 g itaconic acid

<i>Expt. No.</i>	<i>Time (h) at</i>			<i>Weight, mg</i>
	25°C	40°C	60°C	
1	—	—	1	19.5
2	1	—	—	13.4
3	1	1	—	27.2
4	1	1	1	46.4

We may conclude that with polyethylene the results of *Figure 3* are consistent with the presence of initial surface radicals which rapidly become occluded; however, they do not preclude the existence of radicals at a depth of several molecular layers. We return to this point later.

The second technique used to investigate the grafting reaction consisted of grafting polymethacrylic acid to the surface of polyethylene powders, films or fibres and estimating the extent of reactions by dyeing the product with a basic dye (e.g. Sevron Red L). After submitting the specimen to the discharge, grafting was effected by heating in degassed methacrylic acid at 80°C for $\frac{1}{2}$ h. Again it was found that either the initial radicals or peroxidic groups resulting from reaction with oxygen could be utilized for grafting. After washing the specimen with methanol and water to remove free methacrylic acid, and dyeing, sections were prepared for microscopic examination. It was found that the methacrylic acid graft formed a dense

layer on the surface of the polyethylene, about 1μ in thickness. This distance corresponds approximately to the length of a polymethacrylic acid molecule; however, the orientation of these latter molecules relative to the surface was not investigated. The extent of grafting in these experiments was approximately 10 per cent w/w.

It was possible to use the grafted (but undyed) films to obtain additional confirmation that the radicals produced by the high-frequency discharge do, in fact, lie close to the surface. The discharge was applied to a film of polyethylene carrying a surface graft of polymethacrylic acid 1μ thick. The resulting radicals had the e.s.r. spectrum shown in *Figure 6(a)* initially, but the spectrum rapidly changed to that of *Figure 6(b)* in which the broad line is split into five components. As will be seen in (3) below this behaviour is highly characteristic of polymethacrylic acid. There was no evidence of the polyethylene radical spectrum (*Figure 1*), and we conclude that in these experiments radical formation is confined to a layer near the surface extending

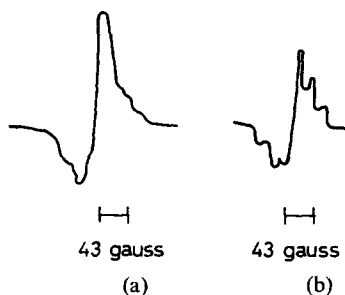


Figure 6—E.s.r. spectra at 77°K of film of low-density polyethylene with surface graft of polymethacrylic acid 1μ thick, after treatment with discharge at 77°K . (a) Immediately after treatment: (b) after 10 min at 20°C

at most to a depth of 1μ . Such a conclusion is quite consistent with the comparatively low penetrating power of β -particles. Thus, for example, it follows from the work of Muramatsu and Sasaki¹¹ that soft β -rays from tritium (energy 18 keV) are 50 per cent absorbed in a thickness of approximately 1μ of octadecane. The electron energies in our systems must be very much less than this, and are probably below 10 eV, hence penetration is likely to be confined to a few molecular layers.

A parallel series of blank experiments was performed which merely involved heating untreated polyethylene film or fibre at 80°C in degassed methacrylic acid for about 20 min followed by washing in methanol and water and subsequent dyeing. Rather surprisingly, some of these experiments—those in which film or fibre were used, but not those with powders—gave surface grafting, though to a smaller extent than with specimens submitted to the discharge. It is thought that these films and fibres were covered with a peroxide layer formed during manufacture. This supposition was substantiated by treating the specimens with an aqueous solution of potassium iodide to decompose the peroxide. After this, grafting was greatly reduced. On submitting to the discharge, however, the surface could be reactivated and grafting could be carried out as before. In a further experiment peroxidized material was prepared from a sample of polyethylene previously treated with potassium iodide, by application of the discharge

followed by oxidation in air. This material readily entered into grafting reactions, but its ability to do so was reduced by a further treatment with aqueous potassium iodide. Complete destruction of peroxide, with consequent elimination of grafting properties, could not be achieved, probably because the iodide is only able to react with the most accessible peroxide groups.

(2) *Isotactic polypropylene*

The observations made on this polymer were generally similar to those on polyethylene although there were some differences. The e.s.r. spectrum of the radicals produced by the high-frequency discharge at 20°C is shown in *Figure 7*. It differs from that produced by irradiation with 2 MeV electrons⁴



Figure 7—E.s.r. spectrum of polypropylene powder after treatment with discharge at 20°C

at 77°K in showing more hyperfine structure. The spectrum probably arises from a mixture of several types of radical, e.g. $\sim\text{CH}_2\dot{\text{C}}\text{HCH}_2\sim$, considered to be formed from polypropylene by the action of fast electrons⁴, together with $\sim\text{CH}_2\dot{\text{C}}\text{MeCH}_2\sim$. Treatment at 77°K gives a similar but stronger spectrum. On warming the specimen to 20°C the latter signal decays without change of shape to 25 per cent of its initial value in 3 min. No spectrum was obtained by Abraham and Whiffen⁶ on γ -irradiation at room temperature, presumably because the concentration of radicals decayed rapidly to a value below the sensitivity of their instrument, but they did find the much sharper peroxy-radical line.

On admitting oxygen to the radicals produced by the high-frequency discharge very rapid reaction occurred, with formation of peroxy-radicals of which the spectrum is shown in *Figure 8*. The amplitude of the derivative spectrum increased sharply on admitting oxygen (by a factor of approximately 5) but the spectrum of the peroxy-radical is narrower and integration indicated that no significant change in the number of unpaired electron spins had taken place. The peroxy-radical in polypropylene appears to be remarkably stable, little decay in concentration occurring after 17 h at room temperature.

Grafts of polymethacrylic acid and polyacrylonitrile on to polypropylene were obtained by the procedure described for polyethylene. The thickness of the surface grafts of polymethacrylic acid was again found to be 1 μ approximately. As with polyethylene there were indications that most of the

untreated polypropylene films and fibres already carried surface layers of peroxidized material, although one fibre specimen definitely did not. These peroxides were found to be rapidly and completely destroyed by treatment with aqueous potassium iodide. A specimen of polypropylene which was free from surface peroxide was submitted to the discharge at 77°K and

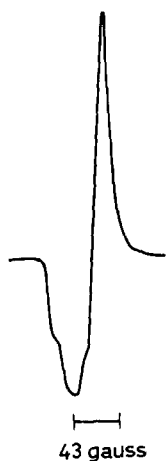


Figure 8—E.s.r. spectrum of peroxy-radical from polypropylene at 20°C after treatment of the specimen of Figure 7 with air at 20°C. The amplification in this figure is 0.42 times that in Figure 7

allowed to oxidize at room temperature to form the stable peroxy-radicals. It was then reacted with acrylonitrile in a dilatometer at 80°C, with results shown in Figure 9. The remarkably rapid initial polymerization has the character of the 'fast reaction' observed in other heterogeneous systems. Under the conditions of the experiment the peroxy-radicals are clearly readily accessible to acrylonitrile.

(3) Polymethacrylic acid and its methyl ester

After treatment with high-frequency discharge at 77°K polymethacrylic acid gives an e.s.r. spectrum consisting of a single broad line with evidence

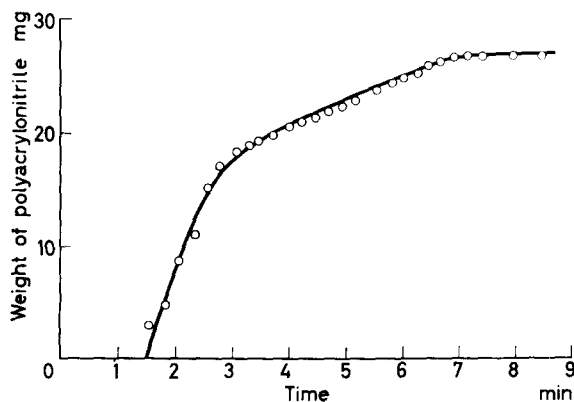
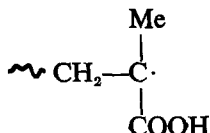


Figure 9—Graft polymerization at 80°C of acrylonitrile on to polypropylene (98 mg) containing peroxy-radicals

of hyperfine structure [Figure 10(a)]. This appears to resemble the spectrum obtained by Ovenall¹² by γ -irradiation of monomer-free polymethacrylic acid at 77°K, and attributed by him to the $\cdot\text{COOH}$ radical. Warming the specimen to 20°C for 3 min brings about a considerable decay of signal and a transformation of the spectrum to that shown in Figure 10(b); this approximates to the familiar 5 lines and 4 shoulders assigned to the



radical which is responsible for chain propagation in the polymerization of solid and liquid methacrylic acid¹³. The same radical is produced by treating crystalline methacrylic acid^{1, 13} with the high-frequency discharge at 77°K



Figure 10—E.s.r. spectrum of polymethacrylic acid after treatment with the discharge at 77°K.
(a) Immediately after treatment:
(b) after 10 min at 20°C

(Figure 11). In the most general terms the 'single' line spectrum [Figure 10(a)] indicates the presence of a radical in which the unpaired spin is not strongly coupled to proton spins. The carboxyl radical suggested by Ovenall¹² may be one possibility; since hydrogen atoms are present in our systems the

adduct of $\text{H}\cdot$ and $-\text{C}-\text{COOH}$, i.e. $-\text{C}-\dot{\text{C}}\begin{array}{l} \text{OH} \\ \text{OH} \end{array}$ may be another (probably

less likely). On raising the temperature these radicals decay, either by eliminating a hydrogen atom, or, particularly in the case of $\cdot\text{COOH}$, by migration and mutual destruction. The residual spectrum [Figure 10(b)] in

our systems is much weaker than the original and may initially have been present but obscured by the stronger spectrum.

Although the radical responsible for the broad line is labile at room temperature its spectrum does not change significantly in 3 min on admitting



Figure 11—E.s.r. spectrum of crystalline methacrylic acid at 77°K after treatment with the discharge at 77°K

air at -80°C . On raising the temperature to 18°C in the presence of air a marked change to the spectrum of Figure 13 occurs in 3 min. This spectrum

probably arises from a mixture of $\sim\text{CH}_2-\overset{\text{Me}}{\underset{\text{COOH}}{\text{C}}}\cdot$ radicals and their

oxygen adducts. Figure 12 shows the spectrum of the latter radicals, these being obtained by repeated action of the discharge on crystalline methacrylic

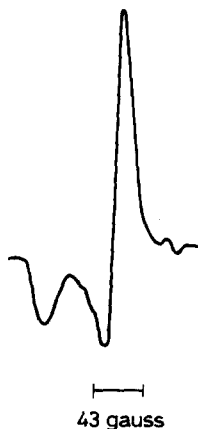


Figure 12—E.s.r. spectrum of $\sim\text{CH}_2-\overset{\text{Me}}{\underset{\text{COOH}}{\text{C}}}\cdot$ radical.

Propagating radicals were produced from crystalline methacrylic acid by repeated action of the discharge at 77°K with intermediate warming to 13°C . After 8 treatments the temperature was raised to 30°C and air admitted¹³

acid followed by admission of oxygen¹³ at 30°C . The results are consistent with the view that the initial radicals giving the broad line are destroyed by oxygen without formation of an appreciable concentration of any other radical.

A similar spectrum consisting of one broad line is obtained from polymethyl methacrylate on submitting it to the discharge. Although the decay properties of this spectrum are the same as those found for polymethacrylic acid the behaviour in the presence of oxygen is different. Admission of air



43 gauss

Figure 13—E.s.r. spectrum from polymethacrylic acid at 77°K. The specimen was treated with the discharge at 77°K, then warmed to 18°C in the presence of air and held at that temperature for 3 min before recooling to 77°K

at -80°C causes extensive conversion to a typical asymmetric peroxy-radical spectrum in 1 min with little decay (Figure 14), while after a further 2 min at 20°C the signal is reduced to a quarter of its intensity without change in shape.

If we assume that the $\cdot\text{COOH}$ and $\cdot\text{COOMe}$ radicals are responsible for the initial broad lines from polymethacrylic acid and its methyl ester, respectively, the difference in the behaviour of the two polymers is understandable. The oxygen adducts with these radicals would be expected to differ in stability, that from $\cdot\text{COOH}$ decomposing particularly rapidly into CO_2 and mobile $\text{HO}_2\cdot$ radicals, so that its spectrum cannot be observed. On the other hand $\cdot\text{O}_2\text{COOMe}$ may have much greater stability with respect to this type of decomposition, and we suggest that this radical is responsible for the spectrum in Figure 14.

It is possible that the broad line obtained by Ungar *et al.*¹⁴ by γ -irradiation of monomer-free polymethyl methacrylate arose from the same source.



43 gauss

Figure 14—E.s.r. spectrum of polymethyl methacrylate at 77°K. The specimen was treated with the discharge at 77°K then warmed to -80°C in the presence of air for 1 min before recooling

If true, this would mean that the $\cdot\text{COOMe}$ radical is stable in the absence of monomer when formed in the interior of the sample, but that in the presence of the monomer it reacts with the latter to give the normal propagating radical. The behaviour of the broad line spectrum of Ungar *et al.*

on admitting oxygen supports this hypothesis. The work of Ungar *et al.* was carried out at room temperature, and it is possible that if their specimens were irradiated and examined at 77°C they would all show the broad line.

(4) Polyvinyl chloride

This polymer gives a strong e.s.r. signal after exposure to the discharge at room temperature, consisting of a single, broad, slightly asymmetric, line with a half-width between points of maximum slope of about 35 gauss. Admission of air produces an immediate change to a peroxy-radical giving a spectrum which is narrower and strongly asymmetric in the opposite sense. The peroxy-radical has a half-life of 10 min at 20°C. The spectra are shown in Figures 15 and 16.

To test the feasibility of grafting to polyvinyl chloride a specimen of the powder was submitted to the discharge and allowed to oxidize in air at room

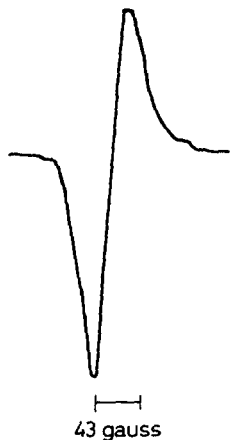


Figure 15—E.s.r. spectrum of polyvinyl chloride at 20°C after treatment with the discharge at 20°C

temperature until the peroxy-radical spectrum had disappeared. Degassed acrylonitrile was then added and the mixture heated to 80°C in a dilatometer. A small amount of reaction occurred, corresponding to a grafting of approximately 4 per cent of acrylonitrile on the polyvinyl chloride. The relatively small extent of grafting suggests that the yield of peroxides formed during the decay of the peroxy-radical is small. This is consistent with the well-known resistance of this polymer to oxidation.

Polyvinylidene chloride gave similar results but the signals were much weaker.

(5) Cellulose

Cotton wool treated under the same conditions (20°C) gives the strong line shown in Figure 17(a). It appears to consist of a narrower line superimposed on a broader one. On heating the material to 50°C, the spectrum decays to half its initial intensity in 10 min. Exposure to the discharge at 77°K gives the spectrum shown in Figure 17(b). On warming the specimen to 20°C the signal decayed to 40 per cent of its initial strength in 3 min.

Figures 17(a) and (b) differ from the spectra obtained by γ -irradiation of cellulose⁶ in showing less hyperfine structure and asymmetry.

Warming the specimen of Figure 17(b) to room temperature in the presence of oxygen failed to produce any evidence of an asymmetric peroxy-radical



Figure 16—E.s.r. spectrum of peroxy-radicals from poly-vinyl chloride at 20°C produced by admitting air to the specimen of Figure 15 at 20°C

spectrum, but merely caused the signal to decay rapidly without significant change of shape. It seems likely that in this case the decay proceeds through formation of mobile $\text{HO}_2\cdot$ radicals. In agreement with this was the observation that no grafting to cellulose could be achieved by the technique described earlier.

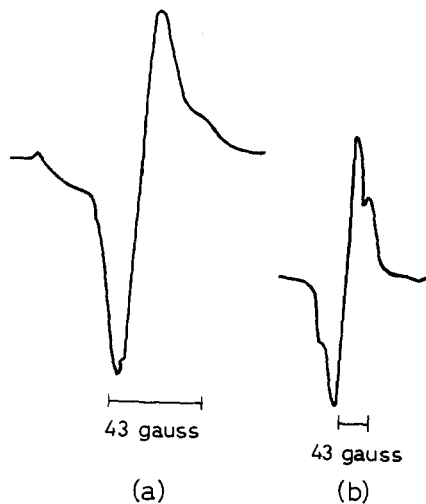


Figure 17—E.s.r. spectra of cellulose after treatment with the discharge (a) at 20°C, (b) at 77°K

The high-frequency discharge produces some degradation of cellulose, a single treatment for 3 min at 77°K giving a decrease in specific viscosity in cuprammonium solution from 21 to 15 dl/g.

CONCLUSIONS

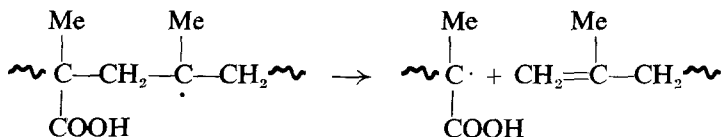
The high-frequency discharge evidently provides an effective way of producing radicals from solid polymers. Indeed, all the polymers which have so far been examined except polytetrafluoroethylene yield radicals when treated with the discharge at 77°K. From the survey of results presented in this paper some general conclusions may be drawn, which, however, at the present stage can hardly be other than tentative.

Most of the radicals identified have structures corresponding to the cleavage of atoms or groups from the main chains (e.g. H, ·COOH, ·COOCH₃). It seems less common to obtain radicals by scission of the chains themselves, perhaps because of a cage effect, although with polymethacrylic acid and its methyl ester such a radical is probably formed. However, it must be remembered that the radicals which are trapped are not necessarily those produced in the primary acts. Although the specimen is cooled, local heating to temperatures considerably above 77°K must occur during the passage of the discharge, and further, 'hot' radicals and other species may be formed. Under these conditions the occurrence of a variety of radical reactions cannot be excluded, tending eventually to the trapping of the least reactive radicals. The appearance of the 'propagating' methacrylic radical referred to above would be consistent with these views; if this radical is not formed in the primary act it could arise comparatively easily by chain rupture on account of the internal strain present in the polymer molecule.

It has frequently been noted that in e.s.r. studies of γ -irradiation polymers only one of the two radicals resulting from chain scission can be identified. This situation may also arise in the present work on polymethacrylic acid and polymethyl methacrylate. If, as suggested, the initial spectrum is that of ·COOH or ·COOMe it might be expected that the radical



would remain and be recognizable, especially since a radical of similar structure in the neighbourhood of the unpaired spin is detectable in irradiated polypropylene. The initial broad line may contain some contribution from this radical, or, alternatively, the latter may decay rapidly by a process such as the following (which may be a hot-radical reaction)



In general, the resemblances between the nature of the radicals formed by the high-frequency discharge and those produced by other methods are more striking than the differences, indicating either that the primary acts are generally similar, or that secondary processes leading to the most stable radicals are important.

On the other hand, the distributions of radicals in the specimens are quite different, since we have shown that the present technique leads to radicals only in a region close to the surface of the polymer. From the practical point of view this may be an important feature of the high-frequency method,

in that it provides a way of modifying the surface properties of a polymer, e.g. by grafting, without affecting the bulk of the material. It may also provide the basis of a technique for identifying thin films on the surface of polymers. The localization of the radicals in a surface layer would be expected to influence their behaviour in at least two ways, by facilitating their rapid decay, and by increasing their accessibility towards reagents.

It will be recalled that radicals formed by the discharge on the surfaces of some crystalline solids (e.g. methacrylic acid¹, *n*-butyric acid¹³) may possess a very high mobility at room temperature, and decay very rapidly. By no means all crystalline solids give mobile surface radicals, however; as already mentioned, itaconic acid is a striking example of one which does not. The mobility clearly depends on the chemical nature and crystal structure of the material, and we intend to explore this aspect further in the future. In the case of polymers the movement of radicals attached to the chains will be relatively restricted, even when the radicals lie close to the surface, hence it is not surprising that the extensive decay of radicals found with crystalline methacrylic acid on passing from 77°K to 273°K is not observed with polymers. It is unlikely that the kinetics of radical decay in a polymer will follow a simple law over the whole course of reaction. If the radicals are attached to polymer chains, then above the glass transition temperature they may have sufficiently mobility to react with neighbouring radicals, and the range of effective interaction will increase with the temperature. At a given temperature a situation will ultimately be reached in which radicals are too widely separated to allow a significant rate of reaction. Thus although the decay may appear second order in the early stages the concentration will seem to be asymptotic to a finite non-zero value. This type of behaviour is, in fact, commonly encountered with radicals trapped in polymers (cf. e.g. Loy⁷). The rate of radical decay at a given temperature will not be a function merely of the concentration, but will depend on the detailed spatial distribution (cf. ref. 5). Since it is not possible to change the temperature of specimens instantaneously, the rate of decay at any temperature may be expected to depend upon the temperature at which the radicals were formed and their original concentration. This fact limits useful comparisons to data obtained under closely similar conditions. For a given radical concentration based on the total volume of the polymer sample, localization near the surface should facilitate the initial rapid portion of the decay at a given temperature, compared with a more nearly homogeneous radical distribution. There are no quantitative data available suitable for examining this.

Our quantitative understanding of these systems is so incomplete that particular caution is necessary when inferring reaction mechanisms from kinetic observations. A similar situation has been shown to exist in some polymerizations under heterogeneous conditions¹⁵. If the radicals are not attached to polymer chains the complications noted above will be less important, and a more extensive second order decay is possible.

The observations described earlier show that the accessibility of surface polymer radicals may be very high. As an example for comparison with radicals produced by γ -irradiation we may cite the work of Florin¹⁶ who has reported that the radicals formed in cellulose decay only slowly in the

presence of air. In our experiments decay under similar conditions is very rapid. Since no peroxy-radical can be detected and the decay probably proceeds through the formation of $\text{HO}_2 \cdot$ this difference implies a difference in the accessibility of the radicals in the two specimens towards oxygen.

We are pleased to thank Messrs E. C. Collingwood and J. Jones-Hewson, and Mrs P. Ginger for assistance with the experimental work and diagrams.

*Courtaulds, Limited,
Research Laboratory,
Maidenhead, Berks.*

(Received February 1961)

REFERENCES

- ¹ BAMFORD, C. H., JENKINS, A. D. and WARD, J. C. *Nature, Lond.* 1960, **186**, 712
- ² BASS, A. M. and BROIDA, H. P. (Editors). *Formation and Trapping of Free Radicals*. Academic Press: New York, 1960
- ³ BASS, A. M. and BROIDA, H. P. (Editors). *Stabilization of Free Radicals at Low Temperatures*. National Bureau of Standards *Monograph 12*: Washington, 1960
- ⁴ LIBBY, D., ORMEROD, M. G. and CHARLESBY, A. *Polymer, Lond.* 1960, **1**, 212
- ⁵ LAWTON, E. J., BALWIT, J. S. and POWELL, R. S. *J. chem. Phys.* 1960, **33**, 395
- ⁶ ABRAHAM, R. J. and WHIFFEN, D. H. *Trans. Faraday Soc.* 1958, **54**, 1291
- ⁷ LOY, R. R. *J. Polym. Sci.* 1960, **44**, 341
- ⁸ ONISHI, S. and NITTA, I. *J. Polym. Sci.* 1959, **38**, 451
- ⁹ CHAPIRO, A. *J. Polym. Sci.* 1958, **29**, 321; 1959, **34**, 439
- ¹⁰ BAMFORD, C. H. and JENKINS, A. D. *Proc. Roy. Soc. A.* 1955, **228**, 220
- ¹¹ MURAMATSU, M. and SASAKI, T. *Science*, 1960, **131**, 302
- ¹² OVENALL, D. W. *J. Polym. Sci.* 1959, **41**, 199
- ¹³ BAMFORD, C. H., JENKINS, A. D. and WARD, J. C. *J. Polym. Sci.* In press
- ¹⁴ UNGAR, I. S., GAGER, W. B. and LENINGER, R. I. *J. Polym. Sci.* 1960, **44**, 295
- ¹⁵ BAMFORD, C. H. and JENKINS, A. D. *J. Chim. phys.* 1959, **56**, 798
- ¹⁶ FLORIN, R. E. Paper presented at American Chemical Society Meeting, New York, September 1960

Branched Polymers. I— Molecular Weight Distributions

T. A. OROFINO

Expressions are derived for the number and weight average molecular weights of branched molecules of a particular structural class as functions of the molecular weight averages of their constituent linear components. The branched structures treated are termed 'comb molecules' and consist of linear backbone chains to which linear side chains are attached by one end at various positions along the backbone. Proper choice of the parameters specifying the structure of the comb molecules reduces them, and the molecular weight relationships presented applicable to them, to the corresponding details characteristic of star shaped branched molecules. The relative effects of the number of side chains attached, the backbone and the side chain heterogeneities on the weight-to-number average ratios of the branched molecule systems are discussed.

IN RECENT years, some physical properties of a number of branched polymer systems have been investigated. Particular emphasis has been placed on the determination of molecular dimensions in solution and comparisons of the values obtained with those found for the corresponding linear polymers¹⁻⁶.

The interpretation of experimental data on these systems has often been complicated by molecular weight polydispersity of the sample, thus rendering difficult or impossible an independent assessment of the effects of branching *per se* on the properties investigated¹⁻³. In such studies, it would clearly be desirable to reduce structure and chain length heterogeneity to a minimum, or at least to obtain an adequate characterization of the various branched molecules constituting the sample.

With the above objective in mind, we have derived some molecular weight relationships applicable to branched polymers of a particular structural class encompassing, in their various architectural ramifications, a number of branched systems currently of interest*.

The branched structures considered consist of a collection of linear backbone chains to each of which a variable number of linear side chains, chosen from an arbitrary distribution, may be attached by one end at various segments of the backbone. We shall refer to the structures so formed as 'comb molecules'. The choice of this particular class of branching affords the following advantages. (1) Theoretically, the exact structures involved may be easily specified by a small number of variables and thus should be better suited in controlled, systematic studies of the effects of branching than would be, for example, randomly branched materials of non-specific architecture. This advantage has already been recognized in

*The original impetus for this work was the need for pertinent molecular weight relationships which would serve as a guide in the synthesis of branched molecules of the types here considered, a programme currently in progress in our laboratories.

recent experimental investigations^{4, 5}. (2) These materials are capable of synthesis and thus afford a practical means of exploiting the foregoing attributes in experimental studies. Moreover, the use of component linear polymers prepared by anionic techniques⁷ in direct coupling syntheses of comb molecules, or, incorporation of side chains or backbones by anionic polymerization at active sites along the main chain, affords possibilities of molecular weight and molecular weight distribution control not heretofore utilized. (3) Proper selection of the pertinent structural variables, for both theoretical and experimental purposes, reduces comb molecules to the star shaped type; the latter materials are also of interest in studies of branched systems and have already been investigated in some detail^{1-3, 8}.

GENERAL MOLECULAR WEIGHT RELATIONSHIPS

We consider a collection of comb molecules formed by the reaction of linear side chain polymer (branches) with linear chains (backbones). One end of each branch molecule is assumed to couple with a backbone segment. Each of the latter has the same probability of reaction, the coupling process being indiscriminate throughout the polymerization in regard to the lengths of the backbone and branch molecules involved and the number of branches already attached to a particular chain. No more than one branch chain, however, may react with any given backbone segment†.

These structures, and the relationship to be presented applicable to them, converge smoothly to the corresponding details characteristic of star molecules (branched molecules consisting of a number of linear chains joined by one end at a common junction), as the ratio of the backbone length to the total number of branch segments approaches zero.

Let the chain length distributions of the original backbone and branch molecules before coupling be specified by the sets:

$$\begin{array}{ll} n_i; x_i & x_i = 1, 2, 3 \dots x^* \\ m_i; y_i & y_i = 1, 2, 3 \dots y^* \end{array}$$

where n_i is the number of backbone molecules of chain length x_i units and m_i is the number of branch molecules of length y_i units. We define for the original linear components in the usual manner:

$$\begin{aligned} \bar{x}_n &= \left(\sum_{i=1}^{x^*} n_i x_i \right) / \left(\sum_{i=1}^{x^*} n_i \right) \\ \bar{x}_w &= \left(\sum_{i=1}^{x^*} n_i x_i^2 \right) / \left(\sum_{i=1}^{x^*} n_i x_i \right) \\ \bar{y}_n &= \left(\sum_{i=1}^{y^*} m_i y_i \right) / \left(\sum_{i=1}^{y^*} m_i \right) \\ \bar{y}_w &= \left(\sum_{i=1}^{y^*} m_i y_i^2 \right) / \left(\sum_{i=1}^{y^*} m_i y_i \right) \end{aligned} \quad (1)$$

†The scheme depicted for the coupling of branches to backbones, although one means of synthesis of comb molecules, has been selected primarily for convenience in the statistical development to follow. The relationships ultimately obtained are equally applicable to comb molecules synthesized by other methods, as for example by propagation of linear chains originating from active sites along the backbone molecules.

For the final branched polymer mixture* we also define the average number of branches per backbone molecule \bar{p}_n :

$$\bar{p}_n = (\sum m_i / \sum n_i) = (\sum m_i y_i / \sum n_i x_i) (\bar{x}_n / \bar{y}_n) \quad (2)$$

The distribution of molecular species in the final mixture of comb molecules may be designated as follows: after reaction, chains of the same x_i , previously indistinguishable, now contain various numbers and permutations of branches. We shall consider any such branched molecule as specified by the values of two parameters: x_i , its backbone length; and s , the total number of branch segments it contains. We let $n_{i,s}$ be the number of branched molecules which contain $Z_{i,s} = x_i + s$ units, and observe that $\sum_{i,s} n_{i,s} = \sum_i n_i$.

The number average degree of polymerization of the final branched polymer mixture thus becomes:

$$\bar{Z}_n = [\sum_i \sum_s n_{i,s} (x_i + s)] / [\sum_i n_i] = \bar{x}_n + \bar{S}_n = \bar{x}_n + \bar{p}_n \bar{y}_n \quad (3)$$

where \bar{S}_n is the number average branch unit content of the backbone molecules.

The weight average degree of polymerization is

$$\bar{Z}_w = [\sum_i \sum_s n_{i,s} (x_i + s)^2] / [\sum_i \sum_s n_{i,s} (x_i + s)] \quad (4)$$

which may be expressed

$$\begin{aligned} \bar{Z}_w &= \bar{x}_w + [\bar{S}_n (\bar{S}_w + \bar{x}_w)] / [\bar{x}_n + \bar{S}_n] \\ &= \bar{x}_w + [\bar{p}_n \bar{y}_n (\bar{S}_w + \bar{x}_w)] / [\bar{x}_n + \bar{p}_n \bar{y}_n] \end{aligned} \quad (5)$$

where \bar{S}_w is the weight average branch unit content of the backbone molecules defined

$$\bar{S}_w = (\sum_s n_s \cdot s^2) / (\sum_s n_s \cdot s) \quad (6)$$

n_s being the number of backbone molecules each of which possesses a total of s branch segments, independent of the value of x_i .

The quantity \bar{S}_w may be explicitly expressed as a function of parameters of the original backbone and branch distributions. In regard to the latter, however, a knowledge of the convenient parameters \bar{y}_n and \bar{y}_w alone is in general insufficient for specification of \bar{S}_w , more detailed information about the branch distribution being required. In the following sections several special cases of interest for which \bar{S}_w may be simply expressed are considered.

*We assume for simplicity that all members of the original backbone and branch chain sets ultimately couple. For the validity of the relationships to be derived, however, it is only necessary that samples of the original backbone and branch components, representative of the respective chain length distributions, take part in the coupling reaction.

MOLECULAR WEIGHT RELATIONSHIPS FOR UNIFORM
BRANCH LENGTHS

(1) *Uniformly spaced branch sites*

We consider here a collection of backbone molecules to which branches of uniform length y are attached at regularly spaced intervals. Such a mixture would result, for example, in the complete reaction of alternating copolymer backbone molecules with uniform branch chains capable of attaching to only one species of repeating unit. The average degrees of polymerization for this case are simply:

$$\bar{Z}_n = \left\{ \sum_i n_i [x_i + y (\bar{p}_n / \bar{x}_n) x_i] \right\} / \left\{ \sum_i n_i \right\} = \bar{x}_n + \bar{p}_n y \quad (7)$$

and

$$\begin{aligned} \bar{Z}_w &= \bar{x}_w (1 + p_n y / \bar{x}_n) \\ \bar{S}_w &= \bar{p}_n y \bar{x}_w / \bar{x}_n \end{aligned} \quad (8)$$

(2) *Randomly distributed branch sites*

If the x_i are arbitrary, y is fixed and if the branches are distributed in random fashion over the collection of backbone segments, the number of x_i molecules which on the average contain $0 \leq k \leq x_i$ branches is given by a Bernoulli distribution of mean $x_i \bar{p}_n / \bar{x}_n$. Thus the probability that a backbone chain of x_i units contains exactly k branches is

$$P(x_i; k) = \binom{x_i}{k} (\bar{p}_n / \bar{x}_n)^k (1 - \bar{p}_n / \bar{x}_n)^{x_i - k} \quad (9)$$

The average degrees of polymerization for this system are accordingly:

$$\begin{aligned} \bar{Z}_n &= \left\{ \sum_i \sum_{k=0}^{x_i} [n_i (x_i + k) P(x_i; k)] \right\} / \left\{ \sum_i n_i \right\} \\ &= \bar{x}_n + \bar{p}_n y \end{aligned} \quad (10)$$

and

$$\begin{aligned} \bar{Z}_w &= \left\{ \sum_i \sum_{k=0}^{x_i} [n_i (x_i + ky)^2 P(x_i; k)] \right\} / \left\{ (\bar{x}_n + \bar{p}_n y) \sum_i n_i \right\} \\ &= \bar{x}_w (1 + \bar{p}_n y / \bar{x}_n) + [\bar{p}_n y^2 (\bar{x}_n - \bar{p}_n)] / [\bar{x}_n (\bar{x}_n + \bar{p}_n y)] \\ \bar{S}_w &= \bar{x}_w \bar{p}_n y / \bar{x}_n + y (1 - \bar{p}_n / \bar{x}_n) \end{aligned} \quad (11)$$

In terms of the number fraction of branch units in the final mixture $N_y = \sum m_i y_i / (\sum n_i x_i + \sum m_i y_i) = 1 - N_x$, where N_x is the number fraction of backbone units, the equations (10) and (11), for example, become:

$$\begin{aligned} \bar{Z}_n &= \bar{x}_n / N_x \\ \bar{Z}_w &= \bar{x}_w / N_x + (N_y / N_x) (y N_x - N_y) \\ \bar{S}_w &= [N_y / N_x] [\bar{x}_w + (\bar{x}_n / \bar{p}_n) - 1] \end{aligned} \quad (12)$$

LIMITING MOLECULAR WEIGHT RELATIONSHIPS
 FOR ARBITRARY BRANCH LENGTHS

If the number of side chains attached to each backbone in a mixture of comb molecules is sufficiently large, it is possible to derive limiting expressions for the weight average molecular weight of the system as a function of the weight and number average chain lengths of the constituent linear molecules. The expressions so derived should also serve as useful approximations for moderate degrees of branching.

(1) *Uniformly spaced branch sites*

Consider a collection of backbone molecules of various lengths to which are attached at regular intervals branch chains selected at random from the side chain distribution $[m_i; y_i]$. The probability that an attached branch chain, chosen arbitrarily, contains y_i units is $m_i/\sum m_i$. The mean value of y_i is \bar{y}_n and the variance of the distribution σ^2 is given by the relation

$$\sigma^2 = \sum_i [(y_i - \bar{y}_n)^2 (m_i / \sum m_i)] = \bar{y}_n^2 (\bar{y}_w / \bar{y}_n - 1) \quad (13)$$

Now it is intuitively plausible that if the number of branches k attached to a given backbone chain containing a total of s branch segments is large, then the ratio s/k will be more likely to lie within prescribed limits of \bar{y}_n than would the number of segments in any *single* branch chain arbitrarily selected. This statement may be made more precise by the Central Limit Theorem, which for our application, states that if k is large deviations of s from the mean value $k\bar{y}_n$ are approximately governed by the relationship

$$P\{a < \left| \frac{s - k\bar{y}_n}{\sigma k^{1/2}} \right| < b\} \simeq \Phi(b) - \Phi(a) \quad (14)$$

where Φ is the normal distribution

$$\Phi(t) = (1/2\pi)^{1/2} \int_{-\infty}^t e^{-r^2/2} dr; \quad \Phi(\infty) = 1 \quad (15)$$

For each backbone chain containing k branches we may now express its possible values of s as multiples of a constant increment q from the mean $k\bar{y}_n$. The probability that $|(s - k\bar{y}_n)/\sigma k^{1/2}|$ lies between $a=0$ and $b=q$, or, in the limit of small q equals $q/2$, is the probability that $s = k\bar{y}_n \pm \sigma k^{1/2} (q/2)$. In general, if we let $\Phi([j+1]q) - \Phi(jq) = \Delta\Phi_j$, then according to equation (14) the number of backbone chains containing k branches with a total branch unit content

$$s = k\bar{y}_n \pm \sigma k^{1/2} [(2j+1)/2] q \\ j = 0, 1, 2, \dots$$

is $n_k \Delta\Phi_j$, where n_k is the total number of backbone molecules containing exactly k branches.

Bearing in mind that for regularly spaced branch locations $k = (\bar{p}_n / \bar{x}_n) x_i$, we have for the number average degree of polymerization of the branched polymer mixture

$$\bar{Z}_n = (1 / \sum_i n_i) \sum_i \sum_j [2x_i + 2\bar{y}_n \bar{p}_n / \bar{x}_n] n_i \Delta\Phi_j \quad (16)$$

We observe that

$$\lim_{q \rightarrow 0} 2 \sum_i \Delta \Phi_i = \Phi(\infty) = 1 \quad (17)$$

which substitution reduces equation (16) to the general result of equation (3).

We have for the weight average degree of polymerization

$$\begin{aligned} \bar{Z}_w = & [1 / (\bar{Z}_n \sum_i n_i)] \sum_i \sum_j \{ [x_i + \bar{p}_n \bar{y}_n x_i / \bar{x}_n + \sigma q (\bar{p}_n x_i / \bar{x}_n)^{1/2} ((2j+1)/2)]^2 \\ & + [x_i + \bar{p}_n \bar{y}_n x_i / \bar{x}_n - \sigma q (\bar{p}_n x_i / \bar{x}_n)^{1/2} ((2j+1)/2)]^2 \} n_i \Delta \Phi_j \end{aligned} \quad (18)$$

for which we observe

$$\lim_{q \rightarrow 0} 2q^2 \sum_j [(2j+1)/2]^2 \Delta \Phi_j \sim (1/2\pi)^{1/2} \int_{-\infty}^{\infty} r^2 e^{-r^2/2} dr = 1 \quad (19)$$

With the value of σ given in equation (13), equation (18) becomes

$$\bar{Z}_w = \bar{x}_w (1 + \bar{p}_n \bar{y}_n / \bar{x}_n) + [\bar{p}_n \bar{y}_n^2 (\bar{y}_w / \bar{y}_n - 1)] / [\bar{x}_n + \bar{p}_n \bar{y}_n] \quad (18a)$$

which we note can be reduced to equation (8) for uniform branch lengths when \bar{y}_n equals \bar{y}_w .

(2) *Randomly distributed branch sites*

Generalization of the preceding methods for the branched polymer mixture in which the number of side chains per molecule is governed by the Bernoulli distribution leads to the results:

$$\bar{Z}_n = (1 / \sum_i n_i) \sum_i \sum_j \sum_k [2x_i + 2k\bar{y}_n] n_i P(x_i; k) \Delta \Phi_j = \bar{x}_n + \bar{p}_n \bar{y}_n \quad (20)$$

and

$$\begin{aligned} \bar{Z}_w = & \bar{x}_w (1 + \bar{p}_n \bar{y}_n / \bar{x}_n) + [\bar{p}_n \bar{y}_n^2 (\bar{x}_n - \bar{p}_n)] / [\bar{x}_n (\bar{x}_n + \bar{p}_n \bar{y}_n)] \\ & + [\bar{p}_n \bar{y}_n^2 (\bar{y}_w / \bar{y}_n - 1)] / [\bar{x}_n + \bar{p}_n \bar{y}_n] \end{aligned} \quad (21)$$

which can be reduced to the associated equation (11) when $\bar{y}_n = \bar{y}_w$.

It should be emphasized that both of the equations (18a) and (21) are strictly valid only when every backbone molecule in the respective system considered contains a large number of branches. In the system to which equation (21) applies, this situation is never really achieved by the nature of the branching mechanism assumed. It is likely, however, that both of the above mentioned equations are good approximations over a wide range of \bar{p}_n values.

THE RATIO \bar{Z}_w / \bar{Z}_n

The weight-to-number average quotient \bar{Z}_w / \bar{Z}_n , as given by the general equations (3) and (5), can be shown always to equal or exceed the corresponding ratio \bar{x}_w / \bar{x}_n for the constituent backbone molecules. From the general relationship

$$\sum_i n_i (A_i - \bar{A}_n)^2 = \sum_i n_i A_i^2 - \bar{A}_n^2 \sum_i n_i \geq 0 \quad (22)$$

where the A_i are arbitrary quantities and $\bar{A}_n = (\sum n_i A_i) / \sum n_i$, it follows that for molecules of backbone length x_i in the final branched polymer mixture we have the inequality

$$\sum_s n_{i,s} \cdot s^2 \geq (\sum_s n_{i,s} \cdot s / \sum_s n_{i,s})^2 \cdot \sum_s n_{i,s} \quad (23)$$

The quantity in parentheses in the above equation is the number average branch segment content of backbone molecules of length x_i , $(x_i \bar{p}_n \bar{y}_n / \bar{x}_n)$. Substitution and summation over all values of i yields

$$\sum_i \sum_s n_{i,s} \cdot s^2 = \bar{S}_w \sum_i m_i y_i \geq (\bar{p}_n \bar{y}_n / \bar{x}_n)^2 \bar{x}_w \sum_i n_i x_i \quad (24)$$

from which we deduce

$$\bar{S}_w \geq \bar{x}_w \bar{p}_n \bar{y}_n / \bar{x}_n \quad (25)$$

Combination of equations (3), (5) and (25) shows

$$\bar{Z}_w / \bar{Z}_n \geq \bar{x}_w / \bar{x}_n \quad (26)$$

the equality applying when the total number of branch segments attached to each molecule is in proportion to the number of backbone units.

It is clear from the result of equation (26) that molecular weight homogeneity (as expressed by the weight-to-number average ratio) of branched polymer mixtures of the type considered here is enhanced by minimizing the original ratio of backbone molecular weights \bar{x}_w / \bar{x}_n .

The effect of branch chain polydispersity on the ratio \bar{Z}_w / \bar{Z}_n for high degrees of branching may be analysed from the results of the preceding section. For random comb molecules, division of equation (21) by equation (20) yields

$$\bar{Z}_w / \bar{Z}_n = \bar{x}_w / \bar{x}_n + \bar{p}_n \bar{y}_n^2 (\bar{x}_n - \bar{p}_n) / \bar{x}_n (\bar{x}_n + \bar{p}_n \bar{y}_n)^2 + \bar{p}_n \bar{y}_n^2 (\bar{y}_w / \bar{y}_n - 1) / (\bar{x}_n + \bar{p}_n \bar{y}_n)^2 \quad (27)$$

We note that at equal values of the ratios \bar{x}_w / \bar{x}_n and \bar{y}_w / \bar{y}_n , the contribution of the last term in the above equation, at most $(1/\bar{p}_n)(\bar{y}_w/\bar{y}_n - 1)$, is always substantially less than the contribution of \bar{x}_w/\bar{x}_n . Thus, as anticipated, variations in the lengths of attached branches tend to compensate, rendering the effect of side chain heterogeneity on the value of \bar{Z}_w/\bar{Z}_n almost inconsequential in many cases. It is likely that this subdued effect of branch chain polydispersity remains operative down to moderate degrees of branching.

The effect of the parameter \bar{p}_n on the ratio \bar{Z}_w/\bar{Z}_n may be investigated for the case of random comb molecules containing branches of constant length by means of the equations (10) and (11). The weight-to-number average ratio for such a mixture is

$$\bar{Z}_w / \bar{Z}_n = \bar{x}_w / \bar{x}_n + \bar{p}_n y^2 (\bar{x}_n - \bar{p}_n) / \bar{x}_n (\bar{x}_n + \bar{p}_n y)^2 \quad (28)$$

which can be shown to exhibit a maximum when

$$\bar{p}_n |_{\max.} = \bar{x}_n / (2 + y) \simeq \bar{x}_n / y \quad (29)$$

for which

$$\bar{Z}_w / \bar{Z}_n \simeq \bar{x}_w / \bar{x}_n + y / 4\bar{x}_n \quad (30)$$

Thus for random comb molecules of constant branch length, molecular weight heterogeneity is minimized by selection of \bar{p}_n values either much less or much greater than \bar{x}_n / y . In any event, we deduce from equations (26) and (30) that for any given \bar{x}_n and y , \bar{Z}_w / \bar{Z}_n for mixtures of these branched polymers lies within the limits

$$\bar{x}_w / \bar{x}_n \leq \bar{Z}_w / \bar{Z}_n \leq \bar{x}_w / \bar{x}_n + y / 4\bar{x}_n \quad (31)$$

A similar calculation for random comb molecules of arbitrary branch distribution [equation (21)] yields for the analog of equation (29)

$$p_n |_{\max} = \bar{x}_n / (\bar{y}_n + 2\bar{y}_n / \bar{y}_w) \simeq \bar{x}_n / \bar{y}_n \quad (32)$$

For these molecules we deduce

$$\bar{x}_w / \bar{x}_n \leq \bar{Z}_w / \bar{Z}_n \leq \bar{x}_w / \bar{x}_n + \bar{y}_w / 4\bar{x}_n \quad (33)$$

In summary, the ratio \bar{Z}_w / \bar{Z}_n , and hence in rough measure the molecular weight polydispersity, of random comb branched molecules, each of which contains at least a moderate number of branches, depends primarily upon the value of the ratio \bar{x}_w / \bar{x}_n . To a lesser extent, branched molecule heterogeneity also depends upon the heterogeneity of the constituent side chains and the average number of these attached.

APPENDIX

Expressions for the weight-to-number average ratio \bar{Z}_w / \bar{Z}_n for the particular comb molecules treated and for other structures derivable from them are summarized in tabular form below.

Definitions: regular comb molecules, a collection of backbone chains of arbitrary lengths to which branches of any lengths are attached by one end in uniform sequence such that the number of backbone units separating adjacent branch points in each molecule is constant; *random comb molecules*, a collection of backbone molecules of arbitrary lengths to which a specified total number of branches of arbitrary lengths are attached in random locations along the backbone chains, multiple occupancy of backbone segments being excluded; *regular star molecules*, a collection of star molecules each of which consists of the same number of constituent linear chains, not necessarily common in length; *random star molecules*, a collection of star molecules formed by the random placement of a specified total number of linear chains on to a specified number of common junction points, each of which procures at least one linear chain.

BRANCHED POLYMERS—I

Table 1

Structure	\bar{Z}_w/\bar{Z}_n
<u>Regular comb</u>	
(1) Constant x, y	1
(2) Arbitrary x , constant y	\bar{x}_w/\bar{x}_n
(3) Arbitrary x, y	$\bar{x}_w/\bar{x}_n + \bar{p}_n \bar{y}_n^2 (\bar{y}_w/\bar{y}_n - 1)/(\bar{x}_n + \bar{p}_n \bar{y}_n)^2;$ $\bar{p}_n \gg 1$
<u>Random comb</u>	
(1) Constant x, y	$1 + \bar{p}_n y^2 (x - \bar{p}_n)/[x(x + \bar{p}_n y_n)^2]$
(2) Arbitrary x , constant y	$\bar{x}_w/\bar{x}_n + \bar{p}_n y^2 (\bar{x}_n - \bar{p}_n)/[\bar{x}_n (\bar{x}_n + \bar{p}_n y)^2]$
(3) Arbitrary x, y	$\bar{x}_w/\bar{x}_n + \bar{p}_n \bar{y}_n^2 (\bar{x}_n - \bar{p}_n)/[\bar{x}_n (\bar{x}_n + \bar{p}_n \bar{y}_n)^2]$ $+ \bar{p}_n \bar{y}_n^2 (\bar{y}_w/\bar{y}_n - 1)/(\bar{x}_n + \bar{p}_n \bar{y}_n)^2; \quad \bar{p}_n \gg 1$
<u>Regular star</u>	
(1) Constant y	1
(2) Arbitrary y	$1 + (1/p) (\bar{y}_w/\bar{y}_n - 1); \quad p \gg 1$
<u>Random star</u>	
(1) Constant y	$1 + 1/\bar{p}_n; \quad \bar{p}_n > 1$
(2) Arbitrary y	$1 + \bar{y}_w/\bar{y}_n \bar{p}_n; \quad \bar{p}_n \gg 1$

This work has been supported in part by the Office of Naval Research.

Mellon Institute,
Pittsburgh, Pa

(Received February 1961)

REFERENCES

- ¹ THURMOND, C. D. and ZIMM, B. H. *J. Polym. Sci.* 1952, **8**, 447
- ² FLORY, P. J. *Ann. N.Y. Acad. Sci.* 1953, **57**, 327
- ³ ZIMM, B. H. *Ann. N.Y. Acad. Sci.* 1953, **57**, 332
- ⁴ JONES, M. H. *et al. J. Colloid Sci.* 1956, **11**, 508
- ⁵ MELVILLE, H. W., PEAKER, F. W. and VALE, R. L. *J. Polym. Sci.* 1958, **30**, 29
- ⁶ BERRY, G. C. *Thesis*. University of Michigan, Ann Arbor, Michigan, U.S.A. 1960
- ⁷ WENGER, F. *Tech. Rep. No. 4*, Office of Naval Research, Task No. NR 356-407, March 1960 (to be published)
- ⁸ FLORY, P. J. and SCHAEFGEN, J. R. *J. Amer. chem. Soc.* 1948, **70**, 2709

Branched Polymers. II— Dimensions in Non-interacting Media

T. A. OROFINO

Theoretical expressions for the mean square radii of some random flight 'comb' type branched molecules are derived. The structures considered consist of linear backbone chains to which linear side chains are attached by one end at various positions along the backbone. Expressions for the (light scattering) z-average radii of some mixtures of star and comb molecules likely to be obtained in the syntheses of these materials are also presented.

IN THE preceding paper, expressions for the average molecular weights and molecular weight distributions of a particular class of branched polymers, termed 'comb molecules', were presented. It is the purpose of the present communication to derive expressions for the mean square radii of comb molecules obeying random flight statistics. The particular structures treated correspond, in part, to those examined in Part I. The present selection of specific branched systems encompassed in the general category of 'comb molecules', as in the previous instance, has been made on the basis of the practicality of synthesis of such materials, their importance in systematic studies of branching and the relative ease with which they may be treated theoretically.

The expressions derived here, applicable to various distinct branched structures and to mixtures of branched molecules, should find use in studies of the Θ -point dimensions of such materials, as obtained for example from intrinsic viscosity or light scattering investigations.

RADI OF GYRATION OF SPECIFIC BRANCHED MOLECULE STRUCTURES

The mean square radius \bar{s}^2 of any polymer molecule may be defined

$$\bar{s}^2 = \langle (1/n) \sum_{i=1}^n \mathbf{s}_i^2 \rangle \quad (1)$$

where \mathbf{s}_i is the vector distance from the centre of mass to the i th segment of the chain in one particular conformation of the molecule and n is the total number of segments. The angular brackets denote a linear average over all possible conformations of the molecular chain.

The computation of the mean square radius of any polymeric structure whose constituent elements obey random flight statistics (which we denote by a subscript zero on pertinent quantities) may often be simplified through application of the Kramers relationship¹

$$\bar{s}_0^2 = (b/n)^2 \sum j(n-j); \quad n \gg 1 \quad (2)$$

where b is the length of one freely jointed chain element. The summation is extended over all possible divisions of the molecule into two parts, one containing j and the other $n-j$ segments.

Either of the equations (1) or (2) yields for long chain linear polymers the well-known random flight result*

$$\overline{s_0^2} = nb^2/6; \quad n \gg 1 \quad (3)$$

The particularly convenient equation (2) will be employed as an operational definition of the mean square radius in subsequent calculations for various branched structures.

(1) *Star molecules*

Expressions for the random flight dimensions of star molecules (and other branched polymer structures) were presented more than ten years ago in a pioneer paper by Zimm and Stockmayer^{3, 4}. For the sake of continuity, however, we shall derive equivalent relationships for this type of branched structure which, in our arbitrary system of classification, may be considered as a special case of the more general comb molecules.

Application of equation (2) to a star molecule consisting of p linear chains, each containing y units, yields

$$\overline{s_0^2} = [(3p-2)/6p] b^2 y = [(3p-2)/p] \overline{s_{0,u}^2} \quad (4)$$

$$y \gg 1$$

where $\overline{s_{0,u}^2} = yb^2/6$ is the mean square radius of one isolated linear chain of y units.

For a star molecule consisting of p branches of lengths y_1, y_2, \dots, y_p units, application of equation (2) yields

$$\overline{s_0^2} = b^2 \overline{y}_w \left(\frac{1}{2} - \frac{1}{3} \overline{y}_z / p \overline{y}_n \right) \quad (5)$$

$$y_i \gg 1$$

where

$$\overline{y}_n = (1/p) \sum_{i=1}^p y_i \quad \overline{y}_w = \left(\sum_{i=1}^p y_i^2 \right) / \left(\sum_{i=1}^p y_i \right)$$

and

$$\overline{y}_z = \left(\sum_{i=1}^p y_i^3 \right) / \left(\sum_{i=1}^p y_i^2 \right)$$

are the number weight and z -average lengths, respectively, of the collection of p linear chains constituting the branched molecule.

*The form of the relationship (3) is applicable to real polymer chains in media where the *net* segment-solvent interaction is nil (Θ -solvent), even though the chemical repeating units are not freely jointed. It is merely necessary to redefine n and b in terms of the number of Kuhn statistical elements². For convenience, we shall assume throughout that linear components of the branched structures treated are chemically identical and that 'segments' referred to are always freely jointed.

(2) *Regular comb molecules*

The relationship in equation (2) may be applied to regular comb molecules, each consisting of a linear backbone chain of x units to which p linear chains of uniform length y units are attached at regular intervals to form the repeating unit

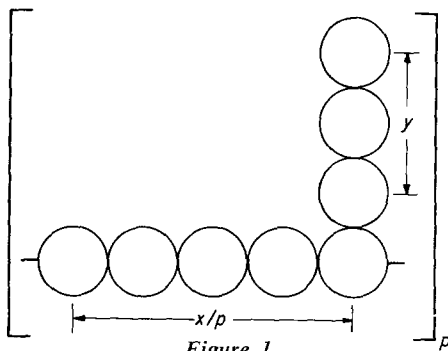


Figure 1

The mean square radius so formulated is

$$\overline{s_0^2} = (b/Z)^2 \left\{ \sum_{i=0}^{p-1} \sum_{j=0}^{x/p-1} [j(x/p+y) + j] [Z - i(x/p+y) - j] + p \sum_{j=0}^y j(Z-j) \right\} \quad (8)$$

where $Z = x + py$ is the total number of segments in the molecule. For x and y large, equation (8) may be simplified to

$$\overline{s_0^2} = \overline{s_{0,x}^2} (1 + N_y/p^2) + \overline{s_{0,y}^2} (3 - 2/p) N_y \quad (8a)$$

$$x, y \gg 1; \quad p \geq 1$$

where the subscripts x and y on the symbol for mean square radius denote the values of this quantity for the denuded linear backbone and one detached side chain, respectively, and $N_y = py/Z$ is the number fraction of branch units in the comb molecule.

We note that in the special cases $y=0$ and $y \gg x$, equation (8a) can be reduced to the expression for the linear backbone chain and to equation (4) for a p -functional star molecule, respectively.

Theoretical expressions for the mean square radii of similar regular comb molecules have been given by Wales, Marshall and Weissberg⁵, by Berry⁶, and, for small values of p , by Zimm and Stockmayer³.

In principle, these structures can be obtained from the complete coupling reaction of side chains with one species of repeating unit in a regularly alternating copolymer of uniform chain length.

Z-AVERAGE RADII OF GYRATION OF BRANCHED POLYMER MIXTURES

The z -average mean square radius, as obtained experimentally from light scattering measurements, is defined for any collection of polymer molecules by the relation

$$\langle \overline{s_0^2} \rangle_z = (\sum n_i Z_i^2 \overline{s_i^2}) / (\sum n_i Z_i^2) \quad (9)$$

where n_i is the number of molecules containing Z_i segments and possessing mean square radius \bar{s}_i^2 . Expressions for $\langle s_0^2 \rangle_z$ pertaining to some branched polymer mixtures of interest are presented below.

(1) *Random star mixtures*

We consider a collection of random star molecules (see Part I) for which the branch length y is fixed. The mean square radius of a member of the mixture containing p branch chains (and hence, degree of polymerization py) is given by equation (4). If the number of branches per molecule is randomly distributed, with a mean value \bar{p}_n , application of equation (9) yields

$$\langle s_0^2 \rangle_z = (yb^2/6) [3 - 2/(1 + \bar{p}_n)] \quad (10)$$

$$y \gg 1$$

(2) *Regular comb mixtures*

A collection of regular comb molecules for which the branch length y is fixed and for which the molecular weight distribution of the constituent backbone molecules is characterized by the three molecular weight averages \bar{x}_n , \bar{x}_w and $\bar{x}_z = (\sum n_i x_i^3) / (\sum n_i x_i^2)$, where n_i is the number of backbone chains containing x_i units, yields according to equations (9) and (8a)

$$\langle s_0^2 \rangle_z = (b^2/6) [\bar{x}_z + 3yN_y + (N_y \bar{x}_n / \bar{p}_n \bar{x}_w) (\bar{x}_n / \bar{p}_n - 2y)] \quad (11)$$

$$x, y \gg 1; \quad \bar{p}_n \neq 0$$

where $N_y = \bar{p}_n y / (\bar{x}_n + \bar{p}_n y)$ is the number fraction of segments belonging to branch chains in any given molecule.

We note that equation (11) can be reduced to equation (8a) when the backbone molecular weight averages are equal.

(3) *Random comb mixtures*

We consider here a distribution of backbone chains to which branches of fixed length y units are attached at random. Individual members of the final mixture will thus vary in backbone length, in the number of branches attached, and, for specified values of these two variables, in the particular arrangement of the branches along the backbone.

In a mixture of these molecules, the distribution of the number of branches attached to a backbone of specified length may be represented by the Bernoulli function used previously in the treatment of the molecular weight distribution for the same system (see Part I). The effect of variations in the positions of attached chains on the z -average mean square radius of the mixture may be taken into account by suitable averaging of the Kramers expression [equation (2)] over all species. The details of this calculation are given in Appendix A. The final result is

$$\langle s_0^2 \rangle_z = (b^2/6 \bar{Z}_w \bar{Z}_n \bar{x}_n) \{ \bar{Z}_n^2 \bar{x}_w \bar{x}_z + \bar{p}_n y^2 [3 \bar{x}_w \bar{Z}_n + y(\bar{x}_n - 3\bar{p}_n)] \} \quad (12)$$

where \bar{Z}_n and \bar{Z}_w are the number and weight average degrees of polymerization, respectively, of the final branched polymer mixture; in the preceding paper, these quantities are expressed in terms of the chain length averages of the component linear backbones and branches.

For the special case of backbone molecules homogeneous in chain length, equation (12) becomes

$$\langle \bar{s}_0^2 \rangle_z = (b^2/6\bar{Z}_w\bar{Z}_n)\{\bar{Z}_n(x\bar{Z}_n + 3\bar{p}_n y^2) + \bar{p}_n y^3(1 - 3\bar{p}_n/x)\} \quad (13)$$

Random comb mixtures of the type treated would be obtained, for example, in the complete or partial coupling reaction of homogeneous side chains with a collection of linear backbone molecules containing reactive sites randomly distributed among the backbone segments.

DISCUSSION AND CONCLUSIONS

In the preceding sections expressions for the mean square radii of a number of branched molecule structures and mixtures of structures are given. These relationships are applicable to materials which are likely to be obtained in syntheses designed to provide polymers for systematic studies of the effect of branching on molecular dimensions. With this ultimate utilization in mind, it may be desirable to examine briefly the foregoing relationships in regard to (1) the range of structural variables best suited for observations of the effects of branching and (2) the influence of molecular heterogeneity on the mean square radii of mixtures.

The dependence of \bar{s}_0^2 for regular comb molecules on the number of branches attached is shown in *Figure 2*, where values of the mean square radii, divided by $\bar{s}_{0,x}^2$ of the parent backbone molecule, are plotted versus $1/p$. The various curves are parametric in the branch-to-backbone chain length ratio $q = y/x$ and were constructed with the aid of equation (8a). The lowermost, corresponding to a zero y/x ratio, represents the linear molecule; as q increases, the successive curves exhibit increasing degrees of star molecule character. Thus, for example, the curve for $q=10$ may also be used to describe a star molecule ($x=1$) containing branches of length 10 units.

At fixed branch and backbone lengths, the mean square radii of regular comb and star molecules approach asymptotic limits with increasing p . These limiting values are easily computed from pertinent equations of preceding sections; for comb molecules, we find

$$\lim_{\substack{p \rightarrow x \\ x, y \gg 1}} (\bar{s}_0^2)_{\text{comb}} = (b^2/6)(x + 3y - 2y/x) \quad (14)$$

while for star structures

$$\lim_{p \rightarrow \infty} (\bar{s}_0^2)_{\text{star}} = \frac{1}{2}b^2y \quad (15)$$

From data used in the construction of the curves of *Figure 2*, one may deduce as a rough guide that for comb molecules this upper limit is essentially attained (within ca. 5 per cent) at p values of the order $25q^{-1/5}$; for star molecules, equation (15) is applicable when p is about fifteen or greater.

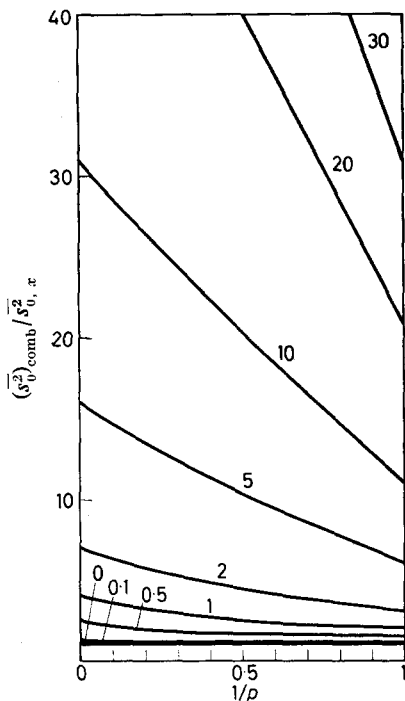


Figure 2—Plots of the ratio of \bar{s}_0^2 for regular comb molecules to \bar{s}_0^2 for the constituent linear backbones, versus $1/p$, for various values of the parameter $q=y/x$

The progressive addition of branch chains to a given linear backbone or star centre is thus seen to involve, initially, a substantial augmentation of the mean square radius of the resulting branched molecule; this effect diminishes as the number of branches attached increases, however, and eventually contributes insignificantly to \bar{s}_0^2 upon further addition of branch chains*. We may therefore conclude that in studies where the distinguish-

*The insensitivity of \bar{s}_0^2 to p for relatively large values of this parameter presents some interesting possibilities in regard to the controlled variation of molecular parameters in Θ -solvent solutions or in bulk polymers. An observable phenomenon in one of these media may, for example, be suspected to depend, to some degree independently, upon the polymer molecular weight M and upon either the molecular size, as characterized by \bar{s}_0^2 , or, the density of segments ρ within the domain of an isolated polymer coil. For a given random flight linear polymer, M , \bar{s}_0^2 and ρ are interrelated and cannot therefore be independently varied. In a series of comb or star molecules of moderately large and varying p values, however, polymers comprising a wide range of molecular weights, but differing insignificantly in mean square radii, could be made available for study. Likewise, systematic variations in \bar{s}_0^2 (or ρ) at constant molecular weight could be realized through alteration of comb or star structure subject to the condition that the total degree of polymerization should remain constant.

able effects of branch addition in such molecules are of interest, samples for which p varies from zero to about $25 q^{-1/5}$ (see above) would appear to be most suitable.

The effects of variations in x at fixed y and p/x (fixed branch spacing), and variations in y at fixed x and p on the mean square radii of regular structures more or less parallel those which would be observed for these linear components if detached from the branched molecule, i.e. constancy of the ratios $(\bar{s}_0^2)/x$ and $(\bar{s}_0^2)/y$ [see equation (3)], provided that the x or y components of the molecule, as the case may be, represent the major constituent of the branched structure. This is illustrated by the behaviour of the curves in *Figure 2*. In regard to variations in x at fixed y and p/x , we may compare the ordinate values of two curves, q_1 and q_2 , at abscissa values $1/p_1$ and $q_2/q_1 p_1$, respectively. This amounts to comparing the two ratios of mean square radius of the branched molecule to that of the backbone when x assumes two values at the same y and p/x . The two ratios are identical for the respective, isolated, backbone chains; they do not differ greatly for the branched molecules in the range where py is of the order of magnitude of x , or less, i.e. wherever the backbone constitutes the major portion of the branched molecule.

Variations in y at fixed x and p may be similarly analysed from *Figure 2*. At q values greater than unity, the approximate agreement at given p of the ordinate values for two curves q_1 and q_2 , divided by q_1 and q_2 , respectively, is in accord with the constancy of such ratios for the isolated branch chains.

An indication of the effect of heterogeneity in the number of branches attached to comb and star molecules may be obtained from the curves of *Figure 3*, where the z -average mean square radii of some random structures (x and y constant) divided by \bar{s}_0^2 for the corresponding regular structure of the same \bar{p}_n are plotted versus p . These values were calculated

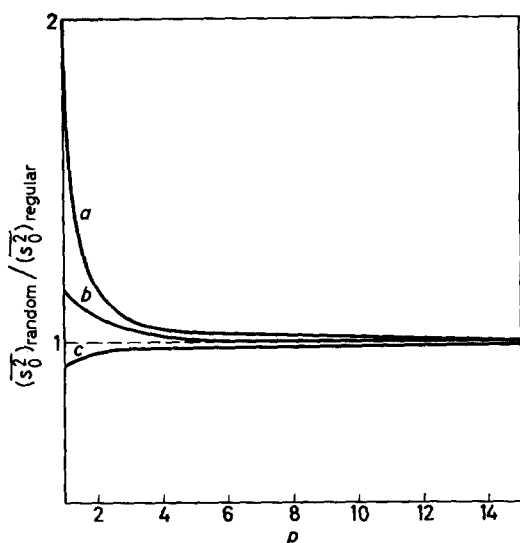


Figure 3—Plots of the ratio of \bar{s}_0^2 for random structures to \bar{s}_0^2 for the corresponding regular systems, versus p ($p_{\text{regular}} = \bar{p}_n, \text{random}$). Curve *a*, star molecules; *b*, comb molecules with uniform backbones $x=y=100$; *c*, comb molecules with uniform backbones, $x=100$, $y=10$

with the aid of equations (4), (8a), (10) and (13), together with pertinent molecular weight relationships from Part I. As would be expected, the effect of this type of heterogeneity becomes vanishingly small as p increases. In studies where p values of about five or greater are chosen for investigation, regular structures, presumably synthesized with greater difficulty, would appear to afford no important advantages in regard to elimination of the effects of this kind of heterogeneity. As mentioned previously, however, in connection with the asymptotic behaviour of \bar{s}_0^2 with increasing branch chain content, if the above mentioned range of p values is to be investigated, some thought should be given to selection of appropriate y/x ratios in order to render significant effects of the number of branches attached on the mean square radius of the branched molecule.

The effects of molecular weight heterogeneity in backbone and branch chain length are more difficult to assess in detail. From an analysis of the theoretical expressions for the z -average mean square radii of mixtures exhibiting such heterogeneity, however, it appears that the effects are similar to those which would be shown if the same heterogeneity were present in the corresponding linear components, particularly of course when the linear component considered constitutes the major portion of the branched chain.

Expressions for the mean square radii of gyration of the various branched structures considered are summarized in Appendix B. Here, these are expressed in terms of the dimensionless parameter g , the ratio of mean square radius of the branched molecule to that of a linear molecule of the same molecular weight³. In the case of mixtures, g is expressed in terms of the z -average mean square radius of the branched molecule and the z -average square radius of a mixture of linear molecules each of which has the same molecular weight as its counterpart in the branched sample.

APPENDIX A

THE z -AVERAGE MEAN SQUARE RADIUS FOR MIXTURES OF RANDOM COMB MOLECULES

We consider a collection of backbone molecules, with chain length distribution represented by the set $[n_i; x_i]$, to which branches have been attached at random positions. The z -average radius of the mixture is given by the right hand side of equation (9), the numerator of which is the sum over all species of the product of the square of the degree of polymerization and the mean square radius (averaged, for a given molecule, over all molecular conformations). For each member of the collection of branched molecules, this product, which we designate P_{ti} with the subscripts denoting the t th member of that portion of the sample whose members possess a common backbone length x_i units, may be expressed in accordance with equation (2) of the text

$$P_{ti} = b^2 \left[\sum_{j=1}^{x_i} K_{jti} + K_{yti} \right] \quad (16)$$

Here, K_{jti} is the Kramers product for the division of a selected molecule at backbone segment j , i.e. the product of the numbers of segments in the

two portions of the molecule resulting, and K_{yti} is the total Kramers product for all divisions along the branches of the molecule. The numerator of the defining equation (9) may now be expressed as the double sum of P_{ti} over all values of t and i . The members of the sum may be grouped into terms pertaining to branched molecules of common x_i and we may accordingly write

$$\begin{aligned} \langle \bar{s}_n^2 \rangle_z (\sum_i n_i \bar{Z}_i^2) &= \langle \bar{s}_0^2 \rangle_z \bar{Z}_w \bar{Z}_n (\sum_i n_i) = b^2 \sum_i \left\{ \sum_t \left[\sum_{j=1}^{x_i} K_{jti} + K_{yti} \right] \right\} \quad (17) \\ &= b^2 \left[\sum_i \sum_j n_i \bar{K}_{ji} + \sum_i n_i \bar{K}_{yi} \right] \end{aligned}$$

where \bar{K}_{ji} is the mean (number average) Kramers product for division of molecules of backbone length x_i at a given backbone segment j , averaged over all (n_i) species, and \bar{K}_{yi} is the analogous mean total product for divisions of the molecule at its branch segments. The mean quantities defined by the foregoing equations are easily evaluated.

We consider first the computation of \bar{K}_{ji} . If the average number of branches per molecule in the entire branched polymer mixture is \bar{p}_n , then the probability that a backbone segment selected at random is the origin of a branch chain is \bar{p}_n/\bar{x}_n . In a molecule of backbone length x_i severed at the j th backbone segment, the combined probability that one portion contains $r_1 \leq j$ and the other $r_2 \leq x_i - j$ branch chains is

$$P_i(r_1, r_2, j) = \binom{j}{r_1} \binom{x_i - j}{r_2} (\bar{p}_n/\bar{x}_n)^{r_1+r_2} (1 - \bar{p}_n/\bar{x}_n)^{x_i - r_1 - r_2} \quad (18)$$

$j = 1, 2, 3, \dots, x_i$

The number average Kramers product for separations at backbone segment j is thus

$$\begin{aligned} \bar{K}_{ji} &= \sum_{r_1=0}^j \sum_{r_2=0}^{x_i-j} P_i(r_1, r_2, j) \cdot (j + yr_1)(x_i - j + r_2y) \quad (19) \\ &= (\bar{Z}_n/\bar{x}_n)^2 (jx_i - j^2) \end{aligned}$$

We consider next the evaluation of the quantity \bar{K}_{yi} . In an x_i molecule containing p branch chains, the total Kramers product for divisions along the branch segments is

$$K_{yi} = (\rho y^2/6) (3Z_i - 2y) \quad (20)$$

where $Z_i = x_i + py$. The probability distribution of the number of branches attached to x_i molecules is given in Part I. That expression, in conjunction with equation (20), yields for the desired mean product

$$\bar{K}_{yi} = (y^2 \bar{p}_n x_i / 6 \bar{x}_n) [3x_i + y + (3\bar{p}_n y / \bar{x}_n)(x_i - 1)] \quad (21)$$

Insertion of equations (19) and (21) into equation (17) and performance of the required summation yields after simplification

$$\langle \bar{s}_0^2 \rangle_z = (b^2 / 6 \bar{Z}_w \bar{Z}_n \bar{x}_n) \{ \bar{Z}_n \bar{x}_w \bar{x}_z + \bar{p}_n y^2 [3\bar{x}_w \bar{Z}_n + y(\bar{x}_n - 3\bar{p}_n)] \} \quad (22)$$

the result given in equation (12) of the text.

APPENDIX B

THE RATIO g FOR VARIOUS BRANCHED STRUCTURES AND MIXTURES

Branched molecule	g
Regular structures	
(1) Star, y constant	$3/p - 2/p^2$
(2) Star, y_i arbitrary	$3\bar{y}_w/p\bar{y}_n - 2\bar{y}_z/p^2\bar{y}_n^2$
(3) Regular comb	$1 - N_y + N_y/p^2 + 3N_y^2/p - 3N_y^3/p^2$
Branched molecules	g
Mixtures	
(1) Random star, y constant	$(3\bar{p}_n + 1)/(\bar{p}_n^2 + 3\bar{p}_n + 1)$
(2) Regular comb, y constant, x_i arbitrary	$\bar{x}_n/\bar{x}_z [\bar{x}_z N_y/\bar{p}_n y + 3N_y^2/\bar{p}_n + (\bar{x}_n N_y^2/\bar{x}_w \bar{p}_n^2 y) (\bar{x}_n/\bar{p}_n - 2y)]$
(3) Random comb, x, y constant	$\frac{\bar{Z}_n (x\bar{Z}_n + 3\bar{p}_n y^2) + \bar{p}_n y^3 (1 - 3\bar{p}_n/x)}{\bar{Z}_n^3 + 3\bar{Z}_n \bar{p}_n y^2 (1 - \bar{p}_n/x) + (\bar{p}_n y^3/x^2) (x - \bar{p}_n) (x - 2\bar{p}_n)}$
(4) Random comb, y constant, x_i variable	$\frac{\bar{Z}_n^2 \bar{x}_w \bar{x}_z + \bar{p}_n y^2 [3\bar{x}_w \bar{Z}_n + y (\bar{x}_n - 3\bar{p}_n)]}{\bar{x}_z \bar{x}_w \bar{Z}_n^3/\bar{x}_n + 3\bar{x}_w \bar{Z}_n \bar{p}_n y^2 (1 - \bar{p}_n/\bar{x}_n) + \bar{p}_n y^3 (1 - \bar{p}_n/\bar{x}_n) (\bar{x}_n - 2\bar{p}_n)}$

This work has been supported in part by the Office of Naval Research.

Mellon Institute,
Pittsburgh, Pa

(Received February 1961)

REFERENCES

- ¹ KRAMERS, H. A. *J. chem. Phys.* 1946, **14**, 415
- ² KUHN, W. *Kolloidzshr.* 1939, **87**, 3
- ³ ZIMM, B. H. and STOCKMAYER, W. H. *J. chem. Phys.* 1949, **17**, 1301
- ⁴ STOCKMAYER, W. H. and FIXMAN, M. *Ann. N.Y. Acad. Sci.* 1953, **57**, 334
- ⁵ WALES, M., MARSHALL, P. A. and WEISSBERG, S. G. *J. Polym. Sci.* 1953, **10**, 229
- ⁶ BERRY, G. C. *Thesis*. University of Michigan, Ann Arbor, Michigan, U.S.A. 1960

The Crystallization of Polyethylene Terephthalate by Organic Liquids

W. R. MOORE and R. P. SHELDON

The development of crystallinity in essentially amorphous polyethylene terephthalate film following immersion in a range of organic liquids at 25°C has been studied. The rate of development of crystallinity varies markedly with the liquid and although molecular size of the liquid may be a contributory factor it is not the only one. Both the equilibrium degree of crystallinity and swelling of the film vary with the liquid and in a similar manner and it would seem that polarity, type and solubility parameter of the liquid are important factors governing both equilibrium crystallinity and swelling. It is suggested that solvation of the polymer occurs and that interaction of solvated polymer and liquid leads to conditions favourable to crystallization.

THE ability of some organic liquids to induce crystallization of a potentially crystallizable but otherwise essentially amorphous polymer has been known for some time but little quantitative information is available. Spence¹, using films of cellulose triacetate, found that the better the solvent the sharper was the X-ray diagram, suggesting a greater degree of crystallinity. Baker *et al.*² drew similar conclusions from work on cellulose triacetate and tributyrate. Kolb and Izard³ showed that some organic and inorganic liquids would induce crystallization of polyethylene terephthalate at temperatures well below those at which rates of crystallization are appreciable in the absence of liquid. A recent study⁴ of the effects of a homologous series of methyl ketones on the crystallization of polyethylene terephthalate suggested that, if allowance were made for any absorbed liquid, apparent densities could be corrected to true densities which were independent of the amount of liquid absorbed. The rate of crystallization appeared to decrease with increasing size of the ketone. There was some evidence that not only the rate of crystallization but also the equilibrium degree of crystallinity might depend on the nature of the liquid. In a further study of factors affecting the crystallization of polyethylene terephthalate in liquids this work has been extended to cover a range of organic liquids of differing chemical types and properties.

EXPERIMENTAL

The polyethylene terephthalate used was essentially amorphous film, 0.008 in. in thickness. Preliminary measurements showed it to have a density of 1.340 g/cm³ at 25°C, corresponding to a degree of crystallinity of 4.2 per cent. The following liquids were used: hexane, carbon tetrachloride, ethanol, *n*-butanol, benzyl alcohol, acrylonitrile, dioxan, ethyl formate, *m*-cresol, aniline, nitromethane, nitroethane, acetic acid, dimethyl phthalate, benzene, toluene, nonyl methyl ketone, *n*-amyl methyl ketone, ethyl methyl ketone and acetone. The best available grades were further purified, dried by appropriate agents and fractionally distilled before use.

Known weights, approximately 0.07 g, of polymer were immersed in each of the liquids at $25^\circ \pm 0.01^\circ\text{C}$ for varying periods of time. Surface liquid was then removed by lightly blotting with filter paper and the sample stored in an evacuated vacuum desiccator for at least 24 hours. It was then weighed, all weighings being made with a semi-micro balance reading to 0.00001 g. With less volatile liquids such as dimethyl phthalate a surface washing with ethanol preceded blotting. After reweighing the density of the sample was determined by immersion in 10 cm³ of carbon tetrachloride at $25^\circ \pm 0.01^\circ\text{C}$ and addition, with agitation, of dry ethanol from a micro burette until the sample neither rose nor sank in the mixture. The density of the sample was then obtained from a graph showing the variation of density with composition of the carbon tetrachloride-ethanol mixtures. Preliminary experiments showed that such mixtures did not induce crystallization, at least within 24 hours. The method was quite reproducible and densities could be estimated to 0.001. With *m*-cresol some solution of the polymer occurred and dissolved polymer was precipitated by addition of ethanol and recovered by centrifuging and drying in a vacuum oven at 50°C , the weight of recovered material being used to correct the apparent density of the undissolved material to the true density. The influence of this procedure on the results will be discussed later.

Swelling of the polymer in the different liquids was obtained from the weight of liquid absorbed when density had reached its equilibrium value and expressed as a percentage of the original volume of the polymer. With volatile liquids such as acetone and benzene weighings were made as a function of time and followed by extrapolation to zero time to obtain the true weight.

As pointed out previously⁴ some liquid is retained by the polymer after evacuation and the density d_a obtained by the flotation method is not that of the polymer d_p but of the polymer plus retained liquid.

$$d_a = (m_p + m_l) / (v_p + v_l)$$

where m_p and v_p are the mass and volume of the polymer and m_l and v_l those of the liquid. Assuming, from previous work⁴ and direct measurements of swelling in a density bottle, that the liquid is uncompressed, then

$$d_a = (m_p + m_l) / (m_p/d_p + m_l/d_l)$$

from which the density of the polymer d_p is given by

$$d_p = d_a / [(m_l/m_p) (1 - d_a/d_l) + 1]$$

RESULTS

Plots of density against time of immersion are shown in *Figure 1*. An equilibrium density is reached with each liquid and these densities are collected in *Table I* together with corresponding percentage crystallinities x_c obtained from

$$x_c = 100 (d_p - d_A) / (d_c - d_A)$$

where d_A is the density of the completely amorphous polymer, taken⁵ to be 1.335 and d_c that of the completely crystalline, taken⁶ as 1.455. Values for

THE CRYSTALLIZATION OF POLYETHYLENE TEREPHTHALATE

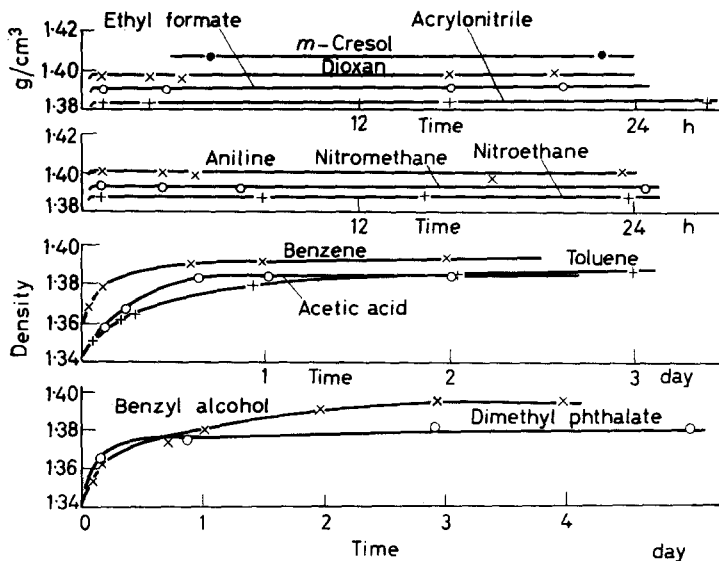


Figure 1—Rate of crystallization of polyethylene terephthalate in various liquid media at 25°C

Table 1

Equilibrium values of density, swelling and degree of crystallinity

Liquid	$\delta_{25^{\circ}}$ (cal/cm ³) [†]	Density (g/cc)	Swelling (% vol.)	Crystallinity (% vol.)
Hexane	7.3	1.340	Nil	4.2
Nonyl methyl ketone	7.9	1.340	Nil	4.2
<i>n</i> -Amyl methyl ketone	8.45	1.358	6.3	19.2
Carbon tetrachloride	8.6	1.340	Nil	4.2
Toluene	8.9	1.381	14.7	38.1
Benzene	9.15	1.390	18.8	45.8
Ethyl methyl ketone	9.15	1.395	18.7	50.0
Ethyl formate	9.40	1.390	20.0	45.8
Acetone	9.75	1.405	30.8	58.3
Dioxan	10.05	1.396	21.0	50.8
Acrylonitrile	10.5	1.384	12.6	40.8
Dimethyl phthalate	10.6	1.385	9.9	41.7
Nitroethane	11.1	1.389	17.7	45.0
Benzyl alcohol	11.3	1.396	22.3	50.8
<i>n</i> -Butanol	11.4	1.340	Nil	4.2
Aniline	11.5	1.400	36.8	54.2
<i>m</i> -Cresol	11.9	1.41 ₃	125	63
Nitromethane	12.6	1.394	14.3	49.2
Acetic acid	12.9	1.390	13.1	45.8
Ethanol	13.2	1.340	Nil	4.2

the ketones are somewhat lower than those previously reported⁴ and the reason for this is not clear. As mentioned previously, some polymer, presumably of low molecular weight, was soluble in *m*-cresol. By taking into account the weights of precipitated and undissolved polymer and also a presumably proportional loss of *m*-cresol from the sample by extraction with ethanol, corrections were applied to the density and swelling of the undissolved polymer. Since the soluble fraction may behave differently from the insoluble and very low molecular weight polymer may not be precipitated by ethanol the corrected value given in *Table 1* should be regarded as approximate. The development of crystallinity was always accompanied by increasing opacity of the film and, when absorbed solvent was removed, by increased brittleness. The latter effect has been previously noted⁷ after prolonged heating in an aqueous dye bath at 100°C. Values of equilibrium swelling are also given in *Table 1*.

DISCUSSION

Figure 1 shows that the rate of increase of density and hence of crystallinity varies markedly with the liquid. In some cases crystallization is rapid while in others it occurs at a rate convenient for measurement. *Figure 1* also shows that although molecular size may be a factor affecting the rate of crystallization it is not the only one. Dioxan, ethyl formate, acrylonitrile, *m*-cresol, aniline, nitromethane and nitroethane induce much more rapid crystallization than benzene, toluene, acetic acid, benzyl alcohol and dimethyl phthalate. Kinetic studies of this induced crystallization will be discussed in a later communication and are not further considered here, but it may be noted that the rate of disappearance of available amorphous content at any given time seems to follow a first order equation.

The equilibrium values of density and crystallinity also vary with the liquid. The non-polar hexane and carbon tetrachloride do not induce crystallinity and neither do ethanol and *n*-butanol. The polarizable aromatic hydrocarbons benzene and toluene do so, however, and so does benzyl alcohol. Other liquids inducing crystallinity are polar but there seems to be no obvious relationship between the equilibrium density of the polymer and the polarity of the liquid. Results for acetone and *n*-amyl methyl ketone and for nitromethane and nitroethane suggest that molecular size may be a factor with liquids of the same type but this is not general.

Table 1 shows that, in general, the greater the equilibrium density the greater the swelling of the polymer although density and swelling are not linearly related. Swelling may be regarded as a measure of the interaction between polymer and liquid and the development of crystallinity may depend on such interaction. *Figures 2* and *3* show equilibrium density and swelling respectively as functions of the solubility parameter δ of the liquid.

$$\delta = [(L_e - RT)/V]^{\dagger}$$

where L_e is the molar latent heat of vaporization of the liquid and V is molar volume, both at the absolute temperature T . Values of δ , which are given in *Table 1*, were taken from published values^{8,9} or calculated using values of L_e obtained by use of the Hildebrand rule¹⁰. The difference

between the solubility parameters of a liquid and a not too polar amorphous polymer can be related to the heat change in their mixing and the interaction of polymer and liquid will therefore depend, in part, on the solubility parameter of the latter.

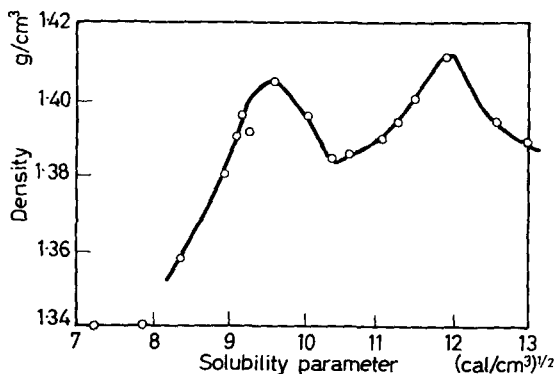


Figure 2 — Equilibrium density as a function of solubility parameter of liquid

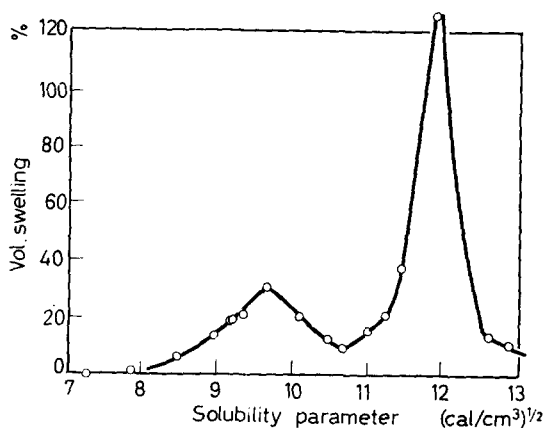


Figure 3—Equilibrium swelling as a function of solubility parameter of liquid

Figure 2 shows two maxima at δ values of approximately 9.7 and 12.0 and similar maxima are seen in Figure 3. The first maximum is associated with liquids such as ketones and esters which may be regarded as basic in the Lewis sense. Benzene and toluene, which are associated with this region of the plots, can also be regarded as basic¹¹. The second maximum is associated with liquids of acidic type such as *m*-cresol, acetic acid and nitromethane. The existence of two maxima may be a consequence of the presence of basic carbonyl groups in the polymer and acidic hydrogen atoms in CH_2 groups adjacent to oxygen atoms. Giles *et al.*¹² have suggested that ester groups in polyethylene terephthalate may act as proton donors. Liquids containing acidic groups should solvate basic polymer groups and those containing basic groups should solvate acidic ones. Alternatively, dipolar attraction may lead to solvation by both types of liquid.

Swelling will occur in liquids whose solubility parameters do not differ too greatly from that of the solvated polymer and be a maximum when these solubility parameters are equal or nearly so. The solubility parameter of the solvated polymer will presumably vary with the solvating liquid but variations for the polymer solvated by liquids of similar type may not be large. It has been pointed out that in cases of polymers containing both acidic and basic groups there will be two ranges of solubility parameter within which swelling or solution can occur, corresponding to the polymer solvated by basic and acidic liquids respectively¹³. Behaviour of this type has been observed with secondary cellulose acetate¹⁴. Dependence of induced crystallinity on solubility parameter of liquid has also been noted for crystallizable polymethyl methacrylate¹⁵.

This correlation of equilibrium density and swelling with solubility parameter of liquid should perhaps be regarded as an approximation and other factors may be operative. A number of the liquids used—ethanol, butanol, benzyl alcohol, *m*-cresol and acetic acid—are known to be associated. Latent heats of vaporization will often include energy required to overcome forces causing association and it is perhaps doubtful to what extent solubility parameters obtained from such latent heats can be related to forces between associated molecules in the liquid state. Association might account for the lack of swelling and density increase in ethanol and butanol. The marked effect of benzyl alcohol, with almost the same solubility parameter as butanol, may be due to the influence of the phenyl group. The points for aniline in *Figures 2* and *3* fall amongst those for acidic liquids although aniline is generally regarded as basic. There is some evidence, however, that the hydrogen atoms of the NH₂ group can take part in hydrogen bonding to basic carbonyl groups¹⁶.

Reasons for the correlation between swelling and development of crystallinity are not entirely clear. It is possible that the solvated polymer imbibes the solvating liquid in swelling and that the imbibed liquid acts as a plasticizer or molecular lubricant, reducing internal stresses and permitting movement of the polymer chains at the temperature of the experiments and the adoption of more favourable conditions for the development of crystallinity. Here it may be relevant to note that the amount of dimethyl phthalate absorbed at equilibrium reduced the glass temperature of the polymer, determined by a dilatometric method, from 67° to 62°C. The value of 62° refers, of course, to the polymer after crystallization. The glass temperature of the amorphous polymer containing dimethyl phthalate may be much lower.

If this picture of the action of liquids is correct it follows that the actual degree of crystallinity attainable may also depend on such aspects of the nature of the polymer as its molecular weight and previous thermal history. This may be supported by the fact that although aniline and *m*-cresol both cause high degrees of swelling the equilibrium level of crystallinity is not very different from that resulting from the use of other liquids, such as acetone, which cause smaller degrees of swelling.

We are grateful to Imperial Chemical Industries Ltd, Plastics Division, for the gift of polyethylene terephthalate film.

*Polymer Research Laboratories,
Department of Chemical Technology,
Institute of Technology, Bradford, Yorks.*

(Received March 1961)

REFERENCES

- ¹ SPENCE, J. J. *phys Chem.* 1941, **45**, 401
- ² BAKER, W. O., FULLER, C. S. and PAPE, N. R. *J. Amer. chem. Soc.* 1942, **64**, 776
- ³ KOLB, J. and IZARD, E. F. *J. appl. Phys.* 1949, **20**, 571
- ⁴ MOORE, W. R., RICHARDS, D. O. and SHELDON, R. P. *J. Text. Inst.* 1960, **51**, T438
- ⁵ THOMPSON, A. B. and WOODS, D. W. *Nature, Lond.* 1955, **176**, 78
- ⁶ BUNN, C. W. in *Fibres from Synthetic Polymers* edited by R. HILL. Elsevier: Amsterdam, 1953
- ⁷ SHELDON, R. P. Unpublished Results
- ⁸ MOORE, W. R., EPSTEIN, J. A., BROWN, A. M. and TIDSWELL, B. M. *J. Polym. Sci.* 1957, **23**, 23
- ⁹ BURRELL, H. *Interchemical Review*, 1955, Spring, 3
- ¹⁰ HILDEBRAND, J. L. and SCOTT, R. L. *Solubility of Non-Electrolytes*, 3rd ed. Reinhold: New York, 1950
- ¹¹ BARKER, J. A. and SMITH, F. J. *chem. Phys.* 1954, **22**, 375
- ¹² ALLINGHAM, M. M., GILES, C. H. and NEUSTADTER, E. L. *Disc. Faraday Soc.* 1954, **16**, 92; ARSHID, F. M., GILES, C. H. and JAIN, S. K. *J. chem. Soc.* 1956, **260**, 1272
- ¹³ MOORE, W. R. *J. Soc. Dy. Col.* 1958, **74**, 500
- ¹⁴ MOORE, W. R. and RUSSELL, J. J. *Colloid Sci.* 1953, **8**, 243
- ¹⁵ Aus. Patent No. 36684
- ¹⁶ MOORE, W. R. and RUSSELL, J. J. *appl. Chem.* 1954, **4**, 369

A Study of Short Chain Branching in Hydrocarbon Polymers by the Irradiation Method. I—The Detection of Side Chains

D. A. BOYLE, W. SIMPSON and J. D. WALDRON

A large number of hydrocarbons of different structure have been irradiated and the gaseous products analysed. The major constituents of the paraffins formed are those corresponding in both carbon number and skeletal structure to the side chains in the hydrocarbon. In any given hydrocarbon, ethyl side chains are more easily detected by this technique than methyl side chains; n-butyl, propyl and methyl are approximately equal in ease of detection, and higher n-alkyl side chains become progressively more difficult to detect.

DUE TO the discovery of new methods of polymerization of olefinic monomers in recent years, polyethylene is now available with a wide range of physical properties, and there is much evidence to indicate that a major factor responsible for the variation in properties is the number and type of 'short' branches in the main polymer chain. The investigation of the nature of short chain branching is therefore of considerable importance. Present knowledge of the extent of short chain branching in these polymers rests largely on the evidence of infra-red spectroscopy; a knowledge of the total number of side groups and some information on their structure has been obtained¹.

An alternative approach to the problem of determining the structure of the branches was suggested by some preliminary work of Harlen *et al.*² who analysed the hydrocarbon products resulting from the high energy irradiation of polymethylenes containing branches of known lengths. Their results indicated that branches are effectively removed as complete units by high energy irradiation, and appear in the gaseous products as the corresponding paraffins.

The present report gives a more complete account of this work.

EXPERIMENTAL

Materials

The experiments were carried out on low molecular weight pure hydrocarbons of known structure and on hydrocarbon polymers. The polymers were prepared by methods chosen to give a preponderance of side chains of one type although the precise structures were not known unequivocally in some cases. These methods were (a) the polymerization of a diazoalkane or copolymerization of a diazoalkane with diazomethane³, and (b) the polymerization of an olefine or copolymerization of an olefin with ethylene using the low pressure catalytic processes of Ziegler or the Phillips Petroleum Company.

The sources and methods of preparation of the materials are shown in the appropriate tables of results.

Irradiation technique and analysis

Breakseal ampoules of approximately 10 ml capacity containing 0.1 g samples of material were evacuated for 16 h at 70°C to a residual pressure of 10^{-4} to 10^{-5} mm of mercury and then sealed off. (The pure hydrocarbons were evacuated at liquid nitrogen temperature.) The vacuum line consisted of a liquid nitrogen cold trap, oil diffusion pump and rotary pump. The ampoules were then irradiated at room temperature with electrons from a 4 MeV Orthotron⁴ at a dose rate of 1 Mrad per minute to a total dose of 100 Mrad. In the most recent experiments, groups of samples were irradiated simultaneously on a rotating stage to ensure equality of dose; all of the polymers examined in an attempt to establish a quantitative relationship between hydrocarbon yield and concentration of side chains were irradiated in this way (i.e. those summarized in *Table 5*). The pure hydrocarbons were irradiated stationary at 0°C. To aid liberation of the gases from the polymers the ampoules were maintained at 100°C for 30 minutes immediately prior to analysis. The breakseal was then broken and the gases admitted to the inlet system of a mass spectrometer while the ampoule was still hot. (The low molecular weight pure hydrocarbons were not heat-treated prior to analysis.) Usually about 1 ml of gas at n.t.p. was liberated. The products were analysed mass spectrometrically in the usual way, the instrument being a type M.S.2 made by Associated Electrical Industries (Manchester) Limited. Blank runs on un-irradiated polymers did not produce any detectable hydrocarbon, indicating that the polymers were unaffected by the heat treatment.

It is difficult to give a value for the accuracy of the analyses, as this varies with the hydrocarbon and the particular mixture analysed, but as a general indication the accuracy may be taken as 10 per cent of the total indicated concentration or 0.02 mole per cent whichever is greater.

The numbers of side chains per 1 000 carbon atoms were estimated from the infra-red absorption spectrum using the $1\,378\text{ cm}^{-1}$ band. The concentrations of side chains in the *n*-deuterobutyl branched polymers were established from the deuterium content¹.

RESULTS

The analyses of the irradiation products of polymers are shown in *Tables 1* to *3*, and of pure low molecular weight hydrocarbons in *Table 4*. In a few typical cases the results of the analyses are shown graphically in *Figure 1*, and the results of the most important quantitative experiments are shown in *Figure 2*.

DISCUSSION

The qualitative detection of side chains

The results for the polymers containing known types of side chains (*Tables 1* to *3*) confirm the claim previously made² that the paraffin corresponding in carbon number to the side chain present in the polymer forms a major constituent, commonly the main constituent, of the products of irradiation.

The only apparent exception to this conclusion is the relatively high

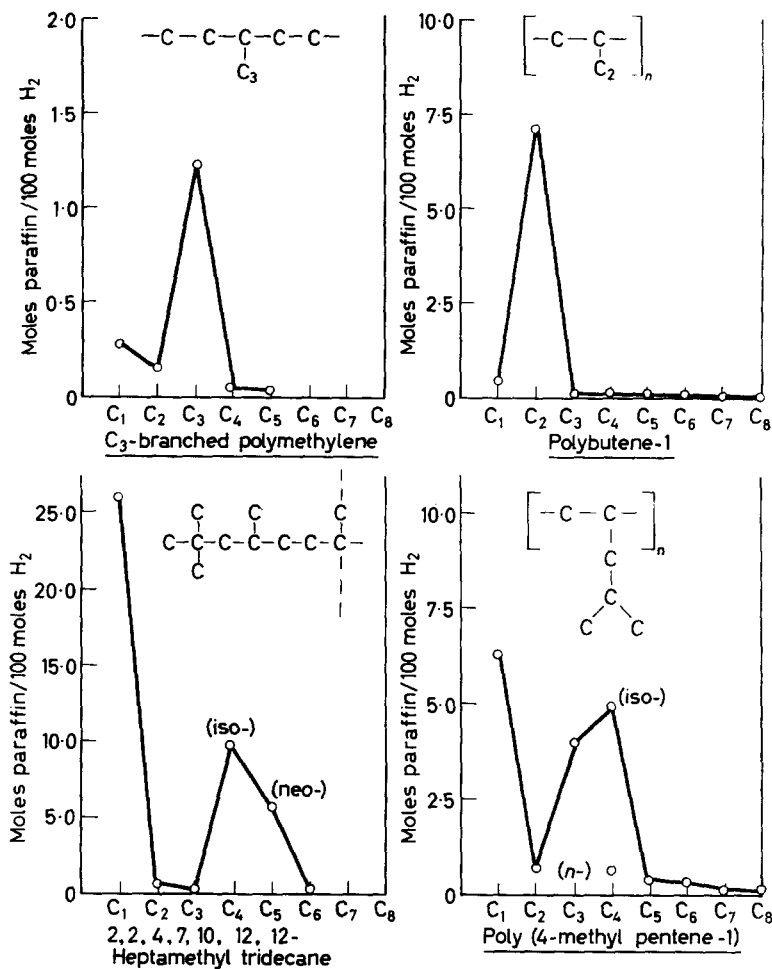


Figure 1—Yields of paraffins from typical hydrocarbons

yields of methane obtained from polymethylenes. (The low methane yield from the unbranched polymethylene reported in ref. 2 must now be regarded as fortuitous.) However, it appears that this high methane yield is anomalous and occurs only with polymers prepared by the diazoalkane synthesis, and even in these cases, the introduction of methyl side groups gives rise to an increase in the methane yield.

In the general case the effect has been demonstrated conclusively for polymers containing methyl, ethyl, *n*-propyl, *n*-deuterobutyl, *n*-amyl and *n*-heptyl side chains. Thus, analysis of the paraffin hydrocarbons evolved on irradiation of polymers provides a unique method of demonstrating the presence of short side chains in these materials. The results for pure hydrocarbons (Table 4) and for poly(4-methyl pentene-1) (Table 3) effectively

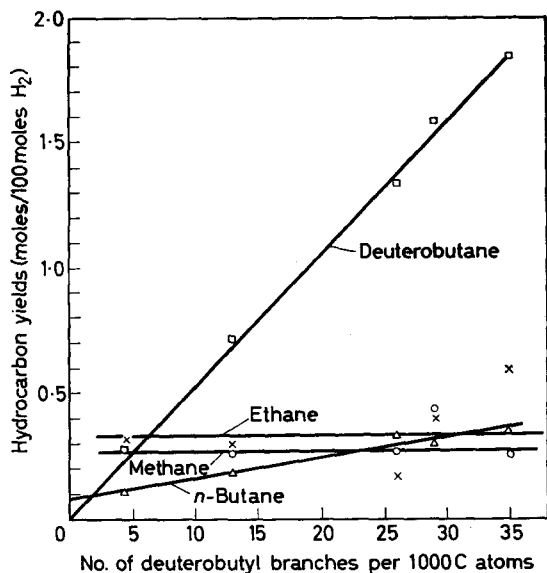


Figure 2—Yields of paraffins from deuterobutyl branched polymethylenes

demonstrate that selective scission occurs at all tertiary and quaternary carbon atoms and indicates the possibility of a unique method of distinguishing between isomeric alkyl side chains. The method may be considered to extend to C_7 side groups at least. It is difficult to assess the upper limit in size for detection of side chains, but it is unlikely that the effect ceases abruptly at C_7 , although the efficiency may decrease with longer side chains.

In addition to the paraffins, olefins are also found on irradiation. In general, however, the olefin concentration pattern is similar to that of the paraffins; further, the olefin concentration is lower, rather less reproducible, and more sensitive to variation in temperature than that of the paraffins. These facts have led to the conclusion that as far as the present technique is concerned the paraffin yield is of greater importance.

The relative efficiency of detection of side chains

In considering the establishment of the relationship between hydrocarbon yield originating from a side chain and the concentration of the latter, the most informative experiments are those on the series of *n*-deuterobutyl branched polymers (Table 2 and Figure 2). (Certain aspects of these experiments were discussed previously by Willbourn¹.) As expected, the main hydrocarbon product formed on irradiation is *n*-deuterobutane. This must originate only from the side chains and Figure 2 shows a linear plot through the origin of the yield of *n*-deuterobutane against the number of side chains.

There is no reason for supposing that *n*-deuterobutyl side chains are in any way unique and hence the results of Figure 2 provide good evidence for concluding that the yield of paraffin hydrocarbon produced on irradiation

Table 1. Irradiation of diazoalkane synthesized polymers

Source	Monomers	Catalyst	Expected side chain	No. of side chains/1000 total C atoms	Analysis of product* (Moles gas relative to 100 moles H ₂)													
					C ₁	C ₂ ^a	C ₂ ^b	C ₃ ^a	C ₃ ^b	C ₄ ^a	C ₄ ^b	C ₅ ^a	C ₅ ^b	C ₆ ^a	C ₆ ^b	C ₇ ^a	C ₇ ^b	C ₈ ^a
A.E.I. (Manchester) Ltd	CH ₂ N ₂	BF ₃ -etherate	Nil	—	0.75	0.09	0.10	0.05	0.06	0.05	0.05	0.06	0.06	0.06	0.01	0.01	0.01	0.01
A.E.I. (Manchester) Ltd	CH ₂ N ₂	Trimethyl borate	Nil	—	1.15	1.10	<0.15	0.05	0.03	0.12	0.03	0.03	0.03	0.03	0.01	0.03	0.03	0.02
Dr A. Ledwith, Liverpool University	CH ₂ N ₂	Copper naphthenate	Nil	—	0.81	0.56	0.14	0.20	0.04	0.20	0.01	0.01	0.01	0.01	0.01	0.01	0.01	0.01
A.E.I. (Manchester) Ltd	CH ₂ N ₂	Trimethyl borate	Ethyl	—	0.47	2.44	0.22	0.15	0.06	0.05	0.03	0.03	0.01	0.01	0.01	0.01	0.01	0.01
A.E.I. (Manchester) Ltd	CH ₂ N ₂	Trimethyl borate	Propyl	15.7	0.30	1.22	0.04	0.05	0.04	0.05	0.03	0.03	0.01	0.01	0.01	0.01	0.01	0.01
I.C.I. Ltd, Plastics Division	CH ₂ N ₂	Trimethyl borate	<i>n</i> -Amyl	—	0.33	0.10	0.05	0.08	0.29	0.08	0.08	0.29	0.01	0.01	0.01	0.01	0.01	0.01
A.E.I. (Manchester) Ltd	CH ₂ N ₂	Trimethyl borate	<i>n</i> -Heptyl	—	0.31	0.03	0.07	0.04	0.02	0.04	0.02	0.02	0.02	0.02	0.00	0.26	0.04	0.04
Dr A. Ledwith, Liverpool University	CH ₂ N ₂	Trimethyl borate	Methyl	—	7.19	1.46	0.64	1.14	0.40	0.64	1.42	0.40	0.18	0.18	0.18	0.41	0.25	0.36
I.C.I. Ltd, Plastics Division	CH ₂ N ₂	Trimethyl borate	Methyl	—	1.11	0.05	0.28	0.19	0.14	0.22	0.14	0.14	0.04	0.04	0.04	0.05	0.05	0.01

*C^a*n* and C^b*n* refer to yields of paraffins and olefines respectively.

Table 2. Irradiation of deuterobutyl branched polymethylenes

Source	Monomers	Catalyst	Expected side chain	No. of side chains/1000 total C atoms	Analysis of product (Moles gas relative to 100 moles H ₂)																
					Undeuterated hydrocarbon					Deuterated hydrocarbon											
					C ₁	C ₂ ^a	C ₂ ^b	C ₃ ^a	C ₃ ^b	C ₄ ^a	C ₄ ^b	C ₁	C ₂ ^a	C ₂ ^b	C ₃ ^a	C ₃ ^b	C ₄ ^a	C ₄ ^b			
I.C.I. Ltd, Plastics Division	CH ₂ N ₂ C ₆ H ₁₃ CHD ₂ CHN ₂	Trimethyl borate	1-deutero- <i>n</i> -butyl	4.3	0.28	0.32	0.00	0.11	0.08	0.11	0.08	—	—	0.07	—	—	—	0.28	0.16		
				13	0.27	0.30	0.00	0.06	0.03	0.06	0.03	—	—	—	—	0.09	0.04	0.04	0.16		
				26	0.27	0.17	0.00	0.02	0.08	0.02	0.08	0.02	0.02	0.08	—	—	—	—	0.10	0.09	
				29	0.44?	0.40?	0.00	0.04	0.09	0.04	0.09	0.04	0.04	0.09	—	—	—	—	—	0.26	0.26
				35	0.26	0.60?	0.00	0.36	0.03	0.36	0.03	—	—	—	—	—	—	—	—	0.58	0.02

Table 3. Irradiation of polyolefins

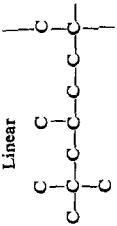
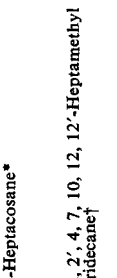
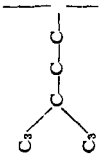
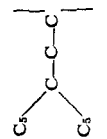
Source	Polymer	Method of preparation	Expected side chain	No. of side chains/1000 total C atoms	Analysis of product (Moles gas relative to 100 moles H ₂)											
					C ₁	C ₂ C ₃	C ₃ C ₄	C ₄ C ₅	C ₅ C ₆	C ₆ C ₇	C ₇ C ₈	C ₈ C ₉				
Distillers Co. Ltd	Polyethylene (Marlex 50)	Phillips' process	Nil	—	0.14*	0.13	0.04	0.04	0.02	0.01	0.01	0.01	0.01	0.01	0.01	0.01
Carbide & Carbon	Ethylene-Propylene copolymer	Probably Ziegler	Methyl	25	0.36	0.04	0.03	0.03	0.02	0.01	0.01	0.01	0.01	0.01	0.01	0.01
Distillers Co. Ltd	Ethylene-Propylene copolymer	Phillips' process	Methyl	15	0.20	0.12	0.05	0.02	0.03	0.03	0.02	0.02	0.02	0.02	0.02	0.01
Distillers Co. Ltd	Ethylene-Propylene copolymer	Phillips' process	Methyl	33	0.34	0.06	0.06	0.02	0.03	C ₅ and above	C ₅ and above	C ₅ and above	C ₅ and above	C ₅ and above	C ₅ and above	C ₅ and above
Distillers Co. Ltd	Ethylene-Propylene copolymer	Phillips' process	Methyl	54	0.42	0.06	0.06	0.02	0.03	C ₅ and above	C ₅ and above	C ₅ and above	C ₅ and above	C ₅ and above	C ₅ and above	C ₅ and above
Distillers Co. Ltd	Ethylene-Propylene copolymer	Ziegler process	Methyl	15.3	0.33	0.26	0.05	0.10	0.10	0.03	0.03	0.03	0.03	0.03	0.03	0.01
Distillers Co. Ltd	Ethylene-Propylene copolymer	Ziegler process	Methyl	37.2	0.80	0.32	0.07	0.20	0.01	0.01	0.01	0.01	0.01	0.01	0.01	0.01
Distillers Co. Ltd	Ethylene-Propylene copolymer	Ziegler process	Methyl	92(?)	2.58	0.38	0.06	0.43	0.01	0.01	0.01	0.01	0.01	0.01	0.01	0.01
Distillers Co. Ltd	Ethylene-Butene-1 copolymer	Phillips' process	Ethyl	2.5	0.08	0.20	0.07	0.07	0.01	0.01	0.01	0.01	0.01	0.01	0.01	0.01
Distillers Co. Ltd	Ethylene-Butene-1 copolymer	Phillips' process	Ethyl	22.5	0.10	0.12	0.04	0.02	0.04	C ₅ and above	C ₅ and above	C ₅ and above	C ₅ and above	C ₅ and above	C ₅ and above	C ₅ and above
Distillers Co. Ltd	Ethylene-Butene-1 copolymer	Ziegler process	Ethyl	12.2	0.10	0.44	0.06	0.03	0.03	C ₅ and above	C ₅ and above	C ₅ and above	C ₅ and above	C ₅ and above	C ₅ and above	C ₅ and above
Distillers Co. Ltd	Ethylene-Butene-1 copolymer	Ziegler process	Ethyl	16.5	1.25	0.70	0.06	0.03	0.03	0.03	0.03	0.03	0.03	0.03	0.03	0.03
Distillers Co. Ltd	Ethylene-Butene-1 copolymer	Ziegler process	Ethyl	45.9	3.21	1.25	0.06	0.03	0.03	0.03	0.03	0.03	0.03	0.03	0.03	0.03
Distillers Co. Ltd	Ethylene-Butene-1 copolymer	Ziegler process	Ethyl	333.0	5.64	0.14	0.15	0.15	0.24†	0.07	0.07	0.07	0.07	0.07	0.07	0.07
Distillers Co. Ltd	Polypropylene	Ziegler process	Methyl	250.0	0.86	0.18	0.00	0.20	0.11	0.10	0.10	0.10	0.10	0.10	0.10	0.10
Distillers Co. Ltd	Polybutene-1	Ziegler process	Ethyl	250.0	1.16	7.14	0.00	0.00	0.08	0.02	0.02	0.02	0.02	0.02	0.02	0.02
Professor Natta, Milan	Polybutene-1	Probably Ziegler	Ethyl	—	0.36	1.35	0.00	0.14	0.12	0.01	0.01	0.01	0.01	0.01	0.01	0.01
Phillips Petroleum Co.	Hydrogenated polybutadiene	—	Ethyl	—	6.35	7.05	0.00	0.08	0.02	0.02	0.02	0.02	0.02	0.02	0.02	0.02
Dr M. Gordon, Arthur D. Little Research Assocn	Poly(4-methyl pentene-1)	Probably Ziegler	Isobutyl	167.0	—	1.80	0.10	0.10	0.04	0.04	0.04	0.04	0.04	0.04	0.04	0.04

* Mean results of three experiments. † Contains oxygenated compounds.

Only ethane results reliable due to presence of oxygenated compounds

C₅ and above 0.02
C₆ and above 0.05
iso' 0.21
n' 0.35
iso 0.09

Table 4. Irradiation of pure hydrocarbons

Hydrocarbon	Structure	Analysis of product (Moles gas relative to 100 moles H ₂)									
		C ₁	C ₂ ^a C ₂ ^b	C ₃ ^a C ₃ ^b	C ₄ ^a C ₄ ^b	C ₅ ^a C ₅ ^b	C ₆ ^a C ₆ ^b	C ₇ ^a C ₇ ^b	C ₈ ^a C ₈ ^b		
<i>n</i> -Heptacosane*	Linear 	0.55	0.81	0.42	0.39	0.39	0.24	0.20	0.06		
2, 2', 4, 7, 10, 12, 12'-Heptamethyl tridecane†		26.0	0.5	0.2	iso' 9.9 iso' 24.8	neo 5.7 0.5		C ₇ ^a and higher 0.6 C ₈ ^a and higher 2.0			
4, 9-Dipropyl dodecane†		2.2	1.8 2.6	10.1 1.5	0.1 1.0	0.2 0.6					
6, 11-Diamyl hexadecane†		0.98	1.25 0.57	1.28 0.28	1.21 0.36	4.00 0.57	0.04 0.01	0.03			

Source of hydrocarbons: *Professor Chibnall, Cambridge; †American Petroleum Institute Res. Proj. 42.

is a linear function of the concentration of side chains from which it originates.

In addition to the expected yield of deuterobutane, small quantities of methane, ethane, *n*-butane and pentane were also produced. Of these, *n*-butane is to be expected because the *n*-amyl intermediate used in the preparation of the polymer was not fully deuterated and consequently a small number of undeuterated butyl branches would be present in the polymer. However, it is interesting to note that the slope of the *n*-butane line does not pass through the origin but intercepts the axis at 0.09 mole per cent. This suggests that some *n*-butane would be produced from a polymer without side chains, i.e. that a little *n*-butane comes from the main chain itself. It is probable that this is also the origin of the methane and ethane produced, as a tenfold increase in the number of side chains has little effect on the yield of these hydrocarbons. The same is probably true of the higher hydrocarbon products, for although the accuracy of analysis of these hydrocarbons is not high, no trend of increasing yield with number of side chains can be distinguished.

Thus it appears that small quantities of paraffin hydrocarbons are also produced from the main chain. This is supported by the results on other materials. *Marlex 50* is generally accepted as a linear polymer and yet this polymer (Table 3) and pure *n*-heptacosane (Table 4) give varying quantities of low molecular weight hydrocarbons on irradiation.

It is difficult to postulate a completely satisfactory mechanism for the formation of main chain hydrocarbons, but the mechanism given by Willbourn¹ on a suggestion of Bawn seems a likely one. Degradation of a paraffinic free radical formed by chain scission might give rise to methylene radicals which could in turn abstract hydrogen atoms to form methane or react with other degradation products. A further possibility on this basis is that the high methane yields from polymethylenes arise due to depolymerization following scission at a relatively weak catalyst-polymer bond⁵.

It follows from the above that the relationship between hydrocarbon yield originating from a side chain and the concentration of the latter can only be obtained by correction of the total observed yield for the paraffin originating from the main chain. The only method of avoiding this is by the use of specially prepared polymers having labelled side chains. This has only been done with deuterobutyl branched polymethylenes. In those cases where a series of similar polymers containing varying numbers of the same side chains were available, however, a reasonably good estimate of the relationship may be obtained from the slope of the main paraffin yield versus concentration of side chains. For single polymers no correction for hydrocarbon originating from the main chain could be made, but it is thought that the errors involved are not likely to be large since the yield is small in comparison with that originating from the side chain, particularly for those polymers with large extents of branching.

The efficiency of detection of a side chain is defined as the ratio of the moles of paraffin (per 100 moles of hydrogen) originating from a particular type of side chain, to the number of side chains of that type in the polymer per 1 000 total carbon atoms. (The total number of carbon atoms rather

than the number of main chain carbon atoms has been used as a basis for estimating side chain concentration, as the same method is employed in infra-red and combustion methods of estimating side chain concentration.) The efficiencies of detection of a number of different types of side chains are shown in *Table 5*. Where more than one value for a given side chain is available, the value is seen to vary over a fairly wide range according to the type of hydrocarbon irradiated.

Table 5. Absolute efficiencies of detection of side chains

<i>Side chain</i>	<i>Hydrocarbon</i>	<i>Table ref. no.</i>	<i>Detection efficiency</i>
Methyl	Ziegler copolymers	3	0.023
	Phillips' copolymers	3	0.006
	Polypropylene	3	0.017
	Poly(4-methyl pentene-1)	3	0.019
	Heptamethyl tridecane	4	0.058
Ethyl	Ziegler copolymers	3	0.068
	Phillips' copolymers	3	0.016
	Polybutene-1	3	0.028
Propyl	C ₃ -branched polymethylene	1	0.078
	Poly(4-methyl pentene-1)	3	0.024
	4,9-Dipropyl dodecane	4	0.046
<i>n</i> -Deuterobutyl	C ₄ -branched polymethylenes	2	0.053
Isobutyl	Poly(4-methyl pentene-1)	3	0.03
	Heptamethyl tridecane	4	0.1
<i>n</i> -Amyl	Diamyl hexadecane	4	0.026
Neo-amyl	Heptamethyl tridecane	4	0.057

In view of the fact that the physical form of the polymer may well affect the probability of recombination reaction of the radicals produced in the primary act, variations in the absolute value of efficiency of detection with hydrocarbon type are to be expected. Nevertheless the differences between the values for Phillips and Ziegler type polymers are surprising and not completely understood at present.

In *Table 6* the relative efficiencies of detection of two side chains either from similar types of hydrocarbon or from the same hydrocarbon are calculated. The ratios obtained are in closer agreement than the individual absolute values and appear to be independent of the hydrocarbon irradiated. The important points to note are as follows. In the methyl-ethyl case where three different types of polymer are available and in the methyl-isobutyl and methyl-propyl cases where two separate ratios can be calculated from each of two hydrocarbons of widely differing molecular weight, the ratios obtained are to a first approximation constant.

Table 6 provides fairly conclusive evidence that in any given hydrocarbon C₂ side chains are relatively more easily removed than C₁ side chains, *n*-C₄, C₃ and C₁ are approximately equal in ease of removal, and the trend of results suggests that higher *n*-alkyl side chains become

Table 6. Relative efficiencies of detection of side chains

Side chains	Hydrocarbon or hydrocarbon type	Ratio of efficiencies
Ethyl/Methyl	Ziegler copolymers	3.0
	Phillips' copolymers	2.7
	Ziegler homo-polymers	1.7
Propyl/Methyl	Poly(4-methyl pentene-1)	1.3
	Pure hydrocarbons	0.8
Isobutyl/Methyl	Poly(4-methyl pentene-1)	1.6
	Heptamethyl tridecane	1.7
<i>n</i> -Amyl/Methyl	Pure hydrocarbons	0.4
Neo-amyl/Methyl	Heptamethyl tridecane	1.0
Propyl/ <i>n</i> -Butyl	Polymethylenes	1.5
<i>n</i> -Butyl/Methyl	Calculated*	0.9

* The *n*-butyl/methyl ratio was obtained by dividing the propyl/methyl ratio (1.3) by the propyl/*n*-butyl ratio (1.5).

progressively more difficult to remove. Relative to the methyl removal efficiency as unity therefore, a consistent set of efficiencies for other side chains may now be calculated and is shown in Figure 3. There is little

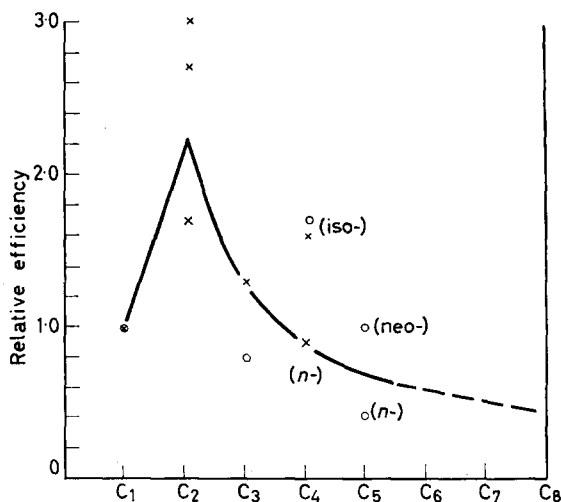


Figure 3—Relative efficiencies of detection of side chains in hydrocarbons
 × Calculated from polymer data
 ○ Calculated from pure hydrocarbon data

doubt that more cross checks on polymers with labelled side chains and prepared by a variety of methods would improve the accuracy of these determinations. Nevertheless the results form a logical pattern and considering the differences in molecular weights of the materials used to establish the values, the variation is not considered large, and the relative efficiencies cannot be greatly in error. As might be expected, the relative efficiency appears to decrease with increasing size of the side chains, presumably

because it is more difficult for a long chain radical to diffuse away and recombination of the radicals produced in the primary act becomes more probable. The reason for the low efficiency of methyl side chains relative to ethyl is not clear but it is probably more difficult to break the carbon-methyl bond than any other carbon-alkyl bond. It should be noted that the detection efficiencies for iso-alkyl side chains are higher than those for *n*-alkyl side chains of comparable carbon number and this might be expected due to the weaker bond between the side chain and main chain.

CONCLUSIONS

(1) The major constituents of the paraffinic products formed during irradiation of hydrocarbon polymers are those corresponding in carbon number and skeletal structure to the side chains in the polymer. This has been demonstrated to be applicable to both *n*-alkyl and iso-alkyl side chains from methyl to heptyl.

In polymers prepared by the diazoalkane synthesis, methane may also be a major component even when methyl side groups are absent, and considerable variation in hydrocarbon yields from linear polymers prepared by this method may be observed. The reason for this behaviour is unknown.

(2) Experiments on polymers containing labelled side chains show unequivocally that the relationship between the paraffin yield originating from the side chain and the concentration of the latter is accurately linear. The ratio of the paraffin yield to the side chain concentration is defined as the efficiency of detection of the side chain.

(3) The efficiencies of detection of side chains from methyl to amyl have been measured. The observed values vary considerably according to the type and molecular weight of the hydrocarbon used for the determination, but in hydrocarbons obtained by the same synthesis, the ratios of the efficiencies of detection of any two side groups appear to be constant and independent of hydrocarbon type.

(4) In any given hydrocarbon, C_2 side chains are more easily detected than C_1 side chains; *n*- C_4 , C_3 and C_1 are approximately equal in ease of detection, while higher (*n*-alkyl) side chains become progressively more difficult to detect. Iso-alkyl side chains are more easily detected than *n*-alkyl side chains of comparable carbon number.

The authors are indebted to the numerous individuals and companies who have helped during the course of this work by supplying polymer samples, for many stimulating discussions and permission to quote their analytical data; particularly Drs A. H. Willbourn and P. P. Manning and their colleagues at Imperial Chemical Industries Ltd, Plastics Division; and Dr K. H. C. Bessant, Research Department, Distillers Company Ltd. They also thank Dr R. W. Sillars for his continuous advice and encouragement and Sir Willis Jackson, F.R.S., Director of Research and Education, Associated Electrical Industries (Manchester) Ltd, for permission to publish.

*Associated Electrical Industries (Manchester) Ltd,
Trafford Park, Manchester 17*

(Received March 1961)

REFERENCES

- ¹ WILLBOURN, A. H. *J. Polym. Sci.* 1959, **34**, 569
- ² HARLEN, F., SIMPSON, W., WADDINGTON, F. B., WALDRON, J. D. and BASKETT, A. C. *J. Polym. Sci.* 1955, **18**, 589
- ³ BUCKLEY, G. D., CROSS, L. H. and RAY, N. H. *J. chem. Soc.* 1950, 2714
- ⁴ MILLER, C. W. *Metrop. Vick. Gaz.* 1953, **25**, 121
- ⁵ BAWN, C. E. H., LEDWITH, A. and MATTHIES, P. *J. Polym. Sci.* 1959, **34**, 93

A Study of Short Chain Branching in Hydrocarbon Polymers by the Irradiation Method. II—The Side Chain Structure of High Pressure Polyethylene

D. A. BOYLE, W. SIMPSON and J. D. WALDRON

An investigation of the relative concentrations of side chains in a commercial high pressure polyethylene, Alkathene 2, has been made by the irradiation technique. There is strong evidence that the side chains in Alkathene 2 are mainly C₂ and C₄ together with apparently significant concentrations of C₅, C₆, C₇ and C₈ side chains. This result adds support to the theory of branching in this polymer by multiple intramolecular transfer insofar as it is consistent with the existence of ethyl, butyl, 2-ethyl hexyl, 2-ethyl butyl and possibly higher iso-alkyl side chains in the polymer.

IN PART I of this study¹ the absolute value of the efficiency of detection by irradiation scission of any given side chain was shown to vary according to polymer type, and the concept of constant relative efficiencies was introduced. There was considerable evidence to indicate that in any given polymer the efficiency of detection of ethyl groups was approximately twice that of methyl groups; the efficiencies of detection of *n*-butyl, propyl and methyl groups were approximately equal; and normal alkyl groups higher than butyl become progressively more difficult to detect.

It is important to note that on the basis of this conclusion, absolute determinations of the concentrations of side chains in an unknown polymer are precluded. However, relative concentrations of the different side chains can be determined and in this paper the possibility of applying the technique to the determination of the side chain structure of commercial high pressure polyethylene is investigated.

EXPERIMENTAL

The polymer examined was *Alkathene 2*, a typical high pressure polyethylene manufactured by Imperial Chemical Industries Ltd.

The polymer samples were irradiated on a rotating stage and the gases examined as in a previous report¹. Eleven experiments were carried out and the mean results and standard deviations are shown in columns 2 and 3 of *Table 1*.

CALCULATION OF THE RELATIVE CONCENTRATIONS OF SIDE CHAINS IN *Alkathene 2*

The previous work¹ on known polymers indicated that, in addition to the hydrocarbon evolved from the side chains, a small quantity of hydrocarbon

Table 1. Calculation of concentrations of side chains in *Alkathene 2*

Carbon No.	Hydrocarbon yield (moles/100 moles H ₂)	Standard deviation	Main* chain correction	Corrected yield = yield of hydrocarbon from side chain	Relative efficiency†	Relative conc. of side chains	Absolute No. of side chains per 1 000 C atoms‡
1	2	3	4	5	6	7	8
C ₁	0.24	0.042	0.24	—	1.0	—	—
C ₂	1.33	0.061	0.22	1.11	2.2	0.50	4.0
C ₃	0.21	0.020	0.11	0.10	1.3	0.08	0.7
C ₄	1.05	0.063	0.07	0.98	0.9	1.09	9.0
C ₅	0.24	0.019	0.04	0.20	0.7	0.29	2.5
C ₆	0.23	0.032	0.02	0.21	0.6	0.35	3.0
C ₇	0.17	0.033	0.02	0.15	0.5	0.3	2.5
C ₈	0.10	0.020	0.02	0.08	0.4	0.2	2.0

* Calculated from the relative hydrocarbon yields¹ from *Marlex 50* and assuming that all the methane originates from the main chain.

† Values obtained from Figure 3, ref. 1.

‡ Calculated from Willbourn's value of 24 side chains per 1 000 C atoms².

originated from the main chain. Strictly, therefore, the observed hydrocarbon yield must be corrected for this main chain hydrocarbon before it can be used in any calculation of side chain concentration. There are three possible methods of approach to the problem.

(a) If no correction is applied, maximum values for concentration of side chains will be obtained.

(b) The hydrocarbon concentration pattern obtained¹ from *Marlex 50* may be used directly as a correction on the basis that this polymer is linear and all hydrocarbons must come from the main chain.

(c) It can be assumed that, although the main chain hydrocarbon yield varies from polymer to polymer, the *relative yield* of the various components is constant. This seems reasonable in the light of the constancy of relative efficiencies for side chain detection. Then if it can be assumed that the entire yield of any single hydrocarbon originates from the main chain, a correction for other hydrocarbons originating from the main chain can be calculated on the assumption that the relative yields are the same as that for *Marlex 50*.

In actual fact the method used does not materially affect the result; in *Table 1* method (c) was used because this gave the maximum correction; it was further assumed that all the methane originated from the main chain. (The assumption of main chain origin for any other hydrocarbon results in negative yields for some products.) The main chain correction and the resulting yield from side chains are shown in columns 4 and 5 of *Table 1*. Division of each yield by the appropriate relative efficiency of detection¹ (column 6) gives the relative concentration of *n*-alkyl side chains in column 7. (Extrapolated values of relative efficiencies for C₆ to C₈ side chains from *Figure 3* of ref. 1 have been used to compute the concentration of these.) The 'absolute' number of side chains has been calculated in column 8 from the infra-red data which indicate a total of 24 side chains per 1 000 carbon atoms in this polymer².

These results indicate that the side chains are predominantly C₂ and *n*-C₄ but with significant concentrations of C₅, C₆, C₇ and C₈. The concentration of C₃ side chains is very small.

DISCUSSION

Inssofar as the above results indicate that the side chains in *Alkathene 2* are predominantly C_2 and $n-C_4$, they are in broad general agreement with the results obtained by Willbourn from infra-red data². The difference in detail is that the irradiation method also indicates significant concentrations of C_5 , C_6 , C_7 and C_8 side chains which have so far not been detected by infra-red. The indirect evidence from infra-red is that these side chains are absent because the total concentration of side chains estimated at the methyl absorption band is equal to the sum of ethyl and butyl groups estimated independently².

Nevertheless, the conclusions of the present study, i.e. that there are significant concentrations of C_5 , C_6 , C_7 and C_8 side chains remain unchanged unless

(a) the main chain hydrocarbon correction is totally different from the *Marlex 50* pattern ('Elimination' of the C_5 to C_8 yield using the latter can only be done at the expense of producing negative yields of C_1 and C_3 hydrocarbons), and/or

(b) the relative detection efficiencies for C_5 to C_8 are much too low.

Table 2. Comparison of observed* and calculated† paraffin yields

Polymer	(a) Observed yield (b) Calculated yield							
	C_1	C_2	C_3	C_4	C_5	C_6	C_7	C_8
Ethylene-Propylene copolymer	(a) 0.33	0.26	0.05	0.10	0.10	0.03	0.01	0.01
	(b) Branch	0.26	0.13	0.08	0.05	0.03	0.03	0.03
Ethylene-Propylene copolymer	(a) 0.80	0.32	0.06	0.20	0.05	0.04	0.02	0.01
	(b) Branch	0.32	0.16	0.10	0.06	0.03	0.03	0.03
Ethylene-Propylene copolymer	(a) 2.58	0.38	0.18	0.43	0.06	0.09	0.06	0.03
	(b) Branch	0.38	0.20	0.10	0.08	0.04	0.04	0.04
Ethylene-Propylene copolymer	(a) 0.20	0.06	0.11	0.02	0.01	$n-C_5+0.01$		
	(b) Branch	0.06	0.03	0.02	0.01	0.005	0.005	0.005
Ethylene-Propylene copolymer	(a) 0.34	0.04	0.07	0.04	0.006	$n-C_5+0.03$	0.003	0.003
	(b) Branch	0.04	0.02	0.01	0.006	0.003		
Ethylene-Propylene copolymer	(a) 0.42	0.06	0.06	0.02	0.01	$n-C_5+0.01$		
	(b) Branch	0.06	0.03	0.02	0.01	0.005	0.005	0.005
Ethylene-Propylene copolymer	(a) 0.36	0.12	0.05	0.09	0.04	0.03	0.02	0.01
	(b) Branch	0.12	0.06	0.04	0.02	0.01	0.01	0.01
Ethylene-Butene copolymer	(a) 0.08	0.12	0.04	0.02		$n-C_5+0.02$		
	(b) 0.08	Branch	0.03	0.02	0.03	0.02	0.02	0.02
Ethylene-Butene copolymer	(a) 0.10	0.44	0.06	0.03		$n-C_5+0.01$		
	(b) 0.10	Branch	0.04	0.03	0.03	0.01	0.01	0.01
Polymethylene C_3 branches	(a) 0.30	0.16	1.22	0.05	0.04			
	(b) —	0.16	Branch	0.05	0.03			
Polymethylene C_7 branches	(a) 0.31	0.09	0.07	0.04	0.02	0.00	0.26	0.04
	(b) —	0.09	0.05	0.03	0.02	0.01	Branch	0.01

*Ref. 1 polymers.

†Calculated on the assumptions that:

- (i) the yields are in the same ratio as those¹ from *Marlex 50*, and
- (ii) the observed yield shown black originates from the main chain.

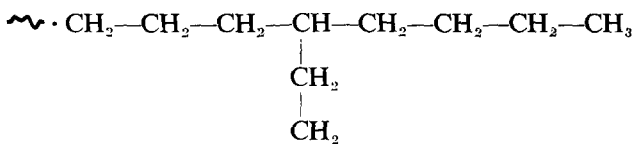
The method used to derive the main chain correction cannot be conclusively justified, but in support of the present argument *Table 2* shows the C_5 to C_8 yields for a number of polymers previously reported¹ compared with those calculated on the basis of the *Marlex* pattern, i.e. in the same way as that used for *Alkathene 2* in *Table 1*. It is evident that a large proportion of the calculated yields is the same as that observed within the experimental error. In those cases, therefore, where C_5 to C_8 side chains (other than those deliberately introduced) are extremely unlikely, the entire C_5 to C_8 yield may be calculated with reasonable accuracy by the present

method. It is inferred therefore that *Alkathene 2* either contains C_5 to C_8 side chains which raise the yields of these hydrocarbons to their observed high value or it is unique, among polymers of comparable total side chain concentration¹, in exhibiting a much higher main chain paraffin yield in the C_5 to C_8 range. This unique behaviour must be regarded as extremely unlikely, and the differences between irradiation and infra-red data cannot be reasonably accounted for on this basis.

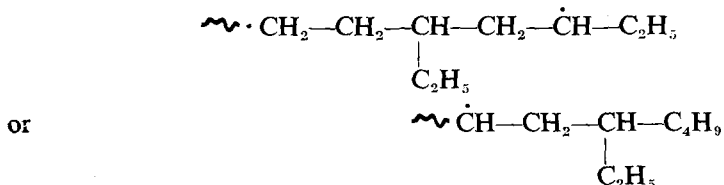
The second alternative would require the relative detection efficiencies of C_5 to C_8 side chains to be too low by factors of 3 to 6 in order to reduce the relative concentrations of these side chains to that of the C_3 for example. The detection efficiencies for iso-alkyl side chains are higher than those for *n*-alkyl side chains of the same carbon number¹ and on the assumption that the C_5 to C_8 side chains are branched, it follows that smaller concentrations than those calculated in *Table 1* would be obtained. This remains a distinct possibility, and in fact the irradiation and infra-red data may be reconciled on this basis.

The irradiation data are best explained in terms of an extension of the Roedel intramolecular chain transfer mechanism of formation of short branches³. This extension was suggested by the authors⁴ some years ago and more recently and independently by Turner of Canadian Industries Ltd². The principle of the extension of the Roedel mechanism is as follows.

The initial (Roedel) transfer occurs to give a secondary radical with a butyl group at one end of the chain. The addition of a monomer unit gives a new primary radical.



A second transfer through a six-membered ring in the transition state will now give a secondary radical with either two ethyl side chains or one ethyl and one butyl side chain as part of a 2-ethyl hexyl group.



The idea has been developed by Manning, Small and Willbourn⁵ who calculate that the second transfer has to be four to ten times more favourable than the first in order to provide ethyl and butyl groups in the ratio observed by the infra-red method. They consider that this probability is not unlikely and that the ethyl and butyl groups occur in 'clusters' along the main polymer chain, either as such or in the form of complex iso-alkyl side chains.

The important point now arises that while a group such as 2-ethyl hexyl will be indicated by infra-red to be equal concentrations of ethyl and butyl

groups, the irradiation technique will indicate the presence of ethyl, *n*-butyl, iso-octyl and *n*-heptyl because selective scission by high energy radiation will occur at all tertiary carbon atoms, either in the main chain or side chains¹.

Table 3. Types of branch clusters obtained by multiple intramolecular transfer

	Branch structure	Infra-red	Groups indicated by Irradiation
First transfer		C ₄	C ₄
Second transfer		C ₂	C ₂
		C ₂ , C ₄	C ₂ , C ₄ , <i>n</i> -C ₇ , iso-C ₈
Third transfer		C ₂	C ₂
		C ₂	C ₂ , <i>n</i> -C ₅ , iso-C ₆
		C ₂ , C ₄	C ₂ , C ₄ , <i>n</i> -C ₇ , iso-C ₈ , iso-C ₁₁ , iso-C ₁₂
		C ₂ , C ₄	C ₂ , C ₄

This theory of branch formation requires that *n*-C₅, iso-C₆, *n*-C₇, iso-C₈, iso-C₁₁, iso-C₁₂, etc. (Table 3) should be present in the irradiation products. While no C₁₁ or C₁₂ products have been observed in the paraffin yield of high pressure polyethylene, the detection efficiencies must be small. The mass spectrometric evidence is that the C₄ is certainly a normal paraffin, the C₅ probably normal and that the C₆ to C₈ paraffins certainly contain some iso-paraffin. The irradiation results therefore provide support for the latest theory of branch formation in high pressure polyethylene. In interpreting the results in this way, it should be noted that the relative efficiency of detection of branched alkyl side chains is higher than that for normal alkyl side chains of the same carbon number¹, and the relative concentrations of C₆ and C₈ side chains may therefore be lower than those indicated in Table 1.

CONCLUSION

An examination of the hydrocarbon irradiation products of high pressure polyethylene indicates that the side chains are mainly ethyl and *n*-butyl together with apparently significant concentrations of C₅, C₆, C₇ and C₈.

This result is shown to support the recent theory of branching by multiple intramolecular transfer in the high pressure polymerization of ethylene, insofar as it is consistent with the existence in the polymer of ethyl, *n*-butyl, 2-ethyl hexyl, 2-ethyl butyl and possible higher iso-alkyl side chains.

The authors are indebted to Drs A. H. Willbourn and P. P. Manning and their colleagues at Imperial Chemical Industries Ltd, Plastics Division, and Dr R. W. Sillars for many helpful discussions during the course of this work. They also thank Sir Willis Jackson, F.R.S., Director of Research and Education, Associated Electrical Industries (Manchester) Ltd, for permission to publish.

*Associated Electrical Industries (Manchester) Ltd,
Trafford Park, Manchester 17*

(Received March 1961)

REFERENCES

- ¹ BOYLE, D. A., SIMPSON, W. and WALDRON, J. D. *Polymer, Lond.* 1961, **2**, 323
- ² WILLBOURN, A. H. *J. Polym. Sci.* 1959, **34**, 569
- ³ ROEDEL, M. J. *J. Amer. chem. Soc.* 1953, **75**, 610
- ⁴ SIMPSON, W. and WALDRON, J. D. Private communication to A. H. WILLBOURN, 1956
- ⁵ MANNING, P. P., SMALL, P. A. and WILLBOURN, A. H. *J. Polym. Sci.* 1959, **34**, 591

The Assignment of the Infra-red Absorption Bands and the Measurement of Tacticity in Polypropylene

M. P. McDONALD and I. M. WARD

By comparison of the spectra of polypropylene, poly(2d-propylene) and poly(333d₃-propylene), band assignments for polypropylene are derived. These assignments confirm the suggestion of Brader that several bands characterize the portions of isotactic chains existing in the helical configuration and therefore give an effective measure of tacticity. The results show that the method of extraction with cold heptane does not give a true indication of the degree of tacticity in polypropylene. The amount of extractable material seems to depend on the molecular weight of the polymer.

IN THIS paper infra-red (i.r.) data for polypropylene and a number of deuterated polypropylenes will be presented. The aims of this work were twofold. First, it was hoped to obtain band assignments for isotactic polypropylene and secondly to examine the possibility of obtaining an i.r. method for measuring the tacticity of the polymer.

In view of the increasing importance of polypropylene as a plastic and synthetic fibre, there has been considerable interest in the characterization of this polymer by physical methods such as i.r. spectroscopy, nuclear magnetic resonance (n.m.r.) and X-ray diffraction, and several papers on these topics have appeared in the literature. The i.r. papers have fallen into two classes: those attempting detailed assignments of the i.r. absorption bands, and those concerned with the differences between the i.r. spectra of different samples—differences which have been variously attributed to crystallinity, tacticity and absorptions characteristic of the helical configuration of the polypropylene chain.

The unit cell of polypropylene contains at least twelve molecules. Thus if there were both large intra-molecular and inter-molecular interactions, the i.r. spectra would be very complex and it would be difficult to make detailed vibrational assignments. Peraldo¹ has considered the fundamental vibrations of a helix containing three monomer units. This assumes that inter-molecular interactions can be ignored, but that we should consider the intra-molecular interactions between each monomer unit and its nearest neighbour along the chain. This is an extremely interesting assumption since it can be related to a definition of tacticity. In none of these papers has tacticity been explicitly defined, but we shall now attempt to do so. We shall define tacticity by stating that it refers to the chain environment of a given monomer unit and that where both its adjacent neighbours on the chain are substituted in a sterically identical manner to itself, this monomer unit is in an isotactic environment.

Tacticity as defined here will not correspond to tacticity inferred from X-ray measurements, which require a longer sequence of stereoregular

structure before discrete reflections can be observed. It will correspond closely with a high-resolution n.m.r. value since this is only concerned with the interactions between nearest neighbours on the chain. This definition implies that even where random substitution occurs, 25 per cent of the monomer units will have both nearest neighbours in an identical stereo-relationship and thus the i.r. and n.m.r. measurements will give an isotacticity value of 25 per cent in this case.

Provided that the chain configuration is that of the helix, this monomer unit will then show the specific molecular vibrations associated with the threefold helix of polypropylene. On this view, in the absence of inter-molecular interactions, it follows that the i.r. spectrum cannot distinguish either crystallinity (which is related to inter-molecular specificity as well as to the helical configuration) or tacticity *per se* but only a chain configuration state.

Peraldo¹ gives a detailed theoretical account of the expected vibrations of polypropylene on the basis of the threefold helix, but he does not attempt to make complete assignments for the spectrum as without deuteration studies it is not possible to distinguish clearly even the principle CH, CH₂ and CH₃ deformation vibrations. Tobin², on the other hand, does attempt to make a more complete analysis. Our deuteration studies, however, show that many of Tobin's assignments in the range 1 200 to 1 500 cm⁻¹ are incorrect. Tobin also considers that the 'doubling' of molecular vibrations arises from inter-molecular interactions, whereas we shall seek to show that it is more plausible to attribute it to intra-molecular interactions.

Krimm³ included a survey of Peraldo's and Tobin's work in his review article on the i.r. spectra of high polymers. He accepts Peraldo's analysis of the modes of vibration of the chain and gives his own band assignments. Our deuteration studies have for the most part confirmed Krimm's assignments except that it becomes clear that several absorptions which Krimm assigns to skeletal vibrations (i.e. combinations of C—C chain stretching vibrations) cannot be pure skeletal vibrations as large shifts in these absorptions are obtained in the spectra of the deuterated polymers.

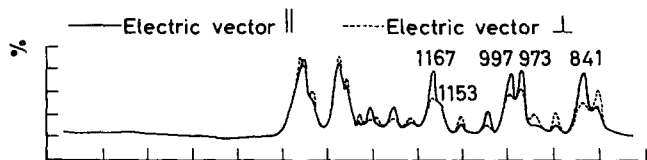
It is clear that the examination of deuterated derivatives is the key to the solution of these assignment problems. Some preliminary measurements on three deuterated derivatives have been reported in a short note by Liang, Lytton and Boone⁴. Assignments are given for the CH, CH₂ and CH₃ stretching vibrations and four deformation vibrations only.

In what follows the i.r. spectra of isotactic and atactic polypropylene, together with those of isotactic poly(2d-propylene) and poly(333d₃-propylene) will be discussed. It will be shown that the band assignments of the isotactic spectra follow from the assumption of a threefold helix and that several of the bands are specific to this configuration.

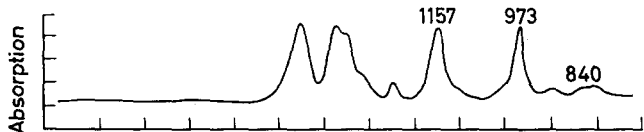
EXPERIMENTAL

Measurement of i.r. spectra

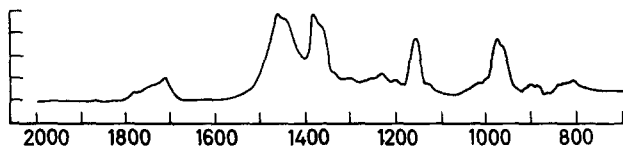
The i.r. spectra were measured using a Grubb Parsons single beam spectrometer Type S3, with a rock salt prism for the region 6.5 to 15 μ and a lithium fluoride prism for the region 3 to 7.5 μ .



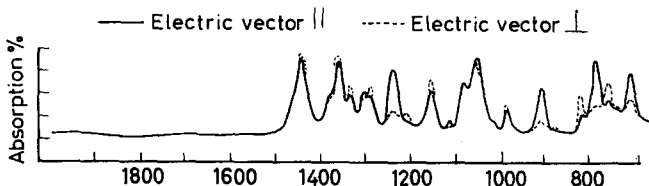
Polypropylene, '80% isotactic', room temperature



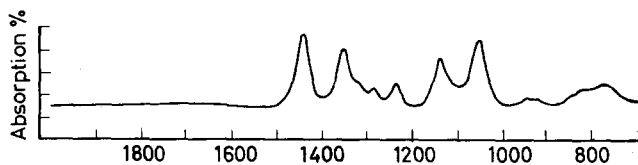
Polypropylene, '80% isotactic', temperature 180°C



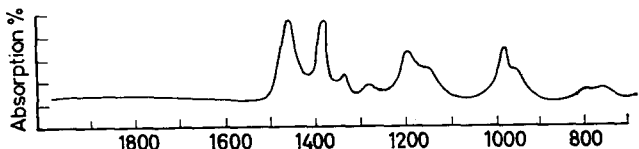
Atactic polypropylene



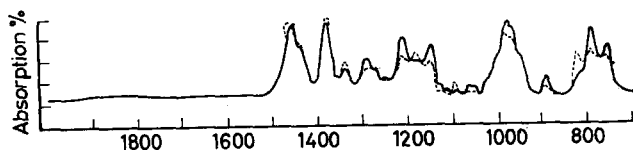
Poly (333 d₃-propylene), '80% isotactic', room temperature



Poly (333 d₃-propylene), '80% isotactic', temperature 180°C



Poly (2 d-propylene), '80% isotactic', room temperature



Poly (2 d-propylene), '80% isotactic', temperature 180°C

Figure 2

Figure 3

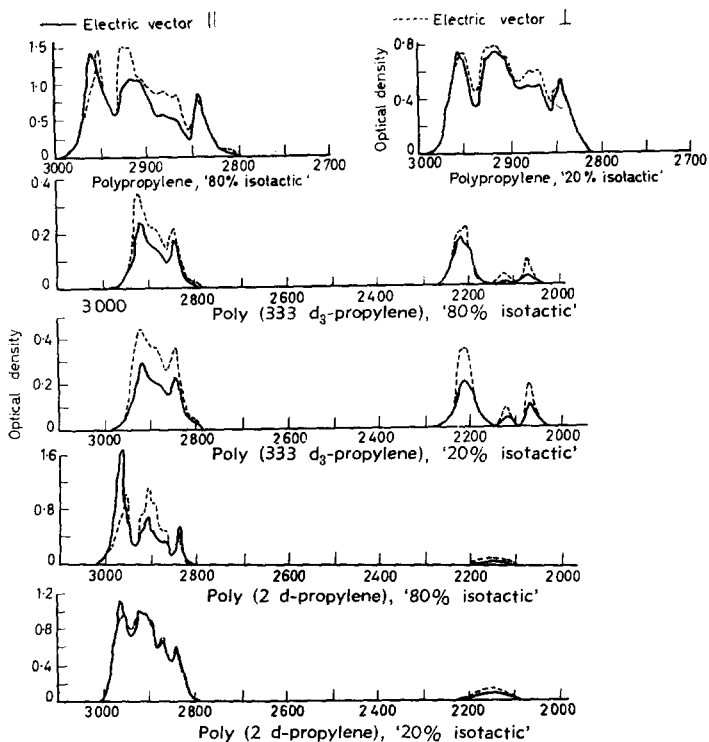


Figure 4

vibrational modes. Vibrations within each monomer unit of the helix can occur with zero phase difference or with a phase difference of $\pm \frac{2}{3}\pi$ between neighbouring units. This gives rise to 25 species A vibrations, where the resultant dipole moment changes are parallel to the axis of the helix (giving parallel absorption bands) and 52 species E vibrations, where the resultant dipole moment changes are perpendicular to this axis (giving perpendicular bands). Both species of vibration are found to occur in the crystalline polymer and also without change, in samples which have been quenched from the melt. In molten polymer a simpler spectrum is observed, corresponding to a single absorption for each molecular vibration.

The C—H stretching vibrations

None of the stretching vibrations in the spectrum of normal polypropylene can be separately resolved and most of the peaks are seen to have perpendicular dichroisms. In some of the assignments it must be assumed that the weak parallel dichroism of certain bands is swamped by the strong perpendicular dichroism of neighbouring absorptions.

This would be expected from the I_A/I_E ratios calculated by Krimm. In the two cases where $I_A/I_E > 1$, parallel dichroism is observed.

Asymmetrical —CH₃ stretching vibration

From their data on pure hydrocarbons Fox and Martin⁵ give a frequency of 2967 cm^{-1} for the doubly degenerate asymmetrical —CH₃ stretching

vibration. Peraldo resolves two bands near this frequency, at 2950 and 2960 cm^{-1} respectively and these have been assigned by Krimm to the E and A species of the asymmetrical $-\text{CH}_3$ stretching vibration.

We observe the two bands at 2951 and 2956 cm^{-1} .

In the spectrum of poly(333d₃-propylene) the corresponding $-\text{CH}_3$ vibrations give rise to a more clearly resolved doublet with peaks at 2214 and 2203 cm^{-1} . It is not clear why both peaks should show perpendicular dichroisms.

Table 1. Characteristics of polypropylene absorption bands

80% isotactic: room temp.	80% isotactic: temp. 180°C	20% isotactic: room temp.	20% isotactic: temp. 180°C	Atactic	Mode of vibration
2956(S, π)		2956		2956	Asymm.—CH ₃ stretching (A)
2951(S, σ)		2951			(E)
2925(sh, σ)		2925		2926	Symm.—CH ₃ stretching
2916(S, σ)		2915		2918	Asymm.—CH ₂ stretching
2907(sh, σ)		2907		2906	2 × Asymm.—CH ₃ bending
2880(S, σ)		2880			2 × —CH ₂ bending
2868(S, σ)		2868		2868	Symm.—CH ₃ stretching
		2851			
		2843		2844	Symm.—CH ₂ stretching
2843(S, π)					—CH stretching
2808(W, σ)					
1459(sh, σ)		1459	1465	1459	Asymm.—CH ₃ bending (E)
1454(S, π)	1451	1454	1452		(A)
1437(sh, σ)		1435		1438	—CH ₃ bending (E)
1377(S, σ)	1373	1375	1370	1378	Symm.—CH ₃ bending (E)
1359(M, σ)	1353	1358	1353	1360	—CH bending (E)
1329(W, σ)	1317	1327		1329	—CH ₂ wagging (E)
1305(W, π)		1303		1302	—CH bending (A)
1297(W, σ)		1294			—CH ₂ twisting (E)
1257(W, π)	1248	1252	1241	1248	—CH wagging (A)
1219(W, σ)		1220		1231	—CH wagging (E)
				1198	
1167(S, π)		1165			—CH ₃ wagging (A) C—C stretching (A)
1153(sh, σ)	1150	1156	1151	1157	—CH ₃ wagging (amorphous)
				1129	
1103(W, σ)	1100	1102	1102		Coupled C—H deformation (E) C—C stretching (E)
		1044			C—C stretching (A)—CH ₃ wagging (A)
1044(W, π)		1014		1016	
997(S, π)	996	997	995	996	C—C stretching (A), —CH ₃ rocking (A), CH ₂ rocking (A)
973(S, π)	971	972	972	973	CH ₃ rocking (A), CH ₂ rocking (A), C—C stretching (A)
941(W, σ)		941		964	Coupled C—H deformation (E) C—C stretching (E)
900(W, σ)	897	899	895	900	Coupled C—H deformation (E) C—C stretching (E)
		887	885	888	End group vibration
				866	
841(S, π)		841		840	CH ₂ rocking (A), CH ₃ rocking (A), C—C stretching (A)
	830		829	827	
809(M, σ)	810	809	810	812	Coupled C—H deformation (E) C—C stretching (E)

Symmetrical $-\text{CH}_3$ stretching vibration

Peak absorptions are observed at 2925 and 2868 cm^{-1} which are assigned to the symmetrical $-\text{CH}_3$ stretching vibrations. The absorption at 2880 cm^{-1} is assigned to the overtone of the CH₂ bending vibration. Thus we have reversed the assignments of the 2868 cm^{-1} and 2880 cm^{-1} bands made by Krimm. Our reasons for this are as follows: first, deuteration of the $-\text{CH}_3$ group produces a large fall in intensity on the low frequency side of the composite absorption at 2880 to 2868 cm^{-1} ; secondly, the corresponding $-\text{CD}_3$ absorptions occur at 2118 and 2066 cm^{-1} in the

deuterated polymer which, using a constant isotopic shift factor of 1.36 on deuteration, suggests $2\ 868\ \text{cm}^{-1}$ for the $-\text{CH}_3$ absorptions.

Asymmetrical $-\text{CH}_2$ stretching vibrations

The slight peak at $2\ 916\ \text{cm}^{-1}$ is assigned to the E species of the asymmetrical CH_2 stretching mode. The A species of this mode should be equal to zero according to the calculated I_A/I_E ratios of Krimm.

Table 2. Characteristics of poly(333d₃-propylene) absorption bands

80% isotactic: room temp.	80% isotactic: temp. 180°C	20% isotactic: room temp.	20% isotactic: temp. 180°C	Mode of vibration
2 915(S, σ)		2 918		Asymm. $-\text{CH}_2$ stretching
2 885(S, σ)		2 887		$2\times -\text{CH}_2$ bending
2 839(S, σ)		2 845		Symm. $-\text{CH}_3$ stretching
2 799(W, σ)		2 804		$-\text{CH}$ stretching
2 214(S, σ)		2 214		} Asymm. $-\text{CD}_3$ stretching
2 203(S, σ)		2 206		
2 118(M, σ)		2 118		} Symm. $-\text{CD}_3$ stretching
2 066(M, σ)		2 066		
1 438(S, σ)	1 444	1 441	1 444	$-\text{CH}_2$ bending (E)
1 376(sh, π)		1 375	1 373	$-\text{CH}_2$ wagging (A)
1 360(S, σ)	1 357	1 360	1 356	$-\text{CH}$ bending (E)
1 332(M, σ)		1 333		$-\text{CH}_2$ wagging (E)
	1 317		1 318	
1 303(M, π)		1 303		$-\text{CH}$ bending (A)
1 290(M, σ)		1 290	1 282	$-\text{CH}_2$ twisting (E)
1 238(S, π)	1 234	1 238	1 232	$-\text{CH}$ wagging { (A)
1 207(sh, σ)		1 207		(E)
1 144(S, σ)	1 139	1 144	1 138	Asymm. $-\text{CD}_3$ bending (A and E)
1 113(W, π)	1 114	1 110		
1 081(M, σ)		1 080		$-\text{CD}_3$ wagging (A), C—C stretching (A)
1 051(S, π)	1 053	1 051	1 052	Symm. $-\text{CD}_3$ bending
1 017(W,)		1 020		C—C stretching (A), $-\text{CD}_3$ wagging (A)
987(W,)		988		Coupled C—D deformation (E) C—C stretching
	955		944	(E)
			922	
908(M, π)		908		C—C stretching (A), CD_3 rocking (A), $-\text{CH}_2$
				rocking (A)
882(W, σ)		882		Coupled C—H deformation (E), C—C stretching
	833			(E)
820(W, σ)		821		Coupled C—H deformation (E), C—C stretching
				(E)
792(S, π)	791	791		CD_3 rocking (A), $-\text{CH}_2$ rocking (A), C—C
				stretching (A)
759(M, σ)		759		Coupled C—H deformation (E), C—C stretching
743(W, σ)				(E)
710(S, π)		710		CH_2 rocking (A), $-\text{CD}$ rocking (A), C—C
				stretching (A)

Symmetrical $-\text{CH}_2$ stretching

The band at $2\ 843\ \text{cm}^{-1}$ in the *Profax* polypropylene spectra has been assigned to both the A and E symmetrical CH_2 stretching modes by Krimm in accord with the position of $2\ 853\ \text{cm}^{-1}$ listed by Fox and Martin for the corresponding vibrations in pure hydrocarbons. In the spectrum of 20 per cent isotactic polypropylene we have resolved two bands at $2\ 843$ and $2\ 851\ \text{cm}^{-1}$ which we presume to be the separate A and E vibrations respectively.

$-\text{CH}$ stretching vibrations

The weak band at $2\ 808\ \text{cm}^{-1}$ is considered to represent the two $-\text{CH}$ stretching vibrations. The $-\text{CD}$ stretching modes in poly(2d-propylene) show as a broad vibration centre at $2\ 154\ \text{cm}^{-1}$.

There are also slight changes in intensity of some peaks in the group of bands around $2\ 900\ \text{cm}^{-1}$ in the poly(2d-propylene) spectrum and the $2\ 916$

cm^{-1} peak cannot be distinguished. It nevertheless seems reasonable to assign this peak to an overtone of a CH_3 asymmetrical bending mode as suggested by Krimm.

The C—H and C—D deformation vibrations

(1) $-\text{CH}_3$ asymmetrical bending vibration—A strong absorption is observed *ca.* $1\,457\text{ cm}^{-1}$. The use of polarized radiation suggests that this is an unresolved doublet, since the peak absorption occurs at $1\,459$ and $1\,454$

Table 3. Characteristics of poly(2d-propylene) absorption bands

80% isotactic: room temp.	80% isotactic: temp. 180°C	20% isotactic: room temp.	20% isotactic: temp. 180°C	Mode of vibration
2 959(S, π)		2 959		Asymm. $-\text{CH}_3$ stretching $\left\{ \begin{array}{l} \text{(A)} \\ \text{(E)} \end{array} \right.$ Symm. $-\text{CH}_3$ stretching Asymm. $-\text{CH}_2$ stretching + 2 \times Asymm. $-\text{CH}_3$ bending 2 \times CH_2 bending Symm. $-\text{CH}_3$ stretching Symm. $-\text{CH}_2$ stretching
2 954(S, σ)		2 954		
2 922(S, σ)		2 919		
2 903(S, σ)		2 904		
2 886(S, σ)		2 894		—CD stretching Asymm. $-\text{CH}_3$ bending $\left\{ \begin{array}{l} \text{(E)} \\ \text{(A)} \end{array} \right.$
2 866(S, σ)		2 869		
2 837(S, π)		2 839		— CH_2 bending (E) Symm. $-\text{CH}_3$ bending (E)
		2 738		
2 154(W, σ)		2 152		— CH_2 wagging (E) — CH_2 twisting (A)
1 459(sh, σ)	1 460	1 459	1 467	
1 454(S, π)		1 454	1 455	— CH_3 wagging (A), C—C stretching (A)
1 437(sh, σ)		1 434	1 434	
1 376(S, σ)	1 378	1 374	1 373	—CD bending $\left\{ \begin{array}{l} \text{(E)} \\ \text{(A)} \end{array} \right.$ —CD wagging $\left\{ \begin{array}{l} \text{(A)} \\ \text{(E)} \end{array} \right.$ Coupled C—H deformation (E), C—C stretching (E) — CH_3 rocking (A), CH_2 rocking (A), C—C stretching (A) C—C stretching (A), CH_3 rocking (A), CH_2 rocking (A) Coupled C—H deformation (E), C—C stretching (E) C—C stretching (A), CH_2 wagging (A) Coupled C—H deformation (E), C—C stretching (E) $\left. \begin{array}{l} \text{CH}_2 \text{ rocking (A), } \text{CH}_3 \text{ rocking (A) C—C stretching (A)} \end{array} \right\}$
1 354(W, π)	1 354	1 353	1 354	
1 333(W, σ)	1 334	1 332	1 327	
		1 300		
1 289(W, π)	1 282	1 288		
1 272(W, σ)		1 271		
1 244(W, π)				
1 209(M, π)		1 206		
	1 194	1 179	1 192	
1 179(M, σ)		1 179		
1 146(M, π)	1 148	1 146	1 151	
1 126(W, π)				
1 110(W, π)		1 107		
1 090(W, σ)		1 091		
1 060(W, π)		1 059		
1 049(W, π)				
1 016(sh, σ)	1 010	1 014	1 008	
1 002(sh, σ)		1 002		
978(S, π)	978	978	975	
969(sh, π)		969		
950(sh, σ)	952	951	952	
881(W, π)		882		
820(M, σ)		819		
791(S, π)	796	791	796	
755(M, π)	762	755	760	

cm^{-1} with direction of polarization perpendicular and parallel to the direction of orientation of the film respectively. These two bands are assigned to A and E species respectively of the 'in plane' $-\text{CH}_3$ asymmetrical bending vibration. In the spectrum of poly(333d₃-propylene) the corresponding $-\text{CD}_3$ absorption occurs at $1\,144\text{ cm}^{-1}$.

(2) $-\text{CH}_3$ symmetrical bending vibration—A strong absorption observed at $1\,377\text{ cm}^{-1}$ is assigned to the E species of the $-\text{CH}_3$ symmetrical bending vibration, found by Sheppard at $1\,380\text{ cm}^{-1}$ in pure hydrocarbons. It has been suggested by Krimm³ that a band at $1\,325\text{ cm}^{-1}$ is the A species of

this vibration in the crystalline polymer, while a further weak band at $1\ 334\text{ cm}^{-1}$ can be assigned to the corresponding vibration in the amorphous regions. We observe one weak band at $1\ 329\text{ cm}^{-1}$ which we have assigned to a —CH_2 wagging vibration and will therefore discuss below.

No other parallel band is observed in this region of the spectrum. It is therefore assumed that the absorption due to a species of the symmetrical —CH_3 bending vibration is masked by the strong absorption at $1\ 377\text{ cm}^{-1}$ and $1\ 359\text{ cm}^{-1}$. This point is not resolved by deuteration. Whereas the E species of the corresponding —CD_3 vibration gives rise to a band at $1\ 051\text{ cm}^{-1}$ in poly(333d₃-propylene) no band corresponding to the A species can be resolved.

—CH_2 bending vibrations

A medium absorption is observed at $1\ 437\text{ cm}^{-1}$. This is the characteristic frequency for the —CH_2 bending vibration and is assigned to the E species of this mode of vibration. No band is observed which can be assigned to the A species of this vibration.

—CH bending vibration

The medium intensity bands at $1\ 359\text{ cm}^{-1}$ and $1\ 305\text{ cm}^{-1}$ are assigned to the E and A species respectively of the C—H bending vibration. In the 2d polymer absorptions at $1\ 090$ and $1\ 060\text{ cm}^{-1}$ are assigned to the corresponding C—D vibrations. These latter assignments are supported by the perpendicular dichroism of the $1\ 090\text{ cm}^{-1}$ band and the closeness of the isotopic shifts $1\ 359/1\ 090$ and $1\ 305/1\ 060$. The neighbouring weak parallel band at $1\ 049\text{ cm}^{-1}$ in the 2d polymer is assigned to a C—D wagging vibration.

—CH_2 wagging vibrations

The spectrum of poly(333d₃-propylene) shows a shoulder at $1\ 376\text{ cm}^{-1}$. A band at this frequency in polypropylene would be masked by the CH_3 symmetrical bending vibration. Taking into account its parallel dichroism, this $1\ 376\text{ cm}^{-1}$ band is assigned to the A species of the —CH_2 wagging vibration.

A weak perpendicular band at $1\ 329\text{ cm}^{-1}$ is assigned to the E species of the —CH_2 wagging vibration. Confirmation of the assignment of this band to a —CH_2 deformation vibration is obtained from the fact that this absorption is present in both the 2d- and 333d₃-substituted polypropylenes.

—CH_2 twisting vibration

The weak perpendicular band at $1\ 297\text{ cm}^{-1}$ is assigned to a —CH_2 twisting vibration. This is presumably the band listed by Peraldo as a weak perpendicular band at $1\ 303\text{ cm}^{-1}$ and tentatively assigned by Krimm to a —CH_2 twisting vibration. Some confirmation for the assignment of this band to a —CH_2 deformation vibration is obtained from the spectra of the deuterated polymers, although this is not conclusive. Poly(333d₃-propylene) shows an identical absorption band. The 2d polymer showed a medium

intensity parallel band at 1289 cm^{-1} with a suggestion of a shoulder at 1297 cm^{-1} which could be this 1297 cm^{-1} band.

—CH wagging vibrations

Weak bands at 1257 and 1219 cm^{-1} are assigned to the A and E species respectively of the C—H wagging mode. Although the few absorptions assigned to —CH wagging vibrations in simpler molecules are not in this region it has been suggested that the bands at 1230 cm^{-1} and 1235 cm^{-1} in polyvinyl chloride and polyvinyl alcohol respectively can be so assigned³.

These assignments are in accord with the deuterated polymer spectra. Both bands are absent from the spectrum of poly(2d-propylene), the corresponding C—D absorptions being identified at 1049 and 1016 cm^{-1} respectively. In the poly(333d₃-propylene) the species A absorption is slightly increased in intensity and occurs at 1238 cm^{-1} with the species E vibration at 1207 cm^{-1} .

Skeletal vibrations

The spectrum of polypropylene shows several bands of strong or medium intensity in the range 1200 to 800 cm^{-1} . The bands at 1167 , 1153 , 997 and 841 cm^{-1} are particularly interesting in view of their large variation in intensity in different samples. As discussed in the introduction these differences have been variously attributed to differences in the degree of crystallinity, tacticity or proportion of helical structure.

Tobin² and Krimm³ have tentatively assigned the 997 and 841 cm^{-1} bands to skeletal vibrations and the 1167 and 1153 cm^{-1} bands to the

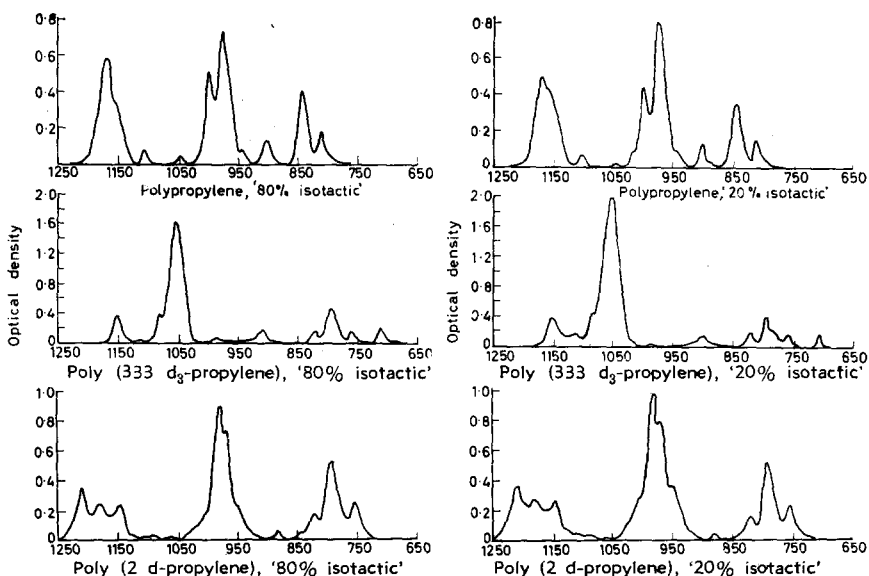


Figure 5

—CH₃ wagging mode in the crystalline and amorphous portions of the polymer respectively.

There are two fundamental C—C stretching vibrations for a monomer unit. These are conventionally called the symmetric and antisymmetric C—C stretching vibrations. Following Peraldo's treatment, we can then derive the stretching vibration of a single helix of three monomer units by considering that these vibrations on a given monomer unit can either be in phase or $\pm \frac{2}{3}\pi$ out of phase with those of the two adjoining units. This is illustrated in *Figure 1*.

If there is no coupling between these skeletal vibrations and C—H deformation vibrations the two species E vibrations will give rise to identical dipole moment changes and are degenerate.

The analysis suggests that there will be two parallel bands from the skeletal vibrations of the helix.

In *Table 4* the principal absorptions between 1200 and 700 cm⁻¹ are shown for polypropylene, poly(2d-propylene), poly(333d₃-propylene) as obtained in this laboratory and for poly(11d₂-propylene) as published by Peraldo and Farina⁶. The isotopic shift ratios (Δ) have been calculated assuming particular correspondences based on approximate intensity relationships.

Table 4. Corresponding i.r. absorption bands in polypropylene, poly(2d-propylene), poly(333d₃-propylene), poly(11d₂-propylene) and isotopic shift ratios

<i>Poly-propylene</i>	<i>Dichroism</i>	<i>Poly(2d-propylene)</i>	Δ	<i>Poly(333d₃-propylene)</i>	Δ	<i>Poly(11d₂-propylene)</i>	Δ
1 167 } 1 153 }	π	1209, 1179(σ) 1 146		1 081 1 050	1·08 1·1	1 185 1 169	
1 103	σ	1 002	1·1	987	1·08	1 018	1·1
1 044	π	881	1·18			961	1·09
997	π	969	1·03	908	1·10	896	1·11
973	π	978		792	1·23	870	1·12
941	σ	950		882	1·07	813	1·16
900	σ	820	1·1	820	1·1		
841	π	791, 755	{ 1·06 } { 1·11 }	710	1·18	691	1·22
809	σ	780	1·04	759	1·06	714	1·13

It can be seen from *Table 4* that deuteration of the tertiary hydrogen atom does not produce large frequency shifts in the case of the parallel bands. On the other hand, with the exception of the 1 167 cm⁻¹ band, all parallel absorptions in this region are appreciably affected by deuteration of either the methyl or the methylene groups.

It appears therefore that there must be considerable coupling of the CH₂ and CH₃ deformation vibrations in this region. Furthermore, it would seem from the large shifts of all bands on deuteration that the parallel skeletal

vibrations which would be expected in this frequency range (Sheppard and Simpson⁷, Table 6) must also be coupled with the C—H deformation vibrations.

The other salient feature of the spectra of polypropylene is the diminution in intensity of many of these bands on melting. The analysis of the C—H deformation vibrations in the isotactic solid polymer depends on the assumption of a threefold helix. The spectra of the molten polymer show only one absorption for each molecular vibration. This suggests that the helical configuration does not exist above the melting point.

It is therefore proposed that the 997, 973, and 841 cm^{-1} are coupled C—C stretching, CH_3 rocking and CH_2 rocking vibrations and that this coupling only occurs in the helical configuration. In the absence of coupling the C—C stretching vibration would be expected to give rise to a weak absorption and the A species CH_2 rocking mode absorption would be of zero intensity according to the I_A/I_E ratios of Krimm³.

It is suggested that the C—C stretching vibration predominates in the 997 cm^{-1} band and the $-\text{CH}_2$ rocking vibration in the 841 cm^{-1} band since these absorptions are appreciably reduced in intensity in the melt.

Similar coupling between these vibrations was proposed by McMurry and Thornton⁸ in their assignments of the spectra of propane, CH_3 , CD_2 , CH_3 , $\text{CD}_3\text{CH}_2\text{CD}_3$ and C_3D_8 in order to explain the observed isotopic shifts on deuteration. From their results they deduced that the 1 155 cm^{-1} and 870 cm^{-1} bands in propane are coupled CH_3 rocking and C—C symmetrical stretching vibrations and bands at 1 336 cm^{-1} and 1 053 cm^{-1} coupled $-\text{CH}_2$ rocking and C—C asymmetric stretching vibrations.

The 1 167 cm^{-1} band shifts to 1 081 cm^{-1} on deuteration of the methyl group, and the 1 153 cm^{-1} band shifts to 1 050 cm^{-1} . In the other deuterated polymers there appears to be some doubling of these vibrations, with their mean frequency remaining approximately unchanged. The 1 044 cm^{-1} band cannot be definitely identified in any of the deuterated polymers.

The 1 167 cm^{-1} band could be assigned to a skeletal vibration or to a $-\text{CH}_3$ wagging vibration (e.g. Sheppard and Simpson⁷, Table 6), but the shift (by a factor of 1.08) on deuteration of the methyl group shows that this band cannot be assigned to either of these vibrations alone.

It is therefore proposed that the 1 167 and 1 044 cm^{-1} bands can be assigned to coupled $-\text{CH}_3$ wagging and C—C stretching vibrations. In the melt, where this coupling vanishes, the C—C stretching vibration absorption is considerably reduced in intensity, and the $-\text{CH}_3$ wagging vibration gives rise to an absorption at 1 153 cm^{-1} . We agree with Krimm³ then, in part, on the explanation of the doublet at 1 167 and 1 153 cm^{-1} . Examination of molecular models suggests that the methyl groups in an irregularly substituted polypropylene chain (i.e. atactic polymer) would have an average separation considerably smaller than that in the helical chain. This could give rise to a difference in the frequency of the $-\text{CH}_3$ wagging vibration quite apart from that caused by coupling with a C—C stretching vibration.

There are four perpendicular bands to be considered in this region. These are shifted appreciably by deuteration of any of the protons [with the possible exception of the 941 cm^{-1} band in poly(2d-propylene)].

It therefore seems that these bands also should be assigned to coupled vibrations. From our initial analysis of the C—C stretching vibrations, at least one perpendicular skeletal vibration band would be expected. Sheppard and Simpson⁷ find a band occurring regularly at about 809 cm^{-1} in a number of hydrocarbons containing isopropyl groups and assign this without doubt to a C—C stretching vibration. The 809 cm^{-1} band in polypropylene, however, is clearly shifted to lower frequencies in all the deuterated polymers and for poly(11d₂-propylene) the shift of 1.13 is much greater than would be expected for a pure skeletal vibration.

It therefore seems most likely that these four perpendicular bands are coupled C—C stretching and C—H deformation vibrations. Since the shifts on deuteration are comparable in each deuterated polymer it does not seem possible to identify these vibrations more closely.

The coupling of skeletal vibrations with certain of the C—H deformation vibrations probably explains the large absolute intensities of the skeletal vibrations and also the unexpected I_A/I_E ratios obtained for some of the other absorption bands. In particular, the E species CH₃ rocking mode would be expected to be a much more intense vibration than the A species but they are both coupled with skeletal stretching modes and the A species vibration has the greater intensity.

DISCUSSION

None of the earlier papers dealing with band assignments makes any attempt to remark specifically on the differences between spectra of different samples, e.g. those loosely described as isotactic and atactic, although Peraldo refers to some bands as being 'amorphous'.

There have, however, been several empirical attempts to use the differences between different samples to measure crystallinity (Heinen⁹), to classify bands as amorphous or crystalline or independent of crystallinity (Abe and Yanagisawa¹⁰), 'to separate the atactic and isotactic fractions of the polymer' (Luongo¹¹), and to measure the portion of isotactic chains existing in the helical configuration (Brader¹²). In addition, Miller¹³ has suggested that the i.r. spectra show that in quenched polymer there exists a non-crystalline form of polypropylene which is an 'aggregation of molecules (or segments of molecules) in which portions of the individual chains maintain the helical structure found in the crystal'.

We have attempted to show that several i.r. absorption bands are, in fact, specific to the helical structure. The assignments, moreover, have been shown to follow directly from Peraldo's analysis of the modes of vibration of threefold monomer units on a helix. Thus it is not necessary to imply either three-dimensional order, i.e. crystallinity, or an aggregation of similar molecules. Our assignments are therefore directly in accord with the suggestion of Brader that these bands characterize the portions of isotactic chains existing in the helical configuration.

The molten isotactic polymer shows a spectrum with only one absorption for each molecular vibration. This suggests that the helical configurations are not present above the melting point. The atactic polymer at room temperature shows a very similar spectrum to this, but weak bands are also observed corresponding to the second species of vibration, as would be expected if small proportions of the material are present in the helical configuration.

It is concluded therefore that the intensities of the 1 167, 997 and 841 cm^{-1} bands will relate to the proportion of material in the helical configuration, i.e. will closely correlate with tacticity.

The intensities of these bands are compared in the spectra of the 20 per cent and 80 per cent isotactic (by extraction) polymers (*Figure 5*). Only slight differences can be observed between the intensities of the 1 167, 997 and 841 cm^{-1} bands in polypropylene and those of the corresponding bands in poly(2d-propylene) and poly(333d₃-propylene). We would therefore conclude from the i.r. assignments that these samples do not differ greatly in tacticity. An alternative explanation is that differences do exist in molecular weight and this is to be preferred for the following reasons:

(a) A band is observed at 888 cm^{-1} in the spectrum of the '20 per cent isotactic' polypropylene material which has been shown by Luongo¹¹ to be an end group absorption.

(b) Measurements of intrinsic viscosity (kindly undertaken by Mr J. F. Lloyd Roberts) on the 333d₃-polymer gave values of 1.8 and 0.9 respectively for the 80 per cent and 20 per cent isotactic samples (measured in decalin at 135°C).

(c) Density measurements were made on all these samples. The data for 80 per cent and 20 per cent tacticity in the normal polypropylene polymer were 0.912 and 0.892 respectively. Earlier workers¹³ give a much lower value of 0.85 for amorphous atactic polypropylene.

(d) The crystallinities of the 333d₃-polymers were measured by X-ray diffraction (Dr G. Farrow) and were found to be 65 per cent and 45 per cent for the 80 per cent and 20 per cent isotactic samples respectively.

Further studies are being carried out using X-ray diffraction and i.r. spectroscopy on extracted materials to investigate the effects of tacticity in greater detail.

We wish to thank Miss J. Horton for her assistance in the experimental work.

*Research Department, Fibres Division,
Imperial Chemical Industries Ltd,
Hookstone Road, Harrogate*

(Received April 1961)

REFERENCES

- ¹ PERALDO, M. *Gazz. chim. ital.* 1959, **89**, III, 798
- ² TOBIN, M. C. J. *phys. Chem.* 1960, **64**, 216

- ³ KRIMM, S. *Advanc. Polym. Sci.* 1960, **2**, 51
- ⁴ LIANG, C., LYTTON, M. R. and BOONE, C. J. *J. Polym. Sci.* 1960, **44**, 549
- ⁵ FOX, J. J. and MARTIN, A. E. *Proc. Roy. Soc. A*, 1940, **175**, 208 and 234
- ⁶ PERALDO, M. and FARINA, M. *Chim. e Industr.* 1960, **42**, 1349
- ⁷ SHEPPARD, N. and SIMPSON, D. M. *Quart. Rev. chem Soc., Lond.* 1953, **7**, 19
- ⁸ MCMURRY, H. L. and THORNTON, V. J. *chem. Phys.* 1951, **19**, 1014
- ⁹ HEINEN, W. J. *Polym. Sci.* 1959, **38**, 545
- ¹⁰ ABE, K. and YANAGISAWA, K. *J. Polym. Sci.* 1959, **36**, 536
- ¹¹ LUONGO, J. P. *J. appl. Polym. Sci.* 1960, **3**, 302
- ¹² BRADER, J. J. *J. appl. Polym. Sci.* 1960, **3**, 370
- ¹³ MILLER, R. L. *Polymer, Lond.* 1960, **1**, 135

The Constitution of Ethylene-Propylene Copolymers

J. VAN SCHOOTEN, E. W. DUCK and R. BERKENBOSCH

Evidence has been obtained from infra-red data that ethylene-propylene copolymers prepared with vanadium-containing catalysts, have methylene sequences of two and four units. The sequence of two methylene units may correspond to head-to-head orientation of propylene units. The conclusions are supported by the results of pyrolysis experiments.

THE properties of an ethylene-propylene copolymer are determined not only by the overall C_2/C_3 ratio, but also by the distribution of the two monomers over the polymer molecules and by their arrangement within a molecule. According to Natta *et al.*¹ the most desirable rubber-like properties are obtained when the two monomers alternate in the molecule. Natta determined the degree of alternation from the infra-red (i.r.) spectrum, using peaks at 13.35, 13.70 and 13.83 μ (750, 731 and 724 cm^{-1}), the one at 13.70 μ being attributed to a sequence of three methylene groups between branch points, presumably due to the insertion of one ethylene between two similarly oriented propylene molecules.

In order to check the correctness of this interpretation we examined the i.r. absorption spectra between 13 and 14 μ of ethylene-propylene copolymers prepared with various catalyst systems and compared them with the spectra of some model compounds, namely 2,5-dimethylhexane, 2,7-dimethyloctane, 4-methylpentadecane, 4-*n*-propyltridecane, polypropylene, polyethylene, polybutene-1 and hydrogenated polyisoprene, the last being considered as an ideally alternating ethylene-propylene copolymer.

An independent support for the conclusions drawn from the spectroscopic investigation was provided by the results of some pyrolysis experiments.

POLYMERS AND MODEL COMPOUNDS INVESTIGATED

Table 1 gives some data on the ethylene-propylene copolymers investigated. The only commercial sample obtainable at the time of the investigation was also included.

The hydrogenated polyisoprene was prepared by hydrogenating a polyisoprene sample, intrinsic viscosity 2.1 (toluene, 25°C), cis content 92.6 per cent, in cyclohexane at a hydrogen pressure of 250 atm and a temperature of up to 185°C with *Ni-on-guhr*. After hydrogenation the product still showed some unsaturation, which could be removed by a subsequent, similar hydrogenation. The product thus obtained was amorphous and completely soluble in *n*-hexane at room temperature. The intrinsic viscosity in toluene at 25°C was 2.3 (in decalin at 135°C: 2.8).

The 2,5-dimethylhexane, 2,7-dimethyloctane, 4-methylpentadecane and 4-*n*-propyltridecane samples were taken from an existing collection of

Table 1. Sample properties

Sample No.	Transition-metal component of catalyst	Intrinsic viscosity*, dl/g	C ₃ in polymer, mole %	Hexane soluble, %
1	TiCl ₃	3.0	50	95
2	VCl ₃	2.7	57	97
3	VCl ₃	2.4	48	93
4	VOCl ₃	3.4	46	92
5	VOCl ₃	3.8	61	90
6	VO(Ot-Bu) ₃	3.1	60	96
7	Not specified†	2.2	52	98

* 0.1 per cent in decalin at 135°C.

† commercial copolymer *Dutral* (Montecatini).

hydrocarbon model compounds. An amorphous butene-1 polymer served as a model compound carrying ethyl groups.

The i.r. spectra of thin films (0.1 to 0.2 mm thick) of the polymers were measured with a Beckman IR-4 spectrometer, operating under the following conditions: prism: NaCl, speed: 0.5 μ /min, scale: 2 in./ μ , gain: 2.5, period: 2, slit schedule: 0.6 mm at 10 μ double beam, reference: air.

The liquid model compounds were measured in a 0.1 mm cell.

SPECTROSCOPIC RESULTS

The i.r. absorption bands between 13 and 14 μ (700 and 770 cm^{-1}) of the various samples are given in *Figure 1*. These bands are due to rocking modes of the CH₂ groups and their frequency depends on the length of the CH₂ sequences. In 2,5-dimethylhexane, hydrogenated polyisoprene and 2,7-dimethyloctane there are two, three and four CH₂ groups between branches, respectively, corresponding to peaks in the i.r. spectra at 13.28 μ (754 cm^{-1}) ($\epsilon_{\text{spec.}}=0.023$ l./g.cm), 13.53 μ (740 cm^{-1}), ($\epsilon_{\text{spec.}}=0.058$ l./g.cm) and 13.75 μ (729 cm^{-1}) ($\epsilon_{\text{spec.}}=0.042$ l./g.cm). Amorphous and crystalline polypropylene do not show any absorption at all in this region, whereas crystalline polyethylene shows two peaks at 13.65 and 13.85 μ (734 and 723 cm^{-1}). The latter peak is also found in liquid low molecular weight hydrocarbons² and in amorphous polymers containing long sequences of CH₂ groups³; the 13.65 μ peak is a crystalline band, attributed to the CH₂ rocking in the polyethylene crystal^{2, 3, 4}. From the spectra of an amorphous butene-1 polymer it was concluded that ethyl side-groups give rise to a peak at around 13.1 μ (765 cm^{-1}) and from the spectra of 4-methylpentadecane and 4-*n*-propyltridecane that *n*-propyl groups absorb at 13.53 μ (740 cm^{-1}), proving that the shoulder at 13.3 μ found in some polymers is not due to ethyl or *n*-propyl end groups. A survey of the various peaks and shoulders present in the spectra is given in *Table 2*.

In the spectra of all copolymers, except sample 6, we find a sharp peak at 13.80 to 13.85 μ which must be ascribed to sequences of CH₂ groups longer than four, i.e. sequences of more than two ethylene units³.

Significant differences are, however, observed between the various spectra in the wavelength region from 13.0 to 13.7 μ . None of the copolymer spectra shows a clear shoulder at 13.53 μ , where hydrogenated polyisoprene

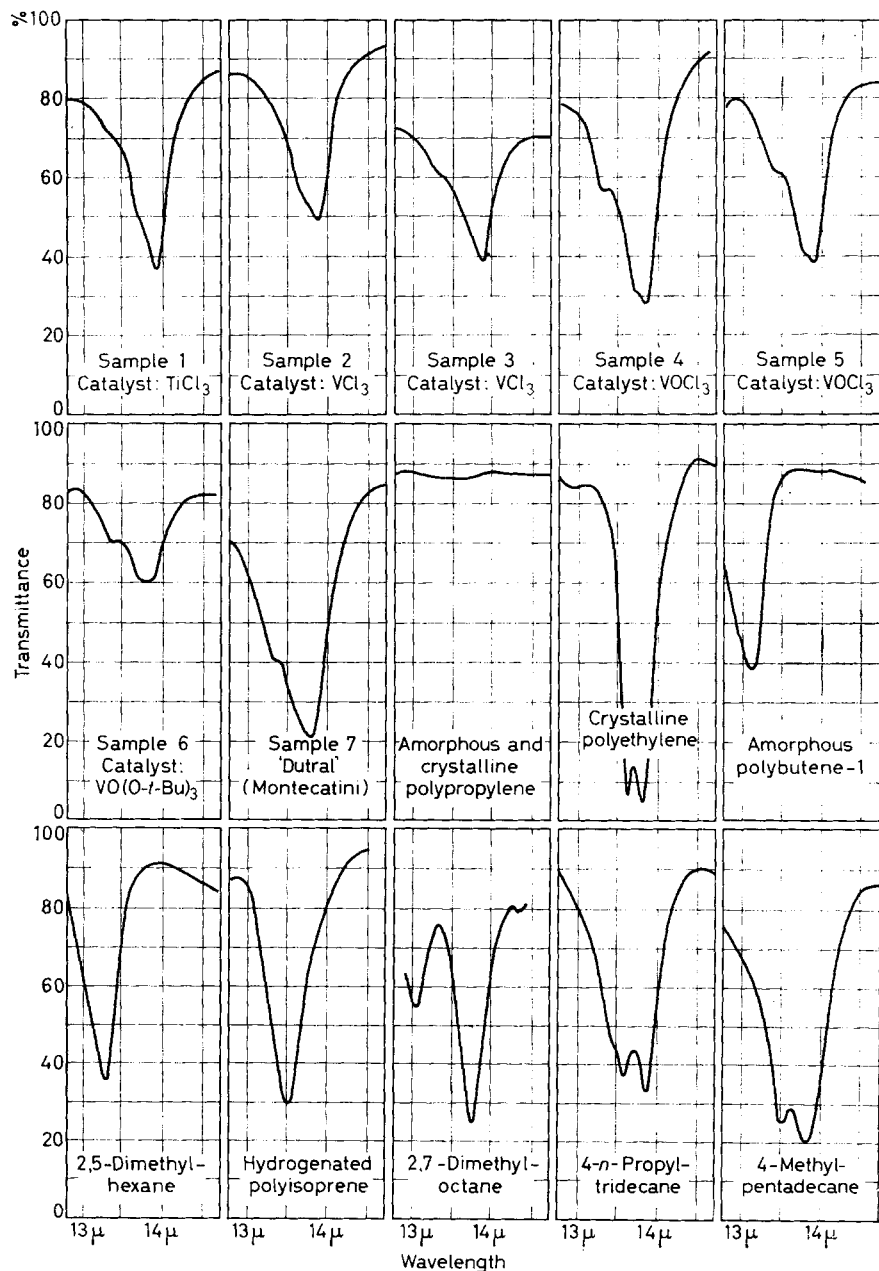


Figure 1—Infra-red spectra between 13 and 14 μ of C₂-C₂ copolymers and model compounds

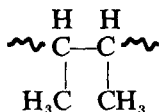
Table 2. Peaks and shoulders between 13 and 14 μ (700 and 770 cm^{-1}) in i.r. spectra of $\text{C}_2\text{-C}_3$ copolymers

Sample	Wavelength, μ				
	13.8 to 13.9	13.7 to 13.8	13.6 to 13.7	13.50 to 13.60	13.0 to 13.35
2, 5-Dimethylhexane	—	—	—	—	Peak at 13.28
Hydrogenated polyisoprene	—	—	—	Peak at 13.53	—
2, 7-Dimethyloctane	—	Peak at 13.73	—	—	—
Amorphous butene-1 polymer	—	—	—	—	Peak at 13.12
4- <i>n</i> -Propyltridecane	Peak at 13.87	—	—	Peak at 13.57	—
4-Methylpentadecane	Peak at 13.85	—	—	Peak at 13.53	—
Cryst. polypropylene	—	—	—	—	—
Cryst. polyethylene	Peak at 13.85	—	Peak at 13.65	—	—
Sample 1. TiCl_3 catalyst	Peak at 13.86	—	—	—	Vague shoulder
Sample 2. VCl_3 catalyst	Peak at 13.85	—	—	Vague shoulder around 13.60	—
Sample 3. VCl_3 catalyst	Peak at 13.86	—	—	—	Shoulder at 13.3
Sample 4. VOCl_3 catalyst	Peak at 13.85	Vague shoulder at 13.7	—	—	Pronounc- ed shoulder at 13.3
Sample 5. VOCl_3 catalyst	Peak at 13.86	Shoulder at 13.75	—	—	Shoulder at 13.35
Sample 6. $\text{VO}(\text{O}-t\text{-Bu})_3$ catalyst	—	Broad peak at 13.75	—	—	Peak at 13.35
Sample 7. <i>Dutral</i>	Peak at 13.82	—	—	—	Pronounc- ed shoulder at 13.3

shows maximum absorption. This can only mean that in all the samples the content of $(\text{CH}_2)_3$ sequences is very low. There are, however, several samples showing a pronounced shoulder at *ca.* 13.3 μ viz. samples 3, 4, 5, 6 and 7. This shoulder must probably be assigned to sequences of two CH_2 groups between branch points (cf. spectrum of 2,5-dimethylhexane). Of these samples two have been prepared with a VOCl_3 -containing catalyst and

one with a VO (O-*t*-Bu)₃-containing catalyst. Only a few of the samples prepared with a catalyst containing VCl₃, (No. 3), showed the shoulder at 13.3 μ. This shoulder was always observed in samples which had been prepared with a catalyst obtained from VOCl₃ or VO (OR)₃. In some of the samples there is also a shoulder or a peak at about 13.7 μ. It might well be that this band arises from the presence of (CH₂)₄ sequences. This holds for samples 4, 5 and 6, which were prepared with catalysts containing VOCl₃ or VO (O-*t*-Bu)₃ and which, as we have seen, also display absorption bands that indicate the presence of C₂ sequences.

None of the copolymer spectra obtained thus far indicates the presence of the structure



which would give rise to absorption at 8.9 μ (1125 cm⁻¹)*. This means that head-to-head orientation of propylene occurs only after addition of an ethylene unit. Experiments to obtain propylene homopolymers with the vanadyl-containing catalysts at best gave poor yields and sometimes no polymer whatsoever. Where polymer was obtained this possessed the normal head-to-tail structure.

PYROLYSIS EXPERIMENTS

Two samples of C₂-C₃ copolymer were pyrolysed in a high vacuum at about 400°C. The volatile reaction products were first led through a receiver cooled in ice water and then into one placed in a dry ice-acetone mixture. Sample A (analogous to sample 1) was prepared with a catalyst containing titanium trichloride, sample B (analogous to sample 5) with a catalyst containing vanadium oxychloride. Some properties of the samples are given in Table 3.

Table 3. Properties of samples A and B

Sample	Catalyst	Intrinsic viscosity Decalin 135°C	%C ₃ in polymer	Hexane-soluble, %
A	TiCl ₃	2.5	50	90
B	VOCl ₃	3.0	57	90

The decomposition products consisted of mixtures of α-olefins and α'-olefins.

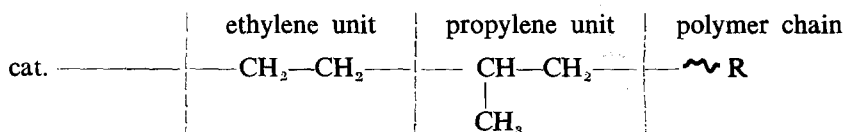
*Unpublished work by Dr C. la Lau of this laboratory. Comparison of published infra-red spectra of iso-paraffins (c.f. *Collection of Infrared Spectral Data*, American Petroleum Institute, Research Project 44) revealed that all compounds with two adjacent tertiary carbon atoms show absorption at 1125 to 1130 cm⁻¹.

The most volatile fractions, collected in dry ice-acetone were hydrogenated to saturated hydrocarbons, which were analysed by gas-liquid chromatography. For both samples, the chromatogram of this fraction showed peaks of 2,4-dimethylheptane, 2-methylheptane, 4-methylheptane, 2,4-dimethylhexane, 3-methylhexane and 2-methylhexane, but only in the chromatogram of the volatile fraction from sample B was a peak of 2,5-dimethylhexane found.

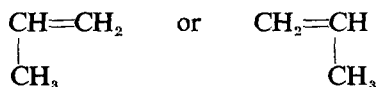
This is an additional indication that polymers prepared with a catalyst containing vanadium oxychloride contains methylene sequences of two units between branches.

DISCUSSION

In order to explain the presence of C_2 and C_4 sequences, we must assume that during polymerization conditions occur under which the propylene may enter the chain head-first or tail-first, e.g.



Propylene entering between catalyst and polymer chain may enter as



Alternation of ethylene and propylene combined with head-to-head orientation of the propylene units in the copolymer chain would thus give rise to $(\text{CH}_2)_2$ and $(\text{CH}_2)_4$ sequences. The occurrence of absorption at the frequency for the $(\text{CH}_2)_2$ and $(\text{CH}_2)_4$ sequences may accordingly be considered as an indication of a high degree of alternation.

The absence of a pronounced shoulder at *ca.* 13.5 μ (740 cm^{-1}) (the peak position in hydrogenated polyisoprene) in the spectra of copolymers prepared with catalysts containing titanium trichloride or vanadium trichloride might similarly be an indication of a low degree of alternation.

CONCLUSIONS

The indications are that ethylene-propylene copolymers prepared with vanadium-containing catalysts, especially those with VOCl_3 or $\text{VO}(\text{OR})_3$, have methylene sequences of two and four units. The absence of an i.r. band assigned to a sequence of three units indicates that the copolymers differ in structure from hydrogenated polyisoprene, which can be regarded as the perfectly alternating C_2 - C_3 copolymer.

The detection of methylene sequences of two units is a strong indication that head-to-head orientation of the propylene units may occur with certain catalysts of the Ziegler-Natta type.

Our thanks are due to Mr A. Kwantes for carrying out the hydrogenation and GLC analysis of the pyrolysis fractions and to Mr H. F. Hazebroek for valuable discussions.

*Koninklijke/Shell-Laboratorium, Amsterdam
Shell Internationale Research Maatschappij N.V.*

(Received April 1961)

REFERENCES

- ¹ NATTA, G. *et al. Chim. e Industr.* 1960, **42**, 125
- ² SHEPPARD, N. and SUTHERLAND, G. B. B. M. *Nature, Lond.* 1947, **159**, 739
- ³ RUGG, F. M., SMITH, J. J. and WARTMAN, L. H. *Ann. N.Y. Acad. Sci.* 1953-54, **57**, 398; *J. Polym. Sci.* 1953, **11**, 1
- ⁴ SUTHERLAND, G. B. B. M. *Disc. Faraday Soc.* 1950, **9**, 279
- KELLER, A. and SANDEMAN, J. J. *J. Polym. Sci.* 1954, **13**, 511
- STEIN, R. S. and SUTHERLAND, G. B. B. M. *J. chem. Phys.* 1954, **22**, 1993
- KRIMM, S., LIANG, C. Y. and SUTHERLAND, G. B. B. M. *J. chem. Phys.* 1956, **25**, 549
- TOBIN, M. C. and CARRAUW, M. J. *J. Polym. Sci.*, 1957, **24**, 93

Book Review

Arbeitserinnerungen

H. STAUDINGER

Dr Alfred Hüthig Verlag: Heidelberg, 1961.

(xii+335 pp.; 5 in. by 8 in.), DM 28.00.

WITH the writing of this book the father of polymer chemistry has rendered another service to his spiritual offspring, because no one else could have made such a meaningful compilation of the prodigious work which he originated. The range of problems and of substances which were investigated under his guidance is staggering, but even more impressive is the scope and penetration of the concepts which were created, many of them ahead of their time betraying the prescience of genius.

The whole tone of the book shows up the character of the author: it is soberly self-assured, free alike from false modesty and boastfulness; good-natured in the references to the author's old opponents and detractors; generous in acknowledgement of the work of his collaborators.

Not the least merit of this account is the frequent reference to unsolved problems. Many of the monomers studied by the author have hardly been touched again, and lie outside the ken of the average chemist. Large parts of the book are thus the most wonderful raw material for creative dreaming—one scans the wealth of strange formulae and of unfamiliar reactions, and thence start multitudinous trains of associative thought. For anyone in search of new problems or, indeed, new materials, the book is as indispensable as the old 'MARK and RAFF'; no industrial pioneering laboratory can afford not to provide its workers with many copies, not only as stimulant, but also that they may have before them an account of how real research should be done. Among the lessons taught by the author, which have been forgotten, one of the most valuable is reiterated in the 'sermon' on the text of 'the need for elementary analysis of polymers'—it is just one aspect of his insistence on utmost thoroughness in all aspects of his work.

This book is so important that its translation into the English language should be treated as a matter of urgency. It is noteworthy as one of the few autobiographical records in which an outstanding scientist gives an account, concisely and methodically, of what he did and why he did it, so that it provides a rich source of material for those interested in the origin and development of scientific ideas.

For a more elegant expression of the reviewer's feelings see J. KEATS, 'On first looking into Chapman's Homer', *Oxford Book of English Verse*, 1939 Ed., p 759.

P. H. PLESCH

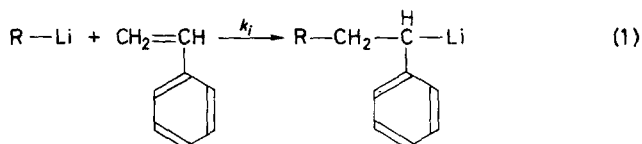
Note

Reactivities of Organo-lithium Compounds as Polymerization Initiators

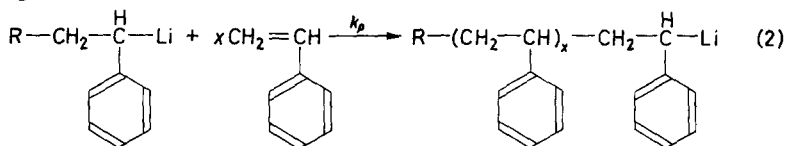
A SIMPLE but useful method for measuring relative reactivities of organo-lithium compounds was used to establish a reactivity series. We have compared five organo-lithium compounds in this respect. The results show that the ability to initiate polymerization is not the same as that expected from the relative thermodynamic stabilities of the carbanions.

Vinyl polymerizations initiated by organo-lithium compounds can be described by two kinetic steps:

Initiation



Propagation



Initiation is addition of a carbanion to a vinyl monomer, thus forming a new and usually different carbanion. Propagation is the addition of monomer to the carbanion formed from the reaction of the initiating organo-lithium species with the monomer. The propagation reaction, then, should be independent of the initiating species. In aprotic solvents there is no termination.

If all the initiator is consumed, the degree of polymerization (D.P.) equals M/C (monomer to catalyst ratio). On the other hand, if only a fraction of the organo-lithium is consumed the $\text{D.P.} = M/C^*$, where C^* is equal to the amount of catalyst consumed.

The relative initiating ability of the organo-lithium species was determined at low M/C values, where the initiation will compete with the propagation, for monomer (styrene), throughout the polymerization. The polymer D.P. is a measure of the activity of organo-lithium, relative to styryl-lithium, toward addition of monomer. These results are given in Table 1.

NOTE

Table I. Standard styrene polymerization initiated by organo-lithium compounds

Organo-lithium compound	Polymer intrinsic viscosity	D.P.*	% R-Li consumed
Butyl-	0.054	29	42
Benzyl-	0.12	86	14
Allyl-	0.15	112	11
Vinyl-	0.24	221	5.4
Phenyl-	0.24	221	5.4
Li-naphthalenide	0.10	69	18

*MAYO, F. R., GREGG, R. A. and MATHESON, M. S. *J. Amer. chem. Soc.* 1951, 73, 1691

The conditions in these polymerizations were $M/C=12$ and concentration of organo-lithium in tetrahydrofuran = 0.250 molar. Temperature 20°C.

The reactivity order, i.e.



does not follow the same pattern as the relative acidities of the corresponding hydrocarbons, or the respective radical reactivities.

The factors affecting the reactivity of organo-lithium toward addition to an olefin are being examined by us, and will be discussed in a forthcoming publication.

R. WAACK and MARY A. DORAN

*Eastern Research Laboratory,
The Dow Chemical Company,
Framingham, Massachusetts*

(Received June 1961)

*The Thermal Depolymerization of Polystyrene. IV—Depolymerization in Naphthalene and Tetralin Solutions**

G. G. CAMERON and N. GRASSIE

The rapid decrease in molecular weight which occurs in the initial stages of the thermal degradation of polystyrene at 325°C occurs at the same rate whether the reaction is carried out in bulk polymer or in solution in naphthalene or tetralin. On the other hand, the radical chain depolymerization process which occurs in bulk polymer and in naphthalene solution, and results in the evolution of volatile products, principally monomer, dimer and trimer, is completely inhibited in tetralin solution. Thus it is deduced that volatilization and molecular weight decrease are manifestations of two distinct processes and this together with previous evidence is taken as proof that the decrease in molecular weight is due to scission of weak links rather than to an intermolecular process involving the depolymerizing free radicals.

DEPOLYMERIZATION reactions, in which polymer molecules break down to lower polymers or monomer, are known to occur by a radical chain mechanism. Radicals are produced somewhere in the system in an initiation step. These may depropagate or 'unzip' giving monomer, or transfer may occur resulting in larger fragments. Finally, it seems probable that the radicals are destroyed by reaction in pairs. The detailed nature of these primary processes and their relative rates vary from polymer to polymer so that the overall characteristics of the depolymerization of different materials can vary widely.

A great deal of experimental work has been done on polystyrene. A great deal of theoretical work has also been carried out with polystyrene either wholly or partly in mind. There remains, nevertheless, fundamental disagreement about certain essential points. This centres around the large but limited decrease in molecular weight which occurs in the early stages of the depolymerization of polystyrene. On the one hand, Jellinek¹ suggested, on the basis of experimental evidence, that it arose from the scission of a limited number of 'weak links' which exist in polystyrene. On the other hand Simha and Wall² proposed that it was due to intermolecular transfer in which polymer radicals abstracted tertiary hydrogen atoms from polystyrene chains, chain scission subsequently occurring at these points. This intermolecular transfer theory has found favour principally as a result of the appearance of a series of theoretical papers by a number of workers²⁻⁷. These theoretical treatments have been applied with varying degrees of success to earlier and sometimes, for this purpose, inadequate experimental results. They have seldom been backed by experiments especially designed to test them.

*Parts I, II and III of this series are cited as ref. 8.

In earlier papers in this series⁸, Grassie and Kerr have given clear evidence that the number of chain scissions which can occur in a polystyrene molecule is a function of the temperature at which polymerization was carried out. This and other evidence suggested to them that the drop in molecular weight under discussion is indeed the result of the scission of a limited number of weak links which are formed during polymerization in some relatively infrequent process occurring in direct competition with the normal head to tail propagation process.

Wall *et al.*⁹ have shown that the rate of decrease in molecular weight is less for poly- α -deuterostyrene than for either polystyrene or poly- β -deuterostyrene. This is claimed to be evidence for the transfer theory since transfer involving a deuterium atom will have a higher energy of activation than that involving hydrogen. This evidence may be used, however, with equal effect in support of weak link scission since the presence of deuterium atoms could affect the rate at which these weak links are broken thermally.

In view of the fact that the transfer theory has received such wide acceptance on such inadequate evidence it seems necessary, before further effective investigations may be made into the finer details of the reaction, to seek a further simple test which will decide unequivocally between transfer and weak links. This is the object of the present paper.

EXPERIMENTAL

Preparation of polystyrene

Monomeric styrene (Forth Chemicals Ltd) was polymerized in bulk under vacuum at 60°C using 0.03 per cent 2,2 azobisisobutyronitrile as initiator. Purification was effected as before⁸.

Naphthalene

Naphthalene (May and Baker Ltd) was purified by the method described by Jellinek and Turner¹⁰.

Tetralin

Tetralin (L. Light and Co.) was purified by the method described by Vogel¹¹. Freedom from peroxides was ensured by storing over sodium, and refluxing for two to three hours and distilling in vacuum from sodium immediately before use. The first 20 to 30 ml of distillate was discarded.

Degradation experiments

(a) Bulk degradations were carried out by the technique previously described⁸.

(b) For degradations in naphthalene solution the procedure was essentially the same as that used by Jellinek and Turner¹⁰ except that in our experiments the polymer (0.24 to 0.25 g) was freed from air by heating it slowly under high vacuum to 200°C. The polymer first sintered then fused to a viscous melt entirely free from bubbles. After cooling, 10 g of naphthalene was sublimed under vacuum into a reaction tube made from heavy walled Pyrex tubing. The mixture was then sealed off under high vacuum.

(c) Tetralin solutions were prepared by dissolving 0.24 to 0.25 g polystyrene in 15 ml of solvent, evacuating and allowing solution to occur under vacuum. It was then transferred to the reaction tube, degassed by repeated freezing and thawing, and sealed off under vacuum.

Solution degradations were carried out by placing the reaction tubes in an electrically heated copper block specially designed to receive them. The temperature was controlled ($\pm 1^\circ\text{C}$) by an Ether Transitrol Controller actuated by a copper-constantan thermocouple.

Estimation of residual polymer

(a) The polymer residue from bulk degradations was estimated as before by weighing the copper tray and its contents before and after each experiment⁸.

For degradations in solution the reaction tubes were removed from the heating block, cooled quickly and the polymeric contents recovered as follows.

(b) With naphthalene as solvent the contents of the tubes were dissolved in the minimum amount of benzene, and the resulting solution poured into 250 ml of methanol from which the polystyrene precipitated as a fine powder.

(c) Since tetralin is not completely miscible with methanol the polymer was precipitated from tetralin by pouring it directly into 250 ml of dry ethanol.

The precipitated polymers were filtered through weighed sintered glass crucibles and, after washing with the appropriate precipitant, were dried to constant weight under high vacuum. For molecular weight measurements the polymer residues were dissolved in benzene, and after further washing with benzene the crucibles were reweighed.

Molecular weight measurements

Number average molecular weights were measured as before using a modified Fuoss-Mead osmometer⁸.

RESULTS AND DISCUSSION

It is generally agreed that the thermal depolymerization reaction in polystyrene is initiated by the formation of radicals at or near the chain ends and that these depropagate to give monomer with decreasing amounts of dimer, trimer and tetramer¹³. Since the rapid initial decrease in molecular weight is accounted for, in the transfer theory, on the basis of a competing reaction of these same depropagating polymer radicals it is clear that the formation of volatile products and the decrease in molecular weight should be closely linked.

On the other hand, Grassie and Kerr⁸ maintain that the decrease in molecular weight is due to the scission of a limited number of weak links to form stable molecules. Thus it should be possible to demonstrate that molecular weight decrease and the production of volatile material are quite separate processes.

In order to test these points degradation experiments were carried out in bulk and in naphthalene and tetralin solutions. It will be obvious that our data on the effect of these solvents on the rate of production of volatile material are qualitatively similar to those previously described by Jellinek and co-workers^{10, 12}.

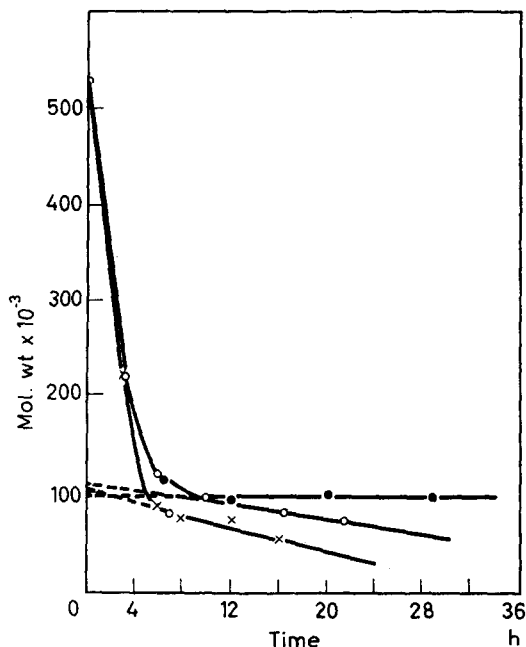


Figure 1—Molecular weight changes with time of degradation of polystyrene at 325°C in bulk, x; in naphthalene solution, o; in tetralin solution, ●

Figure 1 illustrates the changes in molecular weight which occur in each of the three media at 325°C. The rates of the initial rapid fall in molecular weight are, within experimental error, the same in each case. On the other hand the subsequent decrease in molecular weight is less in naphthalene and is completely inhibited in tetralin. Nevertheless the values of molecular weight obtained by extrapolating this later part of the curve back to zero time are identical within experimental error, which emphasizes the close similarity of the extent as well as the rate of the initial molecular weight decrease by contrast with the divergent behaviour in the later stages of the reaction.

The reason for this divergent behaviour is explained by the data in Figure 2. The radical chain depolymerization process is being retarded in naphthalene and completely inhibited in tetralin. Tetralin is a radical chain inhibitor by virtue of the relatively high reactivity of the methylene groups adjacent to the aromatic ring. The reactivity of the hydrogen atoms in naphthalene may be great enough to account for its retardation activity. Alternative explanations are the presence of trace retarders or the greater mobility of the depolymerizing radicals in solution facilitating the disproportionation termination process. This latter explanation seems the more reasonable since it has also been shown to account, under similar

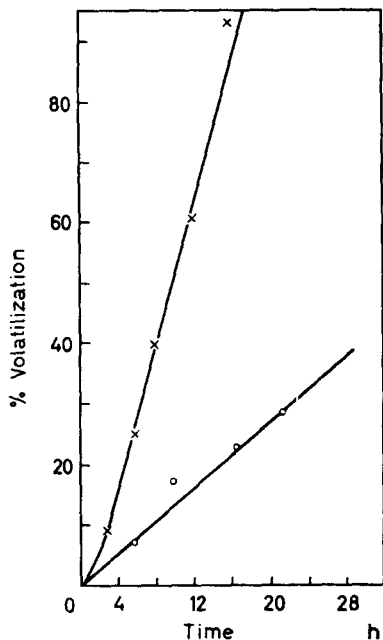


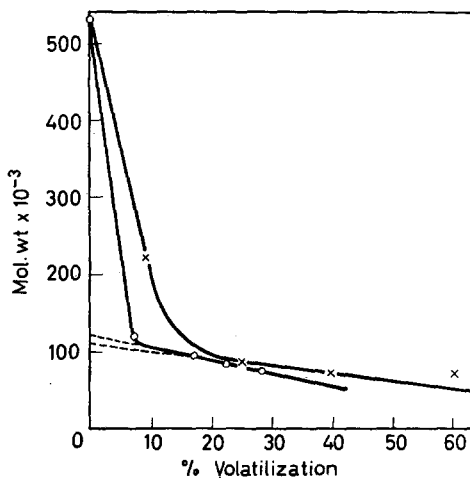
Figure 2—Extent of volatilization versus time relationship for polystyrene at 325°C in bulk, ×; and in naphthalene solution, ○

experimental conditions, for the gel effect which may be observed during polymerization.

By plotting the molecular weight change against the extent of volatilization as in *Figure 3* the lower rate of volatilization in naphthalene solution relative to the constant rate of molecular weight decrease in each medium is clearly illustrated. In this figure the behaviour of the polystyrene in tetralin is represented by the molecular weight axis.

This illustration of the complete inhibition of volatilization while the rate of initial molecular weight decrease remains constant is in complete accordance with, and is indeed strong evidence in support of, Grassie and

Figure 3 — Molecular weight changes versus extent of volatilization of polystyrene at 325°C in bulk, ×; and in naphthalene solution, ○

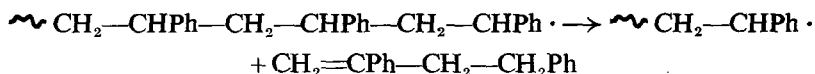


Kerr's weak link theory. It is unaccountable in terms of the transfer theory which requires that the inhibition of molecular weight changes and volatilization should run parallel. There might well be a difference in the relative rates of these two component processes in bulk polymer and solution although it is inconceivable that one should be completely inhibited while the other proceeds at its full rate. Taken in conjunction with the evidence previously presented by Grassie and Kerr⁸ these results prove quite conclusively that the molecular weight decrease in degrading polystyrene is due to weak link scission to non-radical products. Transfer is entirely absent. These findings should be taken into account in any future theoretical treatment of the system.

Nevertheless the potential transfer process between polystyryl radicals and the tertiary hydrogen atoms on polystyrene chains is of considerable interest. These tertiary hydrogen atoms might reasonably be expected to be highly reactive towards radicals. Polystyrene may be regarded in this connection as a substituted isopropyl benzene (cumene) which is a powerful transfer agent in radical processes.

If transfer occurred during depolymerization then it should also occur during polymerization and result in chain branching in view of the high concentration of monomer present. But there is no evidence that polystyrene is highly branched so there seems to be a fundamental difference in behaviour in this respect between polystyrene and the parent cumene structure. It has been suggested that transfer does indeed occur during polymerization but that the radical so formed throws off a hydrogen atom from an adjacent main chain carbon atom to form a double bond. If this occurred the resulting hydrogen atom would initiate a new molecular chain when the molecular weight of polystyrene should be strongly dependent upon the extent of conversion of monomer to polymer, being lower at higher conversions. Such an effect has never been reported.

Again, the dimer, trimer and tetramer which, along with monomer, constitute the volatile products of thermal decomposition of polystyrene have been accounted for in terms of an intramolecular transfer process occurring at the chain ends



No alternative mechanism has been proposed. The molar proportions¹³ in which the products appear are approximately

$$\text{Monomer} : \text{dimer} : \text{trimer} : \text{tetramer} = 40 : 10 : 8 : 1$$

According to this mechanism the transition states for dimer, trimer and tetramer formation should involve 4-, 6- and 8-membered rings respectively. Thus on this basis alone trimer might reasonably be expected to be very much more abundant than either dimer or tetramer. That dimer is even more abundant than trimer may be an indication that the most important factor in facilitating this chain end intramolecular transfer process is the proximity of the radical chain end to the centre at which transfer occurs. The greater the proximity in the same molecule the greater will be the

possibility of internal energy transfer between the bonds made and broken so that the overall energy requirements for the reaction to occur are very much less than would be necessary for an intermolecular process.

One of the authors (G.G.C.) takes this opportunity to thank the Salters' Company and the D.S.I.R. for the award of Fellowships during the tenures of which this work was carried out.

Thanks are also due to the United States Rubber Company for a generous research grant partly used in support of this work.

*Chemistry Department,
The University,
Glasgow, W.2.*

(Received April 1961)

REFERENCES

- ¹ JELLINEK, H. H. G. *J. Polym. Sci.* 1948, **3**, 850; 1949, **4**, 1 and 13
- ² SIMHA, R. and WALL, L. A. *J. phys. Chem.* 1952, **56**, 707
- ³ GORDON, M. *Trans. Faraday Soc.* 1957, **53**, 1662
- ⁴ GORDON, M. and SHENTON, L. R. *J. Polym. Sci.* 1959, **88**, 157 and 179
- ⁵ SIMHA, R. *Trans. Faraday Soc.* 1958, **54**, 1345
- ⁶ BOYD, R. H. *J. chem. Phys.* 1959, **31**, 321
- ⁷ SIMHA, R., WALL, L. A. and BLATZ, P. J. *J. Polym. Sci.* 1950, **5**, 615
- ⁸ GRASSIE, N. and KERR, W. W.
Part I: *Trans. Faraday Soc.* 1957, **53**, 234
Part II: *Trans. Faraday Soc.* 1959, **55**, 1050
Part III: Presented at the International Symposium on Macromolecules, Wiesbaden, October 1959 (Paper III, B11)
- ⁹ BROWN, D. V., HART, V. E. and WALL, L. A. *J. Polym. Sci.* 1955, **15**, 157
- ¹⁰ JELLINEK, H. H. G. and TURNER, K. J. *J. Polym. Sci.* 1953, **11**, 353
- ¹¹ VOGEL, A. I. *Practical Organic Chemistry*, p 825. Longmans, Green: London, 1956
- ¹² JELLINEK, H. H. G. and SPENCER, L. B. *J. Polym. Sci.* 1952, **8**, 573
- ¹³ STAUDINGER, H. and STEINHOFFER, A. *Liebigs Ann.* 1935, **517**, 35

Intermolecular Forces and Chain Flexibilities in Polymers.

III—Internal Pressures of Polymers below their Glass Transition Temperatures

G. ALLEN, D. SIMS and G. J. WILSON

Measurements on polymethylmethacrylate and polyvinylacetate together with literature data for natural rubber and polyisobutene show that internal pressures in the glass are much lower than the corresponding values for the rubber. The freezing in of the chain conformation appears to be a major factor contributing to the low internal pressure values of the glass.

COMPARISON of cohesive energy densities (c.e.d.) and internal pressures (P_i) for simple liquids¹ and for rubbery polymers² shows that, in the absence of strong specific intermolecular interactions such as hydrogen bonding, P_i gives a quantitative estimate of molecular cohesion. For polymers this conclusion is particularly useful because at high molecular weight the internal energy change accompanying vaporization (ΔU^v), and consequently the c.e.d., cannot be measured directly. No estimates of molecular cohesion in polymers at temperatures below the glass transition (T_g) are currently available. Even the indirect methods of estimating the c.e.d. may be of little value here because they are all based on the solution properties of the polymer and consequently involve a transition from rigid to mobile chain conformations. However, direct estimates of P_i can be made below T_g and offer a possible method of evaluating cohesion in the glassy state.

Very few expansivity and compressibility data for polymers below T_g have been published. The most comprehensive study has been made by Scott³ on a vulcanized natural rubber containing 19.5 wt per cent of sulphur and having a glass transition temperature of $T_g = 36^\circ\text{C}$. The internal pressures presented in *Table 1* have been calculated from these data, using the relationship

$$P_i \equiv (\partial U / \partial V)_T \approx T \alpha / \beta_T$$

where α and β_T are respectively the coefficients of expansion and isothermal compressibility.

Table 1. Internal pressure of vulcanized natural rubber*

$T^\circ\text{C}$	P_i cal cm ⁻³	State
15	65	Glass
25	62	Glass
45	122	Rubber
65	117	Rubber

* $T_g = 36^\circ\text{C}$.

A sharp decrease in the magnitude of P_i occurs on cooling through T_g and very recently Dole⁴ has noted a similar decrease for polyisobutene ($P_{i(\text{glass})}$: 100 cal cm⁻³; $P_{i(\text{rubber})}$: 140 cal cm⁻³). In each case the change in P_i arises because α decreases by a factor of 2 or 3 whereas the effect on β_T is much less marked in a rubber-glass transformation.

Intuitively, it is reasonable to suppose that molecular cohesion is greater in the glass than in the rubber. ΔU^v increases and the molar volume of the polymer decreases as the temperature is lowered. Thus, though there are no experimental data, the c.e.d. is almost certain to be larger below T_g . A corresponding increase in P_i might, therefore, have been expected. Inspection of the data for natural rubber and polyisobutene shows that the internal pressure values for the rubbery state are unusually high². Furthermore, measurement of β_T is difficult even for simple liquids and in polymers there is the additional problem of making quasi-equilibrium measurements in the region of T_g . These factors might lead to unreliable values of P_i . In order to study this problem further we have made direct estimates of γ_v [$\equiv (\partial P/\partial T)_v$] and computed P_i in the appropriate temperature range. Preliminary studies on polymethylmethacrylate led to a more extensive investigation of polyvinylacetate for which T_g is located, more conveniently, near room temperature.

EXPERIMENTAL

The apparatus and experimental procedure used for polymethylmethacrylate and for samples 1, 2 and 3 of polyvinylacetate were similar to those previously described for the measurements on natural rubber (ref. 2, *Figure 2*). Only the time-scale of the experiment required modification; below T_g it was usually necessary to thermostat the cell for one or two weeks before consistent values of γ_v were obtained at a particular temperature. This method restricted measurements of γ_v to successively increasing temperatures. A second cell, shown in *Figure 1*, was constructed so that the temperature range could be traversed in the opposite direction. The procedure for measuring γ_v remained unaltered except for the fact that the first measurement was made at the highest temperature. More mercury was then introduced into the cell so that the next measurement could be made at a lower temperature. Further additions of mercury allowed measurements to be made down to -20°C .

MATERIALS

Polymethylmethacrylate

A rod of commercial *Perspex*, 9 in. long \times $\frac{3}{4}$ in. diameter, was baked at 140°C to remove residual monomer. The resulting specimen had a molecular weight of $\bar{M}_n = (15 \pm 5) \times 10^5$ as measured viscometrically. Before use the sample was annealed by heating to 140°C and then cooling to room temperature over a period of 24 hours.

Polyvinylacetate

Shawinigan *Gelva V-7* chips ($\bar{M}_n = 33 \times 10^5$) were cast into a rod 9 in. long \times $\frac{3}{4}$ in. diameter. Four specimens, each with a different thermal

history, were prepared. Samples 1, 2 and 3 were cast at 120°C. Their histories, prior to the measurement of γ_v , were:

- (1) cooled to T_g in 24 hours
- (2) cooled to T_g in 24 hours, heated through 10° and cooled to T_g overnight and kept within 1° of T_g for 4 to 5 days
- (3) quenched to -30°C in a carbon dioxide-methanol mixture.

Sample 4 was cast at 100°C, cooled to room temperature in 24 hours and placed in the cell shown in *Figure 1*. The cell was bolted into the pressure

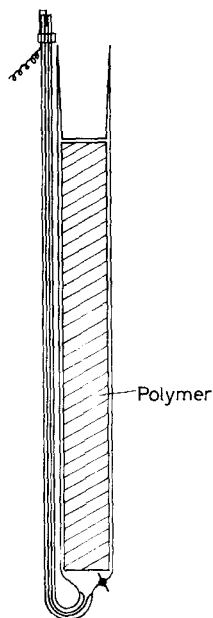


Figure 1—Cell used for measuring γ_v at successively lower temperatures

vessel and the temperature of the surrounding thermostat raised to 80°C, where the first measurement of γ_v was made. Since measurements were made at several intermediate temperatures, the sample was cooled to T_g over a period of several weeks.

RESULTS

Polymethylmethacrylate

Coefficients of expansion of the glass and the rubber, densities, and the glass transition temperature were determined by a pycnometer technique, using mercury as a containing fluid. The results are given in *Table 2* together with literature data for polymethylmethacrylate of similar molecular weights.

Measured values of γ_{obs} (i.e. γ_v for the contents of the cell), corrected values of γ_v for polymethylmethacrylate and the corresponding internal pressures are given in *Table 3*. It will be seen that the correction for the mercury present in the cell and the compressibility of the glass envelope

Table 2. Physical properties of polymethylmethacrylate

Property	This work	Beevers and White ⁵
$10^{-3}\bar{M}_n$	(15±5)	10 to 20
T_g (°C)	97±1	91 to 103
$10^4\alpha_{(\text{glass})}$ [deg ⁻¹]	2.35±0.05	1.9±0.2
$10^4\alpha_{(\text{rubber})}$ [deg ⁻¹]	5.47±0.05	5.5±0.2
Density at 25°C [g cm ⁻³]	1.189±0.002	1.195±0.003

does not exceed 30 per cent of the corrected value of γ_v . Thus, an error of 10 per cent in the correction terms would only introduce a 3 per cent error in the corrected value. We consider that the uncertainty in our corrections falls well within this range and for both polymers reported here the probable error in P_i is:

$$\pm 3 \text{ per cent at temperatures below } T_g$$

$$\pm 1.5 \text{ per cent at temperatures above } T_g$$

Table 3. Thermal pressure coefficients and internal pressures for polymethylmethacrylate*

$T^\circ\text{C}$	$\gamma_{\text{obs.}}$	γ_v atm deg. ⁻¹	P_i cal cm ⁻³
42.9	10.91	8.3 ₀	63.5
61.4	10.40	8.0 ₀	65.0
72.0	10.35	7.9 ₅	66.5
92.7	10.55	8.5 ₅	75.5
106.2	10.77	9.4 ₀	86.5
114.1	11.50	10.2 ₀	95.5

* $T_g = 97^\circ\text{C}$, $\bar{M}_n = 15\,000$.

Polyvinylacetate

The physical properties of the samples actually used for internal pressure measurements are summarized in Table 4. Literature data for a *Gelya V 145* sample⁶ of higher molecular weight are included for purposes of comparison.

Table 4. Physical properties of polyvinylacetate

Property	This work	Meares ⁶
$10^{-3}\bar{M}_n$	33±5	145
T_g (°C)	20.7±1	25.4
$10^4\alpha_{(\text{glass})}$ [deg ⁻¹]	2.28±0.05	2.07
$10^4\alpha_{(\text{rubber})}$ [deg ⁻¹]	5.93±0.05	5.85
Density at 25°C [g cm ⁻³]	1.194±0.001	1.192

Values of P_i for the four specimens of polyvinylacetate are plotted in Figure 2. The main difference between the results for the first three samples and those for the fourth sample lies in the sharpness of the transition from high to low values of P_i .

DISCUSSION

It is clear from the experimental data summarized in *Table 3* and *Figure 2* that polyvinylacetate and polymethylmethacrylate, in common with natural rubber and polyisobutene, show values of P_i which are substantially lower in the glass than in the rubber. Furthermore, the transition occurs fairly sharply in the neighbourhood of T_g and is not strongly dependent on the thermal history of the polymer. In contrast with the values quoted for natural rubber and polyisobutene the observed value of P_i for polyvinylacetate in the rubbery state is of the expected order of magnitude. The c.e.d. for this polymer has been estimated⁷ to be 88 cal cm^{-3} at 20°C ; from

Figure 2—Internal pressure data for four samples of polyvinylacetate

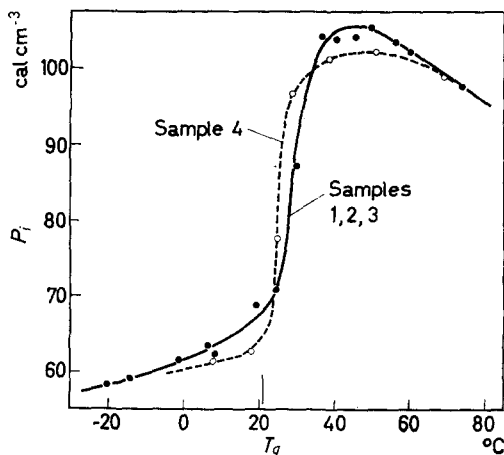


Figure 2 the extrapolated value of P_i at this temperature is 105 cal cm^{-3} so that the ratio $P_i/\text{c.e.d.}$ is 1.2, which compares favourably with ratios reported² for other polymers. A limiting value for P_i above the glass transition temperature cannot be obtained from our measurements on polymethylmethacrylate but Mangaraj⁷ has estimated, from swelling measurements, a c.e.d. of 82.5 cal cm^{-3} at 25°C which suggests that $P_i \sim 95 \text{ cal cm}^{-3}$ at 100°C is quite reasonable.

Before attempting to explain the origin of the decrease in internal pressure associated with a rubber-glass transformation, we recall that, for a system undergoing a reversible isothermal expansion, the First and Second Laws of Thermodynamics give

$$P_i \equiv (\partial U / \partial V)_T = T (\partial S / \partial V)_T - P$$

Since the external pressure P is usually negligible compared with P_i , the decrease in P_i observed in polymers can be discussed in terms of the volume derivative of either the entropy or the internal energy of the sample. If we accept the glass as a state of frozen-in disorder then the simplest explanation of the low value of $(\partial U / \partial V)_T$ is that the application of pressure compresses localized pockets of free volume (i.e. the 'holes' in the solid structure) and has a minor effect on intermolecular separations in regions where the polymer chains are in direct contact.

The complementary explanation, in terms of the effect of vitrification on the volume derivative of the entropy, follows very closely the treatment of glass-liquid transformations recently outlined by Turnbull and Cohen⁸. The essential feature of the argument is that, although the entropies of the rubber and the glass are identical at the glass transition temperature, the volume derivatives of the entropy terms may be very different because communal entropy terms which contribute to $(\partial S/\partial V)_T$ for the rubber will be absent from the rigid glass. A simple calculation, based on a lattice model in which the number of lattice sites is allowed to increase as the polymer expands, illustrates this point.

Consider N_2 molecules of a polymer, of degree of polymerization x , distributed over a lattice which can accommodate one segment on each site. If N_1 is the total number of vacant sites which, taken together, represent the free volume in the polymer sample, then:

$$\begin{aligned} \text{volume fraction of 'holes' in polymer} &= \phi_h = N_1/(N_1 + xN_2) \\ \text{volume fraction of polymer} &= \phi_p = xN_2/(N_1 + xN_2) \end{aligned}$$

The configurational entropy⁹ is

$$S_c = -k[N_1 \ln \phi_h + N_2 \ln \phi_p - N_2(x-1) \ln(z-1)/e] \quad (1)$$

where z is the coordination number of the lattice. Below T_g , S_c will remain constant at a value determined by the amount of free volume frozen in at the glass transition temperature, i.e.

$$(\partial S_c/\partial V)_T = 0 \quad (2)$$

in the glass. Above T_g , however, the polymer chains are mobile and an infinitesimal expansion (dV) of the structure causes an increase (dN_1) in the number of lattice sites available to the molecules. Since the total volume (V) of the polymer is related to the molar volume (V_m) of a segment by the equation

$$V = (N_1 + xN_2) V_m/N$$

where N is the Avogadro's number, then

$$dV = V_m dN_1/N$$

and hence

$$\left(\frac{\partial S_c}{\partial V}\right)_T = \left(\frac{\partial S_c}{\partial N_1}\right)_T \left(\frac{\partial N_1}{\partial V}\right)_T = \frac{N}{V_m} \left(\frac{\partial S_c}{\partial N_1}\right)_T \quad (3)$$

Thus, for the rubber, equations (1) and (3) yield

$$\left(\frac{\partial S_c}{\partial V}\right)_T = -\frac{R}{V_m} [\ln \phi_h + \phi_p(1-1/x)] \quad (4)$$

Combining equations (4) and (2), it is found that the change in P_i accompanying a glass-rubber transformation is

$$\Delta P_i = -\frac{RT}{V_m} [\ln \phi_h + \phi_p(1-1/x)]$$

which for a polymer of high molecular weight can be reduced to

$$\Delta P_i = [-RT/V_m][1 + \ln \phi_h] \quad (5)$$

since $\phi_h \ll 1$.

At the glass transition temperature the free volume fraction ϕ_h is estimated to be of the order of 0.025 for many common polymers¹⁰. For polyvinylacetate $V_m = 72 \text{ cm}^3 \text{ mole}^{-1}$ and thus from equation (5)

$$\Delta P_i = 22 \text{ cal cm}^{-3} \text{ at } 21^\circ\text{C}$$

The observed increment, 40 cal cm^{-3} , corresponds to a fractional free volume of $\phi_h = 0.003$, which is much lower than estimates based on either molecular dimensions or the analysis of the dynamic properties of polymers in terms of the free volume concept¹⁰. One possible explanation⁸ is that only part of the total free volume is available for configurational changes. Our model would require considerable refinement before it could be used to give a reliable estimate of ϕ_h , and we have included the calculation simply to show that the configurational contribution to $(\partial S/\partial V)_T$ probably accounts for a major part of the decrease in P_i observed in a rubber-glass transformation. A first step in improving the model might consider the free volume to be dispersed in pockets smaller than the volume occupied by a segment of the polymer chain, so that a configurational change can occur only when a sufficiently large amount of free volume has been collected in the appropriate region. This procedure immediately introduces another parameter which enables the experimental value of ΔP_i to be realized with $\phi_h = 0.025$. It does not, however, contribute to a further quantitative understanding of the phenomenon.

In conclusion, the lack of internal mobility seems to be the primary cause of the anomalous internal pressures observed in the glassy state. The only useful guides to molecular cohesion in the glass seem to be either c.e.d. values obtained from solution properties of the polymer or internal pressure data extrapolated from temperatures above T_g .

The authors wish to thank Professor Gee for suggesting the problem and for helpful discussions. Two of the authors (D. Sims and G. J. Wilson) are grateful for the awards of D.S.I.R. studentships.

*Department of Chemistry,
University of Manchester*

(Received April 1961)

REFERENCES

- ¹ ALLEN, G., GEE, G. and WILSON, J. G. *Polymer, Lond.* 1960, **1**, 456
- ² ALLEN, G., GEE, G., MANGARAJ, D., SIMS, D. and WILSON, J. G. *Polymer, Lond.* 1960, **1**, 467
- ³ SCOTT, A. H. *J. Res. nat. Bur. Stand.* 1935, **14**, 99
- ⁴ DOLE, M. *Fortschr. HochpolymerForsch.* 1960, **2**, 221
- ⁵ BEEVERS, R. B. and WHITE, E. F. T. *Trans. Faraday Soc.* 1960, **56**, 744
- ⁶ MEARES, P. *Trans. Faraday Soc.* 1957, **53**, 31
- ⁷ MANGARAJ, D. *Ph.D. Thesis.* University of Manchester, 1959

- ⁸ TURNBULL, D. and COHEN, M. H. *J. chem. Phys.* 1961, **34**, 120
- ⁹ FLORY, P. J. *Principles of Polymer Chemistry*, Chap. 12, p 501. Cornell University Press: Ithaca, N.Y., 1953
- ¹⁰ TOBOLSKY, A. *Properties and Structure of Polymers*, Chap. 2, p 85. Wiley: New York, 1960

The Rate of Cure of Network Polymers and the Superposition Principle

M. GORDON* and W. SIMPSON†

Previously reported data on the change of glass transition temperature (T_g) with time during the heat treatment of insulating varnish films have been re-examined from the point of view of Ferry's superposition principle. This principle implies that, at temperatures above T_g all properties governed by the segmental relaxation rate (e.g. viscous flow, mechanical and dielectric relaxation, etc.) will vary with temperature in essentially the same way for all polymers. It is shown that for three insulating varnishes, the rate of increase of T_g at constant temperature is also controlled by mobility of chain segments rather than by chemical structure and that the superposition principle may be applied to these processes. Deviations from the theoretical behaviour occur at advanced stages of the heat treatment and are accounted for by the assumption of a process of constant rate, probably oxidative, to be superposed on the main reaction.

DURING cure of a polyfunctional system, cross links are formed and the glass transition temperature T_g rises and may approach the curing temperature^{1,2}. In this range, the rate of such a reaction often becomes diffusion controlled; physical rather than chemical factors then become of importance and substantially every collision between the reactive functions is effective in producing chemical reaction. The segmental relaxation rate which governs most rate processes that take place in polymers above T_g (e.g. mechanical or dielectric relaxation, growth of crystallites, viscous flow, as well as diffusion and chemical reactions) does of course depend on the chemical structure of the polymer, but these structural effects largely disappear provided the polymers are compared in corresponding states. Thus Tammann³ showed that glass-forming substances generally have the same shear viscosity (about 10^{13} poise) at their T_g and this has often been confirmed for polymer systems. Ferry *et al.*⁴ found that the viscosity decreases essentially in the same way for all such systems, as the temperature is raised above T_g . Thus Ferry's superposition principle may be put in the form

$$\begin{aligned}\log [\eta_T^0 / \eta_{T_g}^0] &= \log (T / T_g) - a\theta / (b + \theta) \\ &\equiv \log (T / T_g) - a + [ab / (b + \theta)]\end{aligned}\quad (1)$$

where

$$\theta = T - T_g \quad (2)$$

$$a = 17.44; \quad b = 51.6^\circ\text{C}; \quad ab = 900.0^\circ\text{C} \quad (3)$$

and η^0 denotes viscosity at very low shear rate.

The important term in equation (1) is the shift function

$$\log a_T = -a\theta / (b + \theta) \quad (4)$$

*Chemistry Department, Imperial College of Science and Technology, London S.W.7.

†Research Department, Associated Electrical Industries (Manchester) Limited, Trafford Park, Manchester 17.

These broad, but often rather accurate, generalizations may be applied to diffusion controlled reaction rates in polymers, especially to crosslinking, which must patently depend on the rate of rotation of chain segments. According to the accepted picture of diffusion controlled reactions, their rate constant k_T is generally proportional to the diffusion constant of a reactant, and therefore inversely proportional to the viscosity of the medium. This suggests that the temperature dependence of such a rate constant would be

$$-\log [k_T/k_{T_g}] = \log (T/T_g) - a + [ab/(b + \theta)] \quad (5)$$

by comparison with equation (1).

The shear viscosity loses its meaning in a gelled system, so that equation (1) may not be used as the proper form of the superposition principle. It is well known, however, that the superposition principle extends to other viscoelastic properties besides the shear viscosity⁵, and in particular to the dynamic shear viscosity η' (the real part of the complex viscosity applicable to vibrations in shear), which retains its meaning in a gel. This quantity depends on the frequency as well as on temperature, and in terms of η' the superposition principle takes the form

$$+\log [\eta' (a_T \omega, T) / \eta' (\omega, T_g)] = \log (T/T_g) - a + [ab/(b + \theta)] \quad (6)$$

[which reverts to equation (1) as the arbitrary frequency ω tends to zero, but this limiting process has meaning only for systems with finite η and not for gels]. For gelled systems, the rate constant of a diffusion controlled reaction may be expected to vary as $1/\eta' (a_T, \omega T)$ instead of as $1/\eta_T^0$. Therefore equation (5) can be derived from equation (6) instead of from equation (1). In fact, equation (5) suggests itself directly from the superposition principle without reference to any form of viscosity.

To analyse measurements of curing rates in terms of equation (5), rather sweeping simplifications are in order. The rate constant k_T may be replaced by the actual rate of crosslinking, or some property proportional to it which can be measured. This amounts to assuming that over the range of reduced temperatures θ to which equation (5) is applied, the concentration of crosslinking functionalities is practically constant despite the formation of new crosslinks. This is plausible, because the formation of a small number of crosslinks considerably increases the T_g (see below). The term $\log (T/T_g)$ in equation (5) will also be treated as constant. It varies but little compared with the term $-ab/(b + \theta)$ and in the sense opposite to the effect arising from the reduction in the concentration of crosslinking functionalities.

The most important assumption to be made is that k_{T_g} is constant. We thus assume that as more crosslinks are introduced, and as in consequence T_g rises, the rate constant of crosslinking is always the same if measured at the T_g prevailing at any stage. This goes beyond the Ferry superposition scheme, since chemically somewhat different systems are involved when working at different stages of crosslinking. The assumption is suggested, rather, by Tammann's observation mentioned above.

Making the simplifications so far suggested, equation (5) can be written

$$\log X = K - [ab/(b + \theta)] \quad (7)$$

where X is some quantity proportional to the rate of crosslinking, and

$$K = \log X_{T_g} - \log (T/T_g) + a \quad (8)$$

is practically constant compared with variations in $(b + \theta)$.

EXPERIMENTAL

It is apparent that dT_g/dt is a useful measurable variable which may serve as the quantity X , because the glass temperature T_g rises markedly with the number of crosslinks introduced, and the relationship between the two would be expected to be linear over the range of interest. It is found to be linear over a range of 120°C in the system styrene-divinyl benzene⁶.

(When interpreting a curing reaction in terms of displacement of T_g caution is required in that chemical reactions other than crosslinking may produce such displacements. However, the theory presented here is, in principle, applicable to any kind of reaction involving diffusion controlled motions of polymer backbone segments.)

Equation (7) can then be verified most simply in two different ways. By keeping θ constant, we find from equation (2)

$$dT_g/dt = dT/dt \quad (\theta = \text{constant}) \quad (9)$$

so that equation (7) becomes (putting $X = dT_g/dt$)

$$dT/dt = \text{constant} \quad (\theta = \text{constant}) \quad (10)$$

The constancy of dT/dt under conditions of constant θ was verified in an earlier paper⁷ on a number of quite diverse (polyaddition and polycondensation) systems, and was presented as the principle of the constancy of isothermal curing rates.

Secondly, one may make isothermal measurements, so that from equations (2) and (7) one finds

$$\log dT_g/dt = \log (-d\theta/dt) = K - [ab/(b + \theta)] = K - [900/(51.6 + \theta)] \quad (11)$$

This differential equation in θ is verified in this paper by reference to isothermal curing rate measurements on systems chosen from those investigated by Bridge and Simpson^{8,9}. Both investigations employed a ball-rebound technique which allows the temperature T of the polymer to be measured directly, and T_g [and hence θ by equation (2)] indirectly. The assumption underlying this indirect measurement of T_g , now to be discussed, is best explained by reference to Ferry's superposition principle. The use we have made of this principle in suggesting equation (7) for the effect of temperature on curing rates is quite independent of what follows; it so happens that the property selected in following the rate is itself subject to the superposition principle. This property is the energy E lost by internal friction when the polymer is impacted by a small steel ball. Such an impact is roughly equivalent to half a cycle of an enforced sinusoidal compression wave, and the frequency of this wave is of the order of $\omega = 10^{3.5} \text{ sec}^{-1}$. The energy loss by internal friction should be proportional to $G''(\omega)$, the imaginary component of the complex bulk modulus, to which the superposition principle applies. It leads to the conclusion that the temperature T_{max} for which E takes a maximum value, which is easily found by the

ball-rebound technique, lies at a nearly constant temperature θ' above the static glass transition T_g . Experimentally, θ' is usually about 40°C for ball-rebound experiments, and this will be assumed for convenience, the results being very insensitive to the value of θ' chosen. [Theoretically, it is found from the shift function {equation (4)} that a displacement of $\theta' = 40^\circ\text{C}$ corresponds to a shift in frequency $\log a_T = 7.65$. Thus $T_{\max.}$ would shift to T_g if the impact time were increased from about $10^{-3.5}$ to about $10^{4.15}$ sec which justifies the description of T_g as 'static'. As follows mathematically from the form of the shift function, $T_{\max.}$ changes very little when the frequency is reduced, or the impact time increased, beyond this very slow region.]

Accordingly, measurements of $T_{\max.}$ as a function of time t may be converted to values of θ by means of the equation

$$\theta = T - T_{\max.} + 40 \quad (12)$$

In the experiments of Bridge and Simpson^{8,9}, films (about 0.010 in. thick) were prepared on stainless steel discs 0.5 in. in diameter and 0.125 in. thick, and all films in a given series were heat treated (from the 'wet' state) for identical periods at the same temperature before the determinations. The varnishes and film preparations are described in *Table 1*. The films

Table 1. Description of materials

<i>Varnish</i>	<i>Description</i>	<i>Film preparation</i>	<i>Heat treatment</i> °C
Silicone	A commercial phenyl methyl silicone impregnating varnish containing some drying oil	Initial heat treatment 6 h at 200°C . Film thickness 0.010 in.	200 220 240
Polyester wire enamel	A commercial glycerol, terephthalic acid, ethylene glycol polyester; probably containing catalytic quantities of tetrabutyl titanate and zinc octoate	Initial heat treatment 1 h at 140°C . Film thickness 0.011 in.	200
Polyester XK	A laboratory polyester preparation from glycerol, glycols, terephthalic and isophthalic acids, containing a small proportion of an epoxide resin	Initial heat treatment 16 h at 162°C . Film thickness 0.010 in.	162 176 200 220 240

were then heated in air circulating ovens at temperatures held constant to within $\pm 1^\circ\text{C}$, and $T_{\max.}$ determined at intervals on a ball-rebound instrument in which a 3/32 in. diameter steel ball was dropped repeatedly from a constant height (16.2 cm) on to the film. The film temperature during the determination was obtained from a chromel-alumel thermocouple and

Cambridge temperature indicator; plots of energy absorption (or rebound height) versus film temperature gave $T_{\max.}$ as the temperature of maximum energy absorption (or minimum rebound height).

To test equation (11), $d\theta/dt$ was calculated at 5°C intervals from the smooth curves drawn through the $T_{\max.}/\text{time}$ data, using equation (12) to convert $T_{\max.}$ to θ . It was assumed in these calculations that the slope of the chord between two successive points (θ_1, T_1) and (θ_2, T_2) was equal to the slope of the tangent to the curve at the point whose ordinate was $\frac{1}{2}(\theta_1 + \theta_2)$. Plots of $\log(-d\theta/dt)$ versus $1/(51.6 + \theta)$ for the three systems are shown in *Figures 1* and *2*. The data for polyester XK and silicone varnishes lie on straight lines at the early stages of cure only; when the reactions become advanced [at high values of $1/(51.6 + \theta)$], the plots for each curing temperature diverge, the deviations from linearity occurring at increasing values of $d\theta/dt$ the higher the curing temperature. The slopes were obtained by fitting best straight lines to the points by the least squares method, omitting points obviously beyond the linear portion; they were close to the theoretical value of $ab = -900^\circ\text{C}$; polyester XK -893°C ; silicone -927°C . The single plot for the polyester wire enamel system conforms well to a straight line of slope -987°C although imminent divergence from linearity at high values of $1/(51.6 + \theta)$ is apparent from the trend of the original results⁹.

DISCUSSION

Throughout this paper the term 'cure' has been used to describe the processes occurring during heat treatment of a polyfunctional system. It will be evident, however, that the time scales of the experiments in question were far in excess of those normally employed to obtain useful products, i.e. the accepted technological 'curing' times. In the present cases (except the polyester wire enamel) the systems had been given an appropriate cure *prior* to the experiments and it is important to note that the results are of interest in what is normally called polymer 'ageing'. In some cases the time scales of the experiments were comparable with the useful lifetimes of the materials⁸. The present theory is therefore to be regarded as an aid in rationalizing the kinetic aspects of the ageing of network polymers.

Rate of crosslinking

The points which lie close to the straight lines in *Figures 1* and *2* support the assumption that the curing reactions, over the ranges concerned, are controlled by mobility of chain segments rather than by chemical structure, and that the superposition principle may be applied to these processes.

For linear polymers, Ferry found that the internal mobility often increased more rapidly than equation (1) predicts when θ is increased beyond 100°C . This effect is linked to the loss of viscoelastic properties in favour of purely viscous flow. In crosslinked systems this transition cannot occur, and the linear portion of the plot for the silicone system extends, for example, to $\theta = 150^\circ\text{C}$. It is not known to what limit θ can safely be taken in superposing the viscoelastic functions of crosslinked polymers.

The vertical spacing of the straight lines drawn in *Figures 1* and *2* depends only on the intercepts K in equation (7). According to equation (8), K

varies from system to system mainly as $\log X_{T_g}$ varies, i.e. the logarithm of the rate of cure dT_g/dt that would exist at T_g . This quantity K is not independently measurable, but can be deduced from the spacing of the plots. It is seen by inspection of *Figure 1* that K is about 10^3 times greater in the wire enamel system than in the silicone. This may be because each crosslink introduced into the polyester wire enamel raised T_g by a much larger amount than in the silicone system; however, it is more likely that

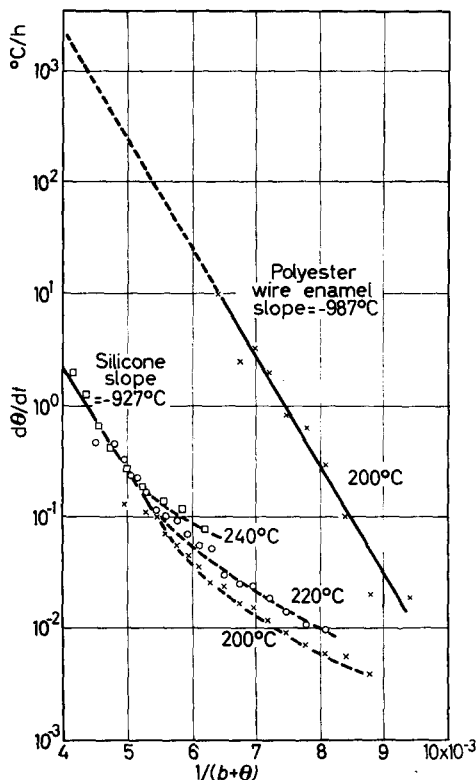


Figure 1—Rate of cure of silicone and polyester wire enamel

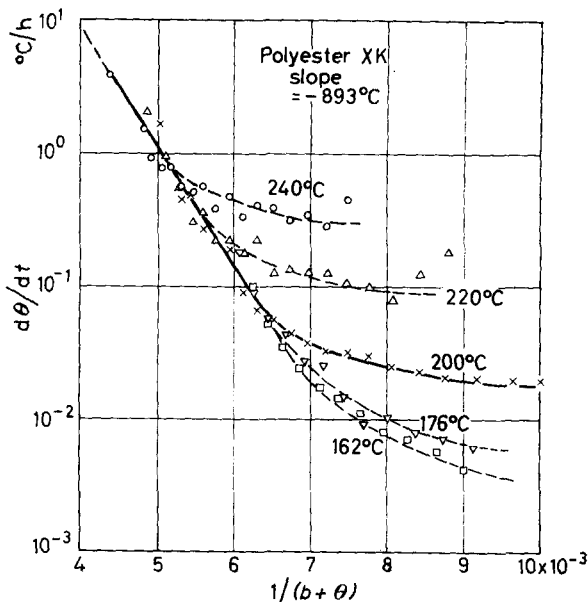
the main reason lies in a much faster absolute rate of increase in the crosslink density in the wire enamel when compared with the silicone system at the same value of θ . Information on absolute rates of crosslinking in various systems undergoing cure remains an important academic and practical objective.

The late stages of cure

The deviations from the theoretical lines in the polyester XK and silicone systems (*Figures 1* and *2*) occur when the reaction is fairly advanced. These deviations may be accounted for by assuming a process of rate K' , independent of T_g and therefore not subject to diffusion control, to be superposed on the main diffusion controlled reaction. On this assumption, equation (11) becomes

$$\log [-(d\theta/dt - K')] = K - [ab/(51.6 + \theta)] \quad (13)$$

Figure 2—Rate of cure of polyester XK



The data pertaining to all the experiments on polyester XK have been replotted on this basis in *Figure 3* and the linearity (slope -771°C) and superposition of this plot support the explanation given. The values of the parameter K' which were chosen are listed in the legend; their variation with temperature—shown in *Figure 4*—corresponds to an activation energy of 25 kcal/mole.

It is well known that diffusion controlled chemical or physical processes may occur side by side with others which are not diffusion controlled. In polymer systems the borderline of diffusion control is generally linked to the size of the chain segments which are involved in various processes, longer chain segments being necessarily slower at diffusing to new locations or configurations. A chemical example is provided by the Trommsdorf effect¹⁰ and a physical example by Rouse's treatment¹¹ of relaxation phenomena such as viscous flow. (This is explicitly based on the notion that short chain-segments are more mobile than whole chains, and in particular the sub-chains diffuse fast enough to maintain a gaussian end-to-end distribution.) Thus the late process with rate K' must involve shorter chain segments than the main earlier process which is diffusion controlled. Probably the late process is oxidative, and possibly it involves merely the introduction of polar substituents on the chains rather than crosslinks between chains. (When observing a rise in T_g , crosslinks need not be involved.) The functionalities deliberately built into the resins for crosslinking are generally rather widely spaced along the chains, while opportunities for oxidative attack occur at short intervals.

In both the silicone and polyester XK systems, the effect of the superposed reaction just attributed to oxidation is swamped by the main diffusion

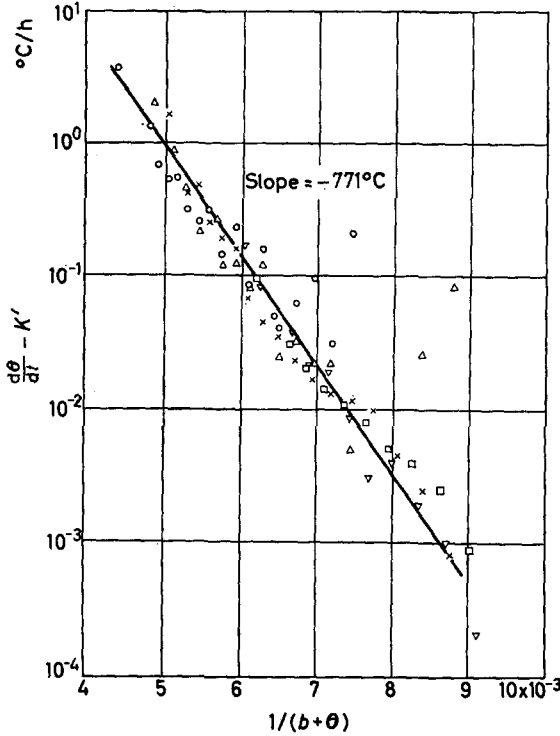


Figure 3—Polyester XK: rate of cure by the diffusion controlled process. At 240°C, $K'=0.25$; 220°C, $K'=0.1$; 200°C, $K'=0.02$; 176°C, $K'=0.006$; and 162°C, $K'=0.0033$

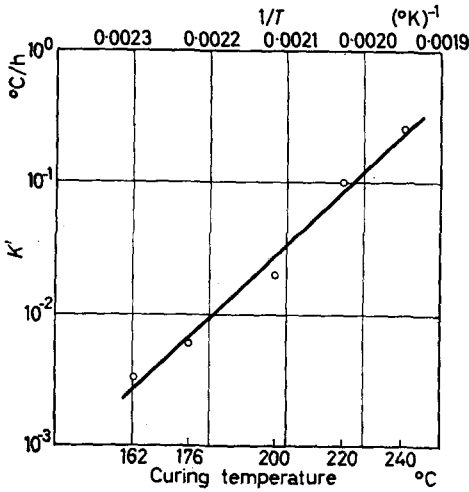


Figure 4—Polyester XK: Arrhenius plot for the superposed process of rate K'

controlled process in the early stages. Oxidative change takes over towards the end when the rise in T_g has effectively frozen out the main process.

The authors wish to thank Dr R. W. Sillars for many helpful discussions and Miss F. Whittaker and Mrs A. Henderson for computing the results. They also wish to thank Sir Willis Jackson, F.R.S., Director of Research, Associated Electrical Industries (Manchester) Limited for permission to publish.

*Chemistry Department, Imperial College
of Science and Technology, London
Research Department, Associated Electrical
Industries (Manchester) Ltd, Trafford Park,
Manchester 17*

(Received May 1961)

REFERENCES

- ¹ LOSHAEK, S. and FOX, T. G. *J. Amer. chem. Soc.* 1953, **75**, 3544
- ² BARRETT, R. M. and GORDON, M. *The Physical Properties of Polymers*, p 183. [Monograph No. 5] Society of Chemical Industry: London, 1959
- ³ TAMMANN, G. *Der Glaszustand*, p 17. Voss: Leipzig, 1933
- ⁴ WILLIAMS, M. L., LANDEL, R. F. and FERRY, J. D. *J. Amer. chem. Soc.* 1955, **77**, 3701
- ⁵ FERRY, J. D., FITZGERALD, E. R., JOHNSON, M. F. and GRANDINE, L. D., Jr. *J. appl. Phys.* 1951, **22**, 717
- ⁶ GORDON, M. *The Structure and Physical Properties of High Polymers*, p 55. Plastics Institute: London, 1957
- ⁷ GORDON, M. and GRIEVESON, B. M. *J. Polym. Sci.* 1958, **29**, 9
- ⁸ BRIDGE, L. and SIMPSON, W. *High Temperature Resistance and Thermal Degradation of Polymers*, p 453. [Monograph No. 13]. Society of Chemical Industry: London, 1961
- ⁹ BRIDGE, L. Unpublished work
- ¹⁰ GORDON, M. and ROE, R-J. *J. Polym. Sci.* 1956, **21**, 57
- ¹¹ ROUSE, P. E., Jr. *J. chem. Phys.* 1953, **21**, 1272

Viscometric Study of the Polyisobutylene–Chlorobenzene System*

H. DAOUST and M. SENEZ

The theta temperature and the interaction parameters have been determined for the polyisobutylene–chlorobenzene system by the viscometric method developed by Fox and Flory (F–F). Improved calorimetric data on the same system (and on the polyisobutylene–benzene and polyisobutylene–toluene systems) give heat parameters which are higher than those calculated according to the F–F treatment. On the other hand, the Kurata–Yamakawa treatment of viscometric data gives interaction parameters which are in better agreement with those determined calorimetrically. A comparison between the two treatments is discussed in this paper.

THE knowledge of the value of the interaction parameters are of first importance to study the behaviour and configurations of macromolecules in solution. Technically, viscometry is by far the easiest way to investigate dilute polymer solutions but the theoretical difficulties encountered in the evaluation of the interaction parameters are considerable in this case and the numerical values obtained depend on the theoretical treatment chosen for the calculations.

The well-known Fox–Flory (F–F) treatment¹ of viscometric data has been widely applied with some success. It gives good relative values of the polymer–solvent interaction parameters from one system to the other. However, comparison of the absolute values with those obtained by more direct methods shows significant differences^{2, 3}. Recently, many investigators^{4–7} have questioned the F–F treatment and have proposed a number of theoretical improvements.

In this work, we have attempted to see how these improvements give values of the interaction parameters in better agreement with our direct calorimetric measurements.

EXPERIMENTAL

Nine polyisobutylene fractions, with viscosity average molecular weights ranging from 93 000 to 2 000 000, have been used in this investigation; they were prepared by the precipitation method⁸. A first cut of a commercial sample of *Vistanex L-100* (generously supplied by Enjay Co. Inc.) has been subsequently fractionated into nine fractions and the first seven of these have been used. The two lower fractions used in this investigation have been obtained from another commercial sample (from Polymer Corporation of Canada) by the same technique.

*This paper has been presented in part at the 9th Canadian High Polymer Forum at Scarborough, Ontario, Canada, 26 to 28 October 1959.

Reagent grade solvents were purified by distillation using a high efficiency column and the concentrations of the filtered solutions were determined by dry weights.

Viscosity measurements were made with a modified Ubbelohde capillary viscometer⁹, at constant temperatures of 12°, 25°, 40° and 54°C. Rate of shear corrections have been applied whenever necessary¹⁰.

The viscosity average molecular weights, \bar{M}_v , of the nine fractions have been determined by measuring the intrinsic viscosity of their cyclohexane solutions¹¹. The intrinsic viscosities in chlorobenzene at the four temperatures are given in *Table 1*.

Table 1. Intrinsic viscosities (in dl/g) of polyisobutylene fractions in chlorobenzene at different temperatures

$\bar{M}_v \times 10^{-6}$	Temperature, °C			
	12	25	40	54
1.99	2.83	3.16	3.46	3.75
1.75	2.64	2.94	3.29	3.45
1.44	2.33	2.62	2.78	(3.11)*
1.24	2.11	2.36	2.59	2.79
0.97	(1.82)*	2.05	2.29	2.42
0.73	1.50	1.77	1.93	2.05
0.485	(1.19)*	1.35	1.49	1.57
0.157	0.62	0.65 ₅	(0.72)*	0.74
0.093	0.43	0.48	0.50	0.54
$K' \times 10^4$	4.01	3.62	3.60	3.20
a	0.611	0.627	0.634	0.648

*Interpolated.

The variation of the intrinsic viscosity with molecular weight at each temperature can also be represented by a Mark-Houwink relation. The parameters K' and a are given at the bottom of the table.

RESULTS AND DISCUSSION

The thermodynamic parameters of the polyisobutylene-chlorobenzene system can be calculated from the data of *Table 1*. Their values will depend on the theory used for the calculations. In this paper, we want to compare two treatments, the well-known Fox-Flory treatment and the more exact theory recently put forward by Kurata and Yamakawa⁵.

The Fox-Flory treatment

The well-known equations of this treatment are the following :

$$[\eta] = KM^{\frac{1}{2}}\alpha^3 \quad (1)$$

and

$$\alpha^5 - \alpha^3 = 2C_M\psi_1(1 - \theta/T)M^{\frac{1}{2}} \quad (2)$$

where K is defined by Φa_0^3 or $\Phi(\bar{r}_0^2/M)^{3/2}$ and C_M by $1.42 \times 10^{-24} \bar{v}_2^2/V_1 a_0^3$. α is the linear expansion factor of the chain due to polymer-solvent interaction characterized by the entropy parameter ψ_1 and by the enthalpy

parameter $\kappa_1 (= \psi_1 \theta / T)$, where θ is the Flory temperature, Φ is a universal constant for linear high polymers of which the mean value is 2.1×10^{21} , a_0 is a structural constant for the unperturbed polymer chain, $(\bar{r}_0^2)^{\dagger}$ being its r.m.s. end-to-end distance, \bar{v}_2 is the partial specific volume of the polymer and V_1 is the molar volume of the solvent.

Thus, in the F-F treatment one determines first the value of K for a given polymer as a function of temperature in a series of θ -solvents (where $\alpha=1$ for all M) and then one obtains the value of α as a function of T and M in a given solvent. By applying this treatment to our data (using the accepted value of K for polyisobutylene¹²) we find $\theta = 261 \pm 2^\circ \text{K}$; the mean value of κ_1 is given in Table 2. The variation of ψ_1 or κ_1 with M , as shown in Figure 1, found by the F-F treatment is general and has been noted for

Table 2. Heat of dilution parameters for polyisobutylene solutions at 25°C

Solvent	Calorimetric	Viscometric	
		Fox-Flory	Kurata-Yamakawa
Chlorobenzene	$0.29 \pm 0.04^*$	$0.13 (0.11)^\ddagger$	0.28 ± 0.02
Toluene	$0.31 \pm 0.04^*$	$0.12^\ddagger (0.10)^\ddagger$	0.28 ± 0.02
Benzene	$0.28 \pm 0.02^*$	$0.15^\ddagger (0.13)^\ddagger$	0.29 ± 0.02

*SENEZ, M. and DAoust, H. To be published.

†See ref. 12.

‡With $\Phi = 2.6 \times 10^{21}$.

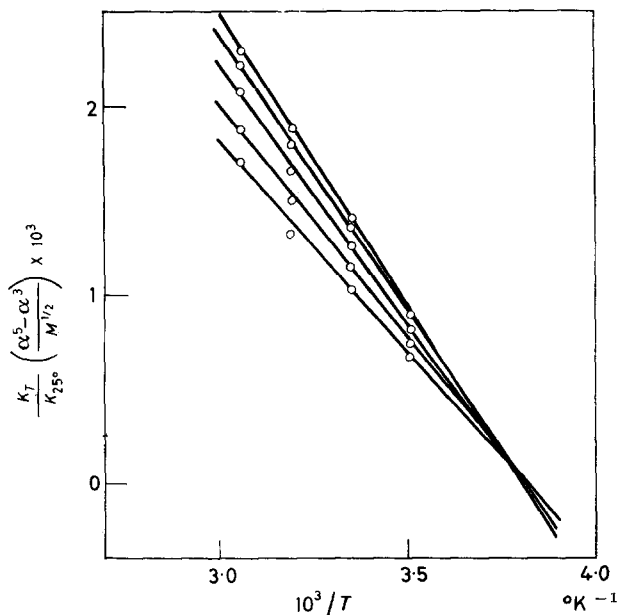


Figure 1—Variation of the slope ($2C_M(25^\circ\text{C})\psi_1\theta$ from equation 2) with molecular weight for five selected values of \bar{M}_v : 2×10^6 (lower curve), 1×10^6 , 5×10^5 , 2×10^5 and 1×10^5 (upper curve)

practically all the systems studied. It is of course attributable to the approximations used in the theory. We can also note that this variation is predictable from equations (1) and (2) and from the fact that the experimental data can be represented, within experimental error, by a Mark-Houwink relation with constant parameters for the whole range of molecular weights studied. In *Table 2*, the parameters found for benzene and toluene¹² are also given.

The parameters θ and ψ_1 or κ_1 can also be evaluated by the excess osmotic pressure as a function of temperature in the neighbourhood of the θ temperature. In general, both methods give practically the same value for θ but not for ψ_1 and this is where the F-F theory fails. The reason for this is twofold: equation (1) is derived from the Kirkwood-Riseman (K-R) theory¹³ of intrinsic viscosity where the distribution of the polymer configurations is assumed to be Gaussian, and because of the further assumption of a uniform distribution of segments in calculating the excluded volume effect on α as given by equation (2).

It can be said that the K-R theory of intrinsic viscosity is, at least semi-quantitatively, verified by the proportionality between $[\eta]$ and $M^{\frac{1}{2}}$ in a θ solvent although this proportionality should (but does not¹⁴) cease when the molecular weight becomes lower. This problem is far from being resolved since there is also some evidence confirming the K-R theory⁵. But, since it is known that at temperatures different from θ the configuration distribution does not remain Gaussian, it is not surprising that equations (1) and (2) are only approximate.

However, the exact calculation of α and $[\eta]$ for a non-Gaussian chain is very difficult and present theories give only the first terms of their infinite series expansion in terms of the excluded volume.

The Kurata-Yamakawa theory

Kurata, Yamakawa and Teramoto¹⁵ have succeeded in obtaining the first terms in the series expansion for α in agreement with results obtained by other approaches¹⁶ as well as with experimental results. Later, Kurata and Yamakawa⁶ have derived an equation for the intrinsic viscosity which is as follows

$$[\eta] = \Phi_0(X) a_0^3 M^{\frac{1}{2}} [1 + p_1(X) z - \dots] \quad (3)$$

where $\Phi_0(X) a_0^3$ is equal to F-F's K when M is sufficiently large, X is the draining parameter and $p_1(X)$, a viscosity function which varies between 1.276 for $X=0$ and 1.55 for $X=\infty$. z represents the excluded volume variable given by

$$z = (6/\pi)^{\frac{1}{2}} (b_0/a_0)^3 (1 - \theta/T) M^{\frac{1}{2}} \quad (4)$$

or, in Flory's symbolism,

$$z = 1.096 \times 10^{-24} \bar{v}_2^2 (\psi_1 - \kappa_1) M^{\frac{1}{2}} / V_1 a_0^3 \quad (4')$$

To make a more explicit comparison with equation (1), they use the following expression for α

$$\alpha^2 = 1 + (134/105) z - \dots \quad (5)$$

and obtain by eliminating z between (3) and (5)

$$[\eta] = KM^{\frac{1}{2}} \alpha^{n(X)} \quad (1')$$

where $n(X) = 2(105/134)p_1(X)$. The exponent $n(X)$ has a maximum value of 2.43, as predicted by the theory, which is in agreement with that found by light-scattering data near the θ temperature^{3, 17}.

The values of the parameters obtained from the K-Y treatment depend of course on the exact value of $p_1(X)$ but we can see in *Table 2* that enthalpy parameters calculated using equation (3) with $p_1(X)$ of ref. 5 are in good agreement with calorimetric determinations*. The use of a somewhat higher value for $p_1(X)$ would decrease all parameters by about 10 per cent¹⁸.

Since equation (3) is valid only near the θ temperature, we cannot apply it directly if data are not available in the vicinity of the θ temperature. Thus, we have either to extrapolate apparent values of ψ_1 using lower and lower M_s (or z) or to establish an empirical general plot of $[\eta]/[\eta]_\theta$ versus $p_1(X)_z$

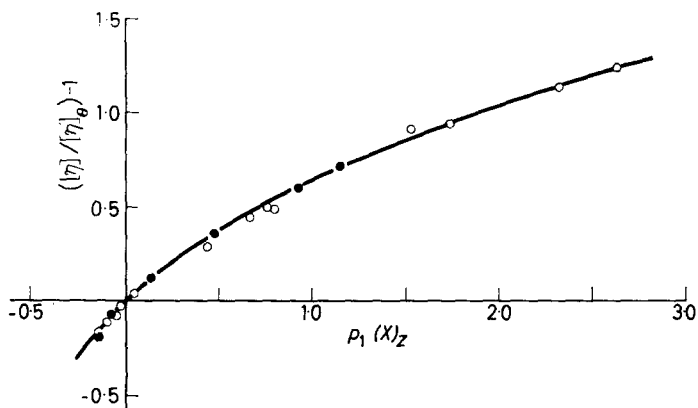


Figure 2—Viscosity function curve used in the calculations of the interaction parameters. Open circles, polyisobutylene-benzene¹²; closed circles, polystyrene-cyclohexane³

as in *Figure 2* using systems where θ temperatures are more easily attained (polyisobutylene-benzene in our case) since in such cases ψ_1 and θ are known and can be used to evaluate z for any other temperature or molecular weight. Those two methods should yield the same values but the second is more appropriate and has been used in this investigation. It should be pointed out that the absolute value of the enthalpy parameter κ_1 can be calculated from calorimetric measurements only after the establishment of such a general curve of the 'excluded volume' function occurring in the second virial coefficient, that is, the observable heat of dilution in infinitely dilute solution.

*The previous values of κ_1 reported by us at the 9th Canadian High Polymer Forum have been redetermined using a better mixing technique.

The absolute value of a_0

It is evident either from equation (1) or (3) that the viscosity analysis gives θ and the ratio ψ_1/a_0^2 . The question then arises whether we have reliable values for the structural constant a_0 or, if we have measured K , whether we have a reliable value for Φ . Since it has been shown that equation (1) is incorrect, the mean value calculated therefrom for $\Phi (=2.1 \times 10^{21})$ must also be incorrect. Indeed, if a_0 is measured directly by light scattering, a higher value is found for Φ in better agreement with the corrected⁵ value from the K-R theory. For polystyrene, the calculated value for a_0 with F-F's Φ is $0.73_5 \times 10^{-8}$ whereas the mean experimental value³ is 0.70×10^{-8} corresponding to $\Phi = 2.4 \times 10^{21}$. For polyisobutylene, the datum obtained with a very sharp fraction in ethyl *n*-octanoate¹⁹, a few degrees above θ , yields $a_0 = 0.76 \times 10^{-8}$ if the measured radius of gyration is corrected to the θ temperature and if a value of 7.25×10^5 is used for M [the required value of ψ_1 in equation (4') has been measured by the authors]. Another datum has been obtained in a mixed solvent¹⁷ and also gives $a_0 = 0.76 \times 10^{-8}$ if the more probable value of $M = 2.5 \times 10^6$ is used in accordance with the measured value of $[\eta]$ in *n*-heptane¹² and if the heterogeneity is taken into account.

At the same time, it should be realized that the assumption making K (or a_0) independent of solvent used is not justified and that variations have been predicted²⁰ and found experimentally²¹. The variation of a_0 with temperature, which is the first thing sought in the F-F treatment, might then be only apparent since it is obtained by using θ solvents somewhat different chemically. In fact, the variation of K with temperature is ill-defined¹². Furthermore, Kunst's¹⁷ viscosity and light-scattering data at two temperatures indicate an increase of a_0 with temperature corresponding to an energy barrier opposing more extended configurations; this is also in agreement with the fact that, for polyisobutylene in cyclohexane where $[\eta]$ is remarkably constant with temperature, a decrease of K or a_0 with temperature implies a positive enthalpy parameter as calculated by Fox and Flory, whereas the experimental heat parameter is negative though very small²². The same applies to the polyisobutylene-*n*-heptane system where a value of zero is assigned to θ by Fox and Flory while the experimental value of the enthalpy parameter is more negative than with cyclohexane²². However, for the aromatic solvents where the heat parameters are positive and much larger, this small temperature effect on a_0 is not important and a_0 can even be considered as a constant. More systematic parallel measurements of viscosity and light scattering in a series of homologous θ solvents would yield more information on that interesting configuration problem.

Thus, a value of $a_0 = 0.76 \times 10^{-8}$ has been used instead of $0.79_5 \times 10^{-8}$ as calculated with $\Phi = 2.1 \times 10^{21}$. If that value is used in applying the F-F treatment, still lower values of κ_1 are found (as shown in parentheses in Table 2).

CONCLUSION

The more exact theory of Kurata and Yamakawa is quite satisfactory and can be used to obtain absolute values of thermodynamic parameters. The

new theory of configuration by Kurata, Stockmayer and Roig⁷ is also very interesting but since there is no expression in closed form for $[\eta]$, it cannot be verified in a non-equivocal manner from viscosity data, although there are some cancellations in the higher terms of equations (3) and (5). However, light scattering would be suitable as a means of testing their new equation in comparison with Flory's approximate equation (2) or alternatively, if equation (1') is established from light scattering (for large z), it could then be verified from viscosity.

We wish to thank the National Research Council of Canada for the generous financial assistance in this investigation. We also thank the Scientific Research Bureau of the Province of Quebec for the award of a bursary to M.S. while doing this research.

Department of Chemistry,
University of Montreal,
P.O. Box 6128, Montreal, P.Q., Canada

(Received May 1961)

REFERENCES

- ¹ FOX, T. G. and FLORY, P. J. *J. Amer. chem. Soc.* 1951, **73**, 1904
- ² FLORY, P. J. and KRIGBAUM, W. R. *J. Amer. chem. Soc.* 1953, **75**, 5254
KRIGBAUM, W. R. *J. Amer. chem. Soc.* 1954, **76**, 3758
- ³ KRIGBAUM, W. R. and CARPENTER, D. K. *J. phys. Chem.* 1955, **59**, 1166
- ⁴ STOCKMAYER, W. H. *J. Polym. Sci.* 1955, **15**, 595
- ⁵ KURATA, M. and YAMAKAWA, H. *J. chem. Phys.* 1958, **29**, 311
- ⁶ PTTITSYN, P. B. and EIZNER, YU. E. *J. phys. Chem. (U.S.S.R.)*, 1958, **32**, 2464
- ⁷ KURATA, M., STOCKMAYER, W. H. and ROIG, A. *J. chem. Phys.* 1960, **33**, 151
- ⁸ FLORY, P. J. *J. Amer. chem. Soc.* 1943, **65**, 372
- ⁹ HENDERSON, D. A. and LEGGE, N. R. *J. Polym. Sci.* 1956, **19**, 215
- ¹⁰ FOX, T. G., FOX, J. C. and FLORY, P. J. *J. Amer. chem. Soc.* 1951, **73**, 1901
- ¹¹ KRIGBAUM, W. R. and FLORY, P. J. *J. Amer. chem. Soc.* 1953, **75**, 1775
- ¹² FOX, T. G. and FLORY, P. J. *J. Amer. chem. Soc.* 1951, **73**, 1909
- ¹³ KIRKWOOD, J. G. and RISEMAN, J. *J. chem. Phys.* 1948, **16**, 565
- ¹⁴ KRIGBAUM, W. R. and FLORY, P. J. *J. Polym. Sci.* 1953, **11**, 37
- ¹⁵ KURATA, M., YAMAKAWA, H. and TERAMOTO, E. *J. chem. Phys.* 1958, **28**, 785
- ¹⁶ ZIMM, B. H., STOCKMAYER, W. H. and FIXMAN, M. *J. chem. Phys.* 1953, **21**, 1716
- ¹⁷ KUNST, E. *Rec. Trav. chim. Pays-Bas*, 1950, **69**, 125
- ¹⁸ KURATA, M. and YAMAKAWA, H. *J. chem. Phys.* 1960, **32**, 1852
- ¹⁹ NEWMAN, S., KRIGBAUM, W. R., LAUGIER, C. and FLORY, P. J. *J. Polym. Sci.* 1954, **14**, 451
- ²⁰ LIFSON, S. and OPPENHEIM, I. *J. chem. Phys.* 1960, **33**, 109
- ²¹ SCHULTZ, A. R. *Thesis*, Cornell University, 1953
- ²² WATTERS, C., DAoust, H. and RINFRET, M. *Canad. J. Chem.* 1960, **38**, 1087

Effect of Radiation and Moisture on the Dynamic Mechanical Properties of Polyethylene Terephthalate

D. E. KLINE* and J. A. SAUER†

Studies of effects of nuclear radiation on the dynamic mechanical properties of a series of polyethylene terephthalate specimens are reported. The investigations cover a temperature range from 80° to 530° K and a frequency range from about 100 to 1300 cycles/sec. Radiation doses greater than 10⁹ rads significantly decrease the temperature of the main glass transition and cause other changes in the internal friction spectra. Addition of water also causes a shift of the glass transition to lower temperatures.

IN RECENT years, several investigations have been reported in the literature concerning the dynamic mechanical properties of polyethylene terephthalate and other related glycol terephthalate polymers¹⁻³. Nuclear magnetic resonance (n.m.r.) studies have also been carried out to study transitions in polyethylene terephthalate and closely related polymers over a wide temperature range⁴⁻⁶. Reddish has reported results of investigations concerning the dielectric properties as a function of frequency and temperature⁷. Little⁸ has shown by X-ray techniques that the polymer is quite resistant to ionizing irradiation and that extensive bridge formation does not result from such treatment. Todd⁹ has shown that pile irradiation dosages up to 450 Mr cause little change in intrinsic viscosity.

It is the purpose of this paper to present and discuss results obtained by studies of the dynamic mechanical properties of a series of irradiated polyethylene terephthalate specimens over the temperature range of 80° to 530°K and at frequencies from about 100 to 1300 c/s. Specimens tested have been subject to irradiation doses in a nuclear reactor ranging up to approximately 4×10^{11} erg/g. Some effects of moisture absorption have also been investigated.

EXPERIMENTAL

The test specimens used in this investigation were turned from injection moulded rods to about 4.40 in. in length and 0.250 to 0.340 in. in diameter. Properties of the polyethylene terephthalate as given by the supplier are density 1.386 g/cm³, crystallinity 52 per cent, and $M_n = 25\,000$. All dynamic mechanical measurements were made using a modified version of an apparatus described elsewhere¹⁰. In this apparatus, rodlike specimens are supported horizontally by two vertical lines. One line, coupled to a transducer, drives the specimen in the first transverse mode while a second line, attached to a detecting device, notes the specimen response. Measurement

*Nuclear Engineering Department, The Pennsylvania State University.

†Physics Department, The Pennsylvania State University.

of the width of the response curve can be used to determine the internal friction, Q^{-1} , by the relation $Q^{-1} = \Delta f / f_0$, where Δf is the 3 dB frequency separation and f_0 is the resonant frequency.

Using the specimen dimensions and the mass, the dynamic modulus can be calculated from the resonant frequency, f_0 . Throughout this investigation, the calculations of dynamic elastic moduli have been made using room temperature values of the dimensions and density. The values obtained are thus nominal values only, as expansion effects have been neglected. It has been shown¹¹ for polyethylene that the error involved from this source is small (< 3 per cent) over the whole temperature range except in the region near the melting temperature. It is estimated that, in this region, the error may rise to 5 to 6 per cent with the true value of the modulus being lower than the nominal one.

Sample irradiations were carried out at the Pennsylvania State University Nuclear Reactor Facility. This is a water-moderated and shielded, heterogeneous, enriched-uranium reactor of the 'pool' type which is described elsewhere¹². Samples were placed in aluminium irradiation containers and lowered into position at the core face. Calculations and experiments^{13, 14} have been made to determine the energy deposited by reactor radiation in polymers similar to polyethylene terephthalate in isotopic percentages, under comparable irradiation conditions. From these one can estimate that for polyethylene terephthalate other radiations (principally fast neutrons) deposit less total energy than the accompanying gamma rays for the irradiation position used. In this case, the ratio of energy deposited by gamma interactions to energy deposited by fast neutrons is about 2:1.

For the PSU Reactor operating at 100 kW the rate of energy deposited (total) for the irradiation position used is about 0.7×10^9 erg/g-h. In

Table 1. Characteristics of polyethylene terephthalate specimens

Specimen	Size		Water content per cent	Total irradiation dose erg/g	History
	Length in.	Diam. in.			
1	4.40	0.340	—*	None	—
2	4.36	0.250	0.00	None	Dried > 150 h at 70°C under vacuum
3	4.37	0.250	0.88	None	Dried > 150 h at 70°C under vacuum, then im- mersed in water at 70°C for > 150 h
4	4.40	0.341	—*	1.2×10^{10}	
5	4.39	0.340	—*	3.6×10^{10}	
6	—†	—†	—*	9.0×10^{10}	
7	4.39	0.340	0.00	18×10^{10}	Dried > 150 h at 70°C, and, after testing from 77° to 300°K, sealed in container before irradi- ation
8	4.34	0.340	—*	37×10^{10}	

*Unconditioned.

†Approximate size 4.4 in. length by 0.34 in. diameter.

Table 1 the total dose in erg/g is given along with the identification of all specimens tested. Because of the substantial rate of energy deposition in polymer materials, the temperature of the specimens rises somewhat above the pool temperature. Based on measurements made on other samples, under somewhat similar conditions, this specimen temperature is estimated to be about 25°C above the reactor pool temperature. For irradiations discussed in this paper, the pool temperature was near 25°C.

RESULTS

The dynamic mechanical data obtained for a sample of un-irradiated as received polyethylene terephthalate are given in *Figure 1* (sample 1), along with the data for two other treated samples (numbers 2 and 3). Results for the internal friction of sample 1 indicate that at least three principal dispersion regions exist in agreement with previously reported data^{1, 2} obtained using a different type of apparatus. A low temperature damping peak is present near 240°K, a large loss peak is present near 380°K, and, above 480°K, the damping again rises as the region of crystallite melting is approached. A corresponding drop and/or an inflection point is noted in the elastic modulus for each of these temperature regions.

(A) Effect of moisture content

To observe the effect of absorbed water on the dynamic mechanical properties, samples 2 and 3 were dried under vacuum near 70°C (see

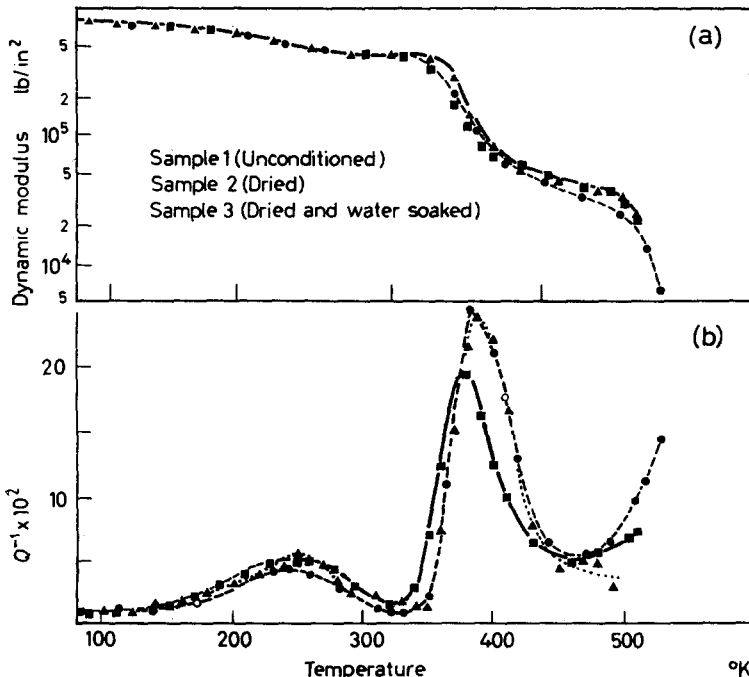


Figure 1—Dynamic modulus and mechanical loss (Q^{-1}) for unconditioned (●), dried (▲), and dried and water soaked (■), polyethylene terephthalate specimens

Table 1). Sample 3 upon subsequent immersion in water at 70°C absorbed about 0.8 per cent water. The results of the dynamic mechanical tests for these two samples are also given in Figure 1 and the change in water content as a function of treatment time is presented in Figure 2. During the testing from 80° to 300°K, little water was lost by sample 3 but during the high temperature tests (300° to 530°K) the water content dropped to 0.2 per cent.

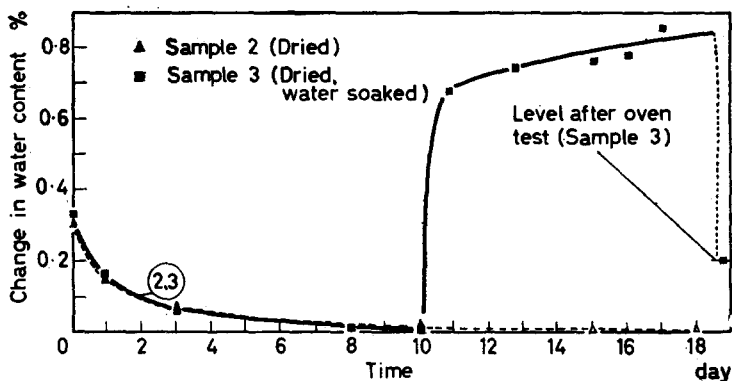


Figure 2—Change in water content of unconditioned specimens with treatment. Sample 2 (\blacktriangle) dried under vacuum at 70°C for 18 days. Sample 3 (\blacksquare) dried under vacuum at 70°C for 10 days, then water soaked at 70°C for 8 days

As a result of the drying treatment, in which the water content was reduced compared to the specimen as received by approximately 0.3 per cent, several changes are apparent in the dynamic mechanical data. The low temperature peak has increased slightly in height, and possibly shifted to a slightly higher temperature. The main damping peak near 380°K has changed little if any in size. The final transition in the temperature region above 450°K shows a slight shift in both damping and modulus data to still higher temperatures, probably as a consequence of increased crystallinity.

For sample 3, where the water content was increased more than 0.8 per cent beyond the dried water content value, the low temperature peak ($\sim 250^\circ\text{K}$) is somewhat increased in value from that of the unconditioned sample (1). Kawaguchi³ has observed a similar increase in undrawn monofilament upon addition of 0.8 per cent water. Our data also show that the primary damping peak is noticeably shifted to lower temperatures with added water and the area under the peak is somewhat decreased. The inflection point in the modulus curve, which appeared at a higher temperature for the dried sample, as compared to the unconditioned sample, now appears at a lower temperature, consistent with the shift in the damping curves.

(B) Radiation effects

In Figure 3 are given the data for samples as received subjected to different irradiations. Sample 1 (unconditioned) data are also shown for comparison. For sample 4 (irradiated to 1.2×10^{10} erg/g), little, if any, change from sample 1 is noted in the modulus and damping values over

most of the temperature range (80° to 400°K). At higher temperatures, there is also little change in modulus, but one significant change is that the damping in the region from about 475° to 520°K no longer rises continuously but comes to a maximum value near 515°K and then falls.

The higher irradiations of sample 5 (3.6×10^{10} erg/g) and sample 6 (9×10^{10} erg/g) result in changes in damping and modulus which are not appreciably different from those of sample 4 except in the high temperature region. Increased dosage seems to cause a shift of the internal friction peak near 515°K to somewhat lower temperatures. For example, this peak shifts

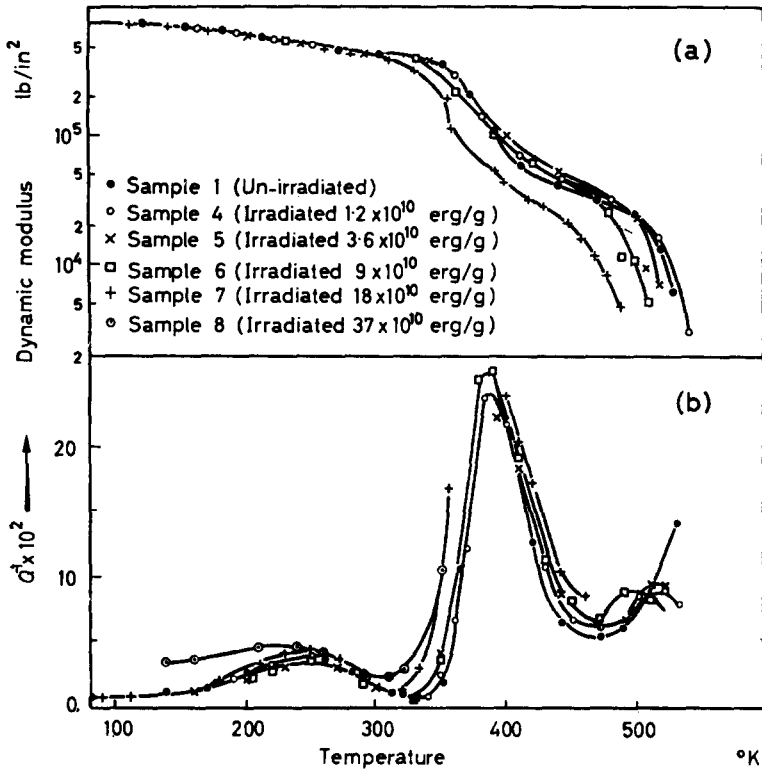


Figure 3—Effect of pile irradiation on the dynamic modulus and mechanical damping (Q^{-1}) of polyethylene terephthalate specimens

from 515°K for sample 4 to 495°K for sample 6. As the irradiation dose increases (samples 4 to 6) the modulus drop, in the region of 515°K, also occurs at lower temperatures, compatible with the shift in the internal friction peaks.

Test measurements were also made on a sample (7) irradiated to 18×10^{10} erg/g. Here the change, upon increased irradiation, of position of the high temperature modulus drop already noted above becomes even more striking. It is also apparent from the data that the modulus drop in the intermediate temperature region ($\sim 330^\circ\text{K}$) occurs at lower temperatures for the irradiated sample. This effect is also visible in the associated

damping data as the primary loss peak begins to rise at temperatures 15° to 20° below that for the un-irradiated specimen. In the temperature region below 300°K there is little change in either modulus or damping as a result of the irradiation. Another sample (8) was irradiated to a still higher dose (37×10^{10} erg/g). This sample became very brittle during irradiation and broke (at 360°K) while the measurements were being made. It appears from the data that the background damping below 240°K has increased from the level of the other samples. A more significant change, however, is that the onset of the large damping peak occurs at still lower temperatures than for the other irradiated samples or even for the high moisture content sample (3).

DISCUSSION

The mechanical loss spectrum of polyethylene terephthalate is generally characterized by three damping regions. From X-ray measurements and other data⁴ it is concluded that there is very little contribution to the loss mechanism from movements within the crystallites until the beginning of the melting range. This is in agreement with the observation that the loss mechanisms of polymers generally arise from the movements of parts of the molecular chains in the amorphous regions¹⁵.

Bateman *et al.*⁴ have investigated the shift of the loss peaks with temperature that occurs on increasing the number of the CH₂ groups in the glycol portion of the molecule to form other terephthalate polymers. As the number of CH₂ links is increased from 2 in polyethylene terephthalate to 3, 4, 5, 6, 9 and 10, the lower loss peak temperature decreases from -30°C or about 240°K to -125°C or about 150°K. The latter is near the temperature of the low temperature peak in polyethylene¹¹, and, in polyethylene, is attributed to molecular rotations and configurational changes of a relatively small number of flexible CH₂ links. A similar situation evidently prevails in polyethylene terephthalate, but the loss peak temperature is higher because of the restrictions to motions of the aliphatic part of the chain caused by the presence of the phenylene groups. From the fact that little, if any, change occurs in this low temperature peak upon irradiation, at least up to doses of 18×10^{10} erg/g, one may conclude that the irradiation has little effect on the mobility of the short chain segments between phenylene groups.

The main damping peak near 380°K is associated^{1, 2} with the motion of a larger number of segments in the amorphous regions, probably involving at least the phenylene carbonyl bond in addition to the glycol residue. Reddish⁷ has also noted this peak and its behaviour with frequency and temperature in dielectric measurements. From the data of the preceding section, it is observed that this peak shifts to lower temperatures with added water content. This shift of the glass-rubber transition is analogous to the plasticizing effect noted in other polymers, for example nylon 6-6¹⁶ when water or other small molecules are added. In 6-6 nylon, the temperature shift is much greater, but the amount of water which nylon absorbs under similar conditions is also much greater.

The effect of irradiation on this primary transition appears to be mostly a broadening effect. As seen in *Figure 3*, the onset of the transition occurs

at lower temperatures with increased dose, and in the temperature range above 430°K the damping decreases somewhat more slowly with temperature. The irradiation appears to be loosening parts of the amorphous structure possibly as a result of some chain scission.

The rise in the damping at temperatures of 500°K and above is attributed to the large scale movements associated with the onset of melting of the crystallites in the polymer. *Figure 3* shows that irradiation produces two effects. The first effect is the occurrence of a peak rather than a monotonic rise as in the un-irradiated specimen. One explanation of this may be the occurrence of some radiation-induced crosslinking which would tend to form a 3-dimensional network and thereby prevent macroscopic slippage of one chain past another. Charlesby has also reported some crosslinking effects in earlier work¹⁷. Normally crosslinking would be expected at high temperatures to produce a rise in elastic modulus. This effect is not seen in *Figure 3* possibly because the crosslinking density is itself not high enough to prevent excessive sagging of the rodlike specimen at these high temperatures. Furthermore any chain scission produced by the irradiation tends to limit the chain lengths. The second effect, clearly visible in both the damping and the modulus data, is to cause a decrease in the melting temperature of the crystallites. This effect is probably a direct result of radiation-induced defects in the crystallites. A similar effect has been observed in both branched and linear polyethylene¹⁸.

The authors wish to acknowledge the assistance of C. Volz, Jr, C. F. Smith, and J. Tomlinson in preparing samples and making experimental measurements, and to thank Professor A. E. Woodward for comments. Dr H. W. Starkweather, Jr of the Polychemical Department of E. I. Dupont de Nemours and Company supplied the polyethylene terephthalate material. The cooperation of the staff of the Pennsylvania State University Nuclear Reactor Facility in carrying out the irradiations is greatly appreciated. This research was supported in part by the U.S. Atomic Energy Commission.

*Pennsylvania State University,
University Park, Pennsylvania*

(Received July 1961)

REFERENCES

- ¹ THOMPSON, A. B. and WOODS, D. W. *Trans. Faraday Soc.* 1956, **52**, 1383
- ² FARROW, G., McINTOSH, J. and WARD, I. M. *Makromol. Chem.* 1960, **38**, 147
- ³ KAWAGUCHI, T. J. *Polym. Sci.* 1958, **32**, 417
- ⁴ BATEMAN, J., RICHARDS, R. E., FARROW, G. and WARD, I. M. *Polymer, Lond.* 1960, **1**, 63
- ⁵ LAND, R., RICHARDS, R. E. and WARD, I. M. *Trans. Faraday Soc.* 1959, **55**, 225
- ⁶ WARD, I. M. *Trans. Faraday Soc.* 1960, **56**, 648
- ⁷ REDDISH, W. *Trans. Faraday Soc.* 1950, **46**, 459
- ⁸ LITTLE, K. *Nature, Lond.* 1952, **170**, 1075; 1954, **173**, 680
- ⁹ TODD, A. *Nature, Lond.* 1954, **174**, 613
- ¹⁰ KLINE, D. E. *J. Polym. Sci.* 1956, **22**, 449

- ¹¹ MERRILL, L. J., SAUER, J. A. and WOODWARD, A. E. *Polymer, Lond.* 1960, **1**, 351
- ¹² JACOBS, A. M., KLINE, D. E. and REMICK, F. J. *Basic Principles of Nuclear Science and Reactors*. Van Nostrand: New York, 1960
- ¹³ KLINE, D. E. and JACOBS, A. M. *J. appl. Phys.* 1959, **30**, 1741
- ¹⁴ JACOBS, A. M. and KLINE, D. E. *J. appl. Polym. Sci.* (To be published)
- ¹⁵ WOODWARD, A. E. and SAUER, J. A. *Fortschr. Hochpolymer Forsch.* 1958, **1**, 114
- ¹⁶ WOODWARD, A. E., CRISSMAN, J. M. and SAUER, J. A. *J. Polym. Sci.* 1960, **44**, 23
- ¹⁷ CHARLESBY, A. *Nature, Lond.* 1953, **171**, 167
- ¹⁸ CHARLESBY, A. and CALLAGHAN, L. *J. Phys. Chem. Solids*, 1958, **4**, 306

The Measurement of Crystallinity in Polypropylene Fibres by X-ray Diffraction

G. FARROW

A method has been devised for the measurement of crystallinity in oriented polypropylene fibres by an X-ray technique. The general level of crystallinity is higher than in similar oriented poly(ethylene terephthalate) fibres. The results also show that the crystallinity so measured is lower than values inferred from density measurements and that no correlation exists between the two methods. A possible method is suggested for the determination of the atactic content of polypropylene polymer by X-ray diffraction.

BECAUSE of its considered importance in determining physical properties of textile fibres various physical methods have been proposed and developed for the measurement of crystallinity in polymers and fibres. Amongst these was an X-ray method for the measurement of the degree of crystallinity in oriented poly(ethylene terephthalate) fibres¹. This has now been adapted to the measurement of the degree of crystallinity in oriented polypropylene fibres.

EXPERIMENTAL

(i) *Sample preparation*

The material used for this work was polypropylene filaments and chip of varying crystallinity. The filaments used in this investigation were prepared by a conventional two-stage process². Molten polymer is first extruded and collected as filaments with slight molecular orientation. Filaments of high orientation are then produced by the application of continuous extension to a pre-set limit. This second drawing stage is carried out by a machine which, in essence, consists of two pairs of rolls with either one or two heating devices in between; the temperature of one heating device is maintained at 95°C and the other, when used, at 145°C. One pair of rolls feeds the undrawn filaments from the spinning machine forward at a constant rate and the second pair moves at a higher velocity, drawing the filaments over the heated surface(s). Filaments of different draw ratios (i.e. ratios of velocity of feed rolls to velocity of draw rolls) were produced by this method.

A further treatment of all the filaments, to give an additional set of samples, was carried out in a vacuum oven at 145°C for half an hour.

(ii) *X-ray determination of crystallinity*

The experimental technique is similar to that already described in detail for the measurement of the degree of crystallinity in oriented poly(ethylene terephthalate) fibres¹. Only a brief summary is, therefore, given here.

Oriented fibres are chopped and made into a randomized sample by a pelleting technique. The preparation of the pellet is rather more critical than

with oriented poly(ethylene terephthalate) fibres for if the fibre is insufficiently randomized quite significant changes occur in the ratios between the principal X-ray reflections when compared with similar measured ratios from a sample of heat crystallized unoriented polypropylene yarn, used as a standard. The prepared sample is placed on the circumference of a focusing camera (evacuated to eliminate 'air scatter') and exposed to a strictly monochromatic beam of X-rays (quartz bent crystal monochromator). The X-ray diffraction lines are recorded on film, which, after processing and drying, is scanned by a microdensitometer. From the resultant trace the crystallinity is determined by measuring the integrated area of the crystalline reflections and the integrated area of the non-crystalline background and comparing the two. With the microdensitometer in use the total area of the trace can be determined automatically³. In order to determine the non-crystalline or amorphous background, however, when the X-ray reflections from the crystalline and amorphous regions overlap as in polypropylene, it is necessary to obtain a diffraction pattern of an amorphous specimen of the same type of material. The trace from this is then used as a template for drawing in the non-crystalline background.

X-ray photographs of polypropylene samples at high temperatures in the melt were obtained and used for this purpose. The samples were held in the inner chamber of the X-ray furnace⁴ (*in vacuo*) in a small cylindrical container made of aluminium foil 0.0005 in. in thickness with a thermocouple placed in contact with one end of the sample. With Cu K_α X-ray radiation (strictly monochromatic, in this case), the absorption of the primary X-ray beam by this thickness of aluminium is negligible. Furthermore, any X-ray diffraction pattern produced from the aluminium foil falls outside the principal X-ray reflections of polypropylene.

Two microdensitometer traces, from high temperature X-ray diffraction photographs, are shown in *Figure 1*.



Figure 1—Traces of two samples of polypropylene in the melt from high temperature X-ray photography

One is a commercial sample of polypropylene (intrinsic viscosity 2.7) and the other a so-called atactic sample of polypropylene (hot heptane extract) of high molecular weight which showed some crystallinity at room temperature. It can be seen that there is a difference in shape between the two curves although not a big difference in area. The curve from the sample of polypropylene is asymmetrical in shape and is similar to published curves used by Natta *et al.*⁵ for measurements of crystallinity, by X-ray diffraction, on unoriented specimens of polypropylene. This curve has been used for our crystallinity measurements.

The drawing in of the non-crystalline background is illustrated in *Figure 2* for some drawn polypropylene filaments.

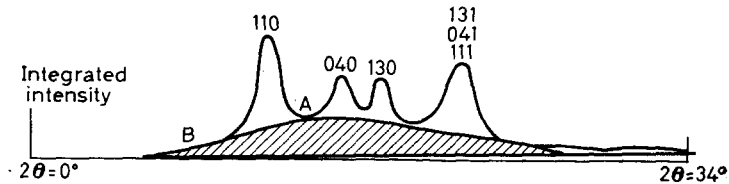


Figure 2—Microdensitometer trace of X-ray diffraction photograph of drawn polypropylene filaments. Shaded area: non-crystalline background; rise in background: incoherent scatter

Points A and B are used as reference points for determining the height of the non-crystalline background, and the crystallinity of a sample is then equal to

$$\frac{\text{area of crystalline fraction}}{\text{area of crystalline fraction} + \text{area of the amorphous fraction} (y)}$$

where y is a factor, necessary to correct for the non-coincidence of the centres of gravity of the amorphous and crystalline reflections⁶. A factor of 0.98 was obtained for polypropylene with the present focusing camera, the crystalline reflections being measured over the range $2\theta = 6^\circ$ to $2\theta = 38^\circ$.

In this set of measurements on drawn fibres of polypropylene the following four assumptions have been made.

- (1) The shape of the non-crystalline background deduced from the high temperature X-ray photographs is the same as that which would exist at room temperature.
- (2) The shape of the non-crystalline background is invariant and only reduced in proportion in a partially crystalline sample even with drawn yarns.
- (3) The thermal motions of the atoms in the crystalline regions do not make an appreciable contribution to the non-crystalline background.
- (4) The scattering efficiencies of the crystalline and amorphous regions are equivalent.

It appears, from *Figure 3*, that the effect of high temperature is not to change the shape of the amorphous curve over the angular range considered but only to increase the mean distance between molecular chains by approximately 0.5 Å.

An amorphous sample of poly(ethylene terephthalate) polymer when examined at room temperature and in the melt also behaved in a manner analogous to the polypropylene sample.

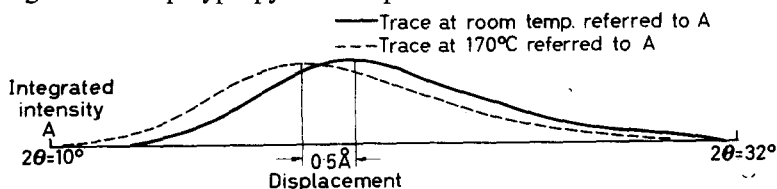


Figure 3—Microdensitometer trace of X-ray diffraction photograph of polypropylene in the melt and its correct angular displacement at room temperature

A number of highly crystalline specimens of drawn and undrawn fibres of polypropylene were examined over a wide range of temperature (-150°C up to the melt). The resolution on the X-ray photographs was sufficiently good to enable the non-crystalline backgrounds to be drawn in to a reasonable approximation without making any assumptions about shape at all. On scaling these curves to the one deduced from the melt they were found to be almost identical except for the angular displacement already referred to in the previous paragraph. This result lends support to assumptions (2) and (3). In particular, if assumption three was invalid the deduced non-crystalline backgrounds should show significant differences at different temperatures. The fourth assumption appears reasonable from an examination of the experimental data. The X-ray diffraction photographs taken under standard conditions and scanned by a microdensitometer gave total integrated areas which were approximately constant irrespective of the actual crystalline/amorphous ratio.

(iii) Density

In the density method of measuring crystallinity in a polymer it is assumed that only two kinds of material exist, viz. crystalline and amorphous. If the densities of a wholly crystalline and a wholly amorphous sample are known, then, by measuring the density of the sample of unknown crystallinity and applying simple proportion the crystallinity of the specimen can be inferred. With polypropylene it is impossible to achieve either of the above two states. The density of the crystallites can, however, be calculated from the crystal structure⁷ and has the value of 0.936 g/cm^3 . On the other hand rapid quenching of polypropylene samples does not produce an amorphous specimen as occurs with poly(ethylene terephthalate) polymer.

In order to determine an amorphous density it is necessary to use indirect methods. The method followed here was to assume that a linear relationship exists [as with unoriented poly(ethylene terephthalate) samples¹] between the crystallinity measured by X-rays and density for unoriented specimens of polypropylene. Samples of different crystallinity were produced by heat crystallization in a vacuum oven at different temperatures.

The best straight line was obtained by a 'least squares' analysis and the results obtained are shown in *Figure 4*. The value deduced for the amorphous density, by extrapolation, is given in *Table 1* together with three other values obtained from the literature.

It can be seen that the value deduced from the X-ray measurements agrees remarkably well with the value obtained by extrapolation for an

Table 1

Polypropylene sample	Density, g/cm^3	Method
Amorphous 'Extrapolated'	0.870	X-ray as described
Amorphous 'Experimental whole polymer'	0.870	Dilatometry ⁸
Amorphous 'Ether extract'	0.855	Extrapolated from melt Dilatometry ⁸
Amorphous 'Ether extract'	0.85 to 0.855	Density gradient column ⁹

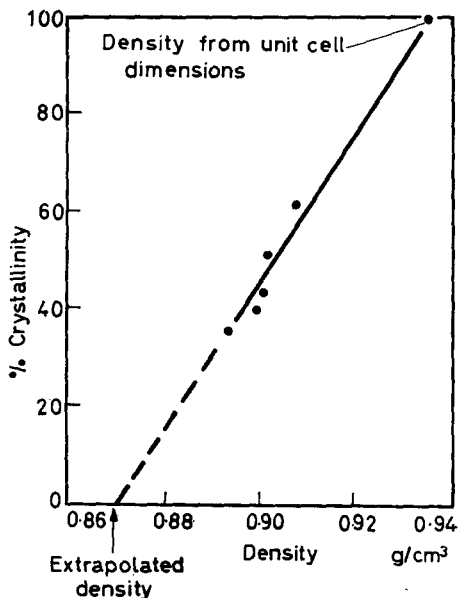


Figure 4—Crystallinity (X-ray) versus density of heat crystallized samples of polypropylene spun fibre

'experimental whole polymer' (such a polymer would be expected to be similar to the polymer used in these experiments) but disagrees with the other quoted values.

It is considered, however, that the value of 0.870 g/cm^3 is a reasonable figure to use for the calculation of crystallinities from density measurements. Specimens obtained at the Fibres Division, by similar extraction techniques, tended to be of low molecular weight and showed X-ray diffraction lines which were probably due to low molecular weight oligomers of polypropylene¹⁰. Furthermore, it is not necessarily true that the density of an atactic polypropylene should have the same density as the non-crystalline regions in a partially crystalline but essentially isotactic polypropylene. It was shown in the previous section that X-ray diffraction photographs of polypropylenes of high and low atactic content respectively showed differences when scanned by a microdensitometer.

(iv) Optical measurements

The optical birefringences of samples used in *Figure 5* were measured using polarized light and a Berek compensator.

Results—The results are presented in *Tables 2* and *3* which list crystallinities measured both by X-ray diffraction and density for a variety of polypropylene filaments. Taking the X-ray measure of crystallinity as the yardstick and knowing the density of the crystalline regions⁶ the density of the non-crystalline material in oriented filaments can be calculated. These values are given in the columns labelled 'oriented non-crystalline'. Some additional results are also presented in graphical form in *Figure 5* and will be referred to in the discussion.

The yarns were kept in a refrigerator after drawing and allowed to condition for 48 hours at room temperature before measurements were taken. The densities were measured in a graded density column¹¹ maintained at 30°C and the results are the means of two separate measurements.

Table 2

Filament draw ratio	Density g/cm ³	% Crystallinity (density)	% Crystallinity (X-ray)	Density oriented non-crystalline
(1) 5.0	0.903	49	37	0.878
(2) 5.5	0.898	44	39	0.873
(3) 6.0	0.902	48	37	0.877
(4) 6.5	0.903	49	37	0.878
(5) 6.9	0.905	52	39	0.879
(6) 5.0	0.909	58	47	0.878
(7) 5.5	0.912	63	48	0.880
(8) 6.0	0.913	64	47	0.880
(9) 6.5	0.920	75	47	0.889
(10) 6.9	0.920	75	49	0.887

Spun yarn crystallinity (X-ray) = 33 per cent.
 Filaments 1 to 5 passed over heating device at a maximum temperature of 95°C
 Filaments 6 to 10 passed over heating device at a maximum temperature of 95°C
 followed by one at a maximum temperature of 145°C

Table 3

Filament draw ratio	Density g/cm ³	% Crystallinity (density)	% Crystallinity (X-ray)	Density oriented non-crystalline
(1) 5.0	0.906	54	52	0.871
(2) 5.5	0.910	60	53	0.875
(3) 6.0	0.911	61	54	0.875
(4) 6.5	0.914	66	58	0.875
(5) 6.9	0.916	69	58	0.878
(6) 5.0	0.910	60	54	0.874
(7) 5.5	0.914	66	58	0.875
(9) 6.5	0.916	69	57	0.878
(10) 6.9	0.917	70	55	0.882

Yarn conditions as in Table 2 but heat crystallized in a vacuum oven for $\frac{1}{2}$ hour at 145°C.
 Heat crystallized chip at 145°C, 66 per cent crystalline.

The X-ray crystallinities have an estimated accuracy of ± 3 per cent.

DISCUSSION

(i) X-ray crystallinity

It can be seen from the results that the method of measuring the amount of crystalline material by X-ray diffraction, developed for oriented polyethylene terephthalate fibres can easily be applied to oriented polypropylene filaments. The general level of crystallinity in oriented polypropylene fibres is higher than that found for similarly treated polyethylene terephthalate fibres; furthermore, polypropylene spun fibre has a crystallinity of 33 per cent which is almost the same as that found in the polypropylene filaments,

Table 2, 1 to 5. There is, however, a marked difference in the widths of the X-ray reflections between the spun fibre and these filaments. The X-ray diffraction lines in the former case are broader indicating that the crystallites in the spun fibre are much smaller than those found in these filaments.

Furthermore the general level of crystallinity in the heat-treated drawn filaments (~ 56 per cent) is less, by X-ray diffraction, than is found for heat-treated unoriented fibre or chip (~ 65 per cent) at the same temperature and under the same conditions. Some recent work has suggested that this is simply a 'rate effect', for on repeated annealing of drawn filaments the crystallinity gradually rises to the same level as that found in undrawn fibres¹⁰. Molecular chains in the oriented state are presumably less mobile than in the unoriented state.

(ii) *X-ray crystallinity and density*

Examination of *Tables 2* and *3* shows that the relationship between X-ray crystallinity and density is different for unoriented and oriented filaments. In the latter case the degree of crystallinity measured by density is higher than the corresponding crystallinity measured by X-ray diffraction. If a lower value (*Table 1*) was used for the density of the amorphous regions of polypropylene then the difference between the results would be even greater.

It is considered that the discrepancy arises between the two methods because [as with oriented poly(ethylene terephthalate) fibres] it is no longer permissible, in drawn filaments, to regard the non-crystalline material as having a constant density¹², i.e. regions of semi-order exist which are non-crystalline but have a higher density. The higher the molecular orientation the higher is the discrepancy between the two methods up to birefringence values of $\Delta = 20 \times 10^{-3}$. This is illustrated in *Figure 5* for filaments which cover a range of $\Delta = 5 \rightarrow 22 \times 10^{-3}$.

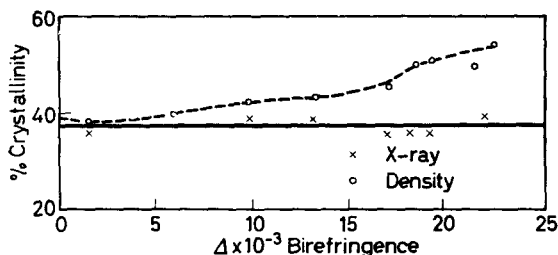


Figure 5—Differences in crystallinity measured by X-ray diffraction and density with increasing molecular orientation

The difference in crystallinity measured by the two methods is quite variable, particularly for the filaments 6 to 10 in *Table 2*. This is reflected in the calculation of an 'oriented non-crystalline density'.

In view of these results, the use of density as a measure of the degree of crystallinity of oriented polypropylene should, therefore, be applied with caution.

(iii) *Atactic content of polypropylene*

There is clearly some connection between the degree of crystallinity and the atactic content of a polymer, for, if considerable lengths of a molecular chain are regularly substituted, and if a number of such chains are brought

together under the correct conditions, crystallization would be expected to occur to a certain degree. It should, therefore, be possible under certain circumstances to relate the degree of crystallinity to the degree of tacticity of the polymer. It is obvious, however, that if the stereo-blocks, as they may be called, are low in number and short in length, then the chances of a number of them coming together to form a three-dimensional network are remote and consequently an estimate of the tacticity, from crystallinity measurements, in such circumstances could be highly inaccurate. Such an extreme situation does not appear to exist with the present polymer in use and it is of interest to calculate a value for the atactic content derived from X-ray measurements.

In order to make this estimate of atactic content it is necessary to crystallize polymer to a maximum degree (a similar idea has been put forward by Nielsen¹³). With the polypropylene used in these experiments values between 65 and 70 per cent have been arrived at. It is also necessary to know the crystallinity of a polymer which is completely regular (i.e. 100 per cent isotactic material). Some estimate for this can be made from measurements of crystallinity of heat-crystallized low pressure polyethylenes¹⁴ (i.e. where very little branching occurs) where values of approximately 85 to 90 per cent have been arrived at. Natta⁵ has also quoted a crystallinity value of 82 per cent for 'isotactic' polypropylene.

If a value of 85 to 90 per cent is assumed for the highest expected crystallinity of a completely isotactic polypropylene (this seems a reasonable assumption because dislocations, entanglements, etc. could account for the other 10 to 15 per cent of the material) a value for the atactic content of the commercial polypropylene, used in these experiments, can then be calculated. Values are assumed intermediate between the limits set out in the previous paragraph. We have, therefore

Maximum attainable degree of crystallinity of a complete iso- tactic polypropylene (87.5 per cent)	-	Maximum attainable degree of crystallinity of commercial sample of polypropylene (67.5 per cent)
= atactic content of commercial polypropylene, \sim 20 per cent.		

It is hoped to check this method of measurement against values obtained by a proposed infra-red method of measurement recently put forward by McDonald and Ward¹⁵. Others, notably Brader¹⁶, have also suggested that certain absorption bands in the infra-red spectra of polypropylene are related to tacticity. McDonald and Ward have, furthermore, defined tacticity in their paper. They state that a monomer unit can be considered in an isotactic environment when both its adjacent neighbours on the chain are substituted in a stereo identical manner. It should be pointed out that this definition, which is perfectly adequate for infra-red purposes, would not be so for X-ray measurements. A randomly substituted polypropylene which might be considered atactic would almost certainly have some isotactic content (on statistical grounds alone) when such short lengths of the molecular chain are considered. Such a polymer examined by X-ray diffraction would almost certainly be amorphous (or atactic).

CONCLUSIONS

An X-ray method has been devised for the measurement of crystallinity in oriented polypropylene filaments. The levels of crystallinity in these filaments are high compared with comparable oriented poly(ethylene terephthalate) filaments.

A method of determining the atactic content of polypropylene by X-ray diffraction has also been suggested.

The author would like to thank Dr K. W. Hillier for helpful criticisms of the manuscript.

*Fibres Division, I.C.I. Ltd,
Hookstone Road, Harrogate, Yorkshire*

(Received August 1961)

REFERENCES

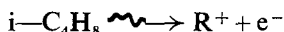
- ¹ FARROW, G. and PRESTON, D. *Brit. J. appl. Phys.* 1960, **11**, 353
- ² HILL, R. (Ed.). *Fibres from Synthetic Polymers*, Chap. 14. Elsevier: London, 1953
- ³ FARROW, G. and PRESTON, D. *J. sci. Instrum.* 1960, **37**, 347
- ⁴ FARROW, G. and PRESTON, D. *J. sci. Instrum.* 1960, **37**, 305
- ⁵ NATTA, G., CORRADINI, P. and CESARI, M. *R.C. Accad. Lincei*, 1957, **22**, 11
- ⁶ HOWELLS, E. R. I.C.I. (Plastics Division). Unpublished
- ⁷ NATTA, G., CORRADINI, P. and CESARI, M. *R.C. Accad. Lincei*, 1956, **21**, 365
- ⁸ NEWMAN, S. *J. Polym. Sci.* 1960, **47**, 111
- ⁹ MILLER, R. L. *Polymer, Lond.* 1960, **1**, 135
- ¹⁰ FARROW, G. To be published
- ¹¹ KOLB, H. J. and IZARD, E. F. *J. appl. Phys.* 1949, **20**, 564
- ¹² FARROW, G. and WARD, I. M. *Polymer, Lond.* 1960, **1**, 330
- ¹³ NIELSON, L. E. *J. appl. Polym. Sci.* 1959, **2**, 351
- ¹⁴ FARROW, G. Unpublished
- ¹⁵ McDONALD, M. P. and WARD, I. M. *Polymer, Lond.* 1961, **2**, 341
- ¹⁶ BRADER, J. J. *J. appl. Polym. Sci.* 1960, **3**, 370

The Effect of Zinc Oxide on the Radiation—initiated Polymerization of Isobutene at -78°C

F. L. DALTON, G. GLAWITSCH* and R. ROBERTS

It has been shown that polymerization rates higher than those previously reported for the radiation induced polymerization of isobutene in the presence of zinc oxide can be obtained if the zinc oxide surface is cleaned by prolonged heating in vacuo before use. The effect on the polymerization rate of varying both the surface area of the additive and the monomer to additive ratio has been studied.

RECENT studies on the radiation polymerization of isobutene at low temperatures have indicated that the reaction proceeds by a cationic mechanism¹⁻⁶, and that the rate of the polymerization can be greatly accelerated by a wide range of solid additives^{2, 3, 5}. It has been suggested that this acceleration is due to a rise in the G value for chain initiation: it has been calculated that the value rises from about 0.1 in the absence of additives to as high as 2.8 when a solid such as zinc oxide is present². The primary radiation chemical act in the polymerization is thought to be



where R^+ may be any of the possible positive ions formed directly, by ion molecule reactions, or by ion breakdown. The majority of the secondary electrons are recaptured within 10^{-12} second by processes which lead to radical formation or the liberation of heat. Since the time required for a single addition of an isobutene molecule to a cation is about 10^{-6} second⁴, polymerization is clearly impossible unless electron recapture processes can be suppressed to a considerable extent. Worrall and Pinner⁵ have suggested that solids such as zinc oxide have sites capable of trapping electrons, and that excess carbonium ions in the solution can then propagate chains which will only terminate when the growing $-\text{C}(\text{CH}_3)_2^+$ ion reaches the solid surface and is neutralized by the bound electron, probably by proton expulsion. It is clear that such a mechanism would suggest that in the absence of additive no polymerization could occur, and Collinson *et al.*⁴ have suggested that the reaction vessel walls and the inevitable sub-microscopic flakes of glass from the walls are responsible for the observed slow polymerization of pure isobutene. The irreproducible nature of such 'additives' may account for the wide rate variations observed in the polymerization.

As yet, little experimental evidence is available to show the effect of the structure of any single additive on the polymerization rate, and such variables as surface area and type and number of lattice dislocations have

*Isotopenlaboratorium der Österreichische Stickstoffwerke Aktiengesellschaft, Linz/Donau, St Peter 224, Austria.

not been investigated. As a first stage of such an investigation it was planned to study the effect of varying the surface area of zinc oxides used as additives in the ^{60}Co γ -ray initiated polymerization of isobutene at -78°C . at a fixed monomer to additive ratio. During this work it was found that if the zinc oxide was treated to remove all traces of adsorbed oxygen, much higher rates than those reported in the literature could be obtained.

EXPERIMENTAL

Preparation of zinc oxide samples

Spectroscopically pure zinc, *ca.* 150g, was dissolved in 'Analar' nitric acid, 1 200 cm³, diluted with an equal volume of water. The residual nitric acid was boiled off and the solution of zinc nitrate diluted to about 2 l. To this solution a saturated solution of ammonium carbonate, 350g, was added. The mixture was heated at 60°C for one hour, after which the precipitate of zinc carbonate was filtered off and washed. This precipitate was dried overnight at 110°C . The zinc carbonate thus prepared was heated at 500°C for two hours in a beryllia crucible in air. The resulting oxide was divided into four equal portions, each portion being heated for a further two hours: the temperature of this heating determined the surface area of the sample. Finally, all the samples were heated for a further two hours at 500°C . The surface area of each zinc oxide sample was determined by the well-known BET method, using krypton as absorbing gas and assuming a value of 19.4 \AA^2 for the area of an adsorbed krypton molecule. The surface areas obtained at the four heating temperatures used are shown in *Table 1*.

Table 1

<i>Heating temperature</i>	<i>Surface area, m²/g</i>
500	17.4
650	7.9
800	3.6
1 200	0.2

Isobutene

The isobutene used in this work was 'research grade' material (Phillips Petroleum Co.). This is claimed to be not less than 99.5 per cent isobutene, the most probable impurity being butene-1. It was introduced to the vacuum line direct from the cylinder and after rigorous outgassing it was distilled from -78°C to -196°C and the middle fraction allowed to stand over a fresh sodium mirror for 16 hours before use. Gas chromatographic methods showed less than 0.2 per cent of butene-1. No other impurity could be detected. This material polymerized at -78°C without additive in a field of 1.90×10^4 rads/h gave a G_{monomer} of 2 100.

Vacuum system

The Pyrex glass system used was evacuated by an all-glass mercury diffusion pump backed by an Edwards two-stage rotary oil pump. The handling line was kept entirely grease-free by the use of greaseless stop-cocks (Springham & Co. Ltd, Harlow), and isolated from the pumping system by a liquid nitrogen trap. Taps on the pumping system were of the usual type and were lubricated with Apiezon L grease.

Source

The source used for this work was 478 curies of ^{60}Co and the design and operation of the facility, typical of those used in this laboratory, has been described by Dove, Murray and Roberts⁷. Dose rates were obtained by the use of the Fricke dosimeter ($G_{\text{Fe}^{3+}} = 15.6$). From known electron fractions the dose received by each dilatometer could be calculated.

Design and filling procedure for dilatometers

In order to follow the initial stages of polymerization with some precision, it was decided to use a dilatometric technique and the design of dilatometer adopted is shown in *Figure 1*. Glassware was cleaned by the

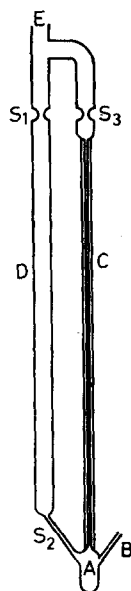


Figure 1—Diagram of dilatometer

method of Davison *et al.*³. The volume of the bulb A was determined and the required amount of additive introduced through the short tube, B, which was then sealed off. The dilatometer was sealed to the vacuum line at E and evacuated, care being taken to avoid blowing the additive out of A. An electric furnace was placed around the dilatometer which was heated to 400°C overnight. After this the tube D, which enabled the outgassing of zinc oxide to be carried out in a reasonable time, was removed by sealing at S_1 and S_2 . Bulb A was cooled to -78°C and isobutene allowed to enter the system and condense in A until the liquid level reached a suitable point in the capillary C. The isobutene reservoir was isolated from the dilatometer and A immersed in liquid nitrogen. This froze the liquid isobutene, together with gaseous isobutene above it and allowance was made for the condensation of this gas to avoid overfilling the dilatometer. The apparatus was then exposed to the pumps and sealed at S_3 . The dilatometer was then ready for use and polymerization was carried out as soon as possible. During any intervening time the dilatometer and its contents were kept at -196°C .

The measurement of polymerization rates

All polymerizations were carried out in a bath of trichloroethylene and drikold: the experimental arrangement is shown diagrammatically in *Figure 2*. Temperature stability was checked by means of a pentane filled bulb of about 5 cm³ capacity attached to a 0.5 mm capillary. By following the change in the meniscus height in this capillary and the capillary of the reaction dilatometer as the bath came to equilibrium temperature, correction for thermal drift during a run was possible, but in practice was found unnecessary. Early attempts to use the more usual acetone/carbon dioxide

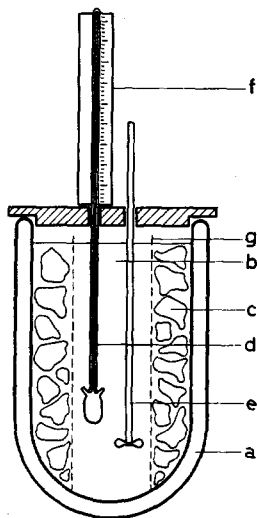


Figure 2—Experimental assembly: (a) Dewar vessel, (b) trichloroethylene, (c) solid carbon dioxide, (d) dilatometer, (e) stirrer, (f) scale, (g) wire gauze

bath proved unsuccessful due to temperature drifts of several degrees per hour. It was considered desirable to ensure adequate ventilation of the radiation chamber and to change the trichloroethylene in the cooling bath at frequent intervals, as radiolysis of trichloroethylene may lead to the formation of small quantities of phosgene. Observation of the meniscus of dilatometers was accomplished by placing a scale behind the capillary and using a telescope and mirror system. The position of the meniscus could be read to 0.5 mm. The protruding stem of the dilatometer is somewhat unusual but makes measurement of change in meniscus level easier. It is, however, necessary to apply a small correction to the measured contraction to allow for the contraction of isobutene in the capillary cooling from room temperature to -78°C . Experimentally it was found that at -78°C , in a capillary of 1 mm diameter, a contraction of 0.595 cm was equivalent to one per cent conversion per gramme of isobutene present. After completion of the run the dilatometer was opened, the unchanged isobutene allowed to evaporate slowly and the residue pumped at 60°C *in vacuo* overnight followed by extraction with carbon tetrachloride. The solution was filtered and polymer obtained by precipitation into a tenfold excess of methanol. The recovered polymer was filtered and dried to constant weight *in vacuo* at 60°C .

Determination of molecular weights

Molecular weights of all the polymer samples were determined by viscometry in carbon tetrachloride solution at 30°C , using a suspended level dilution viscometer. The intrinsic viscosities measured were converted to viscosity average molecular weights M_v by using the equation

$$[\eta] = kM_v^{\alpha}$$

with $k = 2.9 \times 10^{-4}$ and $\alpha = 0.68$. These values are due to Fox and Flory⁸, who showed them to apply for carefully fractionated samples between the limits $530 \leq M \leq 1\,260\,000$.

RESULTS

Preliminary experiments showed that stopcock grease retarded the polymerization and led to the adoption of the grease free system described above. Also, the importance of heating the zinc oxide *in vacuo* to remove oxygen adsorbed on the surface was demonstrated by two runs with '500°' zinc oxide using equal amounts of additive and monomer by weight and a dose rate of 1.90×10^4 rads/h. In one case the additive was pumped for

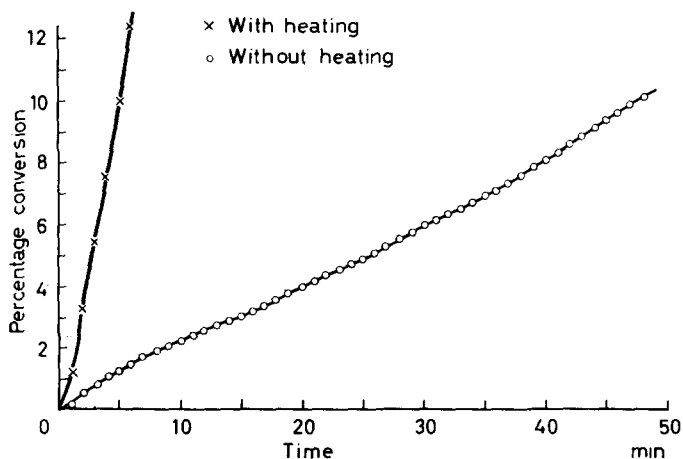


Figure 3—Effect of heating additive, '500°' zinc oxide. Monomer to additive ratio 1 : 1; dose rate 1.90×10^4 rads/h

16 hours at room temperature and in the second at 400°C . The large change in rate caused by heating is shown in Figure 3. A further 24 hours heating did not affect the polymerization rate.

A series of runs was carried out with 0.5 weight fraction additive and a dose rate of 1.90×10^4 rads/h, using zinc oxide samples of all four available surface areas. A similar series was carried out at 410 rads/h and the typical conversion versus time plots for these two series are shown in Figure 4. The plots at the higher dose rate show an initial curvature due to non-isothermal conditions in the dilatometer. All the plots also show a very slight upward curvature throughout, and to normalize rate measurements an arbitrary straight line was drawn between 2 and 7 per cent conversion and the rate

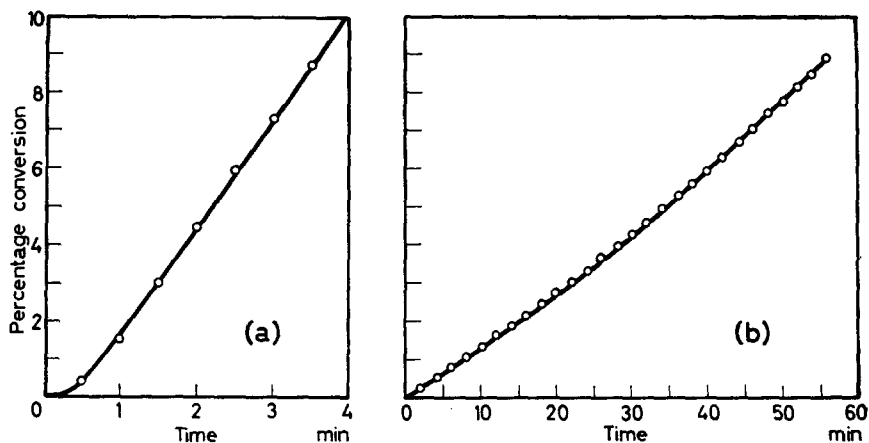


Figure 4—Typical conversion versus time plots: (a) Dose rate 1.90×10^4 rads/h; (b) dose rate 410 rads/h

taken from its slope. All runs were continued to about 10 per cent conversion and molecular weights were determined viscometrically. Polymerization rates and G values calculated from these data are shown in Table 2. Apparent G values for initiation are obtained by dividing overall G values by the degree of polymerization which is obtained from the viscometric data assuming a random molecular weight distribution.

Table 2

Heating temp. of additive °C	Wt fraction of additive	Dose rate rads/h	Rate of polymerization %/min	$M_v \times 10^{-6}$	$G_{\text{overall}} \times 10^{-5}$		$G_{\text{initiation}}$	
					1*	2*	1*	2*
500	0.5	1.90×10^4	2.18	3.06	6.2	11.3	21.2	38.5
650	0.5	1.90×10^4	1.71	2.11	4.8	8.9	24.1	43.6
800	0.5	1.90×10^4	2.35	2.75	6.7	12.2	25.5	46.2
1 200	0.5	1.90×10^4	0.81	3.21	2.33	4.22	7.32	13.25
500	0.5	410	0.155	1.41	20.6	37.3	151	274
650	0.5	410	0.222	3.35	29.5	53.5	91.7	166
800	0.5	410	0.158	2.24	21.0	38.0	101	181
1 200	0.5	410	0.065	3.06	8.6	15.6	29.4	53.1
1 200	0.10	1.90×10^4	0.017	1.86	0.084	0.09	0.47	0.50
1 200	0.20	1.90×10^4	0.200	3.27	0.86	1.0	2.8	3.3
1 200	0.33	1.90×10^4	0.598	3.23	2.2	3.1	7.1	10.0
1 200	0.50	1.90×10^4	0.814	3.21	2.3	4.2	7.3	13.3
1 200	0.67	1.90×10^4	1.31	2.79	2.3	5.9	8.4	20.2
1 200	0.80	1.90×10^4	1.75	4.40	2.2	9.1	5.1	21.4

*In columns headed 1, G values are based on the total energy absorbed in the system; those headed 2 give values based on energy absorbed by isobutene only.

A concurrent series of experiments was carried out in which the ratio of additive to isobutene was varied, other conditions being unchanged. '1 200' zinc oxide was used for these runs since it had a very low powder volume and a wider range of compositions could be studied than with the

other samples. As the fraction of zinc oxide was lowered, the form of the conversion curves changed as shown in *Figure 5*. The curve at 0.33 weight

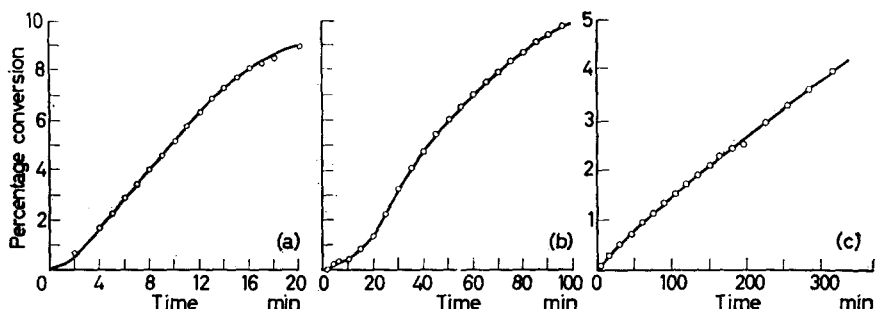


Figure 5—Change of form of conversion versus time curves as the additive to monomer ratio is lowered. '1 200' zinc oxide. Dose rate 1.90×10^4 rads/h: (a) 0.33 weight fraction zinc oxide; (b) 0.20 weight fraction zinc oxide; (c) 0.10 weight fraction zinc oxide (this curve continues linearly to 10 per cent conversion)

fraction of zinc oxide still possessed an almost linear portion from which a rate could be obtained, but at weight fractions of 0.20 and 0.10 zinc oxide only maximum and initial rates could be obtained. It is not surprising, therefore, that plots of G value against weight fraction of zinc oxide showed discontinuities below 0.33 weight fraction zinc oxide (*Figure 6*). Full details of these runs are shown in *Table 2*.

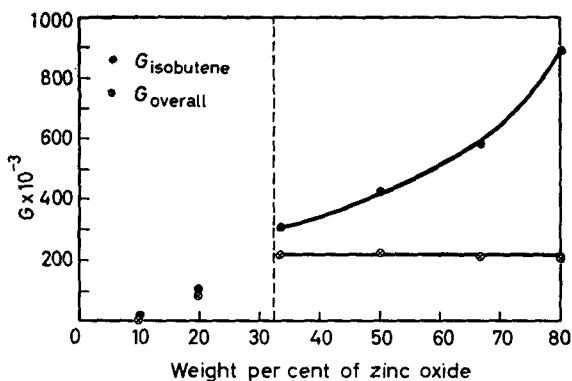


Figure 6—Effect on G values of varying the additive to monomer ratio. '1 200' zinc oxide. Dose rate 1.90×10^4 rads/h. G_{overall} is the G value based on total energy absorbed; $G_{\text{isobutene}}$ is the G value based on energy absorbed by isobutene only

Since the measurements outlined above were made, some experiments have been carried out to investigate the effect of stirring the dilatometers during irradiation. This was done by gripping the end of the dilatometer stem in the chuck of a vibrating stirrer (A.G. für Chemie Apparatebau, Mannedort, Zürich, Switzerland), the agitation being arbitrarily fixed at the highest level which did not cause breakup of the liquid monomer in the

capillary tube. This method showed that in samples containing 0.5 fraction by weight of additive at dose rates of both 1.9×10^4 rads/h and 410 rads/h the rate was unaffected by agitation if 500°, 650° or 800° zinc oxide was used. With 1 200° zinc oxide the rate increased to a value within the range found for the other samples.

DISCUSSION

The most striking result observed in the work described above is the very great increase in rate which is produced by heating the zinc oxide *in vacuo* before use, and it is this change in technique which has led to the wide discrepancy in *G* values between earlier workers and ourselves. The effect is considered to be due to the removal of oxygen from the surface of the zinc oxide during heating. It is well known that adsorbed oxygen is not removed from the surface of zinc oxide in a vacuum at room temperatures, and it has been shown that the gas is given off during irradiation⁹. Free oxygen has been shown to be a retarder for the cationic polymerization of isobutene initiated by ionizing radiation^{3, 4}.

As the surface area of the zinc oxide is varied no significant difference in rate is observed between 17.4 and 3.6 m²/g (500°, 650° and 800° samples) but rates are appreciably lower at both dose rates studied if 0.2 m²/g '1 200°' zinc oxide is used. This latter material does not fill the dilatometer and has a considerable amount of supernatant isobutene, whereas all the other samples spread throughout most of the volume of the dilatometer. Since stirring will restore the rate to the value obtained with the other zinc oxide samples, it is clear that variation of the surface area of the sample does not itself affect the rate of polymerization, but that it is essential for the zinc oxide to be spread throughout the monomer sample. The lower rate obtained with unstirred 1 200° zinc oxide may well be due to the lack of adequate monomer at the more densely packed initiating sites on the surface. Alternatively, it could be caused by the formation of inhibitors such as diisobutene in the supernatant liquid, since it is known that such inhibitors are formed in the gamma ray-initiated polymerization of pure isobutene at -78°. In the marked retardation in samples with weight fractions of zinc oxide 0.33 or less this latter mechanism may again be operative or the zinc oxide may become coated in polymer and inactive. We have noted, however, that if an experiment is carried out with 1 200° zinc oxide at 0.5 weight fraction and a dose rate of 1.90×10^4 rads/h, using double our normal quantities in a dilatometer of the same diameter but of greater length than usual, then a pronounced falling off of the rate is observed at 6 to 8 per cent conversion, whereas under our usual conditions no trace of such an effect can be seen.

Another surprising feature of our results is the extremely high *G* values obtained for chain initiation. There is a certain lack of precision in the degree of polymerization values obtained from our viscometric data, since our molecular weights are somewhat higher than the maximum value for which the intrinsic viscosity molecular weight relationship used has been verified, and we have assumed a most probable molecular weight distribution: however, such factors could make only a relatively small difference

to the value obtained for G initiation. The results are not significantly affected by degradation of polymer chains during polymerization as has been shown to occur in other work, since much lower total radiation doses have been used. The most obvious explanation of our very high apparent G initiation values, coupled with fairly constant molecular weights, is that chain transfer to monomer is occurring to a great extent. This view is strengthened by the fact that the molecular weights remain constant even for runs in which the rate curves show the marked falling off discussed above. There is evidence that chain transfer occurs in the cationic polymerization of isobutene with conventional catalysts¹⁰, but Charlesby⁶ considers that it is unimportant in the radiation-initiated polymerization of pure isobutene when molecular weights are considerably lower than our values. If transfer is accepted as the explanation of the apparent high G initiation value, it is clear that termination must be almost completely suppressed by the additive.

In these laboratories Barry and Klier⁹ have shown that isobutene absorbed on the surface of zinc oxide at both 0°C and -78°C causes a marked increase in the conductivity of zinc oxide on irradiation, and this is due to the absorption of electrons from the isobutene into the zinc oxide, leaving positive ions on the surface. On removing the radiation source a decay of conductivity occurs indicating recombination of the electrons with positive ions, but this process is slow in comparison with the polymerization rates. Further studies on these conductivity effects may well extend our understanding of the system. It must not be overlooked that high G initiation values may well occur if the relevant ionization processes occur in an adsorbed surface layer and it may well be that additives cause a concurrent increase in G initiation and reduction in the rate of termination, but we consider that suppression of the termination process by electron capture by the zinc oxide, coupled with transfer-control of molecular weights, is the most probable explanation of our data. The fact that the polymerization rate is found to be independent of surface area of the zinc oxide used indicates that the electron traps are formed in the bulk of the additive but are highly mobile and can readily migrate to the surface of the solid.

It is apparent from our measurements, although they cover only two dose rates, that the polymerization shows a marked dependence on intensity and this is being studied in some detail at the present time, and will be reported in due course.

The authors of this communication are indebted to Drs K. Klier and T. I. Barry for the conductivity measurements mentioned above, and to Mr E. Jamison for technical assistance.

G.G. would also like to thank the International Atomic Energy Agency for the award of a fellowship during the tenure of which this work was carried out.

*Radiation Branch, Isotope Research Division,
Wantage Research Laboratory (A.E.R.E.),
Wantage, Berks.*

(Received August 1961)

REFERENCES

- ¹ DAVISON, W. H. T., PINNER, S. H. and WORRALL, R. *Chem. & Ind.* 1957, No. 38, 1274
- ² WORRALL, R. and CHARLESBY, A. *Internat. J. appl. Radiation and Isotopes*, 1958, **6**, 8
- ³ DAVISON, W. H. T., PINNER, S. H. and WORRALL, R. *Proc. Roy. Soc. A*, 1959, **252**, 187
- ⁴ COLLINSON, E., DANTON, F. S. and GILLIS, H. A. *J. phys. Chem.* 1959, **63**, 909
- ⁵ WORRALL, R. and PINNER, S. H. *J. Polym. Sci.* 1959, **34**, 229
- ⁶ CHARLESBY, A., PINNER, S. H. and WORRALL, R. *Proc. Roy. Soc. A*, 1960, **259**, 386
- ⁷ DOVE, D., MURRAY, G. S. and ROBERTS, R. U.N.E.S.C.O. International Conference on Radiation in Scientific Research. *Unesco/N.S./R.I.C./19*
- ⁸ FOX, M. and FLORY, P. J. *J. phys. Chem.* 1949, **53**, 197
- ⁹ BARRY, T. I. and KLIER, K. Faraday Society Discussion, Paris 1960
- ¹⁰ EVANS, H. G. and MEADOWS, G. W. *J. Polym. Sci.* 1949, **4**, 359

Normal Stress, Shear Recovery and Viscosity in Polydimethyl Siloxanes

J. J. BENBOW and E. R. HOWELLS

The Weissenberg-Roberts rheometer and a cone and plate viscometer have been used to study the viscous and elastic properties of some polydimethyl siloxane fluids as a function of shear rate and of temperature. Similar experiments with molten polythene provide a comparison between the two types of polymer. It is found that the normal stress is small compared to the tangential stress at low rates of shear, but at high rates the normal stress is the larger; that is, the curves representing the shear rate variation of these stresses cross. The value of the stresses at the cross-over is found to be independent, to a good approximation, of molecular weight and of temperature. The elastic properties determined from normal stresses and recovery measurements are compared in the light of theoretical studies by other workers. It is shown that the so-called 'Hooke's law in shear', i.e. the proportionality between total recoverable strain and shear stress, is not applicable to these materials. Consideration is also given to the criterion required for a material to show normal stresses, and the structural features involved are discussed.

THERE have been several recent communications notably by Philippoff and his co-workers dealing with the correlation of various measurements of viscosity and elasticity in polymeric systems such as solutions of cellulose derivatives¹, polyisobutylene solutions², asphalt³ and polydimethyl siloxanes⁴. In most of this work a wide study was made involving measurements of optical extinction angle and flow birefringence as well as the more usual flow parameters viscosity, normal stress and elastic recovery. Philippoff's paper on silicones⁴ was, however, restricted to optical work and the present paper describes viscosity and elasticity measurements on polymers of the same type.

One of the issues arising from these recent studies is: 'What is the criterion required for a material to show Weissenberg normal stresses?' Our view is that the observation of recoverable elastic strain may be taken as a necessary and sufficient condition for observable normal stresses and that, as a consequence, a qualitative limit can be set on the range of molecular structures which give rise to normal stresses.

A further point of interest is the extent to which polymers showing recoverable elastic strain obey the so-called 'Hooke's law in shear'; that is, the proportionality of the total recoverable strain and shear stress. Philippoff *et al.*^{1, 2, 7} introduce and investigate this idea which was expressed earlier by Weissenberg⁶. In general they appear to regard Hooke's law in shear as a reasonable approximation (though some of their measurements especially those on jellied gasoline⁷ and on polyisobutyl methacrylate in dibutyl phthalate⁸ give cause for doubt) and Bagley⁹ makes use of it in his analysis of capillary flow end effects. The results presented here indicate deviations from Hooke's law at comparatively low shear stresses, namely 2×10^4 dyne/cm² approximately, and Pollett's¹⁰ data suggest that, for low density polythene, deviations occur above a shear stress of about 2×10^5 dyne/cm².

It is worth emphasis that silicone polymers are, in practice, attractive materials for use in viscoelastic studies of this type because at room temperature they have properties similar to those of high polymers such as polythene and polyvinyl chloride in the molten state⁵. The high temperatures required to melt these plastics complicate rheological experiments.

EXPERIMENTAL METHOD

Two instruments were used: (1) a cone and plate rheometer similar to that described by Jobling and Roberts¹¹, for measurements of viscosity and normal stress and (2) a cone and plate viscometer based on a design described by Philippoff and Gaskins¹², which provided elastic recovery measurements as a function of shear stress and strain in addition to viscosity measurements. In each case some modifications were introduced to make the instruments more suitable for the particular requirements in hand.

The general construction of the rheometer is well known and needs no further description. We found it advantageous to use a variable induction gauge rather than the original capacity gauge to measure the total normal thrust. The majority of the normal and tangential stresses referred to are the equilibrium values but a small amount of work was undertaken to determine the time dependence of stresses. To do this the cantilever spring which restricts the vertical motion of the cone was made very stiff in order to reduce the inherent time constant of the apparatus to a fraction of the growth times of the normal stresses. A limit to the stiffness which can be used is determined by the magnitude of the normal force and the sensitivity of the displacement gauge. Another modification was the use of a mirror, galvanometer lamp and scale arrangement to measure the rotation of the torsion bar on which the 'fixed' plate was mounted. Provision was made to rotate the cone continuously, to oscillate it, or to superpose both continuous and oscillating rotation. However, only the results of experiments involving continuous rotation will be described here.

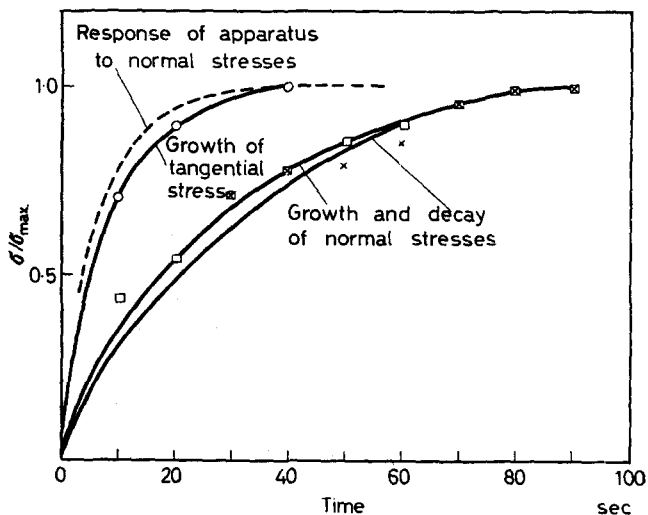


Figure 1
430

The construction and operation of the second cone and plate instrument has already been described in detail elsewhere⁵. It consists essentially of a shearing system in which the cone, in contact at its apex with a flat plate, is rotated under the action of a constant stress. The rotation is measured as a function of time both while the stress is applied and after it has been removed. From the displacement/time curves, the viscosity and shear recovery associated with the particular stress can be calculated; by repeating the experiment with a number of different applied weights, viscosity and recovery can be measured over a large range of stresses. In addition, by using a single weight but removing it after various amounts of rotation, the recovery can be measured as a function of shear strain at constant stress.

RESULTS

In the following description of results and discussion the stress field in the sample under shear is described by reference to the system of orthogonal coordinate axes in which axis 1 is parallel to the flow lines, axis 2 is radial and axis 3 parallel to the axis of the apparatus. Thus the tangential shear stress is denoted by P_{12} and is calculated from $P_{12} = 3T/(2\pi R^3)$, where T is the torque and R the cone radius. Also the relevant difference of normal stresses is $(P_{11} - P_{22})$ and is calculated from $(P_{11} - P_{22}) = 2N/(\pi R^2)$, where N is the total normal thrust on the cone.

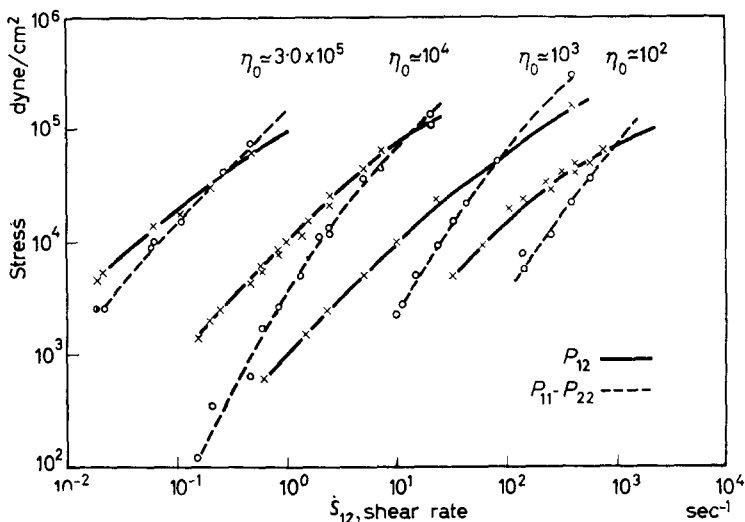


Figure 2

Figure 1 shows examples of growth and decay curves for the total normal thrust observed on the rheometer with one of the silicone polymers. The growth curve reaches its plateau values after about 80 sec and has a shape very similar to the decay curve which has been plotted, for ease of comparison, in the form $N(0) - N(t)$, where $N(0)$ is the steady state value of $(P_{11} - P_{22})$ and $N(t)$ is the corresponding value at time t after the cessation of shear. The indication is that the growth and decay time constants are

appreciably greater than those of the tangential stress growth, though the situation would be clearer if the apparatus response time were further reduced.

Measurements were made on the rheometer of the steady-state values of stress in a number of polydimethyl siloxanes ranging in room temperature Newtonian viscosity from 2×10^3 to 3×10^5 poises. In each case the normal and tangential stresses were measured as a function of applied shear rate. Typical room temperature results are shown in *Figure 2*; other results obtained on polymers of intermediate viscosities fit into this pattern but have been omitted for the sake of clarity. Measurements were also made at different temperatures and an example is shown in *Figure 3*. It is noticeable that, to a first approximation, the normal stress and tangential stress curves cross at a stress value independent of molecular weight and temperature.

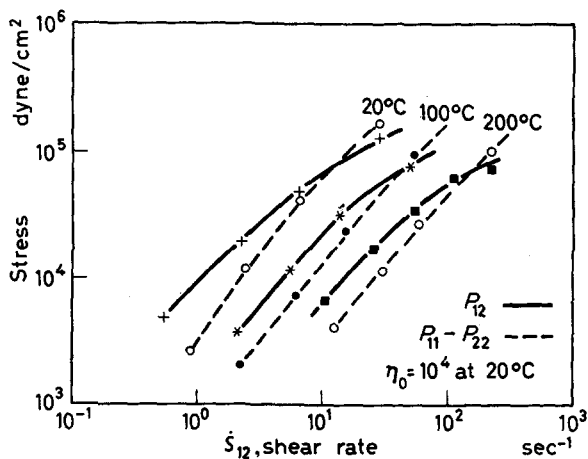


Figure 3

Viscosity measurements made with the simple constant stress cone and plate were found to agree with those obtained from the rheometer and are therefore not described. The recovery experiments made on the cone and plate correspond to the ultimate 'constrained recovery' as defined by Lodge¹³. We have found that the recoverable strain is dependent upon the magnitude of the strain allowed before recovery takes place and reaches a broad maximum value when the initial strain is about 10 units. This agrees essentially with the findings of Pollett¹⁰ and Clegg¹⁴. The recovery values quoted here were made with the shear strain before the stress was removed equal to 10 units, i.e. 50° rotation of the cone of total vertical angle 170°. (The recovery was calculated from the ratio θ/ϕ , where θ is the angular recovery and ϕ the angle between the cone and the plate.) Results obtained for the recovery at different stresses are given in *Table 1*; these are restricted to the three most viscous silicone polymers because of experimental difficulties which arise when measuring recovery in the less viscous samples. Some results for a typical silicone and typical polythenes are illustrated in *Figure 4*—all show appreciable non-linearity. Also

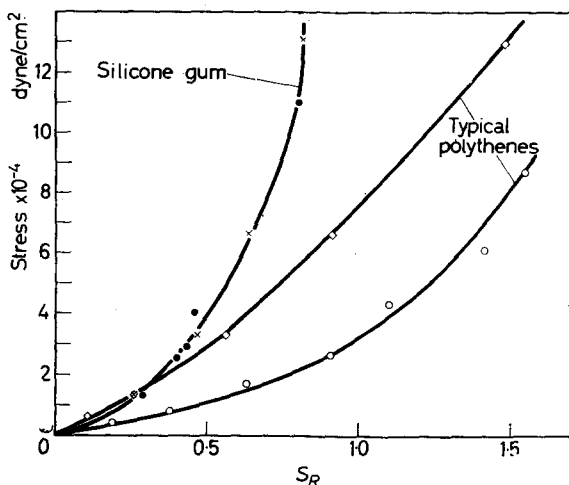


Figure 4

Table 1

Newtonian viscosity poise	Stress dyne/cm ²	Recovery	Newtonian viscosity poise	Stress dyne/cm ²	Recovery
3×10^5	0.33×10^4	0.17	10^4	0.33×10^4	0.07
	0.66×10^4	0.17		0.66×10^4	0.12
	1.3×10^4	0.26		0.99×10^4	0.18
	1.3×10^4	0.29		1.32×10^4	0.33
	2.5×10^4	0.40		2.64×10^4	0.39
3×10^3	2.9×10^4	0.43	3×10^3	0.18×10^4	0.023
	3.3×10^4	0.47		0.33×10^4	0.069
	4.0×10^4	0.46		0.66×10^4	0.17
	6.6×10^4	0.64		0.66×10^4	0.12
	11.0×10^4	0.80		1.32×10^4	0.27
	13.0×10^4	0.81			

included in Figure 4 are results obtained with a coaxial cylinder arrangement in which the imposed steady rotation of the inner cylinder was automatically removed by a mechanical clutch. The agreement between these and the cone and plate results is taken as sufficient evidence to show that the time taken to remove the weight in the cone and plate experiments, and inertia effects, had a negligible effect on the measurements.

Measurements of normal stress can be conveniently compared with the recovery measurements by plotting $(P_{11} - P_{22})$ as a function of S_R^2 as in Figure 5. Here again, the curve is markedly non-linear.

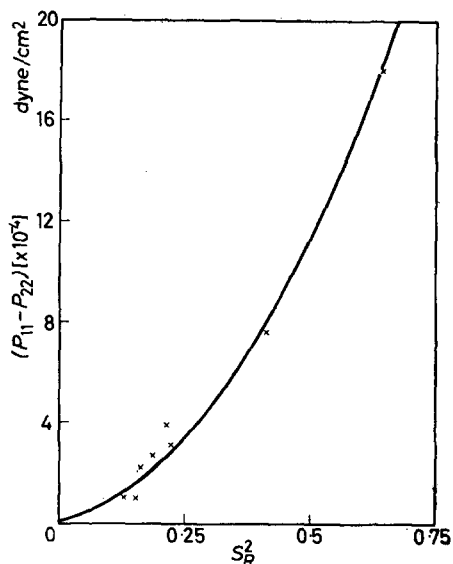
Figure 6 shows one set of rheometer results for a low density polythene. The cross-over of the two curves occurs at a stress value which is about a tenth of that found for the silicone polymers.

DISCUSSION

The observed differences in the time constant for relaxation of normal and tangential stresses are consistent with Lodge's theory¹⁵ which predicts a larger time constant for the normal stress.

The recovery results in *Figures 4 and 5* show that the simple relations

Figure 5



$P_{12} = GS_R$, $P_{11} - P_{22} = G'S_R^2$, where G and G' are constants and S_R is the recoverable strain, are not obeyed. More specifically, the former relation, often called Hooke's law in shear, cannot be retained at shear stresses

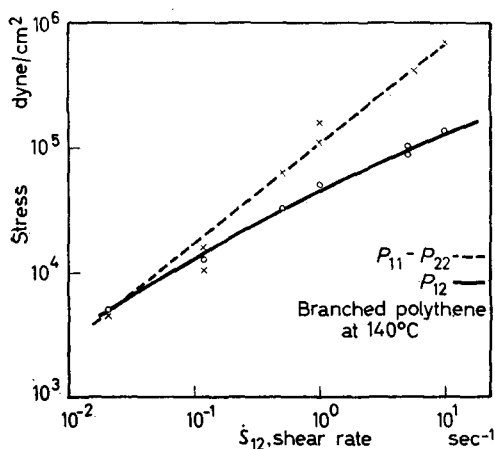


Figure 6

greater than 2×10^4 dyne/cm² for the siloxane polymers studied here. *Figure 5* suggests that $(P_{11} - P_{22})$ and S_R become zero together. In other words the existence of a recoverable shear strain is a criterion for the occurrence of an observable normal stress. This view was implied in the early work of Weissenberg¹⁶. It is of interest to speculate on the molecular characteristics necessary to produce these elastic effects. It has been

shown^{17, 18} that, in principle, elasticity is to be expected in systems composed of elastic solid particles or liquid droplets dispersed in a Newtonian fluid. The present authors suggest, however, that a three-dimensional network is necessary for significant elastic effects to occur, i.e. recoverable strains and normal stresses of the order of 10 per cent of the initial strains and viscous stresses, respectively. The network may be of the obvious rubber elastic type common in polymeric systems¹⁵ or it may arise from molecular association in monomeric materials—this may occur for example in the well known solutions of aluminium dilaurate which are quite strikingly elastic liquids. In terms of an entangled network it is relatively straightforward to describe molecularly the development of elasticity. The entanglement points may be either permanent covalent bonds or transient van der Waals interactions and the application of shear strain causes them to move along the direction of flow.

Figure 7

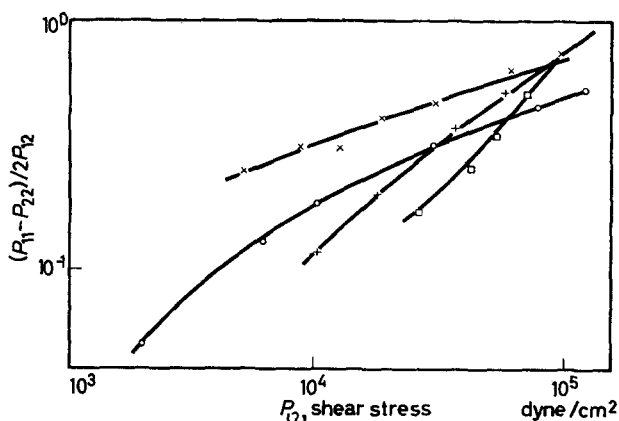
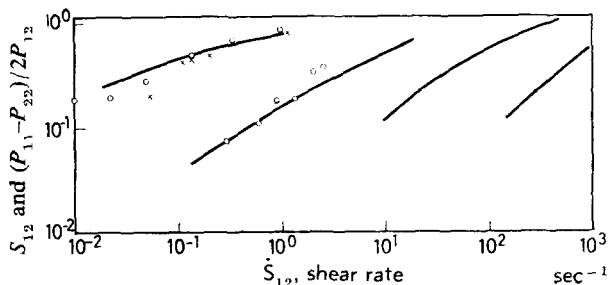


Figure 8

For large shear strains the configurational changes in the network are accompanied by a significant decrease in entropy and a degree of molecular orientation along the direction of flow. This gives rise to a tension along the flow lines and to strain recovery when restraints are removed.

It is more difficult to see how strong interactions can exist between, say, the elastic particles of a suspension and it is not surprising that the observation of significant Weissenberg effects is limited to materials which are polymeric or effectively so.

Lodge's network theory¹³ of viscoelasticity involves the equations $(P_{11} - P_{22}) = GS_R^2$ and $P_{12} = G'S_R$ which we have shown not to be true over the whole range of variables used in the present work. Lodge goes on to calculate the constrained recovery to be expected from his model and obtains the expression $(P_{11} - P_{22})/2P_{12} = S_R$. We find that this equation is a good description of our results. This is shown in *Figure 7* where experimental values of S_R are indicated by circles and crosses with the values calculated from the Lodge equation [using observed $(P_{11} - P_{22})$ and P_{12}] by continuous lines for each of four silicone polymers.

Another feature illustrated in *Figure 7* is that the shear rate dependence of recoverable strain appears to depend upon molecular weight. Similar differences of slope occur when the recovery, again calculated from $(P_{11} - P_{22})$ and P_{12} , is plotted against shear stress (*Figure 8*). Thus a decrease in molecular weight appears to make the elastic properties more rate (or stress) dependent although, as pointed out above, the effect is a second order one since *Figure 2* shows that the four pairs of curves could very approximately be superposed by a shift parallel to the shear rate axis.

Imperial Chemical Industries Limited,
Plastics Division, Bessemer Road,
Welwyn Garden City, Herts.

(Received August 1961)

REFERENCES

- ¹ BRODNYAN, J. G., GASKINS, F. H., PHILIPPOFF, W. and LENDRAT, E. G. *Trans. Soc. Rheol.* 1958, **2**, 285
- ² BRODNYAN, J. G., GASKINS, F. H. and PHILIPPOFF, W. *Trans. Soc. Rheol.* 1957, **1**, 95 and 109
- ³ BRODNYAN, J. G., GASKINS, F. H., PHILIPPOFF, W. and THELEN, E. *Trans. Soc. Rheol.* 1960, **4**, 265 and 279
- ⁴ PHILIPPOFF, W. *Trans. Soc. Rheol.* 1960, **4**, 169
- ⁵ BENBOW, J. J., BROWN, R. N. and HOWELLS, E. R. *Colloques Internationaux du Centre National de la Recherche Scientifique*, XCVIII, Paris, 1960
- ⁶ WEISSENBERG, K. *Rep. Gen. Conf. Brit. Rheologist's Club*, 1946, 36
- ⁷ PHILIPPOFF, W. and GASKINS, F. H. *Trans. Soc. Rheol.* 1958, **2**, 263
- ⁸ GASKINS, F. H. and PHILIPPOFF, W. *Trans. Soc. Rheol.* 1959, **3**, 181
- ⁹ BAGLEY, E. B. 'The separation of elastic and viscous effects in polymer flow'. Paper presented to Rheology Society Pittsburgh Conference, November 1960
- ¹⁰ POLLETT, W. F. O. *Proceedings of the Second International Conference on Rheology*, p 85. Butterworths: London, 1953
- ¹¹ JOBLING, A. and ROBERTS, J. E. *Rheology, New York*, 1958, **2**, 503
- ¹² PHILIPPOFF, W. and GASKINS, F. H. *J. Polym. Sci.* 1956, **21**, 205
- ¹³ LODGE, A. S. *Colloques Internationaux du Centre National de la Recherche Scientifique*, XCVIII, Paris, 1960
- ¹⁴ CLEGG, P. L. Unpublished report, 1956
- ¹⁵ LODGE, A. S. B.R.P.R.A. Conference, 1959.
- ¹⁶ WEISSENBERG, K. *Nature, Lond.* 1947, **159**, 310
- ¹⁷ FRÖLICH, H. and SACK, R. *Proc. Roy. Soc. A*, 1946, **185**, 415
- ¹⁸ OLDROYD, J. G. *Proc. Roy. Soc. A*, 1953, **218**, 122

Book Reviews

Advanced Paint Chemistry

P. M. FISK

Leonard Hill (Books) Ltd: London, 1961.

(viii + 164 pp.; 4½ in. by 7 in.), 21s.

THIS WORK sets out to provide a textbook of organic chemistry for the City & Guilds courses in surface coatings technology. It contains a survey of the principles of organic chemistry, the manufacture of raw materials from petroleum derivatives and from acetylene, the principles of polymer chemistry, the manufacture of polymers and plasticizers, and colour and constitution.

The weakness of the book lies with its presentation of theoretical principles, which is often confused and contains definitions which are insufficiently precise. The confusion is particularly apparent in the treatment of reaction mechanisms; the distinction between polarization effects and polarizability effects is not made clear because of poor definition (or omission) of some of the terms involved, and primary and secondary steric effects are not considered; further, the section on addition polymerization omits the terms 'propagation' and 'chain transfer'. The account of the reactions of naphthalene could have been clarified by a discussion of bond multiplicities. There appears to the reviewer to be an inordinate preoccupation with the resonance theory, the reasons given for omitting molecular orbital descriptions being fallacious. Some of the diagrams are poor, and a number of them could have been clarified by the conventional use of curved arrows to denote mesomeric and electromeric effects.

In spite of these criticisms the main part of the book, which is concerned with synthetic methods, is both comprehensive and succinct and should prove valuable to the young technologist. There are, however, a few surprising omissions even in these pages, e.g. the manufacture of phthalic anhydride, the alcoholysis process for alkyd resins, *in situ* processes for epoxidized oils, thermosetting acrylics and the chemistry of rosin.

I. T. SMITH

Organic Coating Technology, Vol. II: Pigments and Pigmented Coatings

H. F. PAYNE

John Wiley & Sons: London and New York, 1961.

(x + 675—1399 pp.; 5 in. by 8 in.), 140s.

AS COMPARED to Vol. I on the subject which dealt with the binder or polymeric part of the surface-coating, emphasis here is on the pigment, the component added for decorative or protective purposes. A great deal of very useful information has been collected in the present volume but its presentation often lacks direction.

A good start is made on the subject of colour and its physical measurement. The Munsell Colour System and Colour Sphere show how a colour may be defined in terms of hue (red, yellow, green, etc.), lightness and purity (extent to

which greyness has been added to the colour). This system allows of a diagrammatic arrangement of all colours as well as a numerical classification, i.e. 7.5 B 6/8 is a blue containing some green, and having a lightness of 6 and purity of 8. A more accurate numerical designation of a colour is provided by the Hardy system, this defining a colour in terms of dominant wavelength, percentage purity and percentage brightness. The great use of these systems is that they permit one to make a visual assessment of the colour, a thing difficult to do with the familiar *X Y Z* tristimulus values. Some progress has been made towards applying such colour measurement to the very practical problem of matching paint.

Pigments used in paint manufacture are very fully dealt with under white and black pigments, extenders, inorganic and organic pigments. These chapters have been well written and provide all necessary information on pigment manufacture and properties. The great variety of shades and tints obtainable with modern colour manufacture becomes obvious from the text. The chemistry of colour manufacture is clearly and well described. Since lightfastness is often a problem with pigments it is encouraging to note in this American book mention of the British Blue Wool Scale as a standard for measurement of this property. One would have hoped the author would have followed his systematic treatment of pigments with a like study of media and solvents, appropriate to this volume. After pigments however, various media are mentioned and the subject is then dropped until the last chapter of the book when a fuller account is given of vinyls, polyesters, polyurethanes and such modern resins, in a section on chemically resistant coatings. The actual manufacture of paint is well described, mention being made of such modern equipment as the high speed impeller which in part can replace the familiar roller grinder. Surface preparation and methods of application receive full treatment. With regard to formulation most paints are dealt with under industrial or architectural finishes. Since the book is American, emphasis is placed on paints for exterior use to protect wood. An interesting table provides information on the relative rates of disintegration of typical paints applied to a great variety of building woods.

Besides writing on pigments and paints the author has philosophized by heading every chapter with words of wisdom. 'An automobile has no resemblance to the man who made it, likewise creation gives no clue to the attributes of the Creator. Spirit is revealed only through spiritual approach.' All this may make some scientists throw up their hands in horror; however, it is the privilege of the author to include in his work what he chooses. Let us end in the same vein with a quotation from Solomon 'the beginning of wisdom is fear of the Lord'.

A. S. FREEBORN

Chemical Crystallography. An Introduction to Optical and X-Ray Methods (2nd ed.)

C. W. BUNN

Clarendon Press: Oxford University Press, London, 1961.

(xiv+509 pp.; 5½ in. by 8½ in.), 60s.

It is a pleasure to review such an extremely readable book as *Chemical Crystallography: Second Edition* by C. W. BUNN, the first edition of which soon established itself as one of the accepted textbooks on the subject.

The essence of this first edition was first that it integrated in a wholly satisfactory manner the optical and X-ray methods of investigating crystal

Book Reviews

Advanced Paint Chemistry

P. M. FISK

Leonard Hill (Books) Ltd: London, 1961.

(viii + 164 pp.; 4½ in. by 7 in.), 21s.

THIS WORK sets out to provide a textbook of organic chemistry for the City & Guilds courses in surface coatings technology. It contains a survey of the principles of organic chemistry, the manufacture of raw materials from petroleum derivatives and from acetylene, the principles of polymer chemistry, the manufacture of polymers and plasticizers, and colour and constitution.

The weakness of the book lies with its presentation of theoretical principles, which is often confused and contains definitions which are insufficiently precise. The confusion is particularly apparent in the treatment of reaction mechanisms; the distinction between polarization effects and polarizability effects is not made clear because of poor definition (or omission) of some of the terms involved, and primary and secondary steric effects are not considered; further, the section on addition polymerization omits the terms 'propagation' and 'chain transfer'. The account of the reactions of naphthalene could have been clarified by a discussion of bond multiplicities. There appears to the reviewer to be an inordinate preoccupation with the resonance theory, the reasons given for omitting molecular orbital descriptions being fallacious. Some of the diagrams are poor, and a number of them could have been clarified by the conventional use of curved arrows to denote mesomeric and electromeric effects.

In spite of these criticisms the main part of the book, which is concerned with synthetic methods, is both comprehensive and succinct and should prove valuable to the young technologist. There are, however, a few surprising omissions even in these pages, e.g. the manufacture of phthalic anhydride, the alcoholysis process for alkyd resins, *in situ* processes for epoxidized oils, thermosetting acrylics and the chemistry of rosin.

I. T. SMITH

Organic Coating Technology, Vol. II: Pigments and Pigmented Coatings

H. F. PAYNE

John Wiley & Sons: London and New York, 1961.

(x + 675—1399 pp.; 5 in. by 8 in.), 140s.

AS COMPARED to Vol. I on the subject which dealt with the binder or polymeric part of the surface-coating, emphasis here is on the pigment, the component added for decorative or protective purposes. A great deal of very useful information has been collected in the present volume but its presentation often lacks direction.

A good start is made on the subject of colour and its physical measurement. The Munsell Colour System and Colour Sphere show how a colour may be defined in terms of hue (red, yellow, green, etc.), lightness and purity (extent to

which greyness has been added to the colour). This system allows of a diagrammatic arrangement of all colours as well as a numerical classification, i.e. 7.5 B 6/8 is a blue containing some green, and having a lightness of 6 and purity of 8. A more accurate numerical designation of a colour is provided by the Hardy system, this defining a colour in terms of dominant wavelength, percentage purity and percentage brightness. The great use of these systems is that they permit one to make a visual assessment of the colour, a thing difficult to do with the familiar *X Y Z* tristimulus values. Some progress has been made towards applying such colour measurement to the very practical problem of matching paint.

Pigments used in paint manufacture are very fully dealt with under white and black pigments, extenders, inorganic and organic pigments. These chapters have been well written and provide all necessary information on pigment manufacture and properties. The great variety of shades and tints obtainable with modern colour manufacture becomes obvious from the text. The chemistry of colour manufacture is clearly and well described. Since lightfastness is often a problem with pigments it is encouraging to note in this American book mention of the British Blue Wool Scale as a standard for measurement of this property. One would have hoped the author would have followed his systematic treatment of pigments with a like study of media and solvents, appropriate to this volume. After pigments however, various media are mentioned and the subject is then dropped until the last chapter of the book when a fuller account is given of vinyls, polyesters, polyurethanes and such modern resins, in a section on chemically resistant coatings. The actual manufacture of paint is well described, mention being made of such modern equipment as the high speed impeller which in part can replace the familiar roller grinder. Surface preparation and methods of application receive full treatment. With regard to formulation most paints are dealt with under industrial or architectural finishes. Since the book is American, emphasis is placed on paints for exterior use to protect wood. An interesting table provides information on the relative rates of disintegration of typical paints applied to a great variety of building woods.

Besides writing on pigments and paints the author has philosophized by heading every chapter with words of wisdom. 'An automobile has no resemblance to the man who made it, likewise creation gives no clue to the attributes of the Creator. Spirit is revealed only through spiritual approach.' All this may make some scientists throw up their hands in horror; however, it is the privilege of the author to include in his work what he chooses. Let us end in the same vein with a quotation from Solomon 'the beginning of wisdom is fear of the Lord'.

A. S. FREEBORN

Chemical Crystallography. An Introduction to Optical and X-Ray Methods (2nd ed.)

C. W. BUNN

Clarendon Press: Oxford University Press, London, 1961.

(xiv+509 pp.; 5½ in. by 8½ in.), 60s.

It is a pleasure to review such an extremely readable book as *Chemical Crystallography: Second Edition* by C. W. BUNN, the first edition of which soon established itself as one of the accepted textbooks on the subject.

The essence of this first edition was first that it integrated in a wholly satisfactory manner the optical and X-ray methods of investigating crystal

structures and secondly that it presented a good deal of information in a fairly non-mathematical manner, making the book a very good introduction for the newcomer to the subject.

The many excellent diagrams are a particularly valuable feature of this book. Their simplicity and clarity add to the understanding of the text as well as emphasizing the importance of visualizing the three-dimensional nature of X-ray crystallographic problems.

Since 1945, both X-ray techniques and techniques of molecular structure have developed considerably and it is fitting that some revision should have been thought worth while. At the same time it is clear that any attempt to integrate all the new techniques would mean entirely rewriting and changing the complexion of the book.

Dr BUNN has chosen to make comparatively small changes, with the exception of two advances in X-ray crystallography itself—heavy atom and anomalous scattering techniques, and these topics are dealt with very adequately. The use of the optical transform is also described, but in less detail.

The remaining additions are quite small and somewhat uneven in quality. The use of infra-red spectroscopy is mentioned satisfactorily, whereas many of the immense developments in magnetism and magnetic spectroscopy are not considered; for example the general relation between structure and magnetic properties should have received a review reference later than 1937. Again, although there is adequate mention of diffractometer techniques, it seems surprising that neutron diffraction and electron diffraction are not given greater prominence. The use of bond polarizabilities is described in detail. There is, however, considerable divergence of opinion concerning these results, particularly with regard to the values for the C—C bond and it would perhaps have been better to have given this point some prominence.

These criticisms are, however, very minor compared with the general level of discussion which is of a high order. This book is much more than another textbook on crystallography; Dr BUNN has managed to infuse into its text some of his own personal approach to the subject. It is this combination of factual content and scientific insight which makes it such admirable reading for the research worker and undergraduate alike.

The book, while remaining an essential part of the library of any would-be crystallographer does not profess to be an exhaustive textbook on the subject. At its original price of 25s. it was certainly possible for many students to have it in their personal possession. It is indeed unfortunate that its new price of £3 will, in many cases, place it beyond their reach.

I. M. WARD

Handbook of Organometallic Compounds

H. C. KAUFMAN

Van Nostrand: London, 1961.

(iv+1546 pp; 6 $\frac{3}{4}$ in. by 9 $\frac{3}{4}$ in.), 169s.

UNTIL recently, the literature of organometallic chemistry has been dominated by the classic *Die Chemie der metalorganischen Verbindungen*, by KRAUSE and VON GROSE, published in 1937. Consequently, any text which would bring this work up to date would be welcomed by chemists interested in this active field. The present weighty (2.585 kg) volume is, however, unlikely to receive such a welcome. It lists data on (it is said) about 12 000 organometallic compounds, including, where available, formula, name, molecular weight, state of

structures and secondly that it presented a good deal of information in a fairly non-mathematical manner, making the book a very good introduction for the newcomer to the subject.

The many excellent diagrams are a particularly valuable feature of this book. Their simplicity and clarity add to the understanding of the text as well as emphasizing the importance of visualizing the three-dimensional nature of X-ray crystallographic problems.

Since 1945, both X-ray techniques and techniques of molecular structure have developed considerably and it is fitting that some revision should have been thought worth while. At the same time it is clear that any attempt to integrate all the new techniques would mean entirely rewriting and changing the complexion of the book.

Dr BUNN has chosen to make comparatively small changes, with the exception of two advances in X-ray crystallography itself—heavy atom and anomalous scattering techniques, and these topics are dealt with very adequately. The use of the optical transform is also described, but in less detail.

The remaining additions are quite small and somewhat uneven in quality. The use of infra-red spectroscopy is mentioned satisfactorily, whereas many of the immense developments in magnetism and magnetic spectroscopy are not considered; for example the general relation between structure and magnetic properties should have received a review reference later than 1937. Again, although there is adequate mention of diffractometer techniques, it seems surprising that neutron diffraction and electron diffraction are not given greater prominence. The use of bond polarizabilities is described in detail. There is, however, considerable divergence of opinion concerning these results, particularly with regard to the values for the C—C bond and it would perhaps have been better to have given this point some prominence.

These criticisms are, however, very minor compared with the general level of discussion which is of a high order. This book is much more than another textbook on crystallography; Dr BUNN has managed to infuse into its text some of his own personal approach to the subject. It is this combination of factual content and scientific insight which makes it such admirable reading for the research worker and undergraduate alike.

The book, while remaining an essential part of the library of any would-be crystallographer does not profess to be an exhaustive textbook on the subject. At its original price of 25s. it was certainly possible for many students to have it in their personal possession. It is indeed unfortunate that its new price of £3 will, in many cases, place it beyond their reach.

I. M. WARD

Handbook of Organometallic Compounds

H. C. KAUFMAN

Van Nostrand: London, 1961.

(iv+1546 pp; 6 $\frac{3}{4}$ in. by 9 $\frac{1}{4}$ in.), 169s.

UNTIL recently, the literature of organometallic chemistry has been dominated by the classic *Die Chemie der metalorganischen Verbindungen*, by KRAUSE and VON GROSE, published in 1937. Consequently, any text which would bring this work up to date would be welcomed by chemists interested in this active field. The present weighty (2.585 kg) volume is, however, unlikely to receive such a welcome. It lists data on (it is said) about 12 000 organometallic compounds, including, where available, formula, name, molecular weight, state of

aggregation, solubility, refractive index, density, vapour pressure, and, occasionally, other properties.

The range of elements chosen as forming organo-derivatives is distinctly odd—at random, compounds listed include LiAlH_4 (under lithium), NaBH_4 (under boron), neptunium borohydride (the complete entry under neptunium—but no data and no references!), and many halogen compounds, such as VOCl_3 , VF_5 , PCl_5 , PHF_6 and C_2Cl_6 . The nomenclature used in places can only be called perverse—is there anyone who calls $\text{Al}(\text{C}_2\text{H}_5)_3$ 'Triethyl alumine'? In some cases, however, collection of the data may be useful to specialists in, for example, the extensive sections devoted to silicon (394 pages), boron (100 pages), tin (86 pages) and phosphorus (352 pages). Even here, a number of misprints, amongst minor points such as authors' names and journal titles, make one suspect the accuracy of the rest of the text, although, in all fairness, this is not immediately obvious.

Chemists are greatly indebted for the many useful and authoritative works of reference which have appeared over the years from these publishers. The present volume is rather below this high standard.

C. A. FINCH

Notes

A Quasi-soluble Ziegler Catalyst for the Polymerization of Ethylene

THE Ziegler catalysts which are usually employed to polymerize ethylene or alpha-olefins contain a solid crystalline phase insoluble in the polymerization medium. It has been stated¹ that the crystalline phase is essential in this type of polymerization and that no high polymers can be formed without it.

More recently there have been put forward some very convincing claims for truly soluble catalyst systems which can polymerize ethylene to give polymers of high molecular weight. These catalysts are usually complexes of aluminium alkyls with transition metal compounds²⁻⁴.

The work of Beerman and Bestian³, however, gives a very clear demonstration of a catalyst in which a solid crystalline phase is necessary. These workers prepared and isolated methyl titanium trichloride which would only polymerize ethylene after some decomposition had produced insoluble titanium trichloride.

We have recently come across a Ziegler type system which also demonstrates the necessity of a crystalline phase for polymerization. This system is described below.

PREPARATION OF CATALYST AND POLYMERIZATION EXPERIMENTS

Diisobutyl aluminium ethoxide $\text{Al}(\text{iBu})_2\text{OEt}$ and titanium tetrachloride were mixed for 100 minutes at 65°C in isooctane at concentrations of 100 and 200 mmole/l. respectively. The mixture was filtered to separate the brown precipitate, and the clear red filtrate was used to initiate the polymerization of ethylene.

Ethylene was passed into a solution of the red filtrate containing 5 mmole/l. of aluminium at 80°C . Polyethylene began to form only after an induction period of 60 minutes. The rate of polymerization was then similar to that obtained with the unfiltered catalyst mixture. When the original red filtrate was stored for 18 days in the absence of light it contained traces of brown precipitate. A sample of this mixture was withdrawn and used to effect a polymerization at 80°C , the aluminium concentration being 10 mmole/l. Polymerization commenced immediately without an induction period and proceeded at a normal rate. When a similar sample of the red filtrate was carefully re-filtered it could initiate polymerization only after an induction period of 1 hour. It would thus appear that the presence of a very small amount of brown precipitate is necessary to the polymerization.

Further experiments have shown that the induction period tends to increase as the catalyst concentration is reduced so that three reactions performed at 80°C with 5, 10 and 16 mmole/l. of aluminium showed

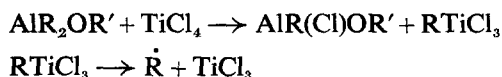
induction periods of 100, 30 and 20 minutes respectively. The induction period decreases with increasing temperature of polymerization. For similar polymerizations performed at 70, 80 and 100°C, the induction periods were 170, 30 and 0 minutes respectively.

The polymers obtained from these experiments were linear polyethylenes of density 0.945 to 0.950.

CONSTITUTION OF CATALYST MIXTURE

We have attempted to analyse the products from the initial reaction of diisobutyl aluminium ethoxide (R₂AlOR') and titanium tetrachloride.

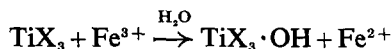
Our standard method (Method A) treats such a mixture with dilute sulphuric acid, adds an excess of ferric salt and back titrates with permanganate. With some mixtures we obtained a higher value when the addition of sulphuric acid and ferric salt was reversed (Method B). We ascribe these differences to the presence of an alkyl titanium compound such as RTiX₃ (X is Cl or OR'). The reaction mixture thus contains both TiX₃ and RTiX₃ from the initial reactions which have usually been represented as:



In Method A the alkyl aluminium compound is decomposed by dilute sulphuric acid and reacts



so that the ferric acid salt is reduced only by TiX₃.



In Method B the ferric salt is reduced by both titanium compounds. The alkyl titanium compound will almost certainly react with two equivalents of ferric salt.



We have established that alkyl aluminium compounds, which are also present, interfere with these titrations to a negligible extent. Our estimations suggest that the proposed alkyl titanium compound, which is present, is very stable.

Table 1

Time, days	Reduction, % (based on original quantity of TiCl ₄)		
	B Apparent total reduction	A Reduction attributed to Ti ³⁺	D = ½(B-A) Reduction attributed to Ti alkyl
Initial analysis	38.9	21.2	8.8
21	36.6	20.1	8.2

When filtering the original catalyst mixture we separate essentially solid TiCl_3 , whereas the other aluminium and titanium compounds remain in the filtrate. *Table 1* shows that the concentration of the proposed alkyl titanium compound falls by only a small percentage when the solution is stored in the dark for 21 days at room temperature. It is also apparent from *Table 1* that the solution contains a major percentage of a trivalent titanium compound. Extensive analyses of the type described, but carried out on the unfiltered mixtures, have demonstrated the stability of the proposed alkyl titanium compound at various temperatures. The compound is quite stable during several hours in the range 60° to 80°C .

The total composition of a typical filtrate used in the above polymerizations was computed to be as follows:

$\text{Al}(\text{iBu})_2\text{OEt}$. . .	10.7 per cent	} Molar percentages based on original TiCl_4
$\text{Al}(\text{iBu})\text{OEtCl}$. . .	39.3 per cent	
TiCl_4	. . .	60.7 per cent	
Ti^{3+} (soluble)	. . .	19.0 per cent	
Ti alkyl	. . .	9.9 per cent	

Apart from the presence of a solid crystalline phase, such as TiCl_3 , the solution appears to contain all the entities required to initiate polymerization. Although we have not attempted to isolate these constituents, our analyses indicate the presence of compounds containing alkyl aluminium bonds, alkyl titanium bonds, titanium tetrachloride and trivalent titanium compounds. The latter are soluble and could be colloidal TiCl_3 , alkoxide derivatives formed by interchange, or some soluble complex of TiCl_3 and an aluminium alkyl derivative. Yet polymerization does not occur until a crystalline phase, such as TiCl_3 , appears.

We would conclude that many of the Ziegler-Natta catalysts can only initiate polymerization on a specific surface without which the polymerization cannot take place.

Conditions for preparation of solution

Concentration	TiCl_4	: 200 mmole/l.
	$\text{Al}(\text{iBu})_2\text{OEt}$: 100 mmole/l.
Solvent		: Isooctane
Temperature		: 65°C
Time before filtration		: 90 min

M. N. BERGER and K. FLETCHER

*Carrington Research Laboratory,
Petrochemicals Ltd,
Urmston, Manchester*

(Received May 1961)

REFERENCES

- ¹ FRIEDLANDER, H. N. and OITA, K. *Industr. Engng Chem. (Industr.)*, 1957, **49**, 1885
- ² NATTA, G. Fifteenth Annual Technical Conference of the Society of Plastics Engineers, Stereospecific Polymers Session, New York, 27 to 30 January 1959
- ³ BRESLOW, D. S. and NEWBURY, N. R. *J. Amer. chem. Soc.* 1959, **81**, 87
- ⁴ CARRICK, W. L. *J. Amer. chem. Soc.* 1960, **82**, 3883 and 3887
- ⁵ BEERMAN, C. and BESTIAN, H. *Angew. Chem.* 1959, **71**, 618

Radiation-induced Conductivity in Irradiated Polythene

SPECIMENS of Alkathene 7F which had been given doses of 25 megarads of 2 MeV electrons were provided with evaporated silver electrodes and exposed to gamma radiation in the manner previously described¹. The induced conductivity σ in this material was a linear function of dose rate (Figure 1). The rise and decay of conductivity followed an exponential

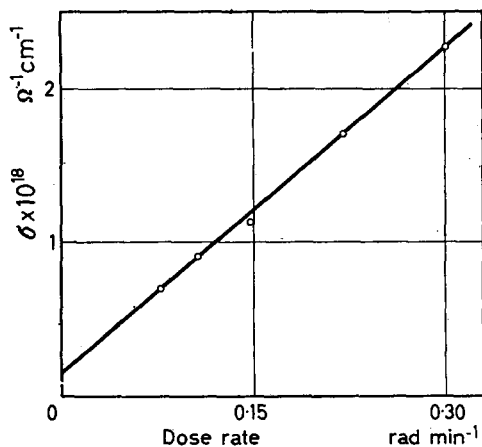
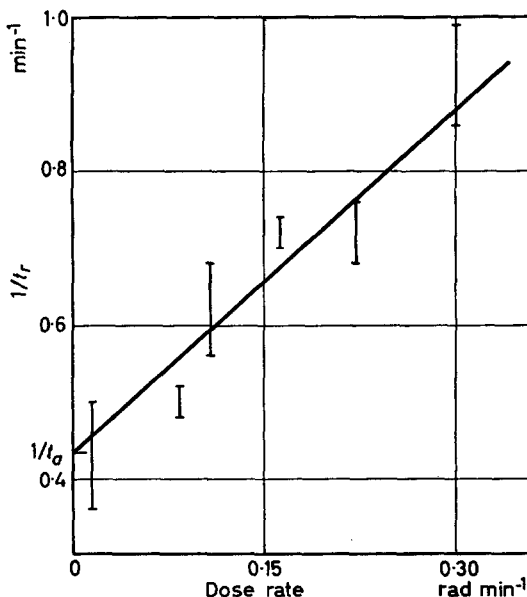


Figure 1—Graph of induced conductivity σ against dose rate

Figure 2—Graph of reciprocal rise time $1/t_r$ against dose rate. The reciprocal of the decay time $1/t_d$ is marked in



form. The reciprocal of the rise time t_r , defined as the time for the first 50 per cent of the conductivity change to take place, is plotted against dose rate in Figure 2. The decay times were closely grouped about a mean value of 2.3 min, and equalled the rise time at zero dose rate. Little difference was found between results obtained at various temperatures in the range 20° to 70°C. The slope of the graph of induced conductivity

against dose rate (*Figure 1*) is $7 \times 10^{-13} \text{ ohm}^{-1} \text{ cm}^{-1} \text{ rad}^{-1} \text{ min}$, which is in agreement with the values obtained in experiments on many insulating substances².

The most reasonable assumption to make about the initial radiation damage is that traps are introduced at one energy level. Since the induced conductivity is linear with the dose rate, these traps lie below the Fermi level of the irradiated material. The probability of disappearance of a free carrier is now the sum of the probability of recombination when the original distribution of traps existed alone and the probability of recombination with the vacancies created when the new traps are filled. The latter probability will be constant at all dose rates and will be written $1/t_c$. From the theory given by Rose³ it can be shown that:

$$\frac{1}{t_r} = \frac{1}{t_c} + \frac{I+J}{0.69BkT}$$

$$\frac{1}{t_d} = \frac{1}{t_c} + \frac{J^2}{(I+J)BkT}$$

and

$$1/t_c = bC/0.69$$

where I is the ionization rate due to irradiation, J the ionization rate in the dark, BkT the density of original traps in an energy depth kT , assumed uniform for simplicity, b the capture cross section and C the concentration of the new traps. Also, in equilibrium

$$\sigma = ne\mu \quad \text{and} \quad I = bnC \quad (C \gg BkT)$$

where n is the carrier density, e the charge and μ the mobility. These equations are consistent with the linear relations found experimentally. Further,

$$d(1/t_r)/dI = 1/0.69 BkT$$

and

$$\frac{d\sigma}{dI} = \frac{e\mu}{bC}$$

whence the ratio of the slopes gives the value of $\mu BkT/bC$ as $2.500 \text{ V}^{-1} \text{ cm}^{-1}$. The decay time will be constant and will equal the rise time at zero dose rate if $J^2/(I+J)BkT \ll 1/t_c$, a condition which is adequately satisfied here if Fowler's data⁴ for B and μ are correct to within two orders of magnitude.

In order to estimate μ/b it will be supposed that C is identical with the concentration of unsaturated carbon-carbon bonds, about $3 \times 10^{19} \text{ cm}^{-3}$ in this material, and that $B = 10^{15} \text{ cm}^{-3} \text{ eV}^{-1}$. With these values, $\mu/b = 3 \times 10^9 \text{ V}^{-1} \text{ cm}^{-1}$, which is a factor of 10^3 greater than the value given by Fowler⁴ for the un-irradiated material. The most probable reasons for this discrepancy are that the trap density may not equal the unsaturation density and that the capture cross section may be different for the original traps and for those produced by radiation. Clearly these reasons depend upon the nature of the traps. No identification of the trap normally present in paraffins has yet been published, but since both the amount of antioxidant

and the initial density of unsaturation will vary with the source of the material, while the induced conductivity in fresh specimens apparently does not², the normal trap would appear to arise from the physical structure of the material.

The author wishes to thank Professor A. Charlesby for his continued interest and encouragement, and the Dean, Royal Military College of Science, for permission to publish this work.

H. J. WINTLE

*Physics Branch,
Royal Military College of Science,
Shrivenham, Swindon, Wilts.*

REFERENCES

- ¹ WINTLE, H. J. *Internat. J. appl. Radiation and Isotopes*, 1960, **8**, 132
- ² For a summary see WINTLE, H. J. *Brit. J. Radiol.* 1960, **33**, 706
- ³ ROSE, A. *R.C.A. Rev.* 1951, **12**, 362
- ⁴ FOWLER, J. F. *Proc. Roy. Soc. A*, 1956, **236**, 464

Determination of the Weight, Viscosity, or Number Average Degree of Polymerization of Cellulose from the Intrinsic Viscosity in Cuprammonium Hydroxide Solution

IN AN earlier publication¹ reference was made to an equation relating the number average degree of polymerization of cellulose to the intrinsic viscosity in cuprammonium hydroxide solution. It is the purpose of this note to explain the derivation of the equation.

When plotted together, the results of three concordant light scattering investigations²⁻⁴ yield the relationship

$$[\eta]_{\Delta} = 0.0083 \bar{P}_w^{0.95} \quad (1)$$

where $[\eta]_{\Delta}$ is the intrinsic viscosity (dl/g) of cellulose trinitrate⁵ in acetone at 25°C and \bar{P}_w the weight average degree of polymerization. In one case² intrinsic viscosities in ethyl acetate have been converted to values in acetone with the divisor 1.38, calculated from published data^{3, 4, 6}.

In the present investigation, cellulose DPs were calculated from intrinsic viscosity measurements on the trinitrate in butyl acetate: to convert from intrinsic viscosities in acetone, use was made of data published by Harland⁷ which, in conjunction with equation (1), lead to the relationship

$$[\eta]_{\text{BuOAc}} = 0.0078 \bar{P}_w^{0.99} \quad (2)$$

The validity of equations (1) and (2) is subject to the influence of DP distribution since intrinsic viscosity is related, strictly, to viscosity average DP⁸ which will, generally, differ from the weight average value by an amount which depends on the DP distribution. However, this effect becomes smaller as the exponent α in the Mark-Houwink equation approaches unity: thus in equations (1) and (2), the values of α of 0.95 and

and the initial density of unsaturation will vary with the source of the material, while the induced conductivity in fresh specimens apparently does not², the normal trap would appear to arise from the physical structure of the material.

The author wishes to thank Professor A. Charlesby for his continued interest and encouragement, and the Dean, Royal Military College of Science, for permission to publish this work.

H. J. WINTLE

*Physics Branch,
Royal Military College of Science,
Shrivenham, Swindon, Wilts.*

REFERENCES

- ¹ WINTLE, H. J. *Internat. J. appl. Radiation and Isotopes*, 1960, **8**, 132
- ² For a summary see WINTLE, H. J. *Brit. J. Radiol.* 1960, **33**, 706
- ³ ROSE, A. *R.C.A. Rev.* 1951, **12**, 362
- ⁴ FOWLER, J. F. *Proc. Roy. Soc. A*, 1956, **236**, 464

Determination of the Weight, Viscosity, or Number Average Degree of Polymerization of Cellulose from the Intrinsic Viscosity in Cuprammonium Hydroxide Solution

IN AN earlier publication¹ reference was made to an equation relating the number average degree of polymerization of cellulose to the intrinsic viscosity in cuprammonium hydroxide solution. It is the purpose of this note to explain the derivation of the equation.

When plotted together, the results of three concordant light scattering investigations²⁻⁴ yield the relationship

$$[\eta]_{\Delta} = 0.0083 \bar{P}_w^{0.95} \quad (1)$$

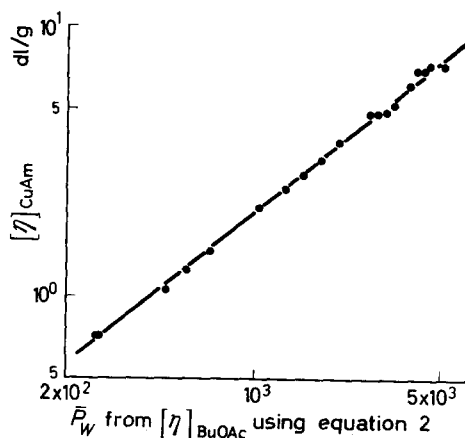
where $[\eta]_{\Delta}$ is the intrinsic viscosity (dl/g) of cellulose trinitrate⁵ in acetone at 25°C and \bar{P}_w the weight average degree of polymerization. In one case² intrinsic viscosities in ethyl acetate have been converted to values in acetone with the divisor 1.38, calculated from published data^{3, 4, 6}.

In the present investigation, cellulose DPs were calculated from intrinsic viscosity measurements on the trinitrate in butyl acetate: to convert from intrinsic viscosities in acetone, use was made of data published by Harland⁷ which, in conjunction with equation (1), lead to the relationship

$$[\eta]_{\text{BuOAc}} = 0.0078 \bar{P}_w^{0.99} \quad (2)$$

The validity of equations (1) and (2) is subject to the influence of DP distribution since intrinsic viscosity is related, strictly, to viscosity average DP⁸ which will, generally, differ from the weight average value by an amount which depends on the DP distribution. However, this effect becomes smaller as the exponent α in the Mark-Houwink equation approaches unity: thus in equations (1) and (2), the values of α of 0.95 and

Figure 1



0.99 correspond to differences between viscosity and weight averages of 1.2 and 0.3 per cent respectively in the case of an exponential or 'most probable' DP distribution (arising, for example, from random degradation). If the material is fractionated, the differences will be smaller still. From this it follows that equations (1) and (2) should apply with acceptable precision to distributions ranging from monodisperse to exponential.

With other solvent systems, the exponent α may differ significantly from unity, when allowance must be made for the divergence between weight and viscosity averages. In deriving a relationship between DP and intrinsic viscosity in cuprammonium, it was thought desirable to employ material of known DP distribution so that any difference between the two averages could be taken into account. Such material is readily obtained by the acid hydrolysis of cotton cellulose, since the hydrolysis has been shown to proceed by random scission, leading to an exponential DP distribution in the hydrolysed product⁹. Accordingly, dewaxed Egyptian cotton was hydrolysed for varying periods in *N* hydrochloric acid at 30°C, providing a range of samples of varying DP. Specimens were nitrated with mixtures of nitric acid, acetic acid and acetic anhydride¹⁰ and the intrinsic viscosity determined in *n*-butyl acetate at 25°C: results were corrected to 14.14 per cent nitrogen content⁵ and to zero rate of shear. Other specimens were dissolved in cuprammonium hydroxide solution¹¹ and the intrinsic viscosity determined at 25°C. Dissolution was carried out in a flask in the presence of 1 per cent cuprous chloride to prevent oxidative degradation of the cellulose¹². The flask was subsequently attached by a ground-glass joint to the jacket surrounding a pipette-type viscometer, the lower capillary orifice of the latter being immersed in the solution. Viscometer dimensions were: capillary length 30 cm, capillary diameter 0.05 cm, mean head 29 cm, capacity 2 ml. It was found necessary first to saturate the interior of the viscometer with vapour from 0.880 s.g. ammonium hydroxide solution: in addition, it was found that filling the viscometer under reduced pressure disturbed the temperature equilibrium due to evaporation of ammonia; so the viscometer was filled by increasing the pressure above the solution in the flask. With these precautions the method gave consistent results in good agreement with those obtained by the B.C.I.R.A. standard procedure¹¹.

In *Figure 1* is shown the logarithmic plot of \bar{P}_w , calculated from intrinsic viscosity in butyl acetate [equation (2)], against intrinsic viscosity in cuprammonium hydroxide solution. The results are well represented by

$$[\eta]_{\text{CuAm}} = 0.0077 \bar{P}_w^{0.81} \quad (3)$$

Since the data refer to material of exponential DP distribution, $\bar{P}_w/\bar{P}_n = 2$, and in addition, from the value of $\alpha (=0.81)$, it follows that $\bar{P}_w/\bar{P}_v = 1.05$, where \bar{P}_n and \bar{P}_v are respectively the number average and viscosity average degrees of polymerization.

Hence

$$[\eta]_{\text{CuAm}} = 0.0135 \bar{P}_n^{0.81} \quad (4)$$

and

$$[\eta]_{\text{CuAm}} = 0.0080 \bar{P}_v^{0.81} \quad (5)$$

Equations (3) and (4) are strictly valid for material of exponential DP distribution; equation (5) is valid for any distribution. The validity of all three is, of course, dependent on that of the original light scattering calibration. It has previously been pointed out that there is a discrepancy between light scattering molecular weights and those obtained from osmotic pressure¹³, the former method yielding values some 50 per cent higher than the corresponding osmotic pressure values. This difference, which has not been explained satisfactorily, creates some uncertainty with regard to absolute DP determination.

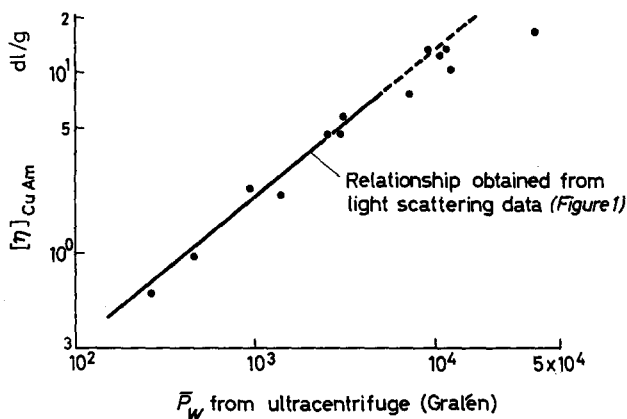


Figure 2

However, it is of interest that the relationship derived from light scattering [equation (3)] agrees quite well with the results obtained by Gralén¹⁴, using the ultracentrifuge to determine the molecular weight of cellulose in cuprammonium: this is illustrated in *Figure 2*. Validity of the light scattering calibration would substantially verify Gralén's molecular weight determinations, which have hitherto been regarded as anomalous^{14, 15}.

R. I. C. MICHIE

Department of Textile Chemistry,
College of Science and Technology,
Manchester, 1

(Received July 1961)

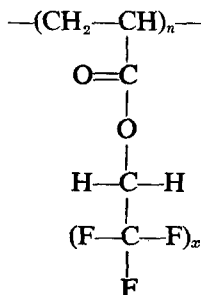
REFERENCES

- ¹ DLUGOSZ, J. and MICHIE, R. I. C. *Polymer, Lond.* 1960, **1**, 41
- ² HUNT, M. L., NEWMAN, S., SCHERAGA, H. A. and F5(x), P. J. *J. phys. Chem.* 1956, **60**, 1278
- ³ HOLTZER, A. M., BENOIT, H. and DOTY, P. *J. phys. Chem.* 1954, **58**, 624
- ⁴ HUQUE, M. M., GORING, D. A. I. and MASON, S. G. *Canad. J. Chem.* 1958, **36**, 952
- ⁵ HARLAND, W. G. *J. Text. Inst.* 1954, **45**, T692
- ⁶ MOORE, W. R. and EPSTEIN, J. A. *J. appl. Chem.* 1955, **5**, 34
MOORE, W. R., EPSTEIN, J. A., BROWN, A. M. and TIDSWELL, B. M. *J. Polym. Sci.* 1957, **23**, 23
- ⁷ HARLAND, W. G. *J. Text. Inst.* 1958, **49**, T478
- ⁸ FLORY, P. J. *Principles of Polymer Chemistry*, p 313. Cornell University Press: Ithaca, New York, 1953
- ⁹ SHARPLES, A. and MAJOR, H. M. *J. Polym. Sci.* 1958, **27**, 433
- ¹⁰ HARLAND, W. G. *J. Text. Inst.* 1954, **45**, T678
- ¹¹ CLIBBENS, D. A. and LITTLE, A. H. *J. Text. Inst.* 1936, **27**, T285
- ¹² LAUNER, H. F. and WILSON, W. K. *Analyt. Chem.* 1950, **22**, 455
- ¹³ MICHIE, R. I. C., SHARPLES, A. and WALTER, A. A. *J. Polym. Sci.* 1961, **51**, 85
- ¹⁴ See HERMANS, P. H. *Physics and Chemistry of Cellulose Fibres*, pp 115-120. Elsevier: New York, Amsterdam, London, 1949
- ¹⁵ GRALÉN, N. and LINDEROT, J. *Svensk. PappTidn.* 1956, **59**, 14

Glass Temperatures of Homologous Series

GRIEVESON has recently proposed an interesting treatment of polymeric homologues as 'copolymers' of the first series member and the growing portion of the repeating unit¹. However, his plot of fluoroacrylate glass temperatures and also his deductions from this plot merit comment.

The data used are the glass temperatures determined refractometrically by other workers² for a series of 1,1-dihydroperfluoroalkyl acrylates of the general formula



Contrary to the author's suggestion, it seems clear that the glass temperature curve versus weight fraction of $\text{---}(\text{CF}_2)_x\text{---}$ cannot be extrapolated to represent poly(acrylic acid) in the limit, for $x \rightarrow 0$. Rather, the extrapolation would correspond to the monofluorosubstituted methyl acrylate

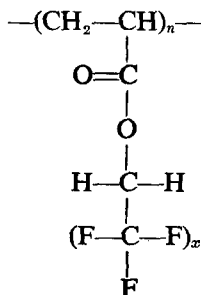
REFERENCES

- ¹ DLUGOSZ, J. and MICHIE, R. I. C. *Polymer, Lond.* 1960, **1**, 41
- ² HUNT, M. L., NEWMAN, S., SCHERAGA, H. A. and F5(x), P. J. *J. phys. Chem.* 1956, **60**, 1278
- ³ HOLTZER, A. M., BENOIT, H. and DOTY, P. *J. phys. Chem.* 1954, **58**, 624
- ⁴ HUQUE, M. M., GORING, D. A. I. and MASON, S. G. *Canad. J. Chem.* 1958, **36**, 952
- ⁵ HARLAND, W. G. *J. Text. Inst.* 1954, **45**, T692
- ⁶ MOORE, W. R. and EPSTEIN, J. A. *J. appl. Chem.* 1955, **5**, 34
MOORE, W. R., EPSTEIN, J. A., BROWN, A. M. and TIDSWELL, B. M. *J. Polym. Sci.* 1957, **23**, 23
- ⁷ HARLAND, W. G. *J. Text. Inst.* 1958, **49**, T478
- ⁸ FLORY, P. J. *Principles of Polymer Chemistry*, p 313. Cornell University Press: Ithaca, New York, 1953
- ⁹ SHARPLES, A. and MAJOR, H. M. *J. Polym. Sci.* 1958, **27**, 433
- ¹⁰ HARLAND, W. G. *J. Text. Inst.* 1954, **45**, T678
- ¹¹ CLIBBENS, D. A. and LITTLE, A. H. *J. Text. Inst.* 1936, **27**, T285
- ¹² LAUNER, H. F. and WILSON, W. K. *Analyt. Chem.* 1950, **22**, 455
- ¹³ MICHIE, R. I. C., SHARPLES, A. and WALTER, A. A. *J. Polym. Sci.* 1961, **51**, 85
- ¹⁴ See HERMANS, P. H. *Physics and Chemistry of Cellulose Fibres*, pp 115-120. Elsevier: New York, Amsterdam, London, 1949
- ¹⁵ GRALÉN, N. and LINDEROT, J. *Svensk. PappTidn.* 1956, **59**, 14

Glass Temperatures of Homologous Series

GRIEVESON has recently proposed an interesting treatment of polymeric homologues as 'copolymers' of the first series member and the growing portion of the repeating unit¹. However, his plot of fluoroacrylate glass temperatures and also his deductions from this plot merit comment.

The data used are the glass temperatures determined refractometrically by other workers² for a series of 1,1-dihydroperfluoroalkyl acrylates of the general formula



Contrary to the author's suggestion, it seems clear that the glass temperature curve versus weight fraction of $\text{---}(\text{CF}_2)_x\text{---}$ cannot be extrapolated to represent poly(acrylic acid) in the limit, for $x \rightarrow 0$. Rather, the extrapolation would correspond to the monofluorosubstituted methyl acrylate

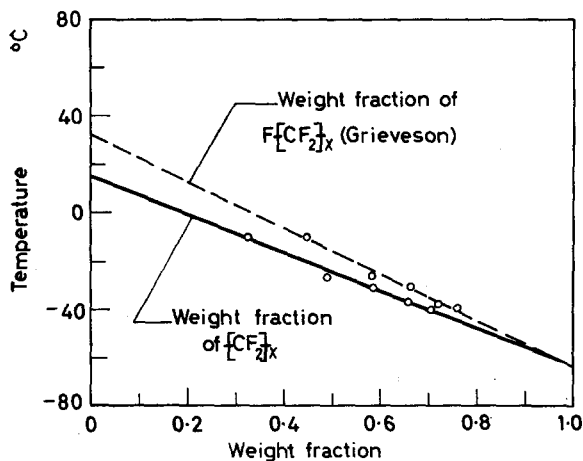
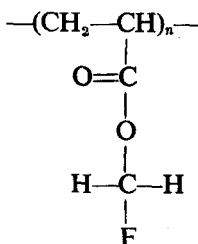


Figure 1—Glass temperatures of a series of 1,1-dihydroperfluoroalkyl acrylates treated as copolymers (ref. 2)



Furthermore, the abscissa values of the plot indicate that the third fluorine atom at the tail end has been included in the computed fluorocarbon weight fractions. This produces an appreciable error in the extrapolation to $x=0$, as can be seen from Figure 1. The glass temperatures of this series have been plotted versus the weight fraction both of $\text{F}-(\text{CF}_2)_x\text{---}$ and $\text{---}(\text{CF}_2)_x\text{---}$, extrapolating to 33°C and 15°C , respectively.

Table 1. (Values from ref. 2)

1, 1-Dihydroperfluoroalkyl acrylate	Monomeric molecular weight	Glass temp. T_g °C	Weight fraction of	
			$\text{F}-(\text{CF}_2)_x\text{---}$	$\text{---}(\text{CF}_2)_x\text{---}$
Ethyl	154.09	-10	0.448	0.324
Propyl	204.10	-26	0.583	0.490
Butyl	254.11	-30	0.664	0.590
Pentyl	304.12	-37	0.720	0.657
Hexyl	354.13	-39	0.760	0.705

Grieverson's plot corresponds to the $\text{F}-(\text{CF}_2)_x\text{---}$ line in Figure 1. His comparison of the extrapolated value of 'about 35°C ' with the much higher value of 106°C found dynamic mechanically by Hughes and Fordyce for the glass transition temperature of poly(acrylic acid) must be irrelevant. Instead, it is suggested that the extrapolation of the $\text{---}(\text{CF}_2)_x\text{---}$ line should be considered, not as being representative of poly(acrylic acid), but rather of the above monofluorosubstituted methyl acrylate. Accounting for the

anticipated effect of the fluorine atom, the value of 15°C compares favourably with the dilatometrically established value of about 9°C for the glass temperature of poly(methyl acrylate).

G. K. DYVIK*

Physics Laboratory,
Rohm & Haas Company,
Bristol, Pennsylvania, U.S.A.

(Received August 1961)

* Present address: Horten Tekniske Skole, Horten, Norway

REFERENCES

- GRIEVESON, B. M. 'Glass transition temperature in homologous series of linear polymers'. *Polymer, Lond.* 1960, **1**, 499-512
- BOVEY, F. A., ABERE, J. F., RATHMANN, G. B. and SANDBERG, C. L. 'Fluorine-containing polymers III. Polymers and copolymers of 1,1-dihydroperfluoroalkyl acrylates'. *J. Polym. Sci.* 1955, **15**, 520-536
- THOMPSON HUGHES, L. J. and FORDYCE, D. B. 'Sorption of water vapor by water-soluble polymers: kinetic, equilibrium, and glass temperature data'. *J. Polym. Sci.* 1956, **22**, 509-526

Mechanisms of Pyrolysis of Epoxide Resins

NEIMAN *et al.*¹ recently reported on the thermal decomposition of a diepoxide monomer prepared by condensing bisphenol A with epichlorohydrin. They² also reported on the pyrolysis of a polymer prepared from the same diepoxide and maleic anhydride. In both cases, they proposed that one of the main steps in the mechanism of decomposition consisted initially of bond scission to produce a radical containing an intact epoxy group which subsequently isomerized to a radical containing a carbonyl group.

Differential thermometric experiments in our Laboratory support the idea that isomerization of an epoxy group to a carbonyl is an important step in the pyrolysis of epoxide resins. For example, when we pyrolysed a diepoxide monomer similar to the one that Neiman *et al.* studied, using the technique of differential thermometry, an exothermic peak was observed in the 350° to 400°C range as shown in *Figure 1*. This peak is attributed to

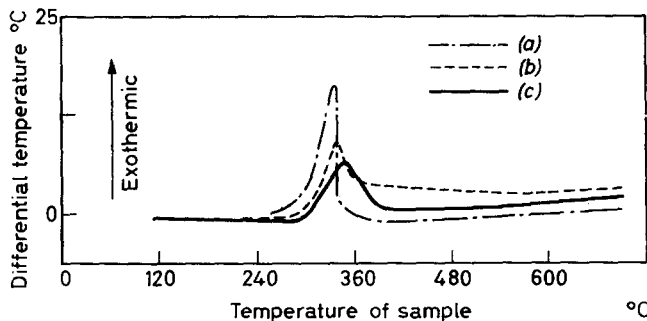


Figure 1—Differential thermometric curves of Dow D.E.R. 332 epoxide: (a) unpolymerized; (b) polymerized with meta-phenylenediamine; (c) polymerized with maleic anhydride. Heating rate: 5°C/min

anticipated effect of the fluorine atom, the value of 15°C compares favourably with the dilatometrically established value of about 9°C for the glass temperature of poly(methyl acrylate).

G. K. DYVIK*

Physics Laboratory,
Rohm & Haas Company,
Bristol, Pennsylvania, U.S.A.

(Received August 1961)

* Present address: Horten Tekniske Skole, Horten, Norway

REFERENCES

- GRIEVESON, B. M. 'Glass transition temperature in homologous series of linear polymers'. *Polymer, Lond.* 1960, **1**, 499-512
- BOVEY, F. A., ABERE, J. F., RATHMANN, G. B. and SANDBERG, C. L. 'Fluorine-containing polymers III. Polymers and copolymers of 1,1-dihydroperfluoroalkyl acrylates'. *J. Polym. Sci.* 1955, **15**, 520-536
- THOMPSON HUGHES, L. J. and FORDYCE, D. B. 'Sorption of water vapor by water-soluble polymers: kinetic, equilibrium, and glass temperature data'. *J. Polym. Sci.* 1956, **22**, 509-526

Mechanisms of Pyrolysis of Epoxide Resins

NEIMAN *et al.*¹ recently reported on the thermal decomposition of a diepoxide monomer prepared by condensing bisphenol A with epichlorohydrin. They² also reported on the pyrolysis of a polymer prepared from the same diepoxide and maleic anhydride. In both cases, they proposed that one of the main steps in the mechanism of decomposition consisted initially of bond scission to produce a radical containing an intact epoxy group which subsequently isomerized to a radical containing a carbonyl group.

Differential thermometric experiments in our Laboratory support the idea that isomerization of an epoxy group to a carbonyl is an important step in the pyrolysis of epoxide resins. For example, when we pyrolysed a diepoxide monomer similar to the one that Neiman *et al.* studied, using the technique of differential thermometry, an exothermic peak was observed in the 350° to 400°C range as shown in *Figure 1*. This peak is attributed to

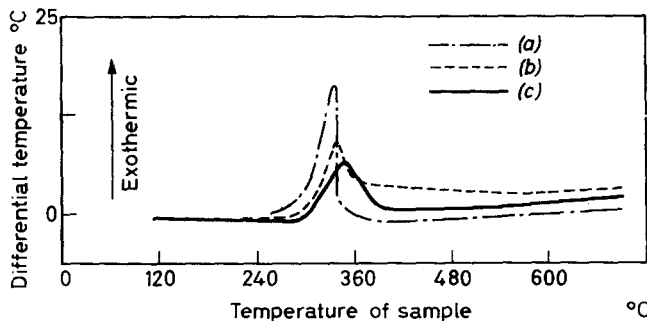


Figure 1—Differential thermometric curves of Dow D.E.R. 332 epoxide: (a) unpolymerized; (b) polymerized with meta-phenylenediamine; (c) polymerized with maleic anhydride. Heating rate: 5°C/min

isomerization of the epoxide groups to carbonyl groups. Exothermic peaks were also observed for two polymers prepared from the diepoxide and maleic anhydride or meta-phenylenediamine. In the case of the polymers, the exothermic peaks were due to isomerization of residual epoxide groups to carbonyl groups.

The thermal isomerization of ethylene oxide to acetaldehyde has been reported^{3,4} to be highly exothermic. Since the above epoxides can be considered to be derivatives of ethylene oxide, it is reasonable to assume that they can behave in a similar manner. These observed exothermic peaks indicate that the heat of isomerization is enough to overshadow the heat absorbed by simultaneous volatilization and bond scission.

We propose that the free radical mechanism of the thermal decomposition of epoxide resins proposed by Neiman and his co-workers can also be accounted for by assuming isomerization of the epoxy group still attached to the resin or polymer. In this case, the rapid isomerization reaction could generate enough instantaneous heat⁴ to initiate many types of free radical reactions.

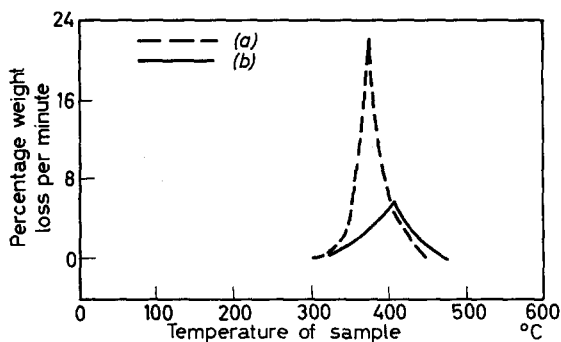


Figure 2 — Differential thermogravimetric curves of Dow D.E.R. 332 epoxide polymerized with: (a) meta-phenylenediamine; (b) maleic anhydride. Heating rate: 5°C/min

The pyrolysis mechanism of epoxide polymers is indeed complex and can be influenced by factors other than isomerization of the epoxy group. The differential thermogravimetric curves obtained in our Laboratory and presented in *Figure 2* show that the maximum rates of pyrolysis differ greatly for two polymers prepared from the same diepoxide mentioned above and maleic anhydride or meta-phenylenediamine. One reason for the higher maximum rate of decomposition of the polymer prepared from the diamine could be the susceptibility of the amino groups to internal oxidation, i.e. oxidation caused by oxygen chemically bound in the polymer, since the experiments were carried out *in vacuo*.

H. C. ANDERSON

*Non-Metallic Materials Division,
U.S. Naval Ordnance Laboratory,
White Oak, Silver Spring, Md*

(Received October 1961)

REFERENCES

- ¹ NEIMAN, M. B., GOLUBENKOVA, L. I., KOVARSKAYA, B. M., STRIZHKOVA, A. S., LEVANTOVSKAYA, I. I., AKUTIN, M. S. and MOISEEV, V. D. *Vyosokomol. Soedineniya*, 1959, **1**, 1531
- ² NEIMAN, M. B., KOVARSKAYA, B. M., STRIZHKOVA, A. S., LEVANTOVSKAYA, I. I. and AKUTIN, M. S. *Dokl. Akad. Nauk S.S.S.R.* 1960, **135**, 1147
- ³ HECKERT, W. W. and MACK, JR, E. J. *Amer. chem. Soc.* 1929, **51**, 2706
- ⁴ PEYTRAL, E. *Bull. Soc. chim. Fr.* 1926, **39**, 306

Contributions to Polymer

*Papers accepted for future issues of
POLYMER include the following:*

*Viscosity-Shear Effects in Polyisobutylene Systems as a Function of
Solution Variables—R. S. PORTER and J. F. JOHNSON*

*The Degradation of Poly(ethylene Terephthalate) by Methylamine: A Study
by Infra-red and X-Ray Methods—G. FARROW, D. A. S. RAVENS and
I. M. WARD*

*A Kinetic Study of the Benzene-induced Crystallization of Polyethylene
Terephthalate—R. P. SHELDON*

*A New Technique for Following High Rates of Crystallization.
II—Isotactic Polypropylene—J. H. MAGILL*

*Thermodynamic Properties of Dilute Solutions of Polymethyl Methacrylate
in Butanone and in Nitroethane—E. F. CASSASSA and W. H.
STOCKMAYER*

*Properties of Dilute Polymer Solutions. I—Osmotic and Viscometric
Properties of Solutions of Conventional Polymethyl Methacrylate
—T. G. FOX, J. B. KINSINGER, H. F. MASON and E. M. SCHUELE*

*Properties of Dilute Polymer Solutions. II—Light Scattering and Visco-
metric Properties of Solutions of Conventional Polymethyl Metha-
crylate—E. COHN-GINSBERG, T. G. FOX and H. F. MASON*

*Properties of Dilute Polymer Solutions. III—Intrinsic Viscosity/
Temperature Relationships for Conventional Polymethyl Methacrylate
—T. G. FOX*

*A Treatment of Static and Dynamic Birefringence in Linear Amorphous
Polymers by an Extension of the Molecular Theory of Viscoelasticity
—B. E. READ*

*Interference Microscopy of Solution-grown Polyethylene Single Crystals
—B. WUNDERLICH*

CONTRIBUTIONS should be addressed to the Editors, *Polymer*, 4-5 Bell Yard, London, W.C.2.

Authors are solely responsible for the factual accuracy of their papers. All papers will be read by one or more referees, whose names will not normally be disclosed to authors. On acceptance for publication papers are subject to editorial amendment.

If any tables or illustrations have been published elsewhere, the editors must be informed so that they can obtain the necessary permission from the original publishers.

All communications should be expressed in clear and direct English, using the minimum number of words consistent with clarity. Papers in other languages can only be accepted in very exceptional circumstances.

A leaflet of instructions to contributors is available on application to the editorial office.

Classified Contents

- Advanced Paint Chemistry*, review of, 437
- Anion exchangers based on cellulose: I—Preparation and general properties, 18
- Anionic polymerization of styrene, 151
- Applications of direct examination of polymer degradation by gas chromatography to polymer analysis and characterization, 27
- Arbeitserinnerungen*, review of, 364
- Assignment of the infra-red absorption bands and the measurement of tacticity in polypropylene, 341
- Branched polymers: I—Molecular weight distributions, 295
- II—Dimensions in non-interacting media, 305
- Butadiene-styrene copolymerization, thermochemical aspects of, 74
- Cellulose, determination of the weight, viscosity, or number average degree of polymerization of, from the intrinsic viscosity in cuprammonium hydroxide solution, 446
- Cellulose and its derivatives, synthesis of block and graft copolymers of, 213
- Chain flexibilities, intermolecular forces and, in polymers: III, 375
- Chemical Crystallography. An Introduction to Optical and X-Ray Methods* (2nd ed.), review of, 438
- Chemistry of Nucleic Acids*, review of, 117
- Constitution of ethylene-propylene copolymers, 357
- Crystallization of poly[3,3-bis (chloromethyl) oxacyclobutane], 1
- Crystallization of polyethylene terephthalate by organic liquids, 315
- Depolymerization in naphthalene and tetralin solutions, 367
- Derivation of Tung's and Wesslau's molecular weight distribution, surface-chemical mechanism of heterogeneous polymerization and, 41
- Detection of the side chains in a study of short chain branching in hydrocarbon polymers by the irradiation method, 323
- Determination of the weight, viscosity, or number average degree of polymerization of cellulose from the intrinsic viscosity in cuprammonium hydroxide solution, 446
- Di-anisoyl peroxide and the anisoyloxy radical, tracer studies of, 265
- Dielectric and dynamic mechanical properties of polyoxymethylene (Delrin), 239
- Dimensions of branched polymers in non-interacting media, 305
- Direct examination of polymer degradation by gas chromatography: I—Applications to polymer analysis and characterization, 27
- Effect of added terminating agent in a test between rival theories for molecular weight distributions in heterogeneous polymerization, 60
- Effect of high-frequency discharge on the surfaces of solids: I—Production of surface radicals on polymers, 277
- Effect of primary radicals in the termination reaction in radiation polymerization in solution, 83
- Effect of radiation and moisture on the dynamic mechanical properties of polyethylene terephthalate, 401
- Effect of zinc oxide on the radiation-initiated polymerization of isobutene at -78°C , 419
- Electron spin resonance studies of irradiated polymers: I—Factors affecting the electron spin resonance spectra of irradiated polymers, 119
- Epoxide resins, mechanism of crosslinking of, by amines, 95
- mechanisms of pyrolysis of, 451

- Ethylene, a quasi-soluble Ziegler catalyst for the polymerization of, 441
- Ethylene-propylene copolymers, constitution of, 357
- Factors affecting the electron spin resonance spectra of irradiated polymers, 119
- Fractionation of radiation-branched polybutadiene, 235
- Glass transition temperatures, internal pressures of polymers below their, 375
—of homologous series, 449
- Growth of pressure fluctuations in concentrated polymer solutions during prolonged shear flow, 195
- Handbook of Organometallic Compounds*, review of, 439
- Infra-red study of the crystallization of poly(vinyl chloride), 143
- Intermolecular forces and chain flexibilities in polymers: III—Internal pressures of polymers below their glass transition temperatures, 375
- Internal pressures of polymers below their glass transition temperatures, 375
- Isobutene, effect of zinc oxide on the radiation-initiated polymerization of, at -78°C , 419
- Isotope Effects on Reaction Rates*, review of, 116
- Macromolecules, soft linear, with finite chain length, streaming birefringence of, 257
- Measurement of crystallinity in polypropylene fibres by X-ray diffraction, 409
- Mechanism of the crosslinking of epoxide resins by amines, 95
- Mechanisms of pyrolysis of epoxide resins, 451
- Miscibility of polymers: II—Miscibility and heat of mixing of liquid polyisobutenes and silicones, 8
- Molecular weight distributions in branched polymers, 295
- Morphology of multilayer polymer crystals, 109
- New method for following rapid rates of crystallization: I—Poly(hexamethylene adipamide), 221
- Normal stress, shear recovery and viscosity in polydimethyl siloxanes, 429
- Nylon 66, proton magnetic resonance in, 203
- Organic Coating Technology, Vol. II: Pigments and Pigmental Coatings*, review of, 437
- Organo-lithium compounds, reactivities of, as polymerization initiators, 365
- Physical and mechanical properties of polypropylene fractions, 161
- Polybutadiene, fractionation of radiation-branched, 235
- Polyisobutenes and silicones, miscibility and heat of mixing of liquid, 8
- Polyisobutylene-chlorobenzene system, viscometric study of the, 393
- Poly [3,3-bis (chloromethyl) oxacyclobutane], crystallization of, 1
- Polyethylene terephthalate, crystallization of, by organic liquids, 315
—effect of radiation and moisture on the dynamic mechanical properties of, 401
- Polydimethyl siloxanes, normal stress, shear recovery and viscosity in, 429
- Poly (hexamethylene adipamide), new method for following rapid rates of crystallization, 221
- Polymorphism of crystalline polypropylene, 185
- Polyoxymethylene (Delin), dielectric and dynamic mechanical properties of, 239
- Polypropylene, assignment of the infra-red absorption bands and the measurement of tacticity in, 341
—crystalline, polymorphism of, 185
- Polypropylene fibres, measurement of crystallinity in, by X-ray diffraction, 409
- Polypropylene fractions, physical and mechanical properties of, 161
- Polythene, radiation-induced conductivity in irradiated, 444
- Poly (vinyl chloride), infra-red study of crystallization of, 143

- Preparation and general properties of anion exchangers based on cellulose, 18
- Production of surface radicals on polymers using high-frequency discharge, 277
- Properties and Structure of Polymers*, review of, 115
- Proton magnetic resonance in Nylon 66, 203
- Quasi-soluble Ziegler catalyst for the polymerization of ethylene, 441
- Radiation-induced conductivity in irradiated polythene, 444
- Rate of cure of network polymers and the superposition principle, 383
- Reactivities of organo-lithium compounds as polymerization initiators, 365
- Rheological properties of concentrated polymer solutions: I—Growth of pressure fluctuations during prolonged shear flow, 195
- Shear recovery, normal stress, and viscosity in polydimethyl siloxanes, 429
- Side chain structure of high pressure polyethylene in a study of short chain branching in hydrocarbon polymers by the irradiation method, 335
- Silicones, miscibility and heat of mixing of liquid polyisobutenes and, 8
- Streaming birefringence of soft linear macromolecules with finite chain length, 257
- Study of short chain branching in hydrocarbon polymers by the irradiation method: I—The detection of the side chains, 323
- II—The chain structure of high pressure polyethylene, 335
- Studies on radiation polymerization in solution: III—Effect of primary radicals in the termination reaction, 83
- Styrene, anionic polymerization of, 151
- Superposition principle, the rate of cure of network polymers and the, 383
- Surface-chemical mechanism of heterogeneous polymerization and derivation of Tung's and Wesslau's molecular weight distribution, 41
- Synthesis of block and graft copolymers of cellulose and its derivatives, 213
- Test between rival theories for molecular weight distributions in heterogeneous polymerization: the effect of added terminating agent, 60
- Thermal depolymerization of polystyrene: IV—Depolymerization in naphthalene and tetralin solutions, 367
- Thermochemical aspects of butadiene-styrene copolymerization, 74
- Tracer studies of di-anisoyl peroxide and the anisoyloxy radical, 265
- Viscometric study of the polyisobutylene-chlorobenzene system, 393
- Viscosity, normal stress, shear recovery and, in polydimethyl siloxanes, 429

Author Index

- ADDINK, Miss E. J. and BEINTEMA, J.: Polymorphism of crystalline polypropylene, 185
- ALLEN, G.: *See* STRETCH, C. and ALLEN, G.
- GEE, G. and NICHOLSON, J. P.: The miscibility of polymers: II—Miscibility and heat of mixing of liquid polyisobutenes and silicones, 8
- SIMS, D. and WILSON, G. J.: Intermolecular forces and chain flexibilities in polymers: III—Internal pressures of polymers below their glass transition temperatures, 375
- ALLEN, J. K. and BEVINGTON, J. C.: Tracer studies of di-anisoyl peroxide and the anisoyloxy radical, 265
- ANDERSON, H. C.: Mechanisms of pyrolysis of epoxide resins, 451
- BAMFORD, C. H. and WARD, J. C.: The effect of the high-frequency discharge on the surfaces of solids: I—The production of surface radicals on polymers, 277
- BARLOW, A., LEHRLE, R. S. and ROBB, J. C.: Direct examination of polymer degradation by gas chromatography: I—Applications to polymer analysis and characterization, 27
- BEINTEMA, J.: *See* ADDINK, Miss E. J. and BEINTEMA, J.
- BENBOW, J. J. and HOWELLS, E. R.: Normal stress, shear recovery and viscosity in polydimethyl siloxanes, 429
- BERGER, M. N. and FLETCHER, K.: A quasi-soluble Ziegler catalyst for the polymerization of ethylene, 441
- BERKENBOSCH, R.: *See* VAN SCHOOTEN, J., DUCK, E. W. and BERKENBOSCH, R.
- BEVINGTON, J. C.: *See* ALLEN, J. K. and BEVINGTON, J. C.
- BOERMA, J.: *See* VAN SCHOOTEN, J., VAN HOORN, H. and BOERMA, J.
- BOYLE, D. A., SIMPSON, W. and WALDRON, J. D.: A study of short chain branching in hydrocarbon polymers by the irradiation method: I—The detection of the side chains, 323
- — —: — II—The side chain structure of high pressure polyethylene, 335
- BROOK, B. N.: *See* JAKUBOVIC, A. O. and BROOK, B. N.
- CAMERON, G. G. and GRASSIE, N.: The thermal depolymerization of polystyrene: IV—Depolymerization in naphthalene and tetralin solutions, 367
- CERESA, R. J.: The synthesis of block and graft copolymers of cellulose and its derivatives, 213
- COOPER, W.: *See* VAUGHAN, J., EAVES, D. E. and COOPER, W.
- DALTON, F. L., GLAWITSCH, G. and ROBERTS, R.: The effect of zinc oxide on the radiation-initiated polymerization of isobutene at -78°C , 419
- DAOUST, H. and SENEZ, M.: Viscometric study of the polyisobutylene-chlorobenzene system, 393
- DORAN, MARY A.: *See* WAACK, R. and DORAN, MARY A.
- DUCK, E. W.: *See* VAN SCHOOTEN, J., DUCK, E. W. and BERKENBOSCH, R.
- DYVIK, G. K.: Glass temperatures of homologous series, 449
- EAVES, D. E.: *See* VAUGHAN, J., EAVES, D. E. and COOPER, W.
- FARROW, G.: The measurement of crystallinity in polypropylene fibres by X-ray diffraction, 409
- FINCH, C. A.: review of *The Chemistry of Nucleic Acids*, 117
- : review of *Handbook of Organometallic Compounds*, 439
- FLETCHER, K.: *See* BERGER, M. N. and FLETCHER, K.

- FREEBORN, A. S.: review of *Organic Coating Technology*, Vol. II: *Pigments and Pigmental Coatings*, 437
- FURUKAWA, J.: See KAWASAKI, A., FURUKAWA, J., TSURUTA, T. and SHIOTANI, S.
- GEE, G.: See ALLEN, G., GEE, G. and NICHOLSON, J. P.
- GLAWITSCH, G.: See DALTON, F. L., GLAWITSCH, G. and ROBERTS, R.
- GOODINGS, E. P.: review of *Isotope Effects on Reaction Rates*, 116
- GORDON, M. and RYONG-JOON ROE: Surface-chemical mechanism of heterogeneous polymerization and derivation of Tung's and Wesslau's molecular weight distribution, 41
- and SIMPSON, W.: The rate of cure of network polymers and the superposition principle, 383
- GRASSIE, N.: See CAMERON, G. G. and GRASSIE, N.
- HOWELLS, E. R.: See BENBOW, J. J. and HOWELLS, E. R.
- ISAMU NITTA: See SHUN-ICHI OHNISHI, YUICHI IKEDA, MICHIO KASHIWAGI and ISAMU NITTA
- JAKUBOVIC, A. O. and BROOK, B. N.: Anion exchangers based on cellulose: I—Preparation and general properties, 18
- JONES, D. W.: Proton magnetic resonance of Nylon 66, 203
- KAWASAKI, A., FURUKAWA, J., TSURUTA, T. and SHIOTANI, S.: An infra-red study of the crystallization of poly(vinyl chloride), 143
- KELLER, A.: See MITSUHASHI, S. and KELLER, A.
- KLINE, D. E. and SAUER, J. A.: Effect of radiation and moisture on the dynamic mechanical properties of polyethylene terephthalate, 401
- LEHRLE, R. S.: See BARLOW, A., LEHRLE, R. S. and ROBB, J. C.
- LODGE, A. S.: Rheological properties of concentrated polymer solutions: I—Growth of pressure fluctuations during prolonged shear flow, 195
- MCDONALD, M. P. and WARD, I. M.: The assignment of the infra-red absorption bands and the measurement of tacticity in polypropylene, 341
- MAGILL, J. H.: A new method for following rapid rates of crystallization: I—Poly(hexamethylene adipamide), 221
- MANABE, T.: See OKAMURA, S. and MANABE, T.
- MASAHIRO HATANO and SHU KAMBARA: Crystallization of poly[3,3-bis(chloromethyl)oxacyclobutane], 1
- MICHIE, R. I. C.: Determination of the weight, viscosity, or number average degree of polymerization of cellulose from the intrinsic viscosity in cuprammonium hydroxide solution, 446
- MICHIO KASHIWAGI: See SHUN-ICHI OHNISHI, YUICHI IKEDA, MICHIO KASHIWAGI and ISAMU NITTA
- MITSUHASHI, S. and KELLER, A.: The morphology of multilayer polymer crystals, 109
- MOORE, W. R. and SHELDON, R. P.: The crystallization of polyethylene terephthalate by organic liquids, 315
- NICHOLSON, J. P.: See ALLEN, G., GEE, G. and NICHOLSON, J. P.
- OKAMURA, S. and MANABE, T.: Studies on radiation polymerization: III—Effect of primary radicals in the termination reaction, 83
- OROFINO, T. A.: Branched polymers: I—Molecular weight distributions, 295
- II—Dimensions in non-interacting media, 305
- ORR, R. J.: Thermochemical aspects of butadiene-styrene copolymerization, 74
- PETERLIN, A.: Streaming birefringence of soft linear macromolecules with finite chain length, 257
- PLESCH, P. H.: review of *Arbeitserinnerungen*, 364

- READ, B. E. and WILLIAMS, G.: The dielectric and dynamic mechanical properties of polyoxymethylene (Delrin), 239
- ROBB, J. C.: See BARLOW, A., LEHRLE, R. S. and ROBB, J. C.
- ROBERTS, R.: See DALTON, F. L., GLAWITSCH, G. and ROBERTS, R.
- RYONG-JOON ROE: A test between rival theories for molecular weight distributions in heterogeneous polymerization: the effect of added terminating agent, 60
- : See GORDON, M. and RYONG-JOON ROE
- SAUER, J. A.: See KLINE, D. E. and SAUER, J. A.
- SENEZ, M.: See DAoust, H. and SENEZ, M.
- SHELDON, R. P.: See MOORE, W. R. and SHELDON, R. P.
- SHIOTANI, S.: See KAWASAKI, A., FURUKAWA, J., TSURUTA, T. and SHIOTANI, S.
- SHU KAMBARA: See MASAHIRO HATANO and SHU KAMBARA
- SHUN-ICHI OHNISHI, YUICHI IKEDA, MICHIO KASHIWAGI and ISAMU NITTA: Electron spin resonance studies of irradiated polymers: I—Factors affecting the electron spin resonance spectra of irradiated polymers, 119
- SIMPSON, W.: See GORDON, M. and SIMPSON, W.
- : See BOYLE, D. A., SIMPSON, W. and WALDRON, J. D.
- SIMS, D.: See ALLEN, G., SIMS, D. and WILSON, G. J.
- SMITH, I. T.: The mechanism of the crosslinking of epoxide resins by amines, 95
- : review of *Advanced Paint Chemistry*, 437
- STRETCH, C. and ALLEN, G.: Anionic polymerization of styrene, 151
- TRELOAR, L. R. G.: review of *Properties and Structure of Polymers*, 115
- TSURUTA, T.: See KAWASAKI, A., FURUKAWA, J., TSURUTA, T. and SHIOTANI, S.
- VAN HOORN, H.: See VAN SCHOOTEN, J., VAN HOORN, H. and BOERMA, J.
- VAN SCHOOTEN, J., DUCK, E. W. and BERKENBOSCH, R.: The constitution of ethylene—propylene copolymers, 357
- VAN HOORN, H. and BOERMA, J.: Physical and mechanical properties of polypropylene fractions, 161
- VAUGHAN, J., EAVES, D. E. and COOPER, W.: Fractionation of radiation-branched polybutadiene, 235
- WAACK, R. and DORAN, MARY A.: Reactivities of organo-lithium compounds as polymerization initiators, 365
- WALDRON, J. D.: See BOYLE, D. A., SIMPSON, W. and WALDRON, J. D.
- WARD, I. M.: review of *Chemical Crystallography. An Introduction to Optical and X-Ray Methods* (2nd ed.), 438
- : See McDONALD, M. P. and WARD, I. M.
- WARD, J. C.: See BAMFORD, C. H. and WARD, J. C.
- WILLIAMS, G.: See READ, B. E. and WILLIAMS, G.
- WILSON, G. J.: See ALLEN, G., SIMS, D. and WILSON, G. J.
- WINTLE, H. J.: Radiation-induced conductivity in irradiated polythene, 444
- YUICHI IKEDA: See SHUN-ICHI OHNISHI, YUICHI IKEDA, MICHIO KASHIWAGI and ISAMU NITTA